MEASUREMENT AND THERMODYNAMIC INTERPRETATION OF HIGH PRESSURE VAPOUR-LIQUID EQUILIBRIUM DATA

Andreas Lorenz Mühlbauer

A thesis submitted

in the

Department of Chemical Engineering

University of Natal at Durban

In partial fulfillment of the requirements for

the degree

Doctor of Philosophy

December 1990

For
My Parents

DECLARATION

This thesis embodies my own original work, except as otherwise specifically acknowledged in the text. It has not been submitted for degree purposes at any other university

---

A. L. Mühlbauer

ACKNOWLEDGEMENTS

I wish to express my gratitude to my supervisor Professor J.D. Raal of the Department of Chemical Engineering for his assistance, interest and guidance during the course of this research program.

I would also like to express my appreciation to others who have helped :

To my parents, for their boundless encouragement and support during the course of this project.

To the workshop staff in the Department of Chemical Engineering under the supervision of the late Mr D Penn and Mr L C Clarence who, with Mr Ken Jack, were responsible for much of the construction of the equipment.

In addition Messers Otto Msomi and Micheal Mthethwa who helped in various ways.

To Messrs Mike Gooch and Johnny Visser for their assistance with the installation of the electrical circuitry.

To Mr Marcus Lussi of the laboratory staff for his guidance and useful suggestions with regard to gas chromatography analysis.

To Mr C Brouckaert for his help with the simplex program.

To Miss Crystal Human, who gave up many hours of her time to typing the numerous drafts of this thesis, and Mrs Loveena Kisson who helped as well.

Mr David Nagessur for his help with the photographs appearing in this thesis.

To Professor C. Buckley for his permission to use the Pollution Research Group Laser Printer.

To Mr Barry Scott from SALVALVE who supplied a number of valves free of charge.

To the Council of Scientific and Industrial Research and Development (CSIR) and South African Coal Oil and Gas Corporation (Sasol) for their financial assistance.

SUMMARY

Detailed experimental and thermodynamic studies of the isothermal phase equilibria for the **volatile / non-volatile** carbon dioxide / toluene and propane / 1 - propanol systems are presented.

Measurements were made in a 350 cm^3 **static** equilibrium cell capable of operating up to 200 bar and 180 °C. The equilibrium cell was mounted in an air bath which provided the isothermal environment. Considerable precautions were taken in the design of the bath to remove vertical temperature gradients induced by conduction and heater element radiation.

The sampling procedures were designed to cause minimal distrubance to the equilibrium condition. The vapour phase was sampled by releasing it into a 0,9 cm^3 evacuated manifold. A liquid phase sample was obtained via a piston-driven sampling rod which removed a 8,8 mm^3 sample, and released it into a previously evacuated jet mixer. Homogeneity of the vapour and particularly the liquid samples, an especially acute problem due to the great volatility difference between the components, was ensured by the use of **novel jet mixers.** Analysis was by gas chromatography.

The measured carbon dioxide / toluene data at 79 °C agree well with published data. Data are presented for the previously unmeasured propane / 1-propanol system at 81,6, 105,2 and 120,1 °C, the volatile component being **supercritical** at each of the above temperatures, with the exception of propane for the 81,6 °C isotherm.

The isothermal phase behaviour of the propane / water system, which shows extremely **limited miscibility** between the two components, was experimentally examined at 100,7 and 119,5 °C. This limited miscibility provided a severe test of the functioning of the experimental equipment and operating procedures. The vapour data agreed well with published data. The liquid data showed an incorrect bias towards the volatile component. The probable source of error was identified and a modification to the equilibrium cell is proposed.

Excellent modelling of the carbon dioxide / toluene system was achieved with the **combined method,** based on the UNIQUAC equation for the excess Gibbs free energy and the Peng-Robinson EOS for the fugacity coefficient. Satisfactory modelling of the propane / 1-propanol system was achieved with the **combined method** using the the UNIQUAC equation with either one of the following EOS : the Group Contribution EOS of Skjold-Jorgenson (1986), Peng-Robinson EOS or two parameter Virial EOS. Since $T_{component} / T_c < 1,8$ for the avaliable data sets, the carbon dioxide and propane components were considered **condensable gases** (Prausnitz, *et al* 1980). The **symmetric convention** for **normalizing** the activity coefficients was therefore used for all components. The "liquid phase" properties of the non-condensable components were evaluated by extrapolation. The **standard state** reference pressure was zero.

UNIQUAC parameters α_{ij} , hitherto unavailable, with **fairly strong temperature dependence** in the 38 to 120 °C and 81.6 to 120 °C range are proposed for the two systems respectively. Analysis of the co-variance matrix indicated a high degree of correlation between the parameters.

Temperature independent classical mixing rule interaction parameters, δ_{ij} , as used in the original Peng-Robinson EOS, are presented for the propane/1-propanol system.

The measured data was tested for **thermodynamic consistency** by two **equal area tests** : The Chueh, *et al* (1965) and a **newly derived equal area test.** The new variation derived from the Gibbs-Duhem equation requires only vapour phase properties and has the following form :

$$\int_{y_2}^{y_2} \ln\left(\hat{\phi}_2^v/\hat{\phi}_1^v\right) dy + \int_{p_1}^{p_2} \left(\frac{V^v}{RT}\right) dp = \left[\ln \hat{\phi}_1 P + y_2 \ln \hat{\phi}_2^v/\hat{\phi}_1^v\right]_{y_2}^{y_2}$$

Useful features of this test are :

1. It can be applied if only P-T-y data are available,
2. The liquid molar volumes required in the Chueh, *et al* (1965) test and which are difficult to calculate are not required,
3. The vapour molar volumes and fugacity coefficients required can both be obtained from a single appropriate EOS.

The consistency tests indicated the measured data to be not inconsistent, except at very low vapour phase concentrations. In this region small changes in total pressure, due to sampling, produce large changes in the relative amounts of vapour and liquid in equilibrium.

A **novel static equilibrium cell design** for measuring **multicomponent multiphase** data based on experience gained in this project, has been developed in principle. The cell design incorporates see-through windows and can conveniently be housed in an air, oil or water bath. Liquid sampling is based on a **single sampling valve** with a **double piston construction** allowing for sampling at **any desired level.** The advantages of the proposed cell lie in the ability to detect multiple phase formation and to subsequently sample each liquid phase with a single sampling valve, **without disturbing equilibrium.** The cell with minor additions can be used to determine volumetric data.

CONTENTS

APPENDICES

FIGURES

PHOTOGRAPHS

TABLES

NOMENCLATURE

LIST OF SYMBOLS

a_{ij}	UNIQUAC interaction parameter (units Kelvin)
a	Peng and Robinson attraction parameter
B	2 nd Virial EOS Coefficient
b	van der Waals volume
C	3 rd Virial EOS Coefficient
f	fugacity
f°	standard state fugacity
f^{OL}	standard state liquid phase fugacity
g, G	Gibbs energy
ΔH	enthalpy change of mixing
k	interaction parameter for EOS
K	equilibrium K values
n	number of moles
P	Pressure
R	gas constant
T	Temperature
v_j^i	number of groups (j) in molecule (i) (Group Contribution EOS)
V	liquid molar volume
$\overline{V}$	partial liquid molar volume
ΔV	volume change of mixing
w	acentric factor
x	liquid phase mole fraction
y	vapour phase mole fraction
z	lattice coordination number
Z	compressibility factor

GREEK LETTERS

δ_{ij}	Peng and Robinson interaction parameter
ϕ	fugacity coefficient
γ	activity coefficient

SUPERSCRIPTS

E	excess property
L	liquid phase
r	reference
s	saturated
V	vapour phase
^	quantity's value when component is part of mixture
–	partial property

SUBSCRIPTS

c	critical property
i , j	component identification
ij	interaction of components i and j
mix	mixture
r	reference

All other symbols are defined locally in text

ABBREVIATIONS

EOS	Equation of State
FID	Flame Ionized Detector
G-C	Group-Contribution
P-R	Peng-Robinson
PHCT	Perturbated Hard Chain Theory
R-K	Redlich-Kwong
S-R-K	Soave-Redlich-Kwong
S & J	Skjold-Jorgensen
TCD	Thermal Conductivity Detector
VLE	Vapour-Liquid Equilibrium

INTRODUCTION

As the known reserves of raw materials diminish; the chemical industry has to design new plants which make more efficient and economical use of the available reserves. Hydrocarbon processing plants involve many separating units which require accurate phase equilibrium data in their design. As products become more complex, both physically and chemically, more economical separation methods and conditions are continuously being sought and high pressure data is of increasing interest. For example, the rapidly developing technology of supercritical extraction in the food and petrochemical industries has led to considerable interest in high pressure vapour-liquid equilibrium data for systems containing carbon dioxide and light hydrocarbons such as propane. Carbon dioxide is especially valued for its non-toxicity, availability and low cost.

Initially most of the high pressure high temperature data required was supplied from experimental studies. The theoretical treatment of experimental data, which at high pressures is a very severe test for the theoretical concepts involved, was before the advent of electronic computers rudimentary. The number of iterations and complexity of the mathematical algorithms required deterred the researcher from performing the rigorous and time-consuming calculations. Today with the help of computers, data can be correlated and sometimes predicted by complex theoretical and / or empirically derived equations. The only limitation on the accuracy of the results is the validity of the equations employed and reliability of the thermodynamic information. Accurate phase equilibrium data, especially for complex systems, is therefore of fundamental importance and interest to the theoretician to aid in the development of new computational techniques. To date however, no adequate method has yet been found to predict high pressure vapour-liquid equilibrium without some form of experimental data input.

Thermodynamic interpretation and modelling of high pressure equilibrium data is a much more difficult proposition than for the low-pressure case. Modelling by either direct methods (which involve the use of equations of state to describe both the liquid and vapour phase) or by the combined methods (which involves the description of the liquid phase non-ideality via an activity coefficient) presents many problems not encountered in low pressure analysis. These include finding an appropriate model for the Gibbs free energy, iterative methods for estimating the vapour phase fugacity coefficients which are composition dependent, evaluation of liquid molar volumes as a function of pressure and temperature and the vexing problem of defining appropriate reference states for the fugacity when one component is non-condensable. In selecting an equation of state to model either the vapour phase (combined method) or both phases (direct method) difficulties arise in choosing appropriate mixing rules for the mixture for equations other than the Viral equation of state. Such mixing rules are empirical and tend to become system specific. Relatively few researchers attempt thermodynamic consistency testing of high pressure VLE data probably because the procedures are complex and tedious and involve estimates of several quantities such as liquid and vapour phase fugacities and liquid molar volumes, all of which may be subject to greater or lesser error.

INTRODUCTION

As the known reserves of raw materials diminish; the chemical industry has to design new plants which make more efficient and economical use of the available reserves. Hydrocarbon processing plants involve many separating units which require accurate phase equilibrium data in their design. As products become more complex, both physically and chemically, more economical separation methods and conditions are continuously being sought and high pressure data is of increasing interest. For example, the rapidly developing technology of supercritical extraction in the food and petrochemical industries has led to considerable interest in high pressure vapour-liquid equilibrium data for systems containing carbon dioxide and light hydrocarbons such as propane. Carbon dioxide is especially valued for its non-toxicity, availability and low cost.

Initially most of the high pressure high temperature data required was supplied from experimental studies. The theoretical treatment of experimental data, which at high pressures is a very severe test for the theoretical concepts involved, was before the advent of electronic computers rudimentary. The number of iterations and complexity of the mathematical algorithms required deterred the researcher from performing the rigorous and time-consuming calculations. Today with the help of computers, data can be correlated and sometimes predicted by complex theoretical and / or empirically derived equations. The only limitation on the accuracy of the results is the validity of the equations employed and reliability of the thermodynamic information. Accurate phase equilibrium data, especially for complex systems, is therefore of fundamental importance and interest to the theoretician to aid in the development of new computational techniques. To date however, no adequate method has yet been found to predict high pressure vapour-liquid equilibrium without some form of experimental data input.

Thermodynamic interpretation and modelling of high pressure equilibrium data is a much more difficult proposition than for the low-pressure case. Modelling by either direct methods (which involve the use of equations of state to describe both the liquid and vapour phase) or by the combined methods (which involves the description of the liquid phase non-ideality via an activity coefficient) presents many problems not encountered in low pressure analysis. These include finding an appropriate model for the Gibbs free energy, iterative methods for estimating the vapour phase fugacity coefficients which are composition dependent, evaluation of liquid molar volumes as a function of pressure and temperature and the vexing problem of defining appropriate reference states for the fugacity when one component is non-condensable. In selecting an equation of state to model either the vapour phase (combined method) or both phases (direct method) difficulties arise in choosing appropriate mixing rules for the mixture for equations other than the Viral equation of state. Such mixing rules are empirical and tend to become system specific. Relatively few researchers attempt thermodynamic consistency testing of high pressure VLE data probably because the procedures are complex and tedious and involve estimates of several quantities such as liquid and vapour phase fugacities and liquid molar volumes, all of which may be subject to greater or lesser error.

The accurate measurement of high pressure vapour liquid equilibrium data is an extraordinarily demanding, intriguing and fascinating task both from an equipment design and operational point of view. Some of the problems encountered in static, circulation or flow-through methods include :

1. The attainment of true equilibrium which can be adversely affected by even the smallest temperature or pressure gradients.
2. Sampling from a high pressure region without disturbing the equilibrium.
3. Proper homogenization of the sample where the relative volatilities of the components may differ greatly and conveyance of the samples without change in composition to a gas chromatograph.
4. In high pressure and temperature work the attainment of leak-free seals in moving parts due to the attrition or deformation of the sealing materials are perennial problems.

The main objective of this project was to perfect the high pressure static equilibrium cell, whose initial development was described by Bradshaw (1985). The measured data would consequently be analysed within an appropriate theoretical framework. The theoretical analysis would involve the **fitting** of the data onto a suitable liquid phase model (UNIQUAC) to determine the model's binary interaction parameters and to check the validity of these parameters using a **correlation** procedure. Thermodynamic **consistency tests** performed on the measured data gave an important indication of the quality of the measured data. A secondary aim of this project was to become familiar with the latest experimental and theoretical developments in the field of high pressure and temperature vapour-liquid equilibrium.

This project forms part of the on-going study of thermodynamic properties in the Department of Chemical Engineering at the University of Natal (Durban). This particular project, the design of a VLE measuring device capable of obtaining high temperature (500 °C) and pressure (200 bar) equilibrium data, was initiated at the request of SASOL in the early 1980's to obtain data for complex coal-derived mixtures that would be present in their proposed coal liquification process. The preliminary design and construction work was performed by Harel in 1982. During this period the operational method (static) was chosen and initial purchases of pressure and temperature measuring devices were made. Bradshaw between 1983 and 1985 was responsible for the selection and initial construction of the liquid and vapour sampling devices. During this period the SASOL requirements fell away and the first experimental data for the carbon dioxide/toluene system were measured. Bradshaw experienced difficulties with cell temperature uniformity and the liquid phase mole fractions measured were rich in the volatile component compared to the literature values. The vapour phase mole fractions however compared favourably with those in the literature.

In the present project (1987-1990) the liquid and vapour phase sampling devices were perfected, the air bath completely redesigned and certain auxiliary equipment constructed to measure the carbon dioxide/toluene, propane/water and propane/1-propanol binaries.

CHAPTER 2

CLASSIFICATION AND DESCRIPTION OF HIGH TEMPERATURE AND PRESSURE VAPOUR-LIQUID EXPERIMENTAL EQUIPMENT

2.1 PRESENTATION OF HIGH PRESSURE HIGH TEMPERATURE VAPOUR-LIQUID EQUILIBRIUM DATA

Experimentally determined *two phase, two component* vapour-liquid equilibrium data can be presented in one of the following forms of phase diagrams depending on how the data was measured :

- isothermal $P - x - y$
- isobaric $T - x - y$
- isopleth $P - T$ data.

Before discussing the different experimental methods used to measure the above data it is essential to understand the underlying principles involved in the construction of two component, two phase equilibrium diagrams, a summary of which is given in Appendix A.1. For a more detailed review of this subject the reader is referred to Schneider (1978) and Street (1983).

2.2 CLASSIFICATION OF EXPERIMENTAL EQUIPMENT

Depending on :

the kind of data required,
operating conditions (temperature, pressure) of interest,
properties of the substance (volatility, thermal stability,
corrosive properties, explosive tendencies) being investigated, and
the investigator (his experience, location and financial means),

there are a variety of experimental methods from which he can choose.

Accurate experimental measurements of the **field** variables usually presents fewer difficulties than the **density** variables. For this reason Dieters and Schneider (1986) in their review of high-pressure, high-temperature phase equilibria experimental methods classify the methods according to the densities which are primarily observed. Dieters and Schneider (1986) distinguished between the so called **synthetic method** and **analytic method.**

In the synthetic method a mixture of known composition is prepared and its behaviour observed as a function of pressure or temperature. The problems associated with *analysing* the equilibrium mixture's composition are thus replaced by the problem of *synthesizing* the equilibrium mixture and effectively observing it's behaviour. In contrast to the synthetic method, the analytic method does not have to rely on a precise knowledge of the overall composition. Here temperature or pressure are adjusted to bring about phase separation (preferably with large quantities of both

the vapour and liquid). Samples are then withdrawn from the phases and analysed by appropriate methods. Attempts have been made at combining the features of the synthetic and analytic methods into one equilibrium cell.

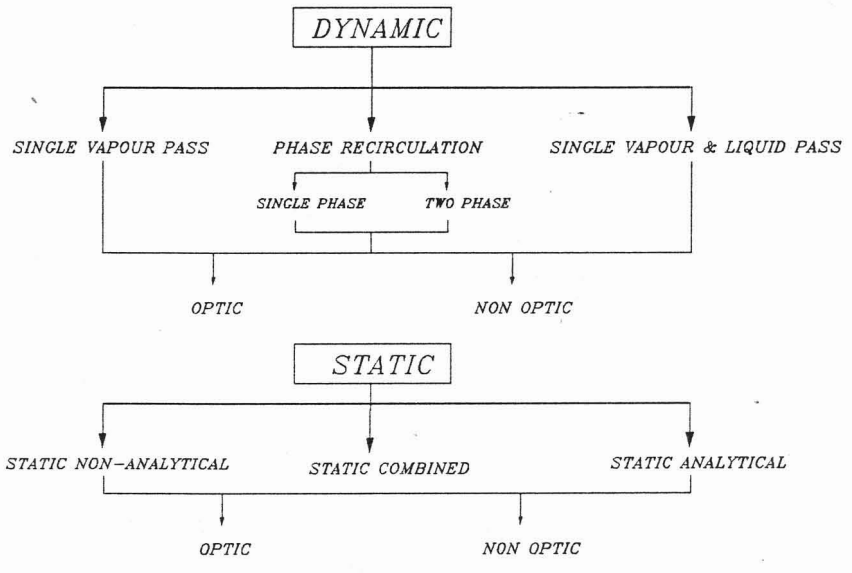

Figure 2.1 : Classification of Experimental High Pressure Vapour Liquid Equilibrium Equipment

A simpler classification of equilibrium cells was adopted in this project and is shown in Figure 2.1. Classification depends on whether either liquid, vapour or both are circulated through the equilibrium cell. If circulation takes place it is known as a **dynamic** or **flow** method and if not a **static** method. Further sub-division of the dynamic category depends on the circulating phase. Sub-division of the static category depends on whether the phases are sampled or not.

The experimental difficulties common to the dynamic and static analytical methods will now be outlined in detail with particular reference to those associated with the static method. The unique and interesting features as well as some of the inherent advantages and disadvantages of the various types of flow and static methods will consequently be described with the aid of examples from the literature. It would not be feasible to cover all the various apparatus reported in the literature; only the more recent apparatus will be covered. Excellent reviews by Tsiklis (1968) and Young (1978) cover the earlier period.

2.3 DYNAMIC AND STATIC ANALYTICAL METHODS

2.3.1 Main Features Of The Analytical Method

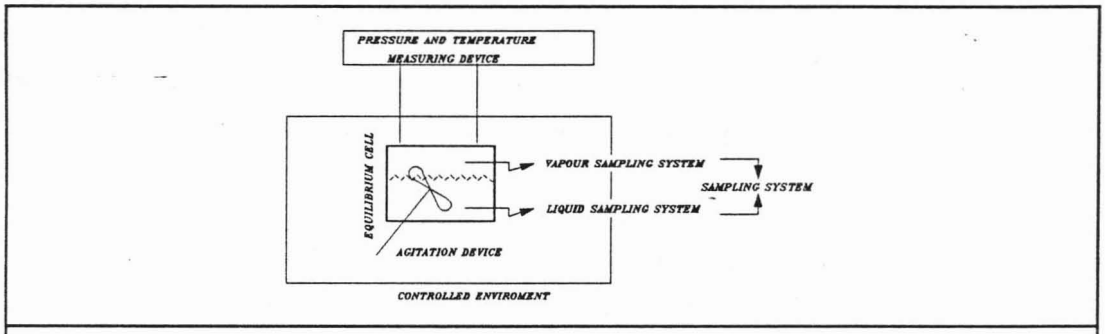

Figure 2.2 : Features of a Typical Analytical Method

A typical analytic apparatus (schematically shown in Figure 2.2) consists of the following :

1. An equilibrium cell in which the vapour and liquid of the mixture are at equilibrium.
2. An environment that controls the temperature of the equilibrium cell : air, oil, water bath or aluminium (Ng and Robinson 1978), copper (Konrad, *et al* 1983) jacket.
3. Some method of agitating the mixture in the equilibrium cell in order to speed up the attainment of equilibrium. Static methods use an internal stirrer, in dynamic methods the circulation of one or more phases fulfils this role. Some vapour recirculation methods do however have an additional internal stirrer. Rocking of the equilibrium cell assembly to attain equilibrium has also been reported Haung, *et el* (1985)
4. Some method of sampling the vapour and liquid phases. In the two phase recirculation and single vapour and liquid pass methods sampling presents few problems. The circulating and effluent streams are diverted through external loops to remove a sample. The vapour recirculation method requires some form of liquid sampling device. Static methods require both a vapour and liquid sampling device.
5. Some means to analyse the withdrawn samples.
6. Pressure and temperature measurement devices.

2.3.2 Difficulties Encountered In Analytical Experimentation

Problems encountered in the measurement of *accurate* isothermal vapour-liquid equilibria common to all analytic methods, and those which received particular attention in this project are :

1. Obtaining truly isothermal equilibrium conditions between the phases.
2. Establishing when equilibrium has been reached.
3. Withdrawal of samples from the equilibrium phases without disturbing equilibrium.
4. Avoiding :
   - 4.1 partial condensation of the heavier component in the sample lines for volitile/non-volitile systems.
   - 4.2 the *flashing phenomenon* (condensation of heavier components and vapourisation of lighter components) when withdrawing samples from a volatile/non-volatile system at high pressure.
5. Accurate analysis of the withdrawn samples.
6. Accurate measurement of temperature and pressure.
7. Degassing of components on entry into the equilibrium cell at the start of the experimentation. The degassing and purging of the sample lines during repetitive samples during experimentation.

2.3.2.1 Obtaining true isothermal conditions

The equilibrium cell must be devoid of any thermal gradients for the analysed vapour and liquid compositions to reflect the true equilibrium conditions, at the temperature under investigation. Obtaining isothermal cell conditions is an especially acute problem when measuring volatile/non-volatile components. Special precautions, usually thermal, are employed when measuring these systems to avoid the potential problems discussed in section 2.3.2.4

Measurement of bath temperature profiles have been reported by various authors in the literature, mainly those using static equipment (among others Rogers and Prausnitz 1970, Figuiere, *et al.* 1980, Legret, *et al* 1981). Measurement of equilibrium cell temperature profiles, although widely reported by various authors, again mainly those using static cells (Toedheide and Franke 1963, Rogers and Prausnitz 1970, Figuiere, *et al* 1980, Legret, *et al* 1981 and Guillevic, *et al* 1983), have seldom been quantitatively given (0.2 K Konrad, *et al* 1983).

2.3.2.2 Establishing attainment of equilibrium

Equilibrium implies a situation in which there is no macroscopic change with respect to time. In thermodynamics, where attention is focussed upon a particular quantity of material, equilibrium is defined as there being no change in the properties of the material with respect to time.

1. Obtaining truly isothermal equilibrium conditions between the phases.
2. Establishing when equilibrium has been reached.
3. Withdrawal of samples from the equilibrium phases without disturbing equilibrium.
4. Avoiding :
   - 4.1 partial condensation of the heavier component in the sample lines for volitile/non-volitile systems.
   - 4.2 the *flashing phenomenon* (condensation of heavier components and vapourisation of lighter components) when withdrawing samples from a volatile/non-volatile system at high pressure.
5. Accurate analysis of the withdrawn samples.
6. Accurate measurement of temperature and pressure.
7. Degassing of components on entry into the equilibrium cell at the start of the experimentation. The degassing and purging of the sample lines during repetitive samples during experimentation.

2.3.2.1 Obtaining true isothermal conditions

The equilibrium cell must be devoid of any thermal gradients for the analysed vapour and liquid compositions to reflect the true equilibrium conditions, at the temperature under investigation. Obtaining isothermal cell conditions is an especially acute problem when measuring volatile/non-volatile components. Special precautions, usually thermal, are employed when measuring these systems to avoid the potential problems discussed in section 2.3.2.4

Measurement of bath temperature profiles have been reported by various authors in the literature, mainly those using static equipment (among others Rogers and Prausnitz 1970, Figuiere, *et al.* 1980, Legret, *et al* 1981). Measurement of equilibrium cell temperature profiles, although widely reported by various authors, again mainly those using static cells (Toedheide and Franke 1963, Rogers and Prausnitz 1970, Figuiere, *et al* 1980, Legret, *et al* 1981 and Guillevic, *et al* 1983), have seldom been quantitatively given (0.2 K Konrad, *et al* 1983).

2.3.2.2 Establishing attainment of equilibrium

Equilibrium implies a situation in which there is no macroscopic change with respect to time. In thermodynamics, where attention is focussed upon a particular quantity of material, equilibrium is defined as there being no change in the properties of the material with respect to time.

As equilibrium requires a balance of all potentials that may cause change, the rate of approach to equilibrium is proportional to the difference in the potential between the actual state and the equilibrium state. The rate of change becomes slow as equilibrium is approached. In phase equilibrium studies therefore, high stirring rates are desirable as the resulting greater contact between the phases decreases the time taken to reach equilibrium. A true state of equilibrium is probably never reached, owing to the continual variations in the surroundings and to retarding resistances. Therefore equilibrium is assumed when changes can no longer be detected with the available measuring devices.

Temperature, pressure, vapour and liquid composition and in some cases stability of the refractive index (Besserer and Robinson 1971) are important indicators in determining whether the equilibrium condition has been reached.

Temperature and pressure indications

The fluctuations in the measured temperature and pressure readings, when less than a predetermined percentage of the measured value for a specific time, have been used by various authors in the literature as an indication of equilibrium. Fredenslund, *et al* (1973) stated that a change in pressure of less than 0,05 % in half an hour was generally taken as an indication of equilibrium.

Compositional analysis

Repeated vapour and liquid sample composition analysis must give reproducible results within the limits of the compositional analysis method. Two samples are usually taken at each equilibrium condition with three consecutive flushings of each sample, Fredenslund, *et al* (1973).

2.3.2.3 <u>Disturbance of equilibrium during sampling</u>

Sampling of either the liquid or vapour phase can entail a change in the volume of the equilibrium cell. The larger the volume change associated with sampling the greater the disturbance to the equilibrium condition. The change in volume can be quantitatively analysed by the pressure change in the cell. Pressure fluctuations of 0,1 and 0,01 bar have been reported by Besserer and Robinson (1971) and Wagner and Wichterle (1989) respectively.

Two volume changes associated with sampling in the static method disturb the equilibrium condition :

the volume change associated with the withdrawn **sample volume** change, and

the volume change associated with the **sampling method** employed.

The ideal sampling method is to remove the smallest **sample volume** possible particular to the **method of sampling** employed. The size of the sample is however dictated by the requirements of the analytical and sampling methods. The method of sample withdrawal should cause the least possible volume change in the equilibrium cell.

Various methods have been developed to overcome this specific problem :

1. A large equilibrium cell volume in comparison to the withdrawn sample volume and sampling method volume change. A large cell volume dampens the two volumetric disturbances as the percentage cell volume change for large cells is smaller. Sagara, *et al* (1972), Klink, *et al* (1975), Aschroft, *et al* (1983) and Reiff, *et al* (1987) all report the use of large equilibrium cells to counteract the volume changes of sampling.
2. A very fast sampling method to minimise the change in equilibrium Figuiere, *et al* (1980). A fast sampling method is however is not as important as having a small sample size.
3. A sampling method were the only volume change the cell experiences is that of the withdrawn sample volume. Rogers and Prausnitz (1970) and Nakayama, *et al* (1987) use a sampling rod which traverses the entire cell. The cell therefore does not experience any sampling method volume change but only the sample volume change.
4. Compensating for the volume change by pressure adjustment Nakayama, *et al* (1987).
5. Analysing the phase compositions in situ by optical methods, Konrad, *et al* (1983).

2.3.2.4 <u>Sampling and analysis of volatile/non volatile mixtures</u>

When the liquid phase of a volatile/non-volatile mixture is sampled it has been observed that there is a tendency for the volatile component to flash preferentially (Kalra, *et al* 1978 and Ng and Robinson 1979). Unless there are some methods of homogenizing the withdrawn sample and the consequent prevention of partial condensation of the non-volitile component, the quantitative analysis of the sample will be in error.

Some solutions to these problems are :

1. Employing some sort of stirred homogenization vessel in the sample line, Wagner and Wichterle (1987).
2. Heating and keeping the carrier gas pressure in the sampling lines low to avoid non-volatile condensation. The temperatures required are usually 50 to 100 K higher than the equilibrium temperature. This causes, without adequate precautions, a thermal disturbance in the equilibrium cell, which is undesirable. This solution does not however address the problem of sample rehomogenization.
3. Keeping the sampling lines at a lower temperature than (2) and employing a circulation system to homogenize the volatile/non-volatile components (Kalra, *et al* 1978, Ng and Robinson 1979, Nakayama, *et al* 1987).

4. Analysing the volatile and non-volatile components separately. The sampling methods of Kobayashi and Katz (1953), Rogers and Prausnitz (1970), Simnick, *et al* (1977) and Inomata, *et al* (1986) basically entailed the separation of the volatile and non-volatile components in the sample by expanding the sample into an evacuated vessel. The amount of supercritical component could be calculated from the total pressure. The condensed non-volatile components were flushed out of the vessel with an organic solvent. A calibration standard was added and the resulting mixture analysed by gas chromatography. A correction was usually made for the amount of supercritical component in the non-volatile component from low pressure phase equilibrium data if such data was available.

In the present study, as discussed in section 4.2.4, this particular problem was solved by use of a novel jet mixer.

2.3.2.5 Accurate analysis of the withdrawn sample

The two most commonly used methods of phase analysis are gas chromatography and spectroscopy.

Gas Chromatography

By far the most common form of analysis in recent years has been by gas chromatography. Refractive index measurements in conjunction with gas chromatograph analysis have also been reported (Besserer and Robinson 1971 and Kalra, *et al* 1978).

The two main types of gas chromatograph detectors used are :

1. Thermal conductivity detectors (TCD) which can be used to detect hydrocarbons and non-hydrocarbons.
2. Flame ionisation detectors (FID) which can be used to detect organics only.

The main disadvantage of this method is that the high-pressure high-temperature equilibrium state is quite different from the input to the chromatograph. Dieters and Schneider (1985) make the observation that the quantitative determination of the compositions does not usually present a problem but the handling and preparation of the sample for analysis does.

Spectroscopic Methods

In situ phase composition analysis by spectroscopy or photometric methods (Beer's Law states that absorbance is proportional to concentration), to overcome the sample preparation difficulties associated with gas chromatographic analysis, have been reported. Konrad, *et al* (1983) and Swaid, *et al* (1986) report the use of infrared spectra (where the absorption bands are often well separated) to determine phase concentrations.

There are however difficulties associated with the use of infrared, visual and ultraviolet spectroscopy or Raman scattering methods these being :

1. The extensive calibration procedures required compared to gas chromatography.
2. The application of visual or ultraviolet spectroscopy is largely restricted to aromatic or coloured compounds.
3. When using infrared spectroscopy there is a strong possibility that absorption bands of different compounds may overlap. There are however methods avaliable to overcome this difficulty.

2.3.2.6 Temperature and Pressure Measurement

Temperature measurement

Thermocouples, platinum resistance thermometers (Pt - 100 Ω), thermistors and quartz thermometers may be used. The relative use of each of the different types may be gauged from Tables 2.1 to 2.4. For work between 0 - 100 °C Platinum (Pt - 100 Ω) thermometers seem to be the preferred device. For temperatures > 150 °C thermocouples seem to be preferred (Table 2.3). The higher sensitivities to temperature change available from thermistors and quartz thermometers are generally not required for the primary measuring device. They are however used as standards against which the primary device is calibrated.

Pressure measurement

Bourdon pressure gauges and in recent years pressure transducers are used as primary measuring devices. Dead weight piston gauges, the most accurate, are seldom used as the primary measuring device. They are however, used as a standard against which the bourdon and pressure transducers are calibrated.

2.3.2.7 Degassing

Degassing the non-volatile component is necessary to remove gases that may compete with the volatile component at low liquid phase mole fractions. Degassing is especially important in systems if the two components are slightly soluble in one another, i.e. the propane-water system. Figuiere, *et al* (1980), Legret, *et al* (1980) and Legret, *et al* (1981) all place great emphasis, more so than many other authors, on their degassing systems and procedures.

2.4 DYNAMIC VAPOUR-LIQUID EQUILIBRIUM METHODS

There are three types of flow apparatus : the single vapour pass method, the phase recirculation method and the single vapour and liquid pass method. The variations will now be discussed.

2.4.1 Single Vapour Pass Method

The features of a typical single vapour pass method are shown in Figure 2.3

Description of the method

A stream of pure gaseous component at a specific pressure is passed through a stationary liquid phase in the equilibrium cell. In well designed equipment more gaseous component progressively dissolves into the liquid phase until equilibrium is finally reached. The claimed equilibrium time is approximately 15 minutes, Young (1978). After equilibrium has been reached the vapour may be analysed by diverting a small sample from the effluent stream. A sample of the liquid phase may be withdrawn from the equilibrium cell.

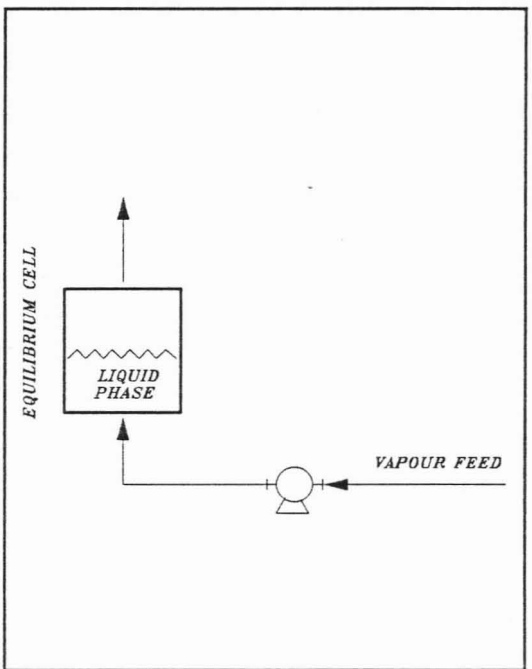

Figure 2.3 : Features of a Typical Analytical Method

The pressure of the gaseous component and the temperature of the liquid phase are regulated to generate the required isobaric or isothermal vapour liquid equilibrium phase diagram.

The original dynamic method, it is the simplest and easiest to operate; it does however, have a number of inherent disadvantages which have led to its replacement by the recirculation methods.

Difficulties encountered in the single vapour pass method are :

1. Ensuring establishing whether the vapour phase is saturated with liquid in the short contact time available. Ensuring equilibrium is obtained in one pass is therefore problematical.

2. Liquid component is constantly being removed. This immediately places constraints on the amount of data obtainable from one experimental run.

3. Large quantities of gaseous components are used. Although this is not an important factor to consider for common gases it does become important for rare, high purity and expensive gases such as the noble gases (xenon).

4. It is difficult to ensure that there is no droplet entrainment in the effluent vapour stream.

5. The partial pressures of the liquids that may be studied by this method are usually low, below 0,01 MPa, Young (1978). A consequence of this is that the method is not suitable for critical region studies.

6. Accurate control of the gas flow rate is vital. The higher the gas flow rate the shorter the time required for the liquid to be saturated with the gas. The liquid component however, requires a longer time to dissolve into the gas phase. It is therefore unlikely that the gas phase will reach saturation if too high a gas flowrate is used. Conversely if the gas flow rate is decreased the conditions for the saturation of the gas phase improve. The conditions for the saturation of the liquid phase however worsen. Therefore if one of the coexisting phases is not at equilibrium errors in the measured data are unavoidable. These errors are particularly pronounced when either the gas is highly soluble in the liquid or the liquid highly soluble in the gas.

7. Some form of mechanical agitation is necessary if the gas is poorly soluble in the liquid or the liquid poorly soluble in the gas.

2.4.2 Phase Recirculation Methods

Two different variations in this equipment have been reported : single phase and two phase recirculation.

The features of a typical phase recirculation method are shown in Figure 2.4

Description of the method

The components are charged into the equilibrium cell. Experience determines the quantities that need to be added to give the desired liquid level, Freitag and Robinson (1986). The temperature and pressure of the mixture are maintained at the required values while either one or both the phases are continuously withdrawn from the cell and recirculated. In two phase recirculation apparatus both phases are circulated counter-currently through the equilibrium cell.

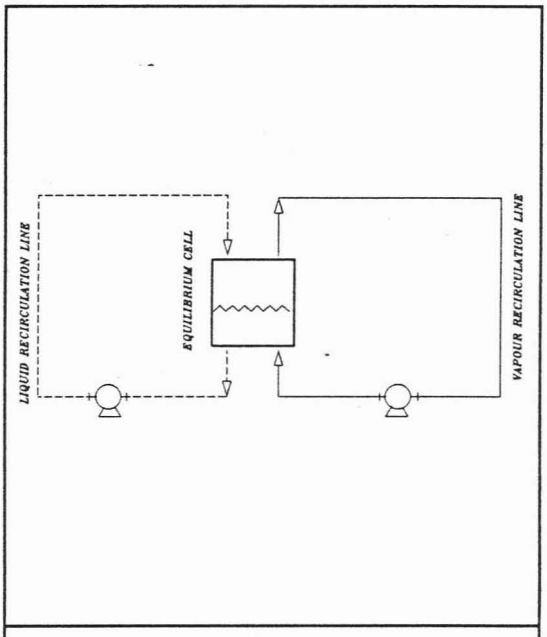

Figure 2.4 : Features of the Phase Recirculation Method

The liquid phase enters the cell at the top and pours through the vapour phase. Conversely the vapour enters at the bottom of the cell and bubbles up through the liquid. Equilibrium between the phases in a well designed equilibrium cell should be achieved fairly rapidly due to good contacting between the two phases.

This method removes some of the problematic factors associated with the single vapour pass method : ensuring equilibrium is reached, the liquid component is not continuously removed from the system, large quantities of the gaseous component are not wasted and liquids of high partial pressures may be studied.

A brief review of single and two phase recirculation methods in the literature is given in Appendix A.2, Table 2.1 and Appendix A.3, Table 2.3 respectively.

The single vapour phase recirculation method, like the single vapour pass method, requires some form of liquid sampling device to remove a sample of liquid from the cell. In the liquid phase and two phase recirculation methods the liquid phase can be sampled by trapping a quantity of the circulating phase in the circulation loop.

For example, the circulating liquid and vapour phases can temporarily be diverted through the external loops of commercially available liquid and or vapour chromatography valves. The use of Rheodyne or Valco valves were reported by D'Souza and Teja (1988), D'Souza, *et al* (1988), Adams, *et al* (1988), Jenning and Teja (1989), Kim, *et al* (1989) and Fink and Herskey (1990). This feature makes liquid sampling relatively easy and straight forward when compared to the static method for example.

The simplicity of sampling in the two phase recirculation method is however somewhat negated by the added complexity of a liquid recirculation loop.

Another reason for the popularity of these methods is the increasing availability of commercially manufactured (usually magnetically driven) pumps. Muirbrook and Prausnitz (1965) and Fleck and Prausnitz (1968) had to design and construct their own pumps which they describe in detail in the abovementioned articles.

Fredenslund's, *et al* (1973) vapour recirculation apparatus had a unique liquid sampling device the principle of which subsequently formed the basis of the liquid sampling devices of Meister (1985) and those developed for the static equilibrium cells of Bae, *et al* (1981), Ng and Robinson (1978) and this project. The device is shown in Figure 2.5. It had a 5 mm diameter rod with a 3,5 μl hole drilled near its tip. The latter being situated such that it was totally immersed in the liquid phase upon insertion of the rod into the equilibrium cell. When the sampling rod was withdrawn into the cell wall the sample hole came into alignment with sample ports drilled into the cell wall. Carrier gas then flushed the sample to a gas chromatograph for composition analysis.

For recirculation methods in general, vapourisation and condensation of the circulating liquid and vapour streams must be avoided. This has been overcome in a number of ways :

1. Having three separately controlled temperature zones. One for the equilibrium cell. Another for the vapour recirculation loop in which the temperature was slightly greater than the equilibrium temperature. The third for the liquid recirculation loop was maintained at a temperature slightly lower than the equilibrium temperature. A good example of this is the equipment of Takishima, *et al* (1986) and Inomata, *et al* (1988). Both have similar circulation loops and sampling systems housed in three different temperature zones, Figure 2.6.
2. Sampling the phases directly from the equilibrium cell which somewhat negates the advantages of a recirculation method.

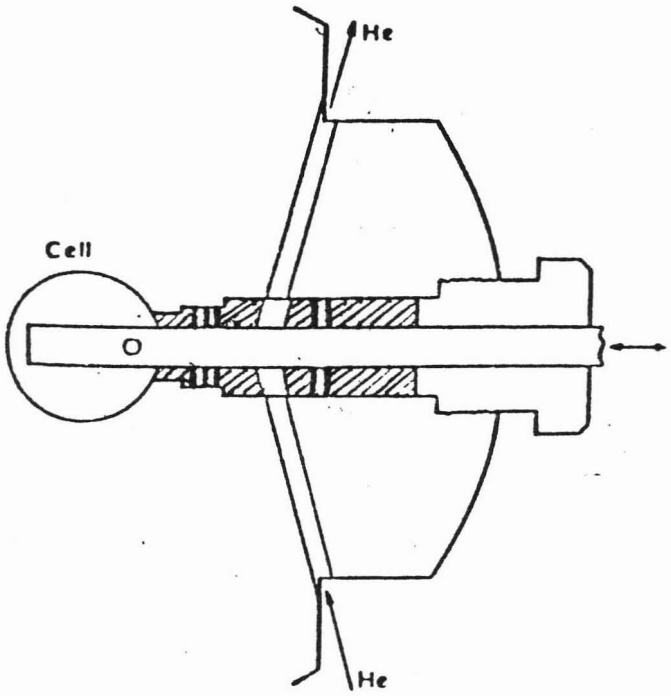

Figure 2.5 Fredenslund, *et al* (1973) liquid sampling device

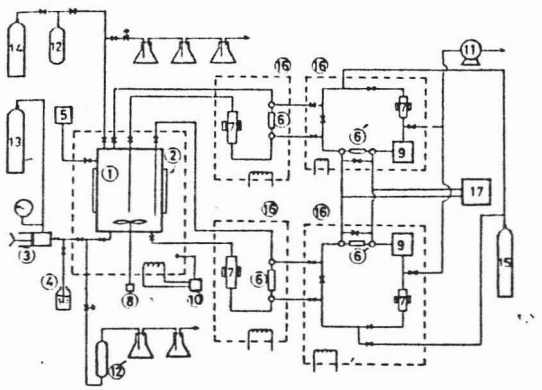

Schematic diagram of experimental apparatus: (1) equilibrium cell; (2) window; (3) sample charging pump; (4) liquid sample; (5) pressure transducer; (6) sampler; (7) magnetic pump; (8) magnetic stirrer; (9) flash tank; (10) temperature controller; (11) vacuum pump; (12) NH_3 sample cylinder; (13) N_2 gas cylinder; (14) NH_3 gas cylinder; (15) He gas cylinder; (16) air bath; (17) gas chromatograph.

Figure 2.6 Experimental apparatus of Inomata, *et al* (1988)

3. Removing samples from the equilibrium cell by some device and transferring these to an analysis device (Dorou, *et al* 1983, Shibata and Sandler 1989 a and Chou, *et al 1990*).

It is interesting to note that Kubota, *et al* (1983), King, *et al* (1983), Takishima, *et al* (1986), Inomata, *et al* (1988) and Suzuki and Sue (1990) all report the use of internal stirrers to aid in the equilibration process.

Difficulties encountered in the recirculation methods are :

1. Maintaining an adequate liquid level in the equilibrium cell. The only authors who mentioned the use of a liquid level measuring device were Muirbrook and Prausnitz (1965). All the other authors appear to rely on visual observations to maintain the desired liquid level.
2. Ensuring no droplet entrainment in the effluent vapour stream. The only specific reference to a demisting device was by Muirbrook and Prausnitz (1965).
3. Ensuring that the pumps used do not contaminate the equilibrium mixture (this problem has largely been overcome by the use of magnetically coupled pumps), or create stagnant spaces.
4. Avoiding the possibility of partial condensation and vapourisation of the circulating vapour and liquid streams respectively.
5. Avoiding undesirable pressure gradients across the equilibrium cell caused by the circulating pump if it is not pulsation free.

2.4.3 The Single Vapour and Liquid Pass Method

A relatively recent development of the dynamic method. The method was specifically developed for high temperature and pressure vapour-liquid equilibrium measurements where thermal degradation of a hydrocarbon could occur.

The features of a typical single vapour-liquid pass method is shown in Figure 2.7

Description of the Method

Separate streams of vapour and liquid components are contacted co-currently at a controlled temperature and pressure in a mixing unit. The combined stream passes into an equilibrium cell where the mixture separates into the vapour and liquid phases. The two phases exit from the equilibrium cell separately and sampling is achieved by the diversion of the effluent streams. A summary of some of the apparatus mentioned in the literature is given in Table 2.3 and Appendix A.4.

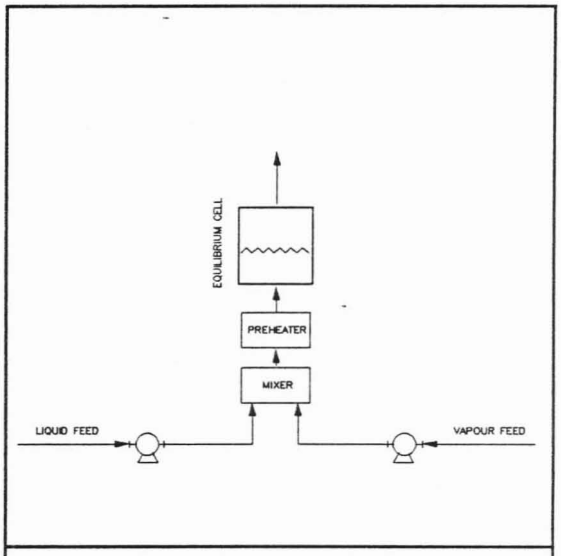

Figure 2.7 : Features of the Single Vapour and Liquid Pass Method

Difficulties encountered in this method are :

1. Ensuring that equilibrium has been reached in one pass.
2. Ensuring complete phase separation in the equilibrium cell.
3. Achieving a steady liquid level in the equilibrium cell.
4. Ensuring no droplet entrainment in the effluent stream.
5. Ensuring the pumps do not contaminate the equilibrium mixture.
6. Avoiding undesirable pressure gradients across the equilibrium cell.

In addition the designer faces material problems due to the very reason these apparatus were designed, namely high temperatures.

2.5 STATIC VAPOUR-LIQUID EQUIBLIBRIUM METHODS

2.5.1 Static Analytic Method

2.5.1.1 Description of the method

The features of a typical static apparatus is shown in Figure 2.8.

The components under investigation are charged into the equilibrium cell. The liquid components may be flushed into the cell by the volatile component or pumped in. The volatile component is usually supplied directly from its storage cylinder. High boiling volatile components such as propane and butane may have to be heated and pumped in by some compressor type device.

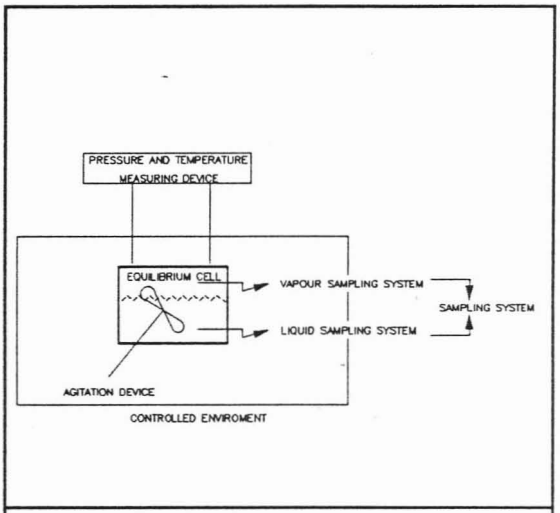

Figure 2.8 : Features of the Static Analytic Method

The contents of the cell are agitated to promote contact between the phases thereby shortening the time taken to reach equilibrium. After equilibrium has been reached the temperature and pressure are noted and samples of the liquid or vapour or both are withdrawn and their compositions analysed. The temperature and pressure of the mixture are regulated to generate the required vapour-liquid equilibrium isothermal phase diagram.

A summary of a few of the important features of a selected number of static apparatus reported in the literature is given in Table 2.4. In the review of static analytic apparatus particular emphasis is placed on :

1. Equipment which displayed similar features to the one used in this project. The liquid and vapour sampling methods of (Ng and Robinson 1979 and Bae, *et al* 1981 and Nakayama, *et al* 1987), equilibrium cell agitation method of (Kalra and Robinson 1973 and Ng and Robinson 1979) and air bath design (Rogers and Prausnitz 1970).
2. The early difficulties experienced in the sampling of a liquid phase whose components displayed large differences in relative volitility. The methods used by Kalra, *et al* (1978), Ng and Robinson (1979) and Wagner and Wichterle (1987) to rehomogenize a withdrawn volatile / non-volatile sample are described.

3. The apparatus of Figuiere, *et al* (1980), Legret, *et al* (1981) and Guillevic, *et al* (1983) which although not directly relevant to this project, are included in Appendix A.5 due to the unique methods employed to sample the liquid phase. The solution of sampling the liquid phase without disturbing equilibrium presented the most challenging and difficult problem to be surmounted for a successful cell design.

4. The equilibrium cell design of Aschcroft, *et al* (1983) and the modified version of the Bessserer and Robinson (1977) cell of Kalra, *et al* (1978) are described. The method of sampling the liquid phase formed the kernel of the idea on which the new cell design proposed in Chapter 10 was based.

5. The equipment of Swaid as described in Konrad, *et al* (1983) is included in Appendix A.5 as an example of the spectographical method of phase analysis.

2.5.1.2 Description of selected static analytic apparatus in the literature

Experimental apparatus of Rogers and Prausnitz (1970).

The equilibrium cell of Rogers and Prausnitz, (1970) is shown in Figure 2.9. Vapour and liquid samples were removed from the equilibrium cell via two sets of moving pistons. Between each set of two pistons was a small variable volume. During sampling this volume was extruded from the equilibrium cell into a cylinder and moved down the cylinder until the sample ports were reached. The sample then expanded through capillary tubes into a low pressure zone. This sampling technique had the primary advantage that the equilibrium cell pressure was not disturbed during withdrawal of the samples since the piston movement did not alter the interior cell volume. A hydraulic drive was used to move the sampling pistons back and forth.

The contents of the cell were agitated with a magnetic stirrer. The stirrer paddle made a 120 degree sweep of the cell and was designed to stir both phases without splashing liquid into the region near the vapour sampling pistons and to dislodge any vapour bubbles near the liquid sampling space. The only areas not reached by the stirring action were the short lengths of tubing leading to the pressure measurement and cell loading systems.

The authors found it necessary to know the position of the vapour liquid interface in order to avoid the withdrawal of a two phase-sample and to aid in the loading of the cell. The interface was located by a movable thermistor whose response depended on whether it was in the vapour or liquid phase.

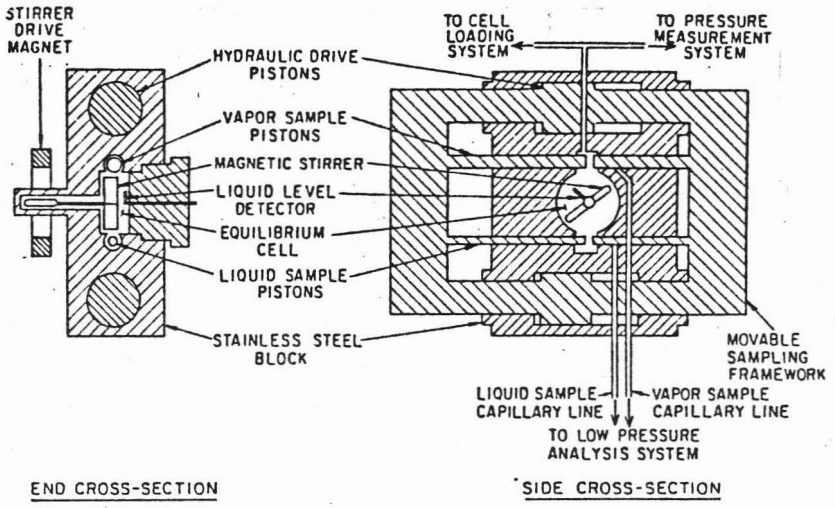

Figure 2.9 Equilibrium cell of Rogers and Prausnitz (1970)

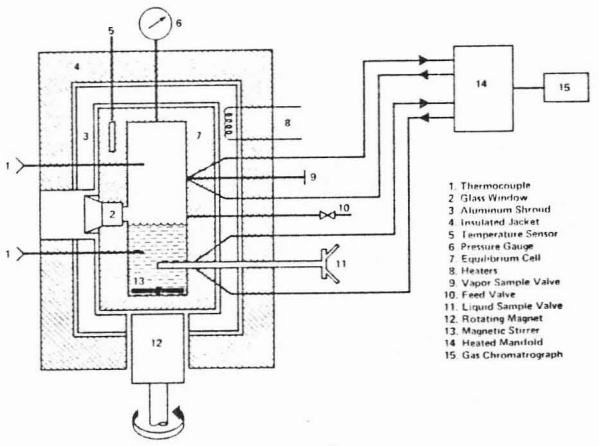

Figure 2.10 Equilibrium Cell of Peng and Robinson (1978)

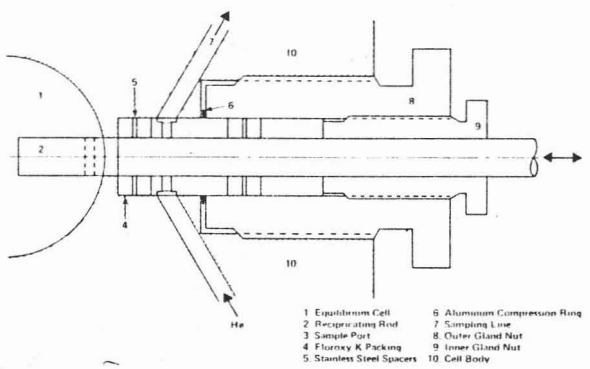

Figure 2.11 Peng and Robinson (1978) Liquid sampling device

Great care was taken in the design of the heating and cooling system in order to achieve isothermal bath conditions. The inside of the bath was constructed of copper plates to promote temperature uniformity and stability. A similar idea for promoting bath temperature uniformity was used in the present project. The equilibrium cell was mounted on steel supports with additional copper plates between them to minimize heat conduction out of the nitrogen bath. Heat transfer lines were hard soldered to the copper walls of the interior to speed up the transfer of energy between the bath and the heating/cooling system.

Experimental apparatus of Kalra and Robinson (1975)

In the equilibrium cell described by Kalra and Robinson (1975) the vapour and liquid phase were sampled through specially designed needle valves which were mounted directly into the wall of the cell. The main features of the valve design were :

1. a sample could be completely removed in a stream of helium from an external supply, and
2. a separate sealing system for the needle and the seat.

The sealing arrangement made it possible to provide the relatively high packing load required to seal off the seat without interfering with the lower load required to seal the delicate sampling needle. The needle was made from a hard chromium plated sewing needle, and the other parts from 316 stainless steel.

To analyse a sample the valves were opened by rotation of an external wheel. The sample was flushed into an evacuated manifold connected directly to the discharge side of the sample valve and to the inlet of the chromatograph. The valve was closed and the residual sample in the valve flushed into the manifold with helium. The manifold pressure was continuously monitored such that it was always maintained below the vapour pressure of the heaviest component in the mixture at the temperature under investigation.

Mixing of the phases was achieved by a teflon coated magnetic stirrer. The driving force for the stirrer was provided by a magnetic pile mounted externally to the cell. The pile consisted of three magnets mounted in mild steel shoes and encased in an aluminium housing. The pile was mounted on a variable speed d.c. motor. The magnetic stirrer remained coupled to the rotating pile at speeds in excess of 500 rpm through 19 mm of 316 stainless steel and a 15 mm air gap. If the cell was half full of liquid the stirrer generated a deep vortex in the liquid phase causing vapour bubbles to be continuously drawn into the underlying liquid phase. According to the authors equilibrium was rapidly attained between the phases, one half to two hours depending on the conditions and the mixture composition being investigated. A similar agitational method was adopted for this project.

Sampling components that showed great difference in relative volitility

At this time more interest was being shown in the field of supercritical extraction. Equilibrium data for volatile/non-volatile systems, especially those containing carbon dioxide, were in great demand. Kalra, *et al* (1978) used an equilibrium cell similar to that described by Besserer and Robinson (1971) to study the carbon dioxide/n-heptane system. Certain *major* modifications were however made to the equipment to overcome the difficulties associated with the analysis of a volatile/non-volatile system which were now becoming apparent.

In a volatile/non-volatile system, during the process of liquid phase sampling, the *flashing* phenomenon occurs. A liquid mixture containing a relatively light and heavy component undergoes a distillation process when it is throttled across a valve from a high pressure region to a low pressure region or to an evacuated space. As a result, the concentration of the light component in the throttled liquid passing through the valve has a higher concentration of light component than the liquid upstream of the valve. Thus the sample obtained for analysis is not representative of the equilibrium liquid phase. Previous methods of sampling the liquid phase, namely those based on opening a valve and releasing liquid phase into an evacuated space (Kalra and Robinson 1975) were not suitable nor applicable to volatile/non-volatile systems. A sampling method similar to that of Rogers and Prausnitz (1970) was required, namely the removal of a representative liquid sample out of the equilibrium cell.

Sample analysis problems similar to these described by Kalra, *et al* (1978) and Ng and Robinson (1978) were encountered in this project.

Modified experimental equipment of Besserer and Robinson (1978).

To overcome the abovementioned *flashing* difficulty, Kalra, *et al* (1978) modified the equilibrium cell of Besserer and Robinson (1977), described in Appendix A.5 by developing a new liquid phase sampling method. The modification consisted of inserting a four-port ball valve in the line connecting the vapour to the liquid space. The liquid level in the cell at equilibrium conditions was raised using a double acting Ruska pump until the liquid flooded one through-port in the ball valve. The valve was rotated 90", whereupon the filled port came in line with hot circulating helium. The helium and sample were circulated until all the liquid sample was vaporised. The flow was switched to the chromatographic sample valve for analysis. The Ruska pump moved the upper and lower pistons simultaneously thus maintaining a constant cell pressure and temperature. The equilibrium condition between the phases was therefore not disturbed.

An additional problem discovered during experimentation was related to the low volatility of the heavy component, n-heptane. During their previous experimental studies the authors had investigated systems in which the components had higher relative volatilities. The high volatility of the components ensured that the vaporised liquid phase sample could be maintained in the gaseous state in a simple electrical,

tape-heated manifold. During these investigations more elaborate precautions had to be taken to prevent partial condensation of the n-heptane during sampling and sample transportation. This was achieved by using an electrically heated and thermostated manifold enclosed in an insulated housing. The manifold was part of a circulation line equipped with a stainless steel bellows type diaphragm pump. The pump circulated the vapourized liquid sample and helium carrier gas. The circulation process ensured homogenization of the liquid sample if any *flashing* occurred during the sampling process and prevented partial condensation of the heavier component prior to injection into the gas chromatograph.

Experimental apparatus of Ng and Robinson (1978).

Figure 2.10 shows the equilibrium cell Ng and Robinson (1978) used to measure carbon dioxide/toluene vapour-liquid equilibrium data. This is the data against which the carbon dioxide/toluene data measured in this project was compared.

The equilibrium cell was equipped with a Pyrex glass bulls-eye window to observe the interface between the two phases. The vapour and liquid phases were sampled by two specially designed valves mounted directly into the cell body. The vapour sampling system had been developed and described earlier in the literature by Kalra and Robinson (1975) and the liquid sampling system by Fredenslund, *et al* (1973). Both sampling valves permitted the removal of micro samples of the particular phase so that the equilibrium conditions between the phases was not disturbed greatly. The liquid sampling device, Figure 2.11, consisted of a 1/4" diameter steel rod which was mounted through packing along a radius near the bottom of the equilibrium cell. A sample of the liquid phase filled a 1/16" diameter hole drilled horizontally along the diameter of the rod near the tip. The nonrotating piston rod and the trapped sample were withdrawn through the cell wall. The withdrawn sample subsequently flashed into an evacuated manifold.

The method of sample homogenization, manifold and stainless steel bellows type diagram pump, to circulate the sample and helium carrier gas was similar to that of Kalra, *et al* (1978).

The equilibrium cell temperature was maintained by a 1" thick aluminium shroud containing eight vertically mounted uniformly spaced pencil-type 250-W electrical heaters.

Equilibrium between the phases could be obtained within 3 hours by using a rotating magnetic stirrer coupled to an externally mounted rotating permanent ceramic magnet as described in the equipment of Kalra, *et al* (1975). The stirring action was allowed to continue overnight however, before the phases were sampled.

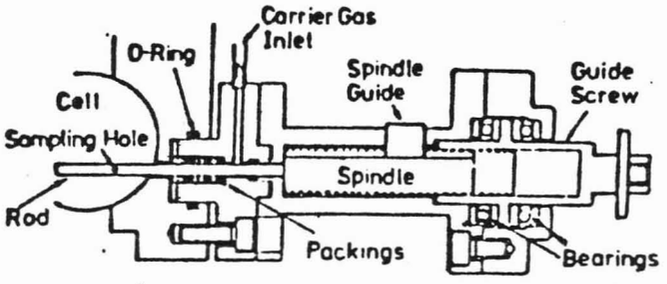

Figure 2.12 Bae, *et al* (1981) Liquid sampling device

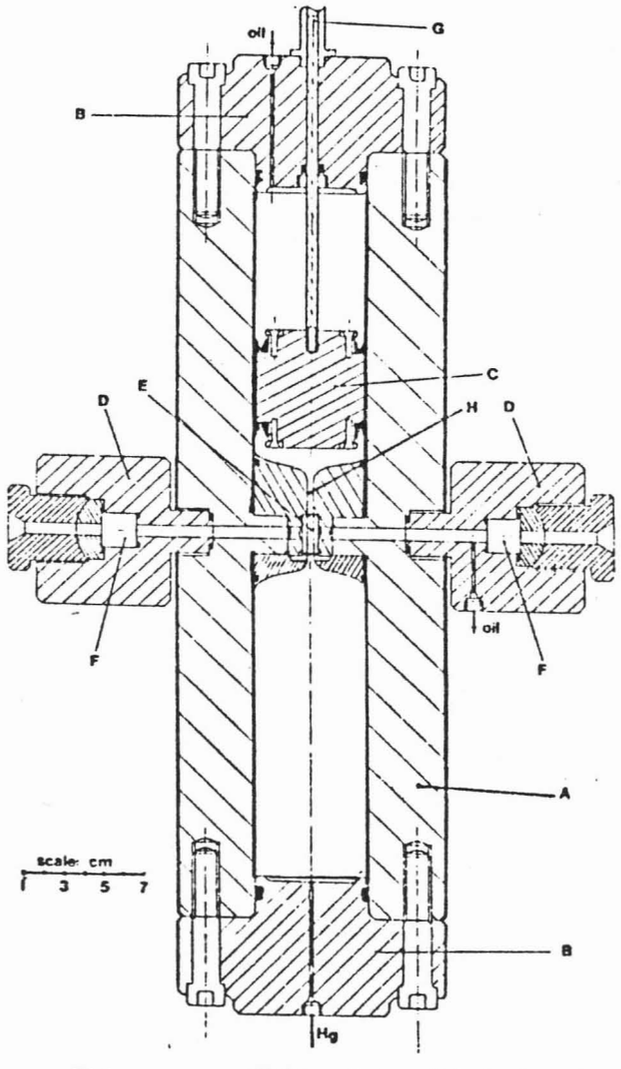

High pressure equilibrium cell. A—cell body. B—end caps. C—piston. D—window assemblies. E—glass capillary. F—toughened glass windows. G—piston indicating rod. H—sampling valve.

Figure 2.13 Equilibrium cell of Ashcroft, *et al* (1983)

Experimental apparatus of Bae, et al (1981)

The windowed equilibrium cell of Bae, *et al* (1981) sports a unique magnetically driven impeller and a specially designed liquid sampling device.

The visibility afforded by the glass window of the cell allowed for the detection of liquid and vapour phases, dew, bubble and critical points.

Mixing in the equilibrium cell was achieved by an internally vaned metallic impeller mounted on a hollow shaft. Vapour entered small holes on the upper part of the shaft, descended down the hollow shaft and dispersed into the underlying liquid phase.

The liquid in the equilibrium cell was sampled through a specially designed device, Figure 2.12, mounted directly into the wall of the cell. The design of the device was based on the methods of Fredenslund, *et al* (1973) and Ng, *et al* (1978). The 5 mm diameter stainless steel sampling rod withdrew an 8 μl liquid sample. The trapped sample was flashed directly into the carrier gas stream of the gas chromatograph. The same device was initially used for vapour phase sampling. It was however found to be unsuitable for sampling the vapour phase as a thin film of liquid was found to have adhered to the equilibrium cell wall in the vapour space. The vapour sampling technique was changed. A small portion of the vapour was released into an evacuated collection device and flushed via a carrier gas stream to the gas chromatograph.

Experimental apparatus of Ashcroft, et al (1983)

Ashcroft, *et al* (1983) have described a variable volume equilibrium cell design with provision for sampling of multicomponent, multiphase systems, visual phase observations and volume measurements. This was achieved by means of a unique sampling valve, optical system and an accurate method of determining the cell volume. The equilibrium cell shown in Figure 2.13 consisted of upper and lower cylinders connected to each other by a glass capillary tube which formed part of the window assembly used for optical observations. The lower cylinder was pressurized with mercury and the upper hydraulically. The lower cell contents could be raised or lowered to allow visual observations of the liquid phase, phase boundary and vapour phase by dual action pumping of the mercury and hydraulic oil. Once it was established that the liquid or the vapour phase occupied the space surrounding the sampling valve a sample of the phase could be taken by the valve in Figure 2.14.

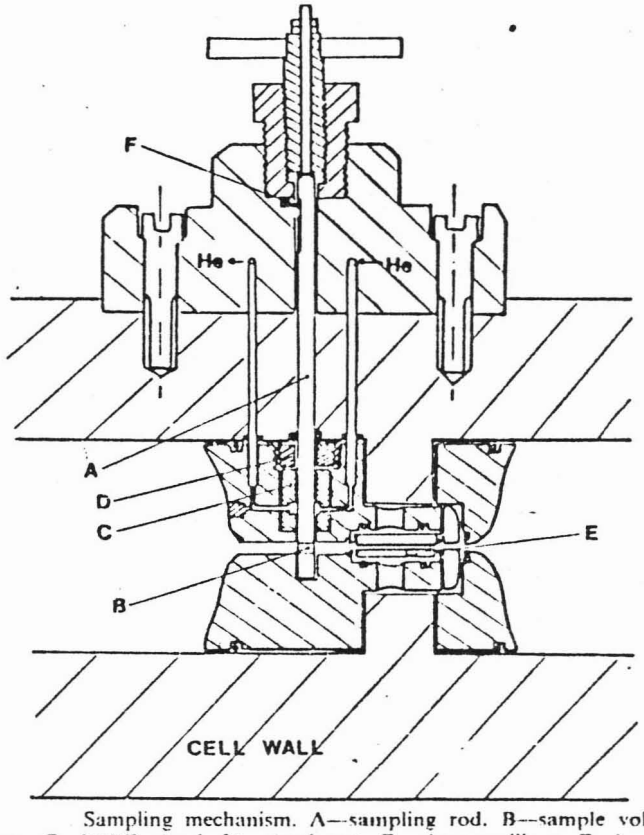

Sampling mechanism. A—sampling rod. B—sample volume. C—PTFE gland. D—gland nut. E—glass capillary. F—key.

Figure 2.14 Ashcroft, *et al* (1983) Liquid sampling valve

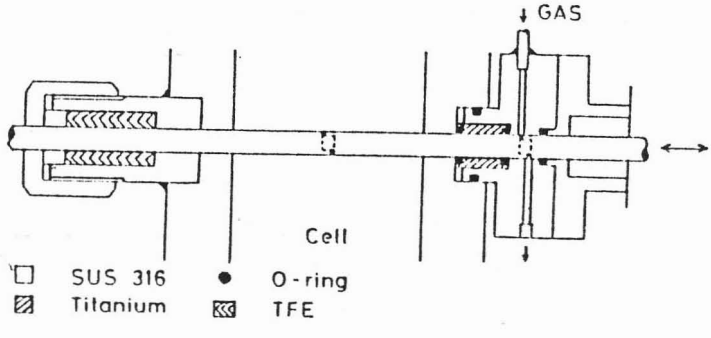

Sliding rod sampler.

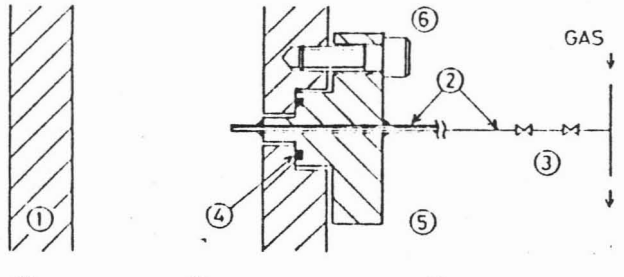

① Cell ② Capillary tube ③ Sampler
④ O-Ring ⑤ Cap ⑥ Bolt

Capillary tube sampler.

Figure 2.15 Nagahama, *et al* (1987) Liquid sampling devices

The 6 mm diameter stainless steel sampling rod (A) had a bored hole (B) of 2 mm diameter into which a sample of approximately 0,06 μl was trapped. As the sampling rod was withdrawn the sample in the bored hole was brought into line with the helium flowing around the teflon gland. Although the teflon gland was held tightly on the steel rod by gland nut (D) there was some leakage of helium into the cell. The authors however claim that this was negligible : during one hundred sampling operations the mole fraction of helium in the cell would rise to 2×10^{-5}. The vapourised sample in the helium carrier gas passed through a heated line via a sample splitter into the gas chromatograph.

Swivel lines were inserted into the mercury and hydraulic oil lines to enable rotation of the cell allowing equilibrium to be reached in about 3 hours by mechanically rocking the cell.

Experimental apparatus of Wagner and Wichterle (1987)

Wagner and Wichterle (1987) used a capillary sampling method to measure binary and ternary data for carbon dioxide, n-hexene and 1-hexene. The authors reported separation of the withdrawn samples for the volatile/non volatile systems due to the pressure drop along the capillary. A 0,8 ml intensively stirred glass homogenizing vessel was inserted in the sampling line to rehomogenize the withdrawn samples. The vessel was kept at approximately 100 K higher than the equilibrium temperature.

Experimental apparatus of Nakayama, *et al* (1987)

Nakayama, *et al* (1987) found an interesting way to compensate for the pressure change that occurs during sampling. The equilibrium cell was connected via a stainless steel diaphram to a buffer tank kept at the equilibrium pressure. The volume of the buffer tank was approximately 5 times greater than that of the cell. The volume and pressure changes that occurred during sampling were automatically compensated for by the action of the diaphragm. Great care had to be taken on filling the cell to avoid rupture of the diaphragm that would have occurred with large pressure differences.

Two sampling devices, Figure 2.15 were used : a capillary and a sliding rod sampler. The latter appears a cross pollination of the ideas of Rogers and Prausnitz (1970) and Fredenslund, *et al* (1973). The sliding rod was brought completely through the equilibrium cell so the only change in volume the cell experienced was that of the sample volume of approximately 0,1 cm^3.

The authors report the capillary tube sampler was simpler to design, operate and maintain. The cell did however experience a larger volume change during sampling 0,25 cm^3. To ensure analysis of equilibrium phase instead of stagnant material, which could be trapped in the thin capillary lines, the first few withdrawals were discarded.

The heavy components that could not be vapourised immediately upon sampling were collected in a cold trap. These components were returned to the air bath to be gasified. The light and heavy components were then homogenized by the magnetic pump in a circulation loop before being injected into the gas chromatograph for composition analysis.

Equilibrium between the phases was obtained by using a stirrer coupled to an externally rotating permanent magnet.

2.5.2 The Static Non-Analytical Method

Description of the Method

In this method a mixture of known composition is prepared and placed into the equilibrium cell. The temperature or pressure of the mixture inside the equilibrium cell is adjusted until phase separation of the homogeneous phase occurs. The moment the homogeneous phase separation starts the pressure and temperature are noted. The mole fractions of substances making up the mixture can be precisely calculated, as the quantities of each substance initially loaded into the equilibrium cell are known. After the appearance of the second phase the temperature and pressure should be readjusted into the homogeneous region in order to avoid demixing and layering of the phases. The temperature or pressure is again adjusted until the formation of a new phase is observed. The pressure, temperature and mole fractions at which these phase separations start define points on the phase envelope.

The initial results of these experiments are sets of isopleths (phase boundaries at constant composition). The method whereby the temperature is varied at constant pressure until a second phase appears is known as the method of temperature variation. Repeating these experiments under different constant pressures defines more points on the $p(T)$ - isopleth. Conversely the method whereby the pressure is varied at constant temperature is known as the method of pressure variation and a $T(p)$ - isopleth is generated. The final results of the synthetic experiments, pressure-mole fraction and temperature-mole fraction phase diagrams must be obtained by cross plotting from the two sets of isopleths.

The equilibrium cell of Meskel-Leasavre, *et al* (1981) an example of this type of apparatus is described in Appendix A.6.

Advantages and Disadvantages of the Synthetic Method :

Advantages :

1. No sampling is necessary and therefore no complicated and expensive analytical devices are required.
2. The experimental method is simple and since there is no need to wait for equilibration between the phases equilibrium data can be generated quickly and efficiently.

3. P , V and T and even orthobaric densities may be obtained if the motion of the pressure transferring element can be recorded with sufficient precision, Meskel-Lesavre, *et al* (1981).
4. Critical states measurements can be carried out on this equipment.
5. A $p(T)$ isopleth can be obtained from one filling of the equilibrium cell.

Disadvantages :

1. Visual observation of iso-optic systems, i.e. where the coexisting phases have approximately the same refractive index is extremely difficult if not impossible.
2. For mixtures with more than two components the information obtained from experimentation is limited.
3. The method is not suitable for measurements away from the critical states i.e. where $(\partial T/\partial C)p$ and $(\partial P/\partial C)t$ is large or infinite.
4. Great care must be taken not to overlook a dew point which can easily happen if the liquid phase condenses not as a mist but as a thin film on the wall of the pressure cell.

2.5.3 The Static Combined Method

In analysing the isobars and isotherms of phase diagrams they are seen to have large gradients far away from the critical states and small gradients near the critical states, (Dieters and Schneider 1986).

Where the isobars and isotherms have small gradients slight disturbances in the temperature and pressure of the mixture in the equilibrium cell can lead to large fluctuations of the phase compositions. Therefore the application of the analytic method for the study of phase behaviour near the critical state should not be considered. As the non-analytic method does not require sampling the above fluctuations are not experienced. Consequently this method is the more accurate near the critical state.

Where the isobars and isotherms have large gradients the non-analytic method is the least accurate of the two methods. An error in the overall composition leads to a large deviation of the temperature in the generated data.

Attempts have therefore been made at combining the features of the analytic and non-analytical static methods into a single equilibrium cell. Provision is made for viewing of the contents, to allow for sampling of the vapour and liquid phase and in recent years some method of accurately determining the volume of the equilibrium cell. The equilibrium cell of Wisotzki (Appendix A.7) is a typical example of this type of apparatus.

TABLE 2.1

Single Phase Recirculation Apparatus Reported in the Literature

Author (1)		Cell Volume cm3	Operating range Temp K	Operating range Press bar	Cell (2)	Measurement Device Temp (3)	Measurement Device Press (4)	Claimed Equilibration time min	Sample size Vap µl	Sample size Liq µl
Vapour Recirculation										
Fredenslund	1973	15	350	373	304 Stainless steel	RT	DWP	120/180	3,5	3,5
Dorau	1983	168	70/100	1/200	Austenitic steel	RT	B	-	60 000	-
Weber	1984	230	223/300	3/180	Chromium-nickel steel	RT	B	-	-	-
Meister	1985	50	70/290	0,1/350	Stainless steel	RT	DWP	-	-	-
Meister	1985	56	70/470	2/400	Stainless steel	RT	DWP	-	-	-
Freitag	1986	100	256/405	1/365	Hastelloy C-276	TC	B	30	50/200	-
Chou	1990	-	-	-	-	TC	B	60	-	-
Shah	1990	-	325/500	83	Saphire	RT	PT	5/10	-	-
Liquid Recirculation										
Kim	1986	100	137	423	316 Stainless steel	TC	PT	10	25	0,5

(1) Due to space limitations only first author mentioned.
(2) Material of construction of equilibrium cell.
(3) TC = thermocouple; RT = Platinum Resistance Thermometer (Pt - 100 Ω).
(4) B = Bourdon pressure gauge; PT = Pressure transducer; DWP = Dead weight piston gauge.

TABLE 2.2

Two Phase Recirculation Apparatus Reported in the Literature

Author (1)		Cell Volume cm3	Operating range Temp K	Operating range Press bar	Cell (2)	Measurement Device Temp (3)	Measurement Device Press (4)	Equilibration time min	Sample size Vap µl	Sample size Liq µl
Muirbrook	1965	200	233-303	1 250	403 Stainless steel	TC	B	-	-	-
King	1983	300	773	500	Stainless steel	TS	B	-	11 500	/34 700
Kubota	1983	106	283-353	800	304 Stainless steel	-	B	120	-	-
Radosz	1984	60	533	350	-	RT	PT	15	100	100
Moris	1985	100	311-588	146-109	-	TC	PT	10/15	20/250	0,5
Yorizane	1985	150	298	90	304 Stainless steel	-	B	-	-	-
Takishima	1986	700	-	-	-	QT	B	-	-	-
Inomata	1988	750	4 130	60	316 Stainless steel	TC	PT	-	-	-
D'Souza a,b	1988	100	353	161	Stainless steel	RT	PT	60	3 001	1 000
Adams	1988	-	313	80	Sapphire	-	-	-	-	-
Kim	1989	150	430	250	316 Stainless steel	RT	PT	10	100	1
Shibata	1989	100	345	422	-	RT	DWP	30/45	-	-
Jennings	1989	40	335	100	Stainless steel	RT	PT	-	1	0,2
Weber	1989	65	300/670	190/103	300 Stainless steel	RT	B	480	20	1
Suzuki	1990	-	453	250	-	RT	B	-	10 000	750
Fink	1990	60	-	-	Hastelloy C	TC	PT	-	-	-
						-	-	-	-	-

(1) Due to space limitations only first author mentioned.
(2) Material of construction of equilibrium cell.
(3) TC = thermocouple; RT = Platinum Resistance Thermometer Pt - 100 Ω.
TS = thermistor; QT = Quartz thermometer.
(4) B = Bourdon pressure gauge; PT = Pressure transducer; DWP = Dead weight piston gauge.

TABLE 2.3

Single Vapour and Liquid Pass Apparatus Reported in the Literature

Author (1)		Cell Volume cm3	Operating range Temp K	Operating range Press bar	Cell (2)	Measurement Device Temp (3)	Measurement Device Press (4)	Hold up time sec	Sample size Vap µl
Simnick	1977	90	703	250	316 Stainless steel	TC type K	B	-	500/2 000
Sebastian	1980	-	-	-	-	TC type K	B	-	1 320/1 860
Lin	1985	10	710	250	316 Stainless steel	TC type K	B	18-36	500/1 000
Inomata	1986	30	710	230	316 Stainless steel	TC type K	B	-	300/1 140
Niesen	1986	250	623	100	316 Stainless steel	RT	B	-	-
Roebers	1990	10-50	673	350	450 Stainless steel	NA	NA	NA	NA

(1) Due to space limitations only first author mentioned.
(2) Material of construction of equilibrium cell.
(3) TC = thermocouple; RT = Platinum Resistance Thermometer Pt - 100 Ω.
(4) B = Bourdon pressure gauge.

TABLE 2.4

Static Equilibrium Apparatus Reported in the Literature

Author (1)		Cell Volume cm3 (2)	Operating range Temp K	Operating range Press bar	Cell (3)	Measurement Device Temp (4)	Measurement Device Press (5)	Equilibration time min	Sample size Vap µl (2)	Sample size Liq µl (2)
Rigas	1958	VV	423	14	304/416 SS	TC	B		0,2	0,75
Todheide	1963	150	623	3 500	-	TC	B	60	200-300 mg	200-300 mg
Rogers	1970	150	423	1 000	SS	TC	PT/DWP	-	VV	VV
Besserer	1971	10/115	310	80	316 SS	TC	PT	5/10 cycles	10^{-3} gmoles	10^{-3} gmoles
Sagara	1972	500	103	100	SS	TC	B	60	-	-
Klink	1975	800			316 SS	-	DWP	300/1 500	-	-
Kalra	1975	250	338	345	316 SS	TC	PT		-	-
Ng	1978	150	315	175	316 SS	TC	B	180	12	-
Figuiere	1980	50	673	400	SS	TC	PT	-	1	1
Legret	1981	100	673	1 000	SS	TC	PT	10	15	15
Bae	1981	300	323	100	304	RT	B	120	8	8
King	1983	500				TS	DWP	310	-	
Konrad						-	-	-	-	-
(Swaid)	1983	-	300/450	2000	N 90	TC	B	-	N.A	N.A
Konrad						-	-	-	-	-
(Konrad)	1983	100	293/473	2000	N 90	TC	-	-	50	50
Ashcroft	1983	883	333	690	MS	RT	PT	180	0,06	0,06
Guillevic	1983	50	558	70	316	TC	PT	-	-	-
Haung	1985	VV	310/477	185	Saphire	TC	PT	-	-	-
Nakayama	1987	270	450	200	-	TC	B	720	100	250
Wagner	1987	65	323	90	SS	QT	PT	-	-	
Reiff	1987	2 000	473	300	-	RT	-	-	-	-

(1) Due to space limitations only first author mentioned.
(2) VV = Variable volume.
(3) Material of construction of equilibrium cell, SS = Stainless steel ; MS = Manganese steel, N 90 = Ninomic 90 SS
(4) TC = thermocouple; RT = Platinum Resistance Thermometer Pt - 100 Ω.
TS = thermistor; QT = Quartz thermometer.
(5) B = Bourdon pressure gauge; PT = Pressure transducer; DWP = Dead weight piston gauge.

CHAPTER 3

REVIEW OF THEORETICAL ASPECTS OF HIGH PRESSURE VAPOUR-LIQUID EQUILIBRIUM

The measurement of vapour-liquid equilibrium is both expensive and complex, especially for high pressures where acquisition of data is not easy and requires considerable experimental skill, experience and patience. Knap (1986) provides some rough estimates of the financial and experimental time requirements to measure VLE data sets. Theoretical interpretation of experimental data is therefore necessary for interpolating and extrapolating the data to new conditions and for correlating phase behaviour from the minimum amount of experimental data.

Thermodynamics provides the tool for interpreting phase-equilibrium data. While thermodynamic analysis of low pressure phase equilibrium data is common such analysis for mixtures at high pressures, i.e., approaching critical conditions, is much more difficult and far less common.

In this *general* review on the theoretical aspects of high temperature and pressure vapour-liquid equilibrium the more commonly used methods of data analysis will be discussed

Particular emphasis will be placed on the direct and combined methods (Wichterle 1978 a and b). These two methods were employed in the theoretical analysis of the VLE data measured in this project.

The direct method requires the computation of the liquid and vapour phase fugacity coefficients through a single appropriate EOS. The combined method requires the computation of liquid phase activity coefficients using an appropriate liquid phase model and the vapour phase fugacity coefficients using an EOS.

The various relationships that have been proposed to calculate the fugacity and activity coefficients (with particular attention to those specifically used in this project) will be discussed :

Equations of state for the fugacity coefficient : Virial, cubic Peng-Robinson and a Group Contribution EOS proposed by Skjold Jorgenson (1986).

Liquid phase models for activity coefficients : UNIQUAC and NRTL equations.

A brief review of consistency testing of high pressure vapour-liquid equilibrium data is also given. The derivation of the proposed new vapour phase test is shown in this section.

3.1 CRITERION FOR EQUILIBRIUM

Elementary thermodynamic treatment of phase and chemical reaction equilibrium, will not be covered here. The various relationships from which equations (3.6) and

(3.8) have been generated may be found in Smith and van Ness (1975) and Walas (1985). The symbol notation and phraseology for the various thermodynamic properties used here are similar to those of Smith and van Ness (1975).

The criterion for phase equilibrium (Appendix B.1) is :

For multiple phases at the same T and P the equilibrium condition is satisfied when the chemical potential or fugacity of each component in the system is the same in all phases.

$$\hat{f}_i^{\alpha} = \hat{f}_i^{\beta} = \ldots\ldots = \hat{f}_i^{\pi} \qquad (i = 1,\ldots,N) \tag{3.1}$$

3.2 THERMODYNAMIC RELATIONSHIPS TO DESCRIBE THE HIGH PRESSURE VAPOUR-LIQUID EQUILIBRIUM CONDITION

Prausnitz (1986) designates high pressure as any pressure sufficiently large to have an appreciable effect on the thermodynamic properties of all the phases under consideration. Pressures above approximately 20 bar may be considered as high, although this will depend on the nature of the system.

The fugacity of any component i in a system containing m components is a function of temperature, pressure and composition. A description of the fugacity based on first principles may be found from the total differential of the logarithm of the fugacity as given by :

$$d\ln \hat{f}_i = \left(\frac{\partial \ln \hat{f}_i}{\partial T}\right)_{(P,x)} dT + \left(\frac{\partial \ln \hat{f}_i}{\partial P}\right)_{(T,x)} dP + \sum_{(j-1)}^{(m-1)} \left(\frac{\partial \ln \hat{f}_i}{\partial x_j}\right)_{(P,T,x_k)} dx_j \tag{3.2}$$

There is some difficulty in calculating the terms on the right hand side of Eq. (3.2)

The first term may be related to partial molar enthalpy, the second to partial molar volume and the third to the excess Gibbs free energy.

Alternatively a thermodynamic description of phase behaviour may be based on the equality of the fugacities throughout the phases, Eq. (3.1). The criterion which must be satisfied for equilibrium between a liquid and vapour phase at the same temperature and pressure according to Eq (3.1) is given by :

$$\hat{f}_i^V = \hat{f}_i^L \tag{3.3}$$

The fugacities in Eq (3.3) are of little practical value unless they can be related to some measurable values such as temperature, pressure and phase compositions. This is achieved in practice by using auxillary functions.

For example, in the *combined method* the vapour phase fugacity of a component may be written as,

$$\hat{f}_i^V = y_i \hat{\phi}_i^V P \tag{3.4}$$

and the liquid phase fugacity of a component as :

$$\hat{f}_i^L = x_i \gamma_i f_i^o \tag{3.5}$$

Consequently Eq. (3.3) becomes :

$$\boxed{y_i \hat{\phi}_i^V P = x_i \gamma_i f_i^o} \tag{3.6}$$

Alternatively in the *direct method* the liquid phase fugacity is given by :

$$\hat{f}_i^L = x_i \hat{\phi}_i^L P \tag{3.7}$$

The vapour phase fugacity is given by Eq.(3.4) resulting in the equilibrium condition being described by :

$$\boxed{x_i \hat{\phi}_i^L = y_i \hat{\phi}_i^V} \tag{3.8}$$

The effect of temperature, pressure and composition on the fugacity in the liquid and vapour phases are therefore essentially determined by the effect of these variables on the activity and/or fugacity coefficients. The following functional relationships are therefore present :

$$\hat{\phi}_i^V = \phi(T, P, y, \ldots y_n)$$

$$\hat{\phi}_i^L = \phi(T, P, x, \ldots x_n)$$

$$\gamma_i = \gamma(T, P, x, \ldots x_n)$$

$$f_i^o = f(T, P)$$

Another useful quantity in vapour-liquid equilibrium is the equilibrium ratio K defined as :

$$\boxed{K_i = \frac{y_i}{x_i} = \frac{\gamma_i f_i^o}{\hat{\phi}_i^V P} = \frac{\hat{\phi}_i^L}{\hat{\phi}_i^V}} \tag{3.9}$$

The value of K gives an indication as to whether the component will concentrate in the vapour (i.e. the light component, $K_i > 1$ or whether it will concentrate in the liquid phase (i.e. for the heavy component, $K_i < 1$).

The above rigorous description of phase equilibrium applies equally to low and high pressure. The extension of Eqs. (3.6) and (3.8) to high pressures is however not trivial for the following reasons :

1. One of the components is usually supercritical at the equilibrium temperature. In the combined method there is some difficulty in defining an appropriate standard state fugacity f_i^{oL} for the supercritical component since the component cannot exist as a pure liquid at the system temperature.

2. Vapour-phase non-idealities become more pronounced i.e. $\hat{\phi}_i^V \neq 1$

3. The isothermal Gibbs-Duhem Eq. (B.1) includes a total pressure differential term. This term, though negligibly small at low to moderate pressures, becomes significant at high pressures especially near the critical region.

3.3 ANALYTICAL METHODS IN HIGH PRESSURE VAPOUR-LIQUID EQUILIBRIUM : THE DIRECT AND COMBINED METHODS

The two analytical methods developed for high pressure vapour-liquid equilibrium work namely, the direct and combined methods were reviewed in detail by Wichterle (1978 a and b). Only the isothermal forms of these methods, the bubble pressure calculation, will be considered here.

3.3.1 Direct Method

The fugacity coefficients in Eq. (3.8) are calculated from,

$$\ln \hat{\phi}_i^V = \left(\frac{1}{RT}\right) \int_{V^V}^{\infty} \left[\left(\frac{\partial P}{\partial n_i}\right)_{(T,V,n_{j\neq i})} - \frac{RT}{V^V}\right] dV - \ln\left[\frac{PV^V}{n_T RT}\right] \qquad (3.10)$$

and

$$\ln \hat{\phi}_i^L = \left(\frac{1}{RT}\right) \int_{V^L}^{\infty} \left[\left(\frac{\partial P}{\partial n_i}\right)_{(T,V,n_{j\neq i})} - \frac{RT}{V^L}\right] dV - \ln\left[\frac{PV^L}{n_T RT}\right] \qquad (3.11)$$

A suitable pressure-explicit EOS, $p = f(V,T)$ applicable to all components and their mixtures over the entire density range (vapour to liquid) is required for the solution of Eqs. (3.10) and (3.11).

There are literally hundreds of equations of state described in the literature. Selection of the most appropriate one for the particular application in hand is the first problem associated with the application of this method. The main criterion in the selection of the EOS is that it must be *flexible* enough to fully describe the system PVT behaviour for both phases in the temperature, pressure and concentration ranges under study.

Another important factor affecting accuracy in the direct methods arises when the description of phase behaviour is extended to mixtures. Most EOS require a mixing or interaction parameter to extend the pure component EOS form to mixtures. Most mixing rules although derived using theoretical assumptions, are somewhat empirical and may be system specific.

A schmetic diagram showing the computational procedure for the direct method is shown in Figure 3.1.

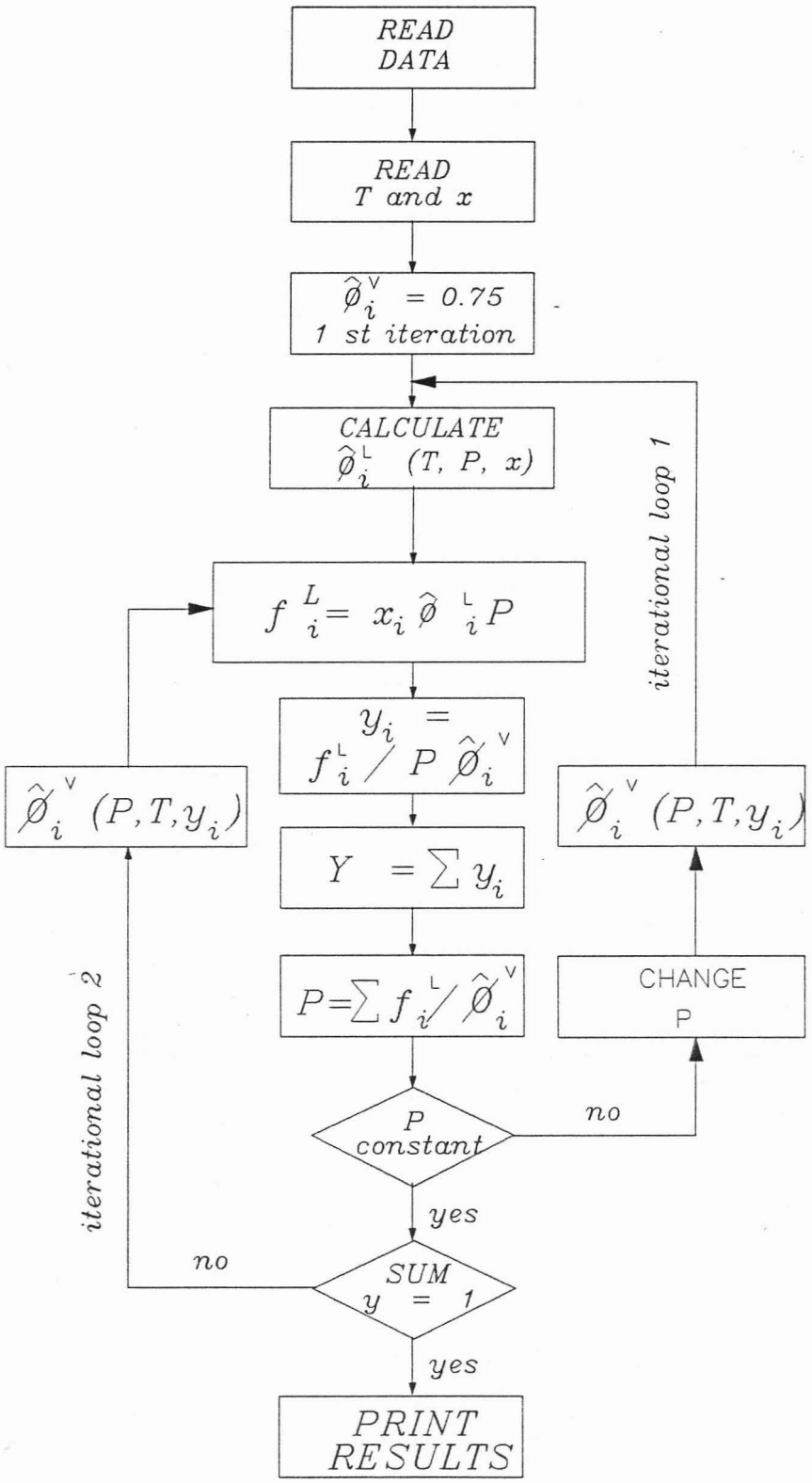

Figure 3.1 : Schematic Diagram for the Bubble-Pressure Program using the Direct Method

3.3.2 Combined Methods

The application of an activity coefficient to describe high pressure phase behaviour (Eq. (3.6)) is a logical extrapolation of the excellent low pressure correlation techniques. The main feature of this method is the use of separate auxillary functions to describe the non-ideality of each phase.

A suitable EOS is used for expressing the vapour phase behaviour through the fugacity coefficient as shown in Eq. (3.10). A semi-empirical equation is used for the activity coefficient, which is only completely defined once the standard state fugacity, f_i^{OL} is specified. The definition of f_i^{OL} is arbitrary and is dictated only by the necessity that f_i^{OL} be the fugacity of pure liquid component i at the system temperature at some chosen pressure. The choice of the reference pressure is arbitrary.

The splitting of the K value as seen in Eq. (3.9) into three different quantities should make the thermodynamic description of phase behaviour simpler. Each of the quantities depends on a smaller number of variables. This is in contrast to the direct method where a single EOS must describe the behaviour of both phases.

One of the main difficulties in the application of this method lies in the selection of a suitable standard state to best describe a supercritical component. The various standard states available for the combined methods will now be discussed.

3.3.2.1 Standard states

For component i in solution the purpose of the activity coefficient γ_i is to relate the fugacity f_i^L at mole fraction x_i, temperature T and pressure P to some other condition where its value is known accurately. This other condition is known as the standard state and represents the known and defined thermodynamic conditions of a component, at which its activity coefficient equals 1.

The standard state is *always* established at the temperature of the system. The conditions of pressure and composition should be chosen such that the numerical values of the activity coefficients are close to unity, i.e., the real conditions should not be very different from the standard ones.

At high pressures the system temperature often exceeds the critical temperature of one of the components. This implies that under these conditions the components liquid phase cannot exist. The component's standard liquid state must then by definition be a hypothetical quantity. Any uncertainties in the hypothetical extrapolation from the subcritical region must affect the evaluated activity coefficients and hence, the fugacities. The condensable and non-condensable components may therefore require different standard states (Appendix B.2).

The most commonly used standard states for condensable and non-condensable components are given in Tables 3.1 and 3.2.

Table 3.1
Standard States Available for Condensable Components

State	Temperature T	Pressure P	Composition x_i	Note
1	T system	P system	1	pure liquid component
2	"	Pr	1	"
3	"	0	1	"
4	"	∞	1	"
5	"	P	1	"

Table 3.2
Standard States Available for Non-Condensable Components

State	Temperature T	Pressure P	Composition x_i	Note
6	T system	P system	0	component i
7	"	Pr	0	infinitely diluted in
8	"	0	0	component j

3.3.2.2 <u>Activity coefficients</u>

The effects of each of the independent variables : temperature, pressure and composition on the liquid phase fugacity is achieved by studying their effects on the activity coefficient. The activity coefficient's dependence on these variables can be determined from the Gibbs-Duhem equation by relating the activity coefficient to the molar excess Gibbs free energy for component i :

$$\Sigma\ x_i d\ln\ \gamma_i = \Sigma\ x_i d\left(\frac{\overline{G}_i^E}{RT}\right) = \left(-\frac{\Delta H}{RT^2}\right)\ dT + \left(\frac{\Delta V}{RT}\right)\ dP \qquad (3.12)$$

For isothermal conditions the variable pressure activity coefficients of the components in a mixture may be summed using the Gibbs-Duhem equation :

$$\Sigma\ x_i\ d\ln\ \gamma_i = \frac{\Delta V}{RT}\ dP \qquad (Constant\ T) \qquad (3.13)$$

The use of a constant pressure activity coefficient is advantageous since a much simpler relation is obtained :

$$\Sigma\ x_i\ d\ln\ \gamma_i = 0 \qquad (Constant\ T\ \&\ P) \qquad (3.14)$$

Eq. (3.14) applies equally to activity coefficients normalized by the symmetric or unsymmetric convention (Appendix B.2). The well known semi-empirical mixture models for example : van Laar, Margules, Scatchard Hildebrand, NRTL and the UNIQUAC with it s derivative UNIFAC are particular mathematical solutions of the integrated form of Eq. (3.14).

At low to moderate pressures the liquid phase activity coefficients are weakly dependent on pressure and for all practical purposes they depend only on temperature and composition. At high pressures however, the pressure dependence must be taken into account. At a constant temperature and composition and where the pressure is specified to be some fixed pressure P (standard state 1), the dependence is given as follows :

$$\left(\frac{\partial \ln \gamma_i}{\partial P}\right)_{T,x} = \left(\frac{\overline{V}_i}{RT}\right) \tag{3.15}$$

Eq (3.15) when integrating between limits p_1 and p_2 yields :

$$\gamma_i^{(P_1)} = \gamma_i^{(P_2)} \exp \int_{P_1}^{P_2} \left(\frac{\overline{V}_i}{RT}\right) dP \tag{3.16}$$

Condensable Component Activity Coefficients

For a component where $T_{critical} > T_{system}$ the constant pressure activity coefficient at constant temperature and composition can be determined by the rigorous thermodynamic relation obtained from intergrating Eq. (3.16) with respect to a standard state at reference pressure p^r :

$$\gamma_i^{(p^r)} = \gamma^{(p)} \exp \int_{p}^{p^r} \left(\frac{\overline{V}_i}{RT}\right) dP \tag{3.17}$$

$\gamma_i^{p^r}$ being the activity coefficient at the arbitrary reference pressure p^r.

Liquid phase fugacity $\hat{f}_i^L$

Liquid phase fugacity $\hat{f}_i^L$ Eq (3.5) for a condensable component may therefore be described by :

$$\hat{f}_i^L = x_i f_i^{OL} \gamma_i^{(pr)} \exp \int_{p^r}^{p} \frac{\overline{V}_i^L}{RT} dP \tag{3.18}$$

This form of describing isothermal systems, where the total pressures usually vary widely with the liquid composition, by the incorporation of $\gamma_i^{(P^r)}$; permits the use of the integrated forms of this isobaric, isothermal Gibbs-Duhem equation such as UNIQUAC equation *without any approximations.*

Standard state reference fugacity f_i^{OL}

For a condensable component in order that $\gamma_i^{(P^r)} \rightarrow 1$ *as* $x_i \rightarrow 1$ the standard state reference fugacity must be that of pure liquid component i at the system temperature and chosen reference pressure :

$$f_i^{OL} = f_i^L$$

At equilibrium conditions the fugacity of a pure liquid component equals the fugacity of the pure gaseous component; the latter is a readily available quantity. It is therefore advantageous to express f_i^L by means of the fugacity at the saturated vapour pressure P_i^s . Therefore :

$$f_i^{L(P_i^s)} = f_i^{V(P_i^s)} = \phi_i^{(P_i^s)} P_i^s \qquad (3.19)$$

If the reference pressure is set equal to zero the integrated form of Eq. (3.18) yields the standard state fugacity as follows,

$$f_i^{OL} = \phi_i^s P_i^s \exp\left(-\frac{V_i^L P_i^s}{RT}\right) \qquad (3.20)$$

If the volume V_i^L is assumed to be independent of pressure (which is not a entirely valid assumption near the critical pressure) Eq. (3.18) may be easily integrated.

Non-Condensable Component Activity Coefficients

The liquid phase fugacity for a non-condensable component may be described analogously to the condensable component's fugacity as shown in Appendix B.3.

In summary : at constant temperature, the constant pressure activity coefficients for the condensable and non-condensable components are functions of composition only and satisfy the two component isothermal isobaric Gibbs-Duhem equation,

$$\Sigma x_i \, d\ln \gamma_i^{(P^r)} = 0 \qquad (3.21)$$

where, for condensable components,

$$\gamma_k^{(P^r)} \rightarrow 1 \quad as \quad x_k \rightarrow 1$$

and for non-condensable components

$$\gamma_k^{(P^r)} \rightarrow 1 \quad as \quad x_k \rightarrow 0$$

3.3.2.3 Fugacity coefficients

The mechanical state of a substance is known when its temperature pressure and volume are fixed. These three properties are related by an equation of state (EOS) in the form, $EOS\ (P,V,T) = 0$. Two of the properties are independent. By itself a suitable EOS can be used to evaluate the : vapour pressures, critical properties, vapour-liquid equilibrium relations, through equations (3.8), (3.10) and (3.11), and the densities of the vapour and liquid phases of pure substances and mixtures.

3.3.2.4 Combined methods in the literature

Chao and Seader Method

The Chao and Seader method was the turning point in high pressure temperature vapour-liquid phase equilibrium calculational procedures as it presented the first easy-to-use general analytical description of high pressure vapour-liquid equilibrium. This method did not require any adjustable parameters making it suitable for predictive calcuations rather than the correlation of experimental data. The method provided reasonable results combining simple generalized relations with commonly available data. A brief description of the method may be found in Appendix B.4 as well as a block diagram outlining the calculational scheme in Figure B.2.

Prausnitz and Chueh Method (1968)

The Chao and Seader Method, although reasonably simple by present standards, represented a new qualitative approach in the development of computational methods. A more exact approach was developed by Prausnitz and Chueh (1968) to yield more accurate results for supercritical components. Prausnitz and Chueh (1968) developed a combined method based on the symmetric / unsymmetric convention for normalization of activity coefficients using standard states 3 and 8 (Tables (3.1) and (3.2)) for the liquid condensable and non-condensable components respectively. The equilibrium condition for component i could therefore be expressed as per Eq (3.6) :

$$y_i \hat{\phi}_i^V P = x_i \gamma_i f_i^o$$

A schematic diagram outlining the calculational scheme is shown in Figure 3.2.

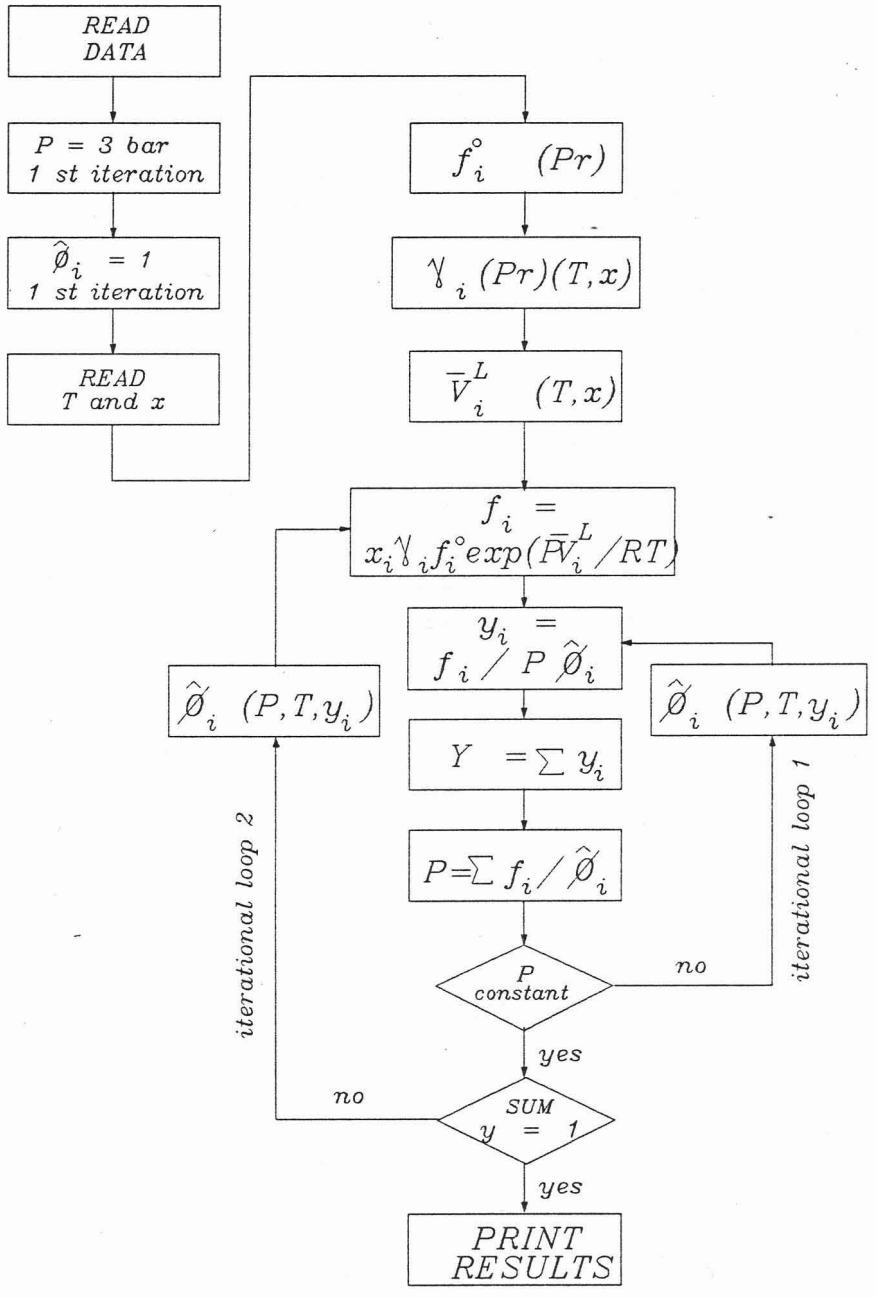

Figure 3.2 : Schematic Diagram for the Bubble-Pressure Program using the Combined Method

The standard state fugacity f_i^o for a condensable component using standard state 3 could be written from, Eq. (3.18), as :

$$f_i^o = f_i^{oL} = f_i^{L(P)} \exp \int_o^P \left(-\frac{V_i^L}{RT}\right) dP \qquad (3.22)$$

A similar expression could be written in terms of Henry's Constant for the non-condensable component using standard state 8. The standard state fugacities were evaluated from polynomial expansions of temperature. Each component required 5 or 6 parameters. The activity coefficients γ_i were derived from Eq. (3.16)

$$\gamma_i^{(P)} = \gamma_i^{(O)} \exp \int_o^P \left(\frac{\overline{V}_i^L}{RT}\right) dP \qquad (3.23)$$

The unsymmetrically normalized activity coefficients at zero pressure $\gamma_i^{(O)}$ were expressed by means of a modified van Laar equation. For a binary mixture the temperature dependence of $\gamma_i^{(O)}$, required seven interaction parameters and one parameter of the pure component. The partial molar volume $\overline{V}_i$ was generalised by means of an 18 parameter relation. The vapour-phase fugacity coefficient was described by the Redlich-Kwong equation of state. Two pure component parameters and three interaction parameters were required.

The complexity of the Prausnitz and Chueh method was reflected in the number of parameters required as seen from Table 3.3.

Table 3.3
Parameters required as function of number of components for the Prausnitz and Chueh (1967) method.

Components	Pure Component Data	Adjustable Pure Binary		Total
2	10	20	34	64
3	15	30	51	96
4	20	40	102	102

Modifications of the Prausnitz & Chueh method have focussed mainly on the use of :

1. Different standard states to describe the non-condensable component.
2. More appropriate liquid phase models to describe complex and polar mixtures.
3. Different EOS to calculate the vapour fugacity coefficient.

An example of modification 2, was developed by Prausnitz, *et al* (1980) for low to moderate pressures (max 20 bar). This method and update of Prausnitz, *et al* (1967) was used mainly as a parameter fitting program for various liquid phase models using experimental data. The method used theoretically more advanced liquid phase models for liquid phase description, among others, the NRTL and UNIQUAC equation. The truncated two parameter Virial EOS was found sufficient for the vapour phase description in the pressure range of interest.

The non-condensable component can be normalised by the symmetric convention. This introduces the hypothetical notion of a pure liquid for the supercritical component at the system temperature, whose properties are evaluated by extrapolation. If the system temperature is not excessively above the non-condensable's critical temperature accurate results can still be obtained by this extrapolation process as shown in this project. If $(T_{system} / T_c < 1.8)$ for the non-condensable, the component can be considered a condensable component as suggested by Prausnitz, *et al* (1980).

Two variations of the combined method were used in this project :

1. A modification of the Prausnitz, *et al* (1980) parameter fitting program. The modification consisted of the inclusion of the Peng-Robinson and the Group Contribution EOS to extend the combined method to high pressures.
2. A modification of the Prausnitz and Chueh (1968) combined method correlation program Figure 3.2. The correlation program used the UNIQUAC liquid phase model in conjunction with either one of the following EOS : the two parameter Virial, Peng-Robinson or Group Contribution. The symmetric convention of normalising activity coefficients was used.

The programs used in this project are fully described in Chapter 8.

3.4 REVIEW OF EQUATIONS OF STATE IN THE LITERATURE

Historical Perspective

Hundreds of equations of state representing the P,V,T behaviour of pure and mixtures of gasses have been proposed to date.

The first EOS for a gas was proposed by Boyle in 1662, $PV = Constant$. The effect of temperature was included by Clapeyron in 1834 in the ideal gas law $PV = R(T + 267)$

It was realized that the ideal gas law was only a rough approximation of the true behaviour of gasses as the inherent assumptions made in its derivation cannot be met by real gases. Real gases have size, shape and structure and as a result molecules occupy space and attract or repel each other physically and/or electrically. These deviations from the ideal gas structure determine the forces between them and

An example of modification 2, was developed by Prausnitz, *et al* (1980) for low to moderate pressures (max 20 bar). This method and update of Prausnitz, *et al* (1967) was used mainly as a parameter fitting program for various liquid phase models using experimental data. The method used theoretically more advanced liquid phase models for liquid phase description, among others, the NRTL and UNIQUAC equation. The truncated two parameter Virial EOS was found sufficient for the vapour phase description in the pressure range of interest.

The non-condensable component can be normalised by the symmetric convention. This introduces the hypothetical notion of a pure liquid for the supercritical component at the system temperature, whose properties are evaluated by extrapolation. If the system temperature is not excessively above the non-condensable's critical temperature accurate results can still be obtained by this extrapolation process as shown in this project. If $(T_{system} / T_c < 1.8)$ for the non-condensable, the component can be considered a condensable component as suggested by Prausnitz, *et al* (1980).

Two variations of the combined method were used in this project :

1. A modification of the Prausnitz, *et al* (1980) parameter fitting program. The modification consisted of the inclusion of the Peng-Robinson and the Group Contribution EOS to extend the combined method to high pressures.
2. A modification of the Prausnitz and Chueh (1968) combined method correlation program Figure 3.2. The correlation program used the UNIQUAC liquid phase model in conjunction with either one of the following EOS : the two parameter Virial, Peng-Robinson or Group Contribution. The symmetric convention of normalising activity coefficients was used.

The programs used in this project are fully described in Chapter 8.

3.4 REVIEW OF EQUATIONS OF STATE IN THE LITERATURE

Historical Perspective

Hundreds of equations of state representing the P,V,T behaviour of pure and mixtures of gasses have been proposed to date.

The first EOS for a gas was proposed by Boyle in 1662, $PV = Constant$. The effect of temperature was included by Clapeyron in 1834 in the ideal gas law $PV = R(T + 267)$

It was realized that the ideal gas law was only a rough approximation of the true behaviour of gasses as the inherent assumptions made in its derivation cannot be met by real gases. Real gases have size, shape and structure and as a result molecules occupy space and attract or repel each other physically and/or electrically. These deviations from the ideal gas structure determine the forces between them and

their P, V, T behaviour. The physical forces due to molecular size and mass are important at small molecular separations. As a result of their structure molecules exhibit electrical properties, they are either :

1. Non-polar symmetrical molecules which are usually electrically neutral.
2. Molecules having residual valences that usually result in association and hydrogen bonding.
3. Polar unsymmetrical molecules usually possess dipole moments.

While forces of repulsion and attraction are present in all molecules they are more pronounced in associating and polar molecules. Consequently the P,V,T correlations proposed to date have been more successful in modeling non-polar substances than polar.

The Cubic Equations of State

The first attempt to quantitatively take the above mentioned factors into account was made by van der Waals in 1873; in his dissertation on the continuity of gas and liquid states :

$$(P + a/V^2)(V - b) = RT \qquad (3.24)$$

The proposed EOS still forms the basis for many of the currently widely used cubic as well as the more modern PHCT and UNIWAALS EOS.

The most successful developments and modifications of the van der Waals equation were those made by Redlich-Kwong in 1949, Soave-Redlich-Kwong in 1972 and the Peng and Robinson in 1976. These cubic equations contain modifications in the form of adjustable parameters, These parameters have either been empirically or arbitrarily derived to fit certain kinds of experimental data such as vapour pressures, densities or enthalpies. The main reason for their popularity and widespread use is that these parameters can be expressed in terms of the critical properties of the pure components with further modifications for temperature and acentric factors. All the pure component properties required are readily available.

The cubic EOS require mixing rules, the values of which are non-trivial, to extend the equations to mixtures. The main disadvantage of this group of EOS is therefore that none of them can be used in VLE *predicition* methods. Experimental data are always necessary to generate the interaction parameters without which no accurate predictions are possible. They can therefore be classified as purely *correlational* equations.

The Virial Equation of State

Continuing studies relating to the forces between molecules led to the statistically mechanically derived Virial EOS by Ursell in 1927. One of the outstanding features of this EOS is that it provides a rational basis for relating the behaviour of mixtures to the composition and properties of pure components.

An EOS similar to the Virial EOS was developed by Benedict, Webb and Rubin in 1940. Due to its complexity this EOS has not found wide spread use other than for the light hydrocarbons and inorganic gas for which the 30 odd constants needed are avaliable.

Recent developments

Recently proposed predictive and correlative models have been aimed at modifying and developing EOS for better representation of the liquid phase and polar mixtures.

One area of developement has been aimed at determining more accurate mixing rules and more appropriate attractive pressure terms (Eq.(B.20)) for the family of cubic EOS.

Example are the three parameter Harmens and Knap (1980) and four parameter Trebble and Bishnoi (1987) EOS. These modified cubic EOS are however not predictive.

The other area of developement that has received particular attention has been directed at the development of truely predictive methods such as the UNIWAALS EOS, the Group Contribution EOS and to a lesser extent the Perturbation Theory family of EOS.

Development of predictive equation of states

The Perturbation Theory was developed on a statistical thermodynamic approach as opposed to the classical thermodynamic approach which yielded the common cubic EOS. This approach was intended to help avoid the, as Prausnitz (1979) so aptly stated, "bureaucratic run-around" involved in classical thermodynamics. In the classical thermodynamic approach one property is related to the next until the last is related back to the first but in most cases one link in the chain is missing. Perturbation theory, although relatively simple, ultimately results in EOS which have complex forms. This computational complexity has resulted in their not being widely used by the production engineer.

Efforts have however been made in recent years to simplify the equations and to develop specific EOS for groups of molecules exhibiting similar behaviour due to their molecular structure. These equations, even if approached with some trepidation due to their complexity, should become widely used in future.

The EOS in the Perturbation Theory family still require some form of interaction parameter. They are however capable of accurate predictions with the neglect of this parameter (i.e. $k_{ij} = 0$) . Only elementary, readily available or calculable pure component data are required. A summary of the underlying theory and some of the EOS derived for specific applications is given in Appendix B.6.

EOS derived from the Huron-Vidal mixing rule

Relating the mixing parameters to the excess Gibbs energy (g^E) by using a expression of g^E as a function of fugacity coefficients was first proposed by Huron and Vidal (1979). These models are sometimes referred to as the density dependent local composition (DDLC) models, Danner and Gupte (1986). The underlying theory of some of the EOS associated with this family are shown in Appendix B.7.

The primary objective of the DDLC models was to extend the traditional cubic EOS, that have been used to model the vapour phase of hydrocarbons and non-polar compounds over a large temperature and pressure range to systems containing polar compounds which have traditionally been described by activity coefficient models over a small temperature and pressure range. The underlying principle, the combination of the two methods would complement each other in the others area of deficiency. This combination of a g^E model and EOS can be viewed as the *modern* combined method.

Of particular interest to the process engineer is when a group contribution g^E liquid phase model is used in conjunction with a cubic EOS. For example the van der Waals EOS when combined with the UNIFAC of Larsen, *et al* (1986) resulted in the UNIWAALS EOS of Gupte, *et al* (1986 a and b) (Appendix B.7.2). This EOS avoids the preliminary interaction parameter fitting step and can therefore be used as a predictive method. The prediction capability of methods such as UNIWAALS come at the expense of simplicity and sometimes of thermodynamic consistency.

Schwartzentruber, *et al* (1989) point out that UNIFAC is valid only for liquid phase descriptions. The group contribution parameters were determined for use in conjunction with a particular EOS such as the ideal gas law in Larsens modified UNIFAC. Larsens modified UNIFAC was used by Gupte in conjunction with the van der Waals EOS. Since the van der Waals EOS is forced to match the UNIFAC (ideal gas law) in the liquid phase the ϕ_i^V calculated by the cubic EOS will not be consistent.

Schwartzentruber, *et al* (1989) avoided the above inconsistency and other shortcomings by proposing a very general rule for mixing parameter determination described briefly in Appendix B.7.3. The interaction parameters were determined directly from a g^E model. The method is entirely general and can be applied to a wide variety of cubic EOSs and g^E models. The resulting EOS can be used as a predictive or correlative consistency test.

Equations of States can therefore be classified as belonging to one of five categories :

1. The n parameter Virial EOS,
2. The traditional cubic EOS with or without modified mixing rules,
3. The complex EOS such as BWR,
4. The Statistical Perturbation Theory EOSs,

5. The DDLC EOS based on the Huron and Vidal (1979) method of incorporating an excess Gibbs energy model (g^E) into the fugacity coefficient.

The EOS relevant to this project will now be reviewed in slightly more detail.

3.4.1 Viral Equation of State

The Viral equation has a sound theoretical foundation for representing the properties of pure gases and mixtures, is free of arbitrary assumptions, and is most commonly used in the power series expansion in volume for the compressibility factor :

$$Z = \frac{PV}{RT} = 1 + \frac{B}{V} + \frac{C}{V^2} + \ldots\ldots \qquad (3.25)$$

Since very little is known about the third virial coefficients and beyond, this EOS is applied mainly in its two parameter form :

$$Z \approx 1 + \frac{Bp}{RT} \qquad (3.26)$$

Smith and Van Ness (1975) recommend the use of the two parameter Virial EOS up to pressures of 15 bar and the three parameter form up to 50 bar.

Extension of the Virial EOS to mixtures (Mixing Rules)

The behaviour of a mixture is affected by the interactions between the molecules making up the mixture. To apply a pure-component EOS to mixtures some indication of the interaction between the molecules needs to be known. One of the most popular and widely used methods of indicating these interactions is provided in the form of interaction parameters.

For an n -component mixture there are : n, $n(n-1)/2$, $n(n-1)(n-2)/6$, etc., possible single, binary, tertiary, etc., interaction parameters. Each interaction is described by a particular virial coefficient. The mixture virial coefficient is a summation of the individual virial coefficients appropriately weighted with respect to the composition of the mixture.

At low to moderate pressures the effects of interactions between dissimilar molecules is usually small (depending ofcourse on whether the molecules are nonpolar or not), and the higher-order interactions (> 2) are usually masked by the imperfections of the EOS being used. The higher order interactions are difficult to measure and therefore usually not available for computational purposes.

Extension of the Virial EOS to gas mixtures is accomplished in a rigourous way which stems from the very nature of the equation itself and is based on theoretical rather than empirical grounds. The interaction parameters follow rigorously from statistical mechanics and are not subject to any assumptions other than those upon which the Virial equation itself is based. The interactions between gases are

incorporated in the 2 parameter Virial EOS as the mixture second virial coefficient which is related to the pure component and cross second virial coefficient for a binary system by the exact expression :

$$B_{mix} = \sum_{i=1}^{2} \sum_{j=1}^{2} y_i y_j B_{ij} \qquad (3.27)$$

Fugacity Coefficient form of the Virial EOS

The integrated form of Eq.(3.10) for the the truncated two parameter Virial EOS Eq (3.26) is :

$$\ln \hat{\phi}_i = \frac{P}{RT} \left[2 \sum_{j=1}^{2} y_i B_{ij} - B_{mix} \right] \qquad (3.28)$$

Inclusion of the third virial coefficient and the integration of the EOS with respect to volume instead of pressure yields :

$$\ln \hat{\phi}_i = \frac{2}{V} \sum_{j=1}^{m} y_j B_{ij} + \frac{3}{2} \frac{1}{V^2} \sum_{j=1}^{m} \sum_{k=1}^{m} y_i y_k C_{ij} - \ln Z_{mix} \qquad (3.29)$$

Prausnitz (1986) regards Eq. (3.29) as one of the most useful equations developed for phase equilibrium thermodynamics as it may be applied to any component in a gaseous mixture regardless of whether that component can exist as a pure vapour at the temperature and pressure of the mixture, i.e. no hypothetical states. In addition it is equally valid for polar and non-polar molecules.

Hayden and O'Connell (1975) provide expressions for predicting pure component and second virial cross coefficients for simple and complex systems requiring only the components' critical temperature and pressure, mean radius of gyration, dipole moment and if appropriate a parameter to describe chemical associations. No such general method has yet been developed for the third virial coefficient in Eq. (3.29).

4.2 Cubic Equations of State

The theory behind the formulation of the empirical cubic equation of states and some of the initial EOS associated with this family are described in Appendix B.5.1. The various methods employed in extending cubic EOS to mixtures, i.e. mixing rules are described in Appendix B.5.2.

4.2.1 Peng and Robinson equation of state

The P-R EOS is closely related to the S-R-K equation and was specifically meant to address the latter's weakness in the area of critical region instabilities and inaccurate liquid density prediction.

To provide accurate prediction of liquid volumetric behaviour, vapour pressure and equilibrium ratios of coexisting phases in VLE calculations; Peng and Robinson proposed an EOS of the form :

$$\left(P + \frac{a(T)}{(V(V+b) + b(V-b))}\right)(V-b) = RT \qquad (3.30)$$

where :

$$a(T) = a\alpha(T_r, w) \qquad (3.31)$$

$$a = \Omega_a R^2 T_c^2 / P_c \qquad (3.32)$$

$$b = \Omega_b RT_c / P_c \qquad (3.33)$$

$$\alpha(T_r, w) = \left[1 + \kappa(1-T_r)^{\frac{1}{2}}\right] \qquad (3.34)$$

$$\kappa = 0.3746 + 1.5422w - 0.26992w^2 \qquad (3.35)$$

$\Omega_a = 0.45724$

$\Omega_b = 0.07780$

The polynomial form of the P-R EOS is :

$$Z^3 + (1-B)Z^2 + (A-3B^2-2B)Z - (AB-B^2-B^3) = 0 \qquad (3.36)$$

where :

$$A = a(T)P/R^2T^2 \qquad (3.37)$$

$$B = bP/RT \qquad (3.38)$$

Fugacity Coefficients

The partial fugacity coefficient of component i in a mixture for the P-R EOS (Eq. (3.10)) is :

$$\ln \hat{\phi}_i = \frac{b_i}{b}(Z-1) - \ln(Z-B) - \frac{A}{2\sqrt{2}B}\left[-\frac{b_i}{b} + \frac{2}{a}\Sigma y_i a_{ij}\right]\ln\left[\frac{Z+2.414B}{Z-0.414B}\right] \qquad (3.39)$$

The Peng-Robinson EOS in the form of Eq. (3.30) and Eq. (3.39) was used in the analysis of experimental data obtained in this project (Chapter 8).

.4.2.2 Modifications of the original Peng and Robinson EOS and Mixing Rules

The "classical mixing rules" adopted by Peng and Robinson (1986) and used in this project are :

$$a = \Sigma\Sigma\ y_i y_j (1-\delta_{ij})\ a_i^{0.5} a_j^{0.5} \qquad (3.40)$$

$$b = \Sigma\ y_i b_i \qquad (3.41)$$

Eq. (3.40) and (3.41) are usually sufficient to enable the P-R EOS to be accurately applied to non-polar and weakly polar system correlations. To describe the strongly polar systems more complex mixing rules usually need to be developed, increasing both the complexity of the EOS and computational times required.

One of the simplest modifications is the temperature dependent form of the P-R EOS as proposed by Lin (1984) and Melhelm, *et al* (1989). They incorporated a dimensionless factor α , which was a function of temperature, into the attraction pressure term, Eq. (B.2). The resulting EOS had the form

$$P = \frac{RT}{(V-B)} - \frac{A_m}{V(V+B) + B(V-B)}$$

where :

$$A_m = \Sigma\Sigma y_i y_j \ (1-k_{ij})(\alpha_i \alpha_j a_i a_j)^{0.5}$$

A more complex modification to the "classical mixing rules" is the incorporation of an interaction parameter η_{ij} in the van der Waals covolume (b) as described by McHugh and Krukorus (1986) and Tsonopoulos and Heidman (1986).

$$b = \Sigma\Sigma \ y_i y_j \ (1-\eta_{ij}) \left(\frac{b_i + b_j}{2}\right) \qquad (3.42)$$

This modification results in the following expression of $\hat{\phi}_i$, for component i in a binary mixture,

$$\ln \hat{\phi}_i = \frac{(bN)}{b}(Z-1) - \ln(Z-B) - \left(\frac{A}{2.828B}\right)\left[\left(\frac{2\Sigma x_j a_{ij}}{a}\right) - \frac{(bN)}{b}\right] \ln\left[\frac{Z+2.414B}{Z-0.414B}\right]$$

where :

$$bN = 2\sum_{k}^{2} y_k b_{ik} - \sum_{j}^{2} y_j b_{jj} - 2\sum_{j-1}^{1}\sum_{j+1}^{2} y_i y_{i-j} b_{ij}$$

When η_{ij} is set to zero in Eq. (3.42) the fugacity coefficient equation reduces to the original expression of the fugacity coefficient as proposed by Peng and Robinson (1975) and shown in Eq. (3.39).

Dieters and Schneider (1976) apply an interaction parameter in the co-volume b to describe high pressure vapour-liquid equilibrium near the critical point using the R-K EOS. For binaries differing in structure, molecular size and/or polarity reasonably good agreement with experimental data was achieved.

Another modification to the "classical mixing rules" was suggested by Mohamed and Holder (1987). They incorporated correction factors $C_a \& C_b$ in Eqs. (3.35) and (3.33) as follows :

$$\kappa = C_a \ (0.37464 + 1.54426w - 0.2699w^2)$$

$$b = C_b \ (0.0778(RT_c/P_c))$$

The values of C_a & C_b were determined by regression of vapour pressure and molar volume data. In addition they proposed a *density dependent adjustable* interaction parameter (δ_{ij}) which was allowed to vary linearly with the phase density of the mixture :

$$\delta_{ij} = \alpha_{ij} + \rho \beta_{ij} \tag{3.43}$$

This modification resulted in a very complex expression for the fugacity coefficient, for component i as shown below, Eq. (3.44). Eq. (3.44) was also briefly used in this project (Chapter 8),

$$\ln\hat{\phi}_i = \frac{b_i}{b}(Z-1) + \frac{A}{2\sqrt{2}B}\left[\frac{2\sum_k x_k\sqrt{a_i a_k}(1-\alpha_{ik}-\beta_{ik}/b)}{a'-c-2d/b} - \frac{b_i}{b}\right]\left[\ln\frac{Z+(1-\sqrt{2})B}{Z+(1+\sqrt{2})B}\right]$$

$$+ \frac{1}{RTb^2}\left[\sum_k x_k\sqrt{a_i a_k}\beta_{ik} + \frac{d}{2} - \frac{b_i}{b}d\right]\left[\ln\frac{Z^2}{Z^2+2ZB-B^2}\right] - \frac{d}{2\sqrt{2}b^2RT}$$

$$\ln\frac{Z+(1-\sqrt{2})B}{Z+(1+\sqrt{2})B}] \tag{3.44}$$

where :

$$a' = \Sigma\Sigma y_i y_j (a_i a_j)^{0.5}$$

$$c = \Sigma\Sigma y_i y_j (a_i a_j)^{0.5}\ \alpha_{ij}$$

$$d = \Sigma\Sigma y_i y_j (a_i a_j)^{0.5}\ \beta_{ij}$$

$$A = \frac{a'-c-2d/b}{R^2T^2}$$

$$B = \frac{bP}{RT}$$

$$D = \frac{dP}{R^2T^2b}$$

Mohamed and Holder (1987) used Eqs. (3.39) amd (3.44) to model several carbon dioxide / aromatic binaries by the direct method. A significant improvement in correlations in the critical region was achieved using the density dependent EOS, Eq. (3.44) as against the original Peng and Robinson EOS Eq. (3.39).

When β_{ij} is set to zero in Eq. (3.43) the fugacity coefficient given by Eq. (3.44) reduces to the original P-R fugacity coefficient form, Eq. (3.39).

.4.3 Group Contribution Equation of State (GC EOS)

The GC EOS was developed by Skjold-Jorgenson (1984) to describe polar and non polar components in the temperature range 100 to 700 K and 30 MPa. The error in

the predicted K values is usually less than 5 %. The GC EOS is suitable for the vapour phase description of the propane / 1-propanol binary for the following reasons :

1. The EOS can be used to *predict* VLE for systems for which information on the groups making up the components, (Skjold-Jorgensen 1988), is available. Only readily accessible pure component data, such as critical pressure and temperature and *group make up* of the component molecules is necessary. No binary information such as mixing rule interaction parameters is necessary.
2. The EOS was developed to describe non-ideal components. The non-idealities introduced in the phase behaviour for the propane / 1-propanol binary by the polar 1-propanol could hopefully be described accurately.

A brief review of some of the theory involved in the derivation of this van der Waals type EOS is given in Appendix B.7.2.

The GC EOS expression for the compressibility factor is :

$$Z = Z_{fv} + Z_{att} + 1 \tag{3.45}$$

Z_{fv} is the free volume contribution and is given by :

$$Z_{fv} = -v\ [3(\lambda_i\lambda_2/\lambda_3) + (\lambda_2^3/\lambda_3^2)(2Y - 1 - 1/Y) + n/Y] \left(-Y^2\frac{\pi\lambda_3}{6V^2}\right) \tag{3.46}$$

Z_{att} is the attractive contribution and is given by :

$$Z_{att} = -\left(\frac{Z}{2n}\right) \sum_{j=1}^{NG} v_j^i q_j\ (H_{5j} + H_{2j} - H_{2j}H_{6j})/H_{4j} \tag{3.47}$$

where H_{ij} are auxillary functions as given in Skjold-Jorgensen (1984).

The fugacity coefficient is derived from the expression for the residual Helmholtz function at constant volume Eq. (B.43)

$$\ln\phi_i = \ln\phi_{i,fv} + \ln\phi_{i,att} - \ln Z \tag{3.48}$$

The free volume contribution to the fugacity coefficient is given by,

$$\begin{aligned}\ln\phi_{i,fv} = {} & 3(Y-1)(\lambda_1\lambda_2/\lambda_3)\ [\lambda'_1/\lambda_1 + \lambda'_2/\lambda_2 - \lambda'_3/\lambda_3 + Y'/(Y-1)] \\ & + (\lambda_2^3/\lambda_3^2)(Y^2 - Y - \ln Y)(3\lambda'_2/\lambda_2 - 2\lambda'_3/\lambda_3) \\ & + (\lambda_2^3/\lambda_3^2)(2Y - 1 - 1/Y)\ Y' + \ln Y + (n/Y)\ Y'\end{aligned} \tag{3.49}$$

The attractive contribution to the fugacity coefficient is given by,

$$\begin{aligned}\ln\ \phi_i, att = {} & -(z/2)\ [\sum_j^{NG} PS_{ij}H_{2j}/H_{4j} + \sum_j^{NG}\theta_j\ (H_{3ij} + MS_iH_{5j})/H_{4j} \\ & - \sum_j^{NG}\theta_jH_{2j}\ (H_{7ij} - H_{4j}MS_i + H_{6j}MS_i)/H_{4j}^2]\end{aligned} \tag{3.50}$$

Application of GC EOS

The components of the binary are broken down into the relevant groups as shown in Table 8.2 for the propane / 1-propanal system. The required group information is given in Skjold-Jorgensen (1984) and revised in Skjold-Jorgensen (1988). The pure component temperatures and pressures are found in the literature for example Reid, *et al* (1987).

The compressibility factor, Eq. (3.45) is solved iteratively for the liquid and/or the vapour phase. The compressibility factor is required to calculate the fugacity coefficients Eq. (3.48). Knowing the fugacity coefficients the K values Eq. (3.9) can be calculated.

An advantage of the GC EOS is that it can easily be incorporated in the direct or combined method flow diagrams, (Figures 3.1 and 3.2), in contrast to the UNIWAAL EOS which requires a completely different computational procedure (Appendix B.7.3).

The computer time requirements are however longer than for most other cubic EOS as a large number of complex auxilary functions need to be calculated. In addition the equations of the compressibility and fugacity coefficients are complex making programming difficult.

The GC EOS equation forms appearing in Eq. (3.45) to Eq. (3.48) and as originally appearing in Skjold Jorgenson (1984) are written in terms of the total volume and number of moles. The auxilary functions (H), not shown here, also appear in the form of total volume and number of moles. All these equations had to be re-written in terms of mole fractions and molar volumes before programming could take place.

3.5 ACTIVITY COEFFICIENT LIQUID PHASE MODELS

Activity coefficients are derived from excess Gibbs energies as follows :

$$G^E/RT = \Sigma\ x_i\ \ln\gamma_i$$

In practice the process is reversed and excess Gibbs energies are evaluated from knowledge of activity coefficients :

$$\ln\gamma_i = G^E/RT - \sum_{k\neq i} x_k\left(\frac{\partial G^E/RT)}{\partial x_k}\right)_{TPx_{j\neq i,k}}$$

Many equations have been proposed for correlating activity coefficients with either composition mole fraction or volume fraction or molecular surface fraction (when the molecules differ widely in size or chemical nature). Some equations were derived on more or less rational grounds while others are purely empirically based on intuition.

There are eight well known correlations of activity coefficients in use today : the Margules, van Laar, Wilson, NRTL, UNIQUAC, the regular solution method of

Scatchard-Hildebrand and the group contribution methods UNIFAC and ASOG. The most comprehensive comparison of the first five methods to date appears in the Dechema Vapour-Liquid Data Collection of Gmehling and Onken (1977).

One of the oldest of the formulas which is still in common use today, and capable of producing highly accurate results, is that proposed by Margules in 1895. The form is equivalent to a power expansion in composition. van Laar in 1910 proposed an equation based on the van der Waals EOS. Wilson in 1964 based his equation on more advanced theory. Wilson proposed that the interactions between molecules depend primarily on local concentrations which can be expressed as volume fractions.

3.1.1 The NRTL (Non Random Two Liquid) Equation

The three parameter NRTL equation proposed by Renon and Prausnitz (1986) was based on two-cell theory and has found a particular niche for itself due to its excellent representation of aqueous binary solutions.

In the derivation for a binary mixture it was assumed that the liquid had a structure made up of a cell of molecules of types 1 and 2 each surrounded by assortments of the same molecules which in turn were surrounded in a similar manner, and so on.

The NRTL equation for the activity coefficients for a binary component system is given as follows,

$$\ln \gamma_1 = x_2^2 \left[\tau_{21} \left(\frac{G_{21}}{x_1 + x_2 G_{21}} \right)^2 + \frac{\tau_{12} G_{12}}{x_2 + x_1 G_{12}} \right] \qquad (3.51)$$

$$\ln \gamma_1 = x_1^2 \left[\tau_{12} \left(\frac{G_{12}}{x_2 + x_1 G_{12}} \right)^2 + \frac{\tau_{21} G_{21}}{x_1 + x_2 G_{21}} \right] \qquad (3.52)$$

where :

$G_{12} = \exp(-\alpha \tau_{12})$ $\qquad$ $G_{21} = \exp(-\alpha \tau_{21})$

$\tau_{12} = (g_{12} - g_{22})/RT$ $\qquad$ $\tau_{21} = (g_{12} - g_{11})/RT$

τ_{12} and τ_{21} are adjustable parameters and α is an empirical parameter related to the non-randomness of the mixture.

A disadvantage of this equation is the necessity for fitting three parameters.

The third parameter was vaguely related by Prausnitz and Renon (1968) to the inverse of the cordination number. The co-ordination number being a function of the number of molecules just touching a reference molecule. α was however found to be a strictly empirical factor not related to any mechanism in general.

Marina & Tassios (1973) found that $\alpha = -1$ gave excellent representation of both miscible and partially immiscible binaries. In the Dechema VLE data collection the authors present recommended values for certain groups of hydrocarbons.

3.5.2 The UNIQUAC (Universal Quasi-Chemical) Equation

Advantages and disadvantages of UNIQUAC

The major characteristics of the UNIQUAC equation are : its applicability to multicomponent mixtures in terms of binary parameters only, applicability to liquid-liquid equilibria, built in temperature dependence valid over at least a moderate range, superior representation of molecules of widely different molecular sizes and its basis for the group contribution method such as UNIFAC. Its only real disadvantage is its greater algebraic complexity than the simpler equations of van Laar, Margules, etc.

UNIQUAC equation form

This semi-theoretical equation was based on the two-liquid model and the concept of local compositions. The excess Gibbs energy was made up of two parts :

$$g^E = g^E(c) + g^E(r)$$

where $g^E(c)$ is the contribution due to differences in sizes and shapes of the molecules (configurational or combinational part), and $g^E(r)$ is the contribution due to energetic interactions between them (residual part). The main steps in the UNIQUAC derivation are shown in Appendix B.8.

The modified UNIQUAC equation of Abrams and Prausnitz (1975) as proposed by Anderson and Prausnitz (1978) was used in this project,

$$\ln\gamma_i = \ln\frac{\bar{\phi}_i}{x_i} + \frac{Z}{2}q_i\ln\frac{\theta_i}{\bar{\phi}_i} + \bar{\phi}_j\left(l_i - \frac{r_i}{r_j}l_j\right)$$

$$+ C\ q'_i\left[-\ln(\theta'_i + \theta'_j\tau_{ji}) + \frac{\theta'_j\tau_{ji}}{\theta'_i + \theta'_j\tau_{ji}} - \frac{\theta'_j\tau_{ij}}{\theta'_j + \theta'_i\tau_{ij}}\right] \qquad (3.53)$$

For a binary,

component 1 : $i = 1,\ j = 2,$ and

component 2 : $i = 2,\ j = 1.$

C is an adjustable binary parameter usually set equal to unity, z is the cordination number usually set equal to ten. r, q, q' are the structural size, area, and modified area parameters respectively which are used in the determination of parameters l, $\bar{\phi}$, θ, θ' and τ_{ij} as follows :

$$l_i = \frac{Z}{2}(r_i - q_i) - (r_i - 1) \tag{3.52}$$

$$\bar{\phi}_i = \frac{x_i r_i}{x_i r_i + x_j r_j} \tag{3.53}$$

$$\theta_i = \frac{x_i q_i}{x_i q_i + x_j q_j} \tag{3.54}$$

$$\theta'_i = \frac{x_i q'_i}{x_i q_i + x_j q'_j} \tag{3.55}$$

$$\tau_{ij} = \exp\left(\frac{-\Delta U_{ij}}{C\ RT}\right) = \exp\left(\frac{\alpha_{ij}}{T}\right) \tag{3.56}$$

The parameters ΔU_{ij} or α_{ij} must be found from binary experimental data. One possible source includes vapour-liquid equilibrium data (P, y, x) at contant T.

If $(C = 1)$ and $(q' = q)$ for both components, the original UNIQUAC equation of Abrams and Prausnutz (1975) is recovered.

The modified structural area parameter (q') was introduced by Anderson and Prausnitz (1978) to obtain better agreement between mixtures containing water or alcohol. For alcohols the surface of interaction q' was found to be smaller than the geometric external surface q indicating that intermolecular attractions are determined primarily by the alcohol OH group.

The two-parameter form of the UNIQUAC equation is sometimes not necessary; if the parameters are highly correlated for example. The UNIQUAC may then be written in its one parameter form as per Abrams and Prausnitz (1975),

$$\Delta U_{ij} = U_{ij} - U_{jj} = \Delta U_x = (U_{ii}U_{jj})^{\frac{1}{2}}(1 - c_2)$$

where

$$U_{ii} = \frac{-\Delta U_i^{vap}}{q_i}$$

ΔU_i^{vap} is the internal energy change of vaporization of component i.

Temperature dependent co-ordination number

To improve the temperature dependence of the UNIQUAC equation the coordination number (z) can be described as a function of temperature as proposed by Skjold-Jorgensen, *et al* (1980) :

$$z = 35.2 - 0.1272T + 0.00014T^2 \tag{3.57}$$

Or as an exponential temperature dependence, Raal and Naidoo (1990) ,

$$z = A + \frac{B}{\exp\left(\frac{T-T_o}{T_o}\right)}$$

where $T_o = 273,15$ and constants A, B were evaluated from h^E data

3.5.3 Group Contribution Liquid Phase Models

The activity coefficient equations mentioned all require experimental data to obtain binary interactions parameters to extend their applicability to mixtures.

Parameters characterising interactions between pairs of structural groups by the suitable reduction of experimentally obtained activity coefficients and the subsequent use of these parameters to predict activity coefficients for other systems have been attempted. The most notable of which are :

1. The Regular Solution Theory and it's modifications as developed by Scatchard Hildebrand. The developed relationships for excess Gibbs energy and hence the activity coefficient were based on solubility parameters.
2. The ASOG model was based on the principle of independent action as proposed by Langmuir. *The properties of complex molecules can be evaluated on the basis that smaller groups of atoms within the molecule contribute in a fixed way to the molecules property, independent of the other groups within the molecule.*
3. The UNIFAC (Functional Group) method as developed by Fredenslund, *et al* (1977) and its subsequent developments, i.e., Superfac, Fredenslund and Rasmussen (1985) was based on the UNIQUAC theory. The activity coefficients are assumed to be made up of two contributions

   $$\ln \gamma_i = \ln \gamma_i^C + \ln \gamma_i^R$$

   γ_i^C being a configuration term and γ_i^R a residual term.

3.6 THERMODYNAMIC CONSISTENCY TESTING FOR BINARY HIGH PRESSURE VAPOUR-LIQUID EQUILIBRIUM DATA

Vapour-liquid equilibrium data are said to be thermodynamically consistent when they satisfy the Gibbs-Duhem equation which can be written :

$$\left(\frac{-H^E}{RT^2}\right)dT + \left(\frac{V^E}{RT}\right)dP = \sum_{i=1}^{2} x_i \, d\ln \hat{f}_i \qquad (3.58)$$

All terms are non-trivial for high pressures.

Relatively few thermodynamic consistency tests for high pressure data have been reported in the literature. This may be due in part to the tedious nature of the test, and the uncertainties inherent in the modelling equations for the Gibbs excess free energy.

A consistency test developed specifically for isothermal high pressure data was proposed by Chueh, *et al* (1965) based on the integral (area) test. The proposed test was a development of the earlier work of Adler, *et al* (1960) and Ibl and Dodge (1953). This test for vapour and liquid data as well as a new area test **based only on vapour phase data** were used in this project.

There are essentially two methods of testing vapour-liquid equilibrium data at low pressures. Van Ness, *et al* (1973) proposed a method whereby the experimental data were tested for consistency by calculating the vapour-mole fractions y from isothermal $(P - x)$ data using the Gibbs-Duhem equation. The calculated y's were compared to the experimentally measured y's (the difference is referred to as a residual) and this comparison of the predicted and observed data provides the basis for consistency. For thermodynamically consistent data this comparison should yield negligible differences, i.e., smaller than some predetermined value usually based on experimental uncertainties. The residuals for thermodynamically consistent data should be randomly spread around the zero mean. The second method makes use of an analytical expression for the excess Gibbs free energy. Barker (1953) developed this technique in which the unknown constants of an assumed algebraic function for the activity coefficient are found through iteration by fitting isothermal $(P - x)$ data.

Christiansen and Fredenslund (1975) and Won and Prausnitz (1973) extended these methods to high-pressure systems respectively. The methods are briefly discussed in Appendix B.9.2. and B.9.3 respectively. The conclusions drawn from the two methods can be misleading as the residuals reflect not only the measurement errors but also any deficiencies of models used.

3.6.1 Equal Area Consistency Test : Chueh, *et al* (1965)

The area test of Chueh, *et al* (1965) is a necessary but not sufficient test of thermodynamic consistency since the areas may contain compensating errors (Van Ness, *et al* 1973). The test is formulated as follows :

$$RHS = \int_{x_2=0}^{x_2} \ln(K_2/K_1)dx_2 + \int_{x_2=0}^{x_2} \ln(\hat{\phi}_2^V/\hat{\phi}_1^V)dx_2 + \frac{1}{RT}\int_{p=p_1}^{p=p_2} V^L dp \quad (3.59)$$

$$LHS = \left[\ln K_1 + \ln\frac{\hat{\phi}_1^V p}{\hat{\phi}_1^s P_1^s} + x_2\left[\ln\frac{\hat{\phi}_2^V}{\hat{\phi}_1^V} + \ln\frac{K_2}{K_1}\right]\right]_{x=x_2} \quad (3.60)$$

For consistency $LHS = RHS$ (3.61)

where :

$\hat{\phi}_i^V$ = *fugacity coefficient of vapour phase*

$K_i = y_i/x_i$

The derivation of the above test is shown in Appendix B.9.1

The above three areas are found by graphical integration of equilibrium data for the composition range $x_2 = 0$ to $x_2 = x_2$. The LHS of Eq. (3.61) depends on equilibrium data at the upper limit $x_2 = x_2$ only. The thermodynamic consistency of the data should be tested for several values of x_2 up to and including the critical composition.

Integration of the first term in Eq. (3.59) from $x_2 = y_2 = 0$ is problematical as it is indeterminate at $x_2 = y_2 = 0$. For graphical integration, i.e., for plots of the three terms and the manual measurement of the corresponding areas this is not a serious limitation. The limit of the first term may be found by extrapolation of the curve. For integration by computer this indeterminate point is problematical. Application of L'Hôpital's rule however yields (Appendix B.9.1) :

$$\ln\left(\frac{K_2}{K_i}\right) = \frac{f_2^{OL}}{P} \text{ or } \frac{H_{21}}{P} \tag{3.62}$$

where :

H_{21} = *Henry's Constant*

This allows the use of a computer for area calculation.

3.6.2 Equal Area Consistency Test : New Vapour Phase Test

A similar yet new consistency based only on **vapour-phase** compositions was derived during the course of this project. This removed the necessity for the determination of the limiting values of K_2/K_1. The liquid phase molar volumes which are difficult to determine are not required.

The test is formulated as follows :

$$RHS = \int_{y_{2i}}^{y_{2f}} \ln\left(\hat{\phi}_2^V/\hat{\phi}_i^V\right) dy + \int_{p_i}^{p_f} \left(\frac{V^V}{RT}\right) dp \tag{3.63}$$

$$LHS = \left[\ln \hat{\phi}_1^V p + y_2 \ln \hat{\phi}_2^V/\hat{\phi}_1^V\right]_{y_{2i}}^{y_{2f}} \tag{3.64}$$

For thermodynamic consistency $LHS = RHS$ (3.65)

Useful features of this test are :

(i) It can be applied if only $P-T-y$ data are available,

(ii) Liquid molar volumes need not be evaluated,

(iii) Vapour-molar volumes and fugacity coefficients can both be obtained from a single EOS.

A full derivation of the test is shown below.

Derivation of Vapour Phase Consistency Test

The Gibbs-Duhem equation for constant temperature is :

$$\Sigma y_i d\ln \hat{f}_i = \frac{V^V}{RT} dp \tag{3.66}$$

Since $\Sigma y_i = 1$,

$$\Sigma y_i d\ln y_i = 0 = \Sigma y_i \frac{dy_i}{y_i} \tag{3.67}$$

Thus, for a binary mixture, from Eqs. (3.66) and (3.67)

$$y_1 d\ln \hat{f}_1 + y_2 d\ln \hat{f}_2 - y_1 d\ln y_1 - y_2 d\ln y_2 = \frac{V^V}{RT} dp \tag{3.68}$$

Rewriting Eq. (3.68) :

$$y_1 d\ln \frac{\hat{f}_1}{y_1} + y_2 d\ln \frac{\hat{f}_2}{y_2} = \frac{V^V}{RT} dp \tag{3.69}$$

Expand the first term of Eq. (3.69) using $y_1 = 1 - y_2$:

$$d\ln \frac{\hat{f}_1}{y_1} + y_2 d\ln\left(\frac{\hat{f}_2 y_1}{y_2 \hat{f}_1}\right) = \frac{V^V}{RT} dp \ . \tag{3.70}$$

Since,

$$d\left(y_2 \ln \frac{\hat{f}_2 y_1}{\hat{f}_1 y_2}\right) = y_2 d\ln\left(\frac{\hat{f}_2 y_1}{\hat{f}_1 y_2}\right) + \ln\left(\frac{\hat{f}_2 y_1}{\hat{f}_1 y_2}\right) dy_2 , \tag{3.71}$$

Eq (3.70) becomes :

$$d\ln \frac{\hat{f}_1}{y_1} + d\left(y_2 \ln\left(\frac{\hat{f}_2 y_1}{\hat{f}_1 y_2}\right)\right) = \frac{V^V}{RT} dp + \ln\left(\frac{\hat{f}_2 y_1}{\hat{f}_1 y_2}\right) dy_2 \tag{3.72}$$

Introducing,

$$\frac{\hat{f}_i^V}{y_i P} = \hat{\phi}_i^V$$

into Eq. (3.72) and rearranging the terms :

$$\ln\left(\frac{\hat{\phi}_2^V}{\hat{\phi}_1^V}\right) dy_2 + \frac{V^V}{RT} dp = d\left(\ln \hat{\phi}_i^V p + y_2 \ln \frac{\hat{\phi}_2^V}{\hat{\phi}_1^V}\right) \tag{3.73}$$

Integrating between $y_2 = 0$ and $y_2 = y_{2f}$ (or to any other intermediate vapour composition) at constant temperature :

$$\int_{y_2=0}^{y_{2f}} \ln \frac{\hat{\phi}_2^V}{\hat{\phi}_1^V} dy_2 - \int_{y_2=0}^{y_{2f}} d\left(\ln \hat{\phi}_1^V p + y_2 \ln \frac{\hat{\phi}_2^V}{\hat{\phi}_1^V}\right) = \frac{-1}{RT} \int_{p_1}^{pf} V^V dp \tag{3.74}$$

$$Area\ 1 - \left[\ln \hat{\phi}_1^V p + y_2 \ln \frac{\hat{\phi}_2^V}{\hat{\phi}_1^V}\right]_{y_2=0}^{y_{2f}} = -Area 2 \tag{3.75}$$

or

$$Area\ 1 + Area\ 2 = [\ln \hat{\phi}_1^V p]_{y_{2c}} - [\ln \hat{\phi}_1^V p]_{y_2=0} + \left[y_2 \ln \frac{\hat{\phi}_2^V}{\hat{\phi}_1^V} \right]_{y_2=0}^{y_{2f}} \qquad (3.76)$$

CHAPTER 4

DESIGN, CONSTRUCTION AND DEVELOPMENT OF HIGH PRESSURE VAPOUR-LIQUID EQUILIBRIUM EXPERIMENTAL EQUIPMENT

4.1 INTRODUCTION

The successful high pressure and temperature static equilibrium cell and associated apparatus, (Photographs 1 and 2), described here are the result of several years of experimentation.

Initial Development

The project was initiated in the early 1980's at the request of SASOL who required vapour-liquid equilibrium data for certain components in their coal liquification process at temperatures and pressures of up to 500 °C and 200 bar. The temperature and pressure requirements however fell away during the initial period of Bradshaw's project as circumstances changed and SASOL no longer required high temperature and pressure data. A more modest operating criterion of 250 °C and 200 bar was then set. The initial development done by Bradshaw is described in his thesis, Bradshaw (1985). Due to numerous difficulties experienced in the sealing of the liquid sampling system and due to time constraints the experimental data measured by Bradshaw was limited. Difficulties he encountered during experimentation were :

1. The non-uniformity of the air bath and equilibrium-cell temperatures.
2. The liquid-phase sample compositions showed an incorrect bias towards the volatile component of the system being measured.

The vapour phase sample compositions were however reproducible and corresponded to the literature values.

Subsequent Development

A re-evaluation of the project direction was undertaken. Decisions were made as to whether the experimental method should be changed, what the temperature and pressure operating ranges would be, and which systems were to be investigated.

It was decided to totally revamp, overhaul and extensively modify the equipment, retaining the original temperature and pressure specifications and principles of liquid and vapour sampling. After the completion of the reconstruction phase, the equipment would be tested on the carbon dioxide/toluene binary. After the successful completion of experimental measurements on this binary the industrially important but very demanding propane/water binary would be measured. Finally a previously unmeasured volatile/non volatile system was to be examined.

Factors Influencing Static Method Choice

Due to the problems faced with the liquid sampling system and the relatively simple sampling systems employed in the dynamic methods, converting the existing equipment to a dynamic method was considered. Conversion of the equipment was however unacceptable for the following reasons :

1. The maintenance work required should be minimal. The work involved with a static method was within the means of one researcher. The work involved in maintaining a dynamic method is however usually beyond the means of one researcher.
2. Since most of the equipment used in dynamic methods is of a specialised nature they are not stock items for the manufacturer's representative (if any) in South Africa. Long delay times for the delivery of equipment and spare parts could therefore be expected.

The static method of operation was therefore retained.

The main experimental aspects covered in this chapter includes :

1. The equilibrium cell,
2. Equipment for agitation of the phases,
3. Equipment for sampling of the liquid and vapour phases,
4. Equipment required for sample preparation for analysis (jet mixer),
5. Equilibrium cell environment (air bath),
6. Measuring equipment : Temperature, pressure and compositional measurements,
7. Safety features.

Additional auxiliary equipment of importance will also be covered briefly :

1. A unique gas chromatograph detector calibration device,
2. A degassing unit,
3. A propane compression device.

The recommended equipment operating procedures will be described in the following Chapter 5. The reasons for the choice of the experimental binary systems investigated are given in Chapter 6. The proposed new equilibrium cell is described in Chapter 10.

4.2 EXPERIMENTAL EQUIPMENT DESCRIPTION

4.2.1 The Equilibrium Cell

Construction

The cylindrical cell was machined from a 15 cm diameter solid billet of type 316 stainless steel and had a diameter of 50 mm and a height of ±180 mm. The resulting cavity had a volume of ±350 mℓ, Figure 4.1 and Photograph 7. The cavity was drilled slightly eccentrically to accommodate the liquid sampling device and sampling port.

The lid was closed with eight M10 stainless steel bolts and sealing was achieved by means of a teflon gasket. Care had to be taken when tightening the lid due to the eccentricity of the cavity. Slight differential tightening of the bolts was however, accommodated by the teflon gasket. The teflon gasket was usually replaced after two tightenings.

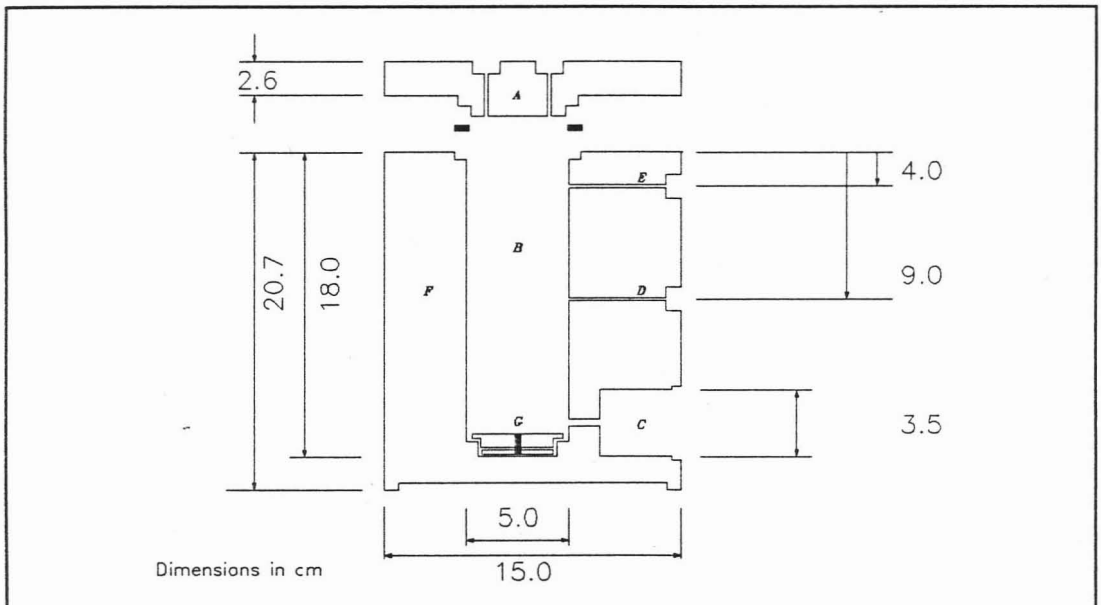

Figure 4.1 : Schematic Diagram of Equilibrium Cell Showing Principal Dimensions. A - lid, B - cell cavity, C - liquid sampling device cavity, D - cell inlet, E - vapour sampling port, F - cell wall, G - stirrer

Type 316 stainless steel was used for the cell and lid due to its inertness to organic materials and amagnetic properties. To eliminate any differential expansion or corrosion problems that could have occurred due to the use of different materials of construction only type 316 stainless steel was used throughout the whole apparatus.

From Tables 2.1 to 2.4 it can be seen that this project's cell cavity volume was large compared to most of those reported in the literature. The larger the cell volume, the smaller the volumetric disturbance of a particular sampling method and the smaller the disturbance to equilibrium.

Pressure and Temperature Limits of Equilibrium Cell

From Photograph 7 it can be seen that the cell can withstand very high pressures. The thinnest part of the cell wall is at the bottom of the cavity with a thickness of 13 mm. This "thinness" was necessary to ensure magnetic coupling between the internal stirrer and external rotating magnet. Even so the pressures the cell can withstand are enormous, certainly greater than 200 bar.

An advantage of thick cell walls is their thermal dampening abilities. Minor thermal disturbances in the air bath become irrelevant with such a large thermal mass. Cyclical or periodical fluctuations would however be noticeable.

The temperature limitation is set by the teflon gasket and rulon packing material in the liquid sampling device which tend to weaken and even become fluid at temperatures approaching 200 °C.

4.2.2 Agitation and Equilibriation of the Phases

Since one of the drawbacks of the static apparatus is the long time required for the phases to reach equilibrium this aspect demands particular attention.

Stirrers rotated by externally mounted magnets have been successfully used by several authors, Kalra and Robinson (1975), Bae, *et al* (1981), Figuiere, *et al* (1980) and Wagner and Wichterle (1987), to produce intensive mixing and hence rapid attainment of equilibrium. An internal stirrer may be rotated by magnetically coupling it to either an externally rotating magnet or by means of an orientable magnetic field induced by coils located outside the cell. Both methods are attractive since they obviate the need for the high pressure seals that would be required for a shaft driven stirrer. The first option was adopted since it did not require complex electronic circuitry to operate effectively. The stirrers designed by Bradshaw (1985) remained unaltered and are briefly discussed here.

Equilibrium cell impeller

The cell impeller was made from two small cylindrical magnets imbedded in a teflon spinner mounted on a stainless steel spindle and support ring. The assembly was located in a small recess in the bottom of the cell cavity, Photograph 7 and Figure 4.1. With a geometrically appropriate impeller and sufficiently rapid rotation a deep vortex is formed in the liquid as can be seen on close observation of Photograph 10. Due to the vortex vapour was entrained in the liquid producing rapid mass transfer and equilibration of the phases.

Externally rotating magnet

This magnet was constructed from three powerflux slab magnets, Photograph 3, with poles aligned along the large faces, mounted in an aluminium holder with rectangular mild steel pole faces. The magnet was driven with a 0,37 kW variable speed motor. This magnet rotated in a sealed well which protruded into the air bath and supported the equilibrium cell. This construction permitted the air in the well to become heated and so reduced the temperature gradient across the cell support plate. Good thermal insulation between the cell body and the asbestos plate was achieved by machining a shallow recess in the bottom of the cell, as shown in Figure 4.1, to entrap a stagnant pocket of air.

This agitation design produced a satisfactory vortex with any depth of liquid.

4.2.3 The Liquid Sampling Device

Accurate liquid sampling is the most difficult problem to overcome in high pressure VLE measurement using static apparatus. A small representative sample of liquid must be removed from a high pressure space without disturbing the equilibrium condition. This can never be fully achieved in practice as sampling by it's very nature implies a change in system volume.

A moveable sampling rod with a small sampling hole was first proposed by Fredenslund, *et al* (1973) and this principle was adopted for this apparatus.

The sampling rod and piston assembly are shown in Figure 4.2 and 4.3 and Photographs 11 to 13. Figure 4.6 shows the auxiliary operating equipment.

4.2.3.1 Description of the sampling device (Figure 4.2)

The sample rod was a 5 mm diameter polished stainless steel rod with a 1,5 mm hole (A) drilled near the tip to give a ±8.8 mm^3 volume. The rod was polished to minimise friction and chafing of the packing and the edges of the sampling hole were slightly flared to prevent chafing of the packing material. Insertion and withdrawal of the rod through the cell wall is accomplished with an air activated piston (I) with guide rods (H). When the rod was inserted the sample hole was positioned just inside the equilibrium cell. When withdrawn it was in alignment with the carrier gas channels (F) drilled through the equilibrium cell body. The guide rods prevented rotation and the consequent misalignment of the sample rod with the sample carrier gas channels. The pressure integrity of the equilibrium cell and sealing of the sampling rod was achieved through an unsupported area seal. The piston rod and unsupported area assemblies were connected to the cell wall by 12 high tensile 8 mm mild steel cap head screws. A teflon spacer between the piston rod and unsupported area seal supplied the necessary freedom of movement required between the two assemblies.

Important features of the liquid sampling device : the principle of sealing (unsupported area seal), the packing material used in the seal, method of operation and piston rod assembly will be examined below in more detail.

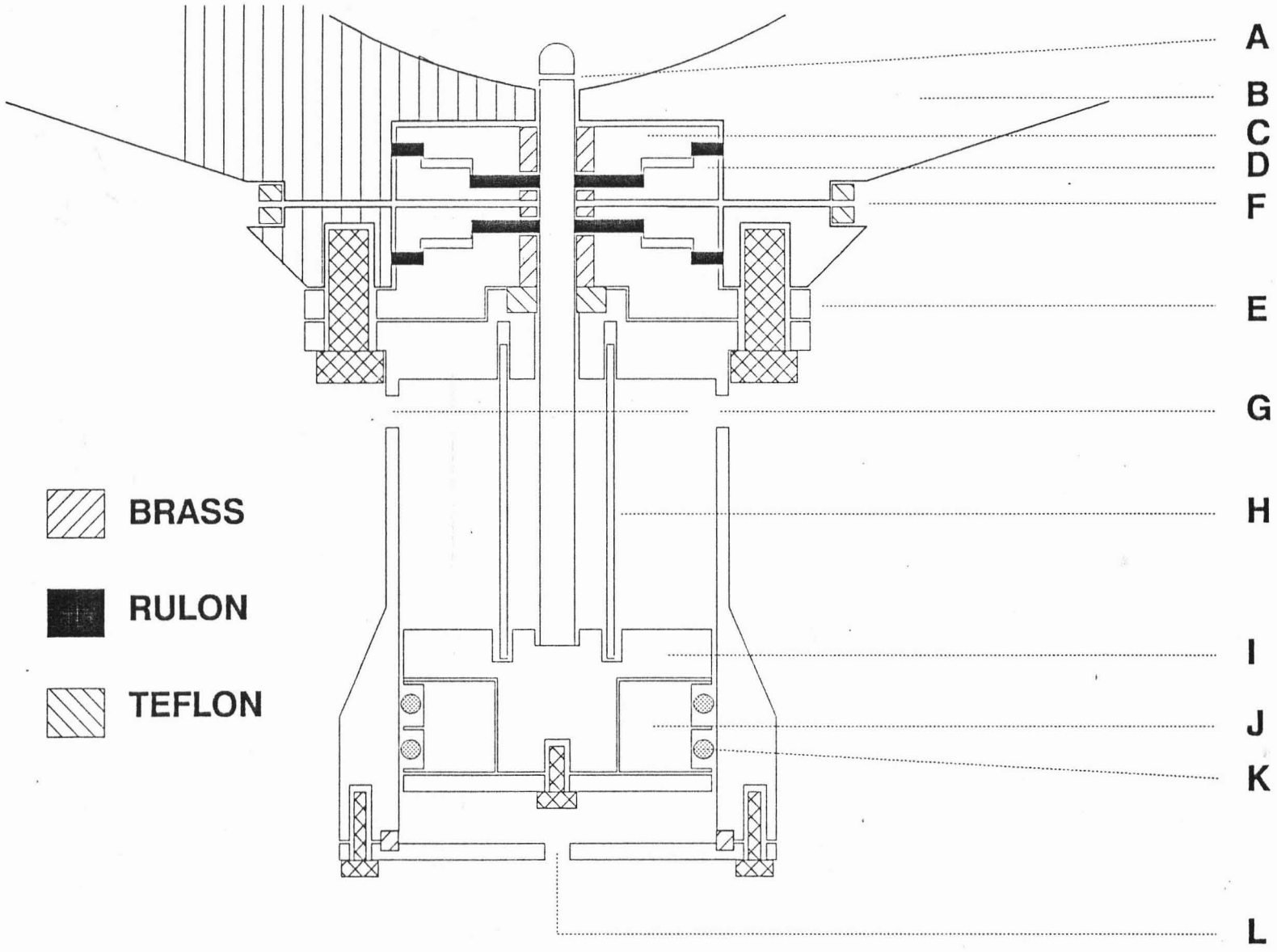

Figure 4.2 : Liquid Sampling Device A - liquid sample hole, B - equilibrium cell wall, C - inner male packing ring, D - female paking ring, E - outer male packing ring, F - carrier gas channels, G - piston withdrawal compressed air parts, H - guide rods, I - Piston, J - brass sleeve, K - viton "O" rings, L - piston insertion compressed air parts

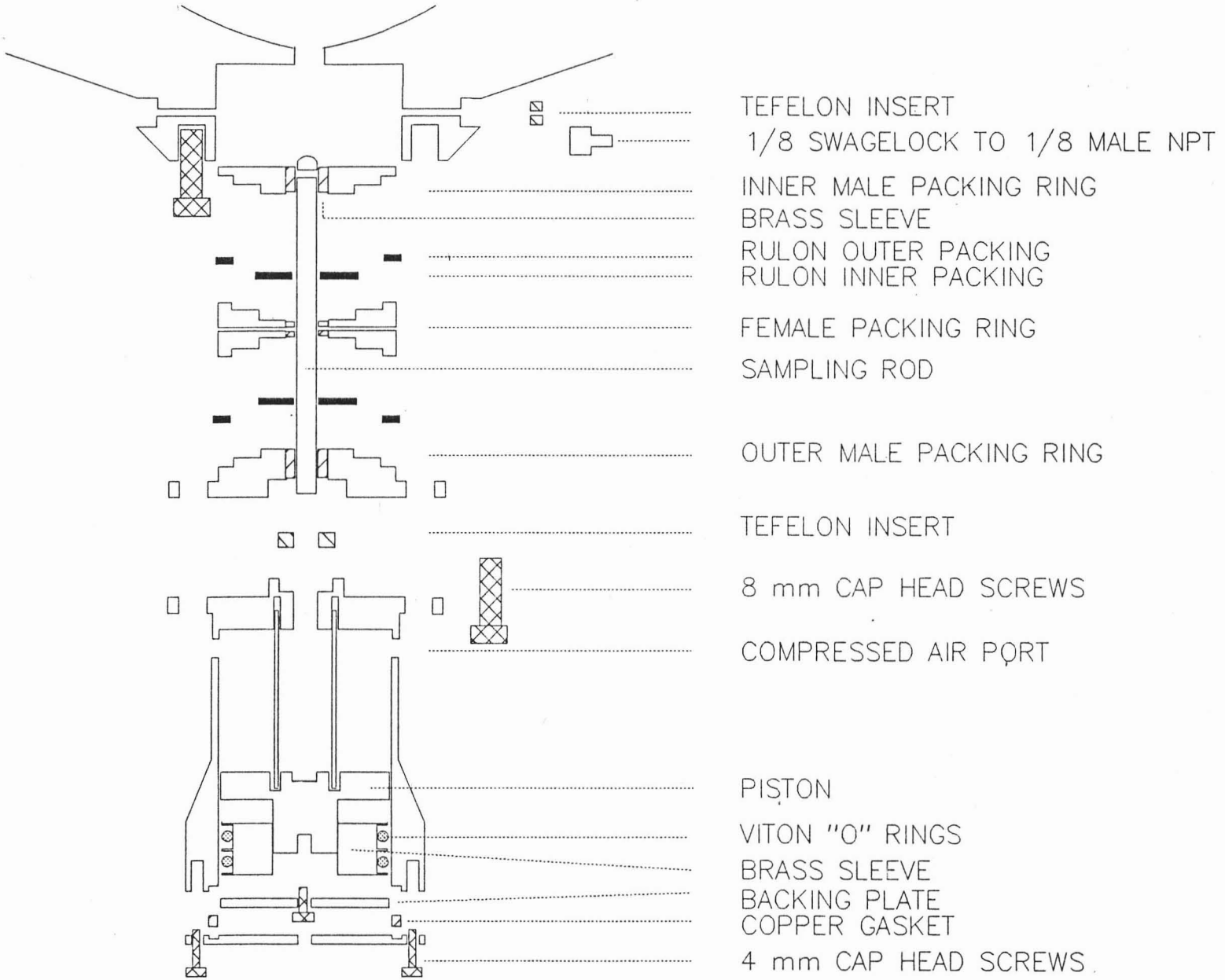

Figure 4.3 : Exploded View of Liquid Sampling Device

4.2.3.2 Sealing of the liquid sampling device : The unsupported area seal

The sealing of the rod surface against the high pressures involved presented considerable problems. A satisfactory solution was found by Bradshaw (1985) using the unsupported area seal principle proposed by Tsiklis (1968).

The basic principle of the unsupported area seal, Figure 4.4, is that the compressive force developed in the packing is greater than the pressure applied to the gland by the ratio of the respective areas.

The gland consists of three stainless steel packing rings (D, F, J) made to slip fit into one another, two being male end pieces (D and J) with a central female piece (F) through which the carrier gas channels were drilled. The pressure P from the interior cell impinges on the substantial cross-sectional area of the front ring D which was restrained from movement by the packing material as shown thereby compressing it by the ratio of their respective areas. The free space shown was important since this provides freedom of movement for the front ring D. The inner packing was responsible for the sealing of the sample rod and the outer for sealing against the cell wall. This isolated the central section from the cell interior and surrounding external environment. Brass rings, to minimise scoring of the sampling rod, were press-fitted into all three packing rings to provide a neat fit around the sample rod.

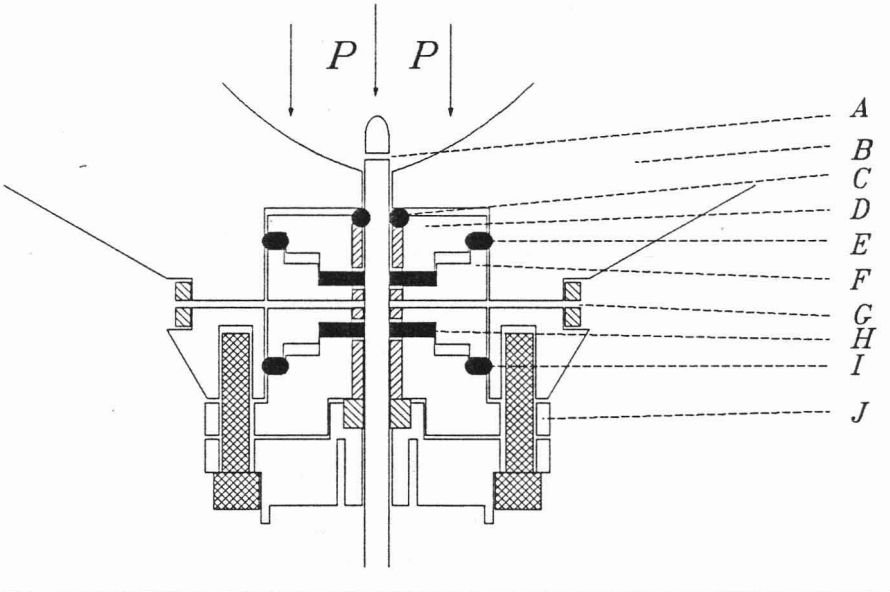

Figure 4.4 : Unsupported Area Seal (Modification 1). A - liquid sample hole, B - equilibrium cell wall, C - nitrile "O" ring, D - inner male packing ring, E & I - outer packing (nitrile "O" ring), F - female packing ring, G - carrier gas channel, H - inner packing (rulon), J - outer male packing ring, P - cell pressure

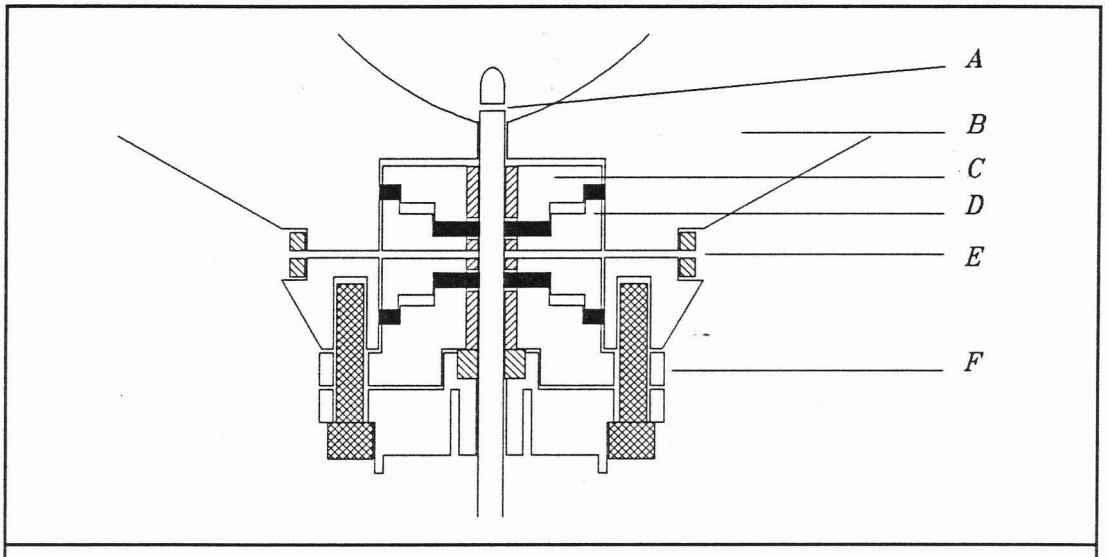

Figure 4.5 : Unsupported Area Seal (Original). A - liquid sample hole, B - equilibrium cell wall, C - inner male packing ring, D - female packing ring, E - carrier gas channel, F - outer male packing ring

4.2.3.3 Selection of packing material (Figure 4.4)

At high temperatures teflon was found to be totally inadequate as a packing material as it showed little resistance to creep. Reinforced teflon (brass or graphite) was adequate in reducing the creep experienced by teflon. Bradshaw mentioned that the reinforced teflon packing material had a life of approximately 3 months but did not mention how many withdrawals. In this project, the graphite impregnated teflon used had a working life on average of 100 withdrawals. Packing life was found to depend on the initial tightening of the unsupported area seal. The tighter the packing compression, the greater the chafing of the packing, the shorter its working life. Tightening the 12 cap head screws to a torque of 35 N x m was found to give optimum packing life. The working life of graphite impregnated teflon although longer than teflon, was found unacceptable. Rulon was tried and this had a significantly longer working life. During the last set of experiments over 500 withdrawals were made without any apparent degradation of the packings.

The packing material was however, found to be very sensitive to temperature variation. If after a particular isothermal experimental data run the equilibrium cell was allowed to cool down to room temperature, on reheating to a new isotherm, the packing's sealing integrity was found suspect. A small leak in the outer packing was discovered. By slightly tightening the cap head bolts the problem was solved. This could only be done once however, as extra compression of the packing material by the tightening

process tended to result in greater extrusion. After the third tightening, extrusion of the packing material resulted in blockages of the sampling hole. The only solution then was to remove the sampling device and machine new packings.

The removal and replacement of the packing material proved time-consuming and troublesome. The packing responsible for sealing against the cell wall usually extruded more than the sample rod packing due to its smaller area. This extrusion resulted in difficulties in the removal of the female and inner male packing rings. A new arrangement shown in Figure 4.4 was tried. The essential differences can be deduced from Figures 4.4 and 4.5 :

1. The replacement of the rulon packings sealing against the outside wall with nitrile "O"-rings (Figure 4.4). "O"-rings made from a more appropriate material viton of the correct size could not be obtained.
2. The addition of a small nitrile "O"-ring to achieve a superior seal on the sampling rod (Figure 4.4).

The arrangement, Figure 4.4, was found to be unacceptable during experimentation for three reasons :

1. Although the original aim of ease of removal of the packing rings was achieved it was at the expense of more removals and replacement of packings. The nitrile "O"-rings which were supposed to withstand 110 °C tended to soften and adopt the shape of the packing ring gap i.e. they acquired flat faces. This meant that they had to be replaced if the equilibrium cell had to be cooled to room temperature between isothermal runs.
2. Rulon and nitrile had different compressibilities. For this reason the whole unsupported area seal had to be tightened more to achieve the same quality of seal. This resulted in greater chafing on the inner rulon packings and consequently shorter working life.
3. The sampling rod nitrile "O"-ring tended to deform and be scraped by the sampling rod resulting in sample hole blockages. A similar problem was experienced by Nakayama, *et al* (1987).

The original system Figure 4.5 was adopted for futher experimentation.

4.2.3.4 Method of operation

The rate of insertion and withdrawal of the sampling rod could be accurately controlled. Figure 4.6 shows the essential features of the control system.

If the sample rod was to be inserted into the cell the Whitey B-43YF2 four way crossover ball valve was set in position such that bottled compressed air, stepped down to a pressure of 80 bar, was routed to the insertion port of the piston rod assembly. To withdraw the sample rod from the cell the four way valve was set in position such that the bottled compressed air was routed to the withdrawal port. In each case the port not connected to the compressed air bottle was connected to the vent. The rate of insertion or withdrawal was controlled by releasing the venting air through a Whitey SS-22RS4 fine metering valve.

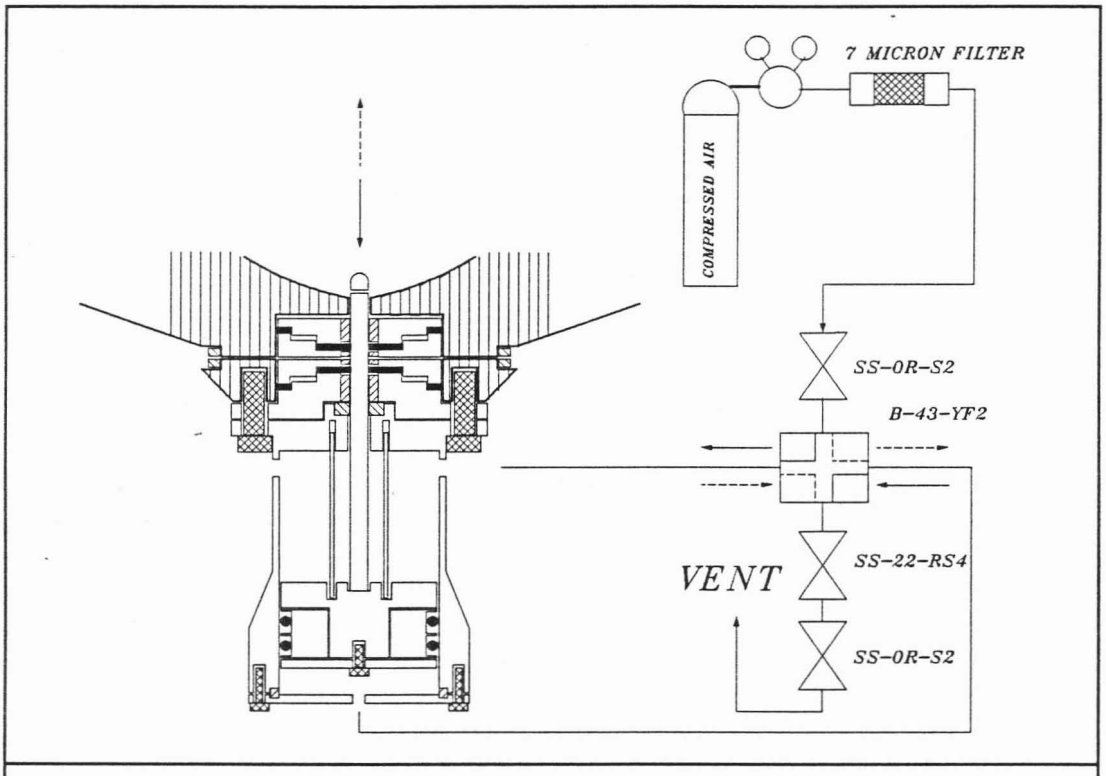

Figure 4.6 : Liquid Sampling Device and Auxillary Equipment

4.2.3.5 Piston rod assembly (Figure 4.2)

This unit was responsible for the insertion and withdrawal of the sampling rod. The system employed by Bradshaw, two solid teflon rings to seal between insertion and withdrawal chambers, was found unsatisfactory.

The two teflon rings were too thick to allow for adequate compression by the backing plate. This meant the piston often contacted the outer chamber walls resulting in scoring and hence leakage across the seal. This leakage resulted in a loss of sampling rod insertion and withdrawal rate control.

This system was replaced with an "O"-ring housing assembly. The piston housing assembly "O"-ring grooves were cut to the dimensions recommended by Dowty Seals (1986), for piston and piston rods used in dynamic alternating pressure applications for P > 100 bar, (Appendix C.1). The viton "O"-rings with two teflon split anti-extrusion rings, not shown in Figure 4.2 but seen in Photograph 11, were fitted in a brass sleeve (J). Brass was used to prevent damage or scoring of the chamber wall. The brass sleeve was attached to the piston with Locktite super glue to prevent any air leakage between them and consequently between the insertion and withdrawal chambers. Any leakage was undesirable as it resulted in a loss of sampling rod withdrawal and insertion rate control. The superglue withstood the operating temperatures well and no leakage was detected. Although only one "O"-ring assembly was necessary they were duplicated to ensure an adequate seal.

A problem encountered during early experimentation, the misalignment of the sampling rod after a few withdrawals, was traced to the withdrawal port. The original piston rod chamber had only withdrawal port (G), Figure 4.2. The compressed air at 80 bar flowing in during withdrawal exerted a force on the one side of the sampling rod thereby misaligning it. This misalignment caused increased packing wear. The addition of a second port directly opposite the original one solved this problem.

A 7 micron air filter was inserted in the compressed air line to prevent any foreign particles entering the piston rod assembly. The introduction of foreign particles into the piston chamber caused scoring of the stainless steel piston and consequently resulted in leakages between the two chambers.

4.2.4 Jet Mixer

One of the most troublesome problems experienced in the sampling of a volatile/non volatile mixture into an evacuated space is the tendency of the volatile component to flash preferentially thus creating a non-homogeneous gas and liquid mixture. Dieters and Schneider (1986) make the observation that sample preparation for analysis and not the quantitative analysis itself is a most demanding aspect. Particular attention is therefore required to obtain successful homogenization of the withdrawn sample. Various methods that have been tried, for example Kalra, *et al* (1978), Nakayama, *et al* (1987), were briefly discussed in Chapter 2.

In the present design a jet mixer (based on a design proposed by Professor J.D. Raal) performed the function of vaporising and homogenizing the liquid sample in preparation for gas chromatography analysis. The liquid sample was flashed into the initially evacuated jet mixer through the nozzle at high velocity to produce a swirling, recirculating flow until the pressure became uniform. Further mixing of the sample was ensured by subsequently flushing helium carrier gas through the passage in the cell wall into the mixer at a controlled pressure. The essential features of the final jet mixer are shown in Figure 4.7 and Photographs 15 and 16.

4.2.4.1 Description of jet mixer

The mixing chamber was fitted with an internally mounted cylindrically shaped baffle. The internal baffle has a restriction nozzle which caused acceleration and hence vaporisation of the liquid sample as the entering sample and carrier gas set up a swirling circulating flow until the pressure equalized. The absence of any moving parts and external devices are distinct advantages in high temperature work.

The inlet was connected to one of the liquid phase carrier gas sampling channels drilled through the equilibrium cell wall. The outlet port leading to the gas chromatograph had a Whitey SS-ORM2-52-19 regulating and shut-off valve tapped into the outer chamber wall. The valve was operated from outside the air bath by fitting a stem extension with a thermal break of teflon. Initially problems were experienced with cross threading of the valve stems due to the rigidity of the stem extension. This was solved using a well oiled universal joint, from a miniature tool kit, in the stem extension giving it the flexibility needed, Photographs 19 and 20.

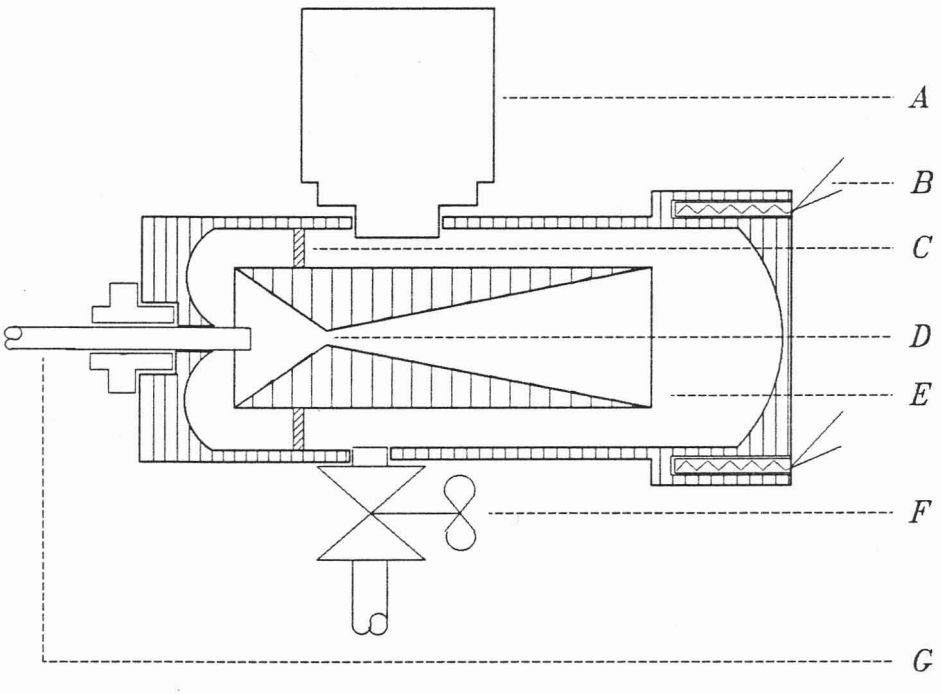

Figure 4.7 : Schematic of Jet Mixer Showing Essential Features. A - sensotec pressure transducer, B - heating elements, C - nozzle support, D - nozzle orifice, E - nozzle, F - Whitey SS-ORM2-S2-A valve, G - inlet from equilibrium cell wall channels

4.2.4.2 Jet mixer temperature control

The jet mixer was kept at a higher temperature than the equilibrium temperature. Heating was achieved by the two 100 W stainless steel cartridge heaters controlled by a Eurotherm 810 (model 810-003-000-003) controller with a thermocouple type K temperature sensor. Stable temperature control was achieved by tuning the controller by the method described by Kinney (1983). The temperature controller was set with proportional band 16 %, integral time 200 seconds, derivative time off, cycle time 20 seconds and maximum power 100. These settings provided stable constant temperature control for settings in the 120 °C to 180 °C range.

4.2.4.3 Jet mixer pressure measurement

A pressure transducer was mounted on the jet mixer to provide useful information on the operation of both the jet mixer and the liquid sampling device. Using this pressure transducer the cause of the non-uniformity of the withdrawn liquid samples as experienced by Bradshaw (1985) was discovered as described in Appendix C.3. Knowing the volume of the jet mixer and liquid sample volume a *rough* indication of the expected pressure rise assuming total vaporisation of the liquid sample could be gained from the ideal gas law as follows,

$$moles\ sample \approx \frac{liquid\ density \times liquid\ sample\ volume}{molecular\ mass\ liquid} \qquad (4.1)$$

$$pressure\ rise \approx \frac{moles\ sample \times R \times T(jet\ mixer)}{V(jet\ mixer)} \qquad (4.2)$$

The temperature specification of 200 °C and absolute pressure measuring capabilities required proved to be troublesome as most transducers available were rated to a maximum of 120 °C due to electronic considerations. Eventually a company specializing in the manufacture of transducers for extraordinary applications was found. Sensotec supplied a Model Z transducer (range 0-3 bar (a), temperature compensated to 204 °C, with an accuracy of ±0,25 % of full scale (0,0075 bar). 2 meters of teflon cable led to a Shimaden (model SD10-900-(1-100 MV)-012-DL) digital indicator with -100 to 400 kPa readout. The pressure transducer screwed directly into the top of the jet mixer. The large opening port eliminated stagnant spaces, an important consideration.

4.2.5 Jet Mixer and Liquid Sampling Device

Using the jet mixer's pressure transducer the cause of the non-reproducibility of the liquid samples as experienced by Bradshaw (1985) was discovered.

Reproducible liquid samples should result from consistent liquid sample volume withdrawals was used. Consistent liquid volume withdrawls must result in reproducible pressure rises in the jet mixer on sampling. The reproducibility of

liquid sample volumes could therefore be detected by the jet mixer's pressure transucer readings. The reason for the inconsistency of the liquid samples was traced to the insufficient inner packing material width as described in Appendix C.3.1

The determination of the final jet mixer volume (75 cm^3) which was dependent on : the withdrawn liquid sample volume and gas chromatograph considerations (gas sampling valve loop volume and detector requirements). This is summarised in Appendix C.3.2. In Chapter 5, the operating procedure developed for the liquid sampling device and jet mixer during the carbon dioxide/toluene studies will be described.

4.2.6 Vapour Sampling System

Sampling of the vapour phase did not present as many problems as the sampling of the liquid phase since preferential flashing of the volatile component did not arise. Partial condensation was prevented by a reduction of the sample pressure and ensuring low partial pressures of the volatile components by adequately diluting the constituent components in helium carrier gas. This ensured a homogeneous sample was available for gas chromatographic analysis.

The principle of the vapour sampling method used in this project was first proposed by Bae, *et al* (1981).

The vapour sample was obtained from the upper part of the equilibrium cell by expanding the vapour phase into a previously evacuated manifold enclosed by three Snotrick SS-410-FP valves capable of withstanding 10 000 psi and 232 °C, Photographs 8 and 14. The Snotrick valves were each fitted with specially constructed extension support and tie rods with thermal asbestos breaks, so they could be opened and closed by air actuators situated outside the air bath. Bradshaw (1985) reported the volume of the manifold to be 0,75 cm^3 (Figure 4.8).

The Snotrick valves and their air actuators had to be rigidly fixed to the air bath as the equilibrium cell could not support their weight. Some flexibility between the cell, which had to be positioned a correct distance above the external rotating magnet and the Snotrick vapour sampling valves, which had to be attached to the cell wall, was desirable.

The 1/4 inch rigid pipe connection between the equilibrium cell and Snotrick valve as used by Bradshaw was the source of continual leaks during the initial phase of experimentation when assembly and reassembly of the equipment was frequent. The 1/4 inch connection was replaced by a flexible 1/16 inch pipe connection, Photograph 14.

Continued operation at high pressures caused blockages in the thin tubes of the teflon inserts press-fitted into the manifold as seen in Figure 4.8. The various options considered to solve this problem are fully described in Appendix C.4. The final design chosen (Option 2 Appendix C.4) is shown in Figure 4.9.

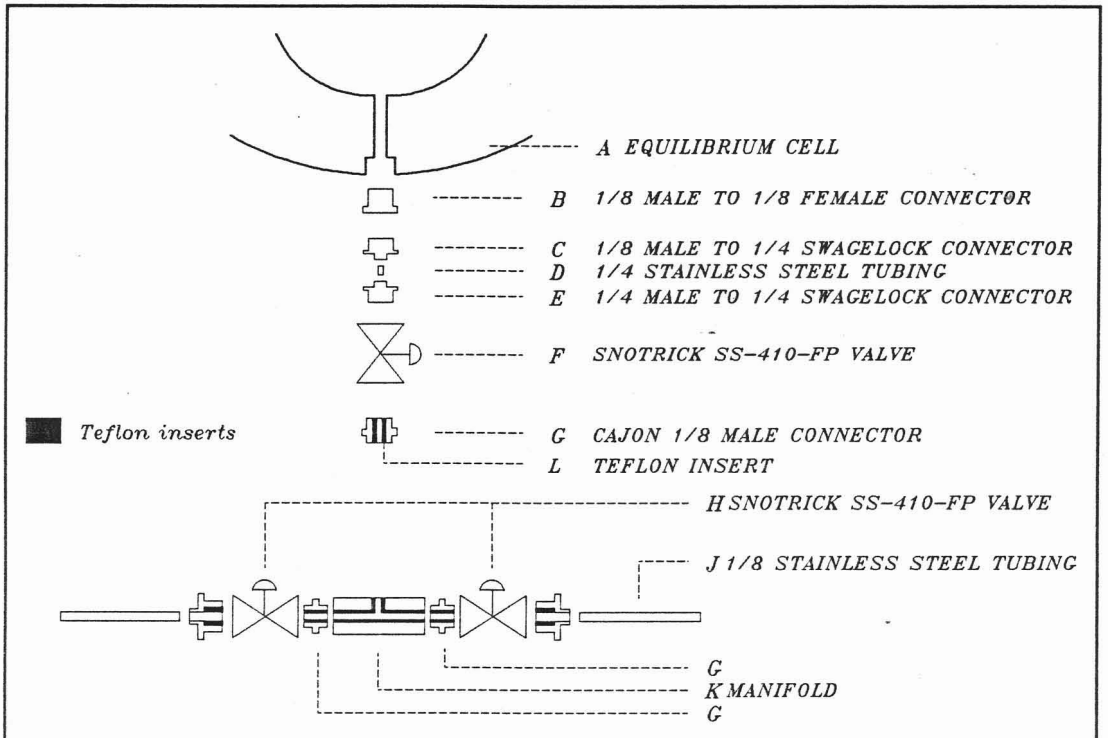

Figure 4.8 : Original Vapour Sampling System of Bradshaw (1985)

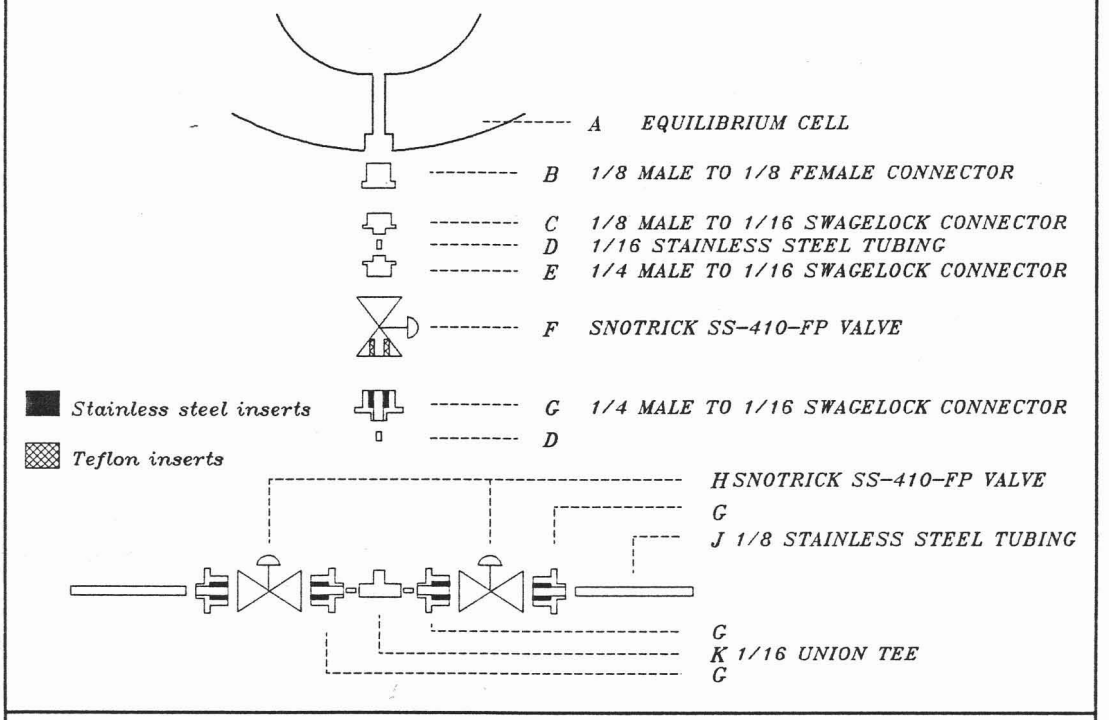

Figure 4.9 : Final Vapour Sampling System

4.2.7 Equilibrium Cell Environment

A stable and uniform air bath temperature is vital for the equilibrium cell to be free of thermal gradients for the establishment of a true vapour-liquid equilibrium state. The following aspects were investigated in the complete redesign of the air bath to improve the temperature stability :

1. Insulation.
2. Interior copper lining.
3. Air agitation methods.
4. Temperature control strategy which includes :

   Controller technology,

   Heating elements,

   Temperature sensing device.
5. Minimizing all possible heat leaks, conductive paths and thermal disturbances.

A schematic diagram of the final air bath design as well as photographs taken during its construction is shown in Figure 4.10 and Photographs 3 to 6.

Each of the above mentioned aspects will now be discussed.

4.2.7.1 Insulation

Two layers of 40 mm fibreglass industrial mineral wool Type IM475 were used as the thermal insulation material. Fibreglass was chosen as it is intrinsically fire safe, does not warp, shrink, sag, rot or slump with time and it can be cut to the shape desired.

Table C.1 (Appendix C) supplies the physical properties of Type IM475 for the design criterion of 200 °C.

Increasing the insulation thickness to greater than 80 mm, which was chosen as the final thickness, would have provided little further improvement in the insulation efficiency.

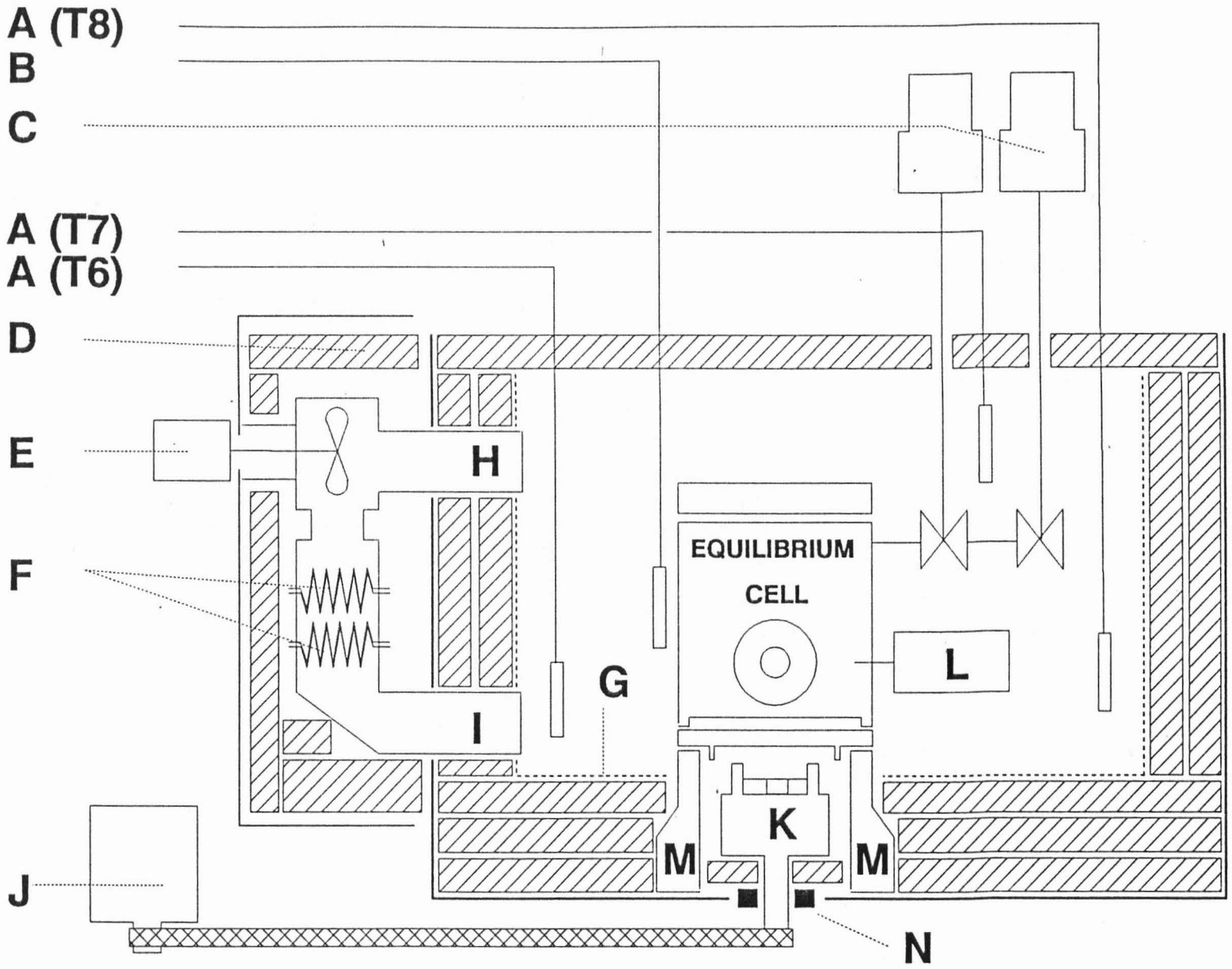

Figure 4.10 : Schematic of Principle Features of Air Bath. A - bath profile measuring thermocouples, B - Eurotherm 818 controller Pt 100 Ω, C - vapour sampling valves, D - fibreglass insulation, E - Siflo fan, F - heaters, G - copper lining, H - air inlet, I - air outlet, J - variable speed motor, K - magnetic stirrer, L - jet mixer

4.2.7.2 Interior copper lining

An inner 26 gauge copper lining was incorporated to keep the insulation in place and to promote air bath temperature uniformity (Photograph 4).

Due to the high thermal conductivity of copper (approximately 388 W/mK at 227 °C) any local temperature disturbance should be quickly dispersed and transmitted to the rest of the bath resulting in a greatly damped disturbance.

Electroplating a thin layer of copper onto the equilibrium cell external surface was also considered. This was found undesirable for the following reasons :

Extreme care would have had to be taken during the electroplating process not to deposit any copper in undesirable places such as the : equilibrium cell walls, liquid sampling device receiving well, carrier gas channels, and sampling rod channel as these had all been machined to fine tolerances. Since the air bath thermal gradients were minimized due to other precautions the necessity for electroplating the cell fell away.

4.2.7.3 Air agitational methods

The only feasible way found of avoiding the radiative heat transfer and consequent local heating effects between the equilibrium cell and the heating elements reported by Bradshaw (1985) was to shield the heating elements from the direct view of the cell. This then necessitated some form of circulation to transfer energy from the heaters to the air bath proper.

Several methods of circulating air over the heating elements were investigated. The heating elements chosen dictated the choice of method. In order to avoid burnout the elements required a flow rate of 2,51 ms^{-1} of air over them. It was therefore decided to circulate air from the bath through an external loop over the heating elements and back into the bath. (Figure 4.10 and Photographs 3 to 5).

The air was drawn in from the top of the bath by a Siflo Universal Fan and blown over the heaters, contained in a heater box, and out at the bottom of the bath Photograph 5. The fan displaced approximately 72 ℓ/s of air under no load conditions through the heater box. The outlet had a deflection plate (Photograph 3) which prevented air being blown directly onto the equilibrium cell and aided in air circulation as it created an upward spiral motion of air.

The bath volume of 65 dm^3 (diameter = 0,455 m, height = 0,400 m) was displaced approximately every 6 seconds. An additional internal convection fan was deemed unnecessary.

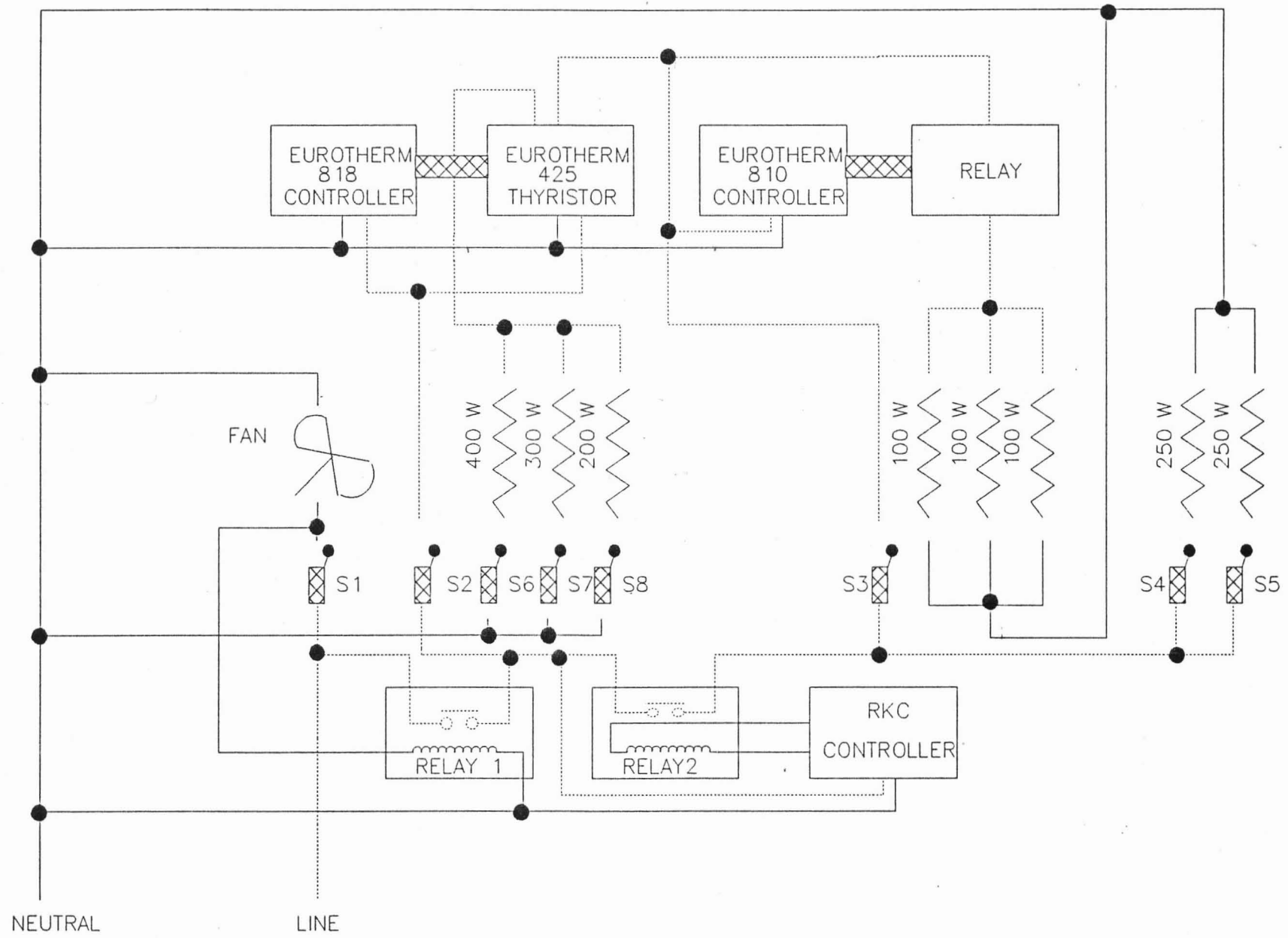

Figure 4.11 : Electric Circuit for Temperature Control

4.2.7.4 Temperature control

The particular temperature controller, heating elements and temperature sensing device were selected to ensure fast response times to air bath temperature disturbances.

The temperature controller was a Eurotherm 818 PID controller with self and adaptive-tune facilities. It's input was from a three-wire Pt 100 platinum resistance bulb mounted in a metal sheath. It's output was a 4 to 20 m Amp dc signal which drove a fast cycle firing Eurotherm 425 thyristor. The thyristor supplied the energy to 3 aluminium finned stainless steel cartridge heaters (Photograph 6).

A schematic diagram of the temperature control system is shown in Figure 5.11. A full description of the temperature control system is given in Appendix C.5.2.

4.2.7.5 Minimizing heat leaks, conductive paths and thermal disturbances

Possible heat leaks and conductive paths identified were : the asbestos well housing the rotating magnet, vapour sampling valve stem extensions, jet mixer and cell inlet valve extensions and the sample lines and electric cables to and from the air bath.

Possible thermal disturbances identified were : the jet mixer.

Magnet housing

Effective thermal insulation between the cell bottom and the rotating magnet required particular attention since the rapid air flow around the magnet produced a high convective heat transfer coefficient between the cold air in the magnet well and the heated supported plate. It was necessary to seal the well, made of asbestos pipe, in the air bath by a graphite (grade MY9D) bush capable of withstanding 200 °C and 2 000 rpm. This allowed the air in the magnet assembly to become heated and reduced the temperature gradient.

Good thermal insulation between the bottom of the equilibrium cell body and its support plate was achieved by machining a shallow recess in the bottom of the cell body to entrap a stagnant pocket of air between the cell and the asbestos supporting plate, Figure 4.1. The asbestos wall housing was insulated from the outside environment by a layer of fibreglass insulation as shown in Figure 4.10.

Valve stem extensions

The vapour sampling system, jet mixer and cell inlet valve stem extensions, all had thermal breaks. Teflon was used for the jet mixer and cell inlet sampling valves, Photographs 4 and 19, and asbestos for the vapour sampling valve stems, Photograph 8.

Sample lines

All the sample lines from and to the cell were routed through at the same place. The outside lines were wrapped in heating tape to prevent thermal gradients.

Electric cables

The electric cables were routed through the top of the air bath and coiled a few times between the two insulation sheets to prevent conductive losses.

Jet mixer

The jet mixer was the source of the two thermal disturbances.

Its higher operating temperature caused a local equilibrium cell disturbance in the liquid sampling device region. This thermal path was nullified by attaching the jet mixer to the cell by a "sandwich" bracket. The stainless steel bracket of the equilibrium cell and jet mixer were separated by a piece of Bakelite, Photograph 7. The only connection between the jet mixer and cell was a piece of piping over which a large quantity of air was continuously flowing. The values of T1 and T2 in Table 4.1 are an indication of this thermal disturbance.

The surface of the jet mixer was also at a higher temperature than the surrounding air bath. The surface was insulated by a few layers of a special insulation tape, to prevent any radiative disturbances (Photographs 19 and 20). T7 in Table 4.1 gives an indication of this thermal disturbance.

4.2.7.6 <u>Cell wall and air bath measured temperature profiles</u>

The cell wall and air bath profiles for three operating temperatures are shown in Table 4.1 to give an indication of the thermal profiles measured during experimentation. The air bath thermocouple positions are shown in Figure 4.10 and cell wall thermocouple positions in Figure 4.12.

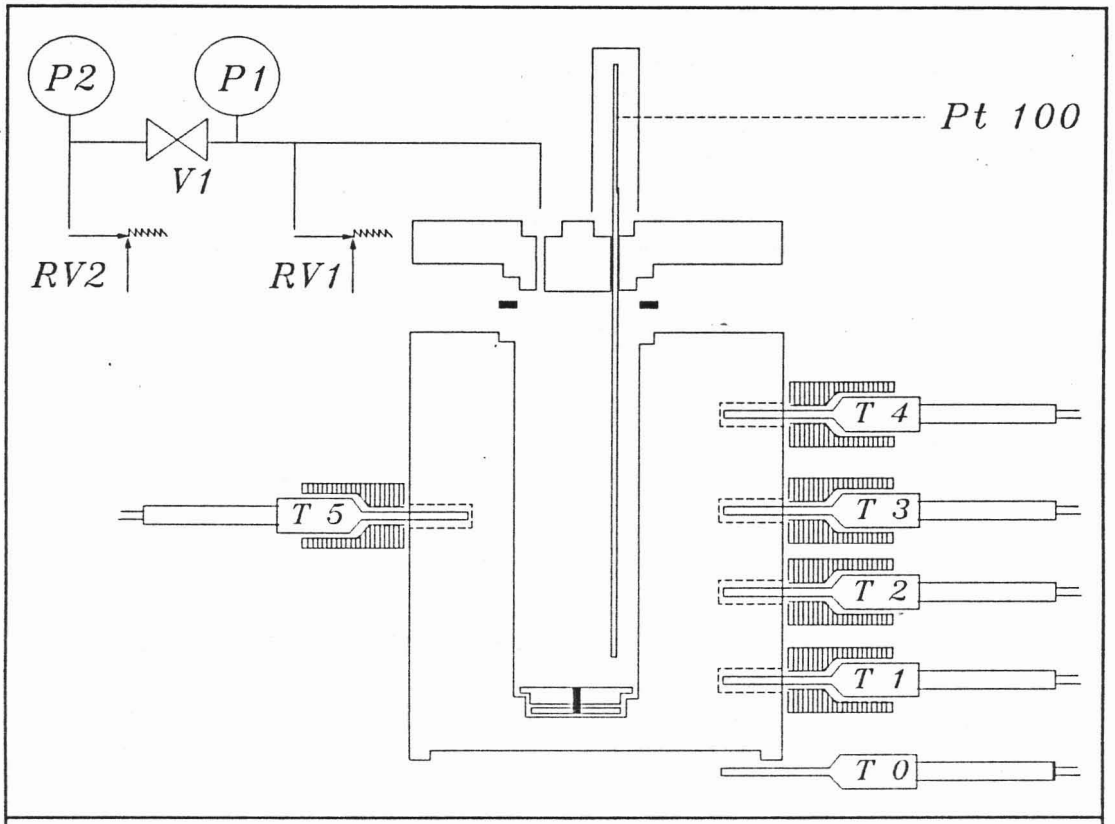

Figure 4.13 : Equilibrium Cell Profile Measuring Thermocouple Positions
P1 - Heise CC 8009, P2 - Heise CC 8008, RV1 - 5 000 psi Relief Valve, RV2 - 500 psi Relief Valve, T - Type J Thermocouple, V1 - Whitey Shuttle Valve

TABLE 4.1
Equilibrium Cell Wall and Air Bath Measured Temperatures

Thermocouple (a)	Approx. Isothermal Operating Temperature (°C)		
	78,64	100	105
T0	74,30	95,20	101,10
T1	78,45	100,50	104,70
T2	78,55	100,60	104,85
T3	78,55	100,70	105,20
T4	78,40	100,70	105,10
T5	78,45	100,60	105,00
T6	81,80	102,60	106,10
T7	78,45	101,40	105,70
T8	78,55	101,50	105,30
Eurotherm 818 TSP(1)	79,00	100,00	105,00
Fluke 8840(2)	79,10	138,52	105,05
Eurotherm 810 TSP(3)	180,00	160,00	180,00

(a) Positions as per Figures 4.10 and 4.12
(1) TSP = Temperature set point air bath.
(2) Converted from ohmic resistance.
(3) TSP = temperature set point jet mixer.

The equilibrium cell was virtually devoid of any thermal gradients. Thermocouples (T1) and (T2) measured the interference as a result of the jet mixer's higher temperature. The values of (T1) and (T2) were similar to temperatures measured at the top of the equilibrium cell wall (T4). All cell wall temperatures were within 0,4 K of each other. The stagnant air pocket under the equilibrium cell had a temperature (T0) slightly lower than the rest of the air bath however. The air as it entered the air bath had a slightly higher temperature (T6) than the rest of the air bath. The temperature in the area around the jet mixer (T7) was hardly different from the rest of the air bath due to the short residence time of air in the bath. The value of (T8), the temperature at the top of the air bath, showed no stagnation of air had occurred in the region around the vapour sampling valve. The temperature was within 0,5 K of the cell wall and air bath temperatures.

The profiles of all the isothermal operating temperatures are given in the experimental results Chapter 7.

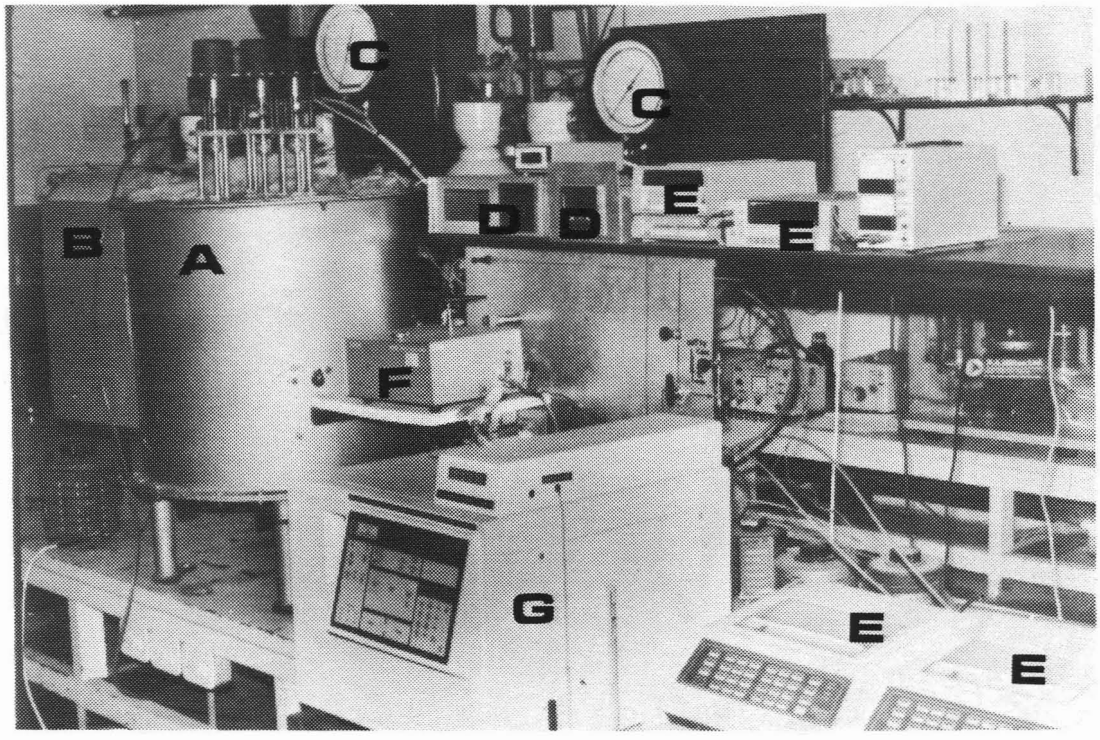

Photograph 1 Experimental Equipment : Frontal Right Hand View
A air bath, B air circulation loop, C pressure gauges, D temperature controllers, E temperature measuring devices, F gas sampling valve oven, G Varian 3000 gas chromatograph, H Varian 4270 integrators.

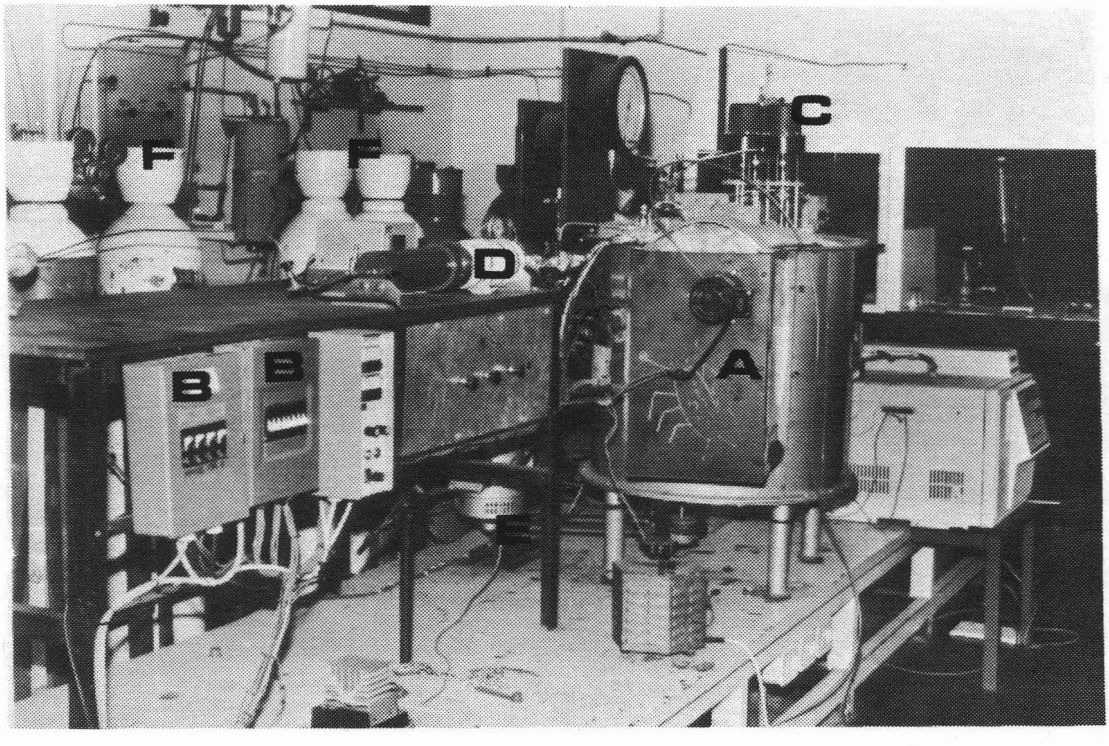

Photograph 2 Experimental Equipment : Frontal Left Hand View
A air circulation loop, B electric switches, C gas sampling valves, D propane compression device, E magnetic stirrer motor, F gas cylinder rack.

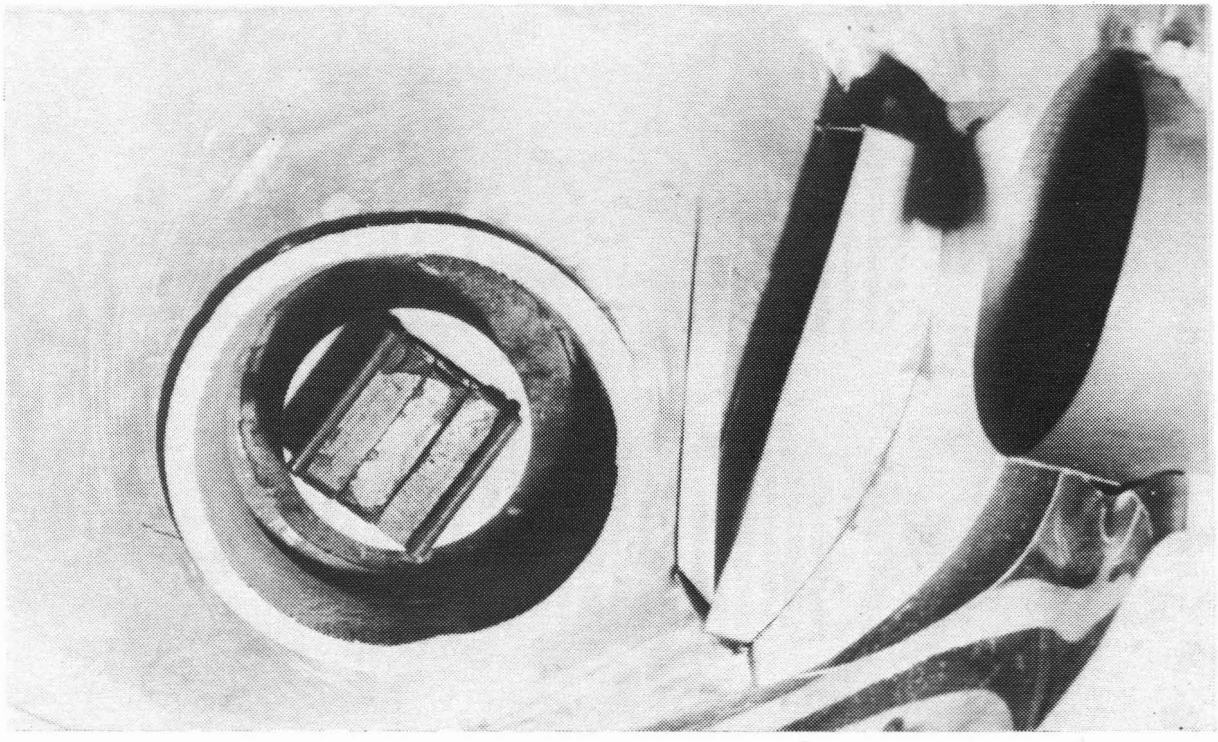

Photograph 3 Magnetic Stirrer Well
Inlet and outlet ports of air circulation loop showing air outlet deflection plate.

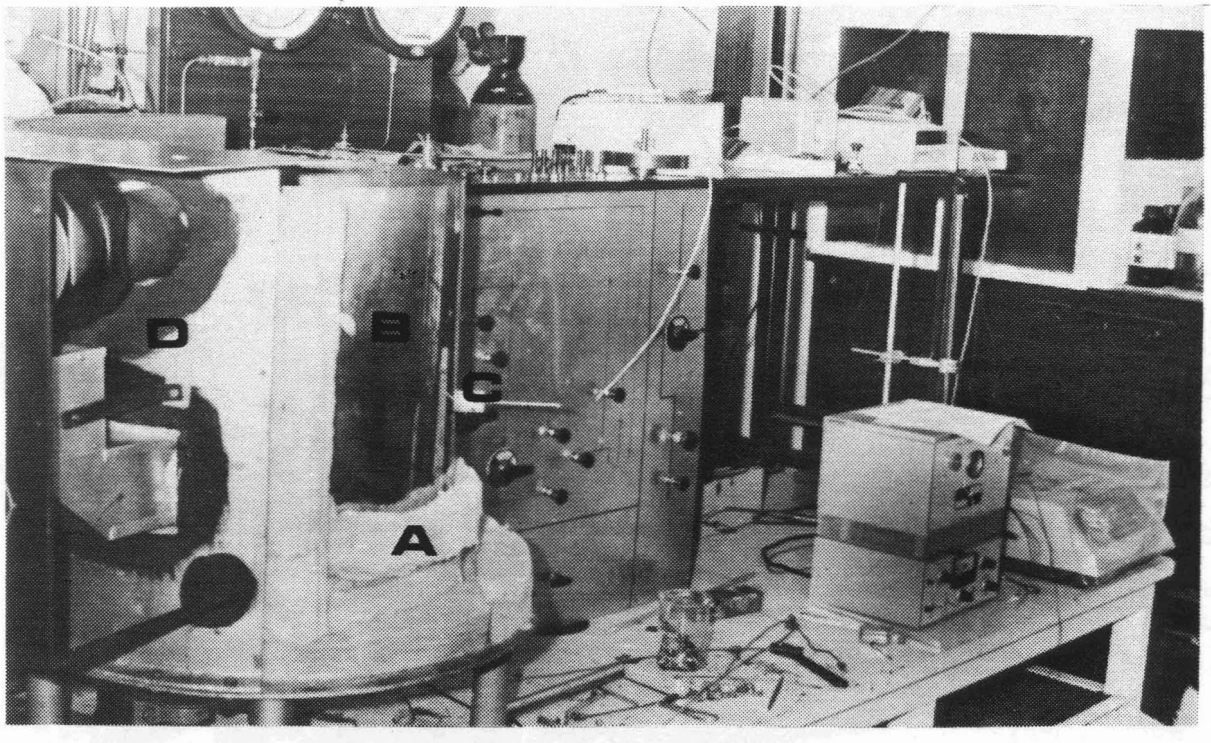

Photograph 4 Air Bath Under Construction
A fibreglass insulation, B copper lining, C jet mixer, valve stem thermal break, D air circulation loop.

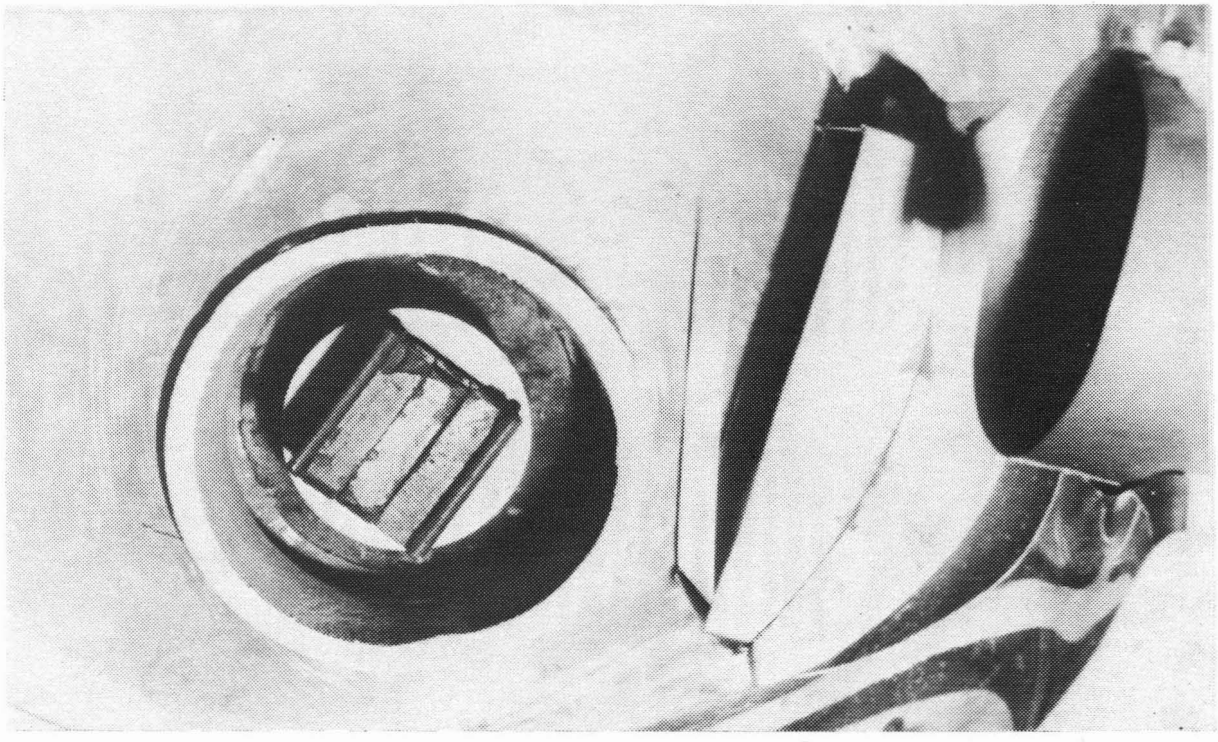

Photograph 3 Magnetic Stirrer Well
Inlet and outlet ports of air circulation loop showing air outlet deflection plate.

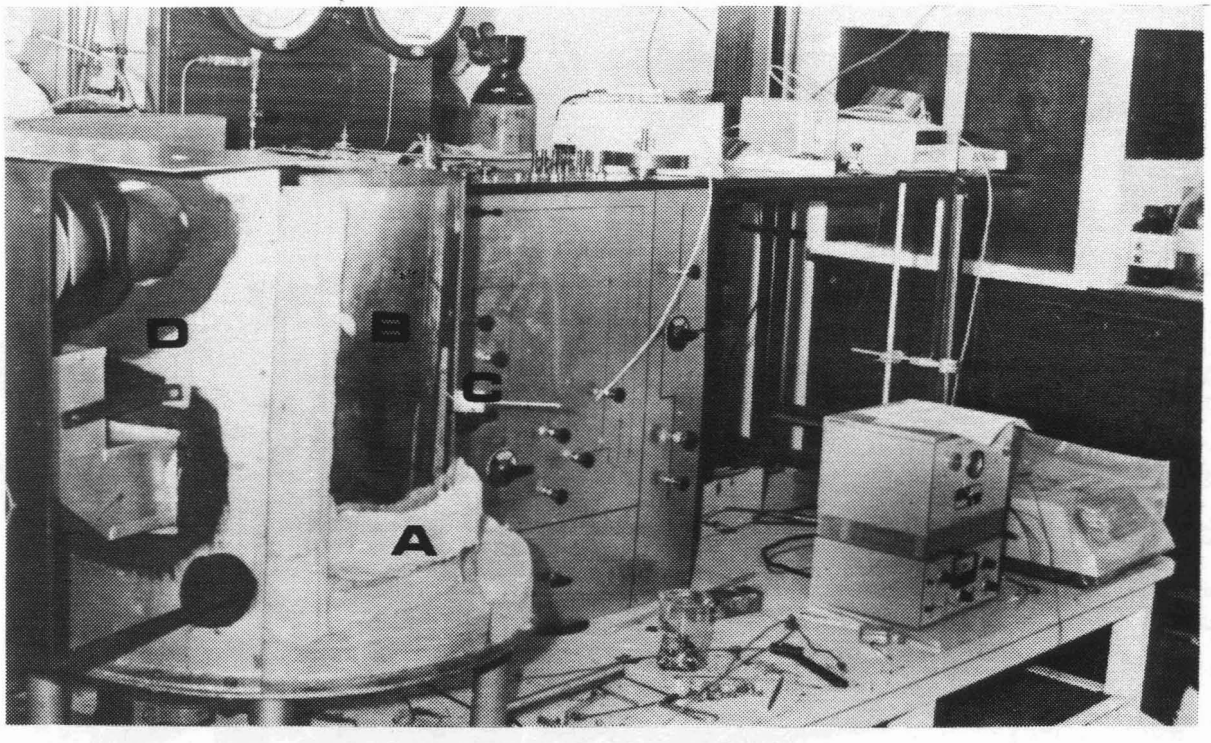

Photograph 4 Air Bath Under Construction
A fibreglass insulation, B copper lining, C jet mixer, valve stem thermal break, D air circulation loop.

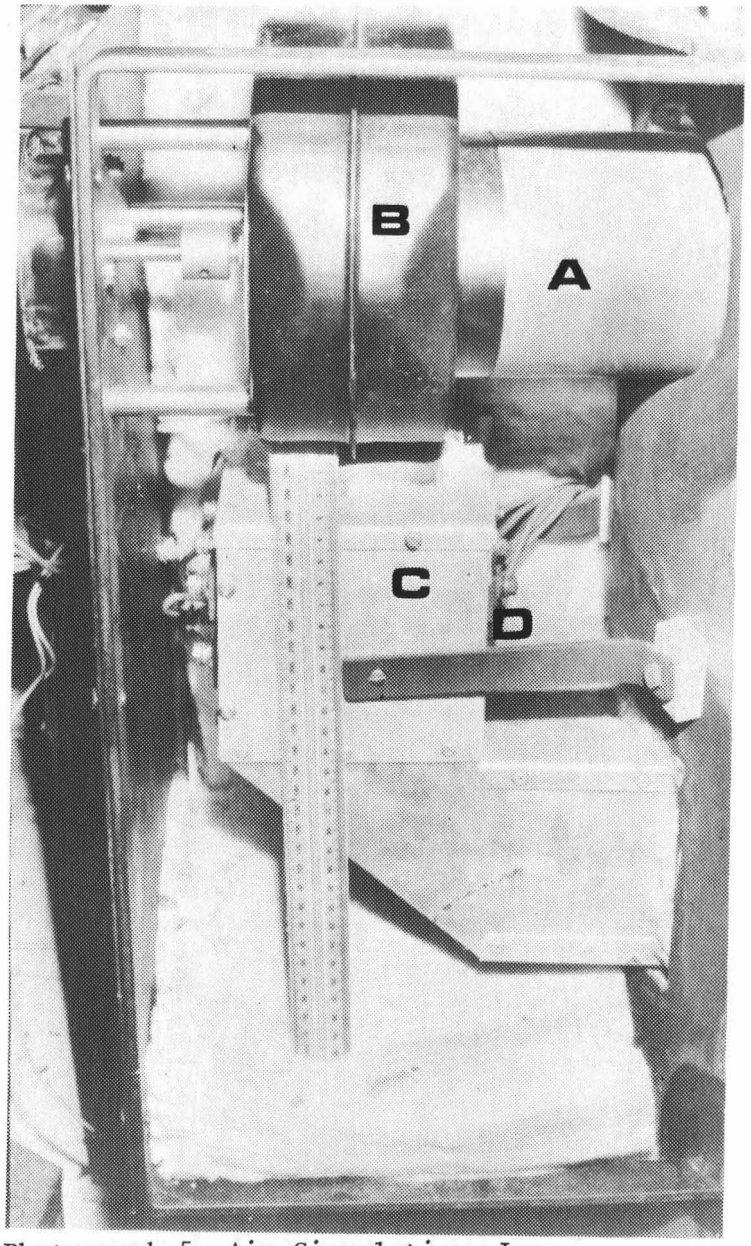

Photograph 5 Air Circulation Loop

A air inlet, B siflo fan, C heater box, D bakelite heater insulation and cartridge heater terminals.

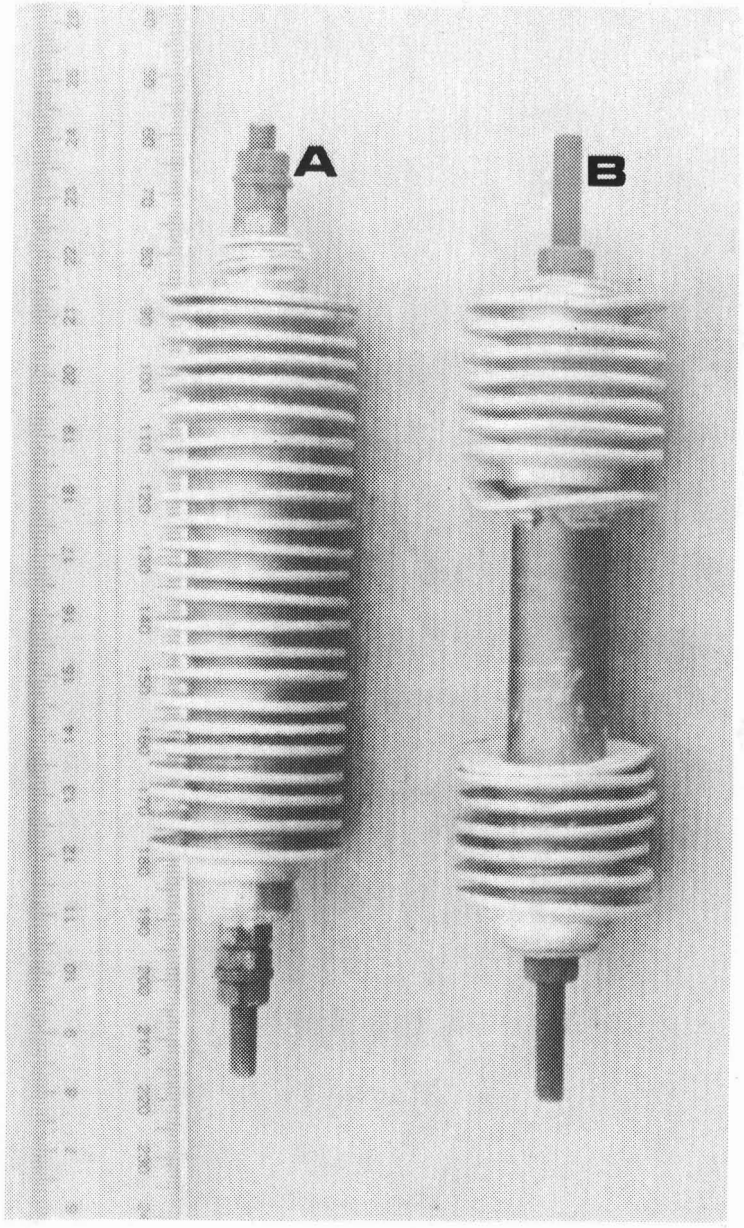

Photograph 6 Cartridge Heater

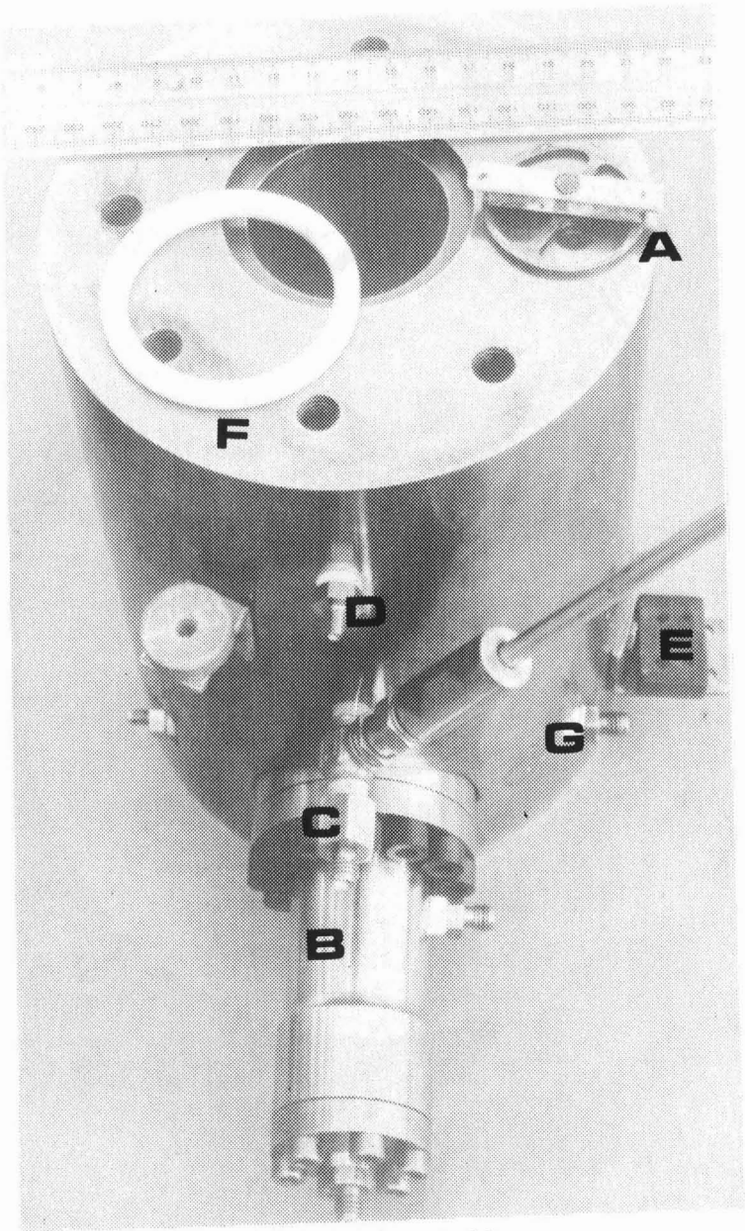

Photograph 7 Equilibrium Cell
A stirrer, B liquid sampling device, C cell outlet, D vapour sampling port, E bakelite, F teflon gasket, G jet mixer port.

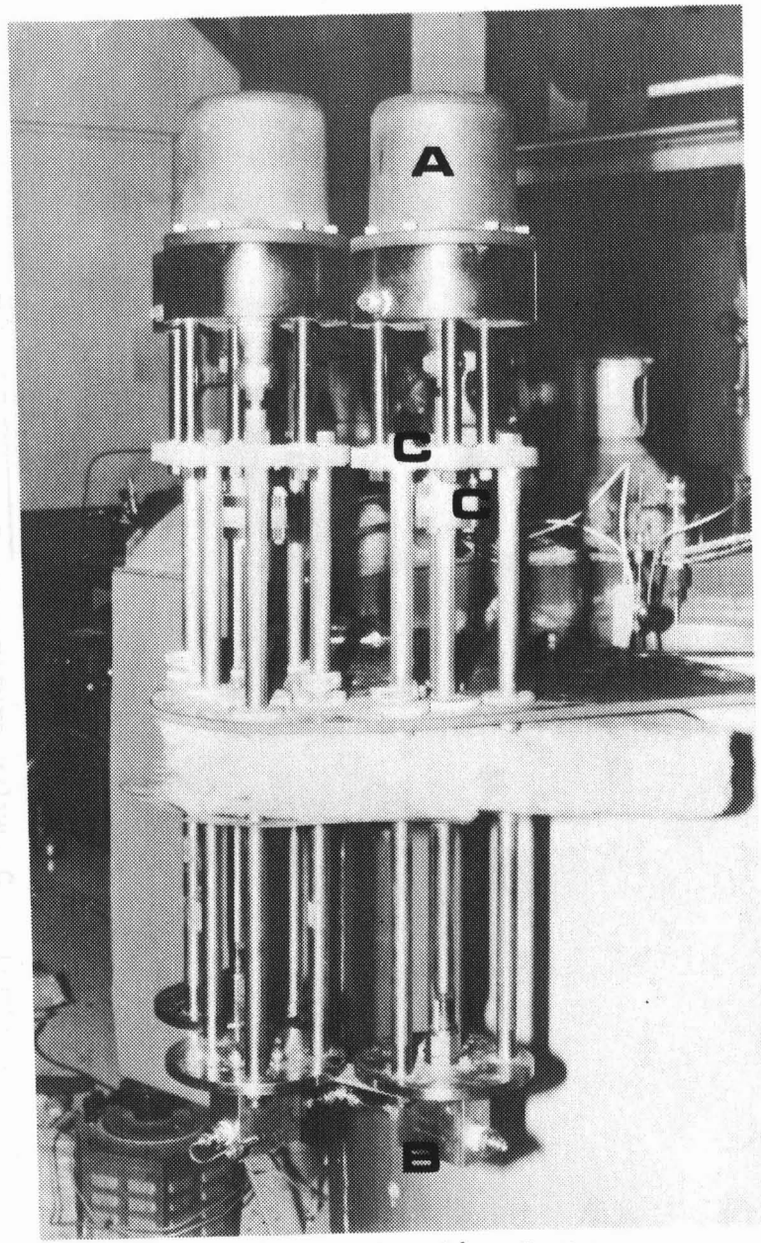

Photograph 8 Vapour Sampling System
A Air actuators, B Snotrick valves, C asbestos thermal breaks

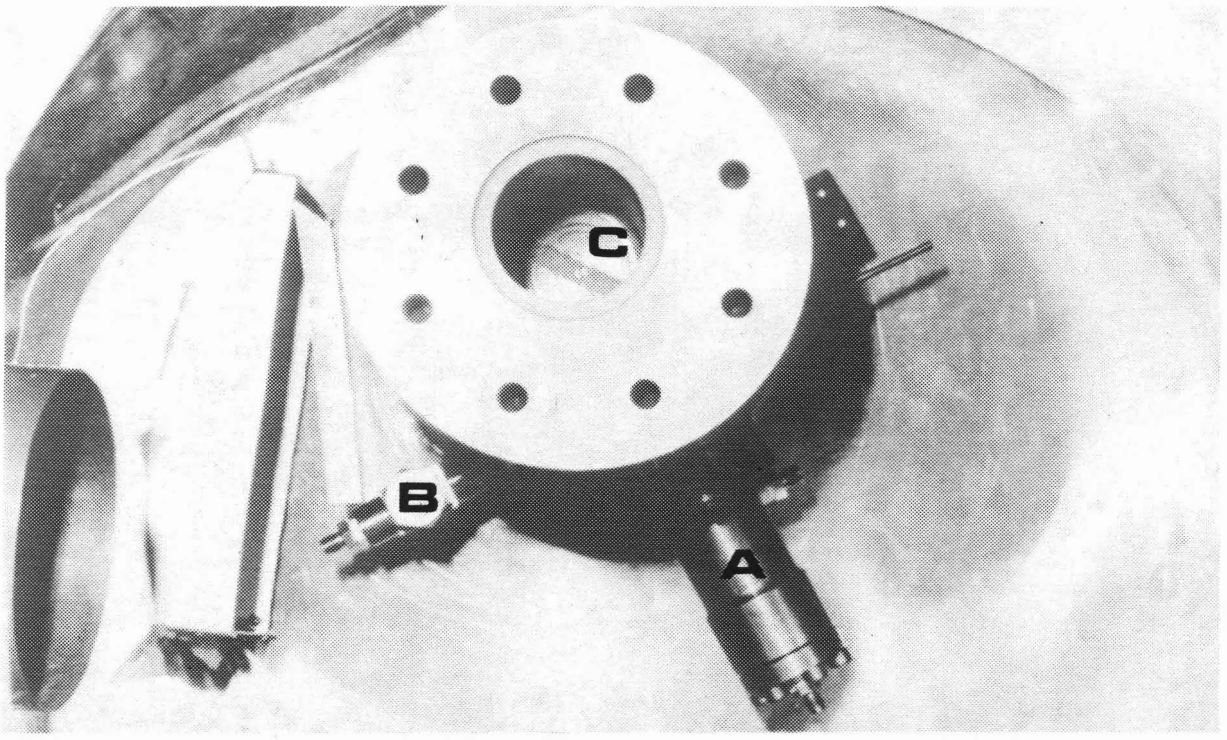

Photograph 9 Equilibrium Cell
A Liquid sampling device, B non-return valve, C internal magnetic stirrer.

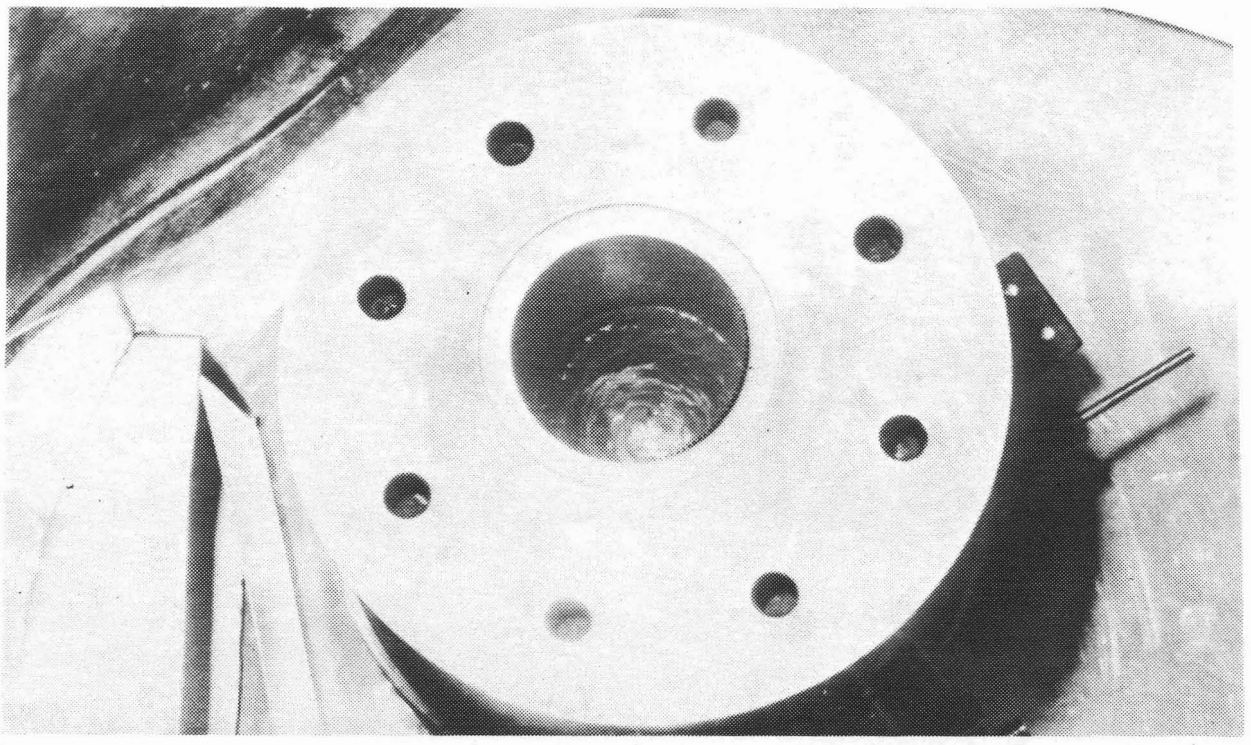

Photograph 10 Magnetic Stirrer Created Vortex

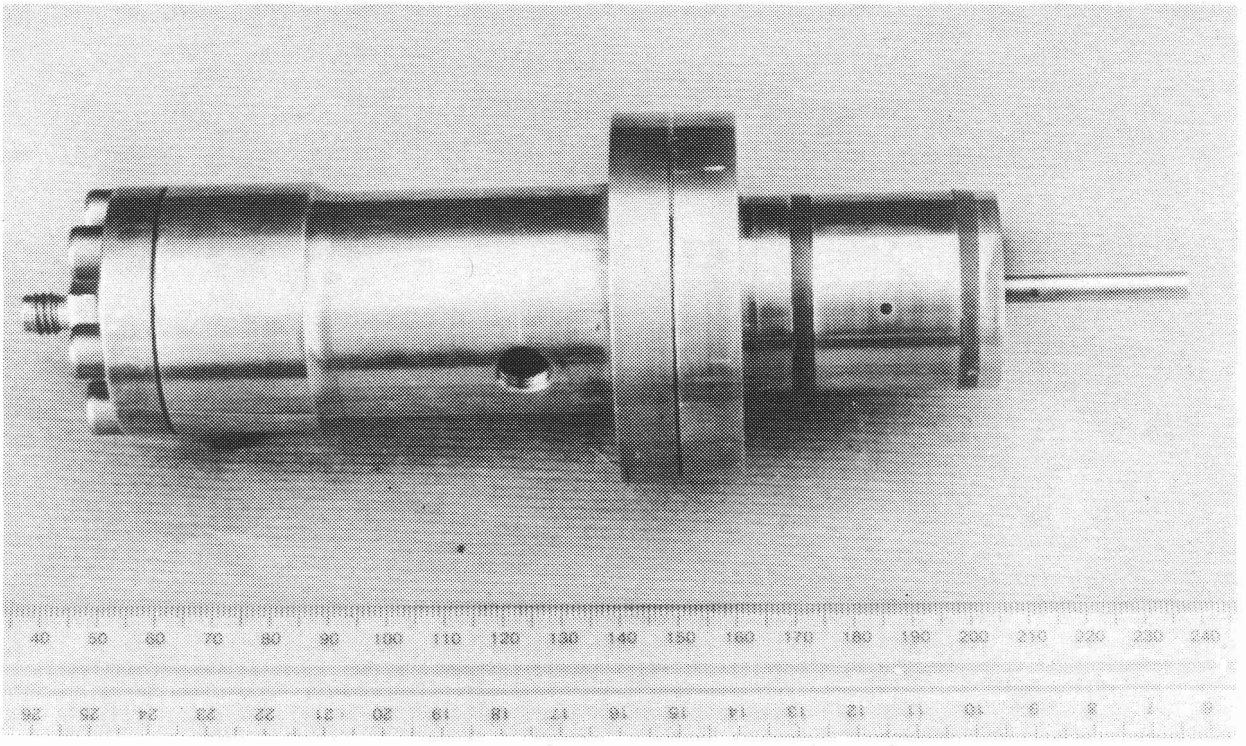

Photograph 13 Assembled Liquid Sampling Device

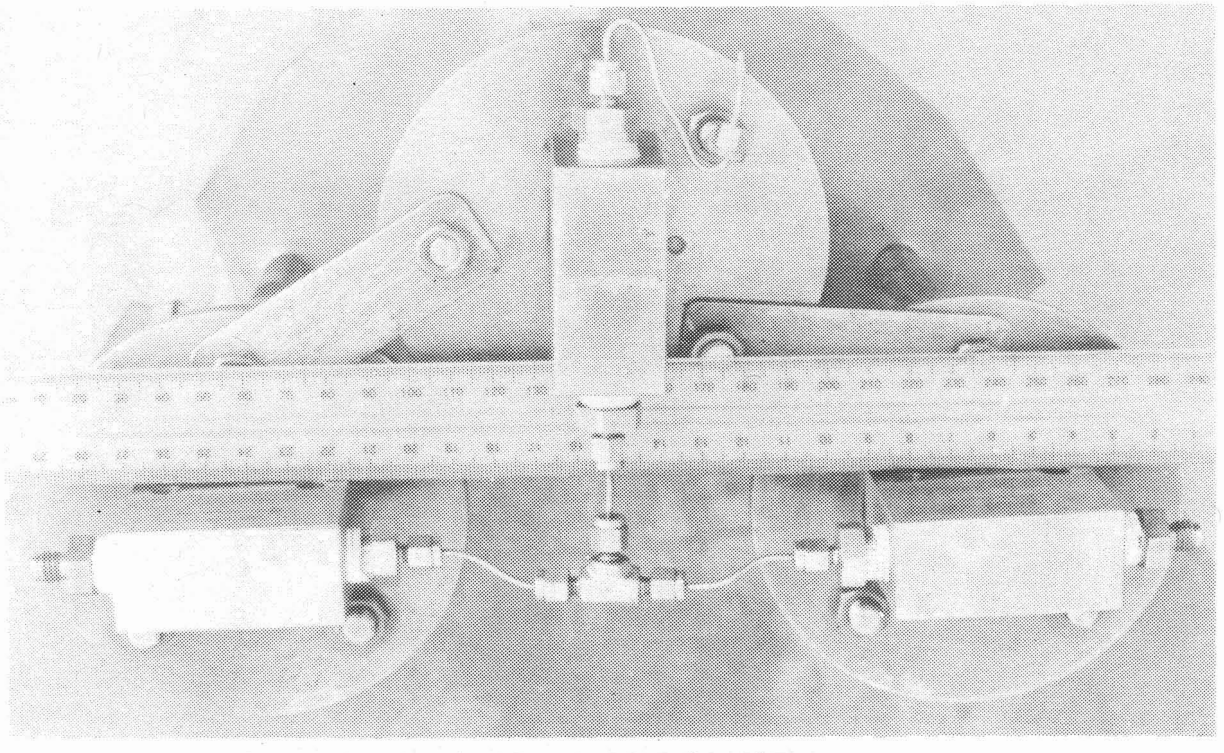

Photograph 14 Vapour Sampling System Manifold

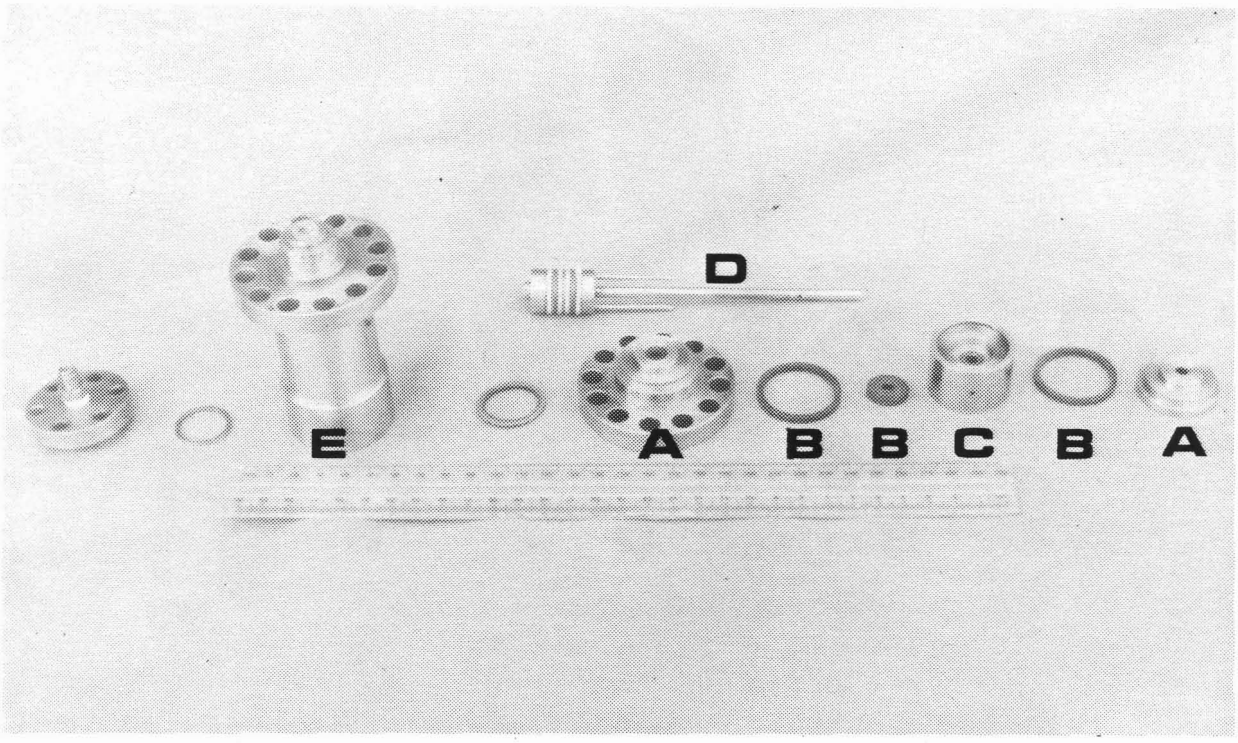

Photograph 11 Vital Parts of the Liquid Sampling Device
A male packing rings, B rulon packings, C female packing ring,
D sampling rod E piston assembly

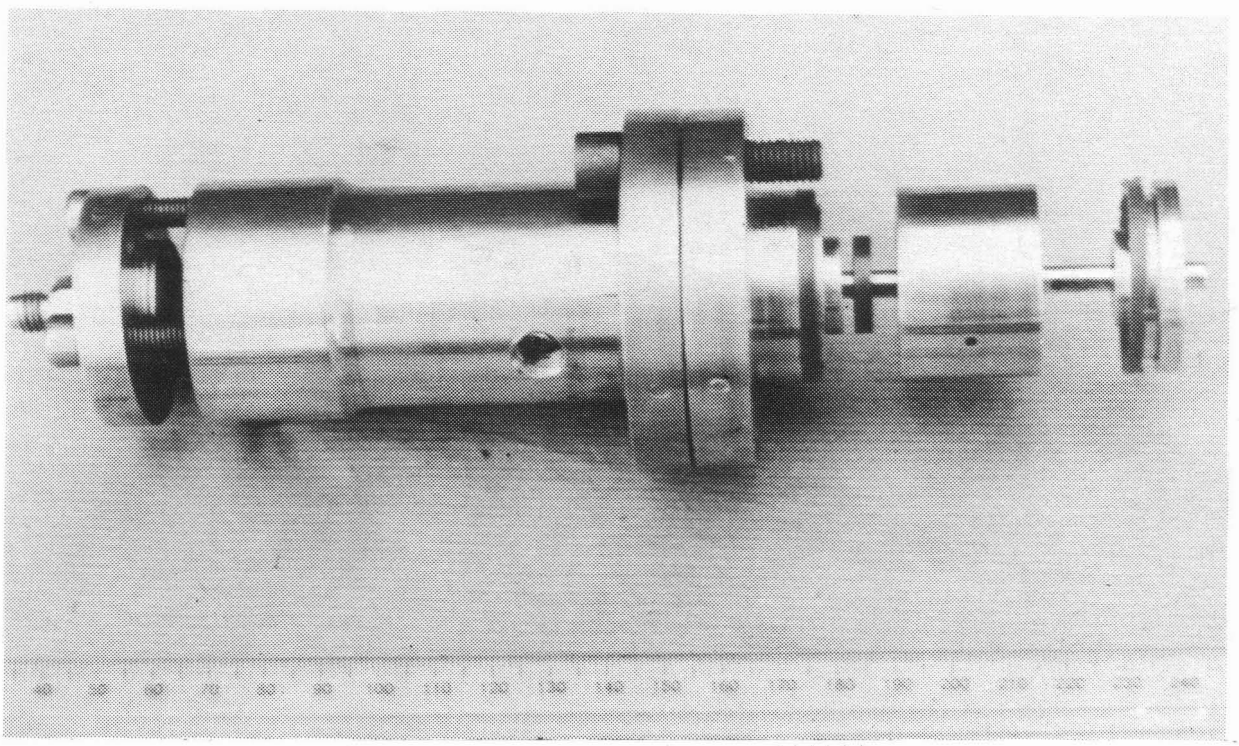

Photograph 12 Liquid Sampling Device being Assembled

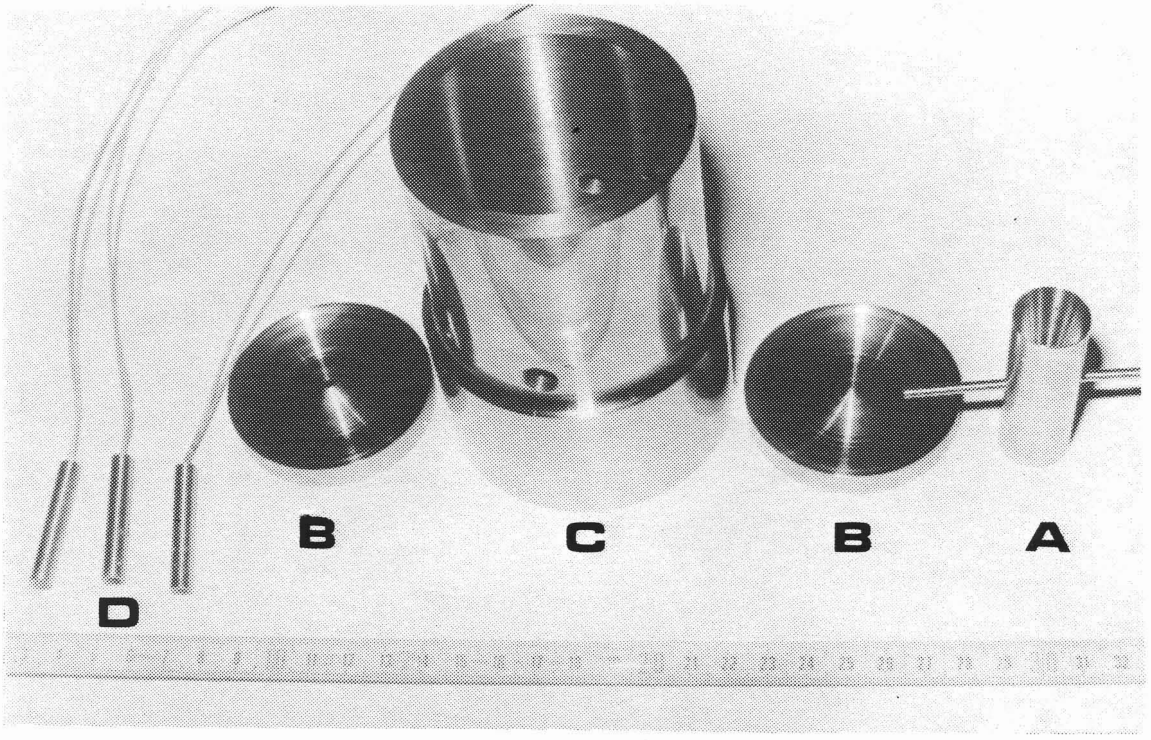

Photograph 15 Vital Parts of the Jet Mixer

A internal baffles, B jet mixer end pieces, C jet mixer body, D cartridge heating elements.

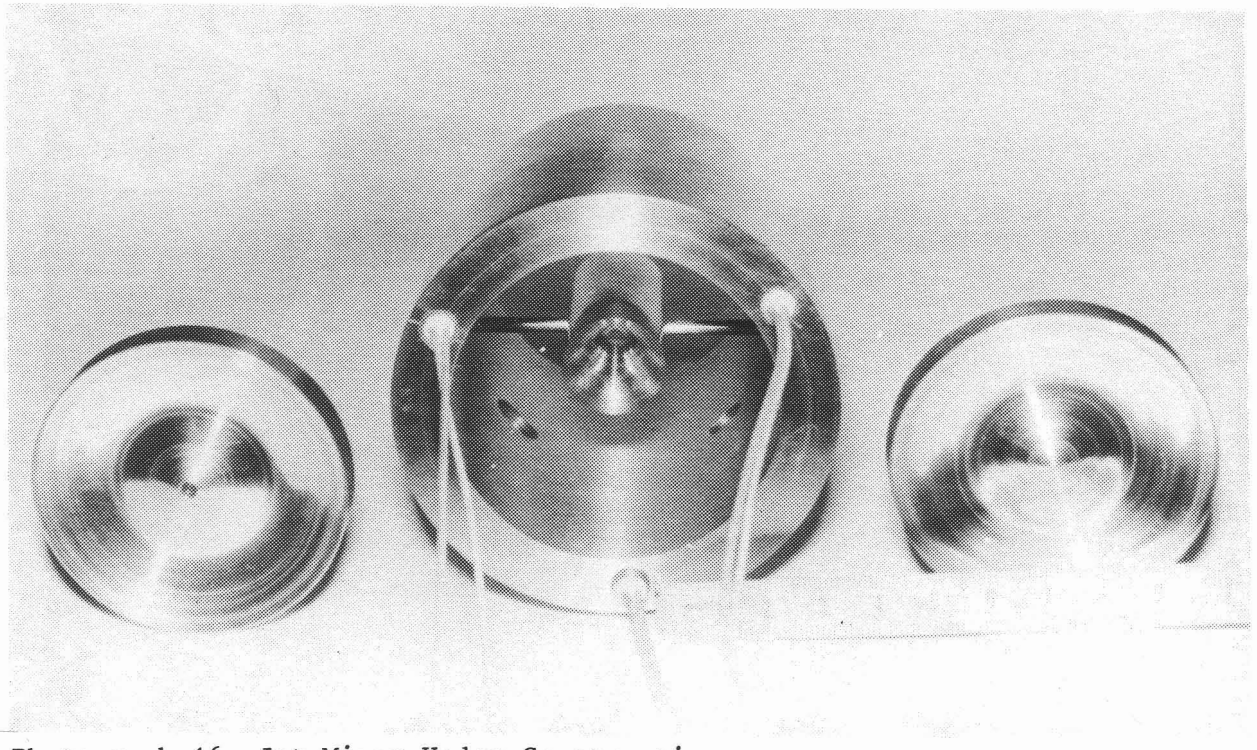

Photograph 16 Jet Mixer Under Construction

The pressure transducer and valve outlet ports are clearly visable.

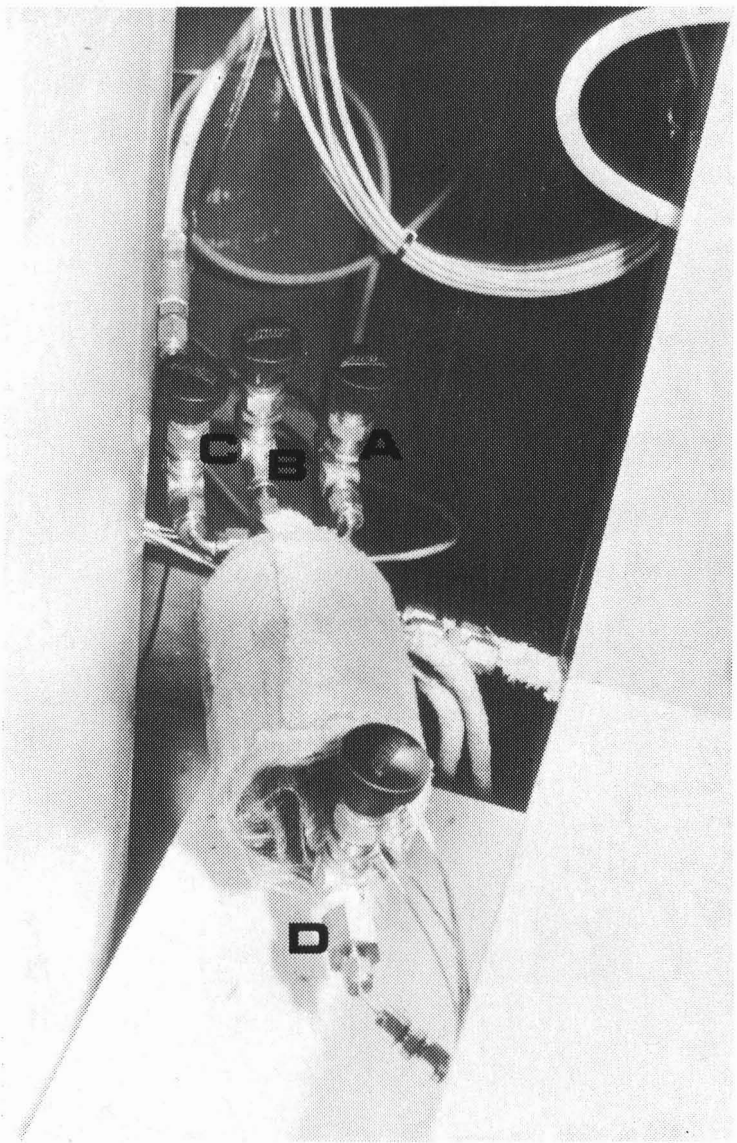

Photograph 17 Jet Mixer 2
A liquid sampling line, B vapour sampling line, C vacuum line, D jet mixer outlet.

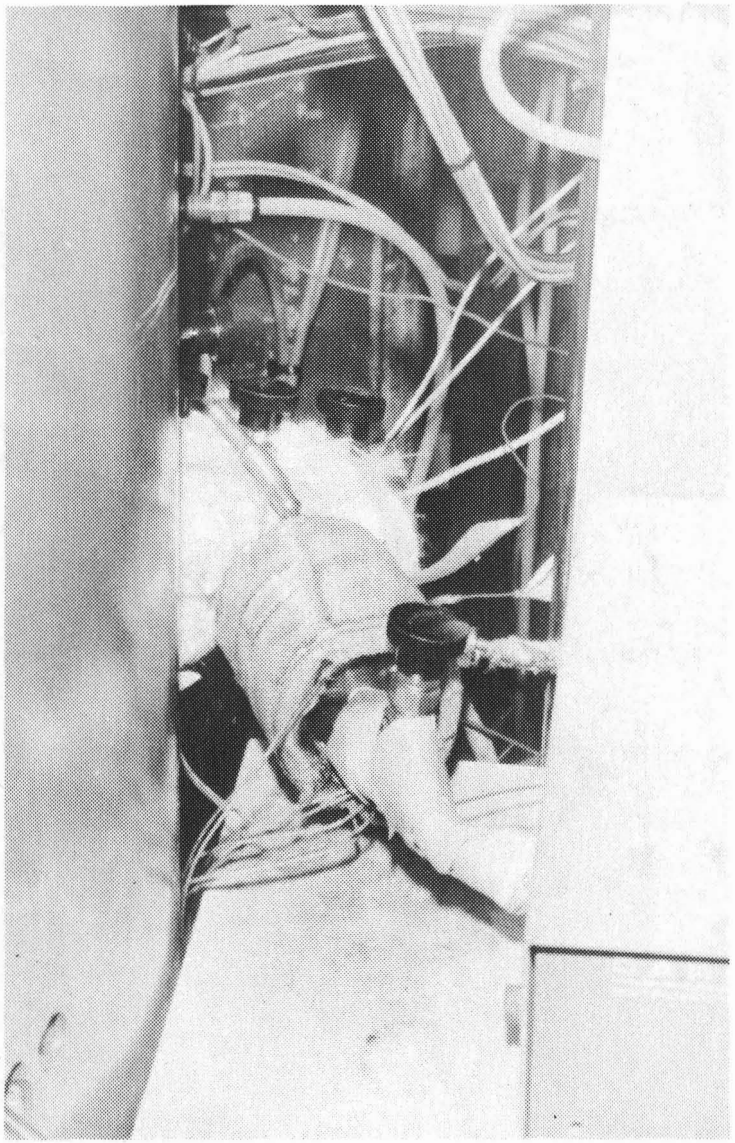

Photograph 18 Jet Mixer 2 suitably thermally insulated

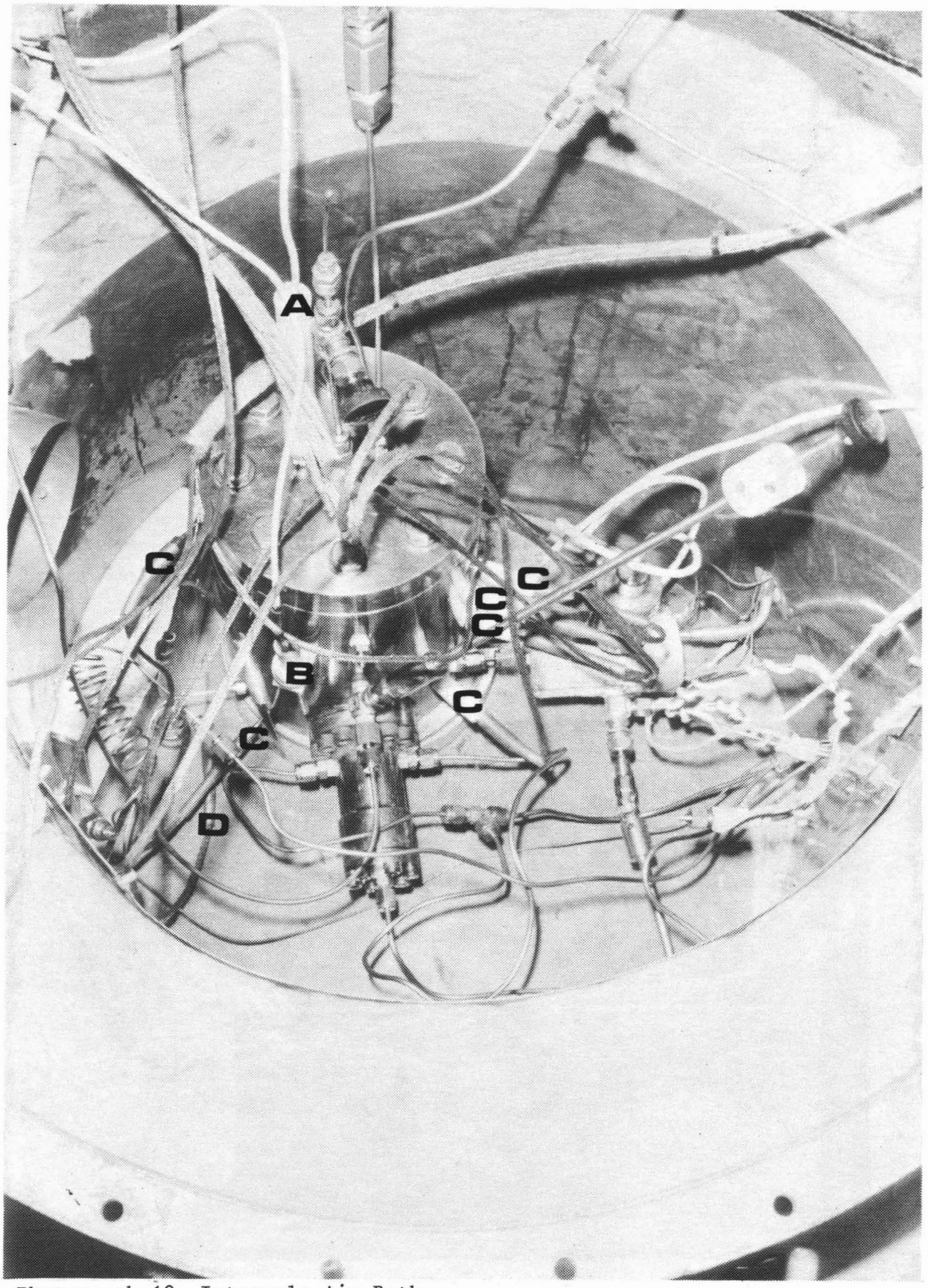

Photograph 19 Internals Air Bath

A platinum resistance thermometer for internal cell measurement,
B Eurotherm 818 controller platinum resistence thermometer
C cell profile measuring thermocouples, D bath profile measuring thermocouples

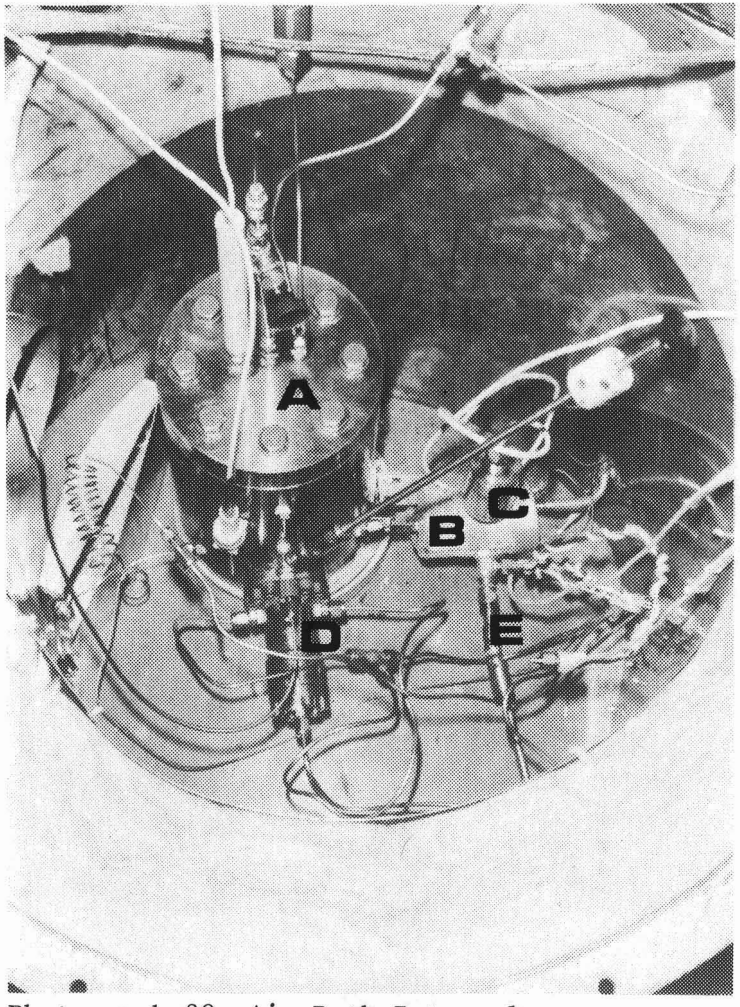

Photograph 20 Air Bath Internals
A equilibrium cell, B jet mixer, C pressure transducer, D liquid sampling device, E jet mixer outlet valve stem extension.

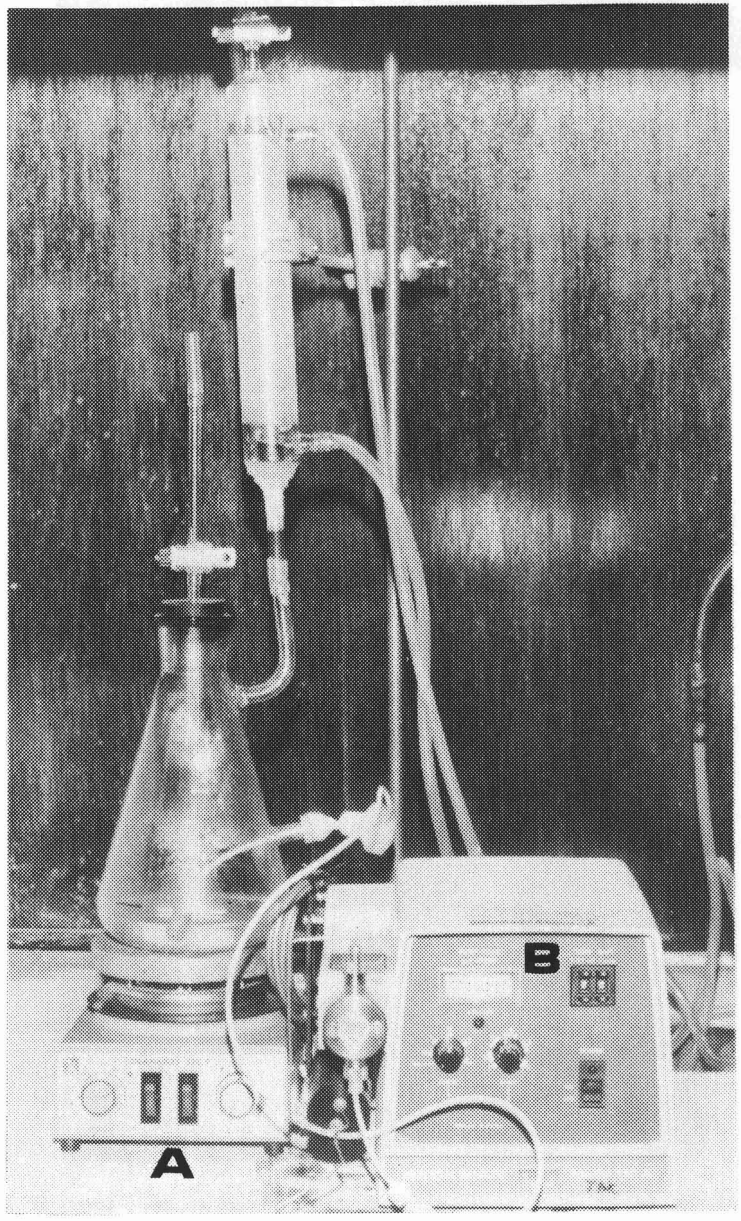

Photograph 21 Degassing Device
A magnetic stirrer/heater, B Beckman pump.

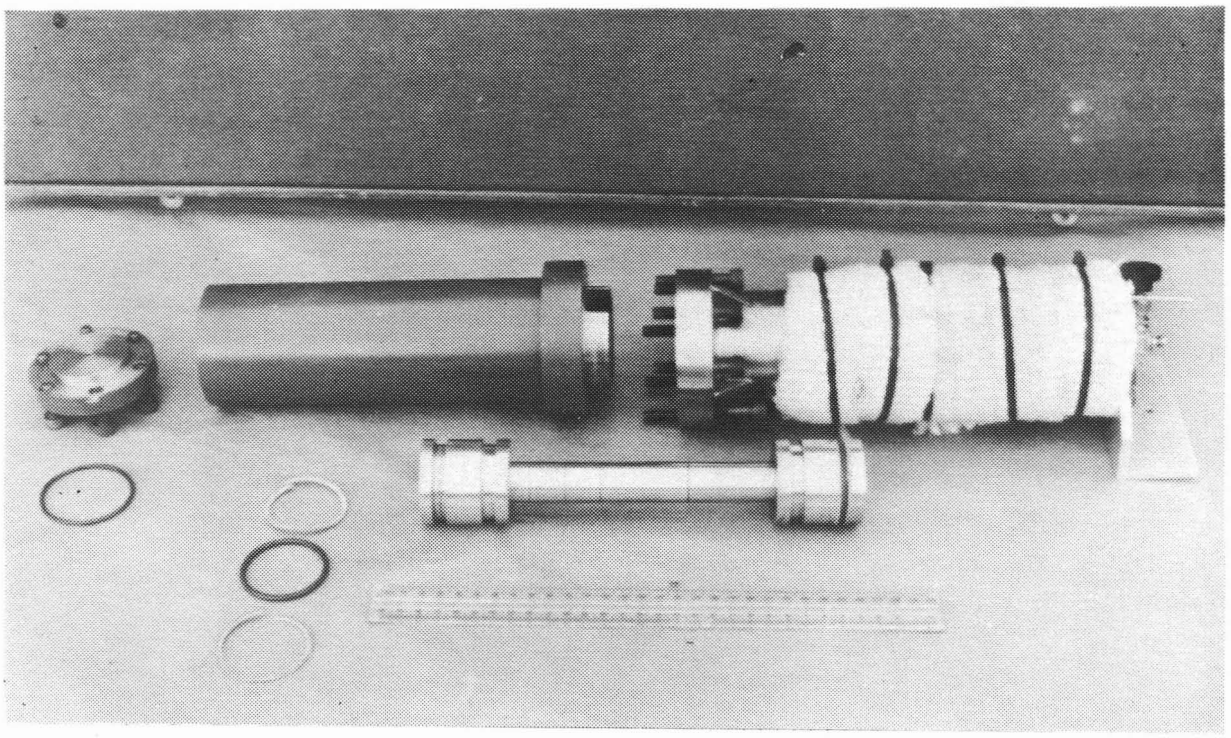

Photograph 22 Vital Parts of the Propane Compression Device

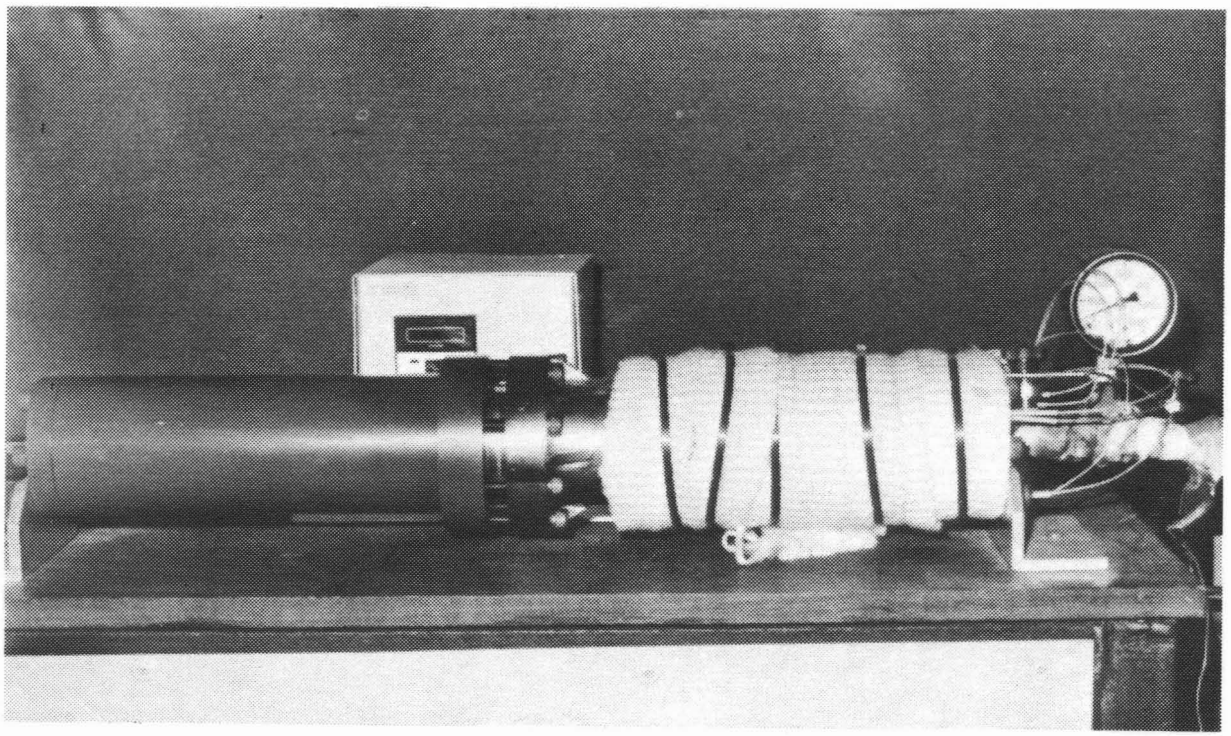

Photograph 23 Assembled Propane Compression Device

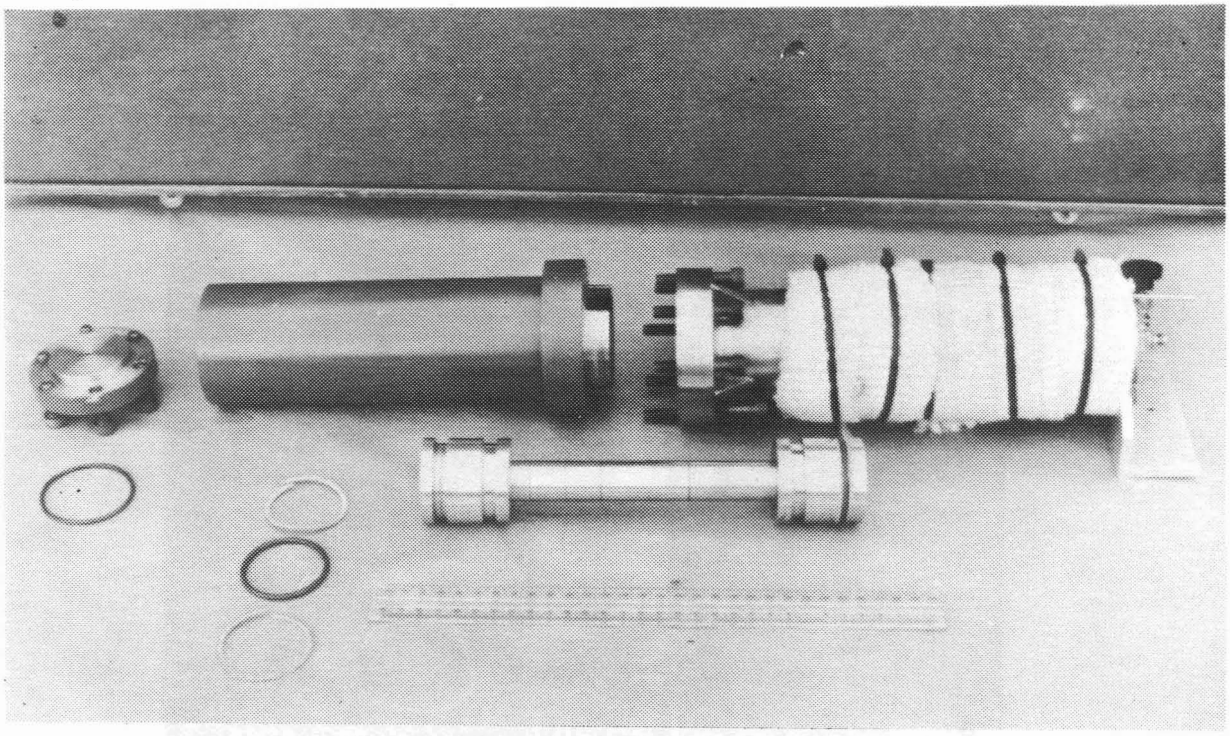

Photograph 22 Vital Parts of the Propane Compression Device

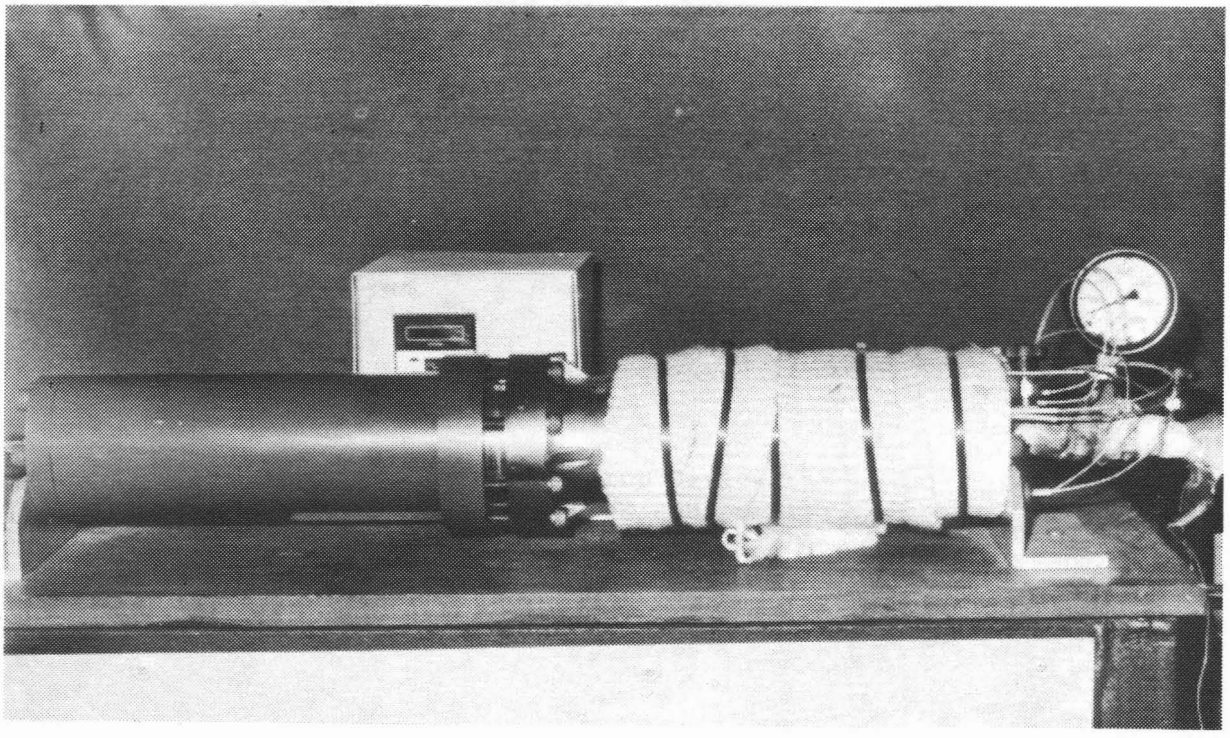

Photograph 23 Assembled Propane Compression Device

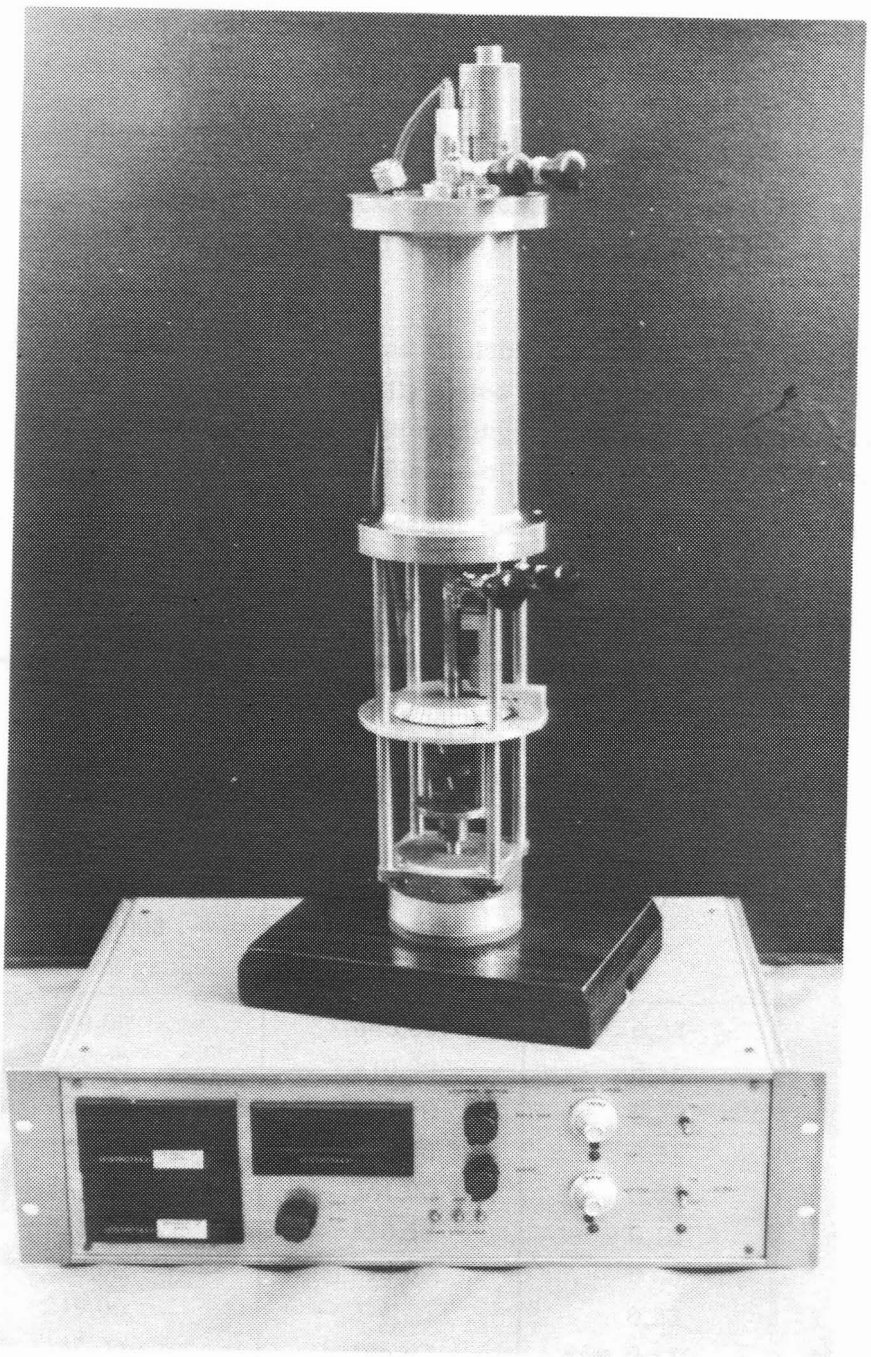

Photograph 24 Gas Calibration Device and associated equipment

4.3 PRESSURE COMPOSITION AND TEMPERATURE MEASUREMENT

Many excellent reviews appear in the literature, on temperature and pressure measurement (Benedict 1977, Nicholas and White 1982, Kennedy 1983, Kardos 1977).

4.3.1 Pressure Measurement

Two Heise bourdon tube type CC pressure gauges with measuring ranges of 0 to 500 psi (CC 8008) and 0 to 5 000 psi (CC 8009) were used.

Calibration

No dead-weight piston gauge was available on which to calibrate the two gauges. Each gauge was however critically tested by the manufacturer to conform to the accuracy of 0,1 % of the full scale reading as claimed. A certified copy of the test results traceable to the National Bureau of Standards was supplied with each gauge.

The two gauges were compared against each other. The results of this comparison are shown in Table 4.2.

TABLE 4.2
Comparison of the Two Heise Bourdon CC Pressure Gauges

Pressure (psi)		% Difference
0 - 500 psi CC 8008 Bourdon gauge	0 - 5 000 psi CC 8009 Bourdon gauge	(1)
439,00	440,05	-0,24
406,90	410,00	-0,76
405,90	408,00	-0,52
381,25	380,00	0,33
361,00	361,00	0,00
321,00	320,50	0,16
290,00	290,00	0,00
219,00	218,50	0,23
147,00	146,00	0,68
62,00	63,50	-2,41

(1) (CC 8008 - CC 8009)/CC 8008 x 100

4.3.2 Temperature Measurement

Accurate temperature measurement is desirable, although it is not one of the principal variables (P,x,y) in isothermal work .

The important temperature measurements were

1. the internal equilibrium cell temperature.
2. cell wall and air bath temperature profiles.

Temperature may be measured with thermocouples, platinum resistance thermometers or thermistors. Thermistors are the most sensitive and thermocouples the least if all the sensing units are of a high quality. The sensitivity of the thermistor is generally not needed for high pressure vapour-liquid equilibrium work, Tables 2.1 to 2.4 (Chapter 2). A good platinum resistance thermometer is of sufficient accuracy and was chosen for the primary cell temperature measurement in this project. Cell wall and air bath temperature profiles were measured using thermocouples. The specifications of the platinum resistance thermometers and thermocouples supplied are given in Appendix C.6.

Calibration of Pt 100 IEC 751 Temperature Senors

The equilibrium cell and Eurotherm 818 platinum resistance Pt 100 IEC 751 thermometers and their respective readouts, were checked against an extremely accurate Hewlett Packard 2801A (Sno 1003 A 00 298) Quartz Thermometer. The results are tabulated in Table 4.3

TABLE 4.3
Pt 100 IEC 751 versus Quartz Thermometer

Quartz Thermometer °C	Fluke equilibrium cell Pt-100 (1) °C	% Difference (2) °C	Eurotherm 818 Pt 100 °C	% Difference (2) °C
34,24	34,34	-0,55	34,50	-0,76
42,33	42,50	-0,40	42,70	-0,87
51,61	51,51	-0,78	52,15	-0,05
61,89	61,91	-0,03	62,40	-0,82
71,40	71,43	-0,04	71,80	-0,56
80,89	80,78	-0,14	81,15	-0,32

(1) Converted from resistance value by °C = (Resistance -100,37)/0,379
(2) % Difference = ((Quartz - Pt 100)/Quartz) x 100

Table 4.3 shows that the temperatures indicated by the two platinum resistance thermometers and their respective readouts were accurate to well within the IEC 751 : 1983 (DIN 43760 : 1980) specified tolerances.

4.3.3 Composition Measurement

The various methods that can be used for compositional analysis were briefly discussed in section Chapter 2. Gas chromatography was used in this project.

Two gas chromatographs were used. For the carbon dioxide/toluene system the composition analysis was performed using a simple Gow Mac Series 150 gas chromatograph equipped with a thermal conductivity detector. For the propane/water and propane/n-propanol binaries a Varian 3000 gas chromatograph equipped with thermal conductivity (TCD) and flame ionisation (FID) detectors connected in series was used. The output of the chromatograph detectors was analysed and converted into a peak area signal by Varian 4270 Integrators.

The Varian gas chromatograph which only became available in the latter part of the project was required for two reasons. In the propane/water binary the propane was only present in the liquid phase in very small quantities. With the liquid sample size and sampling procedures adopted it would not have been detected by the Gow Mac. In addition the Varian has a FID detector which is more sensitive to hydrocarbons than a TCD. For the propane/1-propanol binary a temperature program was needed to separate the two components, a feature not available on the Gow Mac.

The components must be well separated to allow for accurate detection. This separation depends on four factors : column packing type, column temperature, column carrier gas flow rate and component physical properties.

A 1,5 m long, 3,175 mm OD, 2.2 mm ID, stainless steel column packed with 100 to 120 mesh Poropak Q was used in the Gow Mac for the carbon dioxide/toluene binary.

A 2,5 mm long, 3,175 mm OD, 2,2 mm ID stainless steel column packed with 50 to 80 mesh Poropak Q was used in the Varian for the propane/water and propane/n-propanol system after initial trials with a 1,5 m, 3,175 mm OD, 2,2 mm ID, 80 to 100 mesh Poropak Q column.

The gas chromatograph operating conditions used are shown in Table 4.4.

TABLE 4.4
Gas Chromatograph Operation Conditions

Gas chromatograph condition		Gow Mac 150 (1)	Varian 3000 (2)	
		Binary system being separated		
		carbon dioxide /toluene	propane/water	propane/propanol
Column Temperature				
Initial temperature	(°C)	175	85	120
Hold time	(min)	Na	1NF	4
Final temperature	(°C)	Na	Na	170
Hold time	(min)	Na	Na	10
TCD Detector				
Current	(mA)	150	120	120
Attenuation		1	1	1
Range		1	0,5	0,5
FID Detector				
Attenuation		Na	4	8
Range		Na	10	10
Elution Time	(min)			
Carbon dioxide		0,14		
Propane			4,16	2,53
Water			2,19	
Propanol				8,71
Toluene		1,41		

(1) Helium carrier gas flow rate (30 mℓ/min).
(2) Helium carrier gas flow rate (30 mℓ/min).
FID hydrogen flow rate (30 mℓ/min).
FID air flow rate (300 mℓ/min).

4.4 AUXILIARY EQUIPMENT

The description and method of operation of the auxillary equipment used in this project are given in Appendices C.8, C.9, and C.10 for the gas chromatograph detector calibration device, degassing unit and propane compression device respectively

4.4.1 Gas Chromatograph Detector Calibration Device

The gas chromatograph detectors must be calibrated for the region of experimentally generated peak areas. For example Figure 4.13 shows the propane peak area regions for the liquid and vapour phase samples for the propane/water binary.

For the propane/water binary the amount of propane in the liquid phase is small, propane mole fractions are of the order of approximately 0,0001 to 0,0003. The peak areas generated by sampling were correspondingly small. They were too small for any syringe to duplicate by the direct injection calibration method using pure components.

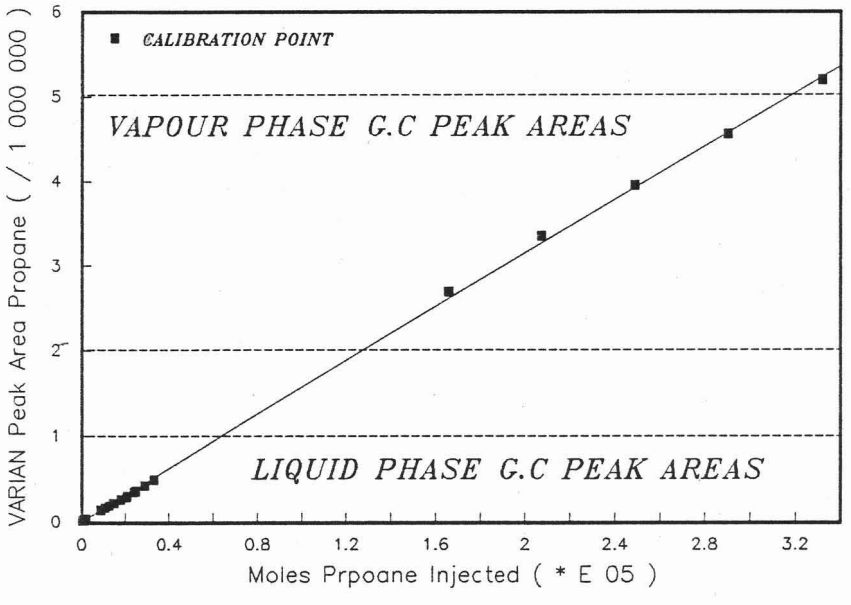

Figure 4.13 : Propane Peak Areas for Propane/Water Binary Liquid and Vapour Phases

A method therefore had to be found to calibrate the gas chromatograph sensors in the low peak area ranges. The only option available was to dilute the propane in another gas to reduce its concentration to the desired level before injection into the gas chromatograph. The British Standards Institution's method BSI 1983, for the preparation of calibration gas mixtures BS4559: Part 3 was not satisfactory for the small amounts of propane that would be required in the solvent gas .

Professor Raal studied this problem and designed, constructed and patented a simple yet highly accurate device in which two gases could be mixed to obtain a *homogeneous mixture* of *known composition* (Figure C.3 and Photograph 24). The propane could be diluted to very small accurately known concentrations in a suitable solvent (eg nitrogen). The gas chromatograph detectors could consequently be accurately calibrated to allow for analysis of propane concentrations in the liquid phase for the propane/water binary.

4.4.2 Degassing Method

The equilibrium cell filling procedures for the carbon-dioxide and propane binaries differed as fully discussed in Chapter 5. The equilibrium cell filling procedure for the propane binaries necessitated that non-volatile component degassing had to take place outside the cell. For the propane/water binary, the propane is only slightly soluble in the liquid phase and conversely water is only slightly soluble in the vapour phase. Any gaseous impurities introduced with water may therefore compete with propane for solubility in the liquid water phase. Extra precautions therefore had to be taken to ensure that all traces of dissolved gases in the water were removed.

A degassing method similar to that by Battino (1971) was adopted and is shown schematically in Figure C.4 and Photograph 21. The liquid was degassed under vacuum and vigorous stirring conditions in a heavy duty vacuum flask. The degassed liquid could be removed directly from the flask and pumped directly into the equilibrium cell with a Beckman HPLC pump.

The toluene was degassed *in situ* in the equilibrium cell under vacuum and vigorous stirring conditions.

4.4.3 Propane Compression Device

A device or method was needed to pressurize the propane/non-volatile binary in the equilibrium cell. A simple device was designed, Figure C.5 and Photographs 22 and 23, to heat and compress propane, supplied from a gas cylinder, to pressures above it's bottle pressure. The heated and compressed propane was then forced into the equilibrium cell thereby pressurizing the cell contents.

4.5 SAFETY FEATURES

Temperature run-away of the air bath due to controller failure was prevented by a RKC controller, shown in Figure 4.10, which acted as an upper temperature switch. The temperature of the RKC controller was set at 10 °C above the air bath temperature setpoint. If the air bath temperature exceeded the RKC set point the relay shut down the electric circuit with the exception of the circulation fan.

If the input from the Pt 100 to the Eurotherm 818 controller failed the controller signal to the thyristor was automatically set to zero. This feature ensured that the controller did not continue to heat the bath on receiving an artificially low (zero) input due to sensor failure.

The cell pressure was limited to pressures below 4750 psig by a pressure relief valve. This protected the 0 to 5 000 psi Heise pressure gauge and prevented cell overpressurisation. The 0 to 500 psi Heise pressure gauge was protected by a pressure relief valve, set to 485 psig, upstream of valve V1 as shown in Figure 4.12.

The jet mixer pressure transducer was protected by a pressure relief valve, set to 2,5 bar (g), in the liquid sampling line as shown in Figure 5.3

CHAPTER 5

EXPERIMENTAL PROCEDURE

Topics covered in this chapter include :

The procedure followed in preparing the equilibrium cell and associated equipment for experimentation. The procedure described was carefully followed to ensure that the equipment was in perfect working order at the beginning of an isothermal run.

The described operational procedures for the sampling of the liquid and vapour phases were the result of constant experimentation and innovation to simplify the sampling procedure and increase the accuracy of the results obtained.

The method of detector calibration as well as the aspects that require particular attention in gas chromatographic work are briefly discussed.

Finally improvements are suggested for any future development of the equipment.

The operating procedures for the auxilary equipment are described in Appendices C.8 to C.10.

5.1 PREPARATION OF EQUILIBRIUM CELL AND ASSOCIATED EQUIPMENT FOR EXPERIMENTATION

5.1.1 Preparation of the Equilibrium Cell and Liquid Sampling Device

Preparation of the equilibrium cell and sampling equipment for an experimental run generally took two days and consisted of the following :

1. Ensuring the correct operation of the liquid sampling rod.

   The liquid sample rod was inserted and withdrawn a few times to check if the sample hole was in correct alignment with the carrier gas channels. This also gave an indication as to whether the unsupported area seal packings were compressed correctly. If the packings were too compressed, they would immediately have been chafed with consequent sample hole blockage.

2. Detection of leaks in the equilibrium cell and liquid sampling device.

   The cell was pressurized to approximately one and a half times the expected maximum operating pressure, and placed in a water bath. A thorough inspection was made around the cell and liquid sampling device to detect the slightest trace of bubbles. Snoop leak detector used on all the Swagelok fittings was found unsatisfactory for the purpose of leak detection around the liquid sampling device. If no leaks were detected the equilibrium cell carrier gas channel was pressurized to one and a half times the carrier gas pressure of 1,25 bar. If no leaks were detected the withdrawal ports of the liquid sampling piston assembly

were pressurized to detect, or test for any leaks from the piston assembly into the carrier gas sampling channel. If no leaks were detected the equilibrium cell and liquid sampling device were ready to be connected to the auxiliary equipment.

It was expedient to discover leaks before connection of the equilibrium cell and liquid sampling device to the sampling equipment took place, as their consequent removal due to a minor leak would be both time consuming and, more importantly, increase wear and tear on the Swagelok fittings. Pipe ferrules had to be replaced after the third or fourth reconnection to ensure 100 % seals. The fittings were damaged if nuts were overtightened to ensure a seal.

5.1.2 Attachment Of Sampling Equipment

The jet mixer was connected to the equilibrium cell carrier-gas port. The liquid sampling line was pressurized to one and a half times the maximum carrier gas pressure. Any leaks in the liquid sampling line would be detected by a decrease in the jet mixer's pressure transducer reading. If after two hours no reduction in pressure was detected the liquid sampling device's piston assembly was connected to its auxiliary equipment. The system (Figure 4.6) was pressurised to 80 bar. If the assembly was leak free the equilibrium cell inlet valve was connected. The vapour sampling valves were connected to the equilibrium cell and their carrier gas lines. The Pt 100 temperature probe and pressure lines were connected to the cell. Snoop leak detector, capable of minute leak detection, was used throughout to check for the sealing integrity of all the fitting connections. The cell was pressurized to one and a half times its maximum anticipated operating pressure and left overnight. The following morning the pressure drop was noted. If the pressure change was within allowable limits, (corrections were allowed for temperature changes), the cell was ready for an experimental isothermal run.

Depending on which system was being measured the start-up procedure varied slightly. Schematic diagrams showing the equipment arrangements used to measure the carbon dioxide/toluene binary and propane/water or propane/1-propanol binaries are shown in Figures 5.1 and 5.2 respectively.

The essential differences between the two arrangements were the degassing and liquid and gas feed systems.

5.2 START-UP PROCEDURE

5.2.1 Carbon Dioxide/Toluene System

The toluene, in a roughly graduated feed container, was held under vacuum for approximately 2 hours and the rate of disappearance measured. Carbon dioxide was bubbled through the toluene to saturate it and remove any traces of residual dissolved gases. The equilibrium cell, at room temperature, was evacuated and filled with carbon dioxide to about 50 bar and subsequently vented to atmosphere after 5 minutes vigorous stirring. This filling and venting procedure was repeated on average seven times. This ensured that only traces of residual air were present in the equilibrium cell. The toluene was then flushed into the vented cell with carbon dioxide at about 2 bar. The toluene was degassed again *in situ* under vigorous stirring and vacuum. This was continued for at least 15 minutes. From the previously measured rate of disappearance the toluene liquid level in the equilibrium cell was brought to between 75 and 100 m*l*.

Carbon dioxide was then added, raising the cell pressure to that of the feed bottle (approx. 80 bar). The controller was set to the desired isothermal temperature and the cell was allowed to heat up slowly (8 hours) to the set point. Venting of the cell proved necessary during this initial heat up period. The cell was left overnight to completely reach thermal equilibrium.

5.2.2 Propane/Water and Propane/1-Propanol Systems

Requirements for a propane compression device

Since propane is subcritical at room temperature the *quantity* of gas that can be added to the equilibrium cell is limited. A rough estimate of the amount could be obtained from the ideal gas law using the vapour pressure of propane at room temperature. Since the vapour pressure of propane at room temperature is 8 bar the final pressure in the equilibrium cell that may be achieved by simple heating, as in the case of carbon dioxide, is limited.

Using the ideal gas law for rough calculational purposes; for a 100 °C rise in the equilibrium cell temperature the cell pressure would rise approximately 2,5 bar if the volume occupied by the vapour phase was assumed constant. As the volatile component is absorbed however, the system total pressure decreases. A small quantity of non-volatile component evaporates to the vapour phase but this quantity is small. Therefore some means of pressurizing the propane and delivering it to the cell had to be found.

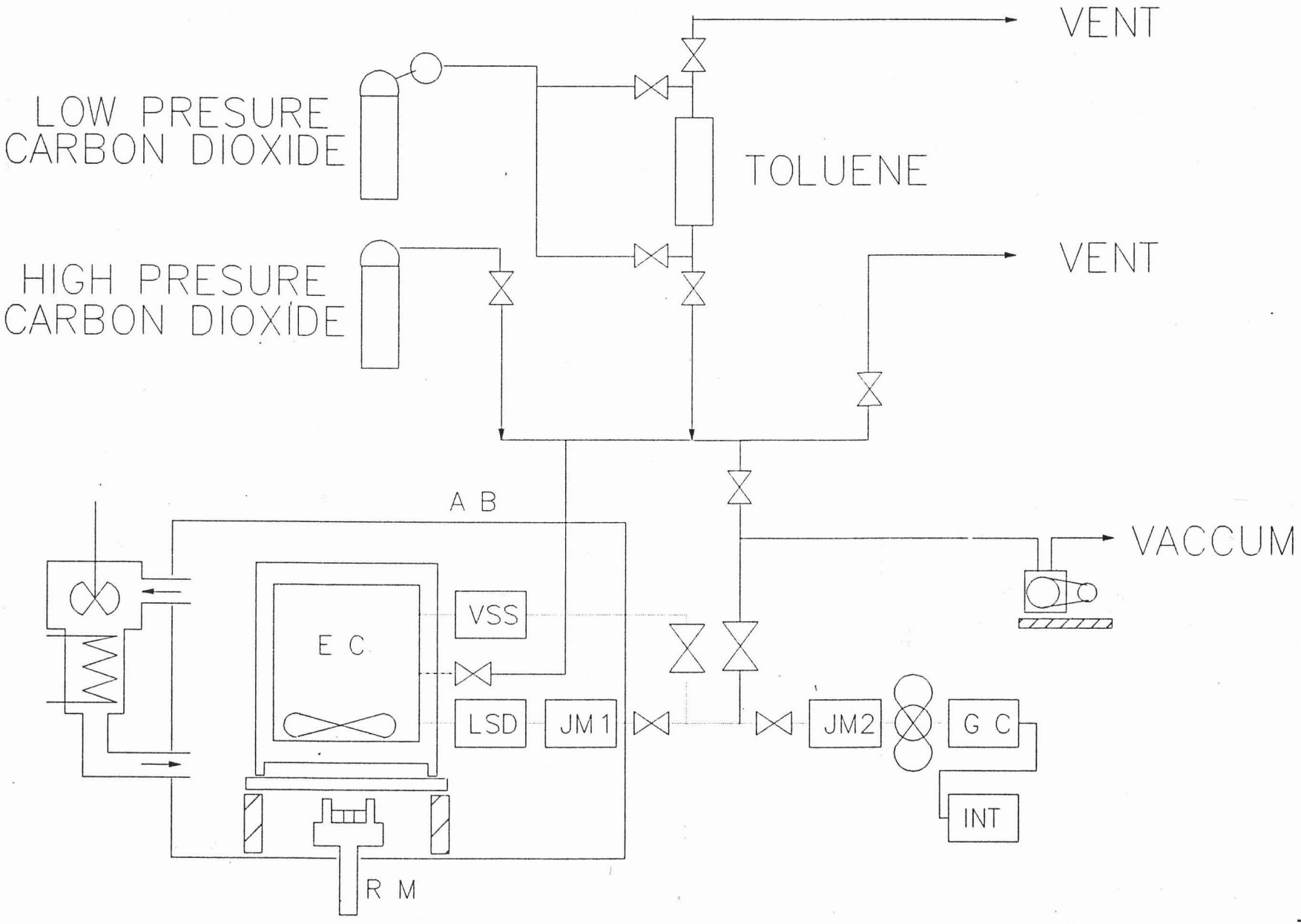

Figure 5.1 : Schematic of Static Equilibrium Cell Equipment : Carbon Dioxide / Toluene Binary AB - Air Bath, EC - Equilibrium Cell, JM - Jet Mixer, FC - Feed Container, GC - Gas Chromatorgraph, INT - Integrator, LSD - Liquid Sampling Device, VSS Vapour Sampling System, RM - Rotating Magnet.

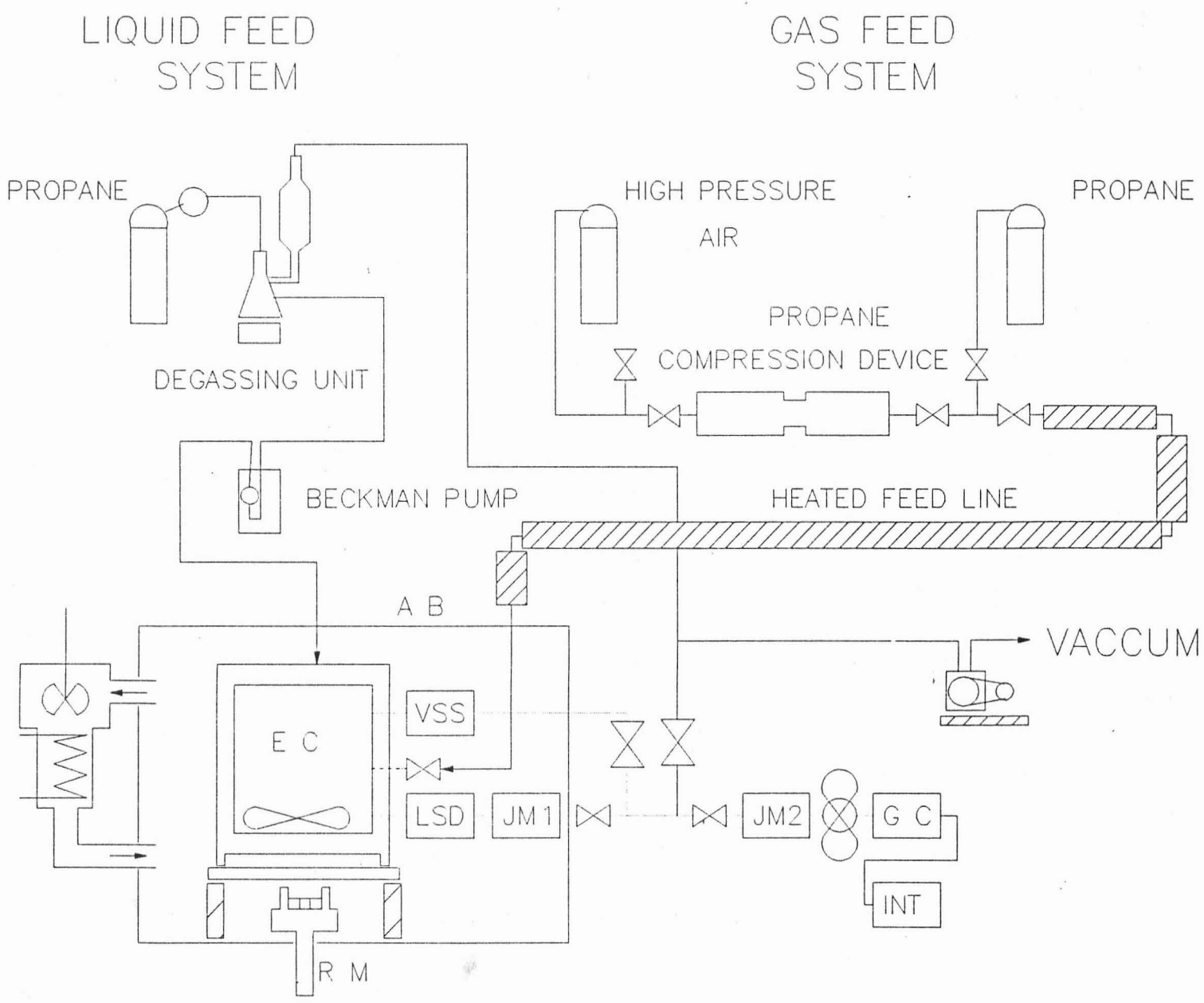

Figure 5.2 : Schematic Static Equilibrium Cell Equipment Setup : Propane Binaries. AB - Air Bath, EC - Equilibrium Cell, JM - Jet Mixer, FC - Feed Container, GC - Gas Chromatorgraph, INT - Integrator, LSD - Liquid Sampling Device, VSS - Vapour Sampling System, RM - Rotating Magnet.

The simplest method would have been to decant the subcritical propane as a liquid into the equilibrium cell. This would have increase the *quantity* of volatile component tremendously. The avaliable propane cylinders, containing propane of the desired purity did not however have a port for liquid withdrawal. The special cylinders would have had to be imported by sea, not a viable option. The simple propane compression device and its operation , described in Appendix C.8, was used to force propane into the cell until the desired cell pressure was obtained.

Liquifying the propane gas was considered but the equipment required for the process was more complex and expensive than the simple propane compression device described.

Equilibrium cell filling procedure

The equilibrium cell, at room temperature, was initially evacuated and flushed out with propane at 8 bar in a procedure similar to that described for the carbon dioxide/toluene system. This equilibrium cell filling and venting ensured that only residual traces of air were present. This was confirmed by gas chromatography analysis. The cell was heated to the desired isothermal equilibrium temperature, after which the propane was compressed into the cell by the compression device. The degassed non-volatile component, obtained from the unit described in Appendix C.9, was then added using a Beckman HPLC pump.

When water was added a marked increase in pressure was observed as very little propane was dissolved in the liquid phase. When 1-propanol was added to the propane a marked decrease in pressure was observed as propane readily dissolved into the liquid phase. The addition of propane was therefore necessary in the case of the propane/1-propanol binaries to increase equilibrium cell pressure. A maximum pressure was obtained after which the increase on each insertion of propane from the compression device created only a slight increase in pressure. Pumping was stopped at this point.

5.2.3 Importance of Initial Liquid Level

The volatile component liquid phase mole fraction rises with an increase in pressure sometimes up to 0,7 near the critical point. The non-volatile component vapour phase mole fraction does not change markedly in the high pressure regions. The non-volitile vapour phase mole fractions rarely rise above 0,3 mole fraction.

As a result the liquid phase level can increase approximately three fold as the volatile component is absorbed into the liquid phase at high pressures. This can lead to vapour phase sampling problems due to too high an equilibrium cell liquid level. Conversely liquid phase is lost during the venting process, (used to achieve a new lower equilibrium cell pressure), if the liquid level is above the equilibrium cell inlet/outlet port. If the initial liquid level is too low the venting process can lead to too low a liquid level at the lower pressures.

The ideal quantity of liquid to add initially to the equilibrium cell was found to be 75 to 100 m*l* . This starting volume was small enough not to interfere with vapour sampling at high pressure but large enough to ensure an adequate liquid level for low pressure measurements.

5.3 LIQUID AND VAPOUR SAMPLING PROCEDURE

Experiments on the carbon dioxide/toluene system were used to determine the optimum operational procedure for obtaining reproducible results for the liquid and vapour phases. The procedure was used essentially unaltered for the propane/water and propane/propanol binary systems.

A schematic diagram of the vapour and liquid sampling lines is shown in Figure 5.3

5.3.1 Liquid Sampling Procedure (Figure 5.3)

Withdrawal of liquid sample

If a liquid sample was desired the line between V1 and the vacuum pump was evacuated to about 3 torr. After the desired evacuation was achieved V3 was closed. After the stirrer had been set to approximately 20 rpm for one minute, to allow for disengagement between the phases, the sample rod was inserted into the equilibrium cell. The sample rod was left in the cell for 10 minutes to ensure a representative liquid sample would be withdrawn. Any bubble formation in the sampling hole due to preferential flashing, on insertion of the sample rod, was dislodged by the gentle stirring motion. Approximately 10 minutes was required to ensure the sample hole was completely filled with liquid. The sample rod was withdrawn quickly (2 to 3 seconds) and the increase in pressure in the jet mixer noted. This immediately gave an indication if a pure liquid or a liquid/vapour sample had been withdrawn. If adequate care was taken to follow the above procedure a liquid sample was always withdrawn.

Flushing of liquid sample to jet mixer

Helium carrier gas delivered through a fine metering valve V2 (Figure 5.3) was immediately allowed to flush the sample into the jet mixer. A fine metering valve was used to produce the setting of a very slow helium flowrate. Depending on the binary system being measured, the helium flowrate was adjusted such that the combined pressure of the liquid sample and helium carrier gas increased by 20 kPa over 3 minutes to a jet mixer pressure of 20 kPa (a). The jet mixer contents were allowed to equilibrate for a further 2 minutes. This procedure (insertion of sampling rod and helium flushing), was repeated a further two times. After each withdrawal the jet mixer pressure increased by 20 kPa. On the final withdrawal a helium carrier gas flowrate was set such that the the final jet mixer pressure had increased to 200 kPa (a) after 15 minutes.

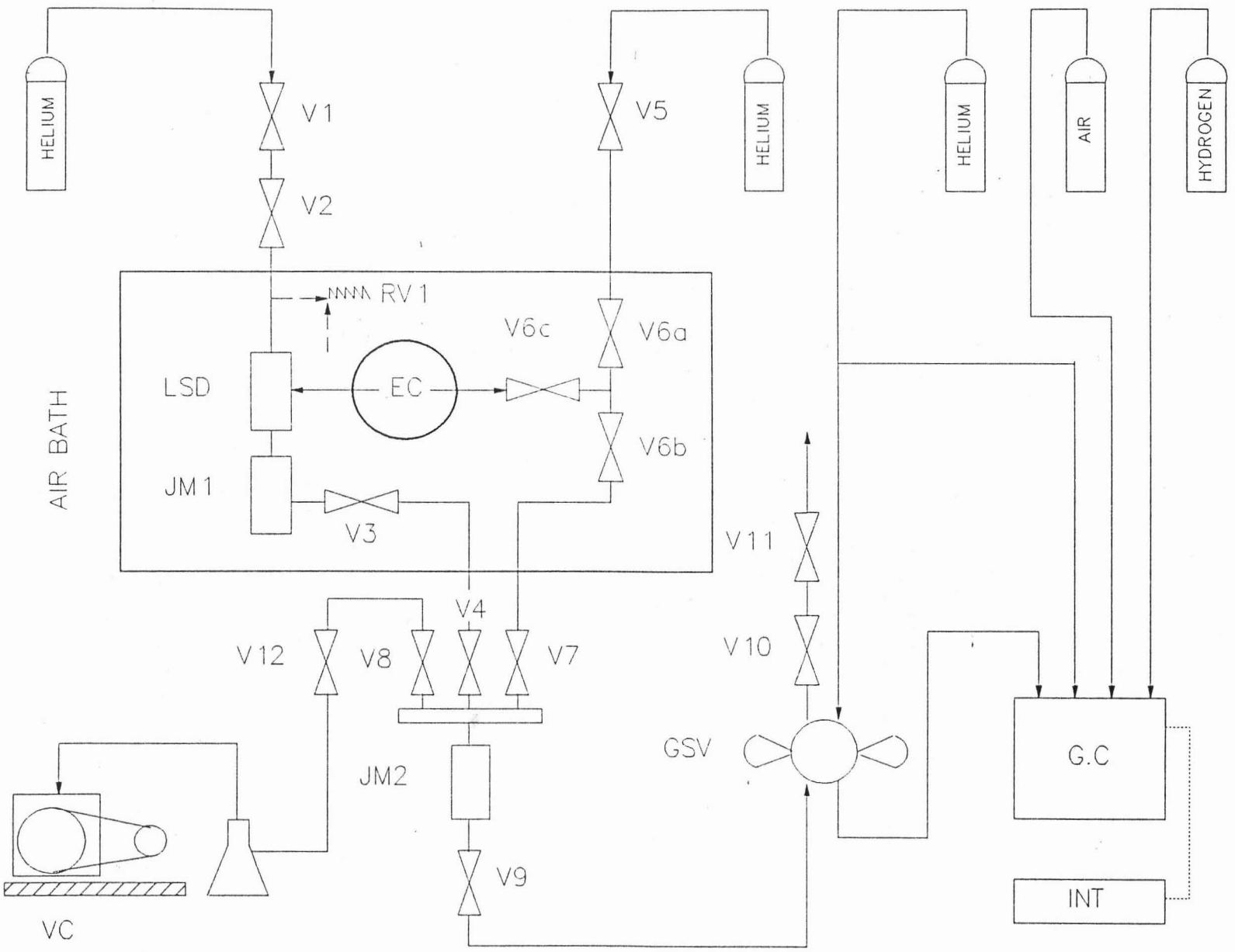

Figure 5.3 : Vapour and Liquid Sampling Lines and Associated Valves. V1 - Nupro SS-4BMG V2, V5, V11 - Whitey SS-OR-S2 V3 - Whitey SS-ORM2-S2-A V4, V7, V8, V9 - Whitey SS-ORM2-S2 V6 - Snotrick SS-410-FP V10 - Nupro SS GSV - Valco 8 port gas sampling valve EC - Equilibrium Cell, GC - Gas Chromatograph, INT - Integrator, LSD - Liquid Sampling Device, JM Jet Mixer, VP - Vacuum Pump

The steady helium flow rate over the 15 minute period ensured that :

1. If any of the non-volatile component had condensed in the line between V2 and the liquid sampling device it was flushed into the jet mixer. The flashing of the liquid sample into the line to V2 was hindered by incorporating 60 cm of coiled 1/16 inch diameter stainless steel tube in the line upstream of the liquid sampling hole. The 1/16 inch diameter tube fulfilled two functions.

   (1.1) It effectively acted as a *non-return* valve. Its small diameter ensured that the withdrawn sample followed the path of least resistance, (smaller pressure drop for distance travelled) and preferentially flashed into the jet mixer. It was essential to the homogenisation process that all the withdrawan sample entered the jet mixer as soon as possible. Initially a Whitey SS-53F2 non-return valve seen in Photograph 9 was attached to the equilibrium cell carrier gas channel upstream of the sampling hole to furfill this purpose. It was however found unsatisfactory due to the stagnant areas present in its construction.

   (1.2) As the helium carrier gas flowed slowly through the 1/16 pipe it was heated to the air bath temperature. Any non-volatile component that may have deposited in the sampling line after flashing would be displaced into the jet mixer.

2. The constant influx of helium ensured that the liquid sample was trapped in the jet mixer.

3. The additional mixing of the sample and carrier gas mixture, due to circulation created by the continuous entrance of carrier gas, resulted in a totally vapourized and homogenized volatile/non volatile liquid sample ready for gas chromatographic analysis.

Overpressurization with helium carrier gas in the jet mixer however had to be avoided. Overpressurization may result in the non-volatile component separating out into the jet mixer thereby converting the jet mixer into a vapour-liquid equilibrium cell.

During this process which took 75 minutes, the line between V3 and the vacuum pump was still being evacuated. V7 was now closed and V3 opened. The sample and carrier gas now flowed through the line to the second jet mixer. The lines were kept short to prevent volitile/non-volitile seperation as they travelled through the lines, (*chromatographic principle*). As an additional measure a slightly smaller jet mixer 2 was added into the vapour and liquid sampling lines and was responsible for sample rehomogenisation (Figure 5.3). The pressure drop due to this increase in sample line volume was about 50 kPa. As an additional measure, to ensure homogenization, the helium carrier gas was again allowed to flow slowly such that the final sample line pressure after 10 minutes was 200 kPa (a). The sample was now ready for gas chromatographic analysis.

Liquid sample gas chromatographic analysis

The 8 port Valco sampling valve connected in the configuration shown in Figure 5.3 had two loops of 8.46×10^{-4} dm^3 and 7.08×10^{-4} dm^3 respectively. The loop volumes were determined such that the sample size trapped and flushed to the gas chromatograph resulted in peak areas which were in the range of the calibration curves available. The sample loops were filled by opening fine metering valve V10 and allowing a very slow flow rate to displace the volume of the loop. The slow flow rate avoided any seperation of the volatile/non-volatile components due to the "chromatographic principle". The pressure of the line was monitored and at 190 kPa (a) a sample was sent to the gas chromatograph. After the sample had eluted from the chromatograph and the latter was ready to receive another sample, the same venting procedure was followed to fill the second loop and a second sample was sent to the gas chromatograph after the pressure had reached 180 kPa (a). with this procedure samples were sent to the gas chromatograph at 170, 160 and 150 kPa (a) respectively. These five samples were analysed for mole fraction of volatile component.

The same procedure was followed to obtain a second liquid sample analysis at the same pressure whenever possible.

The vapour sample line between V5 and V7 was kept at a pressure of 150,0 kPa with pure helium carrier gas during the liquid sampling process.

5.3.2 <u>Vapour Sampling Procedure</u>

The vapour sampling procedure was simpler and quicker than for the liquid.

Vapour phase sampling and flushing to second jet mixer

The line between V5 and the vacuum pump was evacuated to 3 torr. V6a and V6b were closed and V6c opened to allow vapour to evacuate into the manifold after the stirrer speed had been reduced to 20 rpm. The line between V5 and V6a was filled with helium carrier gas at 300 kPa (a).

The first two samples at each new equilibrium pressure were discarded as a precautionary measure. This ensured only vapour withdrawn from the cell interior proper was sampled and not the initial small amount of vapour phase in the connection between the equilibrium cell and valve 6a.

Valve V6a remained open for 5 minutes, after which it was closed. Valve V7 was closed and valves V4, V6a and V6b were opened in that order allowing the vapour sample and helium carrier gas in line V5 to V6a to be flushed into the evacuated jet mixer, resulting in vigorous mixing between carrier gas and vapour sample. Valve V5 was again opened and helium was allowed to flow in until the pressure in the line reached 300 kPa (a). The sample was allowed to homogenization for 10 minutes before being sampled.

A 1/16 inch tube was installed upstream of valve V6 for the vapour sampling line. This fulfilled the same purpose as the 1/16 inch tube in the liquid sample line.

Vapour sample gas chromatograph analysis

The samples were taken after allowing for a certain venting time instead of reaching a certain sampling line pressure as in the liquid sampling procedure. 5 successive samples were sent to the gas chromatograph. The whole sampling procedure was repeated for another vapour sample.

The liquid sample line between V1 and V4 in this case was kept at a pressure of 150 kPa with pure helium carrier gas during the vapour sampling procedure.

5.4 IMPORTANT OBSERVATIONS DURING EXPERIMENTATION

5.4.1 Sample Line Length

The volatile and non-volatile components in the liquid and vapour samples tend to separate (the volatile component travelling faster than the non volatile) as they are flushed from the sampling device to the gas chromatograph. This (*chromatographic principle*) process is very similar to the process occurring in a gas chromatograph column.

This profile was noticeable on analysis by the increase in the non-volatile component concentration over successive flushings to the gas chromatograph.

After identification of this problem area the liquid and vapour sampling lines from the sampling devices to the gas chromatograph were kept as short as possible to prevent this undesirable concentration profile. In addition a second jet mixer was installed at the junction of the vapour and liquid sampling lines, Figure 5.3, to rehomogenize the samples before analysis.

The shortening of the sampling lines and installation of the second jet mixer, resulted in successive liquid sample compositions being randomly spread around a calculated mean mole fraction of all the flushings. The successive vapour mole fractions did however show a non-random spread. The samples were slightly rich in volatile component at the first flushing and slightly lean at the final flushing.

5.4.2 Sample Line Purging And Evacuation Between Successive Sample Analysis

Between successive liquid and vapour samples the following procedure was adopted to ensure that no residual traces of components from the previous sample were present in sampling lines. The same procedure was followed for both the vapour and liquid sample lines.

The sample line was evacuated to 3 torr and kept at this pressure for 15 minutes by an Edwards vacuum pump. The combination of low pressure and high temperature ensured total removal of any residual traces of non-volatile components. The sample line was flushed with helium at 50 kPa for one minute after closing V8 and opening V9, V10 and V11, Figure 5.3. The venting helium was sent to the gas chromatograph for analysis. Usually no traces of the system components were found. If some traces were found the above procedure was repeated until no traces were detectable. The sample line was finally evacuated to 3 torr and kept at this vaccum for 5 minutes. A liquid or vapour sample was then taken by the procedure mentioned in section 5.3.

5.4.3 Time Required To Analyse A Liquid And Vapour Phase Sample

From the evacuation and sampling procedures described it can be deduced that acquiring a liquid and vapour sample was a lengthy procedure. To analyse one pressure, which included at most 2 liquid and 2 vapour samples, on the isothermal $P-x-y$ diagram required 24 hours.

After the pressure had been reduced in the equilibrium cell to the desired value the cell contents were left overnight to reach equilibrium under vigorous stirring conditions. A very similar observation was made by Ng and Robinson (1979). They also reported stirring the cell contents overnight to ensure the attainment of equilibrium.

Liquid sample

One liquid sample took approximately 3,5 hours to analyse which included :

(a) 25 minutes for evacuation (for the first liquid sample taken a longer evacuation time was allowed to ensure contents upstream valve V 2, Figure 5.3, were evacuated out of the sample line).

(b) 60 minutes for withdrawing the 4 successive liquid phase samples.

(c) 15 minutes for liquid homogenization by the slow influx of helium into the first jet mixer.

(d) 15 minutes for sample rehomogenization by the slow influx of helium into the second jet mixer.

(e) 20 minutes for each sample flushing to the gas chromatograph. On average 4 to 5 flushings were sent to the gas chromatograph for each withdrawn sample.

Vapour sample

One vapour sample took approximately 2,5 hours to analyse which included :

(a) 25 minutes for evacuation (a longer evacuation time being allowed for the first vapour sample to ensure contents upstream of valve V5, Figure 5.3, were purged out of the sample line).

(b) 5 minutes to allow for sample manifold filling.

(c) 15 minutes for vapour sample homogenization in the second jet mixer.

(d) 20 minutes for each sample flushing to the gas chromatograph. On average 4 to 5 flushings were sent to the gas chromatograph for each withdrawn sample.

5.5 GAS CHROMATOGRAPH DETECTOR CALIBRATION PROCEDURE

Achieving accurate results from a gas chromatograph requires an understanding of some of the important qualitative and quantitative aspects that can contribute to or adversely affect the accuracies achieved. A summary of these is given in Appendix D.1.1

There are two methods of calibrating a detector to achieve the accuracy of results desired in this project, namely : the very accurate method of internal standardization or the slightly less accurate direct injection method. A summary of these two methods is given in Appendix D.1.2 and D.1.3 respectively.

The internal standardization calibration method could not be applied in this project for two reasons :

1. Volatile/non-volatile systems were studied which precluded the method being applied.
2. The experimental samples to be analysed were supplied directly from a gas sampling valve, which precluded a standard of known quantity being added to the sample before analysis.

The method of direct injection calibration therefore had to be used.

The main concern when using this method is to diminish the errors due to the reliance on injected volumes. The precautions taken and methods of calibration for the gaseous and liquid components are summarized in Appendix D.2.

5.6 RECOMMENDED IMPROVEMENTS TO EXPERIMENTAL APPARATUS

Although the equipment operated satisfactorily, there are a number of improvements that should be considered in the further development of the equipment. Some like 1 and 2 were not implemented due to time constraints.

5.6.1 Equipment Modifications

1. A liquid level measuring device would be useful. The level measuring device would supply information for phase sampling but increase the complexity of the system. Five ways of determining the liquid level were identified. A brief description of each is given in Appendix D.3.

2. Extending the sampling rod through the entire cell such as in the methods of Rogers and Prausnitz (1970) and Nagakama (1987). The sampling rod could have two sample holes, so that one is filled while the other is sampled. These modifications would require the installation of an unsupported area seal in the cell wall directly opposite the existing liquid sampling device to seal the extended sampling rod and an additional jet mixer. This modification would ensure that the cell saw no cell volume change, at least not due to the sampling rod, during liquid phase sampling. Only the amount of liquid sample removed would be noticed by the equilibrium cell.

3. Modify the vapour sampling system as suggested in Option 2 Appendix C.4.

5.6.2 Phase Sampling Modifications

4. Replacement of the SS-ORM2-S2 valves in Figure 5.3 by "83" Series Trunion valves would reduce maintenance requirements dramatically. A desirable feature of these valves is their excellent vaccum operating capabilities. Enquiries would however have to be made, to the manufacturer, if a "special" batch of these valves could be made to accept Snotrik 9/16-18 uniform thread fittings. The use of low volume Snotrick heavy walled fittings, as described in Appendix C.4, would ensure no stagnant spaces in the sampling lines.

5. A fine regulating valve, Nupro SS-4BMG, in place of V5 in Figure 5.3. A fine metering valve would serve the same purpose as the fine metering valve in the liquid sampling line, Section 5.3.1 (**Flushing of liquid sample to jet mixer**).

6. Positioning a pressure transducer on jet mixer 2, Figure 5.3. This pressure transducer would permit the same sample procedure to be applied to vapour samples as was applied to the liquid samples (i.e. based on regular pressure intervals rather than time intervals).

CHAPTER 6

CHOICE OF BINARY SYSTEMS

The carbon dioxide/toluene, propane/water and propane/1-propanol systems were investigated.

Testing of the experimental data against theoretically predicted data is not possible for high pressure high temperature binary systems. The theoretical methods avaliable are not appropriate as testing methods as they are not entirely predictable. The accepted method of testing equipment and procedure is therefore to compare the measured data with data reported in the literature. If the data corresponds to the literature values a high degree of confidence can be placed in the correct functioning of the equipment.

Carbon dioxide and propane are important supercritical fluid extractants as they are non-toxic, non-flammable (except propane) and relatively inexpensive (carbon dioxide). Of increasing importance is that they are reasonably environmentally acceptable, much more than CFHs for example.

6.1 CARBON DIOXIDE/TOLUENE SYSTEM

The food industry has reported the use of carbon dioxide as a suitable foodstuff extractant e.g. Kalra, *et al* (1987). The petroleum industry has also reported the use of carbon dioxide as an extractant e.g. Braun and Schmidt (1984).

Carbon dioxide has been measured as the volatile component of many binaries, Eckert and Sandler (1986), Shibta and Sandler (1989 a), Suzuki, *et al* (1990), Takishima, *et al* (1986), Holsher, *et al* (1989), Weber (1989), Leu (1988), Wagner and Wichterle (1987). Several authors refer to measurements with aromatics : benzene (Nagarajan and Robinson 1987 and Inomata, *et al* 1987), and toluene (Ng and Robinson 1978, Sebastian, *et al* 1980, Morris and Donohue 1985, Kim, *et al* 1986 and Fink and Hershey 1990).

The carbon dioxide/toluene system was used by the above authors as a very severe test of their experimental equipment and procedure due to :

1. The large differences in the relative volatility of the two components. This volatility difference manifests itself in difficulties in obtaining a representative liquid sample.
2. Handling the withdrawn sample. The liquid sample must be vaporized and homogenized before sampling by a gas chromatograph. Partial condensation in the sample lines of the non-volatile component must be avoided.
3. The attainment of equilibrium conditions.

Carbon dioxide and toluene are readily available in high purity at low cost and are relatively non-toxic. These are important considerations during initial experimentation where leaks have to be identified and materials are used in large quantities.

Carbon dioxide is supercritical at room temperature. Pressurization of the cell contents can be achieved by heating. Carbon dioxide therefore does not require a compression device as is the case with propane.

6.2 PROPANE BINARIES

Propane has been identified as a suitable extractant in the petroleum and syngas industries. It is one of the principal components for which equilibrium data are needed.

6.2.1 Propane/Water

The phase behaviour of light hydrocarbon such as methane, ethane and propane in mixtures with water are interesting systems to investigate experimentally. In the liquid phase the two components have very low mutual solubilities and this makes them *extremely* demanding systems to measure experimentally. For example in the propane/water binary the range of mole fractions of propane in the liquid phase range from 0,000130 to 0,0003765 at 100 °C in the pressure range of 222 to 2 787 psia. The vapour phase water mole fractions range from 0,0894 to 0,00919 at 100 °C in the pressure range of 252 to 2 704 psia, Kobayashi and Katz (1953).

Measuring these mole fractions places severe demands on the experimental equipment and operational procedures. Many useful discoveries were made on the operation of the equipment (cell modification Chapter 10). The necessity for accurate calibration of gas chromatograph detectors for low concentrations resulted in the development of the gas calibration device (Chapter 5).

6.2.2 Propane/1-Propanol

Propane has been measured with the alcohols : methanol (Galivel-Solastiouk, *et al* 1986) and ethanol (Gómez Nieto and Thodos 1978).

A review of Chemical Abstracts and the Data Bibliography of Wichterle, *et al* (1973) revealed one reference of the propane/1-propanol system, that of Nagahama, *et al* (1971). The data were measured at low pressures, (1 to 8 bar), and low temperature (19,85) °C. The IUPAC Solubility Data Series (Kertes and Hayduk 1986) and Dechema Chemistry Data Series, Vol. VI (Knap, *et al* 1982) as well as a search of recent literature revealed no reference for the high temperature and pressure propane/1-propanol binary. A recent publication by Suzuki and Sue (1990 b) reviewed measured binaries of importance to the syngas industry. The authors made no mention of high pressure - high temperature data for the propane/1-propanol binary.

The measurement of the propane/1-propanol system at high pressure and temperature would therefore be a logical extension of the propane/methanol and propane/ethanol data.

CHAPTER 7

EXPERIMENTAL RESULTS

The main factors affecting the accuracy of the measured equilibrium results, the purity of the chemicals used and the accuracy of the pressure, temperature and mole fraction measuring devices, will first be discussed.

Each of the three binaries investigated; carbon dioxide/toluene, propane/water and propane/1-propanol, will be considered separately. Representative gas chromatographic calibration curves as well as the measured isothermal vapour-liquid equilibrium data will be presented. Where appropriate the measured data will be compared to values from the literature.

Important observations pertaining to the operation of the equipment, pressure and temperature fluctuations noted during sampling, and the cell wall and air bath temperature profiles will be reported.

7.1 PURITY OF MATERIAL

7.1.1 Gaseous Materials

The gaseous materials used, carbon dioxide, propane, nitrogen and helium were supplied by Air Products South Africa.

Carbon Dioxide

The carbon dioxide, Coleman grade, minimum purity 99,97 %, was supplied in 75ℓ cylinders at 70 to 80 bar.

Propane

Initially, locally refined instrument grade propane was supplied by Afrox. The quoted minimum purity of 99,0 % was found to be closer to 97 % after gas chromatograph analysis.

Certified instrument grade propane, specially imported from the USA, minimum purity 99,5 %, was consequently supplied in an A1 cylinder as a liquified gas under its own vapour pressure from Air Products.

Helium

Helium used for gas chromatographical purposes was supplied in 75 ℓ cylinders, at approximately 200 bar, with a specified minimum purity of 99,995 %.

Nitrogen

Nitrogen used as the solvent gas in the gas calibration device was supplied in 75 ℓ cylinders, at approximately 200 bar with a specified minimum purity of 99,998 %.

The main impurities found in the gaseous materials are listed in Table 1, Appendix E.

7.1.2 Liquid Materials

Toluene

Toluene was available from two sources.

Toluene from Merk was of minimum claimed purity 99,7 %. The main impurity was water at 0,05 %. The toluene supplied by SAR chemicals of analytical grade was of minimum claimed purity of 99,8 %. The main impurities were water 0,02 % and benzene 0,015 %.

1-Propanol

1-Propanol, glass distilled and filtered through 0,5 μ filters of HPLC grade, minimum purity 99,9 %, was supplied from Aldrich. The main impurity was water 0,03 %

Water

Distilled water was initially obtained from the departmental source. Through the courtesy of the Council for Scientific and Industrial Research low thermal conductivity water, of high purity, from a Millipore-RO-4 water purification system with performance characteristics listed in Appendix E.2, was obtained.

Refractive indices, a useful check of purity, were measured with a high precision refractometer and compared to those given in the literature, Weast, *et al* (1984).

TABLE 7.1

Measured Liquid Refractive Indices Against Literature Values

Substance	Refractive Index	
	Measured (1)	Literature (2)
Toluene	1,49625	1,4961
1-propanol	1,38449	1,3850
Water	1,33280	1,3329

(1) 19,99 °C.
(2) 20 °C.

Gas chromatograph analyses for the toluene, water, 1-propanol, nitrogen and carbon dioxide showed no traces of impurities. For the Air Products propane the ethane and isobutane peaks were visible on the G.C. trace. For the lower purity Afrox propane correspondingly larger ethane and isobutane were visible, as well as a butane peak.

All the materials, gaseous and liquid, were used without further refinement. Purification of the Afrox propane was attempted by passing it through a 6 angstrom molecular sieve. No measurable improvement in purity was detected on gas chromatographic analysis. The Afrox Propane was used without any further attempts at purification.

7.2 ACCURACY OF PRESSURE TEMPERATURE AND MOLE FRACTION MEASUREMENTS

Pressure

The estimated inaccuracies of the pressure measurements are taken as the maximum possible as the gauges were not calibrated against a dead-weight piston gauge :

Pressure Range	Inaccuracy
0 to 500 psi range	± 0,5 psi, ±0,034 bar.
500 to 5 000 psi range	± 5,0 psi, ±0,34 bar.

Temperature

The digital Fluke 8840A multimeter had a resistance resolution of the resistance reading of 0,001 Ω ; this corresponds to a temperature uncertainty of 0,0026 K. The real limit to the accuracy of the temperature measurement is therefore the Pt-100 Ω platinum resistance bulb. The tolerance for a class B Pt-100 Ω to DIN IEC751 West, is :-

$$(0,30 + 0,005\ (t))\ K$$

where t is the temperature in °C.

The estimated inaccuracies of the temperature measurements according to DIN IEC 751 are therefore :-

Temperature °C	Inaccuracy K
80	±0,70
100	±0,80
120	±0,90

The Pt-100 Ω resistance bulb and Fluke 8840A multimeter were however calibrated against a quartz thermometer. The Quartz thermometer and Pt 100 Ω readings were found to be within 0,9 % of each other (Table 4.3). The maximum estimated inaccuracy is therefore lower than in the above table, approximately 0,25 K.

Mole Fraction

Some of the difficulties associated with gas chromatograph analysis have been discussed in detail in Chapter 5 and Appendix D.1 and D.2 dealing with gas chromatographical calibration.

Taking into account all the known possible factors affecting accuracy, it can safely be assumed that the conversion of the peak area to moles present in a sample involves a maximum error of ±1,5 % for the non volatile component and ±1,0 % for the volatile component.

Therefore since the mole fraction was calculated from :-

$$\frac{\textit{moles of volatile component}(\pm 1\%)}{\textit{moles of volatile component}(\pm 1\%) \; + \; \textit{moles of non volatile component}(\pm 1,5\%)}$$

The uncertainties in the calculated mole fractions are therefore ± 2,5 % of the calculated value.

7.3 EXPERIMENTAL RESULTS

7.3.1 Carbon Dioxide/Toluene Binary

Gas chromatograph calibration

Representative calibration curves for carbon dioxide and toluene under the conditions of Table 4.4, for the Gow Mac gas chromatograph are shown in Figures 7.1 and 7.2 respectively.

The response of the detector was linear for both materials over the range of volumes injected. The peak areas were fitted to the moles injected by a least squares linear regression program. A linear calibration curve was obtained between peak areas and moles injected. The liquid and vapour samples flushed to the gas chromatograph for analysis were generally within the calibration range.

Daily recalibration of the detector was required as its response, (slope of the calibration curve), decreased slightly during the course of the isothermal runs.

Experimental phase equilibrium results

Two isothermal runs were performed on this binary at temperatures of 79,33 and 78,95 °C. The first isothermal run provided information to 60 bar. During the second isothermal run data were measured at higher pressures.

The phase equilibrium measurements for the carbon dioxide/toluene system are shown in Figure 7.3 and in Table 7.2

Cell temperature and pressure changes during sampling

During the isothermal runs the cell temperature varied approximately 0,5 K, Table 7.2. The *liquid* phase mole fractions, measured at the same pressure, were reproducible to within 1 % of each other, Table 7.2. The vapour phase mole fractions were slightly less well reproduced as witnessed by the relatively larger scatter about the smoothed curve, Figure 7.3. A similar observation was reported by Fink and Herskey (1990).

During sampling the internal cell temperature change, due to the slow impellar stirring speed required for liquid and vapour sampling, did not exceed 0,1 K. The pressure change during liquid and vapour sampling caused a rise and fall of 1 bar at the highest pressure data point measured (110,03 bar) becoming immeasurable at the lowest pressure measured (8,74 bar).

Comparison of results with literature values

Phase equilibrium data for the carbon dioxide/toluene system have been measured at 79,4 °C by Ng and Robinson (1978), 80,0 °C by Morris and Donohue (1985) 79,9 °C by Kim, *et al* (1986) and 80,0 °C by Fink and Hershey (1990). The results measured in this project are compared to those measured by Ng and Robinson (1978) and Kim *et al.* (1986) in Figure 7.4 and to those of Morris and Donohue (1985) and Fink and Herskey (1990) in Figure 7.5.

The liquid phase mole fractions measured in this project are in good agreement with the data of Ng and Robinson (1978), Morris and Donohue (1985) and Fink and Herskey (1990). Close observation of the low pressure vapour-phase region showed disagreement between all five data sets. This region is probably the most difficult to measure. The P-y curve is nearly horizontal which implies that small pressure changes during sampling produce large compositional changes in the vapour phase. This region tends to be neglected experimentally but may be important in design.

Except for the low vapour phase region agreement between the literature values and those measured in this project is good. Taking into account the slight temperature differences, the measured phase components are within the estimated mole fraction uncertainty of 2,25 %.

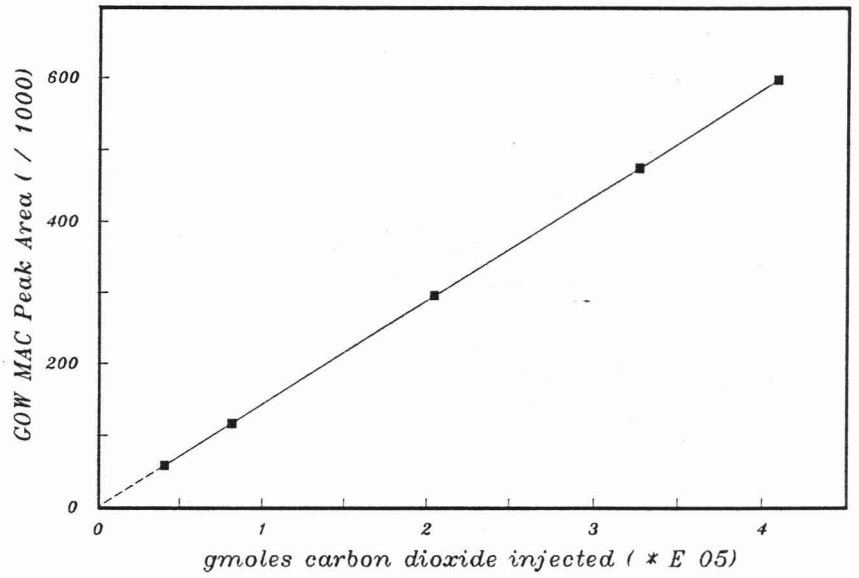

FIGURE 7.1 : Calibration of Gow Mac Gas Chromatograph TCD Detector with Carbon Dioxide

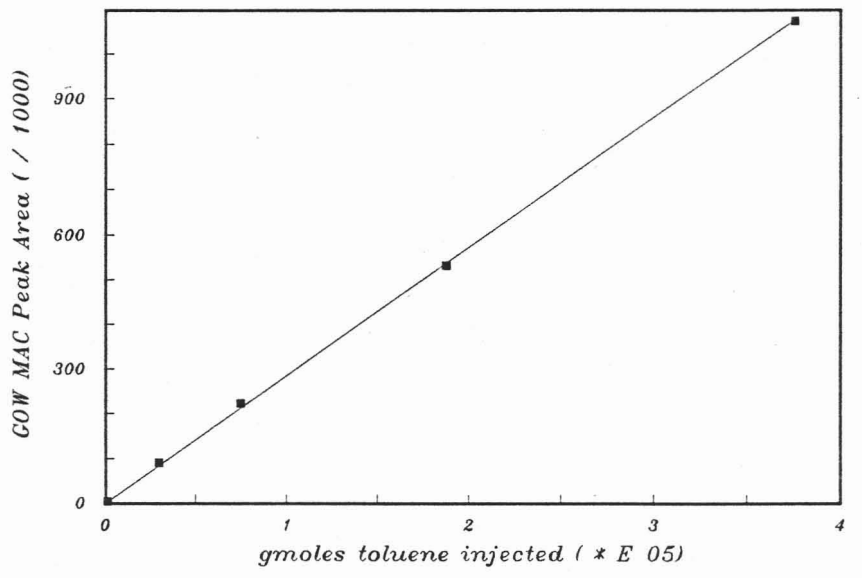

FIGURE 7.2 : Calibration of Gow Mac Gas Chromatograph TCD Detector with Toluene

Table 7.2

Isothermal Phase Equilibrium Data for the Carbon Dioxide/Toluene System. Results for the ±79 °C Isotherm

Pressure	Temperature	Mole Fraction Carbon Dioxide	
		Liquid	Vapour
bar (a)	°C	x	y
First Isothermal Run			
9,60	79,31	0,0678	
36,20	79,43	0,2114	
5,52	79,28	0,2818	
58,00	79,31	0,3366	
5,60	79,33		0,9131
7,84	79,37		0,9297
11,85	79,30		0,9598
30,61	79,35		0,9773
33,79	79,41		0,9753
54,83	79,30		0,9820
61,38	79,31		0,9735
Second Isothermal Run			
8,74	78,95	0,0495	
8,74	78,95	0,0495	
17,57	78,88	0,1100	
30,68	78,86	0,1731	
50,69	78,96	0,2650	
50,69	78,86	0,2640	
54,83	79,30	0,3000	
55,52	78,94	0,3100	
86,57	78,88	0,5006	
103,13	78,84	0,6490	
103,13	78,86	0,6481	
105,89	78,90	0,6693	
110,03	78,95	0,7080	
8,47	79,36		0,9155
60,00	79,31		0,9735
72,94	78,85		0,9836
100,02	78,85		0,9750
103,13	78,86		0,9725
105,89	78,90		0,9720
107,96	78,85		0,9725
110,03	78,95		0,9650

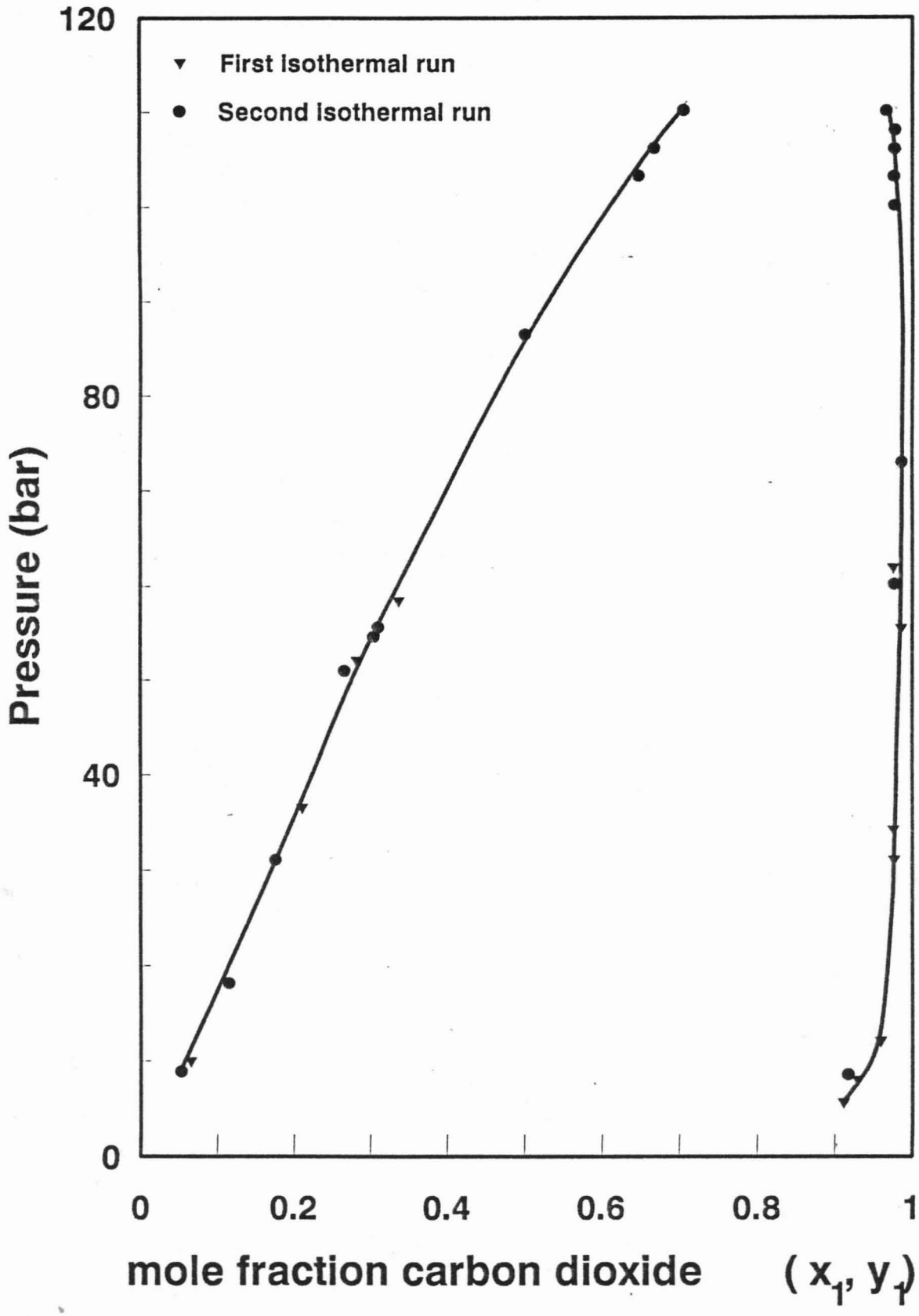

Figure 7.3 : Experimental Results for the Carbon Dioxide-Toluene System at 79 °C

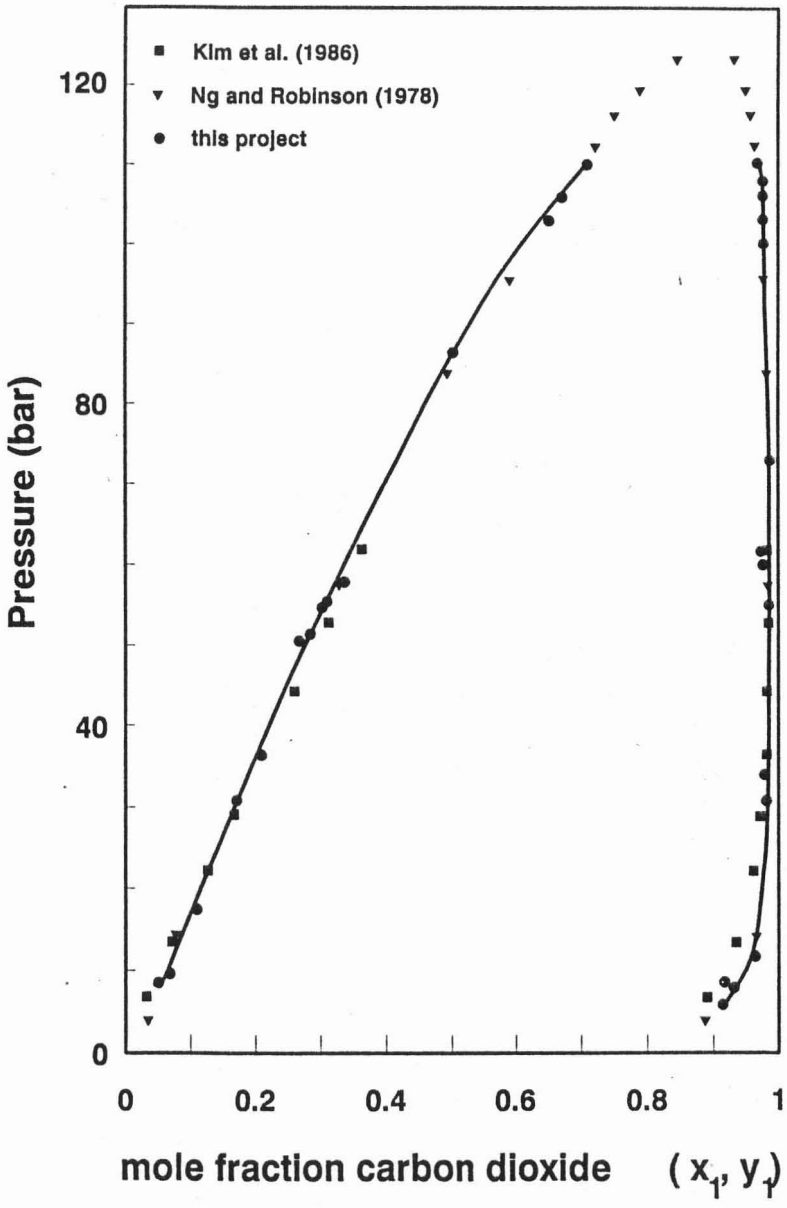

Figure 7.4 : Comparison of Experimental and Literature Values for the VLE of Carbon Dioxide-Toluene System 79 °C

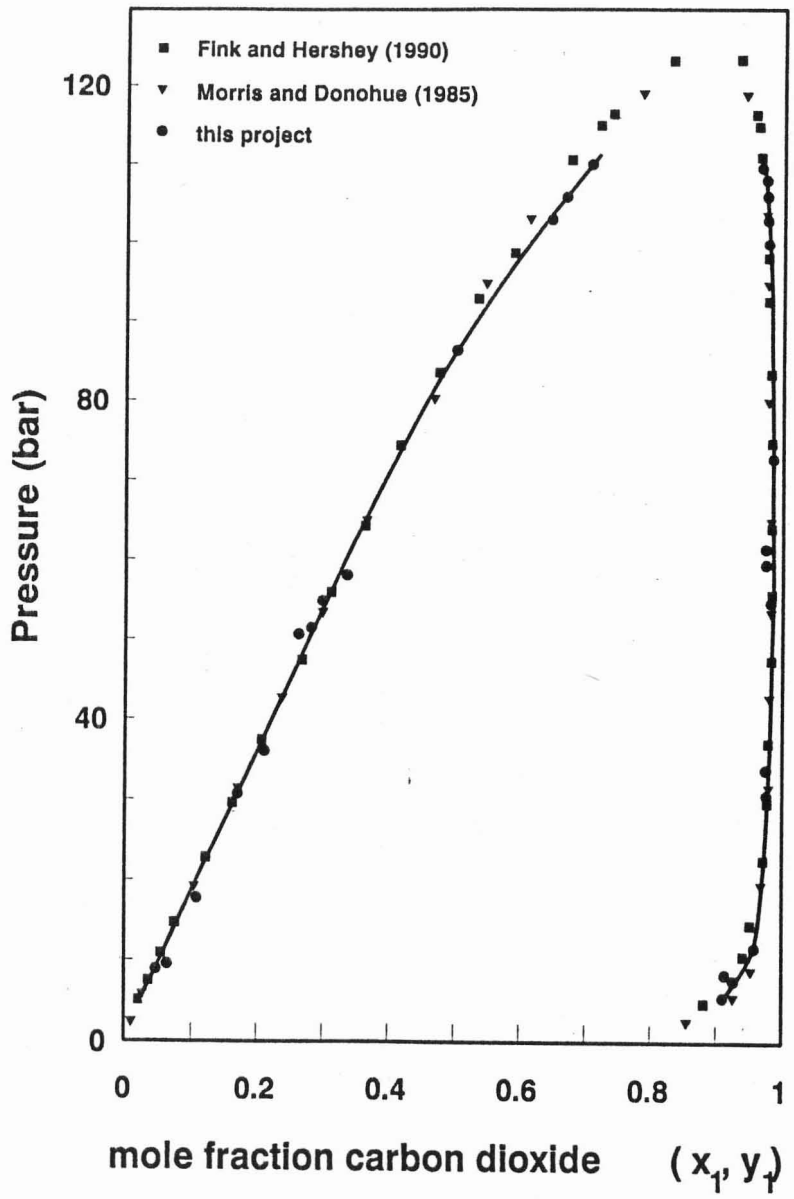

Figure 7.5 : Comparison of Experimental and Literature Values for the VLE of Carbon Dioxide-Toluene System 79 °C

7.3.2 Propane/Water Binary

Gas chromatograph calibrations

Due to the nature of the system being investigated, small quantities of the volatile component present in the non volatile component and vice versa, three calibration curves were necessary to analyse the compositional data. Representative calibration curves for the propane and water for the conditions, Table 4.4, for the Varian gas chromatograph are shown in Figures 7.6 to 7.8.

A calibration curve similar to Figure 7.7 for propane in the liquid phase was generated for the FID detector.

The detectors were calibrated at the beginning of the isothermal run and checked again at the end of the run. Daily recalibration was not necessary for the Varian G.C. as was the case for the Gow Mac G.C due to the former's superior detector and autozero capabilities.

Experimental phase equilibrium results

The experimental phase equilibrium measurements for the vapour phase for the propane/water system at temperatures of 100,72, 100,88 and 119,47 °C are shown in Figures 7.9 to 7.10. The liquid phase measurements at 119,47 °C are shown in Figure 7.12. The data is presented numerically in Tables 7.2 and 7.3

Vapour phase measurements

The vapour phase mole fractions measured at the same pressure were reproducible to 0,35 % of the average mole fraction for that pressure except for the measurement of 5,84 bar (a) at 100,80 °C. This measurement on the "horizontal slope" of the vapour phase curve as discussed in the carbon dioxide/toluene system.

Liquid phase sampling difficulties

A great deal of experimentation was necessary to achieve reproducible liquid-phase mole fractions. On analysing the first liquid sample withdrawn at a particular pressure it was noticed that it was far too propane rich compared with the literature values. Successive withdrawn samples became progressively propane leaner. The fourth sample was virtually the same as the third although still slightly leaner than the third. It was hypothesized that during sample rod withdrawal through the cell wall the stagnant material contained between the sampling rod and cell wall (Figure 4.2) was interacting slightly with the sample contained in the sample hole. This effect was not noticeable with the carbon dioxide/toluene system as this system was not being measured to the same mole fraction tolerances. Insertion and withdrawal of the piston rod approximately 10 times before sample withdrawal resulted in the first and second analysed liquid samples having mole fractions essentially similar, within 3 %, as seen in Tables 7.3 and 7.4 from 31,90 bar (a) downwards.

Modification of the equilibrium cell discussed in the Chapter 10 should resolve this stagnant region problem. An increase in the reproducibility of the liquid phase mole fractions measured at the same pressure to within 0,005 % from the current 0,10 % should result.

The difference between the liquid mole fractions at 119 °C (Figure 7.2) determined from the TCD (which are slightly lower) and FID detectors can be ascribed to the "closeness" of the peak areas or elution times between the water and propane. Detection of very small quantities of propane after the elution of a large quantity of water, by a thermal conductivity change resulted in a small propane peak area being detected. The FID determined mole fraction which is free of water peak area interference is the correct value.

The liquid phase mole fractions show greater scatter at the same pressure than he vapour phase measurements, reproducibility being in the order of 2,5 % for the 119,47 °C isotherm.

Cell temperature and pressure changes

The internal cell temperature varied approximately 0,27 K, 0,78 K and 0,43 K for the 100,70, 100,80 and 119,50 °C runs respectively (Tables 7.3 and 7.4).

The internal cell temperature changes during liquid and vapour sampling process were similar to those experienced for the carbon dioxide/toluene sampling. The pressure changes were negligible as lower total pressure where being investigated P_{max} being 50, The cell liquid level was kept lower (a useful observation made during the carbon dioxide/toluene experimentation to minimise equilibrium disturbances during sampling) than during carbon dioxide/toluene experimentation.

Comparison of results with literature values

VLE data for the propane/water system have been measured at 96,5 °C, 105,0 °C and 121,1 °C by Kobayashi and Katz (1953). Liquid phase data have been measured at 104,45 °C and 121,1 °C by Azarnoosh and McKetta (1958). The vapour phase equilibrium data at ±100 °C are compared to the smoothed data presented by Kobayashi and Katz (1953) in Figures 7.9 to 7.11. The liquid phase results at ±119 °C are compared to the smoothed data presented by Kobayashi and Katz (1953) in Figure 7.12.

Although differences of 0,000 05 mole fraction were detectable, the measured liquid phase mole fractions were generally 100 % greater than those measured by Kobayashi and Katz (1953) and Azarnoosh and McKetta (1958) and can probably be attributed to the stagnant region "problem" discussed.

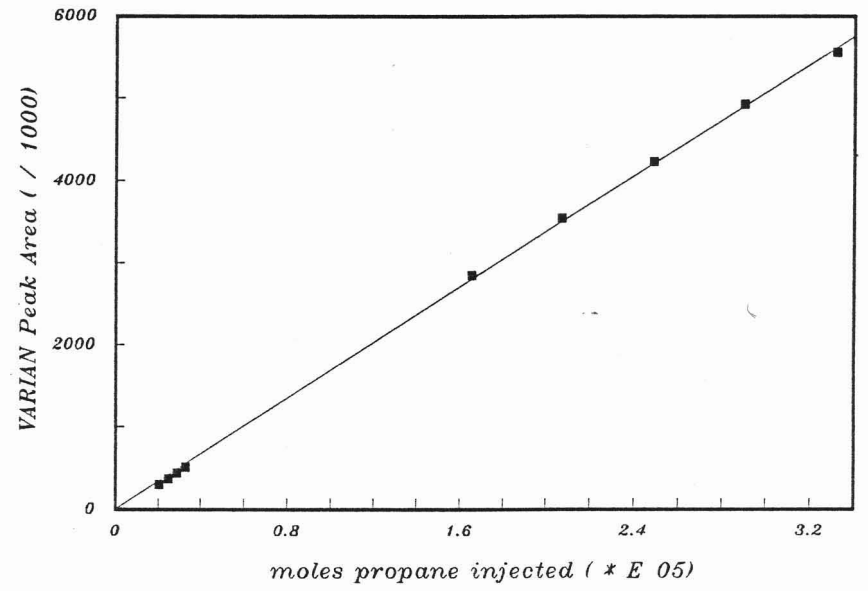

FIGURE 7.6 : Calibration of Varian Gas Chromatograph TCD Detector with Propane for Vapour Phase

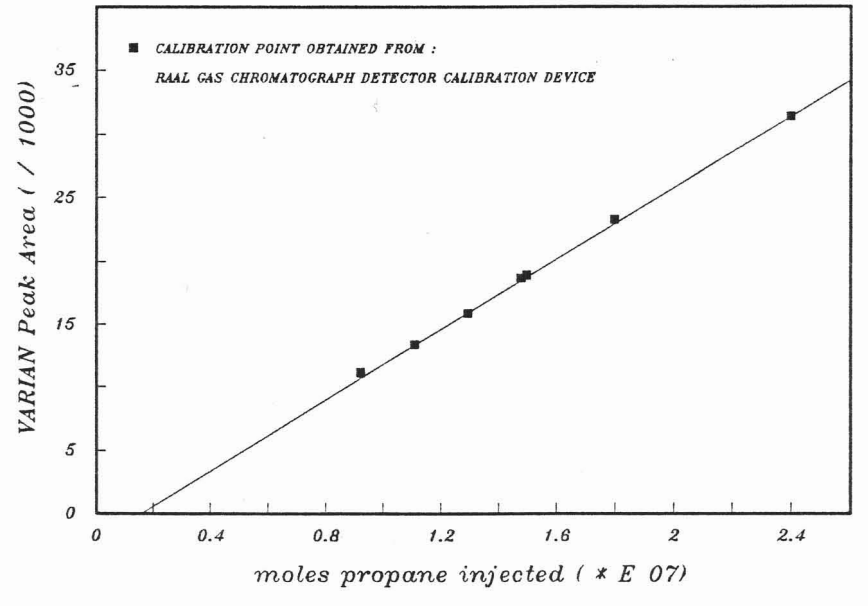

FIGURE 7.7 : Calibration of Varian Gas Chromatograph TCD Detector with Propane for Liquid Phase

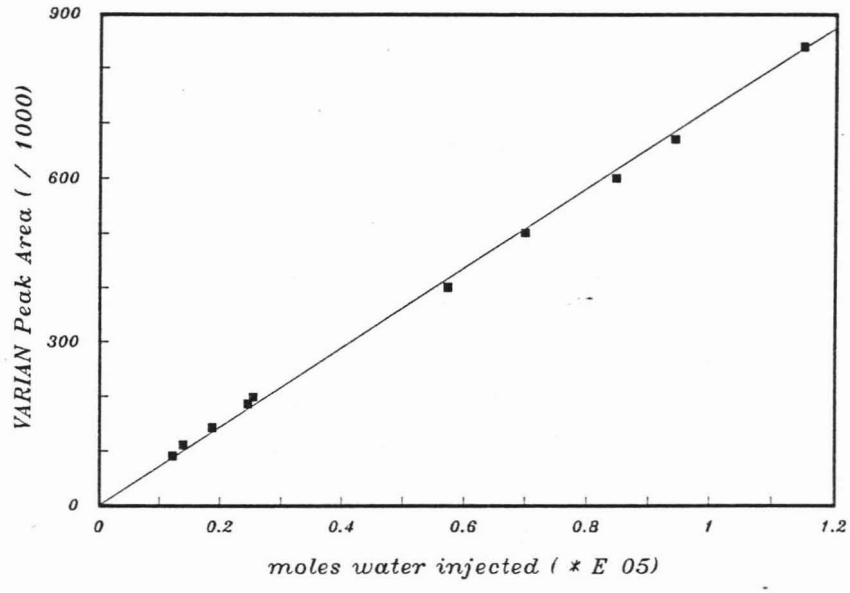

FIGURE 7.8 : Calibration of Varian Gas Chromatograph TCD Detector with Water for Liquid Phase and Vapour Phases

Table 7.3

Isothermal Vapour Phase Data for the Propane/Water System. Results for the ±100 °C Isotherm

Pressure	Temperature	Mole Fraction Propane
bar (a)	°C	Vapour (y)
Afrox Propane December 1989		
39,31	100,60	0,9781
34,13	100,66	0,9726
28,79	100,80	0,9674
28,61	100,69	0,9685
25,85	100,7	0,9619
18,61	100,74	0,9437
18,26	100,69	0,9460
Air Products Propane January 1990		
44,45	100,48	0,9850
44,45	100,50	0,9860
44,45	100,56	0,9850
42,73	100,62	0,9850
39,62	100,63	0,9821
39,55	100,63	0,9820
36,18	100,85	0,9777
36,18	100,33	0,9773
35,49	100,87	0,9751
30,87	100,99	0,9738
30,66	101,01	0,9743
29,21	101,10	0,9687
28,80	100,95	0,9684
25,90	100,99	0,9623
18,80	100,96	0,9514
18,73	101,01	0,9535
14,11	101,09	0,9292
14,11	101,10	0,9303
13,29	101,07	0,9262
13,08	101,07	0,9284
9,77	101,11	0,8851
9,77	101,09	0,8864
9,29	101,05	0,8772
5,84	101,02	0,7841
5,84	101,00	0,7453

Table 7.4

Isothermal Phase Equilibrium Data for the Propane/Water System. Results for the ±119 °C Isotherm

Pressure	Temperature	Mole Fraction Propane	
		Detector	
bar (a)	°C	TCD (1)	FID (1)
Liquid Phase (x)			
54,79	119,58	0,000656	0,001020
49,97	119,51	0,000750	0,001225
42,93	119,43	0,000777	0,001159
42,52	119,45	0,000796	0,001270
38,24	119,42	0,000589	0,000858
31,90	119,56	0,000539	0,000625
31,90	119,48	NR	0,000633
25,70	119,50	NR	0,000441
25,49	119,51	NR	0,000450
17,77	119,43	NR	0,000299
17,63	119,39	NR	0,000374
10,60	119,80	NR	0,000238
10,39	119,53	NR	0,000245
Vapour Phase (y)			
54,79	119,53	0,9809	NR
54,45	119,43	0,9730	NR
54,10	119,65	0,9748	NR
49,83	119,47	0,9687	NR
42,52	119,44	0,9593	NR
38,24	119,54	0,9511	NR
38,18	119,49	0,9500	NR
31,35	119,45	0,9369	NR
31,35	119,46	0,9358	NR
25,28	119,43	0,9174	NR
25,14	119,42	0,9254	NR
16,73	119,38	0,8701	NR
16,73	119,49	0,8825	NR
16,73	119,49	0,8825	NR
10,60	119,50	0,8109	NR
10,39	119,37	0,8202	NR

(1) NR = No Results due to detector limitations.

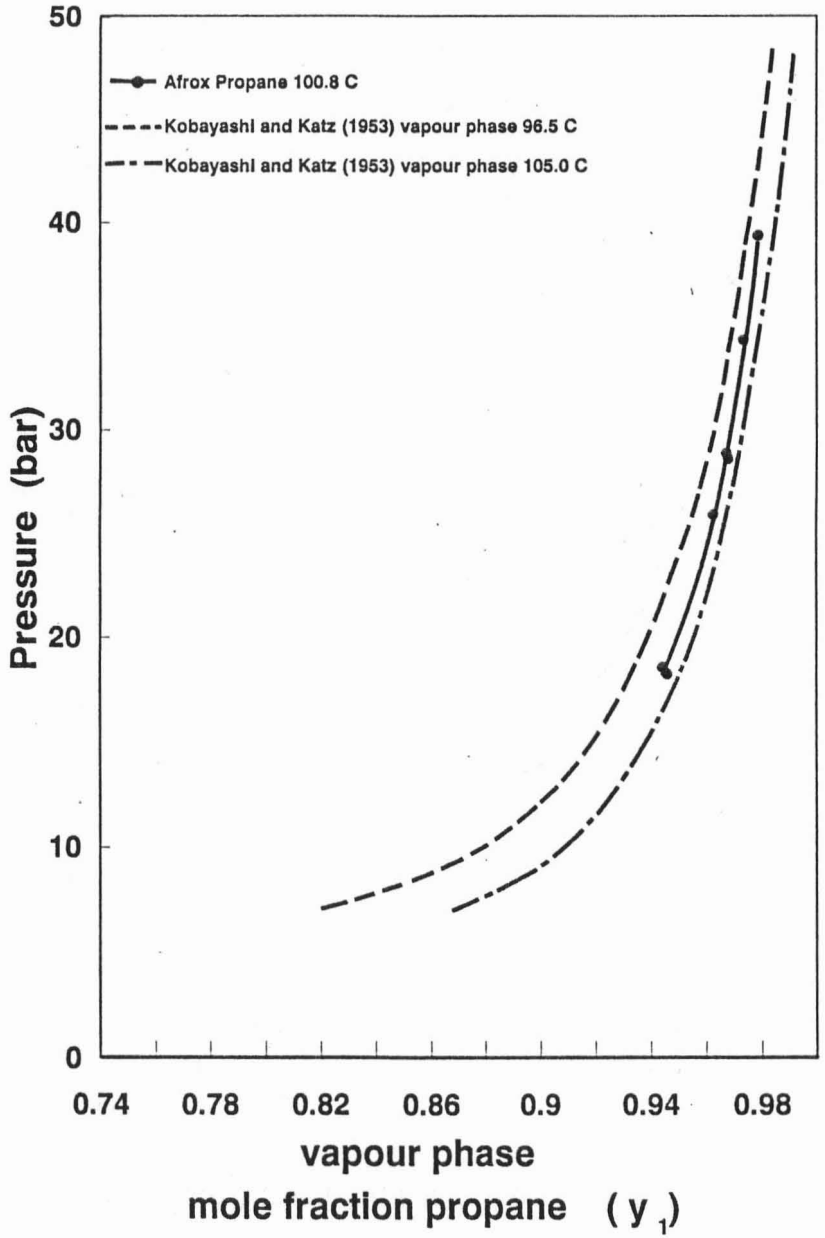

Figure 7.9 : Comparison of Experimental and Literature Values for VLE of Propane-Water System

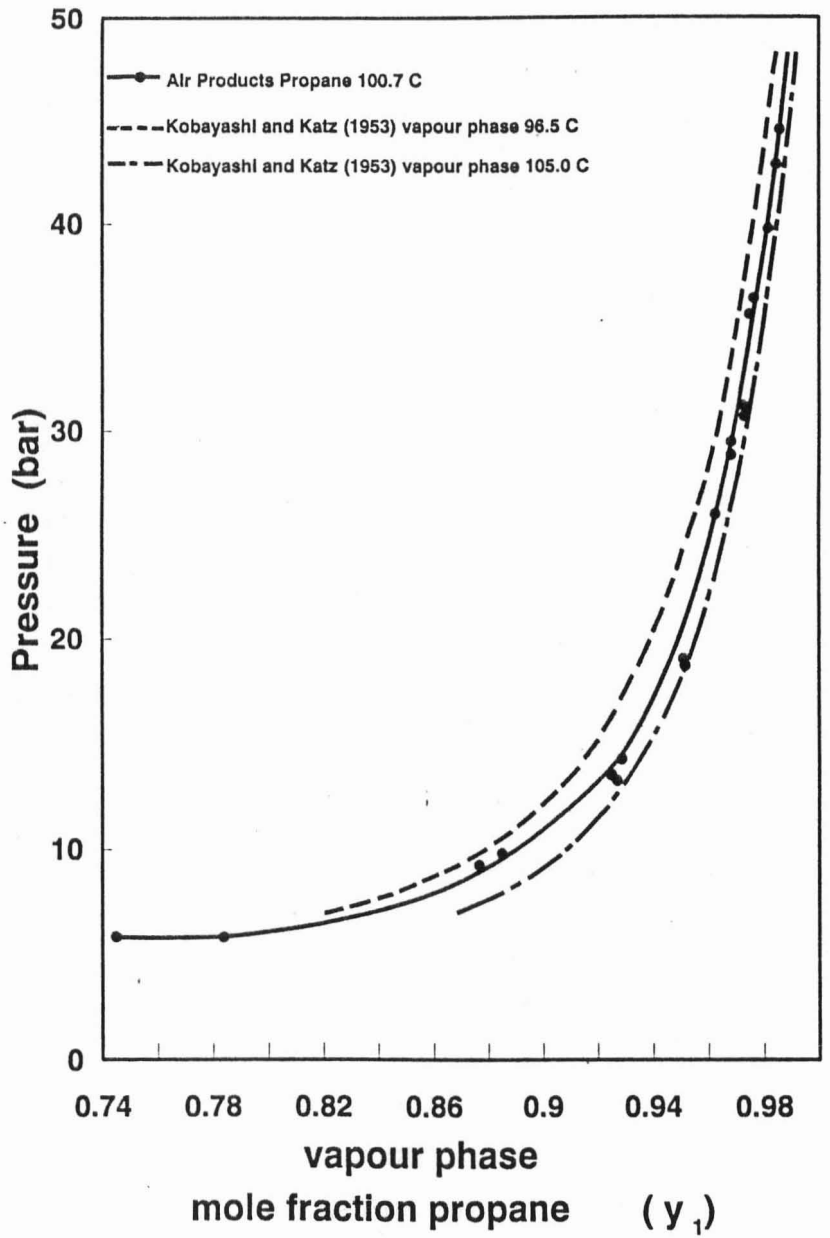

Figure 7.10 : Comparison of Experimental and Literature Values for VLE of Propane-Water System

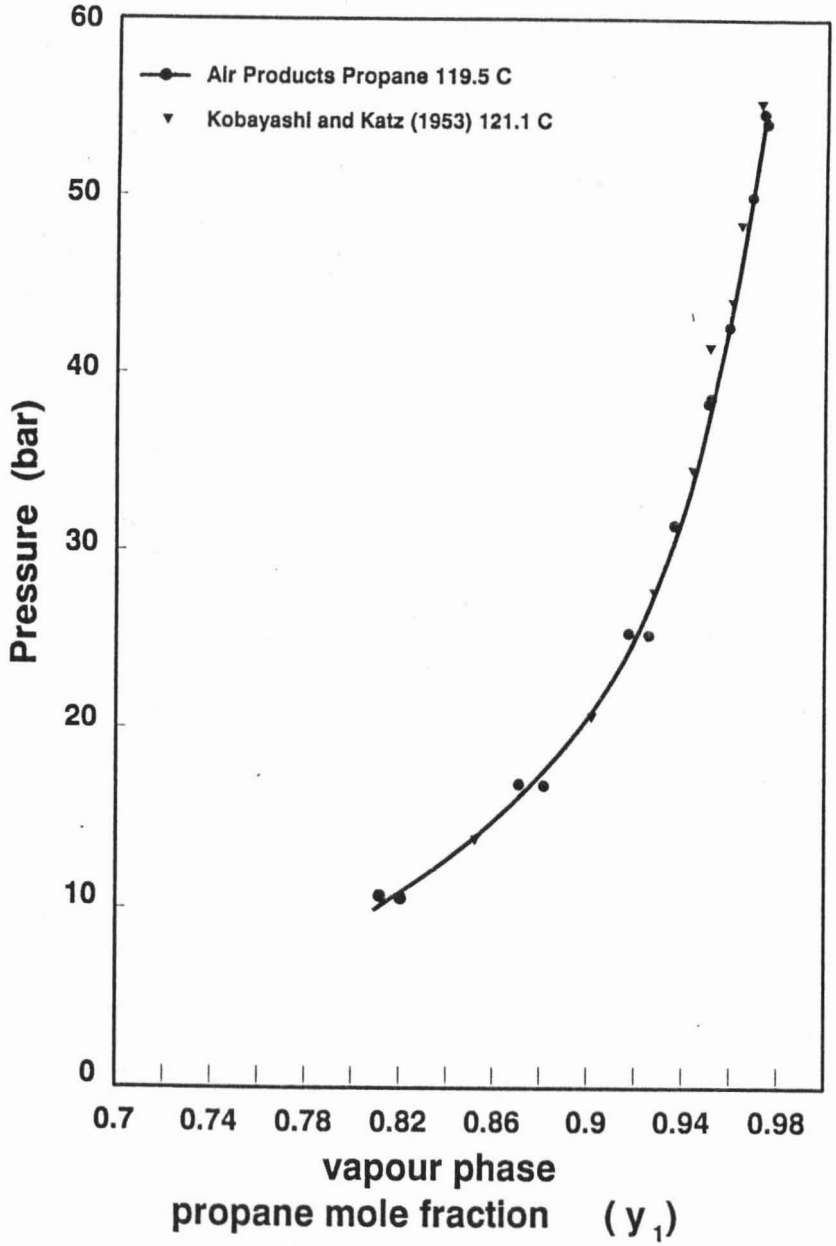

Figure 7.11 : Comparison of Experimental and Literature Values for VLE of Propane-Water System

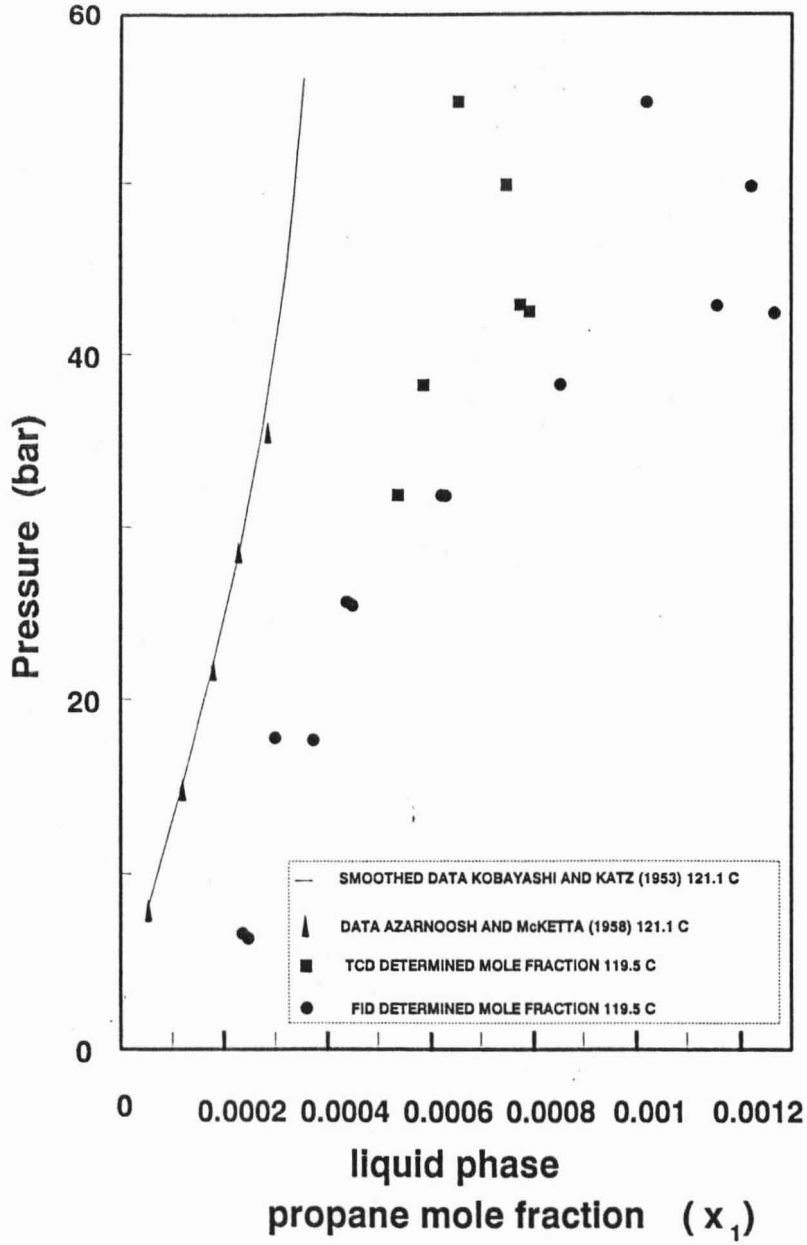

Figure 7.12 : Comparison of Experimental and Literature Values for VLE of Propane-Water System

7.3.3 Propane/Propanol Binary

Three isothermal VLE runs were performed on this binary at 80 °C, 105 °C and 120 °C.

Gas chromatograph calibration

Representative calibration curve for the propane and 1-propanol for the conditions of Table 4.4, for the Varian gas chromatograph are shown in Figures 7.13 to 7.15.

Experimental phase equilibrium results

The experimental phase equilibrium measurements for the propane/1-propanol system at temperatures of 81,62, 105,22 and 120,05 °C are shown in Figures 7.16 to 7.18 and Tables 7.5 to 7.7.

Cell temperature and pressure changes

The temperature varied approximately 0,2, 0,8 and 0,4 K over the entire three isothermal runs at 81,62, 105,22 and 120,05 °C respectively, Tables 7.5 and 7.6 The liquid phase mole fractions, measured at the same pressure, were reproducible to within 1 % of each other. The vapour pressures were reproduced to within 2,5 % of each other.

During the sampling process the internal cell temperature changes did not exceed 0.2 K. The pressure changes observed during sampling were negligible (not measurable).

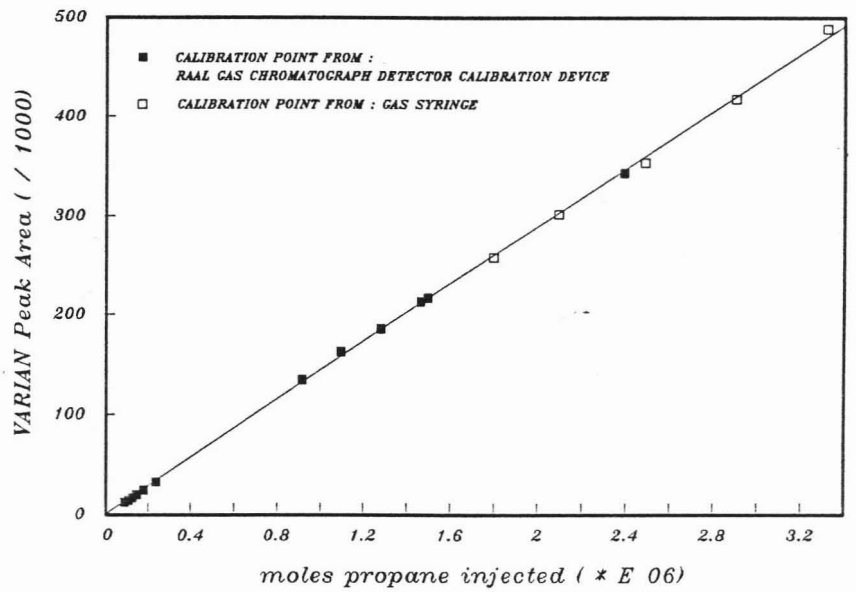

FIGURE 7.13 : Calibration of Varian Gas Chromatograph TCD Detector with Propane for Vapour Phase

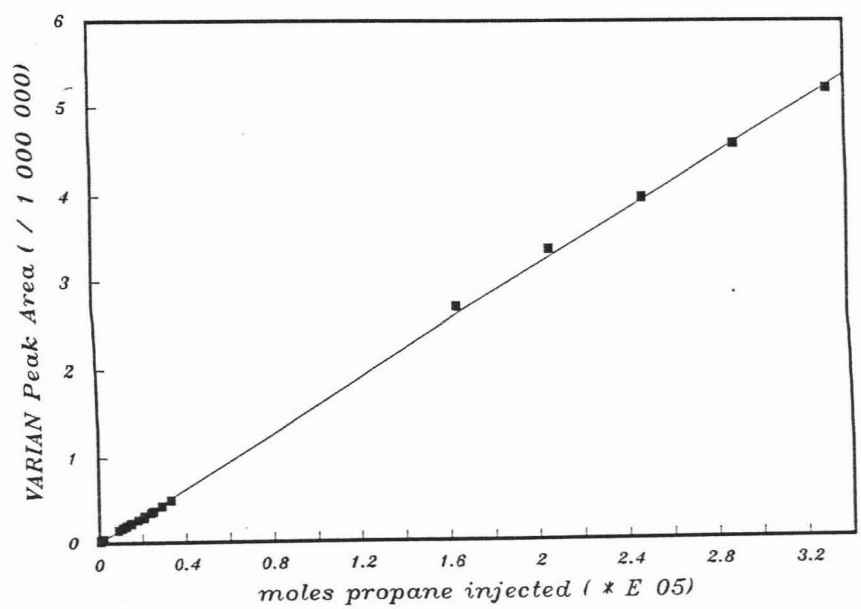

FIGURE 7.14 : Calibration of Varian Gas Chromatograph TCD Detector with Propane for Liquid Phase

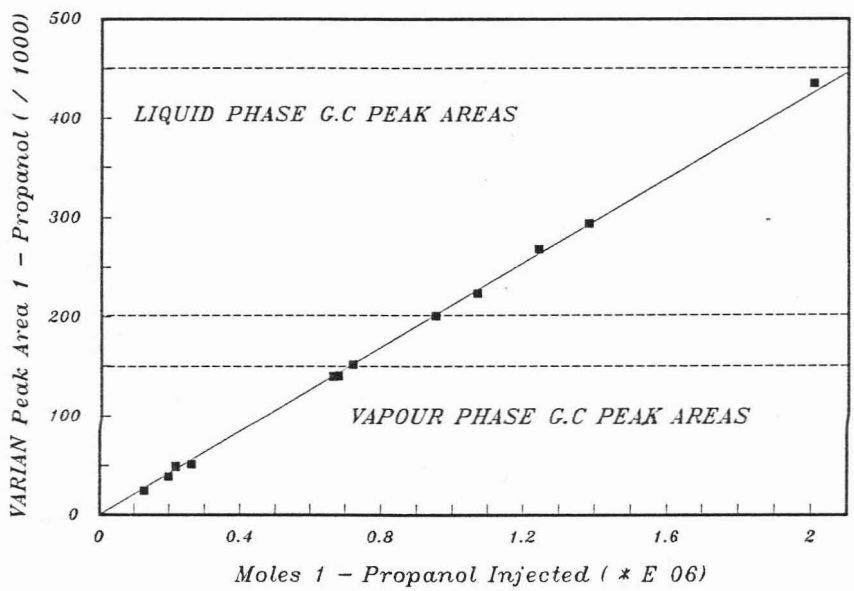

FIGURE 7.15 : Calibration of Varian Gas Chromatograph TCD Detector with 1-Propanol for Liquid and Vapour Phases

Table 7.5

Isothermal Phase Equilibrium Data for the Propane/1-Propanol System. Results for the ±81 °C Isotherm

Pressure	Temperature	Propane Mole Fraction	
		Detector	
bar (a)	°C	TCD	FID
Liquid Phase (x)			
22,39	81,64	0,4709	0,4760
22,39	81,64	0,4765	0,4887
21,70	81,64	0,4346	0,4488
21,70	81,64	0,4336	0,4461
21,49	81,60	0,4353	0,4453
18,53	81,58	0,3469	0,3442
18,25	81,57	0,3378	0,3416
16,18	81,64	0,2883	0,2836
16,11	81,71	0,2876	0,2917
12,80	81,62	0,2198	0,2277
10,53	81,65	0,1690	0,1706
8,18	81,67	0,1258	0,1261
6,53	81,67	0,0973	0,0967
4,53	81,60	0,0647	0,0663
Vapour Phase (y)			
22,39	81,71	0,9819	0,9815
22,39	81,50	0,9843	0,9869
21,35	81,66	0,9796	0,9779
21,35	81,63	0,9760	0,9794
18,11	81,56	0,9752	0,9774
18,11	81,73	0,9719	0,9758
15,97	81,66	0,9714	0,9751
15,97	81,68	0,9687	0,9718
12,80	81,65	0,9665	0,9686
10,39	81,54	0,9665	0,9638
8,18	81,63	0,9530	0,9540
6,46	81,62	0,9472	0,9469
6,46	81,64	0,9404	0,9422
4,53	81,61	0,9264	0,9245

Table 7.6

Isothermal Phase Equilibrium Data for the Propane/n-Propanol System. Results for the ±105 °C Isotherm

Pressure	Temperature	Propane Mole Fraction	
		Detector	
bar (a)	°C	TCD	FID
Liquid Phase (x)			
35,49	105,53	0,5866	0,6012
35,49	105,53	0,5864	0,6002
34,45	105,22	0,5758	0,5872
34,45	105,22	0,5746	0,5863
30,32	105,02	0,4588	0,4737
30,14	105,23	0,4584	0,4693
27,21	105,31	0,3874	0,3953
23,08	105,24	0,3071	0,3058
20,25	105,18	0,2552	0,258
17,49	105,19	0,2139	0,2177
15,56	105,14	0,1877	0,1930
12,80	105,33	0,1484	0,1472
11,05	105,19	0,1220	0,1223
10,80	105,24	0,1219	0,1188
8,46	105,28	0,0887	0,0876
6,11	105,40	0,0601	0,0610
5,00	105,89	0,0424	0,0424
Vapour Phase (y)			
29,97	105,25	0,9161	0,9282
27,21	105,22	0,9296	0,9367
27,14	105,23	0,9294	0,9373
23,08	105,16	0,9230	0,9258
32,08	105,38	0,9204	0,9283
23,08	105,24	0,9159	0,9216
20,18	105,26	0,9129	0,9067
17,49	105,25	0,8935	0,8985
15,49	105,19	0,9014	0,9004
11,15	105,26	0,8864	0,8872
11,15	105,18	0,8871	0,8842
10,80	105,16	0,8779	0,8809
8,46	105,16	0,8513	0,8549
8,46	105,12	0,8489	0,851
6,05	105,16	0,7924	0,8029
4,58	105,15	0,7209	0,7349

Table 7.7

Isothermal Data for the Propane/n-Propanol System. Results for the ±120 °C Isotherm

Pressure	Temperature	Propane Mole Fraction	
		Detector	
bar (a)	°C	TCD	FID
Liquid Phase (x)			
40,45	120,27	0,5613	0,5733
40,31	120,22	0,5652	0,5717
40,31	120,41	0,5627	0,5674
36,73	120,01	0,4782	0,4851
34,97	120,03	0,4448	0,4532
31,21	120,36	0,3689	0,3723
31,21	120,32	0,3674	0,3722
26,52	120,02	0,2999	0,3111
22,46	119,33	0,2414	0,2451
22,46	120,22	0,2402	0,2420
19,97	120,04	0,2045	0,2045
15,84	120,04	0,1585	0,1595
13,29	120,00	0,1288	0,1275
10,05	119,92	0,0904	0,0885
9,22	119,94	0,0787	0,0798
6,39	119,98	0,0493	0,0493
6,39	120,17	0,0485	0,0493
4,53	120,14	0,0297	0,0305
Vapour Phase (y)			
40,31	119,28	0,9335	0,9365
40,11	120,21	0,9327	0,9344
36,73	119,94	0,9273	0,9259
34,80	120,25	0,9304	0,9274
30,66	119,96	0,9199	0,9157
30,66	120,21	0,9350	0,9289
26,52	119,94	0,9100	0,8909
26,18	119,96	0,9149	0,8964
22,32	120,22	0,9036	0,8785
22,32	120,03	0,8968	0,8707
19,63	120,31	0,8900	0,8679
16,11	119,98	0,8681	0,8516
13,22	119,99	0,8701	0,8423
10,05	120,17	0,8356	0,8144
9,22	119,94	0,8144	0,7979
6,32	120,17	0,7364	0,7277
6,32	120,04	0,7122	0,7038
4,53	119,86	0,5890	0,5858
4,46	120,15	0,5762	0,5742

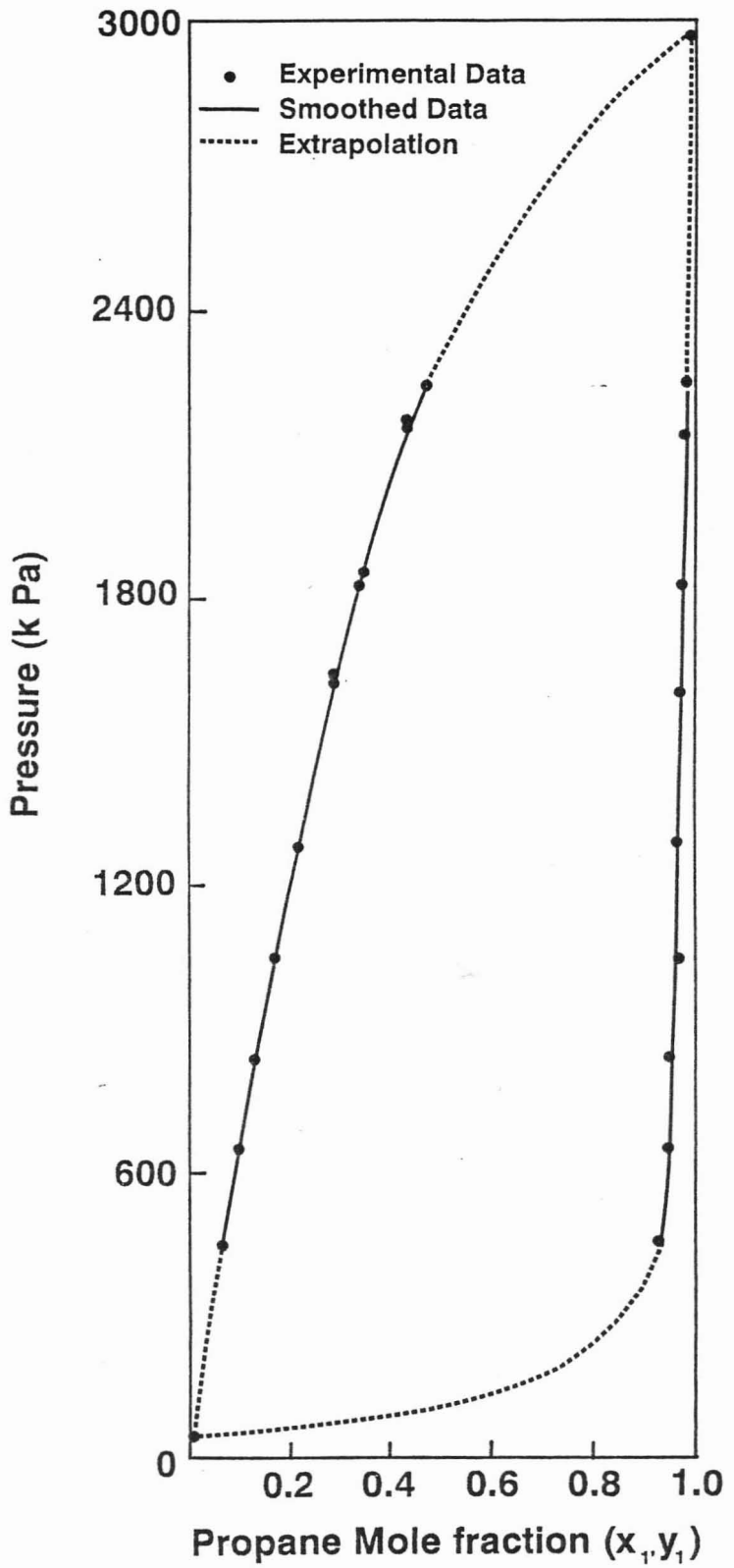

Figure 7.16 : Experimental Results for the Propane / 1-Propanol System at 81.62 ^{o}C

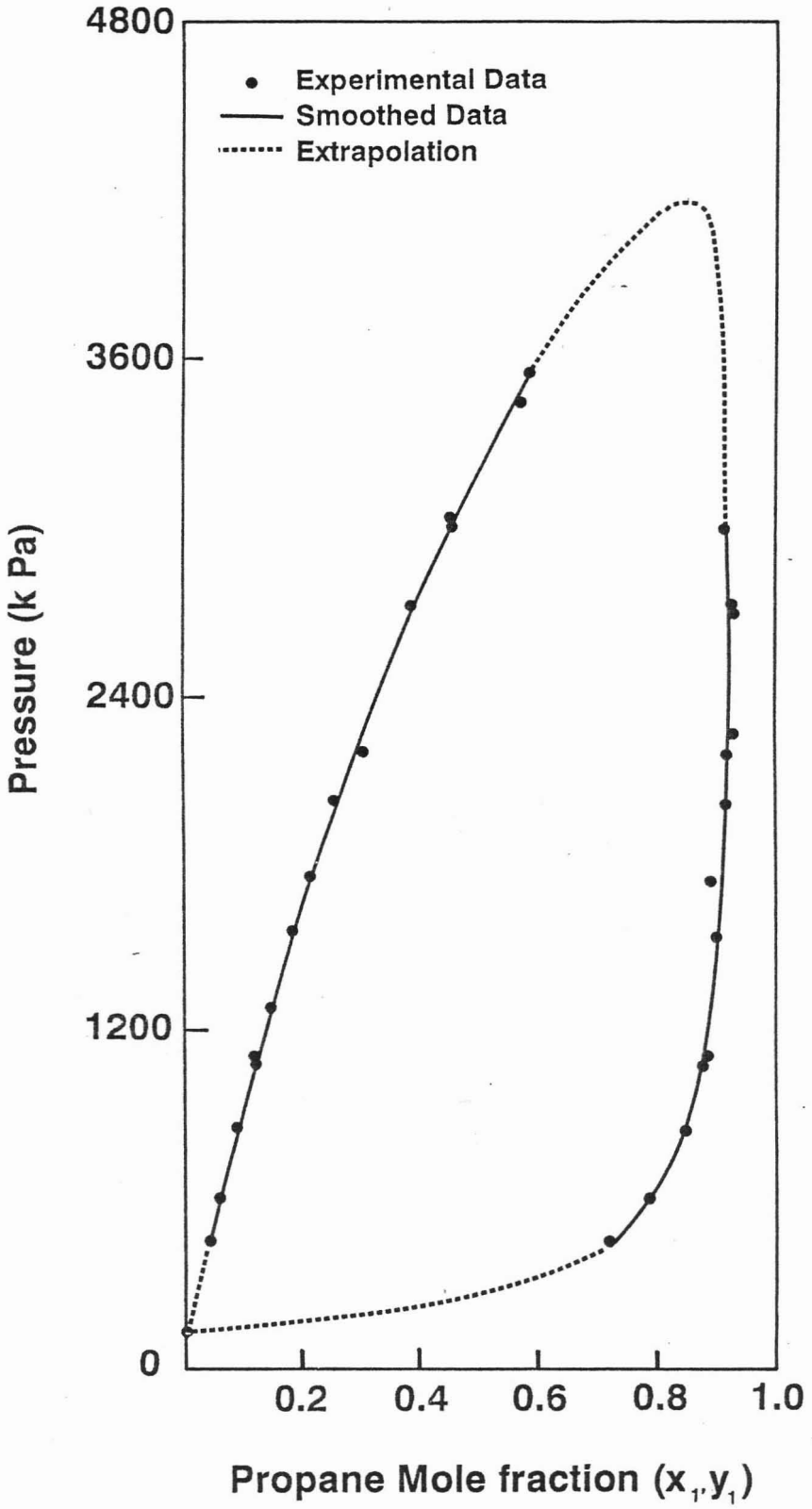

Figure 7.17 : Experimental Results for the Propane / 1-Propanol System at 105.11 °C

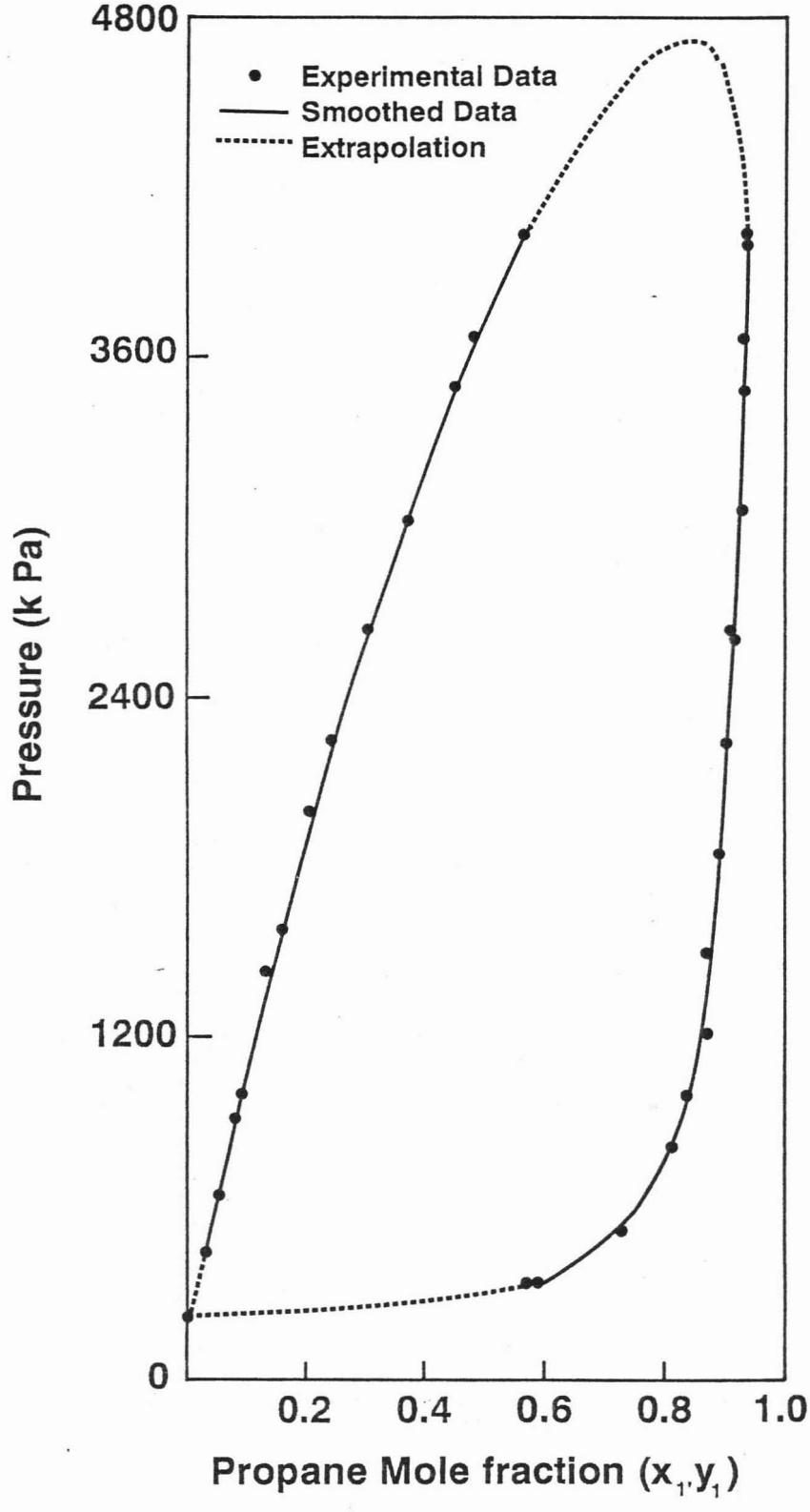

Figure 7.18 : Experimental Results for the Propane / 1-Propanol System at 120.05 ^{o}C

7.4 CELL WALL AND AIR BATH TEMPERATURE PROFILES

The pressure and temperature fluctuations noted during sampling for each of the binaries have already been discussed under the relevant binary experimental data sections.

The cell wall and air bath temperature profiles are listed in Table 7.8.

TABLE 7.8

Air Bath and Cell Wall Temperature Profiles

Temperature measuring device	Operating temperature (°C)				
	±78 (1)	±81 (2)	±100 (3)	±105 (4)	120 (5)
	Temperature Reading of Measuring Device (°C)				
Fluke 2190A Thermocouple Position (6)					
T0	74,30	78,70	95,20	101,10	115,20
T1	78,45	81,20	100,50	104,70	119,35
T2	78,55	81,30	100,60	104,85	119.45
T3	78,55	81,40	100,70	105,20	119,80
T4	78,40	81,50	100,70	105,10	120,00
T5	78,45	81,40	100,60	105,10	119,75
Cell wall difference (7)	0,10	0,20	0,20	0,35	0,65
T6	81,80	81,80	102,6	106,10	121,30
T7	78,55	81,40	101,4	105,70	120,90
T8	78,45	81,40	101,5	105,30	120,10
Air bath difference (8)	3,35	0,40	1,20	0,80	1,20
Eurotherm 818 TSP (9)	79,0	81,0	100,0	105,0	120,0
Fluke 8840 TRM (10)	130,356	131,36	138,468	140,185	145,655
Eurotherm 810 TSP (11)	160	120	170	140	170

(1) carbon dioxide/toluene isothermal run 1.
(2) propane/n-propanol isothermal run.
(3) propane/water isothermal "air products propane" run.
(4) propane/n-propanol isothermal run.
(5) propane/n-propanol isothermal run.
(6) see Figures 4.10 and 4.14 for thermocouple positions.
(7) (highest-lowest) temperature, excluding TO.
(8) (highest-lowest) temperature.
(9) TSP - temperature set point (air bath)
(10) TRM - Ohmic temperature measurement.
(11) TSP - temperature set point (jet mixer).

CHAPTER 8

THEORETICAL TREATMENT OF EXPERIMENTAL DATA

In view of the time-consuming and expensive nature of high pressure VLE data gathering a sound thermodynamic procedure is required to make calculations for other than the measured conditions from the smallest possible number of experiments. It is therefore expedient to consider techniques for calculating phase equilibria from the minimum experimental data possible. Prausnitz, *et al* (1980) suggests that such techniques should require only limited experimental effort and, whenever possible, should be based on a theoretical foundation to provide reliability for interpolation and extrapolation with respect to temperature, pressure and composition.

Theoretical treatment of the experimental data obtained in this project was based on the combined method. The experimental data was *fitted* to the UNIQUAC liquid phase model to obtain binary interaction parameters (a_{12} and a_{21} Eq. (3.30)). The validity of the binary parameters was subsequently tested in a separate *correlation* program. Thermodynamic consistency testing of the data was also performed.

Theoretical analysis of the experimental data involved the correlation of the carbon dioxide/toluene binary with the UNIQUAC and either the Peng and Robinson or Virial EOS.

For the propane/1-propanol binary the UNIQUAC with either the Peng and Robinson, Virial or Group Contribution EOS was used.

The experimental data was also tested for thermodynamic consistency via the Chueh, *et al* (1965) consistency test and the similarly derived vapour phase test.

The propane/water data were not theoretically analysed as they were used primarily as an extremely demanding equipment test and partly due to the lack of accurate experimental liquid phase composition data.

8.1 FUGACITY AND ACTIVITY COEFFICIENT MODELS USED

8.1.1 Correlation and Fitting Programs

Combined method

At the outset of this project it was felt that there was scope for the application of the combined method for the description of phase equilibria in the range of pressures and temperatures under investigation.

From the literature it would appear however, that most of the emphasis in correlating high pressure data has been directed at using an equation of state to describe the liquid and vapour phase behaviour, i.e. the direct method. Combined methods have been used much less frequently with only a few authors referring to this specific method, Appendix F.3 and F.4.

Uniquac equation

The two interaction parameter form of the UNIQUAC equation, Eq. (3.51) was chosen to calculate the liquid phase activity coefficients in the fitting as well as correlation programs written in this project. Eq. (3.51) was derived to describe systems of components which have large size differences (carbon dioxide/toluene) and polarity differences (propane/1-propanol).

The UNIQUAC equation although semi-empirical has a sound theoretical basis. In addition it was felt to be one of the best liquid phase equations available as it uses *pure component properties as well as interaction parameters* to describe specific systems compared to other equations which use only interaction parameters i.e. van Laar, Margules and NRTL.

The use of UNIFAC, which would not have required regressional techniques, and its use in the correlation program, to make it purely predictive, was not desirable. The UNIFAC group interactions were determined from low pressure data and different EOS (i.e Ideal gas law) to those used in this project and consequently would have introduced inconsistencies. In addition the simple EOS are unsuitable for high pressures.

Virial Equations of Sate

The two parameter Virial EOS in conjunction with the UNIQUAC equation as in Prausnitz, *et al* (1980) was expected to be inadequate for the high pressure regions for the carbon dioxide/toluene system. Initial investigations confirmed this.

Peng-Robinson Equations of State

The original P-R EOS was then tried in place of the Virial EOS. Excellent results were achieved for the carbon-dioxide/toluene binary using a combination of the P-R and UNIQUAC equations in the fitting and correlative programs. The use of the P-R EOS in the UNIQUAC fitting program was possible due to interaction parameter information being available for the binary.

Before the UNIQUAC/P-R EOS combination could be applied to the propane/1-propanol system the P-R EOS interaction parameters had to be obtained from the measured VLE data. These parameters were obtained using the simplex regression or fitting program by minimising the errors in the pressure variable. Although the suitability of the P-R EOS for polar substances has been questioned, reasonable correlations were achieved for the propane/1-propanol system.

From the results of the correlations it would appear that the P-R EOS was more comfortable in handling size differences (carbon dioxide/toluene) than polarity differences (propane/1-propanol).

Group-Contribution Equation of State

The group contribution EOS was consequently tried. This EOS has predictive capabilities and no prior data regressions were therefore needed before application in the UNIQUAC fitting program. Similar correlatons were achieved for the propane/1-propanol system using the G-C and Virial EOS in conjunction with the UNIQUAC equation.

8.1.2 Consistency Testing

As discussed in Chapter 3 most EOS require interaction parameters which are found by the regression of the experimental data onto the appropriate EOS. The fitting or regression of data onto an EOS yields residuals which are a form of consistency test.

Even though an area test is a necessary but not sufficient test of thermodynamic consistency since the areas may contain compensating errors, (Van Ness and Abbot 1982), the plot of the areas can yield much useful information.

The Chueh, *et al* (1965) and the new vapour phase equal area consistency tests, which required no fitting procedures, were chosen for consistency testing of the data in this project.

8.2 COMPUTER PROGRAMS USED

Four computer programs were written :

The first, a "*fitting*" program (Program 1) was based on the combined method as suggested by Prausnitz, *et al* (1980). This program was used to fit VLE data at a given temperature to a liquid phase model for activity coefficients. In the original Prausnitz program the two parameter Virial EOS was selected for the description of the vapour phase. The Prausnitz program was expanded in this project to accept the Peng and Robinson and Group Contribution EOS. This program yielded values of the UNIQUAC binary interaction constants α_{ij} Eq 3.56 for each temperature for the binaries experimentally measured.

The second, a "*correlation*" program (Program 2) permitted prediction of total pressures and vapour phase compositions for given experimental temperatures and liquid phase compositions by the combined method, i.e. essentially a bubble point computation. This constituted a test of the accuracy of the UNIQUAC parameters obtained from the fitting program.

The third and fourth were "*consistency test*" programs. These programs allowed for thermodynamic consistency testing of the data according to the Chueh, *et al* (1965), section 3.6.1, and vapour phase, section 3.6.2, consistency tests respectively.

8.3 CALCULATION OF THE LIQUID AND VAPOUR FUGACITIES

8.3.1 Liquid Phase Fugacity ($\hat{f}_i^L$)

As previously mentioned, section 3.3.2.1, a standard state must be chosen when using the combined method.

Activity Coefficient (γ_i)

Following Prausnitz, *et al* (1980) it was convenient to define pressure-independent liquid phase activity coefficients $\gamma_i^{(Pr)}$ by ,

$$\gamma_i^{(p^r)} = \gamma_i^{(p)} \exp \int_p^{p^r} \left(\frac{\overline{V}_i^L}{RT}\right) dp \qquad (8.1)$$

where $\gamma_i^{(p^r)}$ is the activity coefficient at an arbitrary reference pressure p^r and $\overline{V}_i^L$ the liquid partial molar volume.

For isothermal systems, as in the present study, total pressures usually vary widely with liquid composition but the above definition of $\gamma_i^{(p^r)}$ permits the use of integrated forms of the isobaric isothermal Gibbs-Duhem equation such as the UNIQUAC and NRTL equations, without approximation.

Standard State Fugacity (f_i^{OL})

The standard state liquid phase fugacity f_i^{OL} was given in terms of the fugacity of component i in solution, $\hat{f}_i^L$ and $\gamma_i^{(p^r)}$ by :

$$\hat{f}_i^L = x_i \gamma_i^{(p^r)} f_i^{OL} \exp \int_{p^r}^{p} \frac{\overline{V}_i^L}{RT} dp \qquad (8.2)$$

For condensable components in order that $\gamma_i^{(p^r)} \to 1$ as $x_i \to 1$ the standard state fugacity f_i^{OL} must be that of pure liquid i at solution temperature and reference pressure p^r . In this work the reference pressure p^r was taken as zero, i.e. Standard State 3 Table 3.1, which implies :

$$f_i^{OL} = P_i^s \phi_i^s \exp \int_{p_i^s}^{p^r} \frac{V_i^L}{RT} dp \qquad (8.3)$$

V_i^L is the molar liquid volume of pure i at temperature T . Since liquid partial molar volumes are seldom available a considerable simplification can be achieved by assuming that :

$$\overline{V}_i^L = \overline{V}_i^L(T) = V_i^L = V_i^L(T) \qquad (8.4)$$

The fugacity of pure liquid i at zero pressure is thus given by :

$$f_i^{(P^o)} = p_i^s \ \phi_i^S \ \exp - \frac{V_i^L \, p_i^s}{RT} \qquad (8.5)$$

In the Prausnitz, *et al* (1980) program the standard state fugacities were obtained from a five parameter equation of the form :

$$\ln f_i^{P^o} = C_{1i} + C_{2i}/T + C_{3i}T + C_{4i}\ln T + C_{5i}T^2 \qquad (8.6)$$

The constants Eq (8.6) were obtained by fitting the expression to vapour pressure data, as discussed in Prausnitz, *et al* (1980 : Appendix B).

The liquid molar volumes were calculated using Rackett's equation as modified by Spencer and Danner (1972) ,

$$V = \frac{RT_c}{P_c} \ Z_a^{\tau} \qquad (8.7)$$

where

$$\tau = 1 + \left(1 - \frac{T}{T_c}\right)^{\frac{2}{7}} \text{ for } T/T_c \leq 0,75$$

$$\tau = 1,60 + 0,00693026(T/T_c - 0,655)^{-1} \text{ for } T/T_c \geq 0,75$$

The values for the constants C_{Ji} in Eq (8.6) and Z_a in Eq (8.7) were available for carbon dioxide, propane, 1-propanol and toluene in Prausnitz, *et al* (1980).

For the "non-condensables" carbon dioxide and propane a normalization for the pure liquid fugacity based on Henry's law for dilute solutions may be used. This avoids the hypothetical notion of a pure supercritical fluid. In this study, however since carbon dioxide and propane were not excessively above their critical points, $T/T_c < 1,8$, for the available data sets they were considered condensable gases with evaluation of their properties by extrapolation. The symmetric convention for standard state fugacities was used. The validity of Henry's law :

$$\lim_{x_i \to 0} \frac{\hat{f}_i}{x_i} = H_{ij}$$

is in any case questionable for the higher liquid phase concentration regions of the non-condensable component.

8.3.2 Vapour Phase Fugacity ($\hat{f}_i^V$)

The vapour-phase fugacity coefficient can be calculated using the integrated form of the exact thermodynamic relationship, Eq. 3.10, together with any equation of state judged suitable for the system and conditions. In this study it was decided to use the two parameter truncated Virial EOS, Peng and Robinson EOS in its original form (Peng and Robinson (1976)) for the carbon dioxide/toluene system and the

Group Contribution EOS in addition to the above two for the propane/1-propanol system. The integrated fugacity coefficient forms of the above EOS are given under the relevant sections in Chapter 3.

Virial EOS

The Virial EOS is attractive as it is soundly based theoretically and the mixture 2nd virial coefficient B_{mix} is related to the pure component and cross 2nd virial coefficients for a binary by the exact expression :

$$B_{mix} = \sum_{i=1}^{2} \sum_{j=1}^{2} y_i y_j B_{ij} \qquad (8.8)$$

Eq. (8.8) negated the need for **system specific** interaction parameters which would not be available for unmeasured systems. As in the Prausnitz, *et al* (1980) program the B_{ij} 's were evaluated as functions of temperature from the Hayden and O' Connell (1975) corresponding states correlation.

The two parameter Virial EOS cannot be expected to perform well near the critical point and the inclusion of the third virial coefficient, which should be sufficient to describe high pressure behaviour, would be attractive if sufficient information were available. The correlating ability of the Virial EOS is therefore usually limited to low to moderate pressures, eg P < 20 bar.

Peng and Robinson EOS

The original Peng and Robinson EOS is considered one of the most accurate cubic equations of state near the critical point. It does not produce instabilities near the critical point as has been noted for example for the Soave modified Redlich-Kwong EOS (Reid, *et al* (1987)). An important drawback in using this EOS for the vapour phase description is the necessity for interaction parameters, which themselves need to be derived from experimental data. Binary interaction parameters δ_{ij} for the "classical mixing rules" Eq. (3.40) are available for the temperature range 38 to 200 °C for the carbon dioxide/toluene system. The δ_{ij} proposed by various authors are summarized in Table 8.1.

Binary interaction parameters for the propane/1-propanol system were generated using the Simplex Regression program still to be discussed in section 8.5.2.4.

Group Contribution EOS

The Group Contribution EOS is attractive in that it does away with the need for binary interaction parameters and can describe polar substances. This EOS has better high pressure correlational abilities than the two parameter Virial EOS.

The propane/1-propanol components had to be broken down into their appropriate groups. The groups choosen to represent the above two molecules are listed in Table 8.2.

Table 8.1

Peng and Robinson Interaction Parameters for Carbon Dioxide/Toluene

Reference	δ_{ij}	Temperature °C
Ng and Robinson (1978)	0,09	38 to 204
Lin (1984)	0,102	38 to 204
Kim, *et al* (1986)	0,108	
Mohamed and Holder (1987)	0,1056	38
	0,09424	79
	0,09331	120

Table 8.2

Pure Group Parameters for GC EOS for Propane and 1-Propanol

Component	Group	Lit. Ref[1]	Ref No.[2]	υ_j^i
Propane	CH_3	A	1	2
	CH_2	A	2	1
Propane	C_3H_8	B	34	1
1-Propanol	CH_3	A	1	1
	CH_2	A	2	1
	CH_2OH	A	11	1
1-Propanol	CH_3	B	1	1
	CH_2	B	2	1
	CH_2OH	B	20	1

1. Literature Reference
A) Skjold-Jorgensen (1984)
B) Skjold-Jorgensen (1988)

2. Component Reference
A) Skjold-Jorgensen (1984) : Table 2 denoted GC (O)
B) Skjold-Jorgensen (1988) : Table 1 denoted GC (N)

8.4 COMPUTER PROGRAM DESCRIPTION

8.4.1 Parameter "Fitting" Program (Program 1)

In previous parameter estimation methods, parameters were determined by calculation of the dependent variable at each experimental point, summation of the squared differences between the calculated and measured values, and adjustment of the parameters to minimize this sum. Any errors in the measured independent variables were therefore ignored.

The most important feature of the Prausnitz, *et al* (1980) program is the attempt to properly account for all measurement errors. This is in contrast to the previous parameter estimation methods which give only estimates for the parameters and no measure of their uncertainty. The regressional method was based on a general application of the maximum likelihood principle, as described by Anderson, *et al* (1978).

Objective Function

The Prausnitz, *et al* (1980) program used the combined method,

$$x_i \gamma_i f_i^{OL} = y_i \phi_i P$$

to seek the parameters that minimized the objective function (S) :

$$S = \sum_{i=1}^{m} \left[\frac{(P_i^c - P_i^e)^2}{\sigma_p^2} + \frac{(T_i^c - T_i^e)^2}{\sigma_T^2} + \frac{(x_i^c - x_i^e)^2}{\sigma_x^2} + \frac{(y_i^c - y_i^e)^2}{\sigma_y^2} \right] \tag{8.9}$$

where m is number of data points, σ the estimated variance of the particular measurement and superscripts c and e denote the calculated and experimental values respectively.

Parameter Variance and Co-Variance Matrices

The fitted parameter's, variance and covariance matrices which were obtained as a last step in the iterative calculation of the parameters give an indication of the uncertainties of the parameters.

The percentage confidence ellipses (regions within which the parameters can be expected to lie at the confidence level associated with the ellipse) can be calculated from the eigenvalues and eigenvectors of the variance and co-variance matrix.

The parameter correlation coefficients were also obtained from the above matrices. These coeficients give an indication of the interdependence of parameters. Correlation coefficient 0, is an indication of independent parameters and ±1, of highly correlated parameters.

Highly correlated parameters, which can also be deduced from the shape and slope of the confidence ellipses, (the slope of which approaches 45° for highly correlated values), implies there may be some difficulty in obtaining a *unique set* of parameters. When parameters are strongly related some linear combination of the two parameters may represent the data as well as the individual parameters. Eliminating the one parameter would yield a single parameter equation to represent the binary vapour-liquid equilibrium data, as noted by Abrams (1975) and described in section 3.5.2.

Residuals

In addition to the variance-covariance matrix the maximum likelihood method also generates the best estimate w.r.t. the model chosen of each measured variable in the course of the parameter estimation. The differences between these "true" values and experimentally measured values will be refered to as residuals.

Examination of the residuals when plotted against another system variable such as liquid mole fraction may provide useful information on excessive experimental error, systematic error, "bad" data points or lack of model fit.

When a suitable model is used to describe experimental data free of any systematic error the residuals are randomly distributed with zero means.

If there is sufficient flexibility in the choice of model and if the number of experimental data points is large it should be possible to fit data to within the experimental uncertainties of the measurements. If such a fit is not obtained it is either a shortcoming of the model, its inability to describe the system, or greater random measurement errors than expected or some systematic error in the measurements.

8.4.2 Bubble-P Correlation Program (Program 2)

This program performs a bubble-pressure calculation where the temperature and the liquid phase mole fractions are specified. An iterational procedure, based on the combined method, is followed to find the equilibrium pressure and vapour-phase mole fraction. A schematic diagram of the program is shown in Figure 8.1.

It was noticed during some data point iterations in loop 1 (Figure 8.1) that the sum of the y_i's would be greater than 1. This would sometimes result in instabilities and consequently no convergence was achieved in the iterational loop. The y_i's were normalized as shown in Figure 8.1 and convergence was achieved. The convergence criterion was :

$$\left[\left(P_{\text{present iteration}} - P_{\text{previous iteration}} \right) / P_{\text{present iteration}} \right] * 100 < 0{,}5$$

$$\left[\left(1 - \Sigma y_i\right) / 1 \right] * 100 < 0{,}5$$

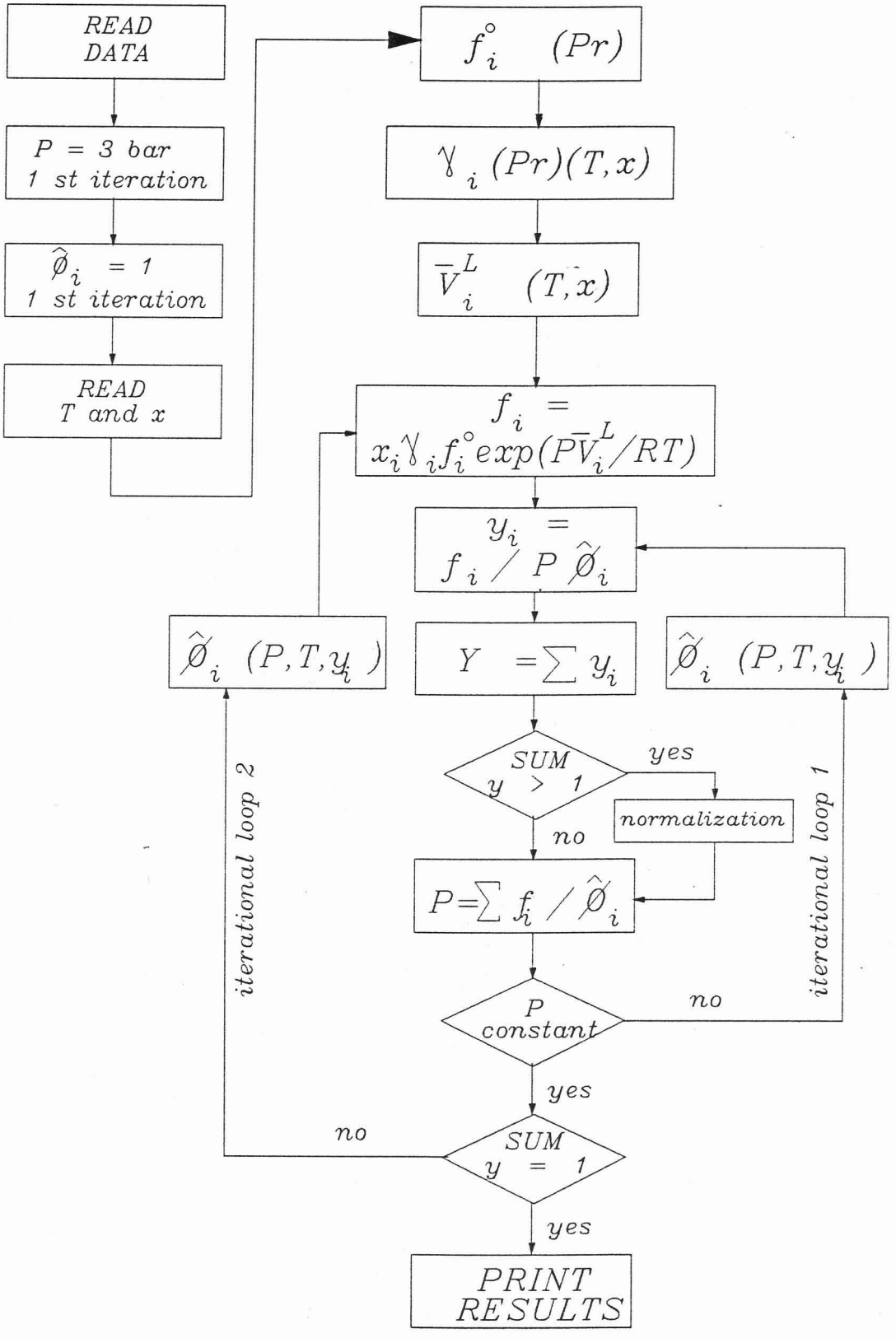

Figure 8.1 : Schematic Diagram of Bubble-Pressure Program used in this project

8.4.3 Consistency Test Programs

In the Chueh, *et al* (1965) and vapour phase consistency tests, integration by graphical methods was not practical. The quantities K_2/K_1, $\hat{\phi}_2/\hat{\phi}_1$, V^L and V^v were calculated at the experimental data points by the program and estimates of the various areas were obtained by numerical integration with the aid of the trapezoidal method (Scheid 1968 or Perry and Green 1984) :

$$\int_{x_0}^{x_n} y(x)dx \simeq \frac{1}{2}h\ [y_o + 2y_i + \ldots + 2y_{n-1} + y_n]$$

In the Chueh, *et al* (1965) Consistency Test for the carbon dioxide/toluene system the Peng Robinson EOS was used to calculate the fugacity coefficient ratio and the Rackett equation for the liquid molar volumes.

In the Vapour Phase Test the fugacity coefficients were calculated as in Chueh's Test however the vapour molar volumes were obtained from the P-R EOS.

For the propane/1-propanol system the Virial, P-R or Group Contribution EOS could be used with the Rackett or GC EOS for the liquid molar volumes. The vapour phase test used a single EOS to obtain the relevant vapour phase fugacity coefficients and vapour molar volumes.

8.4.4 Determination of EOS Compressibility Factors (Z)

The root determination method suggested in Perry and Green (1984) for cubic equations was used to solve the cubic form of the P-R EOS for its roots of Z. These roots of Z were required to calculate the fugacity coefficient. The quartic form of Mohamed and Holder's P-R EOS was solved for its quadratic roots of Z by the method suggested in the Hewelett Packard Maths Pac Manual.

Wegsteins iterational method, (Meyers and Seider 1976) was used to find the compressibility factor Z for the GC EOS which satisfied Eq. (3.45). No problems were experienced in determining Z^{vap} by Wegsteins method. Obtaining Z^{liq} however, was more problematical. Wegsteins method would sometimes diverge and no result would be obtained even if close initial estimates and small interval step changes were specified. Wegsteins method was modified by the inclusion of a relaxation method. The new value generated by Wegsteins Method was limited by a relaxation factor R = 0,005 as follows,

$$F(N+1) = F(N) + R(F'(N+1) - F(N))$$

where $F'(N+1)$ was the new estimate obtained from Wegsteins Method. This factor coupled with close initial estimates produced convergence.

This method is not entirely satisfactory and a method such as Brent's method (Press, *et al* 1987) which is guaranteed to converge so long as the function can be evaluated within the initial interval known to contain a root, would have been more satisfactory. This was not attempted due to time considerations.

8.5 APPLICATION OF PARAMETER FITTING AND CORRELATION PROGRAMS ON THE EXPERIMENTAL DATA

8.5.1 Carbon Dioxide/Toluene System

8.5.1.1 Determination of UNIQUAC (α_{ij}) with the Virial EOS (Program 1)

UNIQUAC parameters

Using the Virial equation for the vapour phase, the UNIQUAC interaction parameters (α_{ij}) were obtained from the fitting program (Program 1) for the experimental data of Ng and Robinson (1978) (38, 79 and 120 °C) , a combination of low pressure, Kim, *et al* (1986), and high pressure, Ng and Robinson (1978), data (79 °C) and this project's data at 79 °C. The data are listed in Table F.1 Appendix F.1.

The fitting program did not converge for a few of the data sets. The changes in parameter values between successive iterations became so small however, (less than 0,1 % of the estimated parameter), that the estimated parameters were considered acceptable. The UNIQUAC parameters obtained are shown in Table 8.3 and Figure 8.2. Convergence was found to be sensitive to the initial parameters chosen at the start of the fitting procedure.

As an experiment, the effect of a temperature-dependent co-ordination number z in the UNIQUAC equation varying in accordance with the universal function proposed by Skjold-Jorgenson, *et al* (1980) Eq. (3.57) was also investigated. The effect on the predictions was generally minor as may be seen from Table 8.3.

Confidence ellipses

Analysis of the co-variance matrices for the data sets permitted plotting of the 90 & 95 % confidence regions as described by Beck and Arnold (1977) and shown for the 38 °C data set in Figures 8.4. The elongated shape of the confidence ellipses are an indication that the parameters are highly correlated. The correlation matrix for the various temperatures had diagonal values of +/- 0,90 a further indication that the parameters are highly correlated.

According to Fabries and Renon (1975) this is to be expected for nearly ideal solutions and suggests the possibility of describing the UNIQUAC equation as a single parameter equation.

Residuals

The residuals for the 38 °C data set are given in Figure 8.6. The T , p and x residuals appear to be randomly distributed and have zero means. The absolute values of the residuals do however appear to increase with pressure. The y -residuals are nearly all negative. Statistical trends for the data sets at higher temperatures were similar.

Table 8.3

Carbon Dioxide/Toluene System : UNIQUAC Parameters as a Function of Temperature

Temp. °C	Regression type	z (b)	Data (a)	Equation of State			
				Virial		PR	
				UNIQUAC Parameter (Kelvin)			
				a_{12}	a_{21}	a_{12}	a_{21}
38	P T X Y	10	1	170,13	112,10	99,35	182,24
79	P T X Y	10	1	232,49	99,09	256,67	84,08
79	P T X Y	10	2	227,55	105,31	250,44	91,53
79	P T X Y	10	3	224,57	115,96	245,17	102,54
120	P T X Y	10	1	237,27	122,35	384,70	37,16
38	P T X Y	S & J	1	173,25	114,05	103,08	183,36
79	P T X Y	S & J	1	240,00	107,40	270,25	86,96
79	P T X Y	S & J	2	235,71	113,01	257,73	99,76
79	P T X Y	S & J	3	232,67	123,87	254,63	109,91
120	P T X T	S & J	1	253,27	133,06	393,31	53,27

(a) (1)Ng and Robinson (1978)
(2)Kim, *et al* (1986)
(3)This Project

(b) S & J Universal function proposed by Skjold-Jorgenson, *et al* (1980)

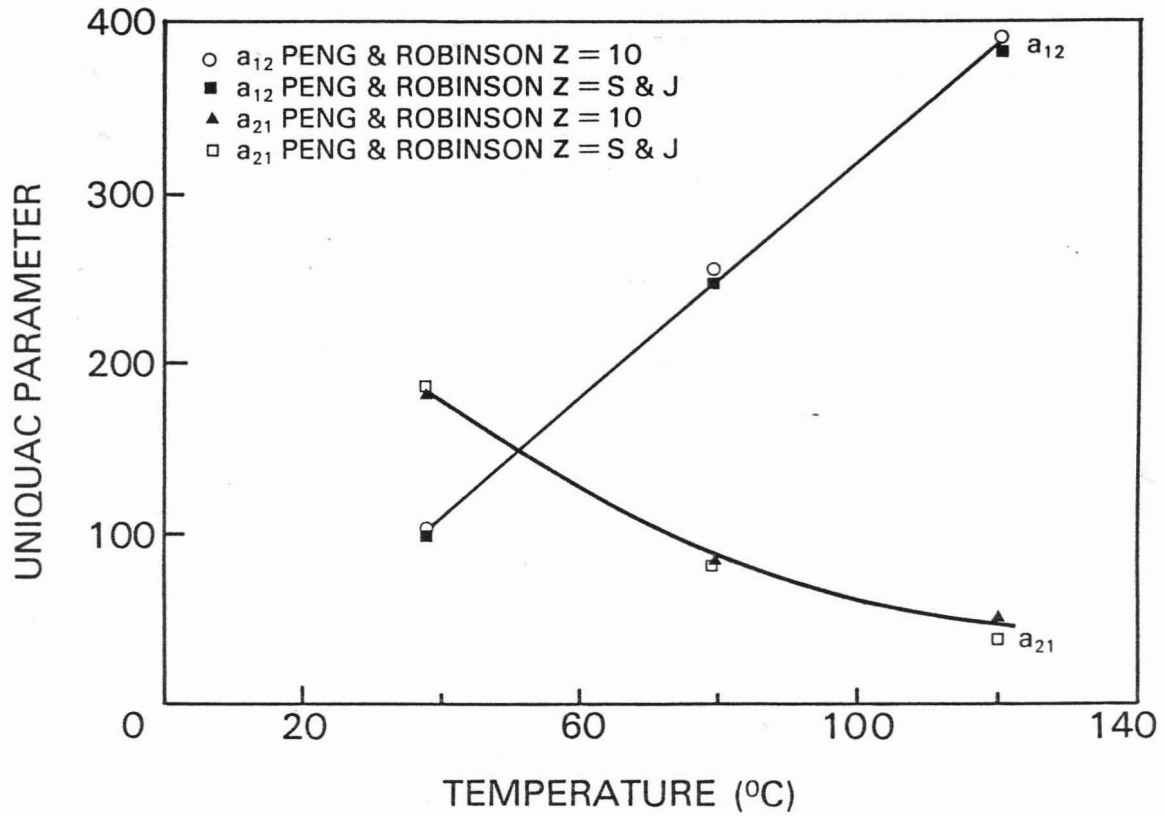

Figure 8.3 : UNIQUAC parameters as a function of temperature for the Carbon Dioxide / Toluene system

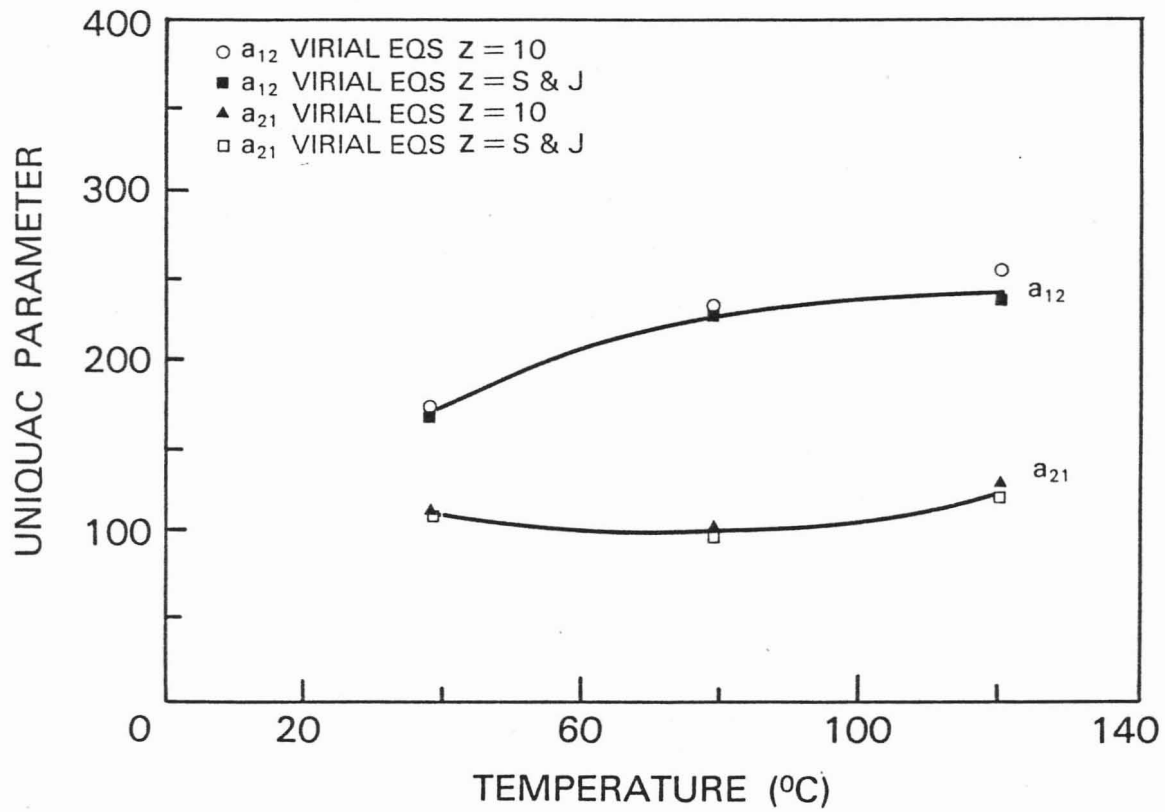

Figure 8.2 : UNIQUAC parameters as a function of temperature for the Carbon Dioxide / Toluene system

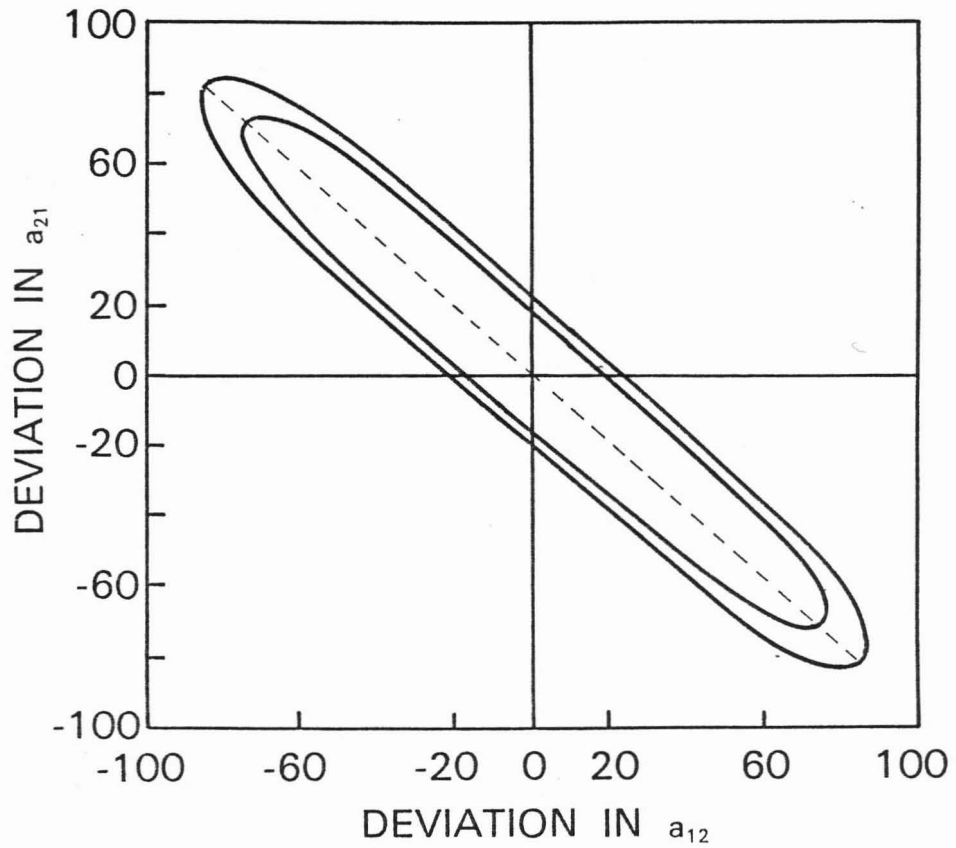

Figure 8.4 : Confidence ellipses for the Carbon Dioxide / Toluene system at 38 °C (Virial EOS)

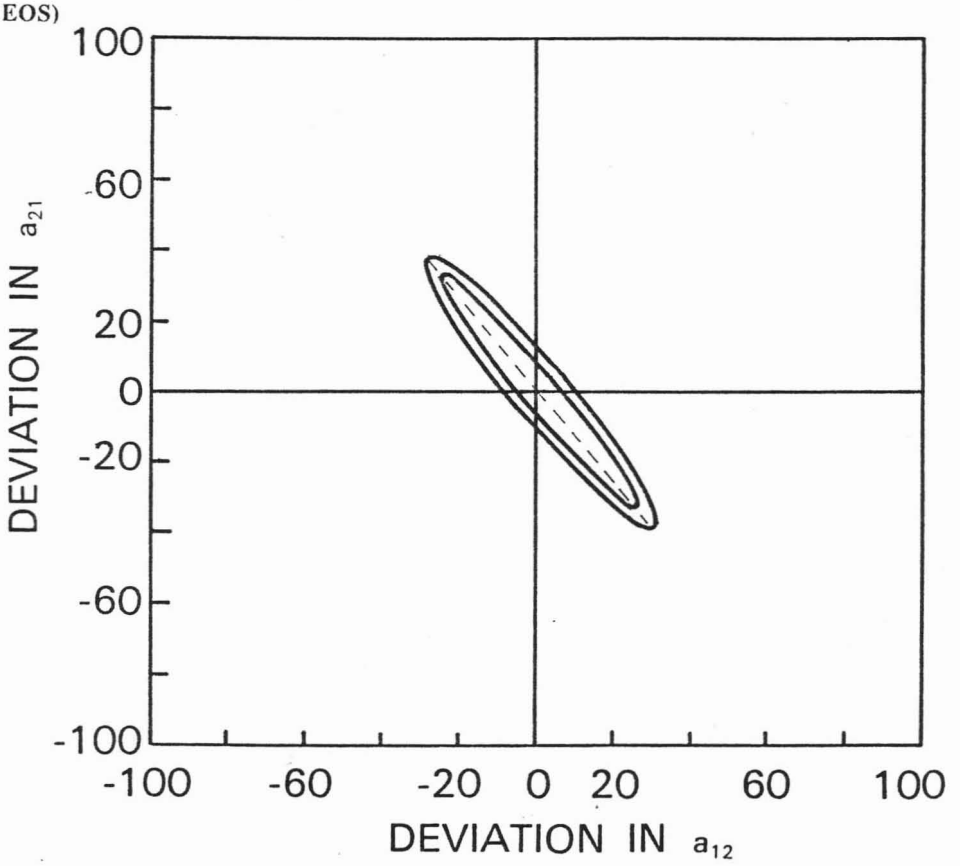

Figure 8.5 : Confidence ellipses for the Carbon Dioxide / Toluene System at 38 °C (P-R EOS)

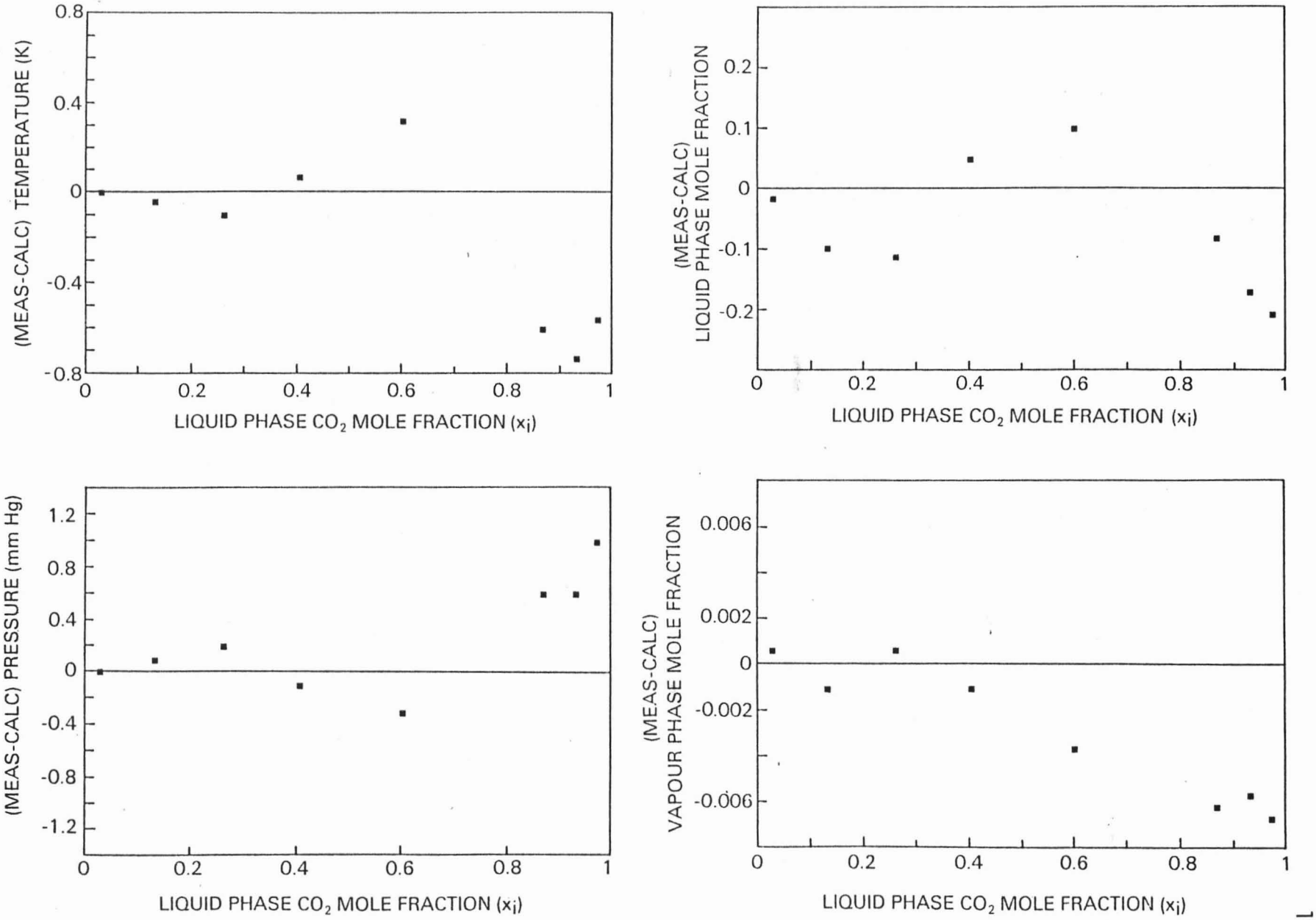

Figure 8.6 : Residuals for Carbon Dioxide / Toluene system at 38 ^{o}C

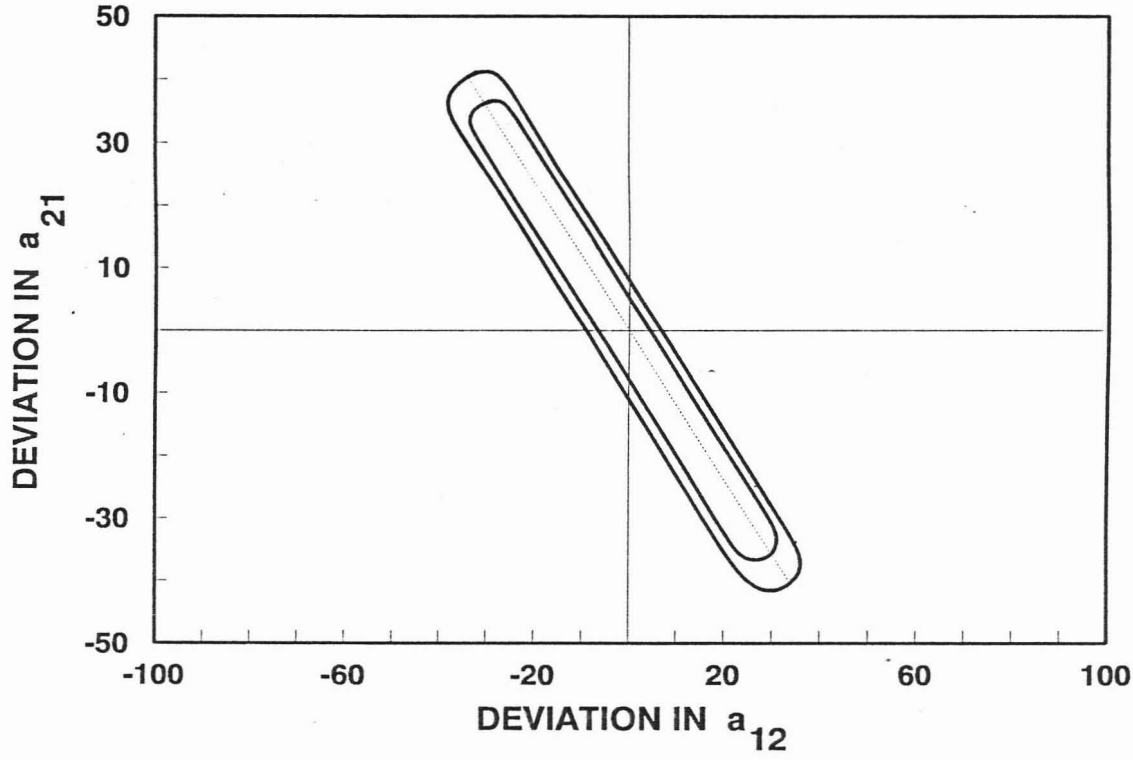

Figure 8.7 : Confidence ellipses for the Carbon Dioxide / Toluene System 79 °C (Z = 10 / P-R EOS)

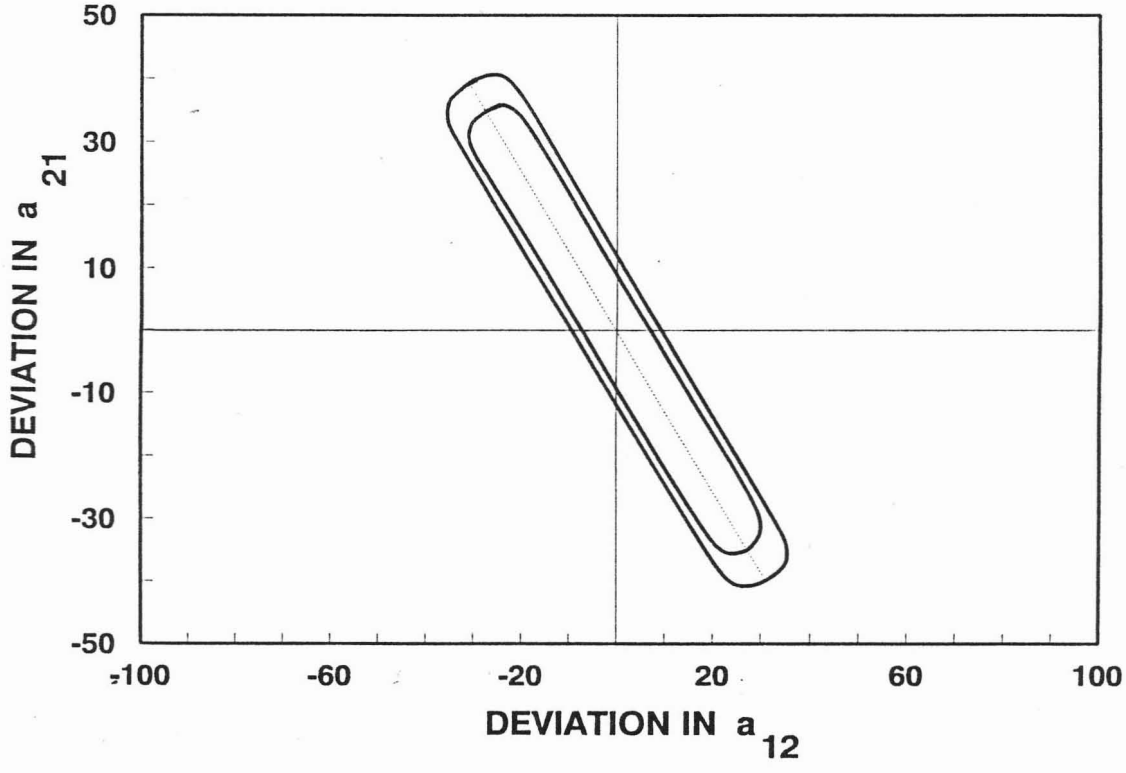

Figure 8.8 : Confidence ellipses for the Carbon Dioxide / Toluene System 79 °C (Z = S&J / P-R EOS)

8.5.1.2 Correlation program applied with UNIQAC/Virial EOS (α_{ij}) parameters (Program 2)

For the UNIQUAC equation with the two parameter Virial EOS the vapour phase mole fractions and total pressures are compared with the experimental data in Figures 8.9 to 8.11 for the Ng & Robinson data, Figure 8.12 for the combined Ng & Kim data, Figure 8.13, for this project's data.

There was no convergence for the higher pressures at the higher temperatures. At low to moderate pressures prediction is good. At higher pressures, as expected, prediction is increasingly unsatisfactory and suggests the need for the third virial coefficient.

As an experiment the P-R EOS was used in the correlational program together with UNIQUAC parameters derived from the Virial EOS. The inclusion of the P-R EOS resulted in a significant improvement in the predictions in the high pressure region.

To improve the fitting program of Prausnitz, *et al* (1980) a Peng-Robinson EOS subroutine for calculation of the vapour phase fugacities was added.

8.5.1.3 Determination of UNIQUAC (α_{ij}) with the Peng-Robinson EOS (Program 1)

The new UNIQUAC interaction parameters obtained using the P-R EOS are shown in Figure 8.3 (for the Ng & Robinson data as a $f\ (T)$) and Table 8.3. They differ substantially from those shown in Figure 8.2 and are strongly temperature dependent.

The P-R EOS interaction parameters (δ_{ij}) used were the temperature dependent values suggested by Mohamed and Holder (1987) and listed in Table 8.1.

Analysis of the co-variance matrix yielded the 90 & 95 % confidence ellipses as shown in Figures 8.7 and 8.8 for this project's 79 °C data.

The confidence ellipses for the P-R EOS fitted parameters are generally smaller than those for the Virial EOS Figures 8.4 and 8.5.

The parameters were still however highly correlated with correlation matrix diagonal values in the order of 0,9.

The P-R/UNIQUAC residuals were similar to those obtained for the Virial/UNIQUAC combination. The magnitudes of the residuals were however, smaller in the high pressure regions.

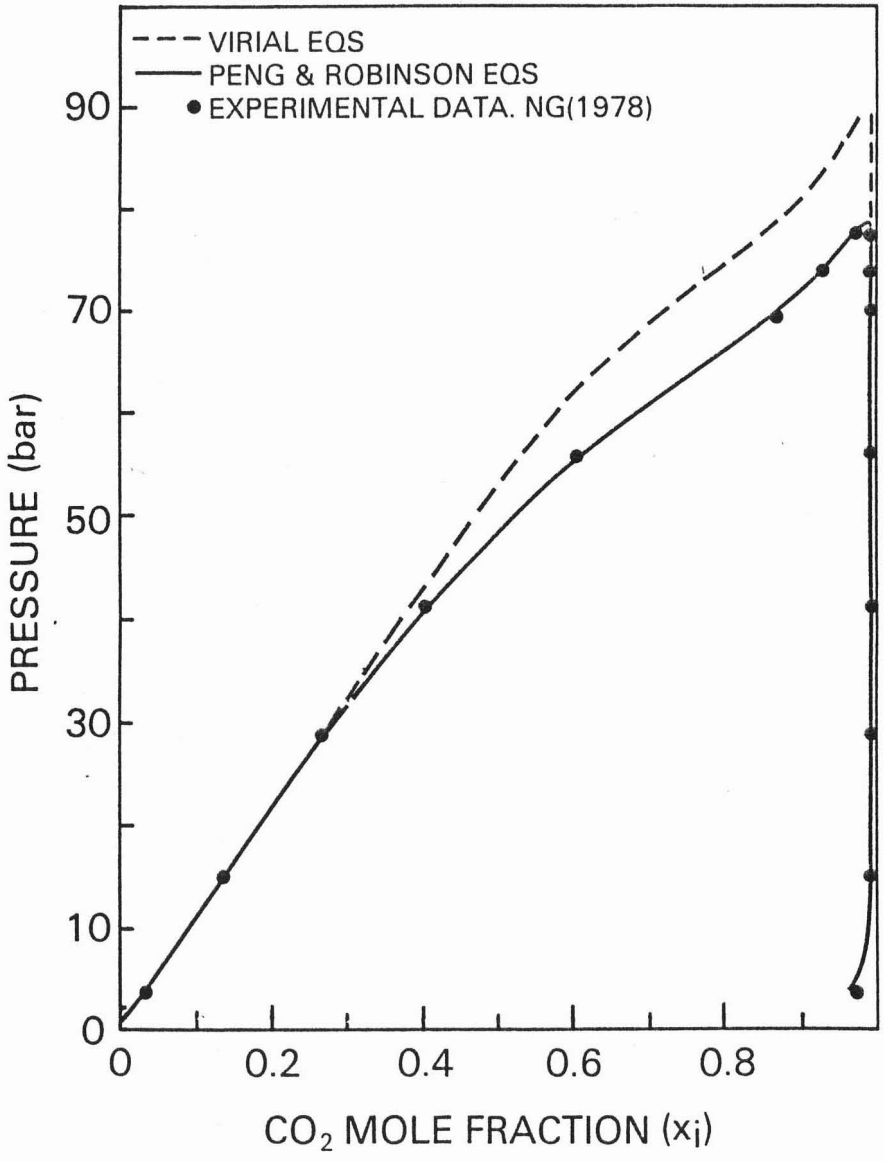

Figure 8.9 : Comparison between theoretically predicted and experimental VLE for the Carbon Dioxide / Toluene system at 38 °C

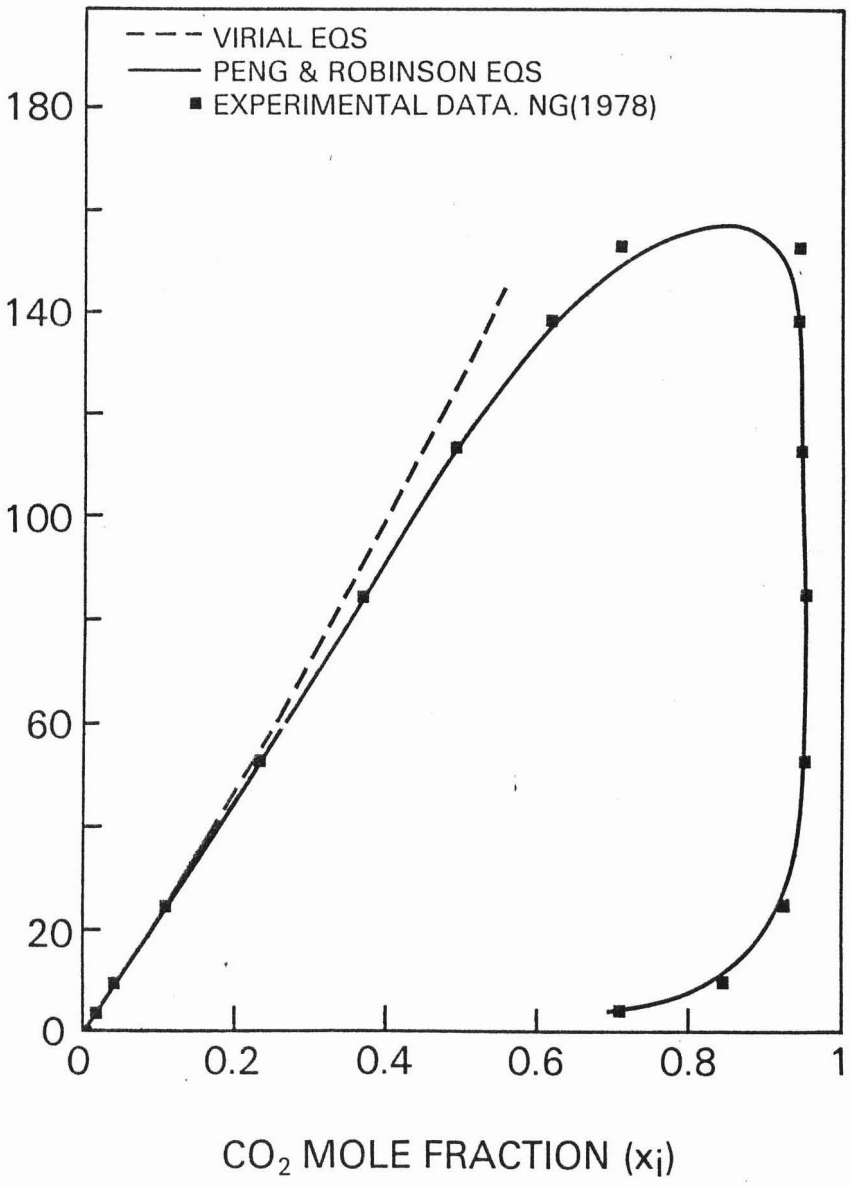

Figure 8.10 : Comparison between theoretically predicted and experimental VLE for the Carbon Dioxide / Toluene system at 120 °C

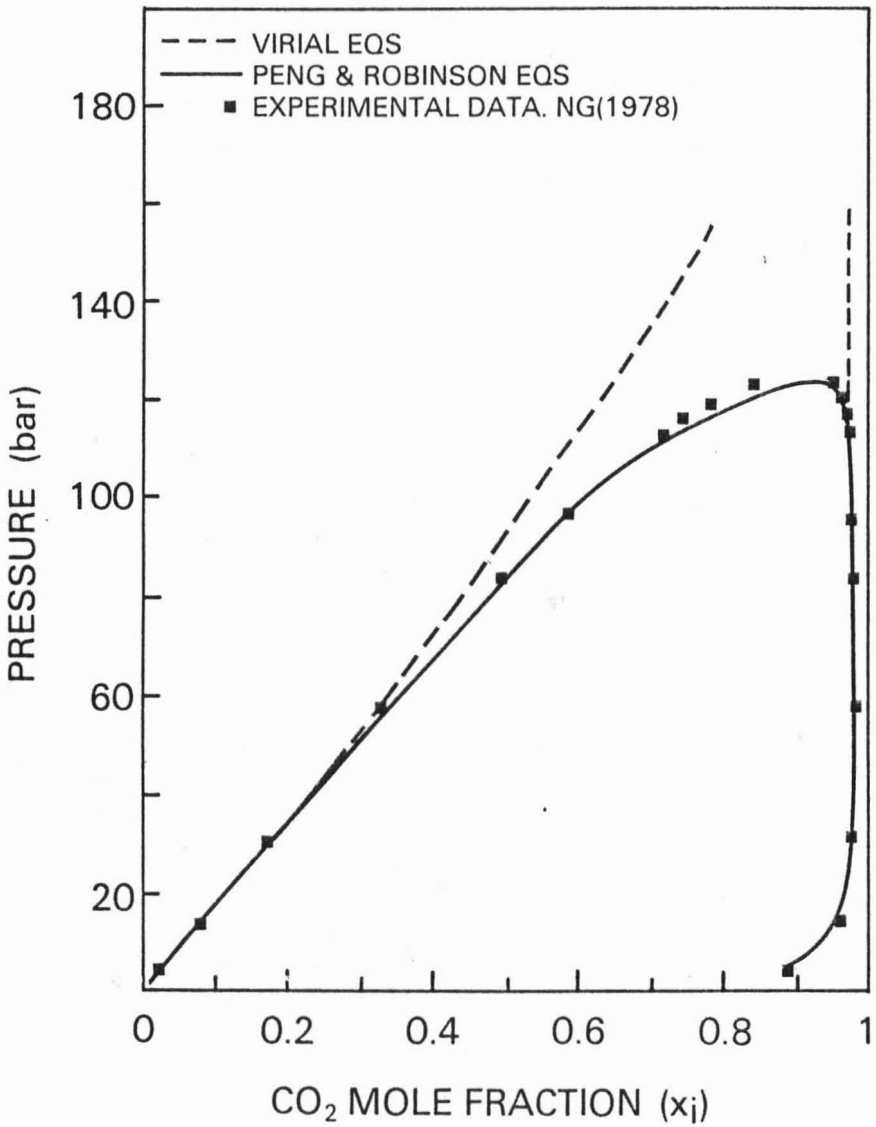

Figure 8.11 : Comparison between theoretically predicted and experimental VLE for the Carbon Dioxide / Toluene system at 79 °C

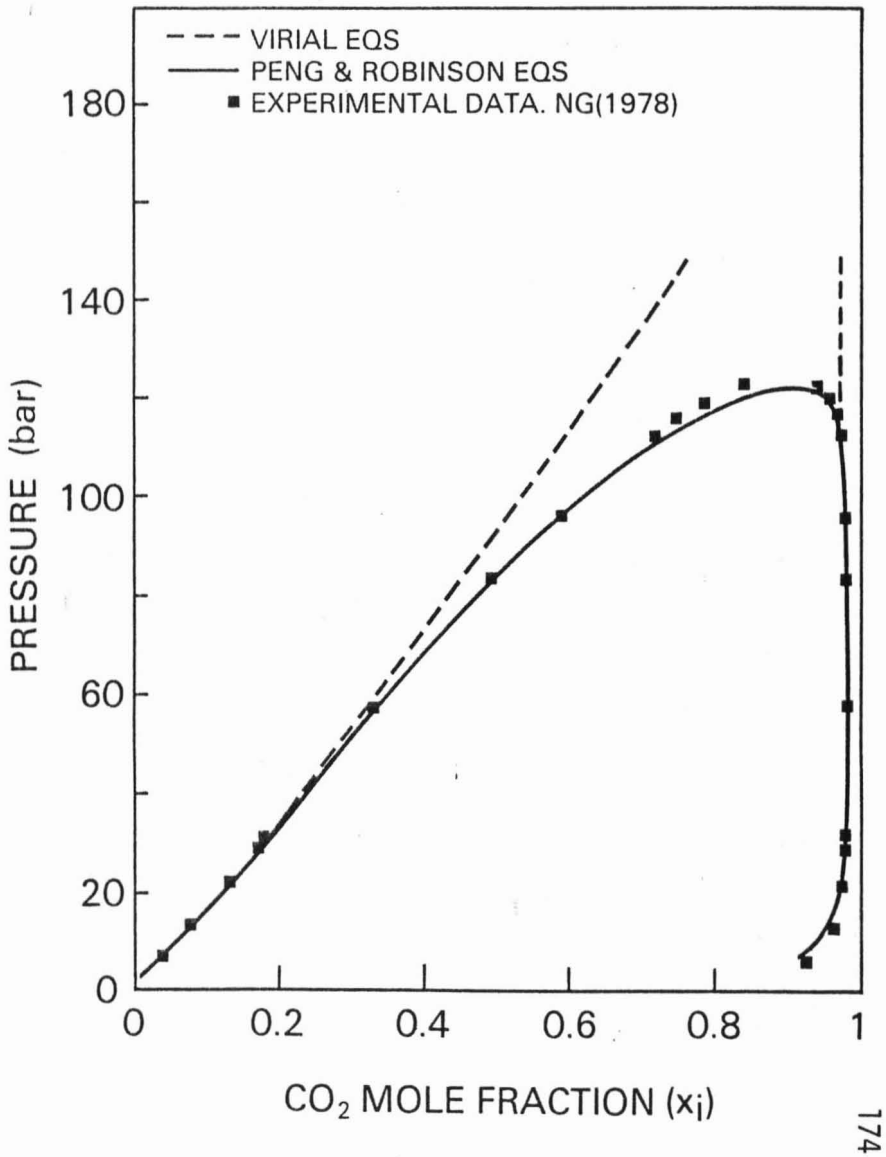

Figure 8.12 : Comparison between theoretically predicted and experimental VLE for the Carbon Dioxide / Toluene system at 79 °C

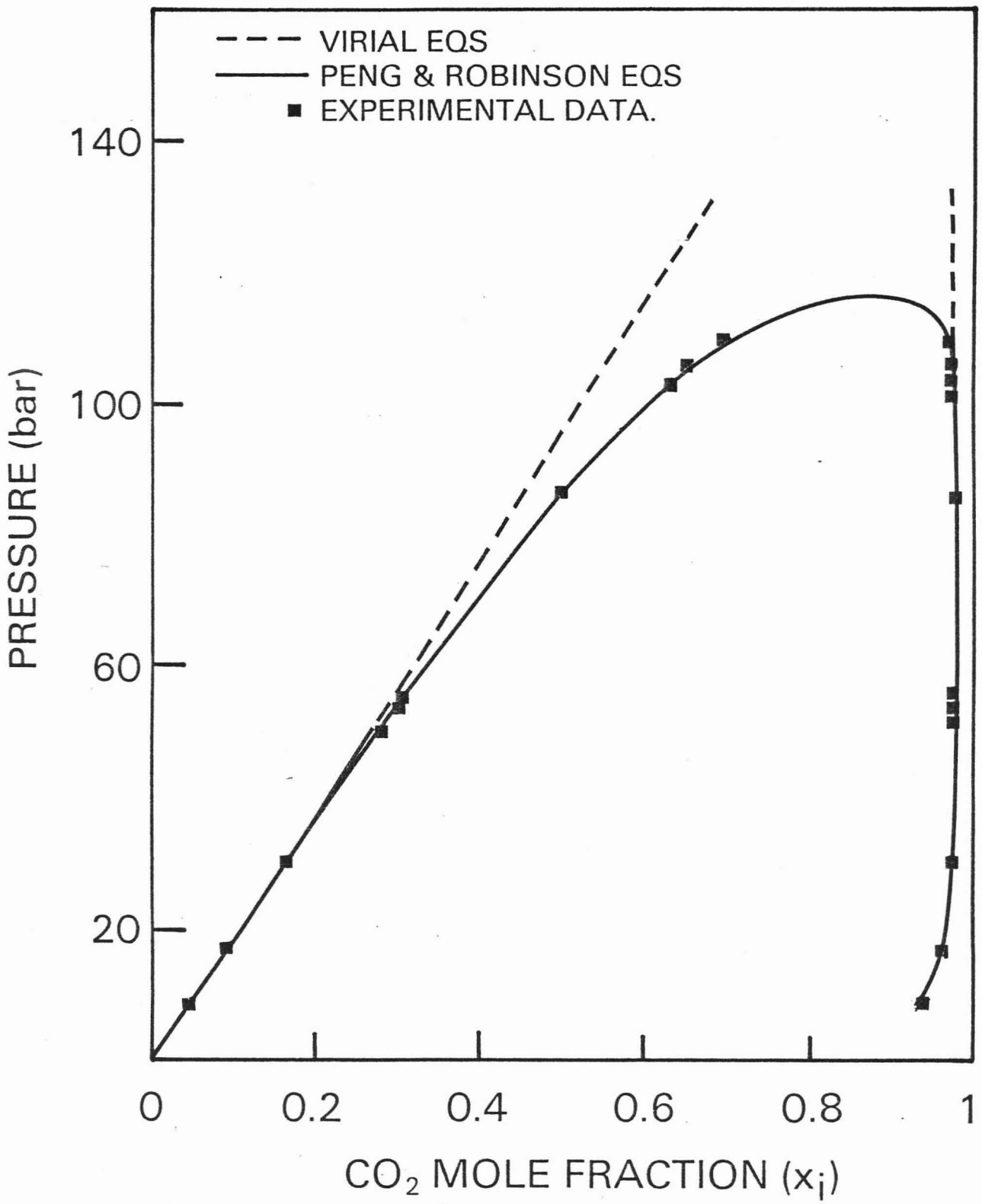

Figure 8.13 : Comparison between theoretically predicted and experimental VLE for the Carbon Dioxide / Toluene system at 79 ^{o}C

8.5.1.4 Correlation program applied with UNIQAC/Peng-Robinson EOS (α_{ij}) parameters (Program 2)

Predicted vapour-phase compositions and total pressures when using the new parameters are compared with experimental values in Figures 8.9 to 8.13.

The correlations based on the combination of UNIQUAC and P-R EOS are in excellent agreement with the experimental values at both high and low pressures, whereas those based on the truncated virial equation depart significantly from measured values at higher pressures.

Subroutines for the Mohamed and Holder (1987) density dependent mixing rule P-R EOS, (Eq. (3.44)), were added to the fitting and correlation programs. No improvement in correlation was achieved when compared with the results of the original P-R EOS.

The UNIQUAC interaction parameter values in Figure 8.3 are recommended for interpolation and prediction for the carbon dioxide/toluene system in the temperature range 38 to 120 °C.

Activity coefficients plots are shown for the three temperatures in Figures 8.14 and 8.15.

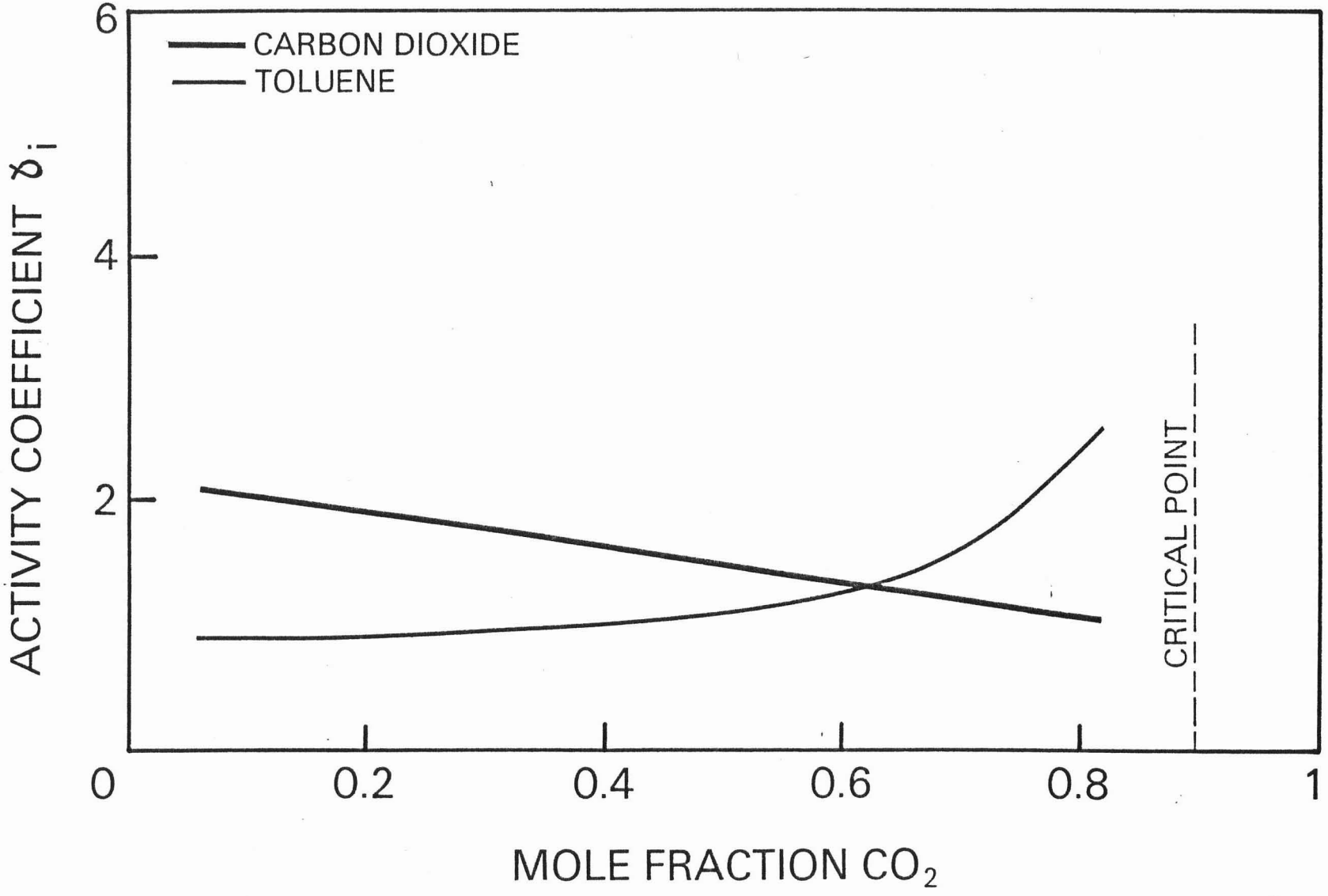

Figure 8.14 : Activity Coefficient Plot for the Carbon Dioxide / Toluene system at 79 °C (this projects data)

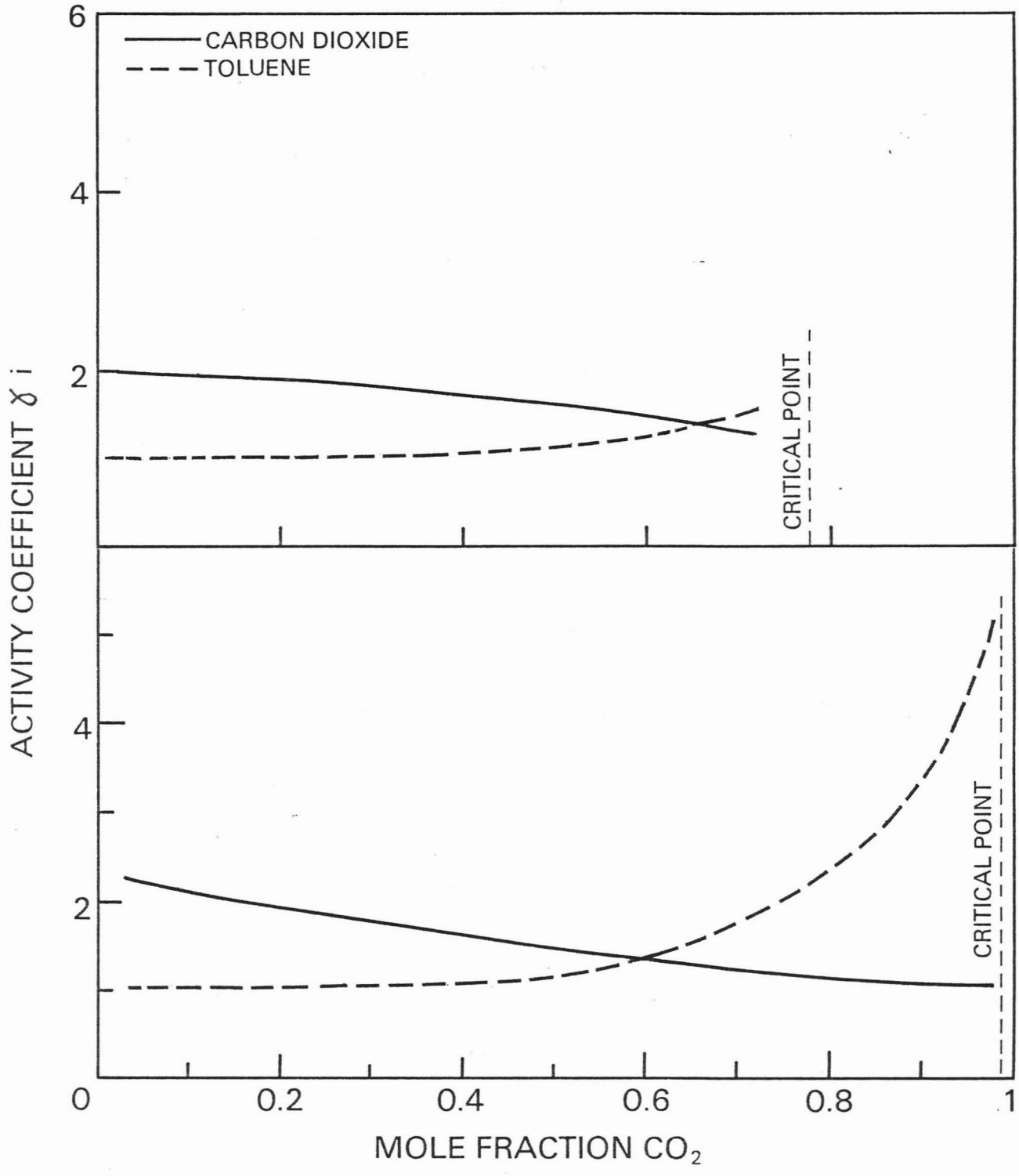

Figure 8.15 : Activity Coefficient plots for the Carbon Dioxide / Toluene system at 38 and 120 ^{o}C

8.5.2 Propane/1-Propanol System

8.5.2.1 Determination of UNIQUAC (α_{ij}) with various EOS (Program 1)

UNIQUAC parameters

Using the Virial, Peng-Robinson and Group Contribution EOS the UNIQUAC interaction parameters obtained from the fitting program on the experimental data sets listed in Table F.2 (Appendix F.1) are shown in Figures 8.16 and 8.17 and Table 8.4.

Confidence ellipses

Analysis of the co-variance matrix for the various data sets permitted the plotting of the 90 & 95 % confidence regions as described by Beck and Arnold (1977). A selected few are shown in Figures 8.18 and 8.20. The elongated shape indicates that the two parameters are highly correlated. The correlation matrices with diagonal values in the region of 0,9 also indicate a high degree of parameter correlation.

All the parameters for this binary are strongly temperature dependent, as is the case with the carbon dioxide/toluene system.

The carbon dioxide/toluene and propane/1-propanol derived UNIQUAC parameters are vapour-phase description dependent. Interestingly enough for the propane/1-propanol binary the parameters follow the same trend, Figures 8.16 and 8.17, for two of the EOS (Virial and GC). The Virial and GC derived parameters also lie within overlapping confidence regions. The exceptions are the α_{12} and α_{21} derived with the Peng Robinson EOS.

A high degree of correlation implies that there are many sets of parameters that can equally well represent the data. Realistic data reduction can therefore only determine a region of parameters. The "non uniqueness" of parameters is not only confined to the combined method. Fink and Hershey (1990) obtained P-R EOS parameters for the carbon dioxide/toluene binary, from various literature sources using the direct method. They report the interaction parameter values to be data-origin-dependent.

Residuals

The P , T , x and y residuals for the three EOS at 81°C are given in Figures 8.21. The P , T and x residuals appear to be randomly distributed and have zero means. The y residuals for this binary, in contrast to the carbon dioxide/toluene binary, are all positive and decrease with increasing pressure. The statistical trends for the higher temperatures are similar and are shown in Figure 8.22.

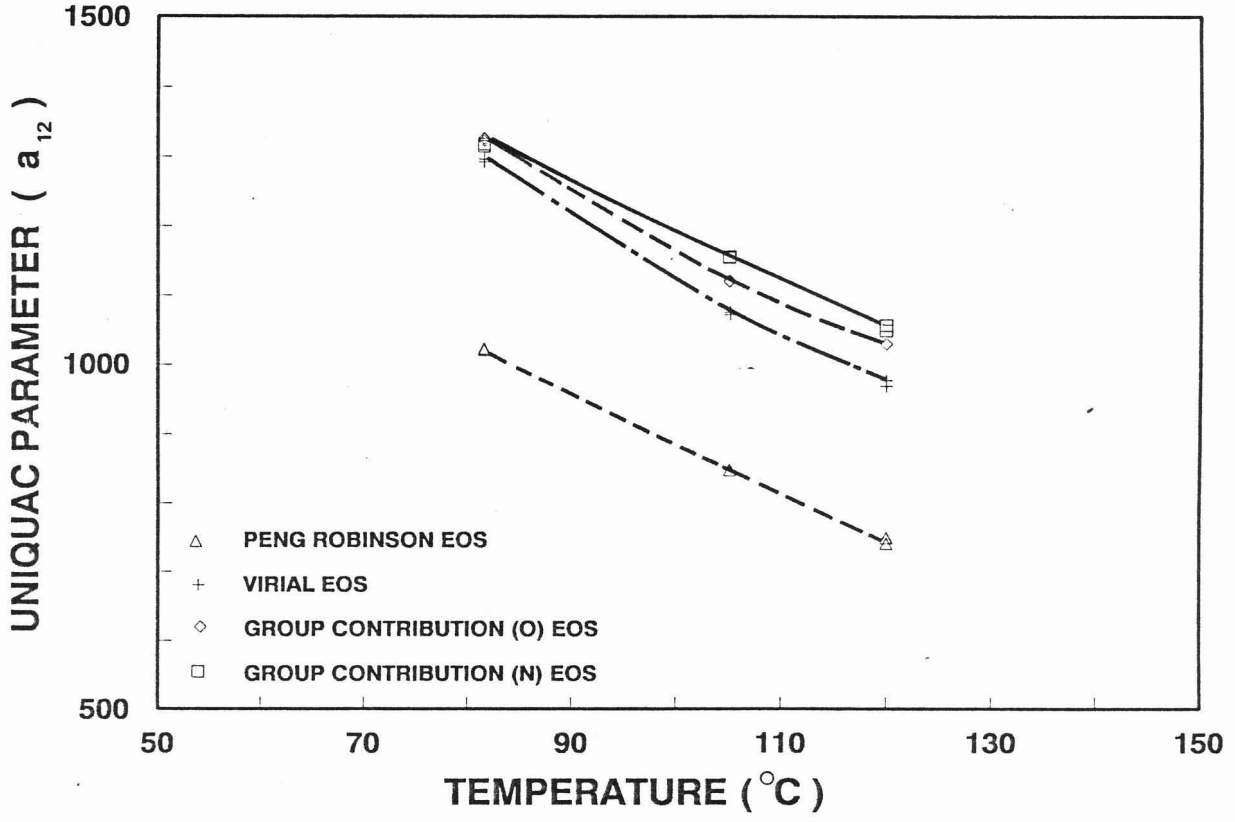

Figure 8.16 : UNIQUAC α_{12} parameters as a function of temperature for the Propane / 1-Propanol system

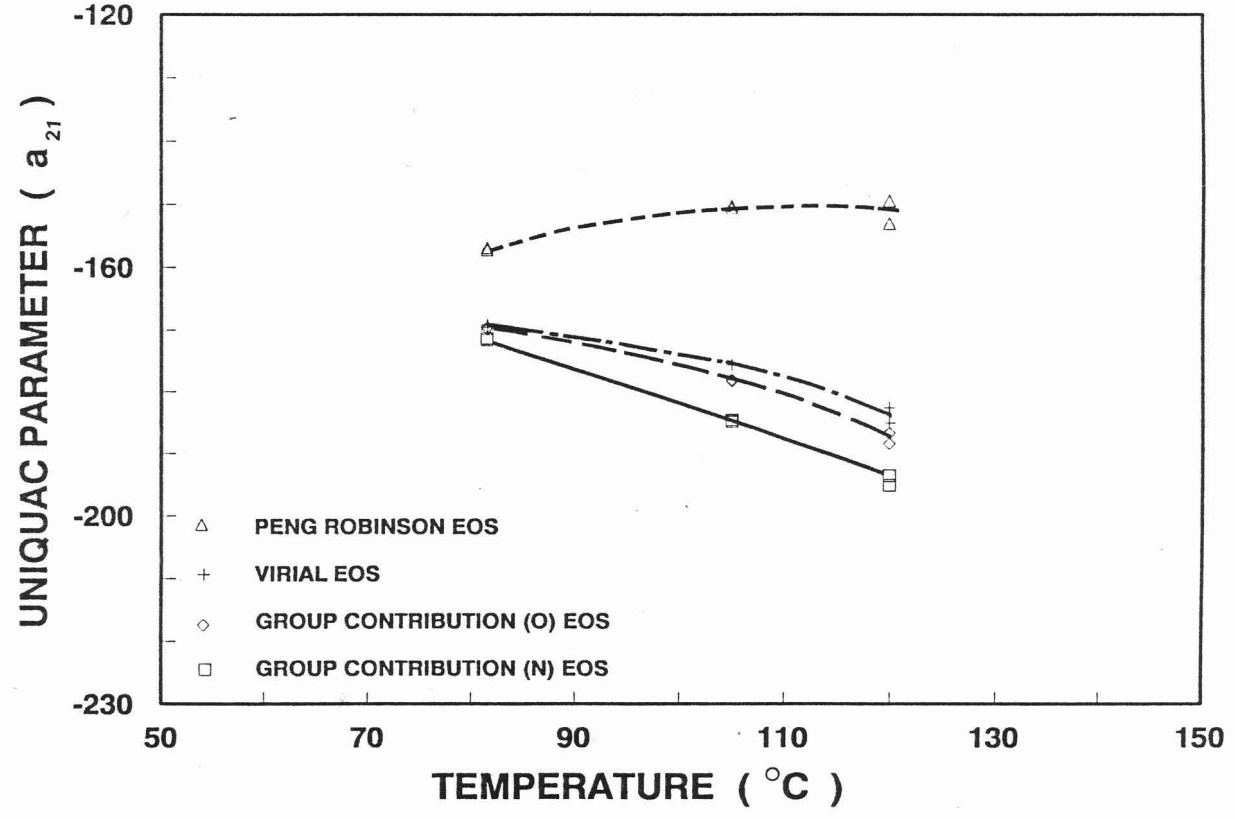

Figure 8.17 : UNIQUAC α_{21} parameters as a function of temperature for the Propane / 1-Propanol system

TABLE 8.4

Propane/1-Propanol System : UNIQUAC Parameters as a Function of Temperature

Temperature °C	Regression type	Equation of State			
		Virial (1)	GC (O) (2)	GC (N) (3)	PR (4)
		UNIQUAC Parameter α_{12} (Kelvin)			
81,62	P T X Y	1 316,94	1 294,66	1 324,97	1 021,14
81,62	P T X	1 313,49	1 290,74	1 321,51	1 019,78
105,11	P T X Y	1 153,25	1 070,53	1 117,77	846,03
105,11	P T X	1 154,52	1 070,56	1 118,84	847,20
120,05	P T X Y	1 055,03	975,28	1 028,47	747,25
120,05	P T X	1 048,77	966,87	1 022,17	739,02
		UNIQUAC Parameter α_{21} (Kelvin)			
81,62	P T X Y	-171,78	-169,63	-169,95	-157,24
81,62	P T X	-171,46	-169,26	-169,64	-156,91
105,11	P T X Y	-184,66	-175,80	-178,20	-150,25
105,11	P T X	-184,90	-175,80	-178,42	-150,58
120,05	P T X Y	-195,08	-185,11	-188,43	-153,09
120,05	P T X	-193,51	-182,67	-186,76	-149,47

(1) Equation (3.26)
(2) Equation (3.45) : Table 8.2 Lit. Ref. A.
(3) Equation (3.45) : Table 8.2 Lit. Ref. B.
(4) Equation (3.30)

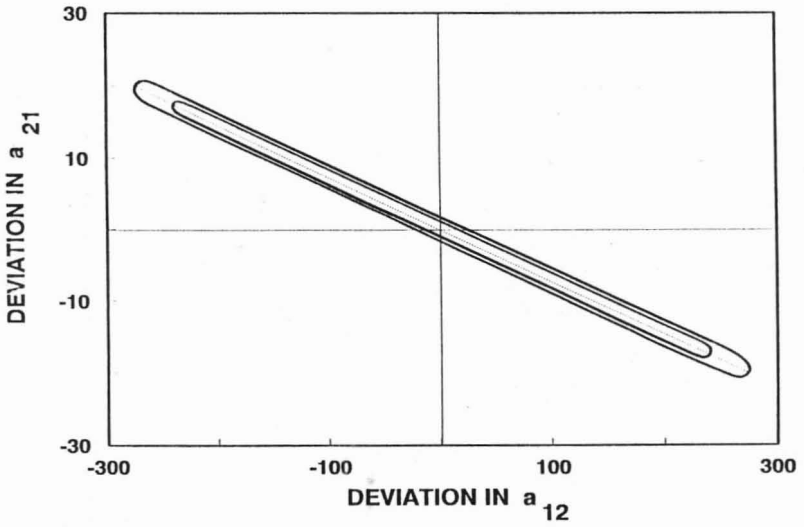

Figure 8.18 : Confidence ellipses for the Propane / 1-Propanol system at 81,6 °C

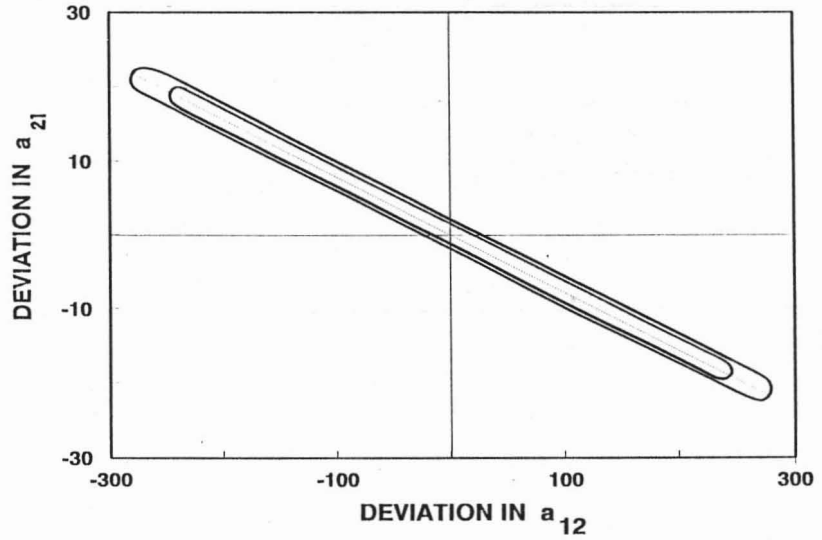

Figure 8.19 : Confidence ellipses for the Propane / 1-Propanol system at 105,1 °C

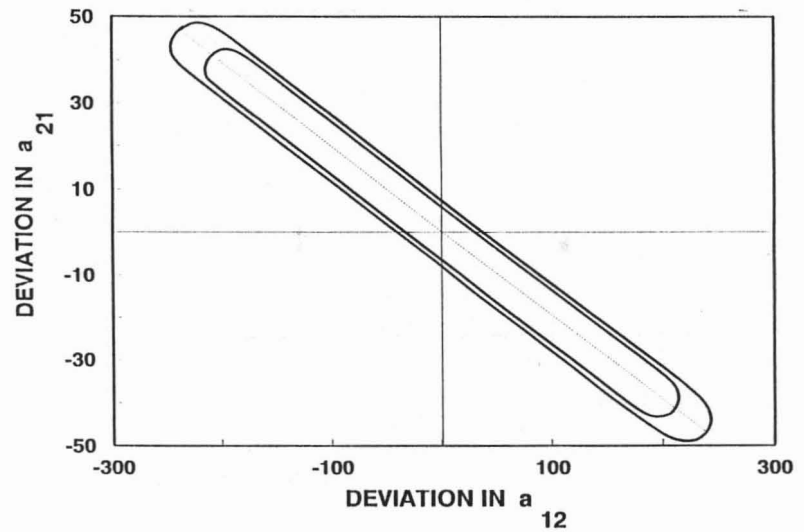

Figure 8.20 : Confidence ellipses for the Propane / 1-Propanol system at 120.1 °C

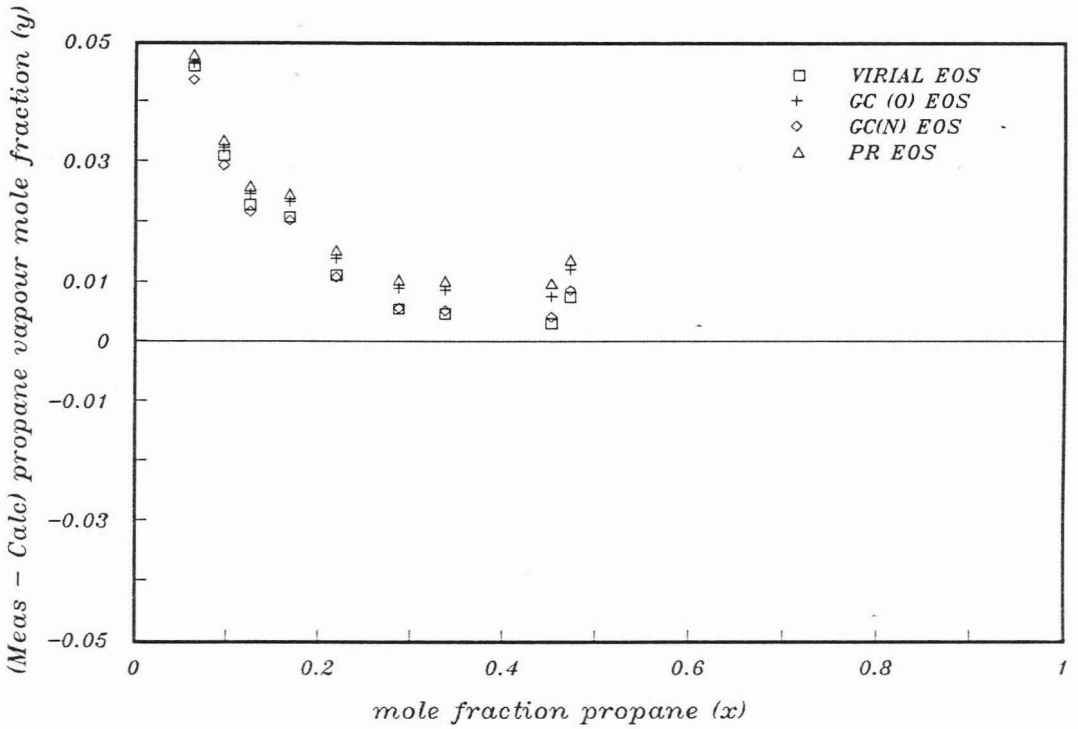

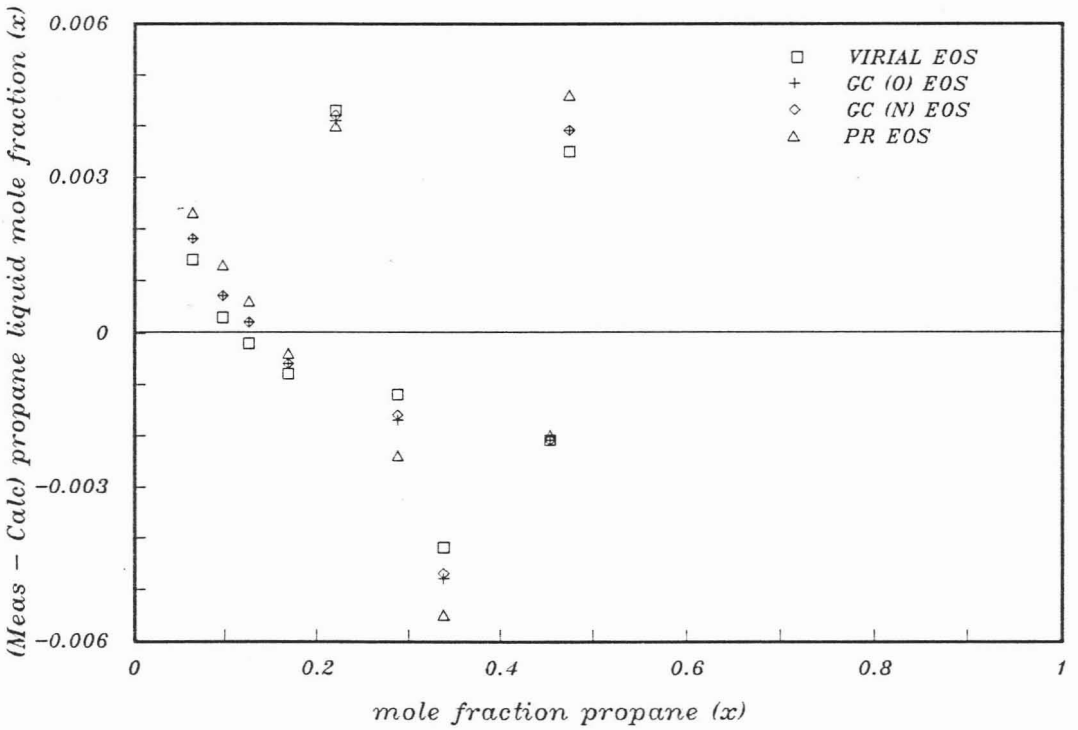

Figure 8.21 continued overleaf

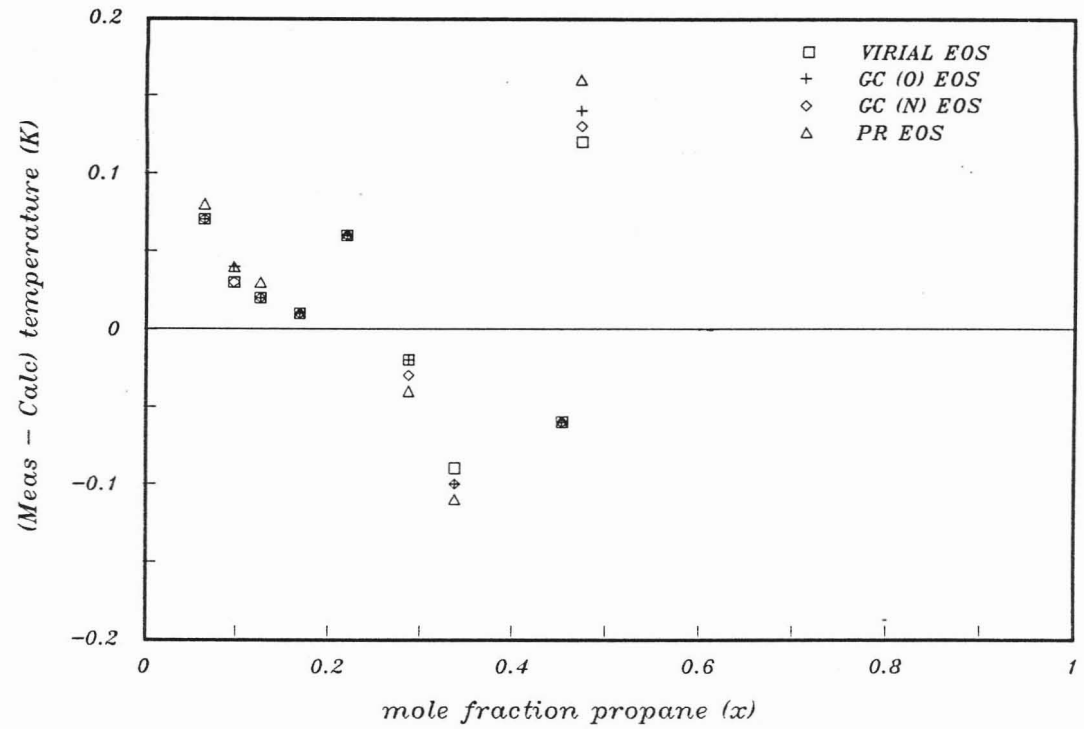

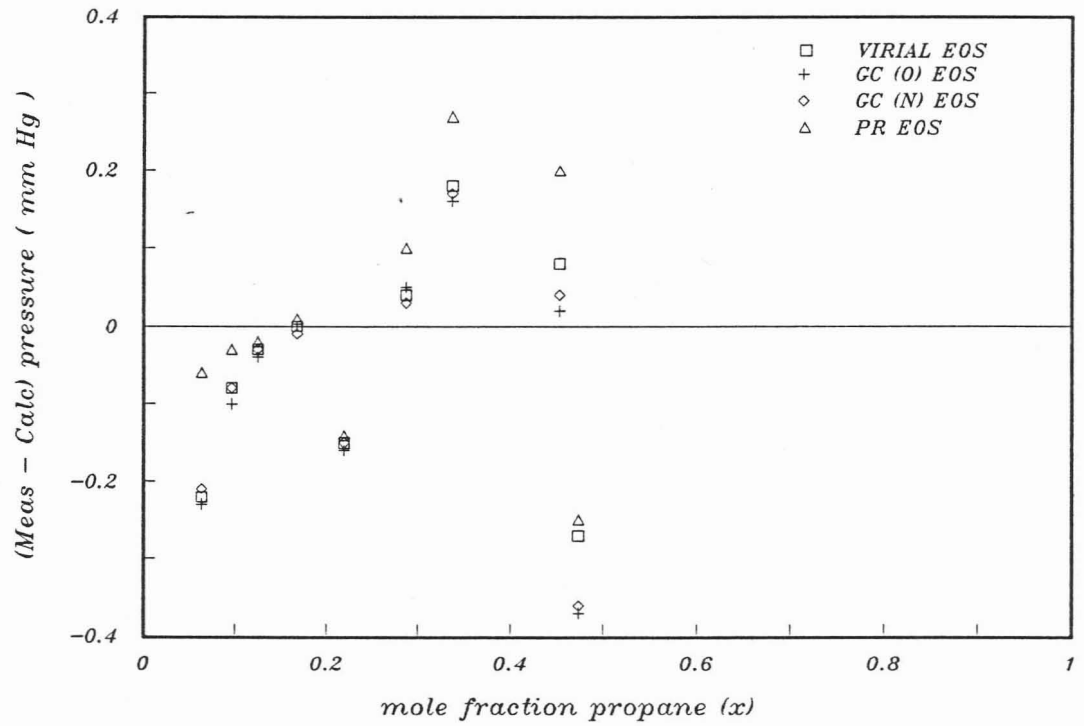

Figure 8.21 : Residuals for the Propane/1-Propanol System at 81,6 °C

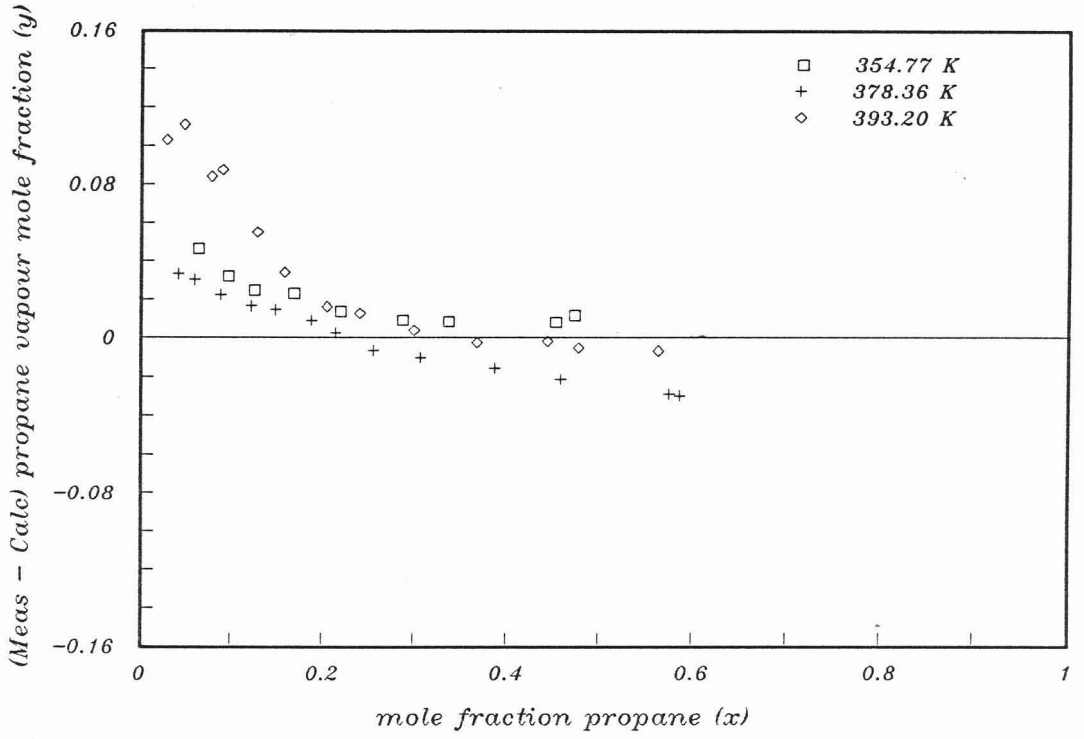

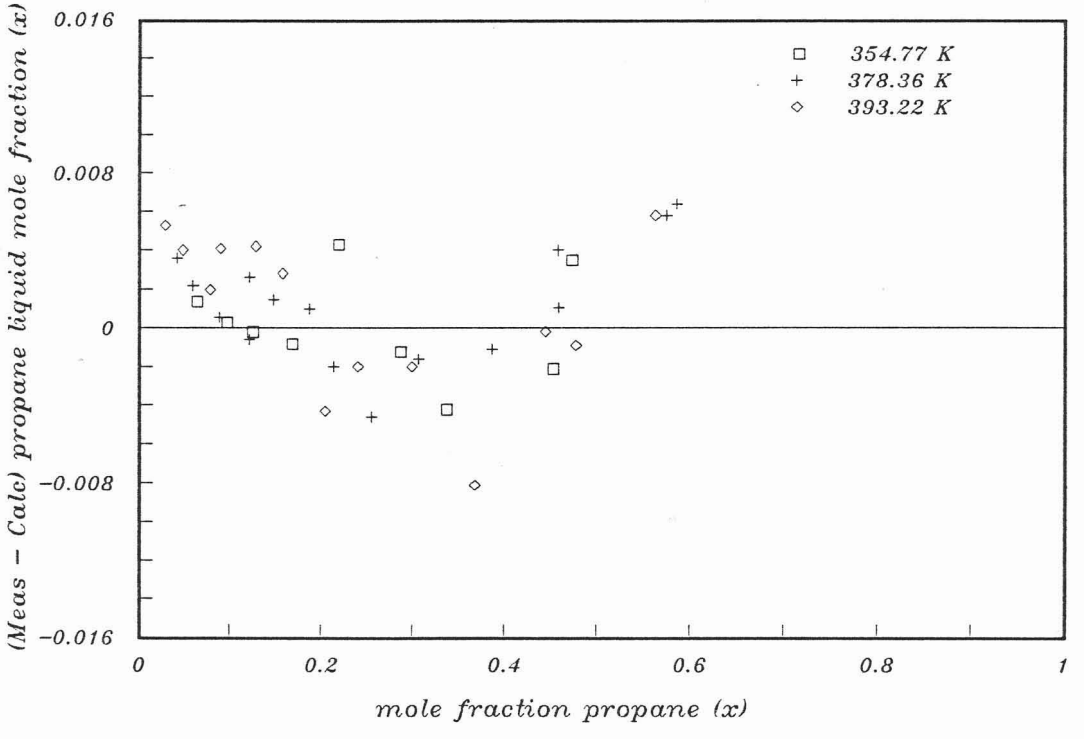

Figure 8.22 continued overleaf

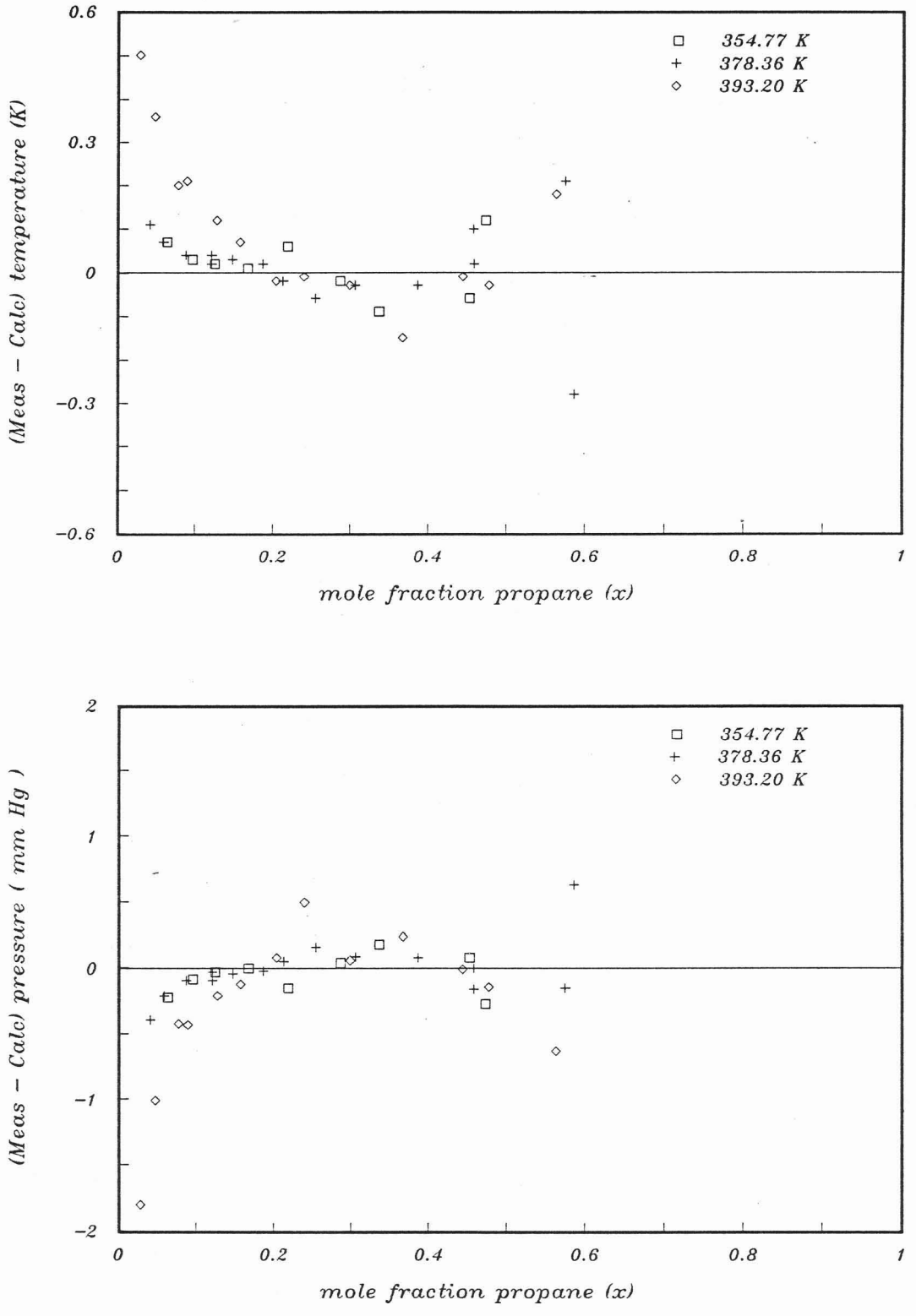

Figure 8.22 : Residuals for the Propane/1-Propanol System at 81,6, 105,1 and 120,1 °C

8.5.2.2 Correlation program applied with UNIQUAC/EOS (α_{ij}) (Program 2)

The predicted vapour-phase compositions and total pressures generated from the correlation program are shown in Figures 8.23 through to 8.34. A plot of the K-values for the GC(N) EOS and UNIQUAC correlation is given in Figure 8.35.

Significant differences between the measured and calculated vapour phase mole fractions are observed for the lower pressure regions for the 81 °C and 120 °C isotherms. This would suggest the measured pressure was either too low if the composition was measured correctly or the measured vapour mole fraction too high if the pressure was measured correctly or a combination of both. The maximum differences certainly are larger than can be accounted for by uncertainties in the experimental measurements.

This would suggest one of the following possibilities :

1. The liquid and vapour phase models chosen, i.e. UNIQUAC and the various EOS were incapable of adequately describing the propane/1-propanol system. Since the predictions for all the different EOS were similar this suggests that either the UNIQUAC equation or the various EOS are not capable of describing the polar component, 1-propanol.
2. The experimental data are incorrect. This is unlikely for experimental data, if measured carefully, are usually more reliable than theoretical predictions. This may be particularly true when EOS are used for polar components such as 1-propanol.
3. Another possible explanation is not related to the measurements or the theory but to the purity of the propane. As already explained the highest purity propane available had contaminants of ethane and butane. The contaminants, effectively diluents in the propane may compete with the 1-propanol at low pressures resulting in a lower 1-propanol presence in the vapour phase than if pure propane had been used. This explanation was deemed unlikely for the following reasons :
    1. It would not explain why the 105 °C correlations are better than those for the other two temperatures.
    2. It would not explain the improved predictions at higher pressures especially for those with the Group Contribution (N) the Virial EOS.
    3. For the propane/water system the correct vapour mole fractions were experimentally determined with a grade of propane containing a greater number and higher quantity of impurities.

The the most likely explanation is therefore the inability of the UNIQUAC and/or the EOS to accurately describe the behaviour of the polar/non-polar binary mixture.

Activity coefficient plots are shown for the three temperatures in Figures 8.36 to 8.38

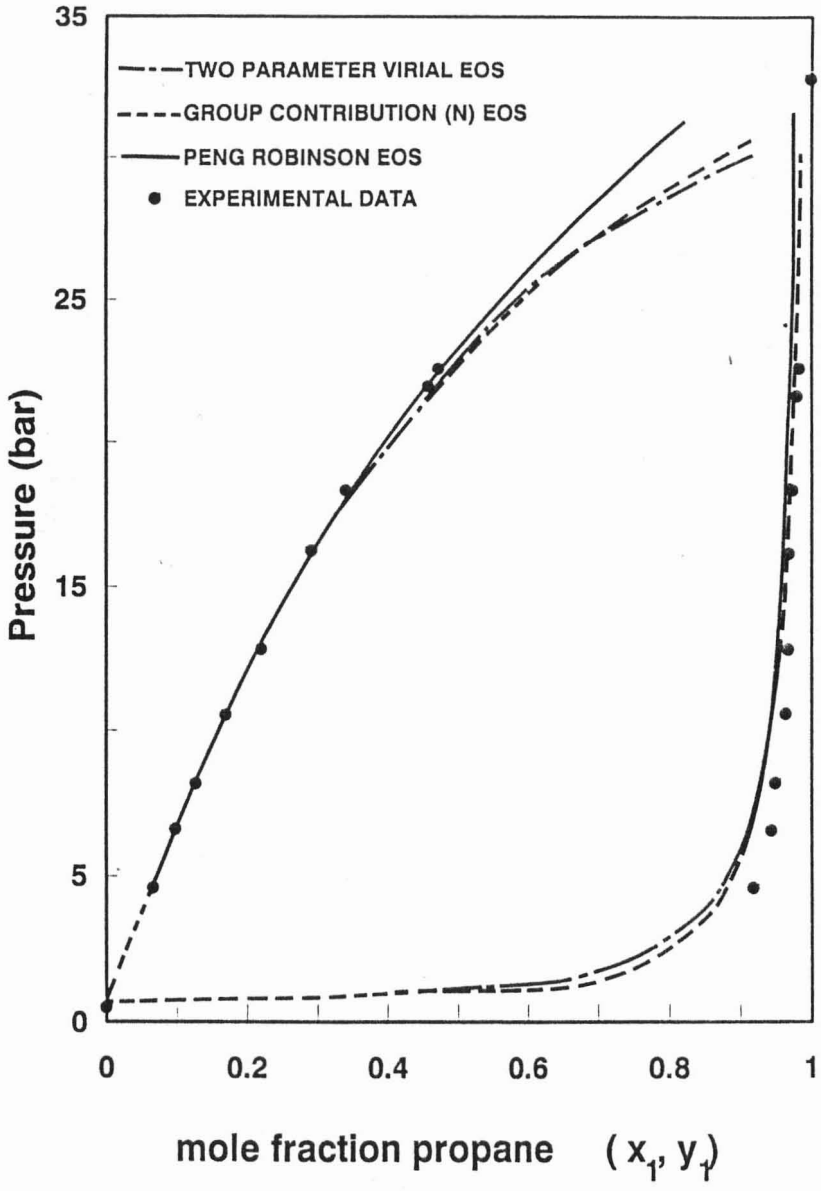

Figure 8.23 : Comparison between theoretically predicted and experimental VLE for the Propane / 1-Propanol system at 81,6 ^{o}C

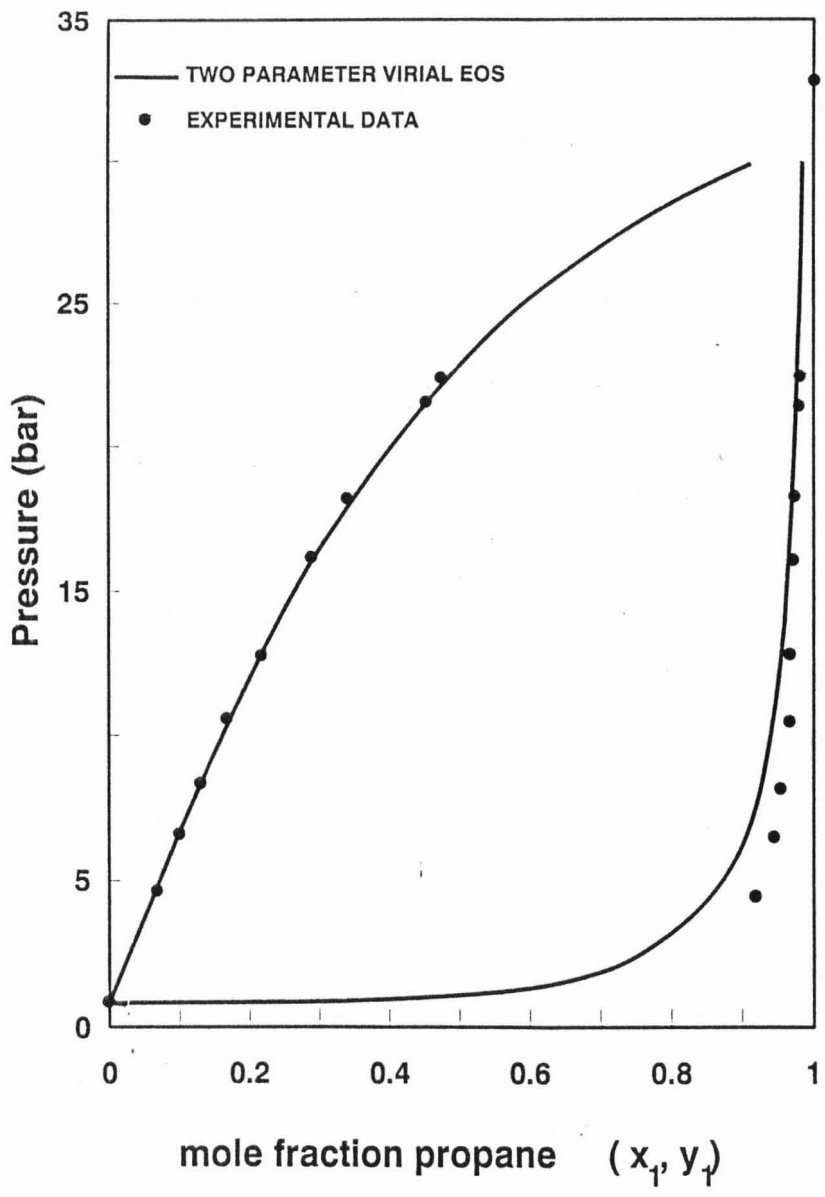

Figure 8.24 : Comparison between theoretically predicted and experimental VLE for the Propane / 1-Propanol system at 81,6 ^{o}C

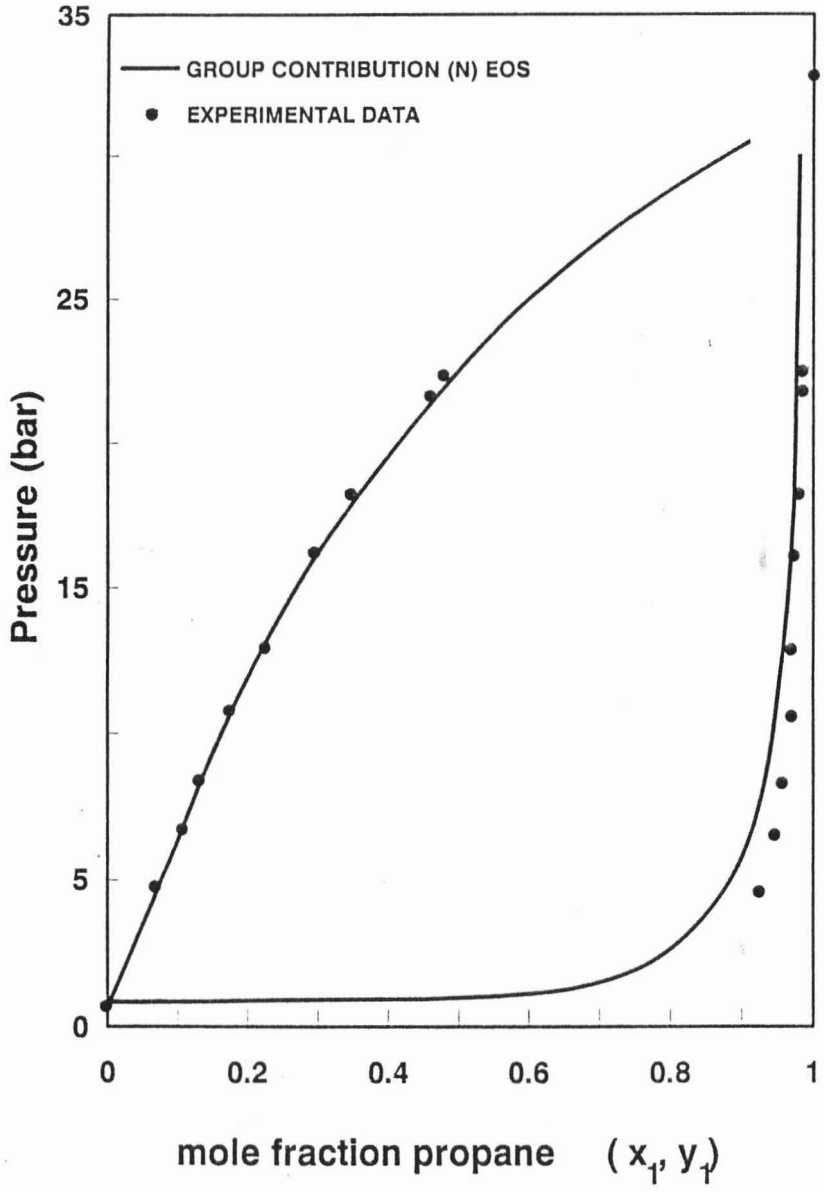

Figure 8.25 : Comparison between theoretically predicted and experimental VLE for the Propane / 1-Propanol system at 81,6 ^{o}C

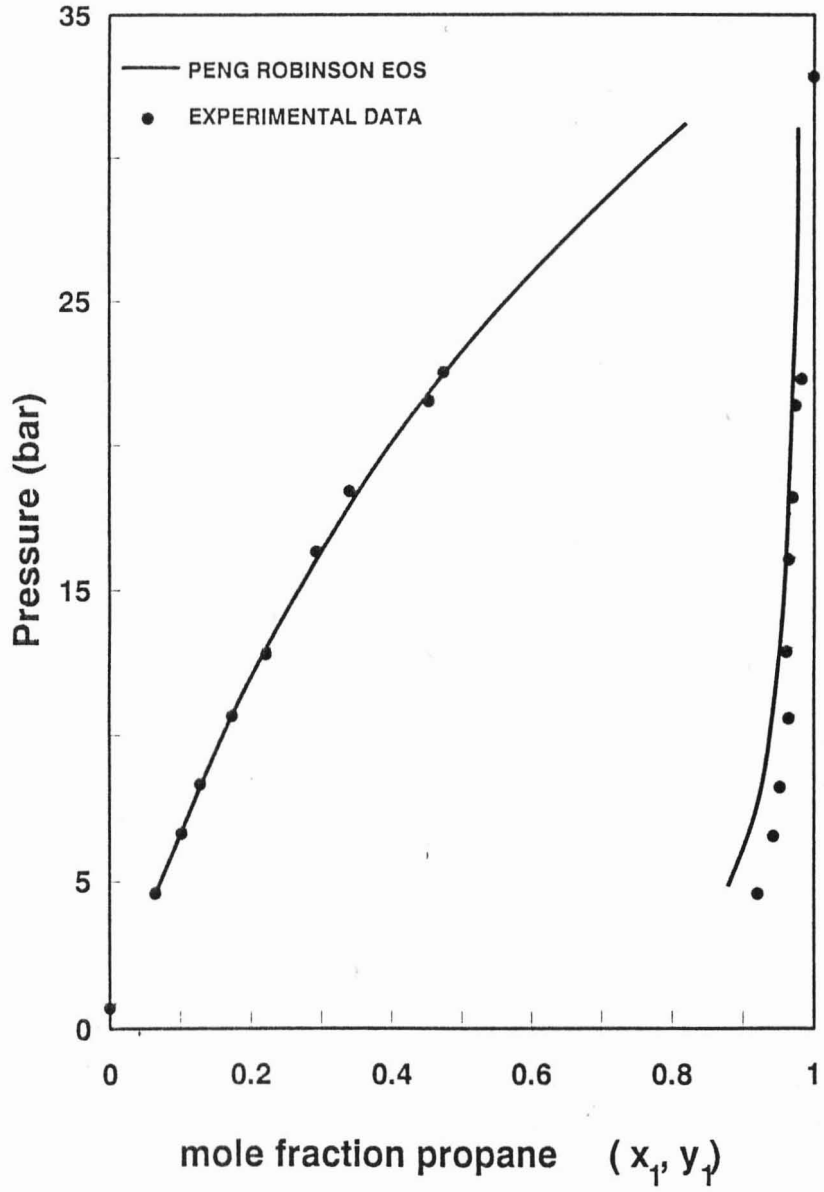

Figure 8.26 : Comparison between theoretically predicted and experimental VLE for the Propane / 1-Propanol system at 81,6 ^{o}C

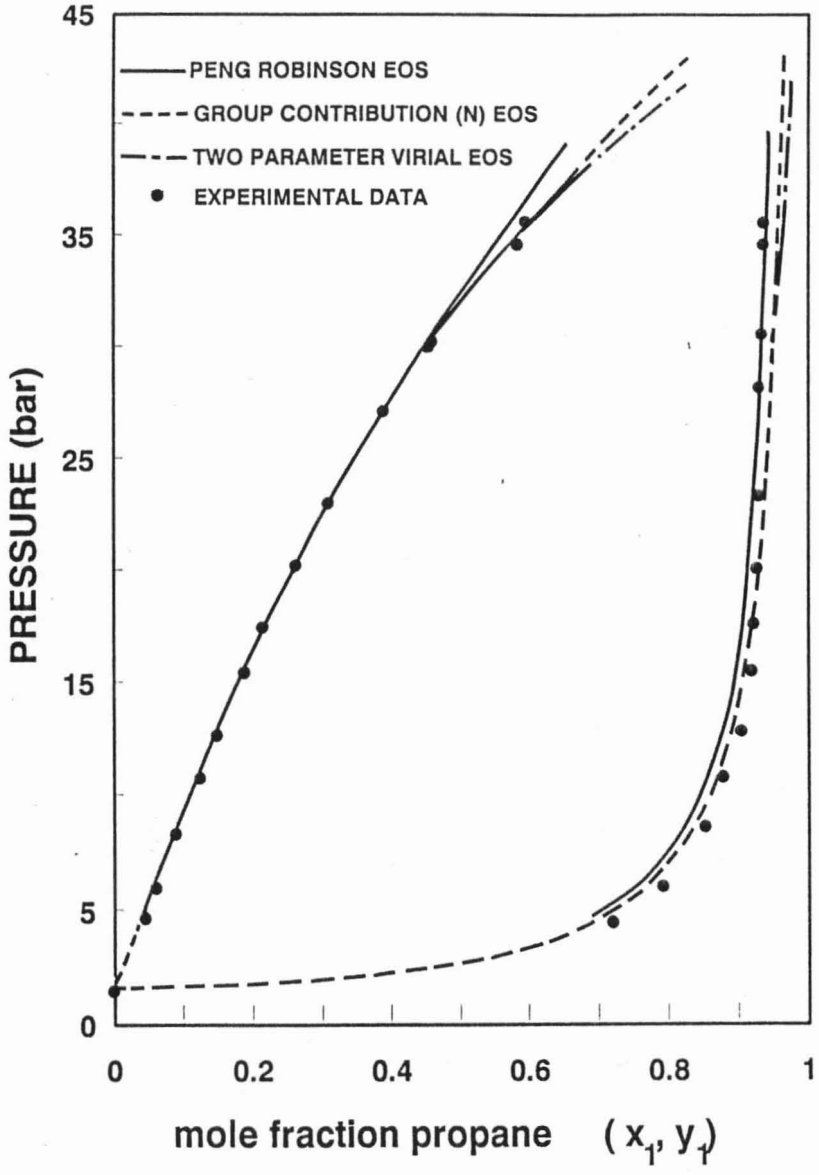

Figure 8.27 : Comparison between theoretically predicted and experimental VLE for the Propane / 1-Propanol system at 105,1 ^{o}C

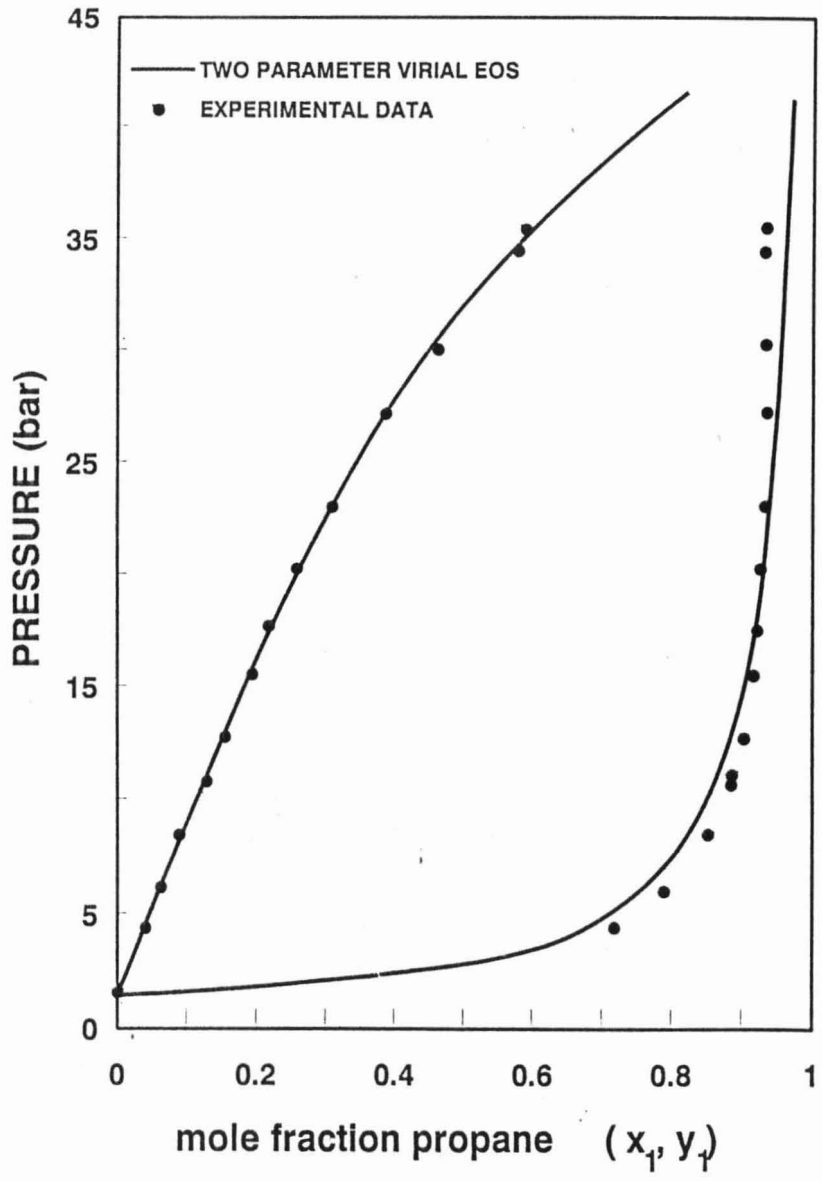

Figure 8.28 : Comparison between theoretically predicted and experimental VLE for the Propane / 1-Propanol system at 105,1 ^{o}C

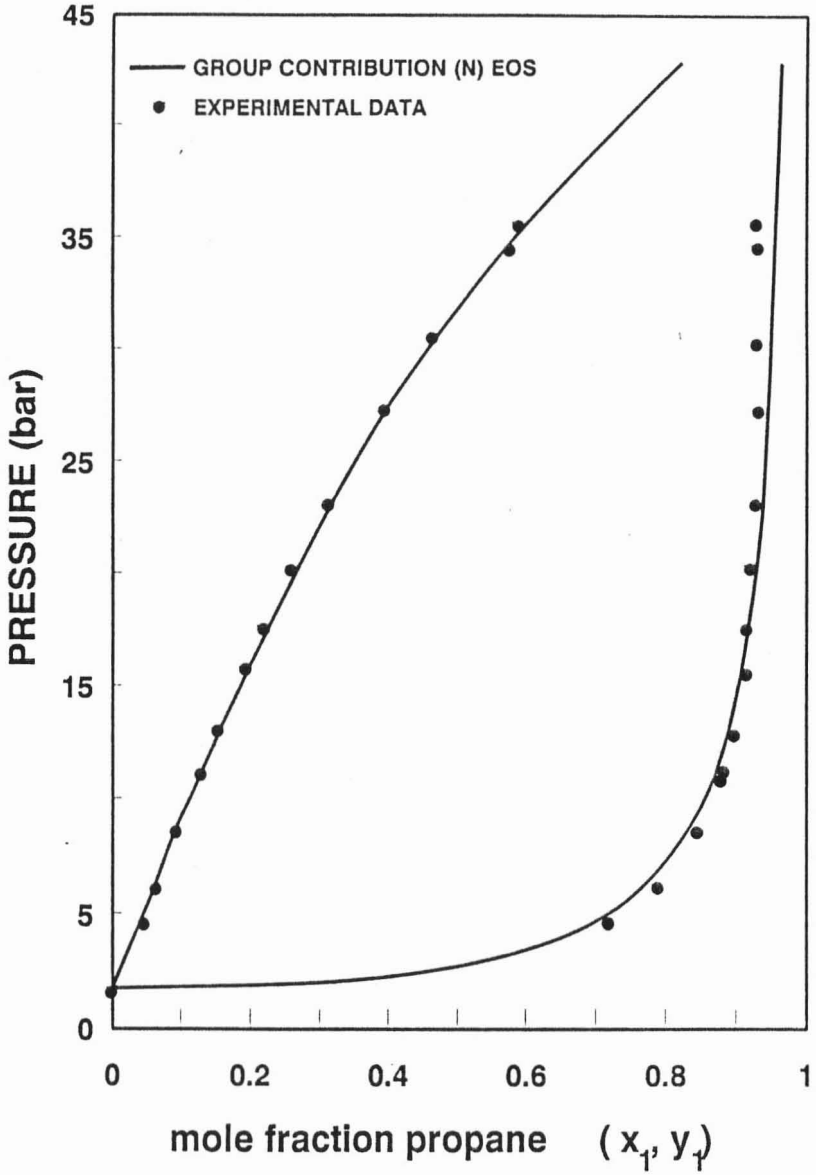

Figure 8.29 : Comparison between theoretically predicted and experimental VLE for the Propane / 1-Propanol system at 105,1 °C

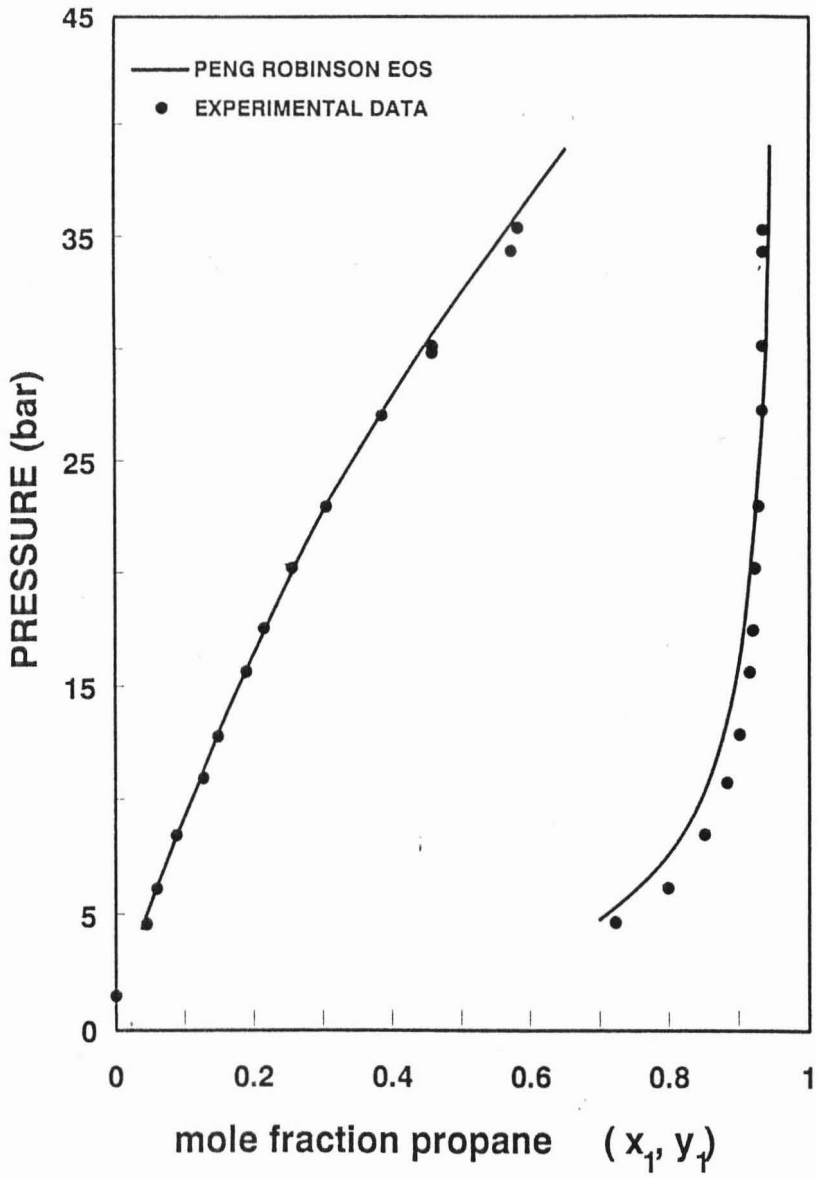

Figure 8.30 : Comparison between theoretically predicted and experimental VLE for the Propane / 1-Propanol system at 105,1 °C

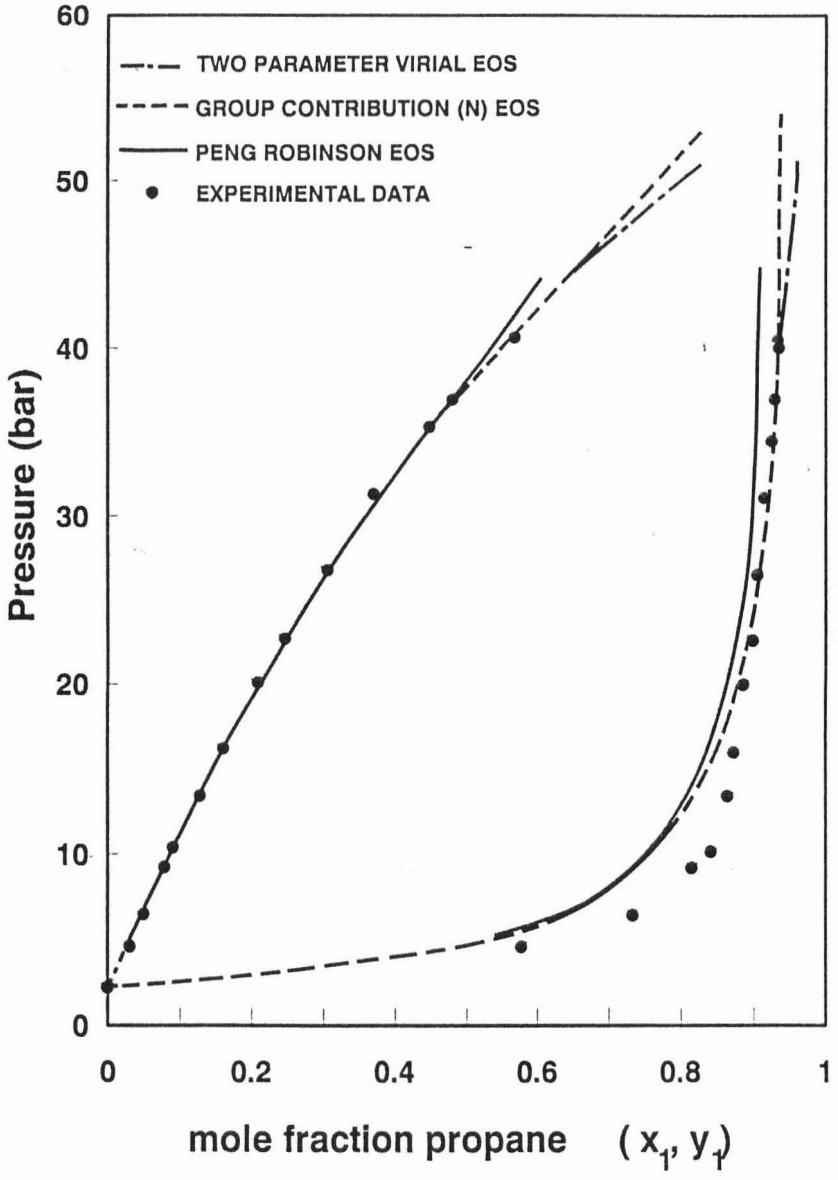

Figure 8.31 : Comparison between theoretically predicted and experimental VLE for the Propane / 1-Propanol system at 120,1 ^{o}C

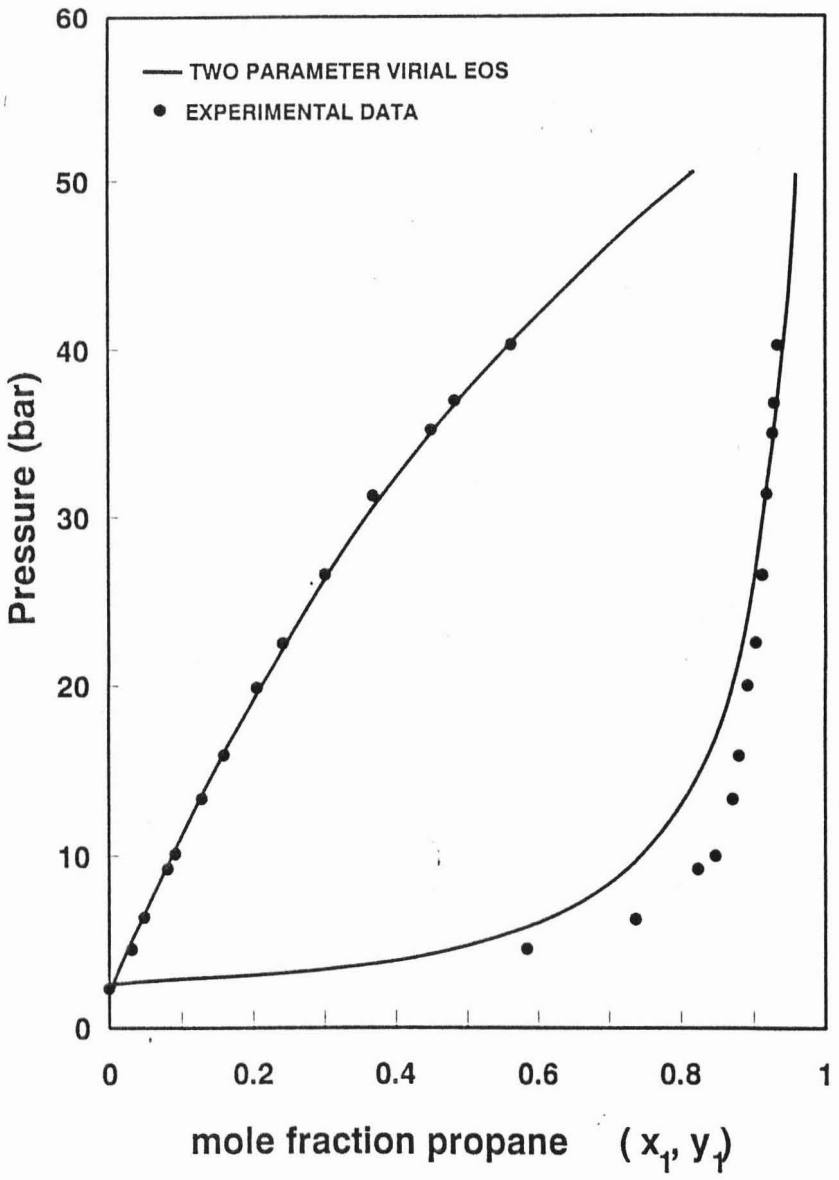

Figure 8.32 : Comparison between theoretically predicted and experimental VLE for the Propane / 1-Propanol system at 120,1 ^{o}C

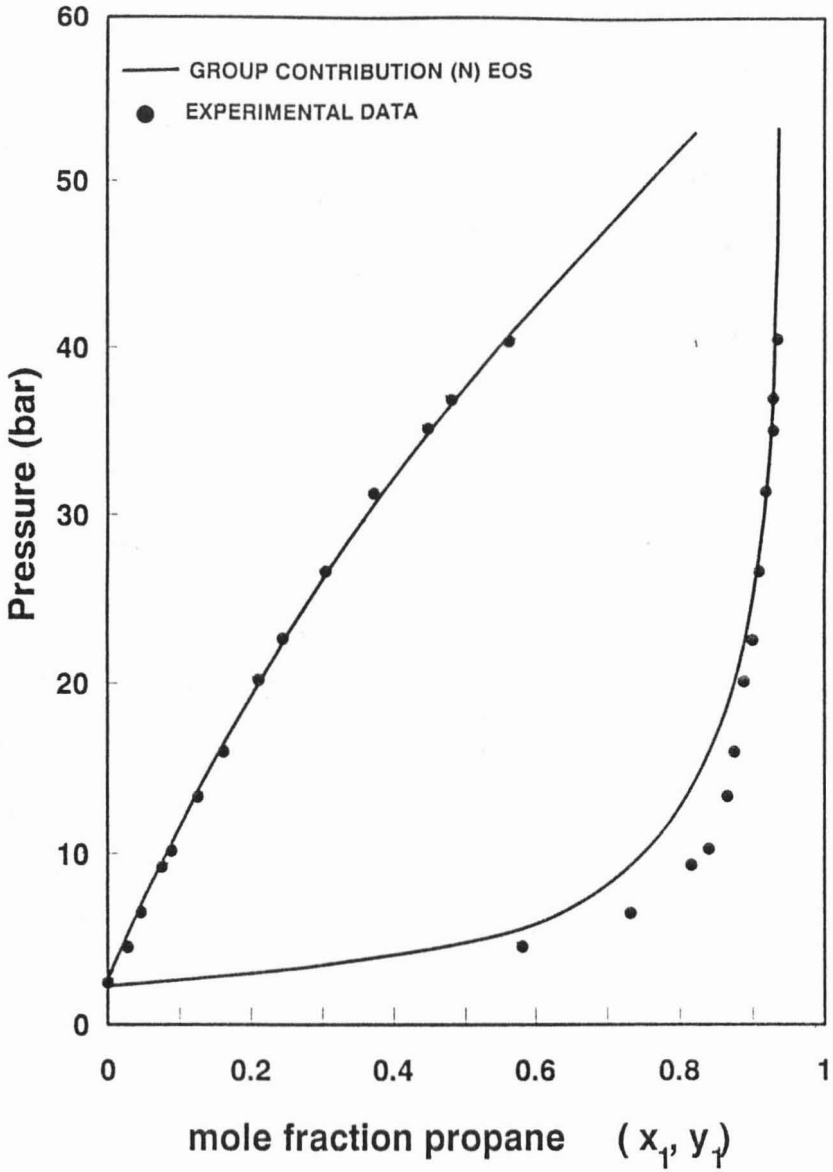

Figure 8.33 : Comparison between theoretically predicted and experimental VLE for the Propane / 1-Propanol system at 120,1 ^{o}C

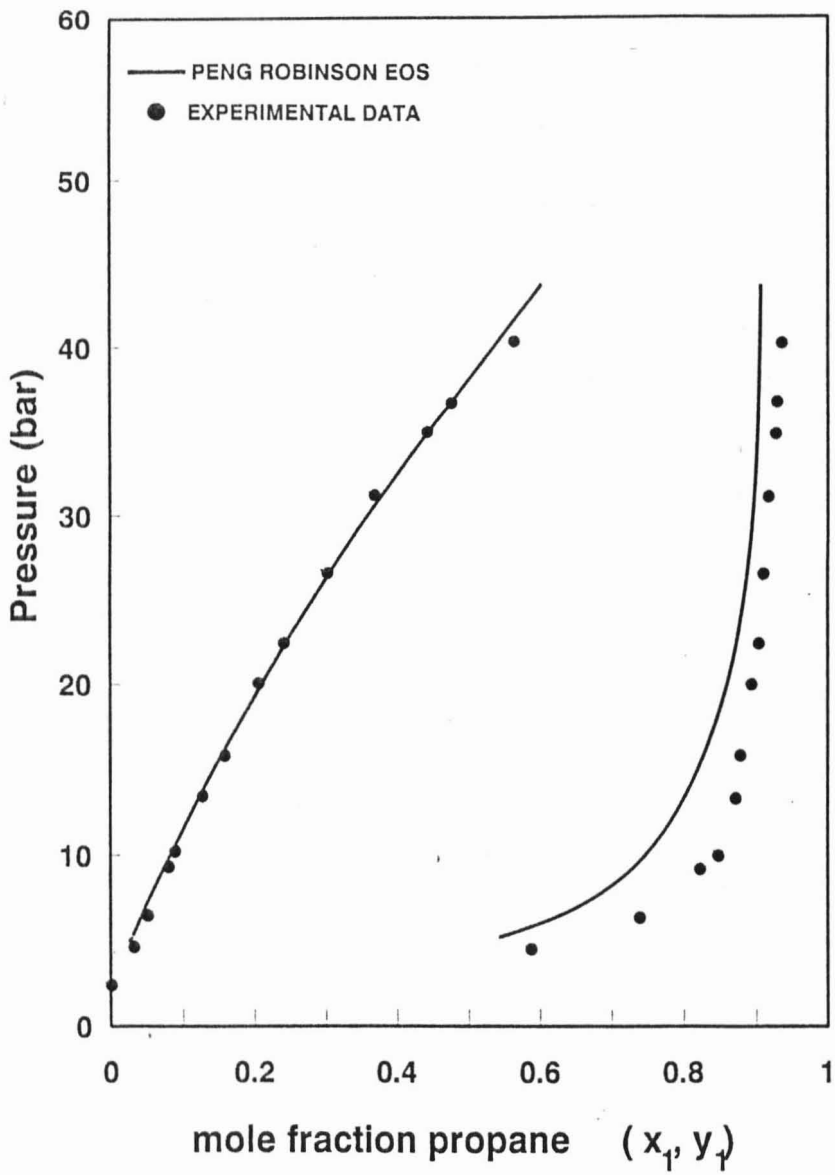

Figure 8.34 : Comparison between theoretically predicted and experimental VLE for the Propane / 1-Propanol system at 120,1 ^{o}C

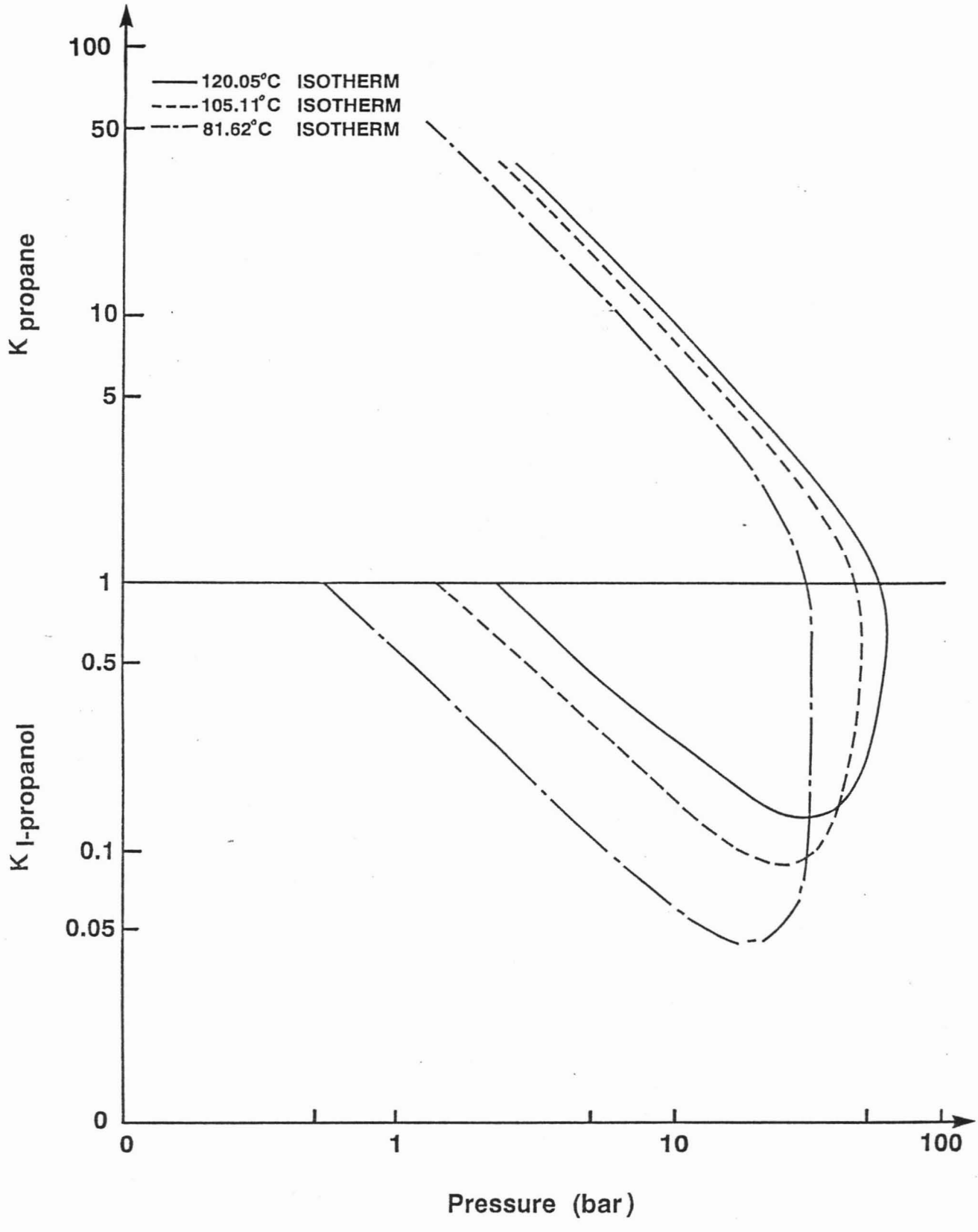

Figure 8.35 : Isothermal relationships of K constants versus pressure for the Propane / 1-Propanol system using the Group Contribution ((N) EOS

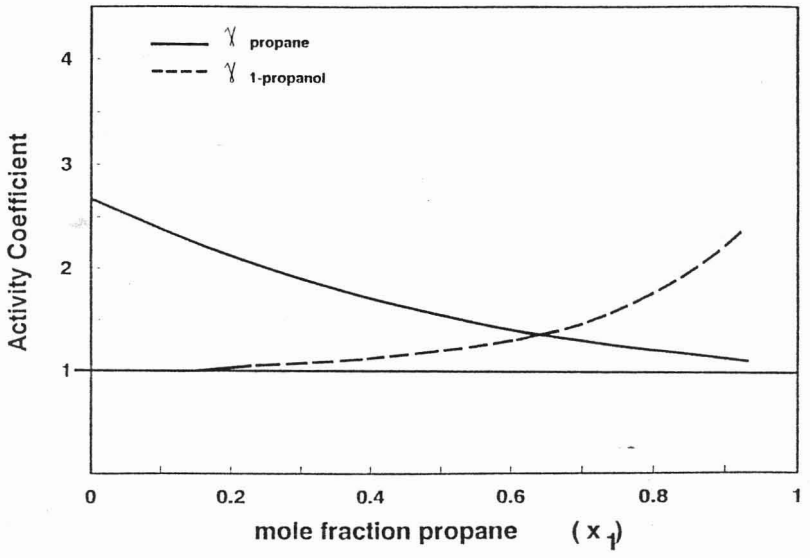

Figure 8.36 : Activity Coefficient plot for the Propane / 1-Propanol system at 81,6 °C

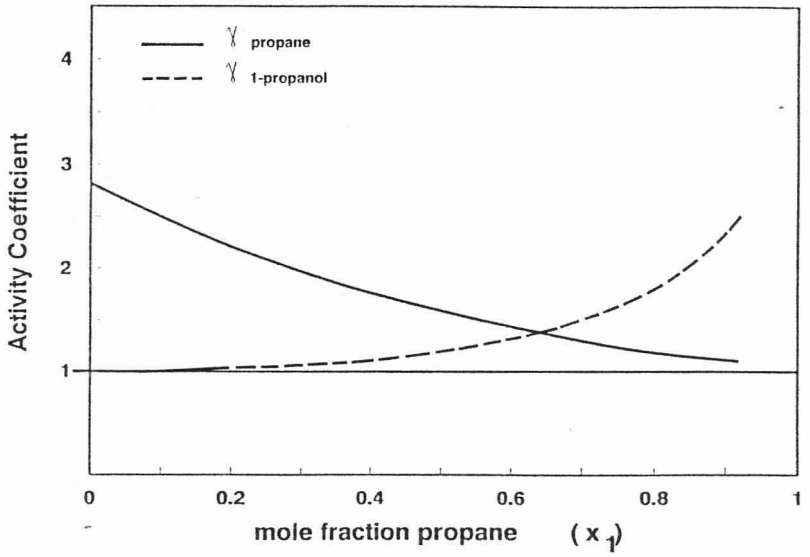

Figure 8.37 : Activity Coefficient plot for the Propane / 1-Propanol system at 105,1 °C

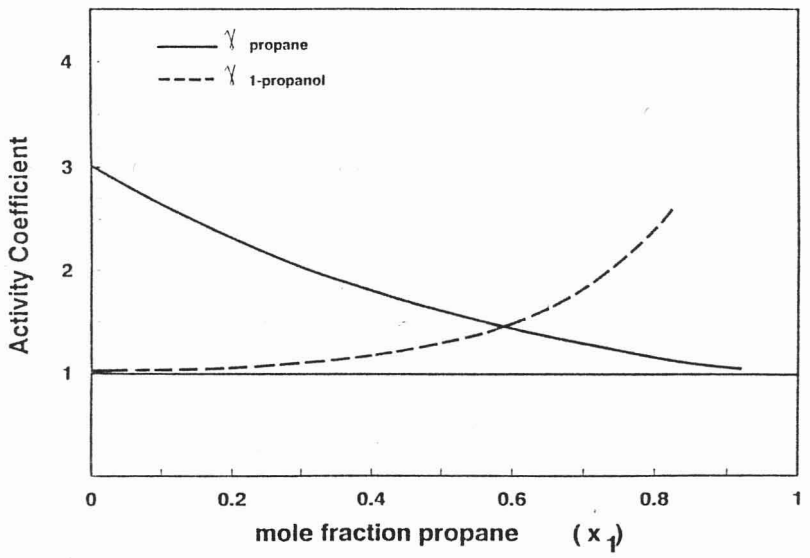

Figure 8.38 : Activity Coefficient plot for the Propane / 1-Propanol system at 120,1 °C

Further fitting program application to the propane/1-propanol experimental data

As an experiment the data were fitted to the UNIQUAC equation by minimizing the objective function ,

$$S = \sum_{i=1}^{m} \left[\frac{(P_i^c - P_i^e)^2}{\sigma_p^2} + \frac{(T_i^c - T_i^e)^2}{\sigma_T^2} + \frac{(x_i^c - x_i^e)^2}{\sigma_x^2} \right] \qquad (8.10)$$

i.e. a regression of $P-T-x$ data only.

The UNIQUAC parameters obtained, listed in Table 8.4 differed slightly from those obtained for the $P-T-x-y$ data regression. The confidence regions were smaller however implying greater confidence in the calculated parameters. The residuals however still showed the same trends and were of similar magnitudes.

As a further experiment, experimental data were fitted using the NRTL equation for the liquid phase parameters with the Virial and Group Contribution EOS for the vapour phase. The third parameter α was set either to -1 or 0,3 according to the recommendations of Marina and Tassios (1973) and Behrens and Eckemann (1979) or allowed to vary freely. No satisfactory convergence was achieved in either case.

Further fitting program application to the propane/1-propanol experimental data

As an experiment the data were fitted to the UNIQUAC equation by minimizing the objective function ,

$$S = \sum_{i=1}^{m} \left[\frac{(P_i^c - P_i^e)^2}{\sigma_p^2} + \frac{(T_i^c - T_i^e)^2}{\sigma_T^2} + \frac{(x_i^c - x_i^e)^2}{\sigma_x^2} \right] \qquad (8.10)$$

i.e. a regression of $P-T-x$ data only.

The UNIQUAC parameters obtained, listed in Table 8.4 differed slightly from those obtained for the $P-T-x-y$ data regression. The confidence regions were smaller however implying greater confidence in the calculated parameters. The residuals however still showed the same trends and were of similar magnitudes.

As a further experiment, experimental data were fitted using the NRTL equation for the liquid phase parameters with the Virial and Group Contribution EOS for the vapour phase. The third parameter α was set either to -1 or 0,3 according to the recommendations of Marina and Tassios (1973) and Behrens and Eckemann (1979) or allowed to vary freely. No satisfactory convergence was achieved in either case.

8.5.2.3 Propane/1-propanol liquid immiscibility

No convergence was achieved in the high pressure region when the correlation program was used with UNIQUAC in conjunction with the Peng-Robinson EOS. A very liberal pressure convergence criterion was adopted. The resulting pressure versus propane mole fraction generated would seem to indicate the formation of a liquid-liquid equilibrium region as in Vidal (1984) and Peschel and Wenzel (1984) for the ethane/methanol system.

A rigorous thermodynamic criterion for the occurrence of phase splitting in a binary system (Reid, *et al* 1987) is ,

$$\left(\frac{\partial^2 g^E}{\partial x_1^2}\right)_{T,P} + RT\left(\frac{1}{x_1}+\frac{1}{x_2}\right) < 0 \qquad (8.11)$$

where g^E is the molar excess Gibbs energy of the binary mixture.

Alternatively, the Gibbs criterion for equilibrium may be used to test for immiscible regions (Walas 1985). A state of equilibrium is characterized as having a minimum Gibbs energy at a given temperature, pressure and composition. If there are unstable states the plot of Gibbs energy versus composition always has at least one local maximum and two or more local minima i.e. the curve has convex portions,

$$\partial G \;/\; \partial x = 0$$

$$\partial^2 G \;/\; \partial x^2 < 0$$

If there are values of composition that satisfy the above mathematical conditions for convexity, immiscibility will occur. The compositions at which the second derivatives are zero are the inflection points and represent metastable states.

A plot of the Gibbs energy for the propane/1-propanol solution versus the propane mole fraction would therefore indicate the presence of phase splitting by a discontinuity of the curve. The Gibbs energy was calculated from the UNIQUAC derived activity coefficients as suggested by Walas (1985) :

$$g = RT \sum_{i=1}^{2} x_i \ln (x_i \gamma_i) \qquad (8.12)$$

Plots of g versus liquid phase propane mole fraction are shown for the activity coefficients derived from the Virial and P-R EOS in Figures 8.39 to 8.41 for the three temperatures. These plots show no discontinuities indicating that there is no liquid phase splitting.

Schwartzenruber, *et al* (1987) do however mention that erroneous phase splitting is often predicted when correlating the vapour-liquid equilibrium of alcohol-alkane systems with a cubic equation of state.

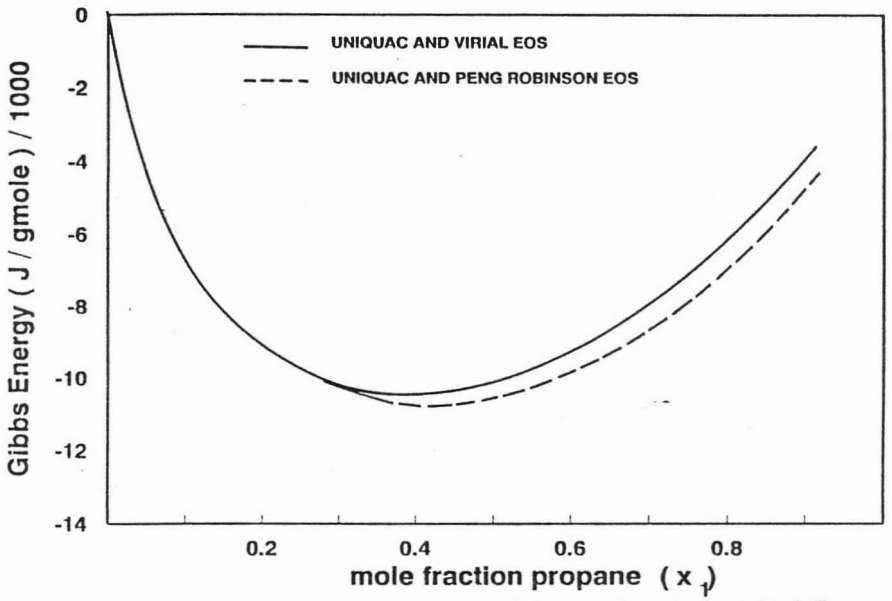

Figure 8.39 : Gibbs Energy plots of Propane / 1-Propanol system at 81,6°C

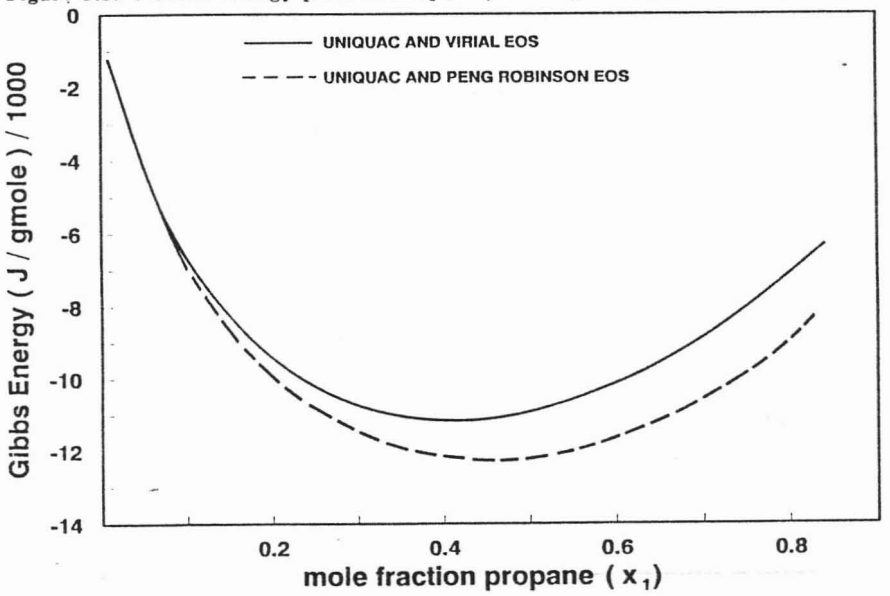

Figure 8.40 : Gibbs Energy plots of Propane / 1-Propanol system at 105,1°C

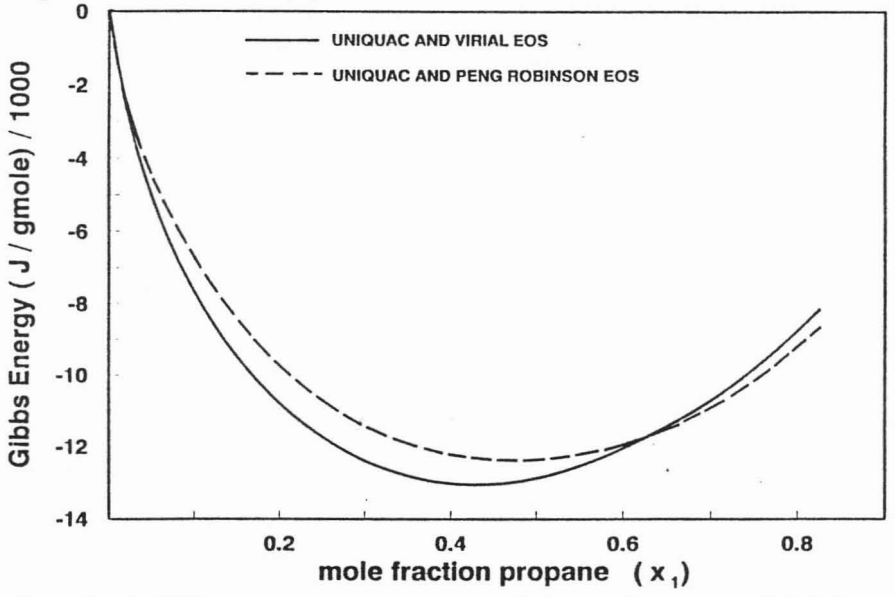

Figure 8.41 : Gibbs Energy plots of Propane / 1-Propanol system at 120,1°C

8.5.2.4 Determination of the Peng and Robinson - classical mixing rule interaction parameters (δ_{ij})

The experimental data obtained in this work (Table F.2) made it possible to calculate the Peng-Robinson EOS binary interaction parameter for the propane/1-propanol system. The optimum interaction parameter δ_{ij} in the relationship ,

$$a_m = (1 - \delta_{ij})(a_i a_j) \qquad (8.13)$$

in the P-R EOS was determined with the help of the Chemical Engineering department's Simplex non-linear least squares regression program. The program developed by ICI contains two main algorithms for minimizing the least squares objective function :

1. The Nelder and Mead simplex, direct search, hill-climbing method.
2. Fitting a quadratic surface to the objective function and solving analytically for the minimum of the approximate objective.

During the course of the search the program decides internally which method is more appropriate, and it may in fact alternate several times between the two.

Due to the nature of the Simplex program, regression on only one dependent variable was possible. For a given set of data the optimum binary parameter depends on the choice of objective function. Minimizing the error in the pressure variable is usually preferred as the pressure objective function gives the sharpest minimum (Reid, *et al* 1987). Since pressure is a crucial measurement in isothermal systems and is measured with better accuracy than compositions, it was chosen as the dependent variable. The vapour mole fraction was chosen for the convergence criterion in the direct method, (Figure 3.1).

The value of δ_{ij} obtained was therefore the one that gave the minimum deviation between the experimental and predicted bubble point pressures in the direct method equation ,

$$x_i \phi_i^V P = y_i \phi_i^L P$$

using a sum of the squares objective function (SS) :

$$SS = \sum_{i=1}^{m} (P_i^{calc} - P_i^{exp})^2 \qquad (8.14)$$

The secant method was used to obtain the calculated pressure corresponding to the estimate of δ_{ij} in each successive regression iterational loop by solving for :

$$\Sigma y_i - 1 \leq \pm 0{,}001 \qquad (8.15)$$

The Peng and Robinson interaction parameters obtained from the experimental data are given in Table 8.4. The parameters are temperature independent for the temperatures for which propane is supercritical.

TABLE 8.5

Peng and Robinson Interaction Parameters for Propane/1-Propanol

Temperature °C	Data (1)	δ_{ij}
81,62	EXP	0,058695
105,11	EXP	0,068586
120,05	EXP	0,068309

(1) EXP experimental data

As a further experiment the δ_{ij} were calculated from the values of P , T , x and y obtained from the UNIQUAC and Virial EOS regression i.e. output from fitting program 1. The δ_{ij} obtained were similar to those listed in Table 8.5.

The P and y residuals for the three temperatures are shown in Figure 8.42. Systematic deviations for the pressure and vapour composition residuals are observed. This would suggest the need for the incorporation of the (η_{ij}) interaction parameter in the van der Waals covolume (b) i.e. Eq. (3.42). Due to time constraints the correlational ability of the two interaction parameter Peng-Robinson EOS could not be examined.

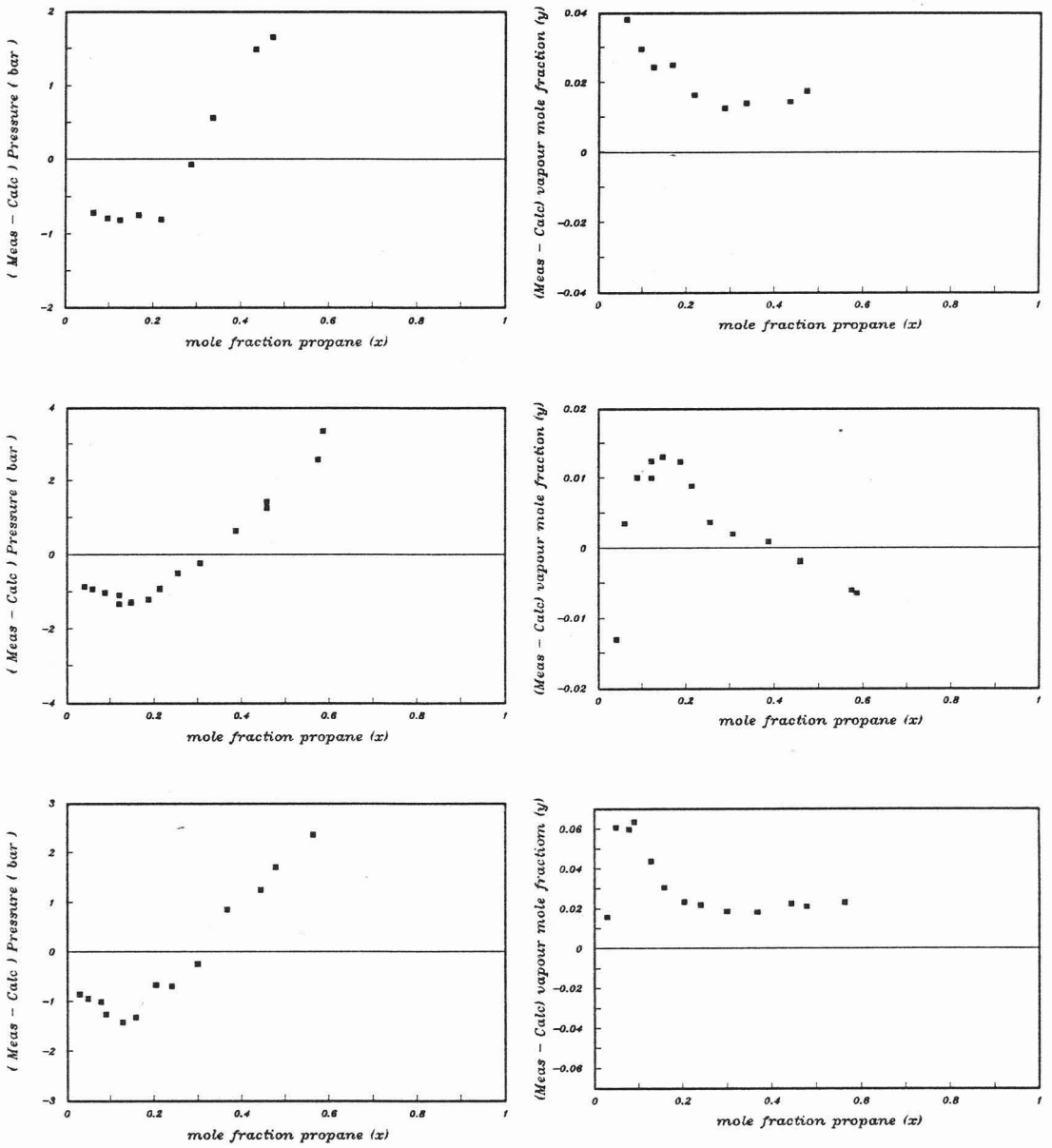

Figure 8.42 : Peng-Robinson δ_{ij} Determination, Residuals for Peng-Robinson EOS for the Propane/1-Propanol system at 81,6, 105,2, 120,0 °C

8.6 THERMODYNAMIC CONSISTENCY TESTING

8.6.1 Carbon Dioxide/Toluene System

Chueh, *et al* (1965) consistency test

The experimental data listed in Table F.1, Appendix F.1, were analysed thermodynamically using the Chueh, *et al* (1965) consistency test (Program 3).

The terms of Eqs. (3.59) to (3.61) were initially integrated from the *lowest reported liquid phase mole fraction* to the extrapolated critical point. The comparison of the LHS and RHS of Eq. (3.61) is given at regular intervals up to and including the critical point for the data of Ng and Robinson at 38, 79 and 120 °C, Table F.3, Appendix F.2. From the table it is apparent that all the terms contribute significantly to the RHS and none could be neglected.

The Chueh, *et al* (1965) consistency test was solved for the indeterminate point $x_2 = 0 = y_2$ by the application of L'Hopitals rule, as shown in Appendix B.9.1. The areas were now integrated from $x_2 = 0$ to the extrapolated critical point. The results for the data listed in Appendix F.1 at regular intervals are given in Table 8.6.

The indicated consistency is generally very good for all the data sets at all three temperatures. At the lowest carbon dioxide mole fraction however, inconsistencies become appreciable. In this region, corresponding to the lowest experimental pressures, the $p-y$ curve is nearly horizontal and a small change in total pressure (e.g. due to sampling) produces a very large change in the relative amounts of liquid and vapour, i.e. large disturbances in the equilibrium state. This region tends to be neglected experimentally but may be important in design.

For the many systems with similar VLE profiles equipment such as that of Nakayama, *et al* (1987) and Rogers and Prausnitz (1970), in which liquid phase sampling via a sliding rod extending the full cell diameter does not disturb the system pressure, may furnish more reliable data in the low mole fraction region. At higher pressures an increase in pressure causes the vapour to condense virtually without change in composition for an appreciable range and sampling affects only the liquid phase.

Illustrative plots of the liquid molar volume, $\ln\ (K_2/K_1)$ and $\ln\ (\hat{\phi}_2/\hat{\phi}_1)$ for this project's 79°C data are shown in Figure 8.43 as functions of pressure or liquid mole fraction of carbon dioxide. From Figure 8.43 the values from the limiting process are slightly inconsistent with the extrapolation of the values from the experimental compositions.

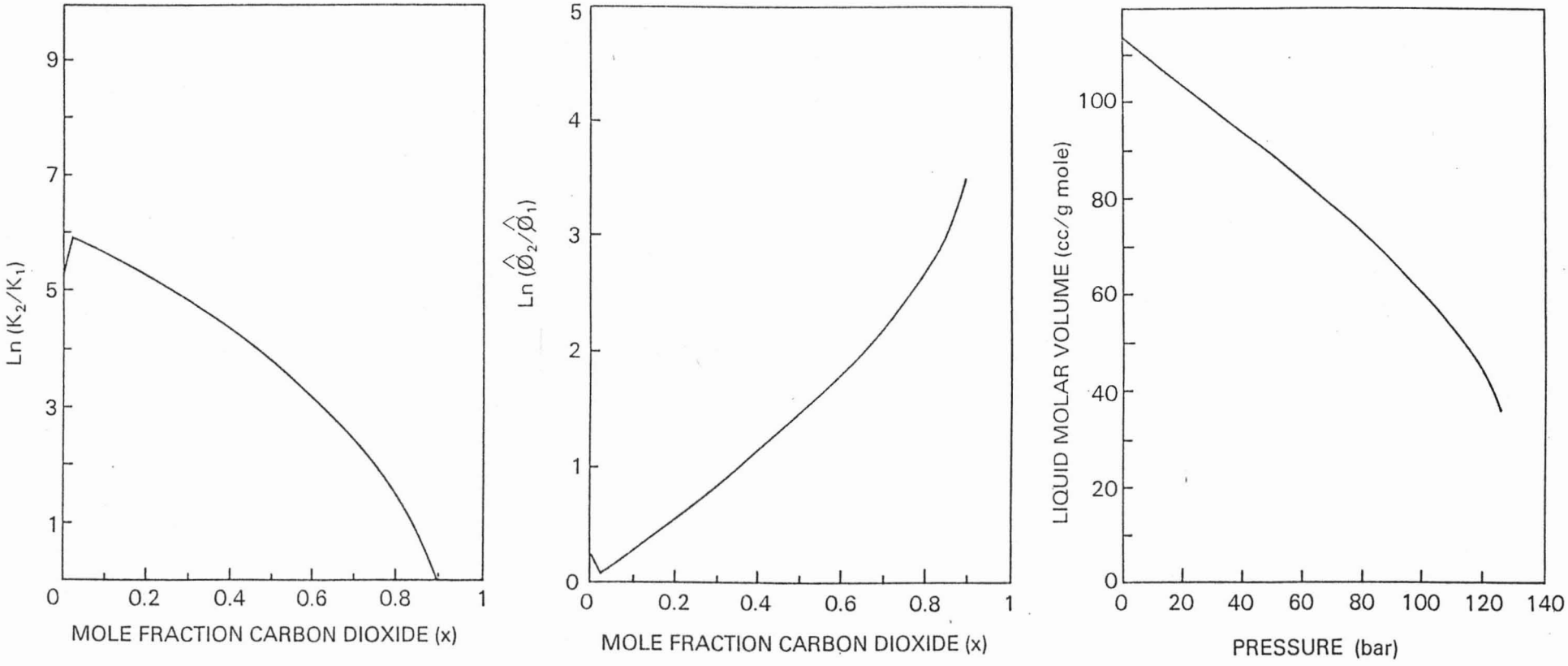

Figure 8.43 : Areas in the Chueh, et al (1965) Thermodynamic Consistency Test for the Carbon Dioxide / Toluene system (79 ^{o}C)

Vapour phase consistency test

Following a similar procedure to that of Chueh, *et al* (1965) a consistency test based on vapour phase properties and compositions was derived as described in section 3.6.2 Eqs. (3.63) to (3.65). This test removed the necessity of limiting values of K_2/K_1 and the assumption $\overline{V}_i^L = V_i$.

The results of applying the test to the data listed in Appendix F.1, Table F.1, are shown in Table 8.7 for several values of carbon dioxide mole fraction from $y_2 = 0$ to $y_{2\ critical}$.

The combination of the two experimental data sets at 79 °C shows the best consistency. Once again the lowest data points (i.e. in the lower y_2 composition range) show large deviations. This could be as a result of the fairly large interpolation necessary due to the scarcity of data in the region between $y_2 = 0$ and the lowest measured vapour composition, Figure 8.44. This implies either error in the lower pressure experimental data region or slightly incorrect values in the saturation pressure of toluene resulting in erroneous extrapolation from $y_2 = 0$ to $y_{2\ measured}$ or a combination of the two.

From Figure 8.44 there are difficulties associated with the accurate numerical integration and also in the explanation of the physical significance of the $\ln\ (\hat{\phi}_2/\hat{\phi}_1)$ curve, due to it's inherent shape. The curve features a point of lowest condensable component (toluene) solubility in the vapour phase before the critical point. The accurate determination of the abovementioned point is essential for the accuracy of the consistency test for systems such as carbon dioxide/toluene. The accuracy of the test also depends to a large extent on the lower pressure region, the accurate definition of which has been experimentally neglected.

This consistency test would therefore be more suitable for data that do not exhibit the feature of a **point of lowest condensable solubility**, such as the carbon dioxide/nitrogen data of Chueh, *et al* (1965).

The argument as to whether the data are thermodynamically consistent is somewhat circular since the interaction parameter δ_{ij} in the Peng Robinson EOS was itself determined by regression of VLE data. The two tests remain useful however, as checks for substantial discrepancies in any composition range.

8.6.2 Propane/1-Propanol System

The experimental data listed in Table F.2 Appendix F.1 as well as extrapolated data for the lower pressure region was tested for consistency by the two tests described above. The results are given in Tables 8.8 and 8.9.

The results are seen to be model dependant; the Group Contribution EOS gave results more consistent than did the Virial EOS. Interestingly the extrapolation of the data in the low pressure region for this system is more consistent than for the carbon dioxide/toluene system, Figures 8.44 and 8.45.

The results of the vapour phase consistency test using the Group Contribution EOS indicate the vapour data to be not inconsistent.

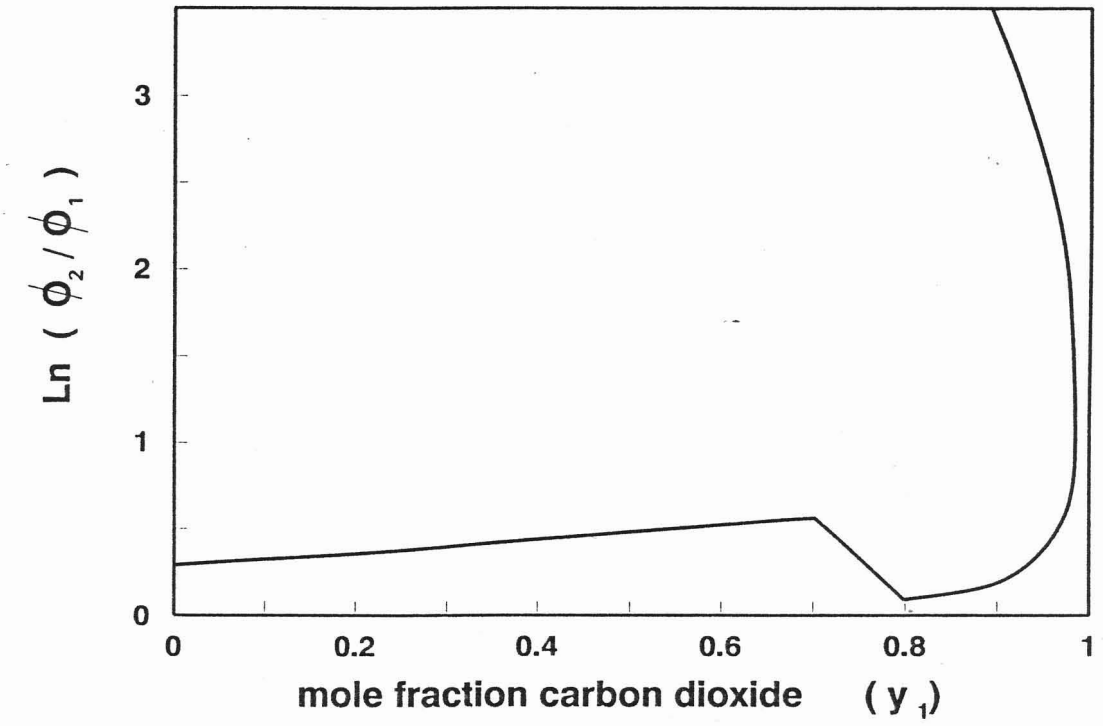

Figure 8.44 : Area 2 in the Vapour Phase Thermodynamic Consistency Test for the Carbon Dioxide / Toluene System (79 °C)

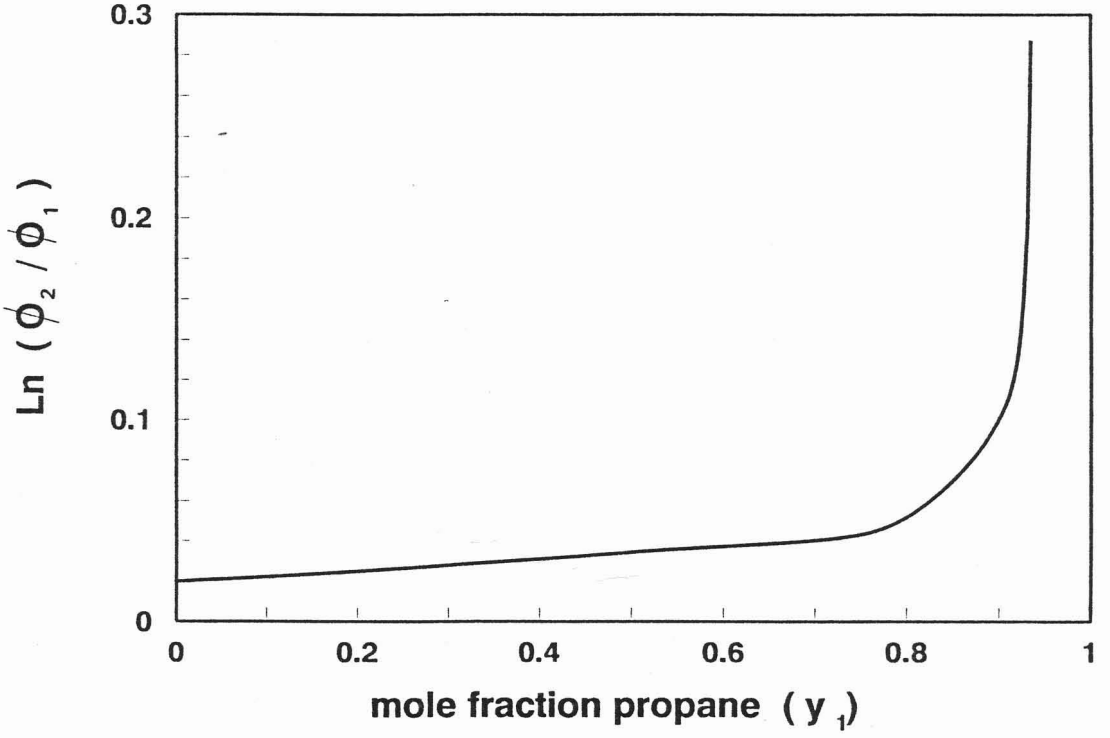

Figure 8.45 : Area 2 in the Vapour Phase Thermodynamic Consistency Test for the Propane / 1-Propanol System (105,1 °C)

TABLE 8.6

Interval Comparison of Chueh, *et al* (1965) Consistency Test
Carbon Dioxide Toluene System

Mole fraction CO_2 in liquid	Area 1 (1)	Area 2 (1)	Area 3 (1)	LHS (1)	RHS (1)	% Diff
Temperature : 38,11 °C						
Data : Ng and Robinson (1978)						
0,264	1,83	0,08	0,11	2,02	1,64	20,88
0,603	3,77	0,41	0,18	4,37	4,39	-0,58
0,931	4,95	0,98	0,22	6,14	6,22	-1,20
0,985	5,04	1,11	0,22	6,37	6,37	-,39
Temperature : 79,44 °C						
Data : Kim, *et al* (1986) and Ng and Robinson (1986)						
0,172	0,97	0,04	0,11	1,13	1,16	-2,58
0,491	2,45	0,35	0,26	3,05	3,08	-0,96
0,720	3,15	0,76	0,32	4,24	4,31	-1,66
0,787	3,28	0,93	0,33	4,54	4,62	-1,80
0,895	3,37	1,25	0,34	4,97	5,05	-1,76
Data : Ng and Robinson (1986)						
0,166	0,86	0,05	0,10	1,01	1,36	-29,48
0,172	0,89	0,05	0,11	1,05	1,16	-9,39
0,491	2,37	0,35	0,26	2,98	3,08	-3,42
0,720	3,07	0,77	0,32	4,16	4,31	-3,43
0,787	3,20	0,93	0,33	4,47	4,62	-3,45
0,895	3,29	1,26	0,34	4,89	5,05	-3,26
Data : Raal and Muhlbauer						
0,173	0,94	0,04	0,11	1,10	1,17	-6,75
0,310	1,63	0,14	0,19	1,96	1,99	1,27
0,635	2,97	0,58	0,31	3,87	3,73	3,45
0,760	3,32	0,84	0,33	4,50	4,49	0,09
0,840	3,43	1,06	0,34	4,84	4,84	0,10
0,900	3,46	1,25	0,35	5,06	5,07	0,16
Temperature : 120,6 °C						
Data : Ng and Robinson (1986)						
0,106	0,50	0,02	0,08	0,61	0,56	6,88
0,368	1,59	0,20	0,26	2,04	2,01	1,69
0,621	2,30	0,57	0,38	3,24	3,28	-1,02
0,790	2,48	0,99	0,42	3,88	3,94	-1,36

(1). Equations (3.59) to (3.61)

TABLE 8.7

Interval Comparison of Vapour Phase Consistency Test
Carbon Dioxide Toluene System

Mole fraction CO_2 in vapour	Area 1 (1)	Area 2 (1)	LHS (1)	RHS (1)	% Diff
Temperature : 79,44 °C					
Data : Ng and Robinson (1979)					
0,500	0,18	1,11	1,29	1,62	-22,77
0,700	0,28	1,34	1,62	1,98	-19,76
0,886	0,32	1,63	1,95	2,24	-13,76
0,981	0,34	4,69	5,03	4,78	5,05
0,984	0,34	4,79	5,14	4,89	4,95
0,973	0,33	5,06	5,39	5,14	4,77
0,954	0,29	5,17	5,46	5,21	4,47
0,931	0,22	5,20	5,42	5,17	4,75
0,895	0,11	5,21	5,32	5,06	4,86
Data : Ng and Robinson (1979) and Kim, *et al* (1986)					
0,700	0,28	1,31	1,60	1,90	-17,19
0,981	0,35	4,32	4,67	4,78	-2,27
0,973	0,34	4,70	5,03	5,14	-2,04
0,954	0,30	4,81	5,10	5,21	-2,00
0,931	0,24	4,83	5,07	5,17	-2,01
0,895	0,12	4,84	4,96	4,96	-2,05
Data : Raal and Muhlbauer					
0,700	0,28	1,53	1,81	2,23	-20,70
0,900	0,33	2,14	2,47	2,85	-13,96
0,930	0,33	2,30	2,63	3,00	-13,16
0,950	0,34	2,43	2,77	3,14	-12,55
0,977	0,35	3,62	3,97	4,25	-6,92
0,982	0,35	4,43	4,78	5,02	-4,92
0,969	0,32	4,67	4,99	5,23	-4,65
0,945	0,26	4,69	4,95	5,20	-4,68
0,900	0,13	4,72	4,84	5,08	-4,78
Temperature : 120 °C					
Data : Ng and Robinson (1978)					
0,300	0,11	0,49	0,61	0,77	-23,42
0,600	0,24	0,72	0,96	1,05	-9,27
0,953	0,30	3,45	3,75	3,51	6,44
0,921	0,25	4,21	4,45	4,45	5,64
0,790	-0,10	4,28	4,18	3,93	6,09

(1). Equations (3.63) to (3.65)

TABLE 8.8

Interval Comparison of Chueh, *et al* (1965) Consistency Test
Propane / 1-Propanol System

Mole fraction propane	Area 1 (1)	Area 2 (1)	Area 3 (1)	LHS (1)	RHS (1)	% Diff
Temperature : 81,62 °C						
Vapour Phase Model : Two Parameter Virial						
0,2198	0,7657	0,01168	0,02213	0,79952	0,93707	-15,84
0,3378	1,2889	0,02618	0,03703	1,35210	1,58351	-15,76
0,4737	1,8525	0,04713	0,04856	1,94820	2,06971	-6,04
Vapour Phase Model : Group Contribution (O)						
0,2198	0,7657	0,0186	0,0262	0,8104	0,8964	-10,07
0,3378	1,2889	0,0447	0,0437	1,3773	1,5166	-9,62
0,4737	1,8525	0,0863	0,0574	1,9962	1,9887	0,37
Vapour Phase Model : Group Contribution (N)						
0,2198	0,7657	0,0113	0,0251	0,8022	0,9287	-14,62
0,3378	1,2889	0,0274	0,0419	1,3581	1,5626	-14,00
0,4737	1,8525	0,0532	0,0548	1,9605	2,0354	-3,74
Temperature : 105,20 °C						
Vapour Phase Model : Two Parameter Virial						
0,1220	0,3220	0,0064	0,0167	0,3451	0,3319	3,87
0,3071	1,0028	0,0319	0,0482	1,0829	1,2707	-15,96
0,5865	1,7830	0,0934	0,0816	1,9580	2,3553	-18,42
Vapour Phase Model : Group Contribution (O)						
0,1220	0,3220	0,0073	0,0200	0,3493	0,3036	14,00
0,3071	1,0028	0,0464	0,0581	1,1073	1,1893	-7,14
0,5865	1,7830	0,1620	0,1001	2,0451	2,2286	-8,58
Vapour Phase Model : Group Contribution (N)						
0,1220	0,3220	0,0050	0,0192	0,3462	0,3255	6,13
0,3071	1,0028	0,0312	0,0554	1,0894	1,2406	-12,98
0,5865	1,7830	0,1102	0,0947	1,9878	2,2839	-13,86

Table 8.8 continued

Temperature : 120,05 °C						
Vapour Phase Model : Two Parameter Virial						
0,1288 0,2999 0,5640	0,3903 0,9785 1,7084	0,0083 0,0336 0,9287	0,0223 0,0564 0,0926	0,4209 1,0685 1,8938	0,3110 1,1943 2,0924	29,99 -11,11 -9,96
Vapour Phase Model : Group Contribution (O)						
0,1288 0,2999 0,5640	0,3903 0,9785 1,7084	0,0096 0,0482 0,1612	0,2705 0,0690 0,1158	0,4270 1,0957 1,9853	0,2760 1,1075 1,9615	42,94 -1,07 1,20
Vapour Phase Model : Group Contribution (N)						
0,1288 0,2999 0,5640	0,3903 0,9785 1,7084	0,0068 0,0312 0,1143	0,0258 0,0337 0,1092	0,4229 1,0778 1,9318	0,3008 1,1594 2,0158	33,74 -7,28 -4,42
0,1245 0,3019 0,5528	0,3525 0,9304 1,6507	0,0101 0,0378 0,0944	0,0223 0,0564 0,0926	0,3849 1,0246 1,8377	0,3973 1,0416 1,8527	-7,17 -1,64 0,81
(1). Equations (3.59) to (3.61)						

TABLE 8.8

Interval Comparison of Vapour Phase Consistency Test
Propane / 1-Propanol System

Mole fraction propane	Area 1 (1)	Area 2 (1)	LHS (1)	RHS (1)	% Diff
Temperature : 81,62 °C					
Vapour Phase Model : Two Parameter Virial					
0,8200	0,0275	1,6649	1,6924	1,6727	1,17
0,9665	0,0333	2,9408	2,9741	2,8777	3,29
0,9831	0,0357	3,6925	3,7282	3,5239	5,63
Vapour Phase Model : Group Contribution (O)					
0,8200	0,0159	1,6659	1,6797	1,6659	0,82
0,9665	0,0235	2,8807	2,9042	2,8742	1,03
0,9831	0,0281	3,5226	3,5507	3,5164	0,97
Vapour Phase Model : Group Contribution (N)					
0,8200	0,0117	1,6681	1,6798	1,6660	0,82
0,9665	0,0164	2,8877	2,9040	2,8740	1,03
0,9831	0,0192	3,5318	3,5511	3,5168	0,97
Temperature : 105,22 °C					
Vapour Phase Model : Two Parameter Virial					
0,4000	0,0225	0,6913	0,7138	0,6965	2,46
0,8489	0,0528	1,8182	1,8711	1,7952	4,13
0,8489	0,0597	2,5431	2,6028	2,4547	5,85
0,9300	0,0620	3,0849	3,1469	2,9011	8,12
Vapour Phase Model : Group Contribution (O)					
0,4000	0,0098	0,6870	0,6967	0,6929	0,56
0,8489	0,0271	1,7745	1,8022	1,7861	0,89
0,8489	0,0339	2,4332	2,4671	2,4464	0,83
0,9300	0,0365	2,8716	2,9081	2,8857	0,77
Vapour Phase Model : Group Contribution (N)					
0,4000	0,0119	0,6833	0,6953	0,6914	0,56
0,8489	0,0367	1,7647	1,8014	1,7852	0,90
0,8489	0,0459	2,4190	2,4649	2,4443	0,84
0,9300	0,4977	2,8523	2,9021	2,8797	0,77

Temperature : 120,05 °C					
Vapour Phase Model : Two Parameter Virial					
0,4000	0,0278	0,5120	0,5399	0,5208	3,60
0,8200	0,0575	1,4112	1,4688	1,3979	4,94
0,8999	0,0662	2,3020	2,3682	2,1997	7,37
0,9335	0,0732	2,8849	2,9581	2,6663	10,37
Vapour Phase Model : Group Contribution (O)					
0,4000	0,0665	0,4984	0,5148	0,5134	0,28
0,8200	0,0537	1,3560	1,3981	1,3861	0,86
0,8999	0,0421	2,1513	2,2050	2,1860	0,85
0,9335	0,0165	2,5926	2,6590	2,6382	0,78
Vapour Phase Model : Group Contribution (N)					
0,4000	0,0136	0,5019	0,5155	0,5140	0,28
0,8200	0,0326	1,3650	1,3976	1,3857	0,85
0,8999	0,0408	2,1666	2,2074	2,1884	0,86
0,9335	0,0498	2,6149	2,6647	2,6439	0,78
(1). Equations (3.63) to (3.65)					

CHAPTER 9

CONCLUSION

EXPERIMENTAL

Static equilibrium equipment used

The static equilibrium equipment described was designed to measure vapour-liquid equilibrium data for temperatures and pressures of up to 200°C and 20 MPa respectively. The results obtained for the very demanding carbon dioxide/toluene test system were in good agreement with published data. This gives a high degree of confidence in the new data for the propane/1-propanol system.

The most troublesome features associated with measuring volatile/non-volatile systems at high temperatures and pressures with a static cell namely , the creation of an isothermal environment, liquid phase sampling (sample withdrawal,vaporization, homogenization and analysis) and the attainment of leak free seals, were adequately solved.

Isothermal bath conditions were achieved with a copper-clad air bath incorporating an external air circulation loop. The loop shielded the equilibrium cell from direct radiative interchange with the heaters.

The liquid sampling method was perfected. Repeated liquid samples were highly reproducible. The individual samples were fully homogenized and showed no volatile/non-volatile concentration profile over successive flushings to the gas chromatograph. The incorporation of two static jet mixers with no moving parts, and relying only on carrier gas to homogenize the liquid sample is a particularly novel and successful feature.

The equipment used contained no device for measurement of liquid level during the cell filling, venting and sampling procedures. The incorporation of a liquid level device in the form of a draft tube capacitor would yield useful information.

Experience gained from measuring the liquid phase concentrations of the extremely demanding propane/water system suggests that, with slight modifications to the equilibrium cell, accurate results for extremely low solubility systems can be obtained.

The incorporation of a liquid level measuring device as well as the cell modification described in Chapter 10 should be considered in any future application of the equipment.

Proposed new equilibrium cell

The principal disadvantage of the equilibrium cell design is the inability to detect and sample multiple liquid phases. Immiscible liquid phases are often encountered when measuring ternary component mixtures, an interesting, challenging an increasingly important area of research. The windowed equilibrium cell design proposed (Chapter 10), with special provision for sampling of vapour and multiple liquid phases, would be ideal for this application.

THEORETICAL

Fitting and correlation

In view of the tedious nature of high pressure vapour-liquid equilibrium data gathering it is highly desirable to obtain the largest prediction capability from the minimum number of experiments. Modified *regression fitting* and *correlation* programs were developed based on those published by Prausnitz and co-workers for the combined method for low to moderate pressure analysis. The non-condensable component for the various difficult condensable/non-condensable systems studied were treated was as condensables whose properties could be found by extrapolation. The modelling procedure based on the UNIQUAC equation and the symmetric convention for activity coefficients was fully vindicated.

The fitting and correlation programs were were implemented with greater success for the carbon dioxide/toluene binary than for the propane/1-propanol binary.

Temperature dependent values of the UNIQUAC interaction parameter α_{ij}, hitherto not available, are proposed for the carbon dioxide/toluene and propane/1-propanol system for temperatures in the 38 °C to 120 °C and 80 °C to 120 °C ranges respectively.

These parameter values were used in the UNIQUAC equation and gave excellent modelling when combined with the Peng Robinson equation in both the fitting and correlation programs for the **carbon dioxide/toluene binary**. With the truncated virial equation satisfactory predictions were obtained only up to moderate pressures (30 bar) as expected. In view of the exact expressions for relating the mixture virial coefficient to composition it is unfortunate that more usable information on the third virial coefficient is not available.

For the **propane/1-propanol binary**, use of the UNIQUAC α_{ij} parameter values gave progressively less satisfactory modelling when combined with the Group Contribution, Virial and Peng Robinson equations of state in the fitting and correlation programs. The deviations between experimental and theoretically calculated values were most marked in the lower pressure regions of the vapour-liquid coexistence curve. The thermodynamic consistency tests performed on the data showed higher absolute inconsistencies than for the carbon dioxide/toluene binary. This can most likely be ascribed to the inability of the equation of state to describe the polar 1-propanol component.

Classical mixing rule interaction parameters (δ_{ij}) for the Peng-robinson EOS were obtained for the propane/1-propanol system. The value of δ_{ij} obtained was the one that gave the minimum deviation for the sum of the squares bubble point pressure objective function. The values of δ_{ij} obtained were temperature independent.

Consistency testing

The proposed new vapour phase consistency test based only on vapour phase compositions is ideally suited for testing P,T,y data. This test may be particulary useful for testing the thermodynamic consistency of older published data often presented in P,T,y form and for data that does not exhibit the feature of a point of lowest condensable solubility (as described in

Section 8.6.1). For systems displaying the feature of lowest condensable component solubility before the critical point, for example carbon-dioxide / toluene, the test is difficult to implement very accurately.

The two equal area thermodynamic consistency tests, the newly developed vapour phase test and that of Chueh, *et al* (1965), nevertheless showed the data sets of Ng and Robinson (1978), Kim, *et al* (1986) and those of the present study, to be not inconsistent.

CHAPTER 10

RECOMMENDATIONS

10.1 PROPOSED NEW CELL DESIGN

A shortcoming of the VLE equipment described is its inability to detect and sample multiple liquid phases. Applying some novel ideas and from experience gained during experimentation a new equilibrium cell design was generated, the principal features of which are shown in Figure 10.1.

The advantages of the proposed cell lie in the ability to detect multiple phase formation through windows and to subsequently sample each liquid phase with a single sampling valve without disturbing equilibrium.

Features of equilibrium cell (Figure 10.1)

The equilibrium cell incorporates see-through windows and can be housed in an air, oil or water bath. The equilibirium cell cavity is contained between two cylindrical end pieces 1 and 2 which are joined together by spacers. The two end pieces and spacers make up piston 2 which can be moved up and down in the cell block by stepper motor 2. The ability to move piston 2 allows the cell contents to be viewed at any level. The formation of multiple liquid phases can therefore be detected and subsequently sampled with a single Rheodyne 6 port valve. Piston 1 is used to adjust the volume of the equilibrium cell, allowing the cell pressure to be set at any desired value.

Sealing

The seal between the circular end pieces 1 and 2 and the cell block is provided by a pair of Viton "O"-rings housed in grooves machined to the Dowty specifications (Appendix C.1). Viton is desirable being chosen due to its chemical inertness and its relative high temperature capabilities (160 °C).

Piston 2

Piston 2 is aligned via the cell block end pieces, Figure 10.1. Aligment is necessary to facilitate operation by preventing misalignment and consequent stress on the "O"-rings. The piston is prevented from turning with the stepper motor by a ball bearing. The ball bearing allows the piston rod to rotate freely in the cylindrical end piece. A similar "O"-ring and ball bearing system is employed on piston 1 which is used for equilibrium cell volume adjustment.

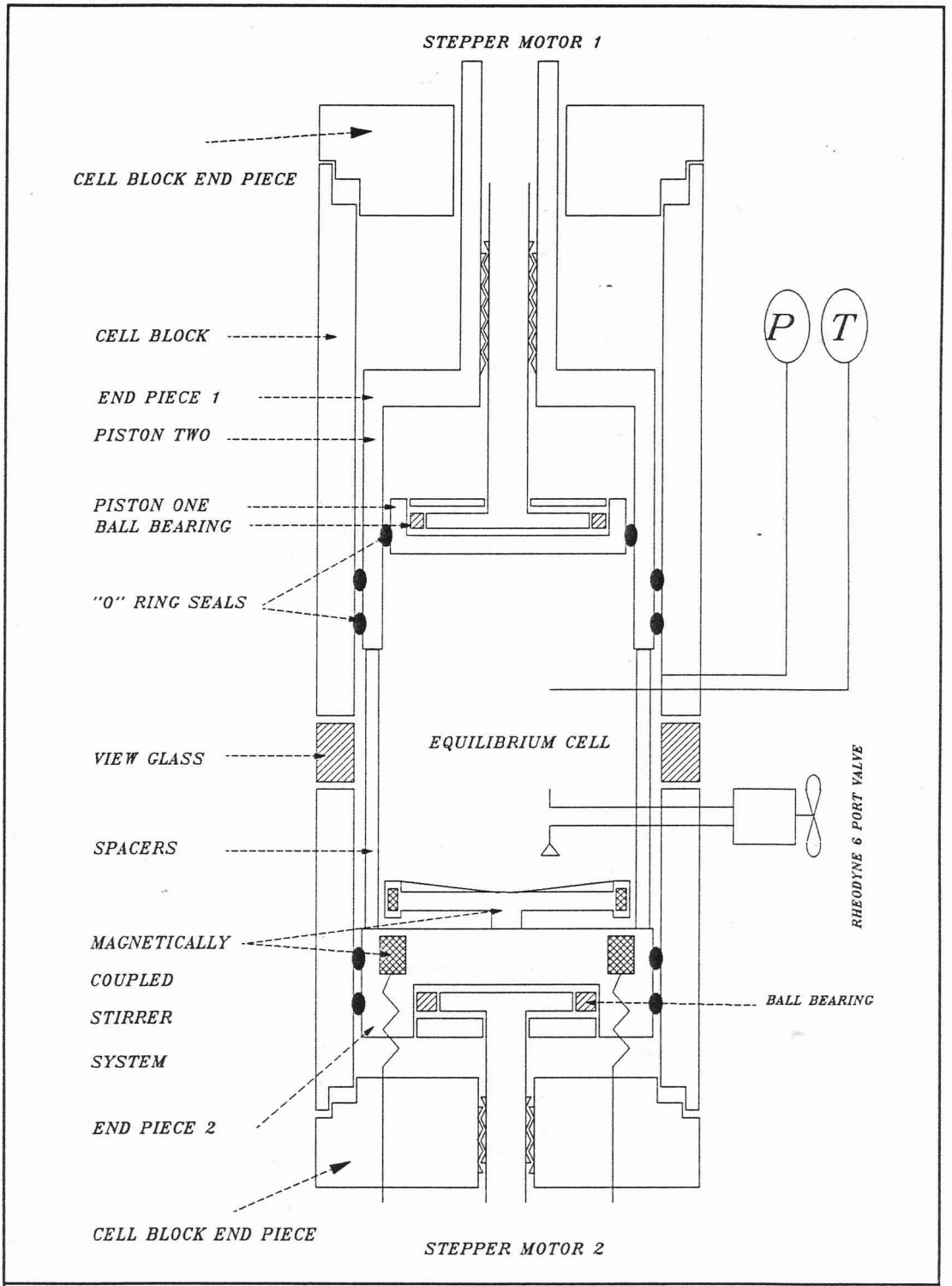

Figure 10.1 : Proposed New Equilibrium Cell

Piston 1

The volume of the cell is varied by piston 1, which is advantageous for three reasons.

Firstly the cell contents can be pressurized. This is a desirable capability for systems containing propane where heating the equilibrium cell is not sufficient to pressurize the cell contents to the critical point and additional forms of pressurization are required.

Secondly the ability to vary cell volume allows the cell to be used in the *synthetic mode* (section 2.5.2).

Thirdly if the piston position is known by graduation, i.e. as in the Raal gas chromatograph detector calibration device the cell can supply volumetric data. To obtain accurate volumetric data the second piston must be moved either manually or via a second stepper motor suitably geared to enable it to move against cell pressure. Hydraulic propulsion was discounted, due to the phenomenon of hydraulic slip.

The above three considerations suggest the cell to be "long and thin" rather than "short and wide". The former configuration allows the volume to be changed very sensitively. A higher liquid level is also produced which allows for more efficient purging of the sample loop.

Liquid sampling

The liquid phase to be sampled is brought into position by piston 2. Liquid sampling is via a single capillary leading to an externally mounted 6 port Rheodyne valve. A sampling rod extending the full diameter of the cell (Rogers and Prausnitz 1970 and Nakayama, *et al* 1987) could also be used. The feature of using a single capillary sampling port and valve (Laugier and Richon 1986 and Renon, *et al* 1989) as opposed to sampling by *multiple* capillaries (Toedheide and Frank 1963) is desirable for a number of reasons :

1. A large number of fittings are required to seal the capillaries. Continual sealing problems can therefore be expected.
2. The large number of capillaries required can create stagnant spaces.
3. The capillary positions are fixed. The capillary inlets are not necessarily always in the correct place to sample the desired liquid phase.

There are problems associated with capillary sampling into an evacuated space due to the volatile component's tendency to flash and consequently create stagnant regions in the thin capillary. Venting, the standard technique employed, to remove the stagnant region creates an undesirable pressure gradient from the cell pressure to the exit pressure of the valve. The stagnant region and venting problems can be overcome by fitting a funnel to the end of the capillary line. As the piston moves up it channels liquid into the funnel, up into the capillary lines and back out into the cell, purging the sample line and sample loop (Figure 10.2). The sample loop is thereby filled with a representative liquid phase sample.

Vapour sampling

Vapour sampling (not shown in Figure 10.1) is achieved by displacing a sample of vapour in one of two sampling loops of an 8 port Valco sampling valve.

Using a Rheodyne or Valco valve holds many advantages over the convential sampling methods discussed in section 2.5.1.2. The main one is that the sample size can easily be manipulated by changing the valve sample loop volume. Changing the sample size for the sampling rod of Nakayama, *et al* (1987) and this project would require extensive machining which is not desirable.

Sample homogenization

The proposed sampling and analysis configurations of the Rheodyne valve are shown in Figures 10.2 and 10.3.

The liquid sample can be pumped through the jet mixer by a suitable pump, as shown in Figure 10.3. The sample can be removed from the loop and sent to the gas chromatograph.

The homogenization scheme shown in Figure 10.3 holds certain advantages over the method outlined in section 5.3.1 as homogeneity of the samples could be achieved more rapidly. However the risks of stagnant spaces are greater.

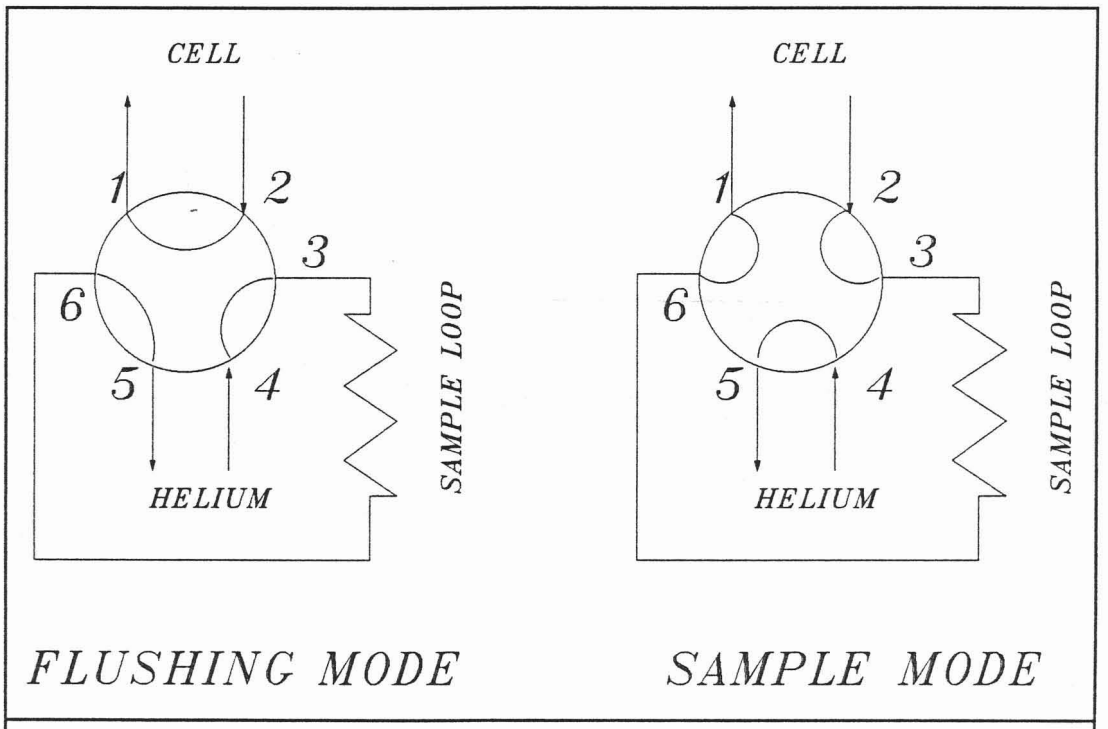

Figure 10.2 : 6-Port Rheodyne Valve Sampling Configuration

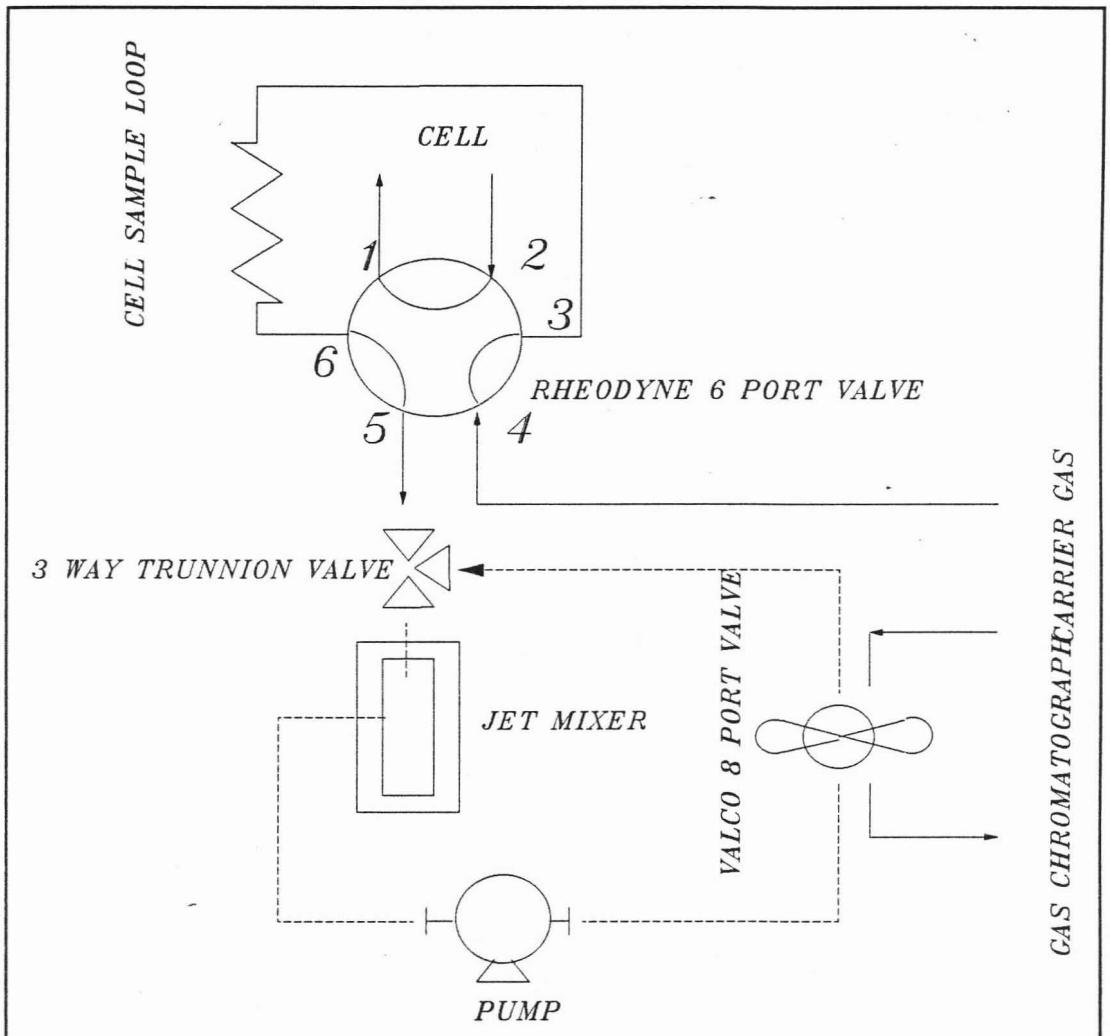

Figure 10.3 : Proposed New Cell's Vapourisation and Homogenisation System

10.2 MODIFICATIONS TO PRESENT EQUILIBRIUM CELL

Equilibrium cell

During the propane/water experimentations it was hypothesized that the stagnant material contained between the sampling rod and cell wall was interacting slightly with the sample contained in the sample hole. The modification shown below, Figure 10.4, i.e. removal of the shaded area, should remove this stagnant region problem.

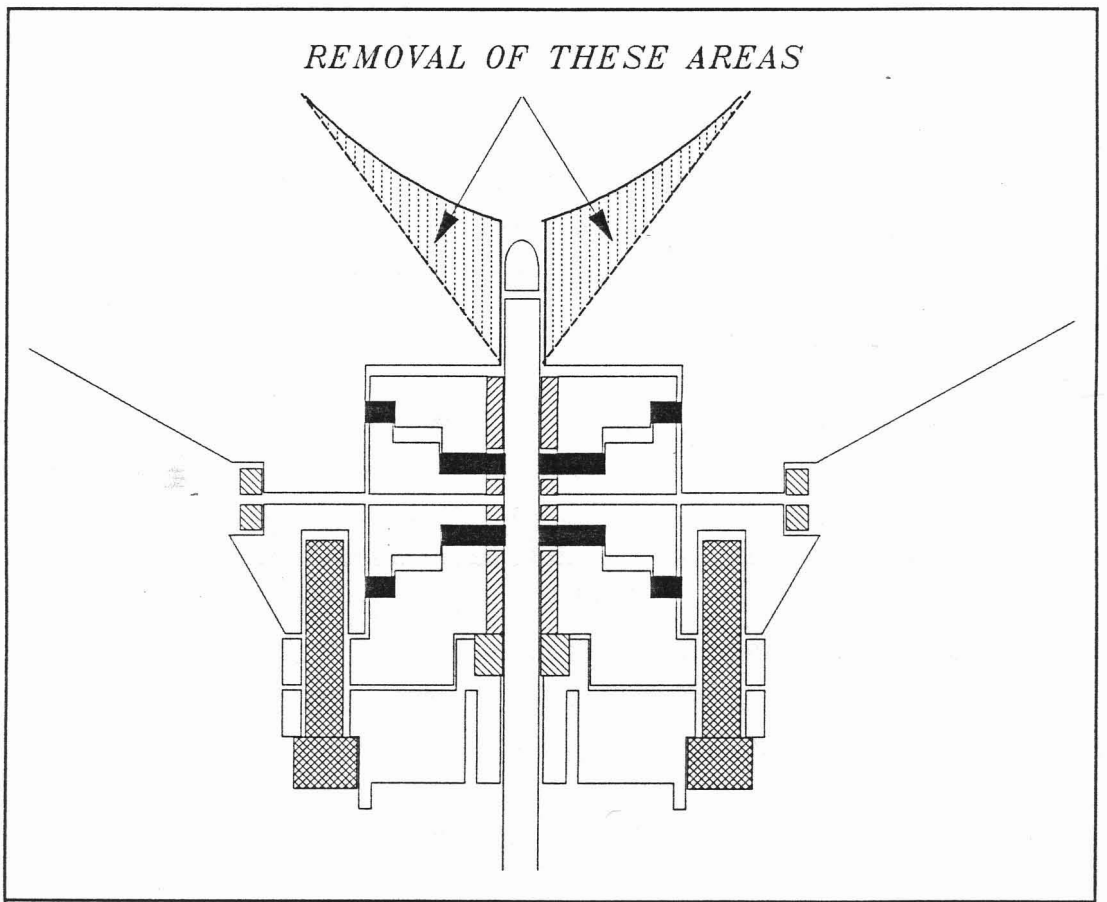

Figure 10.4 : Present Equilibrium Cell Modification

CHAPTER 11

REFERENCES

Abrams, D.S. & Prausnitz, J.M. 1975. Statistical Thermodynamics of Liquid Mixtures : A New Expression for the Excess Gibbs Energy of Partly or Completely Miscible Systems. *AIChE Journal*, 25(1) : 116-128.

Adams, W.R., Zollweg, J.A., Street, W.B. & Rizvi, S.S. 1988. New Apparatus for Measurement of Supercritical Fluid-Liquid Phase Equilibria. *AIChE Journal*, 34(8) : 1387-1391.

Adler, S.B., Friend, L., Pigford, R.L. & Rosselli, G.M. 1960. Thermodynamic Consistency of Binary Liquid-Vapour Equilibrium Data when one Component is above its Critical Temperature. *AIChE Journal*, 6(1) : 104-108.

Anderson, T.F. & Prausnitz, J.M. 1978. Application of the UNIQUAC Equation to Calculation of Multicomponent Phase Equilibria. 1 : Vapour Liquid Equilibria. *Ind. Eng. Chem. Process. Des. Dev.*, 17(4) : 552-561.

Anderson, T.F., Abrams, D.S. & Grens, E.A. 1978. Evaluation of Parameters for Nonlinear Thermodynamic Models. *AIChE Journal*, 24(1) : 20-29.

Ashcroft, S.J., Shean, R.B. & Williams, C.J.J. 1983. A Visual Equilibrium Cell for Mulitphase Systems at Pressures up to 690 Bar. *Chem. Eng. Res. Des.*, 61 : 51-55.

Azarnoosh, A. & McKetta, J.J. 1958. The Solubility of Propane in Water. *Petroleum Refiner*, 37(11) : 275-278.

Baker, J.A. 1953. Determination of Activity Coefficients from Total Pressure Measurements. *Australian J. Chem.*, 6 : 206-210.

Bae, H.K., Nagahama, K. & Hirata, M. 1981. Measurement and Correlation of High Pressure Vapour-Liquid Equilibria for the Systems Ethylene-1-Butene and Ethylene-Propylene. *Journal of Chemical Engineering Japan*, 14(1) : 1-6.

Battino, R., Banzhof, M., Bogan, M. & Wilhelm, E. 1971. Apparatus for Rapid Degassing of Liquids, Part III. *Analytical Chemistry*, 43(6) : 806-807

Beck, J.V. & Arnold, K.J. 1977. *Parameter Estimation in Engineering and Science*. New York : John Wiley & Sons.

Benedict, R.P. 1977. *Fundamentals of Temperature, Pressure and Flow Measurements*. Second Edition, New York : John Wiley & Sons.

Besserer, G.J. & Robinson, D.B. 1971. A High Pressure Autocollimating Refractmeter for Determining Co-existing Liquid and Vapour Phase Densities. *The Canadian Journal of Chemical Engineering*, 49 : 651-656.

Bradshaw, S.M. 1985. *A Static Equilibrium Cell for High Pressure and Temperature Vapour-Liquid Equilibrium Measurements*. M.Sc. Thesis, University of Natal Durban.

Braun, G.S. & Schmidt, H. 1984. High Pressure Extraction of Crude Molten Wax. *Ber. Bunsenges. Phys. Chem.*, 88 : 891-894.

BSI. 1983 BS 4559. *British Standard Methods for Preparation of Calibration Gas Mixtures.* Part 3 : Static Volumetric Methods. London : British Standards Institution.

Christiansen, L.J. & Fredenslund, A.A. 1975. Thermodynamic Consistency Using Orthogonal Collocation or Computation of Equilibrium Vapour Compositions at High Pressures. *AIChE Journal*, 21(1) : 49-57.

Chou, C.F., Forbert, R.R. & Prausnitz, J.M. 1990. High Pressure Vapour-Liquid Equilibria for CO_2 / n-Decane, CO_2 / Tetralin and CO_2 / n-Decane / Tetralin at 71.1 and 104,4 °C. *J. Chem. Eng. Data*, 35 : 26-29.

Chueh, P.L., Muirbrook, N.K. & Prausnitz, J.M. 1965. Part II. Thermodynamic Analysis. *AIChE Journal*, 11(6) : 1097-1102.

Cisternas, L.A. 1988. A Simple Accurate Technique To Obtain Pure Component Parameters for Three-Parameter Equations of State. *Fluid Phase Equilibria.* 39 : 75-87.

Cotterman, R.L., Dimitrelis, D. & Prausnitz, J.M. 1984. Supercritical-Fluid Extraction Calculations for High-Boiling Petroleum Fractions using Propane. Application of Continuous Thermodynamics. *Ber. Bunsenges. Phys. Chem.*, 88 : 796-801.

Danner, R.P. & Gupte, P.A. 1986. Density Dependent Local Composition Models : An Interpretive Review. *Fluid Phase Equilibria*, 29 : 415-430.

Debbrecht, F.J. 1985. Qualitative and Quantitative Analysis by Gas Chromatography. In. Grob, R.L. (editor) *Modern Practice of Gas Chromatography* : 361-420. New York : John Wiley & Sons

Di Andreth, J.R. & Paulaitis, M.E. 1987. An Experimental Study of Three- and Four-Phase Equilibrium for Isopropanol-Water-Carbon Dioxide Mixtures at Elevated Pressures. *Fluid Phase Equilibrium*, 32 : 261-271.

Dieters, U. & Schneider, G.M. 1976. Fluid Mixtures at High Pressures. Computer Calculations of the Phase Equilibria and the Critical Phenomena in Fluid Binary Mixtures from the Redlich-Kwong Equation of State. *Ber. Bunsenges. Phys. Chem.*, 12 : 1316-1321.

Dieters, U.K. & Schneider, G.M. 1986. High Pressure Phase Equilibria : Experimental Methods. *Fluid Phase Equilibria*, 29 : 145-160.

Donohue, M.P. & Vimalchand, P. 1988. The Perturbed-Hard-Chain Theory. Extentions and Applications. *Fluid Phase Equilibrium*, 40 : 185-211.

Dorau, W., Kremer, H.W. & Knapp, H. 1983. An apparatus for the Investigation of Low-Temperature, High-Pressure, Vapour-Liquid and Vapour-Liquid-Liquid Equilibria. *Fluid Phase Equilibria*, 11 : 83-89

Dowty Seals 1986. *"O"-Ring Catalogue. Part 2: Range of "O"-Rings and Anti-Extrusion Rings and Housing Data.* Ashchurch, Glos. : Dwoty Seals Ltd.

D'Souza, R. & Teja, A.S. 1988. High Pressure Phase Equilibria in the System Glucose + Fructose + Water + Ethanol + Carbon Dioxide. *Fluid Phase Equilibria*, 39 : 211-224.

D'Souza, R., Patrick, J.R. & Teja, A.S. 1988. High Pressure Phase Equilibrium in the Carbon Dioxide-n-Hexadecane and Carbon Dioxide-Water System. *The Canadian Journal of Chemical Engineering*, 66 : 319-323.

Dymond, J.H. & Smith, E.B. 1980. *The Virial Cofficients of Pure Gases and Mixtures.* New York : Oxford University Press

Eckert, C.J. & Sandler, S.I. 1986. Vapour-Liquid Equilibrium for the Carbon Dioxide Cyclopentane System at 37.7, 45.0 and 60,0 °C. *J. Chem. Eng. Data*, 31 : 26-28.

Fink, S.D. & Hershey, H.C. 1990. Modelling the Vapour-Liquid Equilibria of 1,1,1 - Trichloroethane + Carbon Dioxide and Toluene + Carbon Dioxide at 308, 233 and 353 K. *Ind. Eng. Chem, Res.*, 29 : 295-306.

Fleck, R.N. & Prausnitz, J.M. 1968. Apparatus for Determination of Liquid-Liquid-Gas Equilibria at Advanced Pressures. *Ind. Eng. Chem. Fundam.*, 7(1) : 174-176.

Fredenslund, Aa., Mollerup, J. & Christiansen, L.J. 1973. An Apparatus for Accurate Determinations of Vapour-Liquid Equilibrium Properties and Gas PVT Properties. *Cryogenics*, 13 : 414-419.

Fredenslund, Aa., Gmehling, J. & Rasmussen, P. 1977. *Vapour-Liquid Equilibria using UNIFAC. A group contribution method.* Amsterdam : Elsevier.

Fredenslund, Aa. & Rasmussen, P. (1985). From UNIFAC to SUPERFAC and back? *Fluid Phase Equilibria*, 24 : 115-150.

Freitag, N.P. & Robinson, D.B. 1986. Equilibrium Phase Properties of Hydrogen-Methane-Carbon Dioxide, Hydrogen- Carbon Dioxide-n-Pentane and Hydrogen-n-Pentane Systems. *Fluid Phase Equilibria*, 31 : 183-201.

Figuiere, P., Hom, J.F., Laugier, S., Renon, H., Richon, D. & Szwarc, H. 1980. Vapour-Liquid Equilibria up to 40 000 kPa and 400 °C : A New Static Method. *AIChE Journal*, 26(5) : 872-875.

Galivel-Solastiouk, F. Laugier, S. & Richon, P. 1986. Vapour-Liquid Equilibrium Data for the Propane-Methanol and Propane-Methanol- Carbon Dioxide System. *Fluid Phase Equilibria*, 28 : 73-85.

Gani, R., Tzouvaras, N. Rasmussen, R. & Fredenslund, Aa. 1989. Prediction of Gas Solubility and Vapour-Liquid Equilibria by Group Contribution. *Fluid Phase Equilibria*, 47 : 133-152.

Gmehling, J. & Onken, U. 1977. *Vapour-Liquid Equilibrium Data Collection Vol I.* Chemistry Data Series, Frankfurt Main : DECHEMA.

Guillevic, J.L., Richon, D. & Renon, H. 1983. Vapour-Liquid Equilibrium Measurements up to 558 K and 7MPa : A New Apparatus. *Ind. Eng. Chem Fundam.*, 22 : 495-499.

Gomez-Nieto, M. & Thodos, G. 1978. Vapour-Liquid Equilibrium Measurements for the Propane-Ethanol System at Elevated Pressures. *AIChE Journal*, 24(4) : 672-678.

Gupte, P.A., Rasmussen, P. & Fredenslund, Aa. 1986a. Equation of State Mixing Rules from G^E Models. *Fluid Phase Equilibria*, 29 : 485-494.

Gupte, P.A., Rasmussen, P. & Fredenslund, Aa. 1986b. A New Group-Contribution Equation of State for Vapour-Liquid Equilibria. *Ind. Eng. Chem. Fundam.*, 25(4) : 636-645.

Harmens, A. & Knapp, H. 1980. Three-parameter cubic equation of state for normal substances. *Ind. Eng. Fundamen.*, 19 : 291-294

Haung, S.S.S., Leu, A.D., Ng H.J. & Robinson, D.B. 1985. The Phase Behaviour of Two Mixtures of Methane, Carbon Dioxide, Hydrogen Sulphide, and Water. *Fluid Phase Equilibria*, 19 : 21-32

Haung, S.S.S. & Robinson, D.B. 1985. The Equilibrium Phase Properties of Selected Mesitylene Binary Systems : Mesitylene-Methane and Mesitylene-Carbon Dioxide. *The Canadian Journal of Chemical Engineering*, 63 : 126-130.

Hayden, J.G. & O'Connell, J.P. 1975. A Generalized Method for Predicting Second Virial Coefficients. *Ind. Eng. Chem., Process Des. Dev.*, 14(3) : 209-217.

Hirata, M., Oke, S. & Nagahama, K. 1975. *Computer Aided Data Book of Vapour Liquid Equilibria*, Tokoyo, Kodansha and Elsevier.

Holscher, I.F., Spee, M. & Schneider, G.M. Fluid-Phase Equilibrium of Binary and Ternary Mixtures of CO_2 with hexadecane, 1-dodecanol, 1-hexadecanol and 2-ethyoxy ethonal at 333.2 and 393.2 K and at pressures up to 33 MPa. *Fluid Phase Equilibria*, 49 : 103-113.

Huron, M.J & Vidal, J. 1979. New Mixing Rules in Simple Equations of State for Representing Vapour-Liquid Equilibria of Strongly Non-Ideal Mixtures. *Fluid Phase Equilibria*, 3 : 255-271.

Ibl, N.V. & Dodge, B.F. 1953. Note on Duhem Equation. *Chem. Eng. Sci.*, 2, : 120-126.

Inomata, H., Tuchiya, K., Arai, K. & Saito, S. 1986. Measurement of Vapour-Liquid Equilibria at Elevated Temperatures and Pressures using a Flow-Type Apparatus. *Journal of Chemical Engineering of Japan*, 19(5) : 386-391

Inomata, H., Arai, K. & Saito, S. 1987. Vapour-Liquid Equilibria for CO_2 / hydrocarbon Mixtures at Elevated Temperatures and Pressures. *Fluid Phase Equilibria*, 36 : 107-119.

Inomata, H., Ihawa, N., Arai, K. & Saito, S. 1988. Vapour-Liquid Equilibria for the Amonia-Methanol-Water System. *J. Chem. Eng. Data*, 33 : 26-29.

Japas, M.L. & Franck, E.V. 1985. High Pressure Phase Equilibria and PVT - Data of the Water-Nitrogen System 673K and 250 MPa. *Ber. Bunsenges Phys. Chem.*, 89 : 793-800.

Jennings, D.W. & Teja, A.S. 1989. Vapour-Liquid Equilibria in the Carbon Dioxide - 1 - Hexene and Carbon Dioxide - 1 - Hexyne Systems. *J. Chem. Eng. Data*, 34 : 305-309.

Kadros, P.W. 1977. Response of Temperature Measuring Elements. *Chemmical Engineering*, August 29 : 79-83.

Kalra, H. & Robinson, D.B. 1975. An Apparatus for the Simultaneous Measurement of Equilibrium Phase Composition and Refractive Index Data at Low Temperatures and High Temperatures. Cyrogenics, 15 : 409-412.

Kalra, H., Kubota, H., Robinson, D.B. & Ng, H.J. 1978. Equilibrium Phase Properties of the Carbon Dioxide-n-Heptane System. *J. Chem. Eng. Data*, 23(4) : 317-321.

Kalra, H. & Robinson, D.B. 1979. Vapour-Liquid Equilibrium in a Six-Component Simulated Sour Natural Gas System at Sub Ambient Temperatures. *Fluid Phase Equilibria*, 3 : 133-144.

Kalra, H., Chung, S.V.K. & Chen. C.J. 1987. Phase Equilibrium Data for Supercritical Extraction of Lemon Flavours and Palm Oils with Carbon Dioxide. *Fluid Phase Equilibria*, 36 : 263-278.

Kennedy, R.H. 1983. Selecting Temperature Sensors. *Chemical Engineering*, August 8 : 54-71.

Kertes, A.S. & Hayduk, W. 1986. *IUPAC Solubility Data Series. Propane, Butane and 2-methylpropane Vol 24.* Oxford : Pergamon Press

Kim, C.H., Vimalchand, P. & Donohue, M.D. 1986 a. Vapour Liquid Equilibria for Binary Mixutres of Carbon Dioxide with Benzene, Toluene and p-Xylene. *Fluid Phase Equilibria*, 31 : 299-311.

Kim, H., Lin, H.M. & Chao, K.C. 1986 b. Cubic Chain - of - Rotators Equation of State. *Ind. Eng. Chem. Fundam.*, 25(1) : 75-84.

Kim, C.H., Clark, A.B., Vimalchand, P. & Donohue, M.D. 1989. High Pressure Binary Phase Equilibria of Aromatic Hydrocarbons with CO_2 and C_2H_6. *J. Chem. Eng. Data.*, 34 : 391-395.

King, M.B., Alderson, D.A., Fallah, F.H., Kassim, D.M., Kassim, K.M., Sheldon, J.R. & Mahmud, R.S. 1983. Some Vapour-Liquid and Vapour-Solid Equilibrium Measurements of Relevance for Supercritical Extraction Operations and their Correlation. In Paulaitis, M.E., Penninger, J.M.L., Gray, R.D. & Davidson, P. (eds) *Chemical Engineering at Supercritical Fluid Conditions* : 31-80, Ann Arbor : The Butterworth Group.

Kinny, T.B. 1983. Tuning Process Controllers. *Chemical Engineering*, September 19 : 67-72.

Klink, A.E., Cheh, H.Y. & Amich (Jr), E.H. 1975. The Vapour-Liquid Equilibrium of the Hydrogen-n-Butane System at Elevated Pressures. *AIChE Journal*, 21(6) : 1142-1148.

Knapp, H., Doring, R., Oellrick, L, Plocker, U. & Prausnitz, J.M. 1982. *Vapour Liquid Equilibria for Mixtures of Low Boiling Substances Vol VI.* Chemistry Data Series, Frankfurt Main : DECHEMA.

Knapp, H. 1986. Physical Properties in Process Design - Past, Present and Future. *Fluid Phase Equilibria*, 29 : 1-21.

Kobayashi, R.S. & Katz, D.L. 1953. Vapour-Liquid Equilibria for Binary Hydrocarbon-Water Systems. *Industrial and Engineering Chemistry*, 45(2) : 440-457.

Konrad, R., Swaid, I. & Schneider, G.M., 1983. High-Pressure Phase Studies on Fluid Mixtures of Low-Volatile Organic Substances with Supercritical Carbon Dioxide. *Fluid Phase Equilibria*, 10 : 307-314

Kubota, H., Inotome, H. Tanaka, Y. & Makita, T. 1983. Vapour-Liquid Equilibria of the Ethylene-Propylene System under High Pressure. *Journal of Chemical Engineering Japan*, 16(2) : 99-103.

Larson, B.L., Rasmussen P. & Fredenslund, Aa. 1987. A Modified UNIQUAC Group Contribution Model for Prediction of Phase Equilibrium and Heats of Mixing. *Ind. Eng. Chem, Res.*, 26(11) : 2274-2286.

Laugier, S. & Richon, D. 1986. New Apparatus to Perform Fast Determinations of Mixture Vapour-Liquid Equilibria up to 10 MPa and 423 K. *Rev. Sci. Instrum.*, 57 : 469-472

Leet, W.A., Lin, H.M. & Chao, K.C. 1986. Cubic Chain-of-Rotators Equation of State II for Strongly Polar Substances and Their Mixtures. *Ind. Eng. Chem. Fundam.*, 25(4) : 695-701.

Lee, R.J. & Chao, K.C. 1986. Cubic Chain of Rotators Equation of State with Density-Dependent Local Composition Mixing Rules. *Fluid Phase Equilibria*, 29 : 475-484.

Legret, D., Richon, D. & Renon, H. 1980. Static Still for Measuring Vapour-Liquid Equilibria up to 50 bar. *Ind. Eng. Chem. Fundam.*, 19 : 122-126.

Legret, D., Richon, D. & Renon, H. 1981. Vapour Liquid Equilibria up to 100 MPa : A New Apparatus. *AIChE Journal*, 27(2), 203-207.

Legret, D., Richon, D. & Renon, H. 1984. Critical Evaluation of Methane-Hydrocarbon High-Pressure Experimental Vapour-Liquid Equilibrium Data Using Equations of State. *Fluid Phase Equilibria*, 17 : 232-350.

Leu, A.D. & Robinson, P. 1988. Equilibrium-Phase properties of the Neopentane-Carbon Dioxide Binary System. *J. Chem. Eng. Data*, 33, 313-316.

Lin, H.M. 1984. Peng and Robinson Equation of State for Vapour-Liquid Equilibrium Calculations for Carbon Dioxide + Hydrocarbon Mixtures. *Fluid Phase Equilibria*, 16 : 151-169.

Lin, H.M., Kim, H., Leet, W.A. & Chao, K.C. 1985. New Vapour-Liquid Equilibrium Apparatus for Elevated Temperatures and Pressures. *Ind. Eng. Chem. Fundam.*, 24 : 260 262.

de Loos, T.W., Weijen, A.J.M. & Diepen, G.A.M. 1980. Phase Equilibria and Critical Phenomena in Fluid (Propane + Water) at High Pressures and Temperatures. *J. Chem. Thermodynamics*, 12 : 193-204.

de Loos, T.W., Poot, W. & Lichtenthaler, R.N 1984. Fluid Phase Equilibria in Binary Ethylene + n-Alkane Systems. *Ber. Bunsenges. Phys. Chem.*, 88 : 855-859.

Marina, J.M. & Tassios, D.P. 1973. Effective Local Compositions in Phase Equilibrium Correlations. *Ind. Eng. Chem. Process Des. Dev.*, 12 : 67-71.

Mc Hugh, M. & Krukonis, V. 1986. *Supercritical Fluid Extraction Principles and Practice.* Stoneham, Butterworths.

Meister, K.H. 1985. Apparatuses for the Determination of High-Pressure Vapour-Liquid Equilibrium Data. *Linde Reports on Science and Technology*, (39) : 23-29.

Melhem, G.A., Saini, R.S., Goodwin, B.M. 1989. A Modified Peng-Robinson Equation of State. *Fluid Phase Equilibria*, 47 : 189-237

Meskel-Lesavre, M., Richon, D. & Renon, H. 1981. New Variable Volume Cell for Determining Vapour-Liquid Equilibria and Saturated Liquid Molar Volumes by the Static Method. *Ind. Eng. Chem. Fundam.*, 20 : 284-289.

Mohamed, R.S. & Holder, G.P. 1987. High Pressure Phase Behaviour in Systems Containing Carbon Dioxide and Heavier Compounds with Similar Vapour Pressures. *Fluid Phase Equilibria*, 47 : 189-237.

Morris, W.O. & Donohue, M.D. 1985. Vapour-Liquid Equilibrium in Mixtures Containing Carbon Dioxide, Zoluene, and 1-methylpaphthalene. *J. Chem. Eng. Data*, 30 : 259-263.

Meyers, A.L. & Seider, W.D. 1976. *Introduction to Chemical Engineering and Computer Calculations.* Englewood Cliffs, New Jersey : Prentice Hall.

Muirbrook, N,K. & Prausnitz, J.M. 1965. Multicomponent Vapour-Liquid Equilibria at High Pressures : Part 1. Experimental Study of the Nitrogen-Oxygen-Carbon Dioxide System ay 0°C. *AIChE Journal*, 11(6) : 1092-1096.

Nagarajan, N. & Robinson, R.L. 1987. Equilibrium Phase Compositions, Phase Densities, and Interfacial Tensions for CO_2 + Hydrocarbon Systems 3. CO_2 cyclohexane 4. CO_2 + benzene. *J. Chem. Eng. Data* : 369-371.

Nagahama, K., Suda, S. Hakuta, T. & Hirata, M. 1971. Determination of Vapour-Liquid Equilibrium From Total Pressure Measurement - C3 -Hydrocarbon-Solvent. *Sekuju Gakkai Shi*, 14(4) : 252-256.

Nakayama, T., Sagara, H., Arai, K. & Saito, S. 1987. High Pressure Liquid-Liquid Equilibiria for the System of Water, Ethanol and 1,1-Difureothane at 323,2 K. *Fluid Phase Equilibria*, 38 : 109-127.

Ng, H.J. & Robinson, D.B. 1978. Equilibrium Phase Properties of the Toluene-Carbon Dioxide System. *J. Chem. Eng. Data*, 23(4) : 325-327

Ng, H.J. & Robinson, D.B., 1979. The Equilibrium Phase Properties of Selected Naphthenic Binary Systems : Carbon Dioxide-Methylayclohexane, Hydrogen Sulphide - Methycyclohexane. *Fluid Phase Equilibria*, 2 : 283-292.

Niesen, V., Palvara, A., Kidnay, A.J. & Esavage. 1986. An Apparatus for Vapour-Liquid equilibrium at Elevated Temperatures and Pressures and Selected Results for the Water-Ethanol and Methanol-Ethanol Systems. *Fluid Phase Equilibria*, 31 : 283-298.

Nichols, J.V. & White, D.R. 1982. *Traceable Temperatures.* New Zealand Department of Scientific and Industrial Research, Wellington, New Zealand.

Peschel, W. & Wenzel, H. 1984. Equation of State Predictions of Phase Equilibria at Elevated Pressures in Mixtures Containing Methanol. *Ber. Bunsenges. Phys. Chem.*, 88 : 807-812.

Peng, D.Y. & Robinson, D.B. 1976. A New Two-Constant Equation of State. *Ind. Eng. Chem. Funda.* 15(1) : 59-64.

Perry, R.H. & Green, D. 1984. *Perry's Chemical Engineers Handbook.* International Edition, Singapore, McGraw Hill.

Prausnitz, J.M., Eckert, C.A., Orye, R.V. & O'Connell, J.P. 1967. *Computer Calculations for Mulitcomponent Vapour-Liquid Equilibria.* Englewood Cliffs, N.J., Prentice Hall.

Prausnitz, J.M. & Chueh, P.L. 1968. *Computer Calculation for High-Pessure Vapour-Liquid Equilibria.* Englewood Cliffs, N.J., Prentice Hall.

Prausnitz, J.M. 1979. Molecular Thermodynamics for Chemical Process Design. *Science*, 205 : 759-766.

Prausnitz, J.M., Lichtenthaber, R.N. & Azevedo, E.G. 1986. *Molecular Thermodynamics of Fluid-Phase Equilibria.* 2nd edition, Englewood Cliffs N.J., Prentice Hall.

Prausnitz, J.M., Anderson, T., Grens, E., Eckert, C., Hsieh, R. & O'Connell, J.P. 1980. *Computer Calculations for Multicomponent Vapour-Liquid and Liquid-Liquid Equilibria.* Englewood Cliffs, N.J., Prentice Hall.

Press, W.H., Flanney, B.P., Teukolsky, S.A. & Vetterling, W.T. 1986. *Numerical Recipes. The Art of Scientific Computing.* Cambridge University Press.

Raal, J.D. & Naidoo, P. 1990. Excess Enthalpy Measurements using a Novel Highly Refined Microflow Calorimeter and the Prediction of Vapour-Liquid Equilibria from such Data. *Fluid Phase Equilibria*, 57 : 147-160.

Radosz, M. 1984. Variable-Volume Circulation Apparatus for Measuring High-Pressure Fluid Phase Equilibria. *Ber. Bensenges. Phys. Chem.*, 88 : 859-862.

Radosz, M., Cotterman, R.L. & Prausnitz, J.M. 1987. Phase Equilibria in Supercritical Propane Systems for the Separation of Continous Oil Mixtures. *Ind. Eng. Chem. Res.*, 26(4) : 731-737

Reid, R.C., Prausnitz, J.M. & Polling, B.E. 1987. *The Properties of Gases and Liquids.* McGraw Hill.

Reiff, W.E., Peters-Gerth, P. & Lucas, K. 1987. A Static Equilibrium Apparatus for (Vapour + Liquid) Equilibrium Measurements at High Temperatures and Pressures. Results for (methane + n-pentane). *J. Chem. Thermodynamics*, 19 : 467-477.

Renon, H. & Prausnitz, J.M. 1968. Local Compositions in Thermodynamic Excess Functions for Liquid Mixtures. *AIChE Journal*, 14 : 135-144.

Renon, H., Laugier, S., Schwartzentruber, S. & Richon, D. 1989. New Determinations of High Pressure Vapour-Liquid Equilibria in Binary Systems Containing n-Propylbenzene with Nitrogen or Carbon Dioxide consistent with the Prausnitz-Keeler Test. *Fluid Phase Equilibria*, 51 : 285-298.

Rigas, T.J., Mason, D.F. & Thodos, G. 1958. Vapour-Liquid Equilibria Microsampling Technique Applied to a New Variable Volume Cell. *Ind. Eng. Chem.*, 50(9) : 1297-1300.

Roebers, J.R. & Theis, M.C. 1990. An Equilibrium View Cell for Measuring Phase Equilibria at Elevated Temperatures and Pressures. *Ind. Eng. Chem. Res.*, 29 : 1568-1570.

Rogers, B.L. & Prausrutz, J.M. 1970. Sample-Extraction Apparatus for High Pressure Vapour-Liquid Equilibria. *Ind. Eng. Chem. Fundam.*, 9(1) : 174-177.

Rousseaux, P., Richon, D. & Renon, H. 1983. A Static Method For Determination of Vapour-Liquid Equilibria and Saturated Liquid Molor Volumes at High Pressures and Temperatures Using a New Variable-Volume Cell. *Fluid Phase Equilibria*, 11 : 153-168.

Sagra, H., Arai, Y. & Saito, S. 1972. Vapour-Liquid Equilibria of Binary and Ternary Systems Containing Hydrogen and Light Hydrocarbons. *Journal of Chemical Engineering Japan*, 54 : 339-348.

Scheid, F. 1986. *Schaum's Outline Series. Theory and Problems of Numerical Analysis.* New York, McGraw Hill.

Schneider, G.M. 1978. High Pressure Phase Diagrams and Critical Properties of Fluid Mixtures. In McGlaston, M.L. (senior reporter) *A Specialist Periodical Report, Vol 2 : Chemical Thermodynamics* : 105-142. London, The Chemical Society.

Schwartzentruber, J., Galivel-Solastiouk, F. & Renon, H. 1987. Representation of the Vapour-Liquid Equibibrium of the Ternary System Carbon Dioxide-Propane-Methanol and its Binaries with a Cubic Equation of State : A New Mixing Rule. *Fluid Phase Equilibria*, 38 : 217-226.

Schwartzentruber, J. & Renon, H. 1989. Extension of UNIFAC to High Pressures and Temperatures by the Use of a Cubic Equation of State. *Ind. Eng. Chem. Res.*, 28(7) : 1049-1055.

Schwartzentruber, J., Renon, H. & Watanasi, S. 1989. Development of a New Cubic Equation of State for Phase Equilibrium Calculations. *Fluid Phase Equilibria*, 52 : 127-134.

Sebastian, H.M., Simmick, J.J., Lin, H.M. & Chao, K.C. 1980. Gas-Liquid Equilibrium in Mixtures of Carbon Dioxide + Toluene and Carbon Dioxide + m-xylene. *J. Chem. Eng. Data*, 25 : 246-248.

Shah, N.N., Pozo de Fernandez, M.E., Zollweg, J.A. & Streett, W.B. 1990. Vapour-Liquid Equilibrium in the System Carbon Dioxide + 2,2-Dimethylpropane from 262 to 424 K at Pressures to 8.4 MPa. *J. Chem. Eng. Data*, 35 : 278-283

Sheng, Y.J., Chen Y.P. & Wong, D.S.H. 1989. A Cubic Equation of State for Predicting Vapour-Liquid Equilibria of Hydrocarbon Mixtures Using a Group Contribution Mixing Rule. *Fluid Phase Equilibria.* 46 : 197-210.

Shibata, S.K. & Sandler, S.I. 1989 a. High Pressure Vapour-Liquid Equilibria Involving Mixtures of Nitrogen, Carbon Dioxide and n-Butane. *J. Chem. Eng. Data*, 34, : 291-298.

Shibata, S.K. & Sandler, S.I. 1989 b. Critical Evaluation of Equation of State Mixing Rules for the Prediction of High-Pressure Phase Equilibria. *Ind. Eng. Chem. Res.*, 28(12) : 1893-1898.

Simnick, J.J., Lawson, C.C., Lin, H.M. & Chao, K.C. 1977. Vapour-Liquid Equilibrium of Hydrogen/Tetralin System at Elevated Temperatures and Pressures. *AIChE Journal*, 23(4) : 469-476.

Skjold-Jorgenson, S., Rasmussen, P., & Fredenslund, Aa. 1980. On the Temperature Dependence of the UNIQUAC/UNIFAC Models. *Chem. Eng. Sci.*, 35 : 2389-2403.

Skjold-Jorgensen, S. 1984. Gas Solubility Calculations II. Application of a New Group-Contribution Equation of State. *Fluid Phase Equilibria*, 16 : 317-351.

Skjold-Jorgensen, S. 1988. Group Contribution Equation of State (GEOS) : A Predictive Method of Phase Equilibrium Computations over Wide Ranges of Temperature and Pressures up to 30 MPa. *Ind. Eng. Chem. Res.*, 28 (12) : 1893-1898.

Smith, J.M. & Van Ness, H.C. 1975. *Introduction to Chemical Engineering Thermodynamics.* 3rd edition, Tokyo : McGraw Hill.

Streett, W.B. 1983. Phase Equilibria in Fluid and Solid Mixtures at High Pressures. In Paulaitis, M.E., Penninger, J.M.L., Gray, R.D. & Davidson, P. (eds) *Chemical Engineering at Supercritical Fluid Conditions* : 3-30, Ann Arbor : The Butterworth Group.

Stryjeck, R. Vera, J.H. 1986. PRSV2: A Cubic Equation of State for Pure Components and Mixtures. *Canadian Journal of Chemical Engineering*, 64 : 323-333.

Suppes, G.J. & McHugh, M.A. 1989. Phase Behaviour of the Carbon Dioxide-Styrene System. *J. Chem. Eng. Data*, 34 : 310-312.

Suzuki, K., Sue, H., Itou, M., Smith, R.L., Inomata, H., Arai, K. & Saito, S. 1990 a. Isothermal Vapour-Liquid Equilibrium Data for Binary Systems at High Pressures. Carbon Dioxide-Methanol, Carbon Dioxide-Ethanol, Carbon Dioxide-1- propanol, Ethene-Ethanol, and Ethane-1-Propanol Systems. *J. Chem. Eng. Data*, 35 : 63-66.

Suzuki, K., Sue, H., Arai, K. & Saito, S. 1990 b. Vaqpour-Liquid Equilibria for Synthetic Alchols Process. *Fluid Phase Equilibria*, 59 : 115-134.

Takishima, S., Saiki, K., Arai, K., Saito, S. 1986. Phase Equilibria for CO_2 - C_2H_5OH - H_2O System. *J. Chem. Eng. Japan*, 19(1) : 48-56.

Toedheide, K. & Franck, E.U. 1963. Das Zweiphasengebiet und die Kritische Kurve im System Kohlendioxid-Wasser bis zu Druken von 3500 Bar. *Z. Phys. Chem.*, 37 : 387-401.

Trebble, M.A. & Bishnoi, P.R. 1987. Development of a New Four Parameter Cubic Equation of State. *Fluid Phase Equilibria*, 35 : 1-18.

Tsiklis, D.S. 1968. *Handbook of Techniques In High Pressure Research Engineering*. New York : Plenum Press.

Tsonopoulos, C. & Heidman, J.L. 1986. High-Pressure Vapour-Liquid Equilibria with Cubic Equations of State. *Fluid Phase Equilibria*, 29 : 391-414.

Vidal, J. 1984. Phase Equilibria and Density Calculations of Mixtures in the Critical Range with Simple Equations of State. *Ber. Bensenges Phys. Chem.*, 88 : 784-791.

Van Ness, H.C., Byer, S.M. & Gibbs, R.E. 1973. Vapour-Liquid Equilibrium : Part 1. An Appraisal of Data Reduction Methods. *AIChE Journal* 19(2) : 238-245.

Van Ness, H.C. & Abbot, M.M. 1982. *Chemical Thermodynamics of Nonelectrolyte Solutions With Applications to Phase Equilibria*. New York : McGraw Hill.

Wagner, Z. & Wichterle, I. 1987. High-Pressure Vapour-Liquid Equilibrium in Systems Containing Carbon Dioxide, 1-hexene and n-hexane. *Fluid Phase Equilibria*, 33 : 109-123.

Walas, S.M. 1985. *Phase Equilibria in Chemical Engineering*. Stoneham, Butterworths.

Weast, R.C., Astle, M.J. & Beyer, W.H. (eds). 1984. *CRC Handbook of Chemistry and Physics*. 65th edition Boca Raton, Fl. : CRC Press.

Weber, W., Zeck, S. & Knapp, H. 1984. Gas Solubilities in Liquid Solvents at High Pressures. Apparatus and Results for Binary and Ternary Systems of N_2 ,CO_2, and CH_3OH. *Fluid Phase Equilibria*, 18 : 253-278.

Weber, L.A. 1989. Simple Apparatus for Vapour-Liquid Equilibrium Measurements with Data for the Binary Systems of Carbon Dioxide with n-Butane and n-hexane. *Fluid Phase Equilibria*, 3 4 : 171 - 175.

Westerford, P. 1987. *Thermodemente und Wilderstandsthermometer*. Frankfurt on Main : Mannesmann Hartman & Braun.

White, P.R. & Brown, G.G. 1942. Phase Equilibria at High Temperatures. *Ind. Eng. Chem.*, 34(10) : 1162-1174.

Wichterle, I., Lineh, J. & Hala, E. 1973. and Supplements 1976, 1979, 1982. *Vapour-Liquid Equilibrium Data Bibliography*. Amsterdam : Elsevier.

Wichterle, I. 1978 a. High-Pressure Vapour-Liquid Equilibrium. IV Quantitative Description. Part 2. *Fluid Phase Equilibria*, 2 : 59-78.

Wichterle, I. 1978 b. High-Pressure Vapour-Liquid Equilibrium. IV Quantitative Description. Part 3. *Fluid Phase Equilibria*, 3 : 143-159.

Wilner, B.L. 1960. Variable Capacitance Liquid Level Sensors. *The Review of Scientific Instruments*, 31(5) : 501-507.

Won, K.W. & Prausnitz, J.M. 1973. High Pressure Vapour-Liquid Equilibria. Calculation of Partial Pressures from Total Pressure Data. Thermodynamic Consistency. *Ind. Eng. Chem. Fundam.*, 12(4) : 459-463.

Yorizane, M., Yoshimura, S., Masuoka, H., Miyano, Y. & Kakimoto, Y. 1985. New Procedure for Vapour-Liquid Equilibria. Nitrogen + Carbon Dioxide, Methane + Freon 22, and Methane + Freon 12. *J Chem. Eng. Data*, 30 : 174-176.

Young, C.L. 1978. Experimental Methods for Studying Phase Behaviour of Mixtures at High Temperatures and Pressures. In McGlaston, M.L. (senior reporter) *A Specialist Periodical Report, Vol 2 : Chemical Thermodynamics* : 71-104. London, The Chemical Society.

Zeck, S. & Knapp, H 1986. Vapour-Liquid and Vapour-Liquid-Liquid Phase Equilibria for Binary and Ternary Systems of Nitrogen, Ethane and Methanol: Experimental and Data Reduction. *Fluid Phase Equilibria*, 25 : 303-322

APPENDICES

APPENDIX A

A.1 PHASE DIAGRAMS

Phase rule constraints on phase diagrams

A phase rule analysis of an equilibrium system serves as an important guide in the construction and interpretation of its phase diagram; through the determination of the system's number of independent variables. The phase rule form for determining the number of independent variables in a non-reacting system is expressed by the relation :-

$$f = C + 2 - p$$

where f = number of independent variables (degrees of freedom).
C = number of components.
p = number of phases.

Knowing the number of independent variables, it is possible to determine the geometrical constraints on the features that describe the co-existence of the phases on the phase diagram. The maximum number of independent variables for a two component equilibrium system is three. The system's phase behaviour can therefore be completely described by means of volumes, surfaces, lines and points in a three dimensional space.

Independent variable type constraints on phase diagrams

Additional geometrical constraints are imposed on the phase diagram features by the distribution of the independent variables between the so called **field** and **density** variables. The distinction between these variables is an important concept in mixture thermodynamics . Field variables such as pressure, temperature and chemical potential have the same value in the coexisting phases at equilibrium. The density variables such as mole fractions, molar volumes, density, internal energy and index of refraction usually have different values in the coexisting phases at equilibrium. For each phase rule variable that is a "field" variable there is a degeneracy that reduces the total number of independent variables by $p - 1$ for $(p > 1)$.

Measurement of Independent Variables in Two Component Two Phase Systems

According to the phase rule, in a two component two phase (vapour-liquid) equilibrium system two independent variables need to be known to completely describe the equilibrium condition. The most conveniently measured independent variables in the study of phase equilibria in fluid systems are pressure and temperature. Changes in these two variables produce dramatic changes in the phase behaviour. As temperature and pressure are both "field" variables it is necessary to measure a third variable to be able to completely describe the two component system.

For qualitative descriptions and comparisons of equilibrium data the most convenient choice of the third variable is a composition. Composition is relatively easily measured and is the most useful in that P , T , x and y diagrams provide the basis for the design of separation process equipment such as distillation and extraction unit operations.

Although only three of the four variables P , T , x and y need to be known to completely define the equilibrium condition; it is difficult to theoretically predict (in high temperature and pressure cases especially) the fourth variable from the three measured variables. Although the measurement of the four variables P , T , x and y , implies an over-specification in terms of the phase rule, it is nevertheless the preferred technique for accurately acquiring high pressure and temperature data. Furthermore this over-determination allows for the thermodynamic consistency testing of the experimental data.

Presentation Of Phase Diagrams For Two Component Two Phase Systems

Presentation of two component vapour-liquid equilibrium data in three dimensional space is both tedious to draw and difficult to interpret. The convention that has been adopted is to use sections of the three dimensional space cut by planes of constant pressure, temperature and composition commonly called isobars, isotherms and isopleths. Data is most frequently reported as isothermal $P-x-y$ data as the measurement of isobaric $T-x-y$ data are experimental more demanding. Theoretical treatment of isobaric data requires the values of excess enthalpy which are scarce for high pressures. Isopleth $P-T-x$ data sets are less common than $P-x-y$ data but more commonly reported than $T-x-y$ data.

A.2 SINGLE PHASE RECIRCULATION APPARATUS IN THE LITERATURE

Vapour phase recirculation apparatus in the literature

Freitag, *et al* (1986) extracted liquid samples directly from the equilibrium cell through a 90 cm capillary tube, at the end of which was located the liquid sampling valve. The 0,23 mm id capillary tube had a 0,15 mm diameter wire inserted along its length. This arrangement provided for the acquisition of a low-pressure vapour sample of the same composition as the high pressure liquid in the cell. All of the sample was captured as it flashed while flowing through the capillary tube and needle valve. The low pressure sample was circulated to ensure homogeneity before being analysed.

Dorau, *et al* (1983) extracted both the vapour and liquid samples directly from the equilibrium cell through capillary tubes. These capillaries led to evacuated flasks attached by rapid connection couplings. In order to achieve representative liquid samples the flask quantity had to be greater than the inventory of the capillary tubing.

The experimental method of Chou, *et al* (1990) was somewhat similar. The equilibrium cell had separate sampling ports for the vapour and liquid phases respectively. A specially designed microcell similar in principle to the ones used by Legret, *et al* (1981) was attached to each sampling port. The microcell collected an equilibrium phase sample at the conditions of the equilibrium cell. The microcells, after a suitable time, were removed and attached to the sample analysis system (enclosed in a separate air bath), for composition analysis. In the sample analysis system the microcell was attached to a variable-volume bellows assembly that acted both as a flash vessel, and pump. The bellows assembly circulated the flashed sample through the gas chromatographic sampling valve until a homogeneous sample suitable for composition analysis was obtained.

The equilibrium cell of Weber, *et al* (1984) showing the principle features of a vapour recirculation equilibrium cell is shown in Figure A.1.

The apparatus of Kim, *et al* (1986 a) was used to measure the carbon dioxide/toluene system. The equilibrium cell was contained in an oil bath. The circulation of the liquid phase resulted in rapid equilibration - the authors claim approximately 10 minutes. The liquid phase was sampled by means of a sampling loop located in the liquid recirculation line. Vapour was allowed to diffuse to the gas sampling valve located outside the oil bath through lines wrapped with heating wire. The vapour and liquid samples were transported with helium carrier gas to a gas chromatograph for composition analysis.

A.3 TWO - PHASE RECIRCULATION APPARATUS IN THE LITERATURE

One of the earliest examples of this type of apparatus was that used by Muirbrook and Prausnitz (1965) to measure the ternary nitrogen-oxygen-carbon dioxide system. Each phase was circulated by specially designed vane pumps through tubing external to the equilibrium cell. The circulation of the phases provided ample agitation to ensure equilibration of the phases. No extra means of liquid agitation was required. Samples for analysis were obtained by blocking off sections of the circulation line. Calibration of these sample spaces permitted the determination of phase molar volumes. Liquid entrainment of the vapour stream was prevented by a simple baffle. The authors reported using a liquid level indicator.

The experimental apparatus of Morris and Donohue (1985) and Fink and Hershey (1990) are of particular interest to this project as they were used to measure the carbon dioxide/toluene system.

The equilibrium cell of Kim, *et al* (1989) was contained in an oil bath and was equipped with two transparent glass windows. With vapour and liquid flow rates of 60 and 6 m^3/min respectively, claimed equilibration time was 10 - 15 minutes. Liquid and vapour samples of 20 to 250 μl respectively were trapped in the external loops of the sampling valves place directly in the liquid and vapour recirculation lines

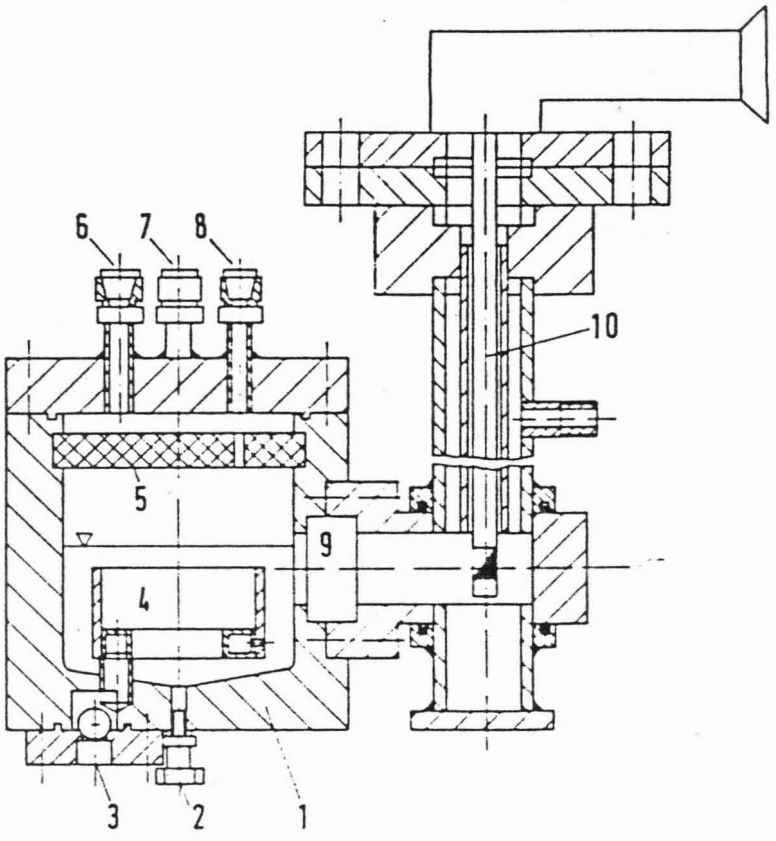

Figure A.1 Equilibrium Cell of Weber, *et al* (1984)

Design of high-pressure equilibrium cell (EC) with optical equipment: 1. cell body; 2. solvent inlet; 3. gas inlet; 4. distribution nozzle; 5. mist separator; 6. gas outlet; 7. connection for temperature sensor; 8. connection for capillary; 9. high-pressure glass window; 10. inspection and illumination device.

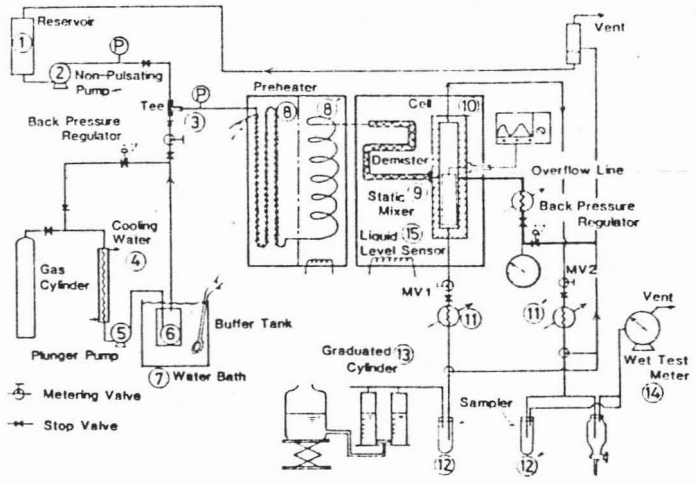

Figure A.2 Experimental Apparatus of Inomata, *et al* (1986)

The experimental apparatus of Kubota, *et al* (1983) used a 6 port valve which (with the appropriate setting) allowed the high pressure pump to circulate either the vapour or liquid phase. Representative samples of the vapour and liquid phases were trapped in the 4 port valve and consequently released into a low pressure line. The sample was circulated until it was homogenized. After sample homogenization it was analysed by gas chromatography. The authors claimed that equilibration of the phases required approximately 2 hours.

The most popular method in recent years of sampling the circulating phases is by using a a commercial sampling valve located in the circulation lines. In contrast Shibata and Sandler (1989 a) used an elaborate method of trapping vapour and liquid samples in sample bombs and transferring these to a gas chromatograph for analysis. The latter are very similar to the methods used by Dorou, *et al* (1983) and Chou, *et al* (1990) in the vapour recirculation methods.

Yorizane, *et al* (1985) describe an unusual method of cell content agitation. The apparatus consists of two equilibrium cells which were connected to each other at both the top and bottom ends by means of flexible stainless steel tubes. One cell was fixed while the other was moved slowly up and down by means of a mechanical device. This motion resulted in a pressure gradient which caused the liquid and vapour phases to flow in opposite directions in an attempt to equalize the pressure. In doing so phase contacting took place.

A.4 SINGLE VAPOUR AND LIQUID PASS APPARATUS IN THE LITERATURE

A schematic diagram of the apparatus used by Inomata, *et al* (1986) to measure a variety of carbon dioxide/hydrocarbon systems is shown in Figure A.2. The essential features common to all flow apparatus of this kind , feed system, preheater, equilibration system (static mixer and equilibrium cell) and sampling system, are present.

The gaseous component was supplied from a buffer tank at its critical pressure. The gaseous and liquid components were contacted co-currently before entering the preheater. The preheater consisted of a tube which was initially heated by an electric line heater and finally by an air bath. The air bath was responsible for adjusting the mixture to the desired equilibrium temperature. The static mixer ensured the mixture was well homogenized in order that rapid equilibriation could take place in the equilibrium cell. The cell design incorporated features to minimise fluid entrainment :

1. The inlet nozzle was inclined so as to minimise liquid entrainment in the vapour phase. As an additional measure a demister was fitted at the vapour outlet.
2. To avoid vapour entrainment of the liquid withdrawn from the cell and to maintain a steady liquid level, the cell was fitted with an overflow-type self-control system and back pressure regulator. The cell liquid level was

automatically controlled at the position of the outlet nozzle which was connected to the overflow line. The pressure was maintained at a fixed value by the back pressure regulator.

The liquid level could be detected by a capacitor sensor and according to the authors proved a useful aid for achieving good steady-state operation.

Liquid was constantly removed from the bottom of the cell while the vapour exited from the top.

Analysis of the sampled liquid and vapour phase (trapped in samplers after steady-state had been achieved), had to be meticulously performed in order to avoid potentially large errors. Cooling and decompression of the trapped samples led to the separation of the samples into a gas and liquid phase. The liquid in the samplers was weighed and analysed by gas chromatography. The volume of gas in the *liquid phase* sample was measured by a graduated cylinder and that in the *vapour phase* sample with a wet test meter. A correction was made for heavy components that vapourised upon decompression.

Simnick, *et al* (1977) combined the final heater and static mixer features in the Inomata, *et al* (1986) apparatus into one unit. They fitted a notched twisted ribbon in the entire length of their heater/mixer. This unit brought the final temperature of the mixture to within 1 °C of the equilibrium temperature.

Provision was made for two methods of sampling :

1. The cell effluents still at high temperatures and pressures were diverted by means of a manifold valve and analysed in a gas chromatograph.
2. The second method was essentially the same as Inomata's, *et al* (1986).

The authors report accuracies of 0,5 % on *volume method* mole fraction determinations.

The auxiliary apparatus of Lin, *et al* (1985) is essentially the same as that of Simnick, *et al* (1977). The equilibrium cell was however, different. Lin, *et al* (1985) found the capacitor level indicator of Simnick, *et al* (1977) to be useless for the system being measured. They therefore had to design an optical cell. The sapphire window created a sealing problem as no organic elastomer could seal at the temperatures of interest. The problem was solved using a gold "O'-ring with a copper shim. Nevertheless the authors consider this seal to be the factor limiting the pressure and temperatures that can be achieved. The auxiliary apparatus of Niesen, *et al* (1986) was essentially the same as that of Lin, *et al* (1985). The equilibrium cell was however different from that of Lin, *et al* (1985). Severe corrosion problems were experienced which ruled out the use of a liquid level measuring device which necessitated the use of a view cell.

The equipment and phase analysis method of Sebastian, *et al* (1980) was essentially the same as described by Simnick, *et al* (1977). The apparatus was used to measure the carbon dioxide/toluene system and carbon dioxide/m-xylene system at high temperatures.

Simnick, *et al* (1977), Sebastian, *et al* (1980), Lin, *et al* (1985) and Inomata, *et al* (1986) indicated that the measured compositions of the vapour and liquid phases were independent of the feed flow rates tested, indicating equilibrium had indeed been reached.

Sebastian, *et al* (1980) and Inomata, *et al* (1986) analysed some samples for traces of thermal decomposition. Gas chromatography and mass spectrometry analysis found these to be negligibly small.

Roebers and Theis (1990) describe a thoroughly well-thought-out and designed equilibrium cell which theoretically has superior temperature and pressure operating ranges to other equilibrium cells. Experimental results using this cell were in press at the time of writing and could therefore not be commented on.

A.5 STATIC ANALYTIC APPARATUS IN THE LITERATURE

Experimental apparatus of Besserer and Robinson (1977).

Besserer and Robinson (1977) have described a variable-volume equilibrium cell, Figure A.3, capable of measuring refractive indexes and vapour-liquid equilibrium data. The cell consisted of three sections; two cylinder-piston end sections and a central window section bolted together. High pressure teflon "O"-rings seals provided an adequate seal. The main functions of the two pistons were to :

1. Isolate the cell contents from the hydraulic fluid,
2. Provide a means of varying the cell volume and
3. Mix the cell contents.

The piston seal was effected by four "O"-rings: one teflon and three neoprene. The central windowed section contained the temperature-and pressure-measuring devices and the sampling and optical systems.

The sampling valves were commercially bought micrometering valves with provision made for flushing out and evacuating the low pressure sampling lines. The average size of each sample taken was 10^{-3} g moles which corresponded to a 0,2 % depletion of the contents of the cell.

A thermocouple proportional-band temperature-controller controlled the heaters in the aluminium environment control shrouds placed over the ends of the cell to within 0,5 K of the setpoint.

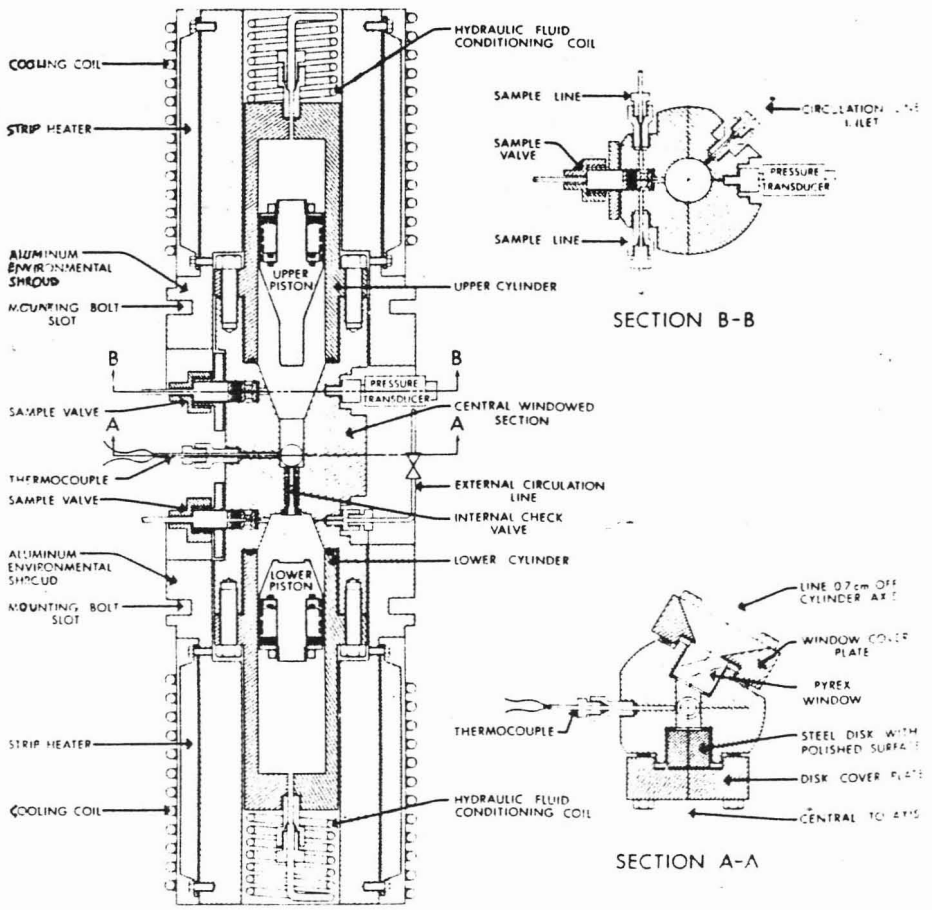

Figure A.3 Equilibrium Cell of Bresserer and Robinson (1977)

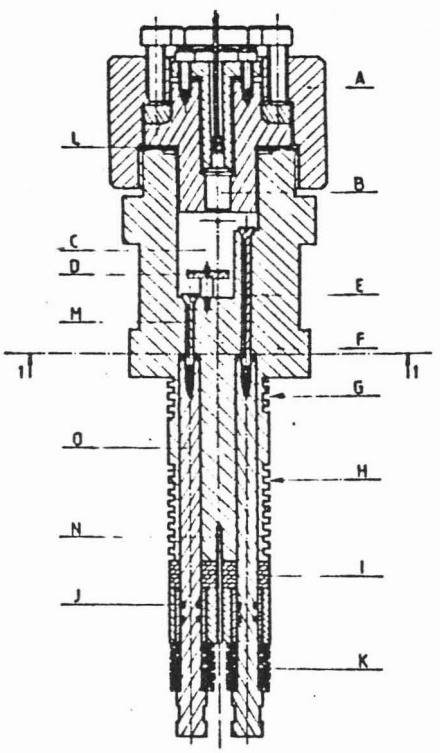

Equilibrium cell: A cell cap, B pressure transducer, C equilibrium compartment, D magnetic stirrer, E valve, F cell body, G heating resistance place, H cooling coil place, I teflon thermal shield, J viton O-ring, K spring washers, L copper gasket, M channel, N thermocouple well, O valve pusher.

Figure A.4 Equilibrium Cell of Figuiere, *et al* (1980)

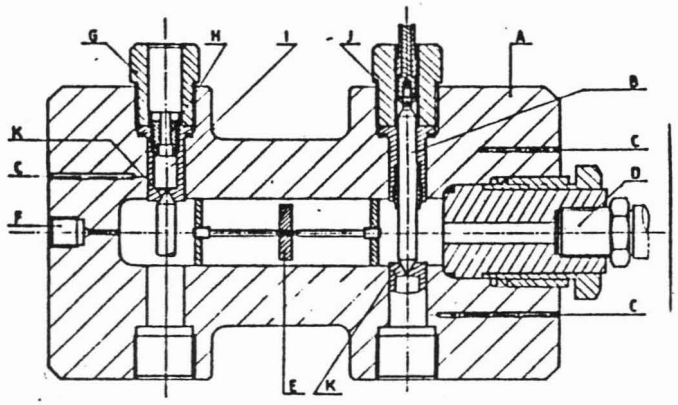

A	Cell body
B	Sampling valve with packing joint
C	Thermocouple well
D	Pressure transducer
E	Magnetic stirrer
F	Connection to filling circuit
G	Microcell bearer fixing-pin
H	Microcell set-screw
I	Microcell
J	Valve fixing-pin
K	Seat of sampling valve stem

Figure A.5 Equilibrium Cell of Legret, *et al* (1981)

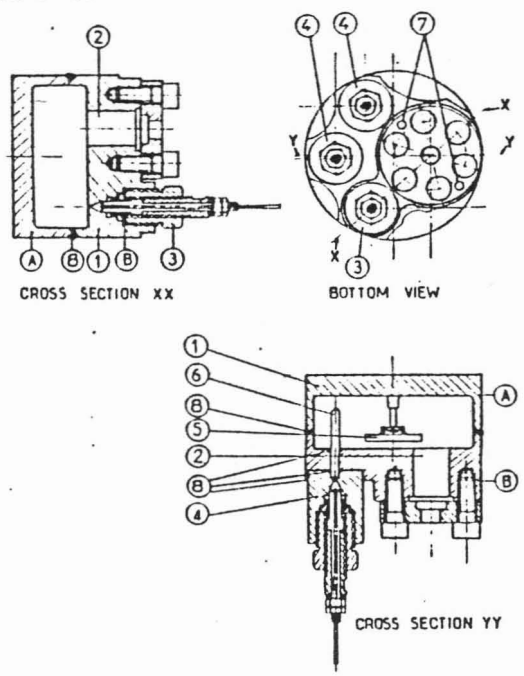

Equilibrium cell: 1, cell body; 2, location of the pressure transducer; 3, feeding valve; 4, sampling valve; 5, magnet; 6, capillary; 7, well for a thermocouple; 8, welding.

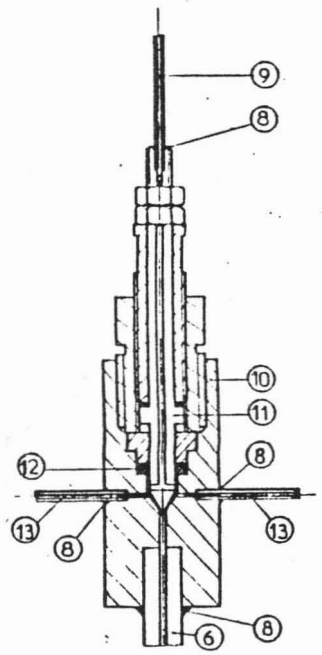

Sampling valve: 6, capillary; 8, welding; 9, carrier gas tubing (outlet); 10, sampling valve body; 11, nonrotating stem; 12, high-temperature resistant polymer O-ring; 13, carrier gas tubing (inlet).

Figure A.6 Equilibrium Cell of Guillevic, *et al* (1981)

Equilibration and mixing of the cell contents was achieved by transferring the contents between the upper and lower cylinders. On the upstroke, the internal check valve in the central section was closed and the fluids in the lower cylinder were forced through the external circulation line into the upper cylinder. On the downward stroke the circulation line valve was closed and the fluids passed from the upper cylinder through the check valve into the lower cylinder. The authors claimed that on average five to ten cycles were required to obtain equilibrium between the phases. Achievement of equilibrium was ascertained once the reflected light image became stable in each phase.

Experimental apparatus of Figuiere, et al (1980)

The experimental system of Figuiere, *et al* (1980) consisted of :

1. A degassing cell to degass liquid before it was fed into the cell,
2. A compressor to feed gases under pressure into the cell,
3. An equilibrium cell, Figure A.4,
4. Cooling and heating systems to control the environment surrounding the equilibrium cell and
5. A gas-liquid-chromatograph .

The unique feature of the apparatus was the vapour and liquid sampling valves. The valves were opened by a hammer activated by an electromagnet and transmitted to the valves by pushers. The valves were returned onto their seats by powerful spring washers. The quantity of the sample withdrawn depended on the opening time of the valve. Opening times of a few hundredths of a second allowed approximately 1 μl to be withdrawn. The withdrawn sample flowed through slits machined along the stems where it encountered the chromatographic carrier gas. The carrier gas carried the sample to a gas liquid chromatograph for composition analysis.

Tightness around the pushers was achieved by means of viton "O"-rings which had to be cooled to prevent thermal damage. The resultant heat transfer from the top to the bottom of the cell was minimized by a teflon thermal break which in turn was prevented from overheating by cooling water tubing wound around the lower part of the cell.

Four thermocouples were located within the equilibrium cell body at different levels, to determine the existence, if any, of thermal gradients in the equilibrium cell.

Equilibration of the phases was achieved by a magnetic stirrer rotating in an orientable magnetic field induced by four coils located outside the cell.

The authors stated that their main difficulty was to achieve a reliable leakproof seal between the valves and their seats. This problem was overcome by depositing smooth metal into the conical part of the valve.

Experimental apparatus of Legret, et al (1981)

The experimental system of Legret, *et al* (1981) consisted of three parts :

1. An equilibrium cell with detachable sampling microcells, Figure A.5

2. A feed assembly consisting of , a degassing cell for the liquid feeds and compressor for gaseous feeds, and
3. An analysis section consisting of a gas liquid chromatograph with special injection ports for receiving sampling microcells.

Accurate analysis of systems containing high-boiling liquids requires heating of the withdrawn sample to a higher temperature than the equilibrium temperature to avoid condensation of the heavier component. Heating the sample in a manifold attached to the equilibrium cell without disturbing the equilibrium between the phases becomes an extremely difficult proposition. The authors developed a sampling system which consisted of detachable sampling microcells. The sampling microcells were transferable to specially designed chromatographic injection ports. According to the authors this system enabled accurate chromatographic analysis of mixtures with high boiling components.

The equilibrium cell and sampling microcells were designed to trap a sample volume of 15 μl between the conical part of the nonrotating stem and the body of the cell in a space limited by "O"-ring. Another "O"-ring, insured a leakproof seal when the sampling microcell was positioned in the equilibrium cell or the injection port of the chromatograph.

When the sampling microcell was placed in the injection port hole its seating pressed against the bottom of the hole. An empty space was left between the microcell seating and the conical part of the stem of the injector valve. The whole injection port assembly was heated by a resistor wire. A thermal shield around the microcell prevented an extremely fast raise of temperature in the sample before it expanded into empty space when the microcell valve was opened.

Efficient stirring was obtained with a permanent magnet rotating in a magnetic field created by four solenoids located outside the cell. Pressure equilibrium was reached within ten minutes according to the authors. Thermal gradients in the equilibrium cell were checked for by thermocouples placed in several parts of the cell.

Experimental apparatus of Guillevic, et al (1983)

The experimental equipment of Guillevic, *et al* (1983), Figure A.6, consisted of four main parts : an equilibrium cell with it's associated capillary sampling systems, pressure and temperature measuring systems, air bath and sample analysis section.

The vapour and liquid phases were sampled by similar sampling valves Figure A.6. The capillary, length, internal section and the shape of the stem were the consequence of an experimental study undertaken to obtain representative samples. The sampling valve with the longest capillary was used to sample the vapour phase while the shortest was used to sample the liquid phase. A sample of either the liquid or vapour phase was obtained by opening the sampling for a short while. As the pressure inside the equilibrium cell was higher than that of the chromatographic circuit the sample flowed through the capillary tube to the stem of the sampling valve. After the sampling valve was closed the sample was flushed through the centre of the stem of

the sampling valve to the chromatograph by carrier gas entering the sampling valve through tubes (13). The authors claim that the withdrawn samples were large enough to allow for chromatographic analysis yet small enough to cause negligible change to the equilibrium condition inside the cell.

Equilibrium between the phases was achieved by means of a stirring magnet rotated around a fixed axis in order to prevent it from damaging the capillary connected to the gas sampling valve. The magnet was driven by a rotating magnetic field induced by four solenoids located outside the cell. The temperature was measured by two thermocouples inserted in wells machined in the cell body and the authors claim that the cell body temperature was kept constant to within 0,1 K.

Experimental apparatus of Konrad and Swaid

Konrad, *et al* (1983) reports the use of two static equilibrium cells to measure equilibrium data for non-volatile systems. The cell developed by Konrad used a sampling technique, the other developed by Swaid used a spectrographical technique to analyse phase composition data.

The equilibrium cell developed by Konrad had two high pressure windows to allow for optical observations of the cell contents. Sampling of the phases was achieved through the use of two capillary tubes (inner diameter 0.1 mm and length 95 mm) located at the bottom of the cell and in the upper third of the cell. The capillary tubes were closed by high pressure valves with small dead-volumes (ca. 2,2 x 10^{-2} cm^3)

The samples, removed from the liquid and vapour phases by the hooping of the valves, separated into two phases. Instead of vapourizing and homogenizing the sample by heating; the sample was decompressed into an evacuated vessel. Here the amount of gaseous component was analysed using PVT data. The non-volatile components were dissolved in a solvent and analysed in a gas chromatograph. The sampling procedure and analysis method was necessary due to the thermoliability and high boiling points of the non-volitile components under investigation.

The temperature of the cell was controlled by an electrically heated thermostating jacket. Additional head and bottom heaters reduced the axial temperature gradients to smaller then 0.2K.

Equilibriation of the phases was achieved by an internal magnetically coupled stirrer whose operation was similar to an axial flow pump, The magnetic field was generated by four solenoids situated outside the cell.

The equilibrium cell developed by Swaid, Figure A.7 used near-infrared spectroscopy to determine composition data in density units according to Beer's Law. In other analytical and synthetic methods composition data are obtained in mole or mass fractions that can only be converted to density units with the knowledge of PVT data for the coexisting phases. This information is normally not available.

Synthetic sapphire windows are situated at the bottom and middle of the cell. Teflon foil was used as a sealing material between the steel window plugs and window. The optical axis of the windows was parallel to the cylinder axis to prevent double refraction and interference of the absorption bands. Near infrared spectroscopy was used in preference to infrared as the absorption bands are usually well separated in the former. Absorbtion data were measured with a Spectrometer. The electric signals of the reference as well as the sample beam were branched out directly behind the detector, digitized and evaluated with the help of a computer. The molar absorbtivity values were determined in the homogenous region as a function of pressure, temperature and composition.

The cell was inserted in a thermosating copper cylinder into which heating elements were installed. Axial thermal gradients were reduced by additional heating elements.

Various different methods have been reported over the years to pressurize equilibrium cell contents. Injecting mercury into the equilibrium cell was reported by Kobayashi and Katz (1953). Huang, *et at* (1985) use a rotary drive mechanism and piston. Konrad and Swaid used a Bridgman piston.

Pressure created by the compression of silicon oil in a screw press was transmitted to the cell contents by a separator system consisting of either a bellows or piston. If the piston was used the cell volumes could be determined by knowing the piston position measured by an inductive coil.

A.6 STATIC NON-ANALYTICAL METHODS IN THE LITERATURE

de Loos, *et al* (1980) and (1986) report the used this type of apparatus to measure phase equilibria and critical phenomena for the propane/water and ethane/2-methylpropane systems respectively.

An example of an application in which volumetric data was generated is the experimental equipment described by Meskel-Lesavre, *et al* (1981). The main feature of the equipment was a very light and small titanium equilibrium cell whose volume could be altered by a pressurising device and whose mass could be accurately determined by a balance due to its light weight. The liquid component was introduced into the cell and after degassing accurately weighed. The second component was added and weighed. The cell was inserted into the pressurising device. The pressure of the cell was increased while the vapour-liquid equilibrium was maintained by vigourous magnetic stirring. The pressure of the cell was known as a function of the total cell volume; a correction for thermal expansion and compressibility of the hydraulic pressurising fluid was taken into account. Accurate values of the bubble pressure and saturated liquid phase molar volume were simultaneously obtained from the pressure volume plot where the discontinuity corresponds to the vapour phase disappearance (bubble point). The mixture pressure was released and when the vapour phase reappeared the process was repeated at another temperature.

It was a fast method of obtaining data, the authors claim it took 1 hour to reach equilibrium and another hour to describe a pressure/cell volume diagram with 10 points. No visual observations were necessary thus avoiding potentially complex sealing problems. A further development of this equilibrium cell capable of withstanding higher temperatures and pressures was described by Rousseaux, *et al* (1983).

Di Andreth and Paulaitis (1987) use a synthetic type apparatus in which the volume of each of the individual phases of a three-or-four phase three-component equilibrium system could be measured.

A.7 STATIC COMBINED APPARATUS IN THE LITERATURE

The equilibrium cell of Wisotzki is shown in Dieters and Schneider (1986), and Figure A.8. The equilibrium cell was used for cryogenic investigations of volatile substances. For mole fractions far away from the critical point the cell was operated in the *analytic mode*. Samples of the liquid and vapour phases were transferred from the equilibrium cell into sample loops connected to six way-valves. From there the samples were flushed to a gas chromatograph for compositional analysis by flowing helium gas. For mole fractions near the critical point the cell was operated in the *non-analytical mode*. The cell contents were pressurized by a Bridgman piston, and separated from the pressurizing fluid by a bellows. The position of the bellows

was accurately determined by a magnetic wire which enabled information on phase densities to be collected. Japas and Frank (1985) and Huang, *et al* (1985) also describe combined method equilibrium cells.

a) pressure vessel
8 - 14: moving piston, 6: magnetic wire attached to it, 15: magnetic stirrer, 16 - 20: sapphire window assembly;
max. pressure 2000 bar, temperature range 20 - 180°C.

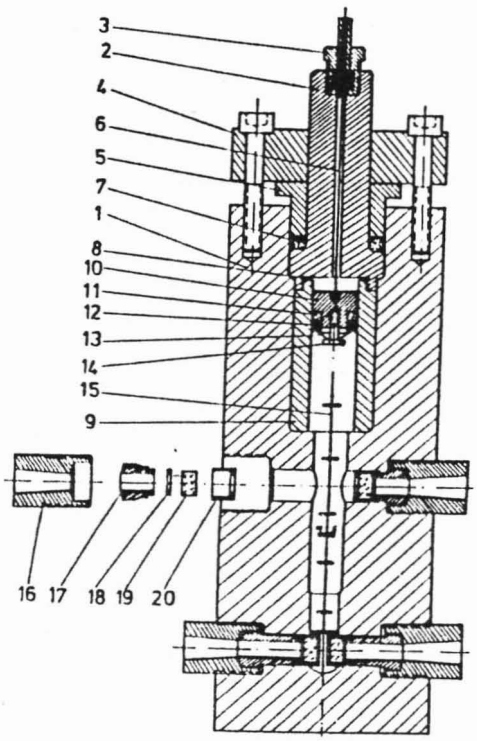

Figure A.7 Equilibrium cell of Swaid

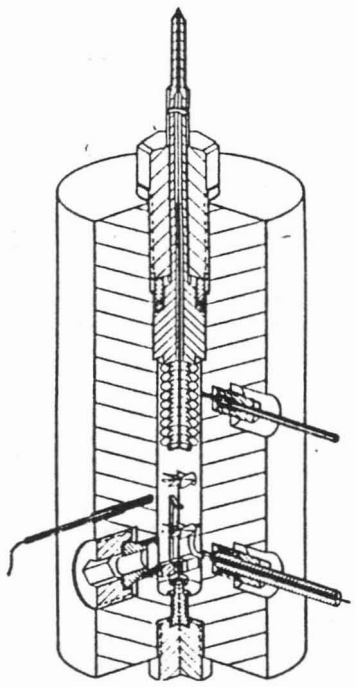

a) pressure cell
This view shows the Bridgman piston with the bellows attached to it, the magnetic stirrer, a sapphire window, and the two sampling capillaries;
max. pressure 3000 bar, temperature range 80 - 373 K.

Figure A.8 Equilibrium cell of Wisotzki

APPENDIX B

B.1 THE CRITERION FOR PHASE EQUILIBRIUM

Theoretical treatment of two phase equilibria in a closed system is possible by considering each phase as an open system each capable of mass transfer to the other. According to Gibbs' criterion the temperature and pressure are uniform throughout both phases at equilibrium. The Gibbs equation for each phase in the mixture is written as;

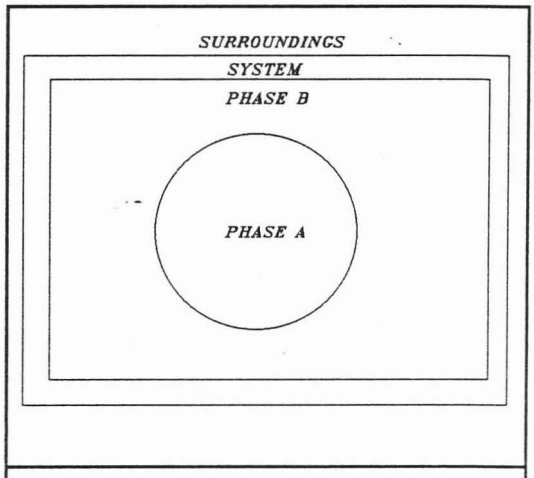

Figure B.1 : Thermodynamic System

$$d(nG)^{\alpha} = -(nS)^{\alpha}dT + (nV)^{\alpha}dP + \Sigma\mu_i^{\alpha}dn_i^{\alpha} \qquad (B.1)$$

$$d(nG)^{\beta} = -(nS)^{\beta}dT + (nV)^{\beta}dP + \Sigma\mu_i^{\beta}dn_i^{\beta} \qquad (B.2)$$

superscripts α and β denote the two phases respectively.

Summation of Eqs. (B.1) and (B.2) gives the total Gibbs energy (G^t) of the system. If the Gibbs equilibrium condition, $(dG^t)_{(T,P)} \leq 0$, is imposed the resulting expression for (G^t) is :

$$(dG^t)_{T,P} = \Sigma\mu_i^{\alpha}dn_i^{\alpha} + \Sigma\mu_i^{\beta}dn_i^{\beta} \qquad (B.3)$$

Since the system is closed and without chemical reaction, material balance requirements necessitate :

$$dn_i^{\beta} = -dn_i^{\alpha} = dn_i \qquad (B.4)$$

As a result (B.3) may be simplified to :

$$\Sigma\ (\mu_i^{\alpha} - \mu_i^{\beta})\ dn_i = 0 \qquad (B.5)$$

Since the quantities dn_i are independent and arbitrary Eq. (B.5) can only be satisfied if the chemical potential of a component is the same in each phase :

$$\mu_i^{\alpha} = \mu_i^{\beta} \qquad (B.6)$$

This result may be generalised to more than two phases by considering the phases by pairs. The general result for π phases with N chemical species is

$$\mu_i^{\alpha} = \mu_i^{\beta} = ... = \mu_i^{\pi} \qquad (i = 1,...,N) \qquad (B.7)$$

No adequate method to calculate the absolute value of the chemical potential has been found to date. An alternative criterion for phase equilibria is readily derived from :

$$d\bar{G}_i = RT \; d\ln \hat{f}_i \qquad (constant \; T) \qquad (B.8)$$

Since $\mu_i = \bar{G}_i$; integrating Eq (B.8) yields :

$$\mu_i = RT \ln \hat{f}_i + \theta_i \qquad (B.9)$$

Since θ_i is dependent on temperature only and since all the phases are at the same temperature, substitution of (B.9) in (B.7) yields,

$$\hat{f}_i^{\alpha} = \hat{f}_i^{\beta} = ... = f_i^{\pi} \qquad (i = 1,...,N) \qquad (B.10)$$

B.2 STANDARD STATES

Standard State of Pure Liquid Component

For components whose critical temperatures are higher than that of the system, i.e., the condensable component, it is customary to normalize the activity coefficient such that :

$$\lim_{x_i \to 1} \gamma_i = 1 \qquad (B.11)$$

As the composition of the solution approaches that of the pure liquid, the component's liquid fugacity becomes equal to the mole fraction multiplied by the standard-state fugacity. The normalization of activity coefficients for these components is said to follow the symmetric convention.

Standard State of Infinitely Dilute Component

This standard state has been introduced for the non-condensable component whose critical temperature is less than that of the system temperature. In this case the activity coefficient is normalized as follows :

$$\lim_{x_i \to 0} \gamma_i^* = 1 \qquad (B.12)$$

For such components, the fugacity of component i becomes equal to the mole fraction multiplied by the standard state fugacity in the limit as the mole fraction of the component i becomes very small. The concentration region where the activity coefficient γ_i^* is essentially equal to unity is called the ideal dilute solution or Henry's-law region. In a binary solution, the characteristic constant for the ideal dilute solution is Henry's constant H defined by :

$$H = \lim_{x_i \to 0} \frac{\hat{f}_i}{x_i} = f_i^o \qquad (B.13)$$

Eq. (B.13) is the standard-state fugacity for any component i whose activity coefficient is normalised by Eq. (B.12). The standard states of this group depend on solvent properties.

In a binary liquid solution containing a condensable / non-condensable component equation (B.11) is used for normalisation of the solvent and Eq. (B.12) for the solute. Since the normalisation for the two components are not the same, they are said to follow the unsystematic convention.

B.3 NON-CONDENSABLE ACTIVITY COEFFICIENTS

Non-condensable component activity coefficients

The liquid phase fugacity for a non-condensable component may be described analogously to the condensable component's fugacity.

$$\hat{f}_i^L = x_i \, f_i^{OL} \, \gamma_i^{*(P^r)} \exp \int_{P^r}^{P_2} \frac{\overline{V}_i^L}{RT} \, dP \qquad (B.14)$$

The hypothetical standard state for non-condensable components is therefore neatly avoided by using the normalization $\gamma^{*(Pr)} \to 1$ as $x_{\,noncondensable\ j} \to 0$ and $x_{condensable\ i} \to 1$. This yields Henry's constant as the standard state fugacity (f_i^{OL}) of the non-condensable component (i) in the condensable component (j) at the temperature of the mixture and reference pressure (P^r) . The pressure dependence of the Henry's constant can be expressed analogously to Eq. (B.17) by :

$$H_{ij}^{(P_2)} = H_{ij}^{(P_1)} \exp \int_{P_1}^{P_2} \left(\frac{\overline{V}_{ij}^{\infty}}{RT} \right) dP \qquad (B.15)$$

Henry's constants are usually measured at the saturated vapour pressures (P_i^S) of the condensable component i. Assuming $\overline{V}_{ij}^{\infty}$ to be independent of pressure, the pressure-correction below converts Henry's constant from the experimental pressure to the desired reference pressure.

$$H_{ij}^{(P^r)} = H_{ij}^{(P_i^s)} \exp \int_{(P_i^s)}^{P^r} \frac{\overline{V}_{ij}^{\infty}}{RT} \, dP \qquad (B.16)$$

If the reference pressure is set to zero (standard state 8 Table 3.2) Eq. (B.14) becomes

$$H_{ij} = H_{ij}^{(P_i^s)} \exp \left(-\frac{\overline{V}_{ij}^{\infty} P_i^s}{RT} \right) \qquad (B.17)$$

B.4 CHAO-SEADER COMBINED METHOD

The combined method equation for the Chao-Seader method (Figure B.2) is :

$$x_i \gamma_i \phi_i^L = y_i \hat{\phi}_i$$

The standard state fugacity in Eq. (B.16) being replaced by the fugacity coefficient of component i as a pure liquid at the T and P of the system (i.e. standard state 1),

$$\phi_i^L = f_i^o / P = f_i^L / P$$

The fugacity coefficient ϕ_i^L was expressed analytically by means of the three parameter corresponding states principle as proposed by Pitzer and as shown in Smith and van Ness (1975),

$$\log \phi_i^L = \log \phi_i^o + w_i \log \phi_i^L$$

where ϕ_i^o were ϕ_i^L are expressed as complex analytical functions of reduced temperature and pressure. The liquid phase activity coefficients γ_i were calculated from the Scatchard-Hildebrand regular solution theory,

$$\ln \gamma_i = \frac{V_i}{RT} (S_i - \bar{S})^2$$

where S is a solubility parameter which is a function of temperature. The vapour phase fugacity coefficients $\hat{\phi}_i$ are based on the Redlich-Kwong equation of state, the parameters required being the critical pressure, temperature and volume.

For supercritical components, fictitious values of ϕ_i, S_i, & V_i had to be used. These values were determined for components by trial so as to produce results in agreement with the data. This solution of dealing with the supercritical components was unsatisfactory and was dealt with far more rigorously by Prausnitz and Chueh (1968) and Prausnitz, *et al* (1980).

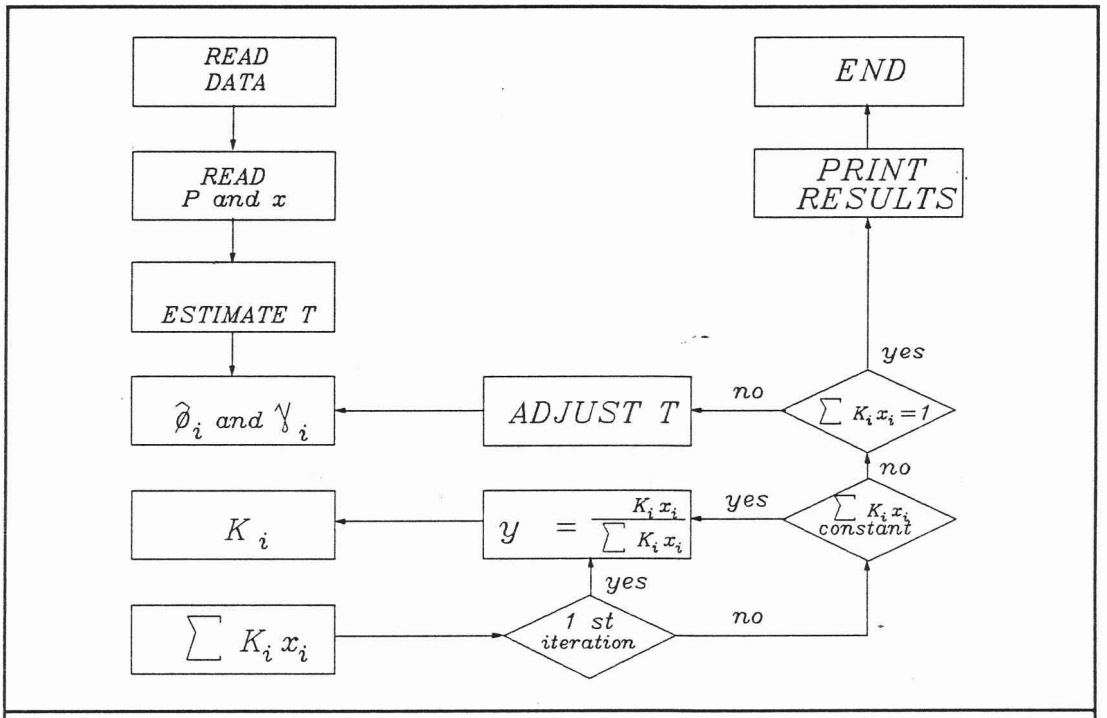

Figure B.2 : Schematic Diagram of Chao-Seader Method

B.5 CUBIC EQUATIONS OF STATE

B.5.1 Formulation of the Empirical Cubic Equations of States

Semiempirical EOS, of which the van der Waals, Redlich-Kwong, (R-K), Soave-Redlich-Kwong, (S-K-R) and Peng and Robinson (P-R) equations are the best known examples generally express pressure as the sum of two terms, a repulsion pressure Pr, and an attraction pressure Pa, as follows :

$$P = Pr + Pa \qquad (B.18)$$

The repulsion pressure term Pr is usually expressed by the van der Waals hard spere equation,

$$Pr = RT / (V - b) \qquad (B.19)$$

where b is a constant related to the size of the hard sphere. The attraction pressure term Pa can be expressed as,

$$Pa = -a/g(V) \qquad (B.20)$$

where a is a constant and regarded as a measure of the intermolecular attraction force and $g(V)$ is a function of the molar volume V.

The values of a and b can be found as functions of the critical properties (temperature and pressure) from the first and second derivatives of pressure with respect to volume at constant temperature.

$$(\partial P/\partial V)_T = (\partial^2 P/\partial V^2)_T = 0 \qquad (B.21)$$

The value of a is constant in the van der Waals and R-K equation. It is however a function of temperature in the S-R-K and P-R equations. Obtaining realistic critical compressibility factors is largely dependent on a suitable function of g (v) being chosen. b is usually regarded as temperature independent and at high pressures the applicability of a cubic EOS is affected by the magnitude of b/Vc.

The first semiempirical EOS was that of van der Waals introduced in 1873. van der Waal predicted the coexistence of the liquid and vapour phases and the critical state by the relation :

$$\left(P + \frac{av^2}{V^2}\right)(v-b) = RT \qquad (B.22)$$

If Z is taken to be :

$$Z = PV/RT \qquad (B.23)$$

The polynomial form of the van der Waals EOS is :

$$Z^3 - (B+1)\,Z^2 + AZ - AB = 0 \qquad (B.24)$$

Over the years several modifications of the van der Waals EOS have been proposed. One of the first was that of Redlich and Kwong in 1949. Redlich and Kwong recognised that the attraction parameter a in the van der Waals EOS was dependent on temperature. Therefore they made an essentially arbitrary but empircally inspired modification to the original van der Waals EOS.

$$\left(P + \frac{a}{\left(T^{\frac{1}{2}}V(V+b)\right)}\right)(V-b) = RT \qquad (B.25)$$

Over the following years several modifications of the R-K EOS were proposed to either improve pure substance (PVT) data fitting or improve pure vapour-liquid equilibrium data correlations. One of the most recent and one that has gained wide acceptance because of its relative simplicity, compared to the more complicated BWR EOS, was that of Soave in 1972.

The temperature dependent attraction term in the R-K EOS was modified by Soave to include the acentric factor (w) and reduced temperature (Tr)

$$\left(P - \frac{a(T,w)}{V(V+b)}\right)(V-b) = RT \qquad (B.26)$$

The R-K and S-R-K EOS are usually able to generate satisfactory vapour densities, but fail to generate satisfactory liquid densities. For example the S-R-K EOS predicts specific liquid volumes greater than the literature values and the derivations increase from about 7 % at Tr < 0.65 to 27 % at the critical point, Peng and Robinson (1976).

B.5.2 Mixing Rules and Interaction Parameters for Cubic EOS

Mixing rules are required to extend the van der Waals, R-K, S-R-K, P-R EOS to mixtures.

For the sake of clarity a distinction is made here between *a mixture's properties*, sometimes known as *pseudocritical properties* Mpc and equation of state *mixture parameters*. Pseudocritical properties refer to properties of the mixture such as mixture critical temperature, pressure, volume and accentric factor. Equation of state *mixture parameters* are use to extend the pure component form of the EOS to a mixture of components.

There are two basic methods of applying a cubic EOS to mixtures.

Method A :

The mixture critical properties (T_{pc} P_{pc}) are calculated by suitable mixing rules. The EOS parameters, Eqs. (B.27) and (B.28) are calculated directly using these values.

Method B :

The pure component EOS parameters, Eqs. (B.27) and (B.28) are calculated using pure component properties (T_{ci} , P_{ci}). A mixing rule for example Eqs. (B.29) or (B.30) is employed to express the EOS parameters for the mixture as some function of the compositions and pure component EOS parameters.

Since the mixing rules are crucial for the application of the EOS to a particular mixture much effort has been devoted to formulating effective combining rules for pseudocritical properties (Method A) and mixture parameters (Method B) from those of the individual components. The simplest of these are mole fraction weighted sums of the corresponding property (Method A and Method B) parameter of the components of the mixture. Other more complicated rules incorporate binary interaction parameters (δ_{ij}) which are specific to the system under investigation.

Combining Rules for Pseudocritical Properties Method A

The various combining rules for the pseudocritical properties T_c, P_c, V_c, Z_c & w such as those proposed by Kay, Prausnitz and Gunn, and Lorentz-Berthelot are covered by Walas (1985) in his review of phase equilibrium in chemical engineering and will not be discussed further here.

Combining Rules for EOS parameters

Most of the mixing rules applied in cubic EOS are purely empirical in contrast to those for the Virial EOS which have a rational basis.

Empirical Mixing Rules used in Cubic EOS

For the van der Waals equation the mixing rules proposed by Lorentz and Berthelot and known as the Lorentz-Berthelot rules are :

$$a = (\Sigma y_i (a_i)^{(0.5)})^2$$

$$b = \Sigma y_i b_i$$

For their EOS, Redlich-Kwong proposed :

$$a = \Sigma y_i y_i a_{ij} \qquad (B.27)$$

$$b = \Sigma y_i b_i \qquad (B.28)$$

where a_{ij} is known as the cross parameter and may be calculated as

$$a_{ij} = (a_i a_j)^{\frac{1}{2}} \qquad (B.29)$$

Soave introduced a binary interaction parameter k_{ij} in the cross parameter as follows :

$$a_{ij} = (1 - k_{ij})(a_i a_j)^{0.5} \qquad (B.30)$$

This form of cross parameter was also adopted by Peng and Robinson for their EOS. Eqs. (B.27), (B.28) and (B.30) are commonly referred to as the *"classical mixing rules"*.

Some of the modifications made to the Peng and Robinson "classical mixing rules" and which have found wide-spread use will now be discussed. The principle applies equally however to all the other van der Waal type EOS.

B.5.3 Further Modifications to the Cubic EOS

Various different temperature dependency models proposed for the attractive term a (for example Stryjek-Vera 1986) Eq. (B.20) for the cubic equations were given in Melhem, *et al* (1989 : Table 2). In a comprehensive review they apply the P-R EOS with the various proposed attractive terms and achieve good results even for highly non-ideal systems. The propane/methanol system at 39,9 and 69,9 °C was satisfactorily modelled using the data of Galviel-Solastiouk, *et al* (1986). The residuals for this system were however high when compared to non-polar systems.

Another area of modifications is related to the denominator of the attraction pressure term $g(V)$ in Eq. (B.20). Some of the various proposals (for example Harmens and Knapp 1980) are given in Cisternas (1988 : Table 1).

B.6 THE PERTURBATION THEORY AND ASSOCIATED EOS

B.6.1 Derivation of The PHCT EOS

Statistical thermodynamics was used on a molecular (microscopic) level to describe the bulk (macroscopic) properties of the molecules and led directly to the Perturbated Hard Chain Theory (PHCT) and its subsequent developments. The original PHCT EOS was derived from differentiation with respect to volume of the molecular partition function Q as follows :

$$P = kT\left(\frac{\partial \ln Q}{\partial V}\right)_{T,N} \qquad (B.31)$$

Ideal gas "molecules" possess only translational energy. The partition function (Q) for a one-component ideal gas was given as,

$$Q = \frac{1}{N!}\left[\frac{V}{\Delta^2}\right]^N [q]^N \qquad (B.32)$$

where :

N = the total number of molecules,
V = the total volume,
q = the molecular energy partition function, and
α = the de Broglie wave length.

Δ can be written in terms of Planck's constant h, molecular mass m and Bolzmann's constant as :

$$\Delta = \frac{h}{(2\pi mkT)^{0.5}} \qquad (B.33)$$

Real gas molecules have finite size and by their nature posses rotational, vibrational and potential energies in addition to the translational energy.

The partition function Q for real fluids in statistical thermodynamics was based on the fundamental ideas of van der Waal namely :

The molecules in a real fluid have finite size resulting in repulsive forces at close molecular separations. Their electronic configurations result in forces of attraction at intermediate molecular separations.

The derivations are taken into account in the partition function (Q) through the concepts of free volume Vf and uniform potential E_o (the potential field experienced by one molecule due to the attractive forces from all other molecules) respectively. The vibrational, rational and potential energies are taken into account through partition function factor q (the contribution per molecule from rotational and vibrational degrees of freedom).

The partition function (Q) for as one component real gas was given as :

$$Q = \frac{1}{N!}\left[\frac{V_f}{\Delta^3}\right]^N \left[\exp\left(\frac{-E_o}{2kT}\right)\right] [q_{r.v.e}] \qquad (B.34)$$

Prausnitz and co-workers in their development of the Perturbed Hard Sphere Theory represent the free volume (Vf) term in Eq. (B.34) by the Carnahan-Starling equation for a hard sphere fluid :

$$Z = \frac{1+\epsilon+\epsilon^2-\epsilon^3}{(1-\epsilon)^3} \qquad (B.35)$$

where ϵ was the reduced density and could be represented as :

$$\epsilon = \frac{b}{4V}$$

where b was a measure of the volume occupied by the molecules. Alternatively :

$$\epsilon = 0.74\left(\frac{V_o}{V}\right) \quad \text{where } V_o = \left(\frac{\sigma^3}{\sqrt{2}}\right)^{N_a}$$

Eq. (B.35) was derived from a potential function representation of a hard sphere (Walas 1985 : pp 80 - 81) shows representations of the various potential functions).

The uniform term (E_o) was represented by an analytical expression obtained from the molecular dynamic studies of Adler,

$$\frac{E_o}{2kT} = c\sum_n\sum_m \frac{A_{nm}}{\bar{T}^n \bar{U}^m} \qquad (B.36)$$

where A, m, n were known constants and $\bar{T}, \bar{U}$ were reduced temperatures and pressures.

The partition function factor q was factored into an internal part (a function of temperature) and an external part (a function of volume).

$$q = [q_{ext}]^N \; [q_{int}]^N \qquad (B.37)$$

Since q_{int} was independent of volume it did not contribute to the EOS. The external part was presented by $q_{ext} = (Vf/V)^{c-1}$ where $3c$ is number of external density dependent degrees of freedom.

The PHCT EOS, which takes into account molecular motions that arise from rotational, vibrational as well as translational degress of freedom in terms of the compressibiltiy factor was given as follows,

$$Z = 1 + c(Z^{cs}_{rep} + Z^{sw}_{att}) \qquad (B.38)$$

where :

Z^{cs}_{rep} = the molecular repulsion term, and

Z^{sw}_{att} = the molecular attraction term.

c = one third the total number of external density -dependent degrees of freedom.

The molecular repulsion term was based on the Carnahan-Starling equation and the repulsive term on the molecular - dynamic studes of Adler.

B.6.2 **Perturbation Theory EOS**

Donohue and Vimalchand, (1988 : Table 1) show the relevant development of these types of EOS.

Developments have largely involved :

1. The modification of the attractive term to simplifiy computations, TPHCT and SPHCT, by the use of a truncated form of Z_{att}

or

2. The addition of perturbation expansions to describe multipolar mixtures, for which PHCT required large interaction parameters.

Eq. (B.38) was simplified by Gmehling who turnacted the perturbation expansion of Adler at the second term. The resulting EOS was :

$$Z = 1 + c(Z^{cs}_{rep} + Z^{sw}_1/T + Z^{sw}_2/T^2)$$

SPHCT EOS

Kim, *et al* (1986) replaced the attractive by a simpler expression, using relatively simple mixing rules. The derived EOS (SPHCT) was simpler to use by the layman than Eq. (B.38). The authors used the SPHCT EOS in conjunction with UNIFAC in a combined method to model the high pressure and temperature vapour-liquid equilibrium phase behaviour for isothermal carbon dioxide / aromatic binaries. They show that smaller numerical interaction parameters were obtained for the SPHCT than for the Peng and Robinson EOS. This would imply that neglect of these parameters would still give fairly accurate vapour-liquid equilibrium predictions. An interesting feature of the plot of the predicted versus the experimental K values for the aromatics shows that the traditional combined method of UNIFAC and SPHCT gave the most accurate results.

COR EOS

The Chain of Rotators (COR) equation approximated the external rotational degrees of freedom by assuming the density dependence of these motions could be calculated by differences between the properties of hard spheres and hard dumb-bell shaped molecules.

CCOR EOS

Kim, *et al* (1986 a and b) developed a *cubic* equation of state of perturbation type to express pressure as contributions due to repulsive, rotational and attractive forces. Use of the equation required the critical temperature, pressures and for strongly polar substance and their mixtures, critical compressibilities. The fugacity coefficient equation of Kim, *et al* (1986 a) although complex, compared to the Peng Robinson and Mohamed and Holder EOS was still simpler that the COR equivalent equation.

Kim, *et al* (1986 b) and Lee and Choa (1986) (who used density dependent mixing rules instead of the one fluid mixing rules of Kim, *et al* 1986 b) modeled several non-ideal systems. Lee and Choa (1986) modeled the propane/ethanol data of Gomez Neito (1978) successfully using their CCOR type EOS.

APACT & COMPACT

APACT was developed to describe hydrogen bonding systems, i.e., non idealities due to physical and "chemical" interactions. It is particularly useful for alchols, water, phenol, carboxylic acid and amino systems. APACT has been simplified to COMPACT.

Attempts have been made to describe Perturbation theory in terms of group-group interactions, (GPSCT).

B.7 LOCAL COMPOSITION EQUATION OF STATES

B.7.1 Huron-Vidal Mixing Rules

The cubic EOS all require an interaction parameter which is system dependent. These parameters need to be found by regression of the particular EOS onto experimental data. Their predictive capabilities are therefore limited since neglect of the interaction parameters in general does not give accurate results except for highly ideal systems.

The introduction of local-composition theory in equations of state or more directly in EOS mixing rules has :

1. extended the application of the more common cubic EOS to more complex mixtures and,
2. enabled their use in purely predictive methods.

In the search for new mixing rules Huron and Vidal (1979) proposed relating the excess Gibbs energy to the pure component ϕ_i and solution ϕ fugacity coefficients :

$$g^E = RT\left[\ln\phi - \sum_{i=1}^{n} x_i \ln\phi_i\right] \qquad (B.39)$$

The fugacity coefficients depend only on the EOS used. ϕ_i and ϕ can be calculated from the same EOS :

$$\phi_i = \phi_i\ (T, P, V_i, a_{ii}, b_{ii} \ldots .)$$

$$\phi = \phi\ (T, P, v, a, b)$$

For the cubic EOS like van der Waals, R-K and P-R having the form ,

$$P = \frac{RT}{v-b} - \frac{a(T)}{g(v)}$$

the volume function $g(v)$ is proportional to b and can be written as ,

$$g(v) = (v + b\lambda_1)(v + b\lambda_2)$$

where λ_1 & λ_2 are numeric constants.

The excess Gibbs energy and the mixing rules implicit in the cubic EOS a and b values were related by limiting the value of g^E at infinite pressure, Huron and Vidal (1979) :

$$g^E_\infty = -\left[\frac{a(T)}{b} - \sum_{i=1}^{n} x_i \frac{a_{ii}(T)}{b_{ii}}\right]\Delta \qquad (B.40)$$

where Δ was a numerical constant which is dependent on cubic equation of state used.

For

1. *Data smoothing and model evaluation* applications Huron and Vidal proposed a Redlich-Kister polynomial expansion of the excess Gibbs energy to achieve a high degree of flexibility in the mixing rule :

$$g^E = RTx_ix_2 \sum_{m=0}^{NP} A_m(x_1-x_2)^m$$

and

2. Predicting VLE from the minimum amount of data a local composition mixing rule to describe the excess Gibbs energy.

Three density dependent local composition theory EOS will now be reviewed, the Group Contribution EOS, UNIWAALS EOS and the method of Schwartzentruber and Renon for determining mixing rules.

B.7.2 Group Contribution Equation of State (GC EOS)

A brief view of some of the theory involved in the derivation of this van der Waals type EOS is given. The principle feature of which is the group contribution principle applied with the statistical thermodynamic van der Waals partition function. The Carnahan-Starling expression for hard spheres and a NRTL like expression for the mixing rules were used to describe the partition function. The Carnahan-Starling expression limits the use of the GC EOS to mixtures with component size ratios of less than 20.

The generalized van der Waals partition function was given by :

$$Q = Q^c * Q_{kinetic} * Q_{internal} \qquad (B.41)$$

The configurational Helmholtz function (A^c) and compressibility factor (Z) form of the EOS were related as follows :

$$A^c = -kT \ln Q^c$$

$$Z = -V \frac{\partial}{\partial V}\left(\frac{A^c}{RT}\right)_{T,\eta} \qquad (B.42)$$

The residual Helmholtz function (A^R) and fugacity coefficient ϕ_i were related as follows :

$$(A^R)_{T,V,n} = [A^c - (A^c)^{idealgas}]_{T,V,n}$$

$$\ln(\phi_i) = \frac{\partial}{\partial n_i}\left(\frac{A^R}{RT}\right)_{T,V,n_{k\neq i}} - \ln Z \qquad (B.43)$$

The residual Helmholtz function, (A^R) , at specified temperature, volume and composition could be divided into an attractive and free volume term :

$$\left(\frac{A^R}{RT}\right)_{T,V,n} = \left(\frac{A^R}{RT}\right)_{att} + \left(\frac{A^R}{Rt}\right)_{fv}$$

The free volume part was described by the Carnahan-Starling expression for hard spheres :

$$\left(\frac{A^R}{RT}\right)_{fv} = 3(\lambda_1\lambda_2/\lambda_3)(Y-1) + (\lambda_2^3/\lambda_3^2)(Y^2-Y-\ln Y) + n\ln Y$$

where λ and Y are auxillary quantities given by,

$$\lambda_f = \sum_j^{NC} n_j d_j^k$$

$$Y = (1-\pi\ \lambda_3/6V)^{-1}$$

where :

n = the total number of moles,
NC = number of components,
V = the total volume, and
d = the hard sphere diameter.

The attractive part can be described by a density-dependent NRTL-type expression :

$$\left(\frac{A^R}{RT}\right)_{att} = -(z/2) \sum_i^{NC} n_i \sum_j^{NG} v_j^i q_j \sum_k^{NG} \left[\theta_k \left(g_{kj}\bar{q}\tau_{kj}/RTV\right) / \sum_i^{NG} \theta_i\tau_{ij}\right]$$

where :

$$\bar{q} = \sum_i^{NC} n_i \sum_j^{NG} v_i^j q_j$$

$$\theta_j = (q_j/\bar{q}) \sum_i^{NC} n_i v_j^i$$

where :

θ_j & q_j = surface fraction and surface area parameters associated with the group
v_j^i = number of group j in molecule i
g_{ij} = attractive energy parameter, and
τ_{ij} = experimental non-randomn weight factor.

The Group Contribution EOS and it's fugacity coefficient form are given in section 3.4.3.

B.7.3 UNIWAALS EOS

Gupte, *et al* (1986 a and b) developed this EOS to be completely predictive by combining modified expressions for the van der Waals EOS (WAALS) and UNIFAC group contribution method (UNI) for the Huron and Vidal mixing rules. Only UNIFAC group interaction parameters, as given by Larson, *et al* (1987), and pure component data are needed as input for VLE predictions.

In contrast to the GC EOS the residual Helmholtz function was given in terms of the van der Waals EOS by :

$$\left(\frac{A^R}{RT}\right) = -\ln\left(1-\frac{b}{v}\right) - \frac{a(T)}{RTv} \qquad (B.44)$$

The fugacity coefficient was obtained from Eq. (B.44) :

$$\ln\phi_i = -\ln\left[\frac{P(v-b)}{RT}\right] + \frac{b_i}{b}\left(\frac{Pv}{RT}-1\right) - \left[\frac{a}{RTb} + n_T\frac{\partial}{\partial n_i}\left(\frac{a}{RTb}\right)\right]\frac{b}{v} \qquad (B.45)$$

The Gibbs excess energy using the van der Waals EOS was written as :

$$\left.\frac{g^E}{RT}\right|_{EOS} = -\ln\left(1-\frac{b}{v}\right) - \frac{a}{RTv} + \sum_i^n x_i\ln\left(1-\frac{b_i}{v_i}\right) + \sum_i^n \frac{x_i a_i}{RTv_i} + \sum_i^n x_i\ln\left(\frac{v_i}{v}\right) + \frac{Pv^E}{RT} \qquad (B.46)$$

Any cubic EOS, i.e. R-K, S-R-K or P-R could, however, have been used in Eq. (B.39).

Eq. (B.46) could be related to the Gibbs excess energy from a liquid phase "model" such as NRTL, UNIQUAC, UNIFAC, ASOG, etc., by :

$$\left.\frac{g^E}{RT}\right|_{EOS} = \left.\frac{g^E}{RT}\right|_{G^E(model)} \qquad (B.47)$$

The mixing rules for mixture parameters a and b were specified as follows :

Combining Eqs. (B.47) and (B.46) resulted in a mixing rule for the a and b parameters.

$$\frac{a}{b}\left(\frac{1}{RT}\right) = \frac{u}{b}\left(\frac{1}{RT}\right)\frac{V}{b}\left[\frac{Pv^E}{RT} - \left[\ln\left[\frac{P(v-b)}{RT}\right] - \Sigma x_i \ln\left[P\frac{(v_i-b_i)}{RT}\right]\right]\right]$$

$$+ \frac{v}{b}\Sigma\frac{x_i a_i b_i}{v_i RT b_i} - \frac{u}{b}\frac{g^E}{RT}\Big|_{G^E(model)} \qquad (B.48)$$

The b parameter was given by the common linear average rule as follows :

$$b = \sum_i x_i b_i$$

The modified version of UNIFAC as proposed by Larsen (1987) was used to calculate the excess Gibbs energy as the group interaction parameters were temperature dependent.

If the system temperature exceeded the critical temperature of one of the components Gupte, *et al* (1986 a) suggested the use of a modified NRTL equation to model the excess value of the a and b parameters as follows :

$$\left(\frac{a}{b}\frac{1}{RT}\right)^E = \frac{1}{RT}\sum\frac{xa_i}{b_i} - \frac{a}{RTb} \qquad (B.49)$$

Eq. (B.48) could thus be written :

$$\frac{a}{b}\left(\frac{1}{RT}\right) = \frac{1}{RT}\sum_i\frac{xa_i}{b_i} - \sum_i x_i n_T \frac{\partial}{\partial n_i}\left(\frac{a}{RTb}\right)^E_{T,P,n_j}$$

For a binary system, for component 1 :

$$\ln\gamma_1 = n_T \frac{\partial}{\partial n_1}\left(\frac{a}{RTb}\right)^E_{T,P,n_2}$$

Gupta, *et al* (1986 a) recommended the use of UNIFAC below reduced temperatures of 0,8 to 0,9 as the modified NRTL has difficuly in accurately reproducing temperature dependence. At reduced temperatures > 0,9 the modified NRTL was recommended as the UNIFAC had difficulty in represtening the composition of $(a/RTb)^E$ accurately.

The temperature dependence of the a parameter was determined from,

$$a = a_c\ \alpha\ (Tr)$$

by fitting pure-fluid vapour pressures to the following expression :

$$\alpha(Tr) = \left[1 + c_i\left(1 - Tr^{\frac{1}{2}}\right) + c_2\left(1 - Tr^{\frac{1}{2}}\right)^2 + c_3\left(1 - Tr^{\frac{1}{2}}\right)^3\right]^2$$

To use the Uniwaal's EOS to predict P and y from T and x is a lengthy procedure but the relative computer time requirement is approximately half that needed for the GC EOS for a $T - x$ flash calculation, Gupta, *et al* (1986 a). Gupta, *et al* (1986 a) fully describe the procedure for determining the equilibrium K values of a binary system which is shown in schematic form in Figure B.3.

Gani, *et al* (1989) revised and extended the Uniwaal's EOS to applications involving mixtures with non-condensable gases and application to broader ranges of temperature and pressure by adding a term to the van der Waals EOS,

$$P = \frac{RT}{v-b} - \frac{a}{v^2} + \frac{p}{v}$$

where

$$p = \frac{da}{dv}$$

and where in turn a and p are functions of (T, P, v, x).

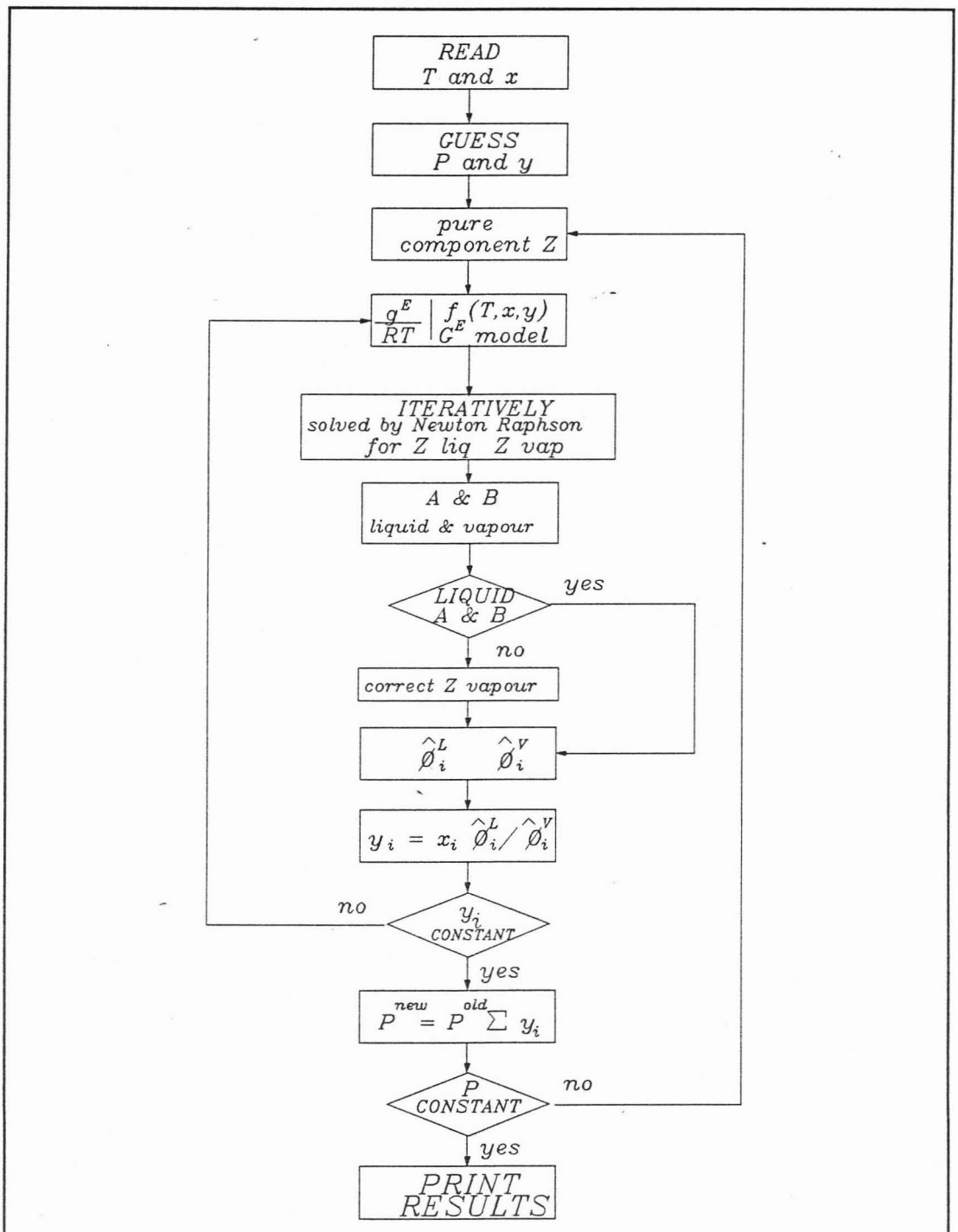

Figure B.3 : Schematic Diagram of UNIWAALS Method

B.7.4 Schwartzentruber and Renon Mixing Rules

Schwartzentruber and Renon (1989) point out some inconsistencies in the derivation of the UNIWAALS EOS :

1. The UNIFAC equation was introduced into the van der Waals equation without using the infinite pressure limit Eq. (B.40) This led to volume-dependent mixing rules from the volume-independent mixng rules of the van der Waals EOS.
2. The modified UNIFAC equation was assumed accurate over a range of temperatures which would only be valid if the temperature dependence of the parameters is known.
3. The EOS uses the UNIFAC expression for both liquid and vapour calculations. It was necessary to use a liquid-like volume of the EOS to calculate vapour phase properties.

Supercritical components cannot be handled by the normal calculational procedure and a different procedure as described by Gani *et al* (1989) had to be used.

Schwartzentruber and Renon (1989) preferred a different approach for determining the mixing rules. The method was completely general and may be applied to any cubic EOS which requires the use of classical mixing rules by using any appropriate g^E model.

Their proposal of applying these mixing rules to a Soave-Redlich Kwong type EOS is outlined below.

Schwartzentruber and Renon (1989) proposed a linear mixing-rule for b :

$$b = \sum_{j=1}^{n} b_i x_i$$

and a pseudoquadratic mixing rule for α :

$$\alpha = \sum_{i=1}^{n} \sum_{j=1}^{n} x_i x_j \, (\alpha_i \alpha_j)^{\frac{1}{2}} \, [1 - K_{ij}(T, x)] \qquad (B.50)$$

The K_{ij} was made a function of not only temperature but also of composition. The functional form of $K_{ij}(x)$ could be generated from an excess Gibbs energy expression using Eq. (B.39).

The use of Eqs. (B.39) and (B.40) is theoretically rigourous, g^E is generally assumed exact at $P = O$. If the working temperature was choosen such that the pure component had a liquid root at $P = O$, (normally true for $T_r < 0.85$, this ensured that the mixing parameters were generated within the temperature validity range of most UNIFAC group parameters.

At a given temperature and pressure Eq. (B.39) was used to relate g^E to mixture parameters a, b. Since b was known a relationship of g^E as a function of a was etablished. The equation was numerically inversed to obtain a as a function of g^E.

For a binary system with components i & j, $a = f(g^E)$ allowed the calculation of K_{ij} as a function of various values of x_i (the composition dependence) at a specific temperature. The values of g^E could be calculated from any appropriate model : NRTL, UNIQUAC, UNIFAC, etc.

The authors proposed the following expression for $K_{ij}(x)$ to describe its composition dependence as a function of T,

$$K_{ij}(x) = k_{ij} + l_{ij}\left(\frac{m_{ij}x_i - m_x x_j}{m_{ij}x_i + m_x x_j}\right)(x_i + x_j)$$

k, l, m are parameters for the temperature dependence and were given as follows,

$$k_{ij} = k_{ij}^{(o)} + k_{ij}^{(1)}T + k_{ij}^{(2)}/T$$

$$l_{ij} = l_{ij}^{(o)} + l_{ij}^{(1)} + l_{ij}^{(2)}/T$$

$$m_{ij} = \frac{1}{2}[1 + \tanh(m_{ij}^{(o)} + m_{ij}^{(2)}/T]$$

If m_{ij} was fixed, ($m_{ij} = 0.5$ was found sufficient for most binary components), K_{ij} could consequently can be expressed as a linear function of mole fraction for the component resulting in,

$$k_{ij} = k_{ij} + l_{ij}(x_i + x_j)$$

Application : Binary Parameter Estimation by UNIFAC

The EOS parameters could be found by computing $K_{ij}(x_i)$ from the UNIFAC g^E for a set of computations and then fitting the parameters to the $K_{ij}(x_i)$ curve. However this took into account only liquid phase non-idealities and Schwartzentruber and Renon (1989) preferred a more rigourous approach.

Isothermal bubble and dew point curves were calculated using UNIFAC and the Hayden - O'Connell EOS. The EOS parameters were fitted directly to this pseudocritical data. The authors found that this approach, EOS with UNIFAC determined parameters, was able to reproduce UNIFAC accurately at low temperatures; and was able to correlate VLE at high temperatures. They therefore considered this approach a powerful extrapolation of UNIFAC to very high temperatures, including the critical region.

Schwartzentruber, *et al* (1989) applied this approach to a three parameter Redlich-Kwong EOS and used the EOS to model the propane / ethanol data of Gomez Nieto (1978) accurately.

B.8 DERIVATION OF UNIQUAC

The derivation of this model is based on a statistical mechanical extension of Guggenheims Quasi Chemical Theory.

Abrams and Prausnitz (1975) postulated that a liquid could be represented by a three-dimensional lattice of equi-spaced lattice sites. The volume in the immediate vicinity of a site being called a cell. Each molecule in the liquid was divided into attached segments such that each segment occupied one cell. The total number of cells being equal to the total number of segments.

The configurational partition function $Z\ (conf)$ was given by,

$$Z\ (conf) = Z\ (lattice) + Z\ (cell)$$

where :

$Z_{lattice}$ refers to the situation where the segment centre is coincident with the lattice site and,

Z_{cell} refers to contributions due to motion of segment about the lattice site.

From Guggenheims theory the lattice partition function was given by,

$$Z_{lattice} = \sum^{\theta} w(\theta)\ \exp\ [-U_o(\theta)/kT]$$

where :

$w(\theta)$ = combinatorial factor : number of ways molecules could be arranged in space,

$U_o(\theta)$ = potential energy of lattice : energy required to remove all molecules from lattice,

k = Botzmanns Constant.

Both w and U_o depend on the molecular configuration of the mixture designated by the variable Θ.

Abrams and Prausnitz introduced a more appropriate variable than Guggenheim, for describing a mixture of molecules differing in size and shape. They proposed describing the micro-composition of the lattice by the use of a local area fraction.

The lattice potential energy which is the sum of all interaction energies between pairs of nonbonded segments in terms of the area fraction was given by :

$$-U_o = (z/2)[q_1N_1(\theta_{11}U_{11} + \theta_{21}U_{21})] + (z/2)[q_2N_2(\theta_{22}U_{22} + \theta_{12}U_{12})]$$

where :

z = Cordination number,

q_i = pure component area parameter of molecule i,

N_i = number of molecules of component i,

θ_{ij} = local area fraction of site belonging to molecules around sites belong to molecule j,

U_{ij} = potential energy characterising the $i = j$ interaction.

No exact method was available to calculate the number of possible configurations or microstructures for local area fractions for a mixture of N_i molecules of component i and N_j molecules of component j. Abrams and Prausnitz therefore based their approximation on that used by Guggenheim by assuming :

$$w = w_1 \; w_2 \; h \; (N_1 N_2)$$

w_i = combinatorial factor which was based on the number of configurations associated with a site occupied by a segment of molecule i ,

h = normalization factor which depended only on N_i, N_j and assured that the w satisfied a physically reasonable boundary condition.

For the boundary condition Abrams and Prausnitz chose the non-exact Staverman combinatorial factor formula which was similar to that proposed by Flory-Huggins for mixtures of molecules with arbitrary size and shape but no attractive forces :

$$w_1 = \frac{(q_1 N_1 \theta_{11} + q_2 N_2 \theta_{12})!}{(q_1 N_1 \theta_{11})! \; (q_1 N_1 \theta_{21})!}$$

w_2 followed similarly. The normalisation factor h could be found from an analysis of the mixture. For the athermal case ($U_o = 0$) the average local area fractions were given by :

$$\theta_{11}^{(o)} = \frac{q_1 N_1}{q_1 N_1 + q_2 N_2}$$

$\theta_{22}^{(o)}$ followed similarly. The superscript (o) denotes zeroth approximation (athermal mixtures).

Mass balance constraints gave :

$$\theta_{12}^{(o)} = \theta_{11}^{(o)} = \theta_1$$

$\theta_{22}^{(o)}$ follows similarly. Therefore :

$$h\ (N_1N_2) = \frac{w^{(o)}(q_1N_1\theta_{11}^{(o)})!\ \ (q_1N_1\theta_{21}^{(o)})!\ \ (q_2N_2\theta_{22}^{(o)})!\ \ (q_2N_2\theta_{12}^{(o)})!}{(q_1N_1\theta_{11}+q_2N_2\theta_{12}^{(o)})!\ \ (q_2N_2\theta_{22}^{(o)}+q_1N_1\theta_{21}^{(o)})!}$$

For the non-athermal case ($U_o \neq 0$) the average local area fractions were given by :

$$\theta_{11}^{(1)} = \theta_1/(\theta_1+\theta_2\ \exp\ [-(U_{21}-U_{11}/RT])$$

where U_{12} are the UNIQUAC binary interaction parameters.

$\theta_{22}^{(1)}$ followed similarly. For a binary non-electrolyte liquid removed from critical conditions, the Helmholtz energy of mixing was given by :

$$\Delta A = \ln \frac{Z_{lattice}(N_1N_2)}{Z_{lattice}(N_1,O)\ \ Z_{lattice}(O,N_2)}$$

The molar excess Gibbs energy was given by :

$$g^E = \frac{\Delta A}{n_1+n_2} - RT\ (x_1\ln x_1 + x_2\ln x_1)$$

The excess Gibbs energy could be written as the summation of two terms,

$$g^E = g^E\ (combinatorial) + g^E\ (residual)$$

where

$$\frac{g^E\ (combinatorial)}{RT} = x_1\ln\frac{\bar{\phi}_1}{x_1} + x_2\ln\frac{\bar{\phi}_2}{x_2} +$$

$$\frac{Z}{2}\left(q_1x_1\ln\frac{\bar{\phi}_1}{\bar{\phi}_1} + q_2x_2\ln\frac{\bar{\phi}_2}{\bar{\phi}_2}\right) \qquad (B.51)$$

$$\frac{g^E\ (residual)}{RT} = -q_1'x_1\ln\ (\theta_1' + \theta_2'\tau_{21}) - q_2'x_2\ln\ (\theta_2' + \theta_1'\tau_{12}) \qquad (B.52)$$

where τ_{ij} the two adjustable parameters account for binary interactions,

$$\tau_{ij} = \exp\left[\frac{-(U_{ij}-U_{jj})}{RT}\right] = \exp\left[\frac{-\Delta U_{ij}}{RT}\right] \qquad (B.53)$$

and where $\bar{\phi}_i$ is the average segment fraction :

$$\bar{\phi}_i = \frac{x_ir_i}{\Sigma x_ir_i}$$

The above two Eqs. (B.51) and (B.52) contain pure-component structural parameters r_i and q_i which can be evaluated from bond angles and bond distances. Only the interaction characteristic energy parameters ΔU_{ij} wer required from experimental data.

B.9 CONSISTENCY TESTING

B.9.1 Equal Area Consistency Test of Chueh, *et al* (1965)

Derivation of Test

For an isothermal binary system Eq. (3.65) was derived as follows from the Gibbs-Duhem equation :

$$x_1 \, d\ln f_1 + x_2 \, d\ln f_2 = (V^L/RT)dP \qquad (B.54)$$

when the identity,

$$x_1 \, d\ln x_1 + x_2 \, d\ln x_2 = 0 \qquad (B.55)$$

was substituted into Eq. (B.54) :

$$\ln\left(\frac{f_2 x_1}{x_2 f_1}\right) dx_2 + \frac{V^L dP}{RT} = d\left(\ln\frac{f_1}{x_1} + x_2 \ln\frac{f_2 x_1}{x_2 f_1}\right) \qquad (B.56)$$

Introducing fugacity coefficients ϕ and K factors

$$\left(\ln\frac{\hat{\phi}_2}{\hat{\phi}_1} + \ln\frac{K_2}{K_1}\right) dx_2 + \left(\frac{V^L dP}{RT}\right) = d[\ln K_1 + \ln\hat{\phi}_1 P + x_2\left(\ln\frac{\phi_2}{\hat{\phi}_1} + \ln\frac{K_2}{K_1}\right)] \qquad (B.57)$$

Subscript 1 refers to the solvent. If Eq. (B.57) was integrated from $x_2 = 0$ to x_2 the following boundary conditions applied :

$$x_2 = 0 \quad : \quad \phi_1 = \phi^s$$

$$P_1 = P_1^s$$

$$K_1 = 1$$

The integrated form of Eq. (B.57) could therefore be written

$$AREA1 + AREA2 + AREA3 = AREA = RHS \qquad (B.58)$$

where

$$AREA\ 1 = \int_{x_2=0}^{x_2} \ln\frac{K_2}{K_1} \, dx_2 \qquad (B.60)$$

$$AREA\ 2 = \int_{x_2=0}^{x_2} \ln\frac{\hat{\phi}_2}{\hat{\phi}_1} \, dx_2 \qquad (B.61)$$

$$AREA\ 3 = \frac{1}{RT}\int_{P_1^s}^{P} V^L \, dP \qquad (B.62)$$

$$AREA = LHS = \left[\ln k_1 + \ln\frac{\phi_1 P}{\phi_1^2 P_1^s} + x_2\left(\ln\frac{\phi_2}{\phi_1} + \ln\frac{K_2}{K_1}\right)\right] \qquad (B.59)$$

Application of L'Hopital's Rule to K Ratio

$$\lim_{x_2 \to 0} \left(\frac{K_2}{K_1}\right) = \lim_{x_2 \to 0} \left(\frac{y_2}{x_2}\right)\left(\frac{x_1}{y_1}\right) = \frac{0}{0} \qquad (B.63)$$

x_2 and y_2 are related by :

$$y_2 \hat{\phi}_2^v P = x_2 \gamma_2 f_2^{OL} \qquad (B.64)$$

By definition therefore ,

$$\hat{\phi}_2^v = \frac{\hat{f}_2^v}{y_2 P} \qquad (B.65)$$

combining Eq. (B.64) and Eq. (B.65) gives :

$$y_2 = \frac{\gamma_2 f_2^{OL} y_2 P}{P \hat{f}_2^v} \; x_2$$

For a binary mixture by definition :

$$\frac{K_2}{K_1} = \frac{\gamma_2 f_2^{OL} y_2 P (1 - x_2)}{P x_2 \hat{f}_2^v (1 - y_2)} \; x_2 \qquad (B.66)$$

as $x_2 \to 0$, $\gamma_2 \to 1$ then :

$$\frac{\hat{f}_2}{y_2 P} = \hat{\phi}_2^v \to 1$$

If :

$$\frac{f_2^{OL}}{P} = A$$

the limit of Eqs. (B.63) and (B.66) can be written

$$\begin{aligned} \lim_{x_2 \to 0}\left(\frac{K_2}{K_1}\right) &= \lim_{x_2 \to 0} \frac{A(1 - x_2)(x_2)}{x_2(1 - A x_2)} \\ &= \frac{d(A(1-x)x)/dx}{d(x_2(1 - A x_2))/dx_2}_{x_2 \to 0} \\ &= \frac{A(1 - 2x_2)}{1 - 2A x_2} \\ &= A \\ &= \frac{f_2^{OL}}{P} \end{aligned} \qquad (B.67)$$

B.9.2 Won and Prausnitz (1973) Consistency Test-Extension of Barkers Method

This method as well as the Christiansen and Fredenslund method was initially developed as a predicitive method to calculate vapour phase-mole fractions for experimental data where the y_i had not been measured.

The method was based on the principle that the total pressure can be represented as the sum of the two partial pressures

$$P = y_1 P + y_2 P \qquad (B.68)$$

for which the Gibbs-Duhem equation can be written as :

$$(1 - x_2) \frac{d \ln \gamma_1}{dx_2} + x_2 \frac{d \ln \gamma_2}{dx_2} = \frac{dP}{dx_2} \qquad (B.69)$$

The standard state fugacities for the condensable (1) and non-condensable (2) components were defined as that of the saturated liquid at system pressure and Henry's constant for solute 2 in solvent 1 at system temperature respectively. This implied the constant temperature (not constant pressure) activity coefficients γ were normalised by the unsymmetric convention.

$\gamma_1 \rightarrow 1 \quad (x_1 \rightarrow 1)$

$\gamma_2 \rightarrow 1 \quad (x_2 \rightarrow 0)$

An arbitrary function $F_2(x_2)$ to represent the variation of the logarithm of γ_2^* along the saturation line and whose unknown coefficients had to be determined from total pressure data, was defined as follows :

$$\ln \gamma_2^* = F_2(x_2) \qquad (B.70)$$

An arbitrary function of pressure $G(P)$ was used to represent the experimental liquid molar volume of the mixture.

Rearranging and integrating Eq. (B.69) an expression for γ_i was obtained :

$$\ln \gamma_1 = F_1(x_2) \qquad (B.71)$$

The above equations were subsitituted into Eq. (B.68) and the working equation was obtained :

$$P = \frac{x_1 f_1^\circ}{\hat{\phi}_1} \exp F_1 + \frac{x_2 f_2^\circ}{\hat{\phi}_2} \exp F_2 \qquad (B.72)$$

Eq. (B.72) was used in the method outlined below :

1. For the first interation the $\hat{\phi}_i$ where set to 1 and F_2 to zero for all x_2. The first estimates of y_1 were obtain by :

$$y_1 = \frac{x_i f_i^o}{P} \exp F_1$$

$$y_2 = 1 - y_1$$

2. f_2^o was determined from experimental $(p-x)$ data where x_2 is small ~ 0.01 ,

$$f_2^o = \left[P - \frac{x_1 P_1^s \phi_1^s}{\phi_1} \exp v_1^L \frac{(P - P_1^s)}{RT} \right] \frac{\hat{\phi}_2}{x_2}$$

3. The constants in F_2 are adjusted to give the best fit of the $(p-x)$ data to Eq. (B.72)

4. The next set of y_i are calculated from :

$$y'_i = \frac{x_i f_i^o}{\hat{\phi}'_1 P} \exp F_i$$

The y_i's were summed. If the sums of the y_i's were found not equal to unity, they were normalised by :

$$y_{i\ (normalised)} = \frac{y_i}{y_1 + y_2}$$

5. A new f_2^o was found from :

$$f_2^o = \lim_{x_2 \to 0} \frac{\phi_2 y_2 P}{x_2}$$

6. The iterational procedure was continued until the constants in F_2 which were continously being adjusted to fit the $(p-x)$ data no longer changed.

The authors state they had no fundamental difficulty in finding a set of thermodynamically consistent equations, Eqs. (B70) and (B.71) to fit $(p-x)$ data and $G(P)$. The difficulty arose in the choice of the EOS for calculation of $\hat{\phi}_i$. Therefore it was *not possible* to reject a set of $P-x-y$ data as thermodynamically inconsistent unless it could be shown that the calculated $\hat{\phi}_i$ used gave the correct representation of the vapour phase properties.

B.9.3 Christiansen and Fredenslund (1975) Orthogonal Collocation Thermodynamic Consistency Test

The Christiansen and Fredenslund method was initially developed as a predictive method, i.e., to predict y_i knowing P, T, x_i. If experimental y_i were available in the method could be used to test the data for thermodynamic consistency by comparing the calculated and experimental y_i. The method was attractive in that it did not require a liquid phase model to calculate γ_i but it did require a vapour phase EOS and some way of calculating excess enthalpies and liquid molar volumes.

Extensions of the low pressure consistency test of van Ness (1973) to high pressures required several modifiactions of which the original test :

1. The non-condensable compenent required the definition of a standard state. The unsymmetric convention was used based on Henry's Constant.
2. The non idealities associated with the vapour phase at high pressures.
3. The non-linearity of the non-isothermal and non-isobaric Gibbs-Duhem equation used to describe the high pressure VLE required powerful numerical technique such as orthogonal collocation.

The consistency test was based on three independent equations for γ_1 , γ_2 , & P for the three unknowns γ_1 , γ_2 , G^E

For γ_i&γ_j :

$$\ln \gamma_i = \frac{G^E}{RT} + x_k \left(\frac{d(G^E/RT)}{dx_i}\right) -$$

$$\frac{x_k}{RT}\left[V\left(\frac{dP}{dx_i}\right)_\alpha - \sum_{j=1}^{2} x_j V_j^\circ \left(\frac{dP_j^\circ}{dx_i}\right)\right] + x_k \frac{H^E}{RT^2}\left(\frac{dT}{dx_i}\right)_\alpha \qquad (B.73a,b)$$

which could be written for $l = 1$, $k = 2$ and $l = 2$, $k = 1$ and,

$$P = \Sigma \frac{x_i \gamma_i f_i^\circ}{\hat{\phi}_i}$$

The consistency test method consisted of calculating the vapour mole fractions y_i^c from experimental (T, P and x) and comparing these to the experimentally measured (y) by the method outlined below :

1. T, P, and x_i are known. f_i°, V_i°, V, H^E, and the slope of the equilibrium curve were assumed known or available by calculation.

   Initially $\hat{\phi}_i = 1$ for $i = 1,2$

2. Eqs. (B.73) (a and b) and (B.74) were solved for γ_1 , γ_2 , G^E for the value of x_i

3. Vapour mole fractions were calculated using :

$$y_i = \frac{x_i \gamma_i f_i^{\circ}}{\hat{\phi}_i P}$$

4. New values of $\hat{\phi}_i$ were calculated using y_i from step 3 and steps 2 and 4 were repreated until the successive calculated values of y_i agreed to within a predetermined tolerance, i.e. 10^{-4}

5. The value of y_i was calibrated at each point by interpolation among the values of y_i last obtained under step 3.

6. The experimentally obtained values of y_i were compared with the calculated values. If

$$|y_i^c - y_i^e| \leq \Delta x_i + \Delta y_i$$

where Δx_i and Δy_i are the uncertainties in the liquid and vapour mole fraction measurements, the data point was deemed thermodynamically consistent in the limit of the methods used to calculate f_i, V and H^E. If however

$$|y_i^c - y_i^e| > \Delta x_i + \Delta y_i$$

two possibilities existed :

1. The data are inconsistent or
2. The methods used to calculated f_i, V and H^E were erroneous.

d3 min = d4 max − 2 (t max)

d3 max = d4 min − 2 (t min)

t and b function of application

"O" RING HOUSING DATA FOR DYNAMIC PISTON SEALING

S and g function of "O" Ring

"O" RING HOUSING DATA FOR AXIAL SEALING APPLICATIONS

Figure C.1 : Dowty "O"-Ring Housing Data

C.2 AVOIDANCE OF STAGNANT SPACES FOR MALE NPT THREADS

The importance of teflon inserts to reduce the stagnant spaces that arise as a result of using Swagelok NPT male thread to pipe connectors is discussed below.

The teflon inserts as shown in Figures 4.2, 4.3 and 4.8 and 4.9 were necessary to remove the stagnant spaces between the NPT male to pipe connectors and the cell wall and Snotrik high pressure valves. The NPT male thread relies on its slight taper to seal on tightening into the female thread. The distance required to tighten the male thread to a specific torque had to be accurately measured and teflon inserts made to fill the stagnant spaces exactly. These stagnant spaces could have caused errors in the liquid and the vapour sample analysis due to any non-volatile components becoming entrained in these spaces.

C.3 JET MIXER AND LIQUID SAMPLING DEVICE

C.3.1 Experimentation to Determine Cause of Non-Uniformity of Liquid Samples

A calculation of a rough estimate of the pressure rise resulting from a 9 mm^3 sample of pure toluene instantaneously flashing in a 90 cm^3 jet mixer (the original jet mixer used by Bradshaw (1985)) using Eqs 4.1 and 4.2 gave a value of approximately 4 kPa. A sample of liquid removed slowly from the cell yielded a massive increase in pressure (>10 bar). The calculations for predicting the pressure rise were checked and found to be correct.

A larger jet mixer with an internal volume of 300 cm^3 was constructed, (shown in Photographs 15 and 16). Two modifications were made compared to the jet mixer described by Bradshaw (1985) :

1. The outlet port was changed. The stagnant outlet area in the jet mixer used by Bradshaw was eliminated by using a Whitey SS-ORM2-S2-A regulating valve with a 1/8 male NPT valve inlet port instead of the 1/8 pipe Whitey SS-OR-S2 regulating valve. The stagnant area occurred in the outlet tube connection to the SS-OR-S2 valve. The stress on the outlet tube connection, that sometimes resulted in leaks due to the valve extension, was hereby eliminated.
2. The thermocouple well in the mixing chamber was removed. The fewer connections the jet mixer chamber had the fewer the connections available in which leaks could develop. This was particularly important as the Swagelock fittings used were not really designed for low-pressure work. In addition the information supplied by this thermocouple was interesting but not necessary.

With the larger jet mixer in place the pressure rise on sampling was found to be a function of the rate of withdrawal of the sample rod. Slow and fast withdrawals caused large and small pressure rises respectively. The conclusion reached was that the cell contents were leaking past the sampling rod packing material as the sampling hole with it's flared edges was wider than the compressed packing. The packing

width was increased from 2 mm to 3 mm and a new sampling rod constructed. The new sampling hole had only slightly flared edges and hole diameter of 1,5 mm giving a 8,8 mm^3 sample volume. Reproducible sample sizes were now achieved.

The 300 cm^3 jet mixer was however too large. Taking into account the sample size requirements of the gas chromatograph the final jet mixer was constructed incorporating the features described in the above 300 cm^3 jet mixer.

C.3.2 Determining Final Jet-Mixer Volume

To produce a vapourized liquid phase sample of the correct magnitude for gas chromatographic analysis the sampling device sample-volume size, jet-mixer volume and chromatograph gas-sampling valve-loop volumes need to be matched to each other.

The crucial volume is the fixed liquid sample size that is withdrawn from the equilibrium cell. Increasing this volume would have required increasing the packing size which would have meant reconstruction of the equilibrium cell and liquid sampling rod, an unacceptable alternative. The jet-mixer volume calculated from the gas chromatograph requirements based on one sample withdrawal would have resulted in a miniature jet mixer of such dimensions that :

1. The construction of the miniature jet mixer would have been extremely difficult.
2. The pressure transducer, which gave vital information on the operation of the liquid sampling device, could not be mounted.
3. The inlet port of the Whitey SS-ORM2-S2-A valve could not be fitted. The Whitey SS-OR-S2 valve with all it's associated problems would have had to be reverted to.

To allow for pressure transducer mounting and ease-of-construction it was finally decided to base the dimensions on four liquid sample withdrawals and a final carrier gas dilution of the 4 withdrawn samples in the jet mixer to 185 kPa (a). The final jet mixer with a volume of 75cm^3 is basically a scaled down version of the 300 cm^3 mixer shown in Photographs 15 and 16.

Thus each sample analysed in the gas chromatograph was the average of four withdrawals. If one withdrawal in the series was for some reason unrepresentative, this could be easily determined from the pressure rise noted on sampling, the procedure was repeated starting from the total evacuation of the jet mixer. The method of withdrawal and dilution is described in Chapter 5.

C.4 DIFFERENT OPTIONS FOR THE VAPOUR SAMPLING SYSTEM

The various options considered to replace the vapour sampling system are given below.

OPTION 1

1. Replacement of the manifold and associated connectors, Figure 4.8, with a 1/16 inch union tee and Snotrick extreme high pressure, heavy-walled uniform male thread-to-swagelock tube-fitting connectors.

   This system would create a manifold with no stagnant spaces and no extrusion problems and consequent tube blockages. The existing SS-410-FP valves would however have had to be remachined to receive the desired Snotrick fittings 9/16-18 inch uniform thread instead of the current 1/4 inch NPT thread. In addition the desired Snotrick fittings (1/16 swagelok to 9/1-18 uniform thread) being a "special" would have been expensive and caused to lengthy a delay in the project. This option should however be seriously considered when the Snotrick valves come up for replacement.

The Snotrick valves could also be replaced with Whitey "83" Series Trunnion ball valves if the correct end pieces to accept the abovementioned Snotrick fittings can be supplied. These valves have better vacuum operating capabilities and are easier to maintain.

This system would result in a reduced vapour sample volume which would be highly desirable.

OPTION 2

2. Replacement of the manifold by essentially the same system described above but using NPT fittings which are readily avaliable. The NPT male thread relies on its slight taper to seal on tightening into the female thread. The distance required to tighten the male thread to a specific torque must be accurately measured and a teflon insert made to fill the stagnant space exactly as described in Appendix C.2. Extreme care had to be taken in the machining of the teflon inserts to manufacture them to the correct dimensions to avoid stagnant spaces. This system adopted due to time constraints had a sample volume of +/- 0.9 mm^3. This volume although slightly larger than Bradshaws was still acceptable in view of the blockage-free operation it provided. Figure 4.9 shows the essential features of this system.

C.5 ASPECTS OF EQUILIBRIUM CELL ENVIROMENT

C.5.1 Fiberglass Insulation Properties

TABLE C.1
Physical Properties of Type IM475 Fiberglass Insulation

Density kg/m³	Insulation thickness mm	Hot face °C	Cold face °C	Heat loss W/m2	Thermal conductivity W/mK	Insulation efficiency %	HCT(1) Outer Surface W/m²K
47,5	80	200	32,6	115	0,055	96,9	9,012

(1) HCT = Heat transfer coefficient.

C.5.2 Temperature Control Equipment

Heating elements

The energy required to heat the circulating air from the air bath was supplied by five aluminium finned stainless steel cartridge heaters. Aluminium fins instead of stainless steel were used due to alumininium's high conductivity wrt stainless steel (237 to 20 W/mK). The heaters however require an air flow rate of greater than 2,51 ms^{-1} over them to prevent melting of the aluminium fins. Cartridge heaters were chosen for safety reasons as mainly flammable organic materials were to be studied.

The five heating elements had power ratings of 400 W, 300 W, 2 x 250 W and 200 W respectively. From circuit diagram, Figure 5.11, it can be seen that the 2 x 250 W heating elements were manually controlled (they could be used to speed up initial heating) while the others were controlled by the Eurotherm 818. Each of the elements could however be individually added or removed from the heating circuit by a switch.

The heating elements were contained in a heater box constructed of aluminium. Copper was not used due to it's lack of rigidity. Aluminium aided in the temperature uniformity due to its relatively high thermal conductivity. The heating elements were insulated from the aluminium by backelite insulation material, Photograph 5.

Eurotherm 818 temperature controller

The Eurotherm 818 is a flexible, advanced technology controller which combines simplicity of operation with powerful control capabilities. It has a low-level I/P analogue-to-digital converter which is continuously corrected for drift. Operating at a speed of 8 updates per second this gives very high stability and rapid response to process changes.

The 818 offers two separate PID loop turning algorithms, self tune and adaptive tune. These facilities automate the tedious part of the commissioning routine, and help to maintain good temperature control despite changing conditions. The abovementioned algorithms may be initiated either individually or separately to suit a variety of requirements and will now be discussed separately.

The self tune feature

The self-tuning algorithm is a manually initiated "one-shot tuner" which is normally used at start up but may be initiated at any time in order to retune for a new set of conditions.

When initiated the self tuner analyses the start up response to give an estimate of the process delay time. The self-tuner then stimulates the process with an on-off sequence which determines the natural response of the process so that new control parameters can be calculated and the proportional, integral and derivative terms automatically set.

The adaptive tune feature

The adaptive-tuning algorithm is designed to run continuously in the background while normal PID control is taking place. The algorithm is activated when load disturbances cause deviations from setpoint in excess of a predefined trigger point. The algorithm then proceeds to analyse the closed loop response while the process value recovers from the initial disturbance and applies expert rules to retune the loop, if necessary. If the loop is already well tuned, no action is taken.

Thyristor 425

The use of a thyristor (basically a semiconductor device which acts as a switch) receiving a logic 4-20 m Amp input signal from a controller holds tremendous advantages over the conventional mechanical on-off relay system for driving the heaters.

The Eurotherm 425 thyristor used to drive the heaters operated in the fast cycle firing mode. This mode is a means of controlling the power of the heaters by time proportioning the available power. Power (P) therefore is switched to the heaters with a regular cycle time (T), for a variable (t), Figure C.1. The heaters therefore see an average power (effective power) of $P_{max} \cdot \frac{t}{T}$. For small systems with fast repsonses such as the air bath (T) has a value of around 1 second.

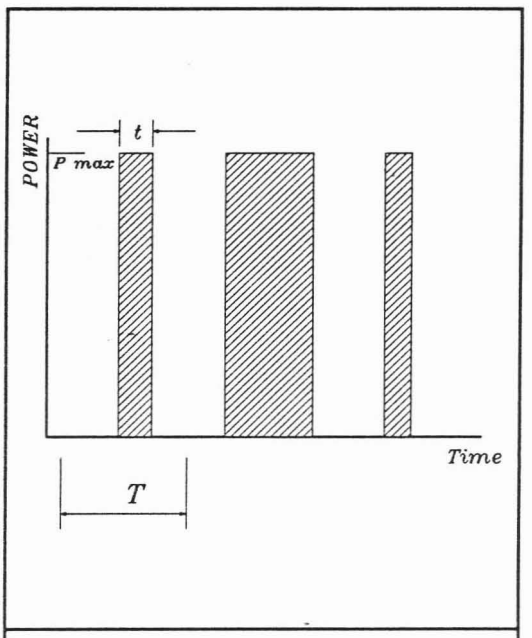

Figure C.2 : Firing Mode of Eurotherm 425 Thyrister

Control inputs for this type of thyristor unit are usually 0-5 V or 4-20 mA and the proportioning ratio t/T will be in a linear relationship with the input signal.

To minimize interference the thyristor unit always switches on when the voltage across the heaters is zero and switches off when the current through the heaters is zero. Each "burst" is therefore a complete number of cycles of the supply.

Temperature Sensing Device

It is important to distinguish between *consistency* of control and absolute *accuracy* of the process variable in this case temperature.

Eurotherm claim that accuracies of ±2 % (for thermocouples) and ±0,5 % (for platinum resistance thermometers) of the temperature range being measured can be expected. Calibration of their controllers against standard tables are better than 0,25 % of the range. Errors in setpoint temperature are consequently quite small, ±0,2 °C for platinum resistance thermometers. These factors add up to the nett *accuracy*, in absolute terms compared to the true temperature. The process temperature may be controlled *consistently* to accuracies less than a fraction of 1 °C.

Due to the desired accuracies in the temperature measurement required, input to the controller is via a three-wire platinum resistance thermometer to BS1904 or DIN 43760 specifications described more fully in Appendix C.6.

C.6 SPECIFICATIONS OF TEMPERATURE MEASURING EQUIPMENT

Great care was taken to obtain the highest quality platinum resistance sensors and thermocouple wire available from the local agent of Mannesmann Hartmann and Braun, West Germany. These agents supplied most of the "speciality requirements" in South Africa. Claims of greater-accuracy sensors and wire were made but on closer investigation manufacture and quality control could match Hartmann and Braun.

Internal equilibrium-cell temperature (Pt 100)

The platinum resistance thermometer was supplied to meet the following specifications : It was a three-wire Class B Pt 100 resistance thermometer conforming to IEC 751:1983 (DIN 43760), with a tolerance of 0,3 + 0,005 ltl where t is in °C for the range -200 °C to 850 °C, Westerfeld (1987). The bulb was mounted in a 120 mm long fully annealed high quality 316 stainless steel hydraulic tube (diameter 3/16 inch).

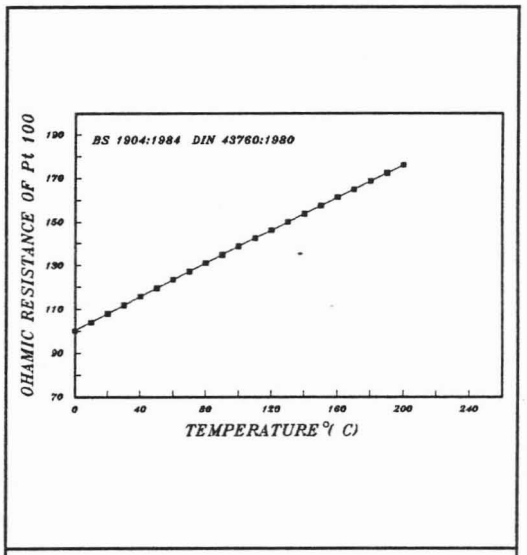

Figure C.3 : Ohmic Resistence versus Temperature for a Pt 100 IEC 751

The tube conformed to ASTM A269 or A213 or equivalent, with hardness Rb80 or less was able to withstand a 200 bar and 200 °C equilibrium cell environment. The tube was minerally insulated and hermetically sealed.

The sensor was mounted 20 mm from the bottom of the cell to ensure that it was always submerged in the liquid phase, Figure 4.12, in order to ensure the fastest possible response times (the liquid phase heat transfer coefficients to metal being larger than the vapours). The sheath was sealed by a 1/8 male to 3/16 pipe Swagelock male connector. The sheath outside the cell was insulated from the surrounding air bath by a teflon jacket as seen in Figure 4.12 and Photograph 19.

The sensor was connected to a high accuracy 6 digit Fluke 8840A multimeter by 3 metres of appropriate high temperature teflon interconnection cable capable of withstanding 200 °C. The resistance reading was converted to temperature from a linear regression curve obtained from fitting the DIN 43760 ohmic resistance versus temperature table values to a straight line. Figure C.2 shows the ohmic resistance versus temperature curve for a Pt 100 IEC 751 Class B platinum resistance thermometer.

The Pt 100 IEC 751 used by the Eurotherm 818 temperature controller conformed to exactly the same specifications but was housed in a shorter 120 mm sheath.

Cell and air bath temperature measuring thermocouples

Thermocouples were used to measure the cell and air bath temperature profiles. The type J (iron/copper-nickel) and type K (nickel-chromium/nickel aluminium) thermocouples supplied conformed to the following specification :-

International thermocouple reference tables : IEC 584-2 : 1982 with tolerance values of ±0,0075 ltl where t is in °C, for the range -40 °C to 750 °C , Westerfeld (1987).

To furfil the requirements that the thermocouples did not deteriorate and continued to produce a measurable stable electric output over a long period of time with the quickest possible response time; they were housed in hermetically sealed, semi flexible sheaths. These sheaths 30 mm by 1,5 mm diameter for type J and 300 m by 3 mm diameter for type K gave the thermocouples complete protection against oxidation and corrosion. The grounded junction configuration used gave a fast response to a temperature change. An exposed junction was considered too delicate while an insulated junction would have had too slow a response time.

The type J thermocouples were chosen as they had a steeper temperature versus mV slope than type K and hence were more sensitive to temperature. The type J thermocouples were inserted into 10 mm wells drilled into the equilibrium cell walls as shown in Figure 4.12. To prevent spurious reading through conduction of energy to the grounded junction tip from the airbath the exposed part of the sheath was insulated by a 15 mm diameter teflon block as seen in Photograph 19.

The sensors were connected to a high accuracy Fluke 2190A digital thermometer with a resolution of 0,1 °C through a Y2001 T/C multipoint selector by 3 metres of appropriate high temperature stainless steel braided interconnection cables capable of withstanding 200 °C. Stainless steel braided cable was used to protect the delicate thermocouple wire from physical damage that could affect its accuracy.

Although the type J thermocouples conformed to the tolerance values specified; the batch supplied by the manufacturer measured temperatures to within a tolerance of 0,1 °C of each other. This was necessary as the absolute accuracy for the thermocouple measurements was not of paramount importance but the relative difference between the readings which gave an indication of the thermal profile.

The type K thermocouples were used as the temperature inputs for the two jet mixer Eurotherm 818 and Eurotherm 103 controllers.

C.7 COMPOSITIONAL ANALYSIS BY GAS CHROMATOGRAPH

Gas chromatography is a method whereby the components of a gaseous mixture are separated in a column and quantified as they elute by a suitable detector, The differences in physical and/or chemical properties of the components are utilized to effect separartion. Although a simple method in principle, to achieve accurate results requires a through investigation to find the correct column packing, optimum separation temperature and detector for the application in question.

Detector Types

Thermal Conductivity Detector (TCD)

This detector is the most simple and widely used in gas chromatography. It is reliable, moderately sensitive and responds essentially to all compounds.

Responses for different substances vary widely and can be non-linear with concentration, so quantitative analysis requires careful calibration of the detector. The analyst is rarely justified in merely-taking peak ratios as an accurate indication of relative amounts, calibration of the peak area versus concentration is the recommended method. Detection limit is about 5 - 10 x 10^{-6} g/mM of effluent gas.

Flame Ionisation Detector

This detector has a wide linear range, high sensitivity and is quite reliable.

The detector does not however respond to water and the permanent gases (N_2, O_2, CO_2 etc.) making it ideal for determining low concentrations of hydrocarbons in water i.e. the propane/water binary's liquid phase. Detection is about 1-5 x 10^{-9} g/mM of sample gas.

Selection of Column Packing and Separation Temperature

The column packing utilizes the differences in the component's physical properties to either effect separation due to differences in charge (e.g. carbowax) or size (e.g. Poropak). Once a decision has been made on which property to effect separation on, a column packing is chosen. A series of experimental injections of the components is made to determine the optimum column length and temperature to give adequate separation.

Poropak Q, a packing material that separates substances on their physical size differences was found suitable for all three binaries.

The propane/water binary was the binary that proved the most difficult to separate. A dual column of Carbowax and Poropak Q was considered so water would elute after the propane. The use of combined columns is however not considered an ideal solution to separation problems. The availability of the Varian gas chromatograph and vigourous experimentation on various lengths of column and temperatures yielded adequate separation with the conditions shown in Table 4.4.

Calibration of the Detectors

Response factors for all components were obtained by calibration. Calibration entailed injecting different volumes of the substances into the column. The signals generated, converted to a peak area in this case, were plotted either directly against the volume injected or the volume converted to moles of substance injected i.e. the direct injection calibration method.

The calibration procedure is discussed in Chapter 5.

C.8 GAS CHROMATOGRAPH DETECTOR CALIBRATION DEVICE

C.8.1 Description Of The Raal Calibration Device

Figure C.3 is a schematic diagram showing the essential features of the device.

In essence it consisted of a cylinder whose internal diameter was accurately known. The cylinder was divided into two chambers by a piston whose position could be accurately measured. The piston was moved up and down the chamber by a stepper motor which allowed the operator to move the piston in very small reproducible increments. The pressure and temperature of the upper mixing chamber were measured by a pressure transducer and Pt 100 resistance thermometer housed in a finned thermowell, respectively. Communication between the upper and lower chambers was accomplished by a ball valve housed in the piston. Both upper and lower chambers had magnetically coupled stirrers to vigorously stir the chamber contents.

C.8.2 Operation Of The Raal Calibration Device

Upper Chamber Volume Determination

The volume of the upper chamber had to be determined first as a function of piston position.

Volume determination as a function of piston position was achieved as follows: The piston was placed in any position after ensuring the chamber was full of gas (nitrogen) by the procedure fully described in the following section (Calibration Mode of Operation). Valves V1, V2 and V3 were closed, Figure C.3. The piston position, temperature and pressure were noted. The piston was moved into another position 2, and after ā suitable equilibration period the piston position, temperature and pressure were noted. This procedure was continued for a number of piston positions. The volume change (ΔV) between the two positions was determined by :

$$\Delta V = \frac{\pi}{4} (Di^2 - do^2)(\Delta L) \qquad (C.1)$$

where :

Di = outer chamber diameter.
di = internal piston guide rod diameter.
ΔL = length of piston travel.

From the temperature and pressure conditions at position 1 (T_1, P_1) and position 2 (T_2, P_2) respectively the number of moles (n_{tot}) in the chamber could be calculated using the 2 parameter truncated virial EOS Eq (3.26) as follows :

Volume at position 1 was ,

$$V_1 = n_{tot} \frac{RT_1}{P_1}\left(1 + \frac{BP_1}{RT_1}\right) \qquad (C.2)$$

and position 2 :

$$V_2 = n_{tot} \frac{RT_2}{P_2}\left(1 + \frac{BP_2}{RT_2}\right) \qquad (C.3)$$

the change in volume was :-

$$\Delta V = V_2 - V_1 = n_{tot}\left(\frac{RT_2}{P_2} + B_2 - \frac{RT_1}{P_1} - B_1\right) \qquad (C.4)$$

Equating Eqs. (C.1) and (C.5) :

$$n_{tot} = \frac{\frac{\pi}{4}(Di^2 - do^2)L}{\left(\frac{RT_2}{P_2} - \frac{RT_1}{P_1} + B_2 - B_1\right)} \qquad (C.5)$$

Since n_{tot} was known; V_1 and V_2 may then be calculated from Eqs. (C.2) and (C.3) respectively.

Operation of Raal calibration device

The upper chamber was filled with the solvent gas. Residual air was removed by moving the piston to the top of its travel and filling and venting the remaining space at least 10 times. The piston was moved down and in the process drew in the solvent gas. Valves V1 and V2 are then shut.

A similar procedure was now followed with the solute gas in the lower chamber. The lower chamber was filled and vented 10 times and solute was drawn in as the piston moved up. Valves V4 and V5 were closed. During this procedure V3 remained closed.

From experience the operator knows the quantity of solute to add to a certain quantity of solvent for the desired peak area required for calibration. The piston was placed in the required position dictated by the quantity of solvent required. Both chambers were vented to atmosphere. They were now at equal pressure, the stirrers were switched off, and valve V3 opened. The piston was moved down and in doing so displaced the required volume of solute into the solvent chamber. After the desired quantity of solute had been displaced valve V3 was closed. The stirrers were switched on, and the mixture in the upper chamber was allowed to homogenize. The upper chamber was slightly pressurized to enable samples of the mixture to be withdrawn from the withdrawal port by a gas syringe. The mixture composition, temperature and pressure were known. The gas chromatograph detector could now be calibrated accurately.

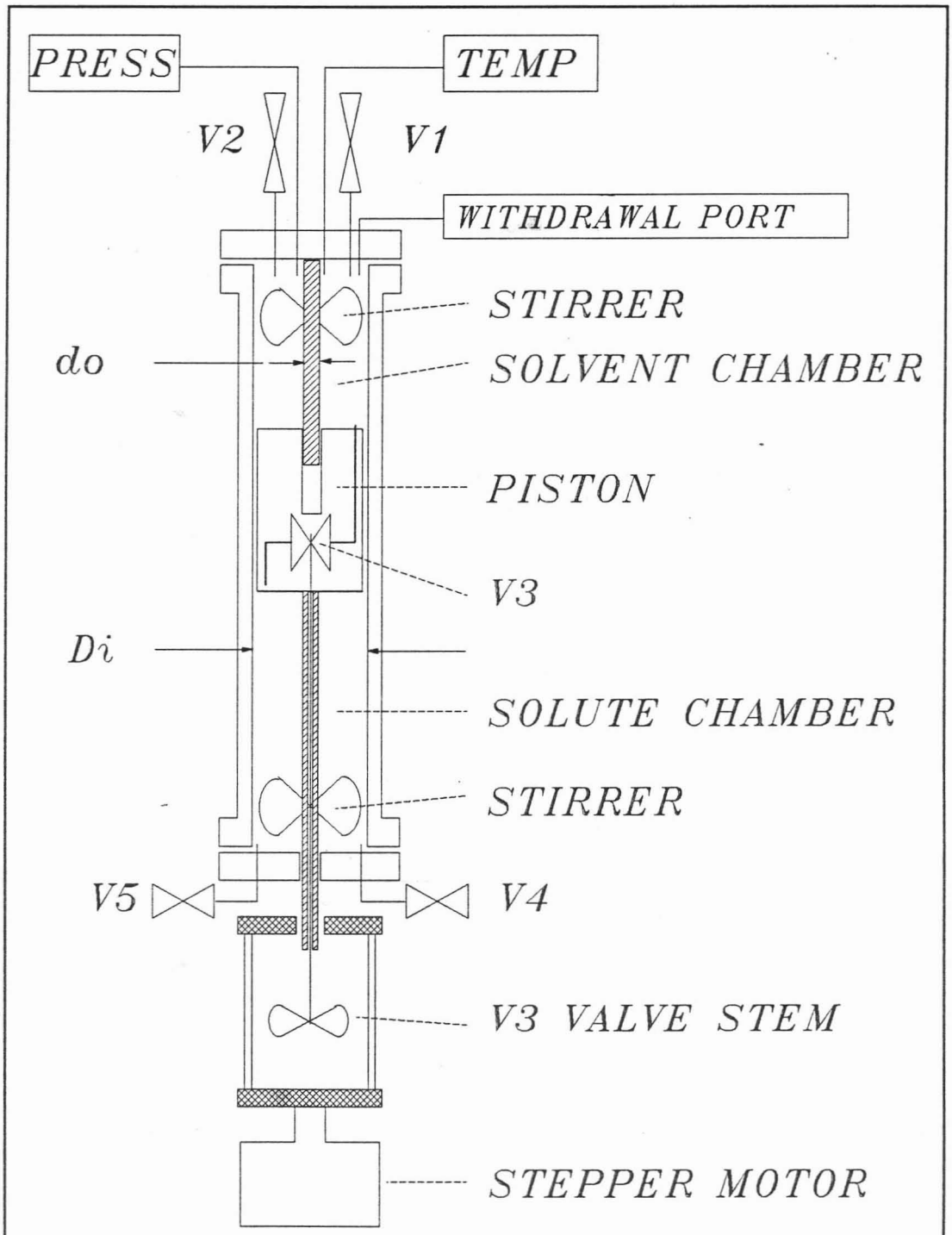

Figure C.4 : Raal Gas Chromatograph Detector Calibration Device

C.9 DEGASSING EQUIPMENT

C.9.1 Description Of Degassing Equipment

The apparatus consisted of a heavy duty vacuum flask with a coiled condensor attached to the vacuum port. The condensor led through a florite 2 mm stop cock (S1) to the vacuum pump. The silicon bun was connected to a propane bottle through an interflon 1,2 mm stop cock (S2). The degassed liquid could be removed directly from the degassing cell with the Beckman 110A pump and pumped directly into the equilibrium cell.

C.9.2 Operation Of Degassing Equipment

Stop cock S2 was closed and S1 opened to vacuum and the liquid (water and subsequently 1-propanol) was brought to boil and stirred by a IKAMAG stirrer hot plate.

The liquid was allowed to degass for 15 minutes under moderate heating and vigorous stirring conditions. After this time S2 was closed and S1 opened to allow pure propane into the evacuated space. The liquid was subsequently pumped into the equilibrium cell by the Beckman 110A pump. The precise amount of liquid added to the equilibrium cell could be determined as both the flow-rate set on the pump, and time pumped were known.

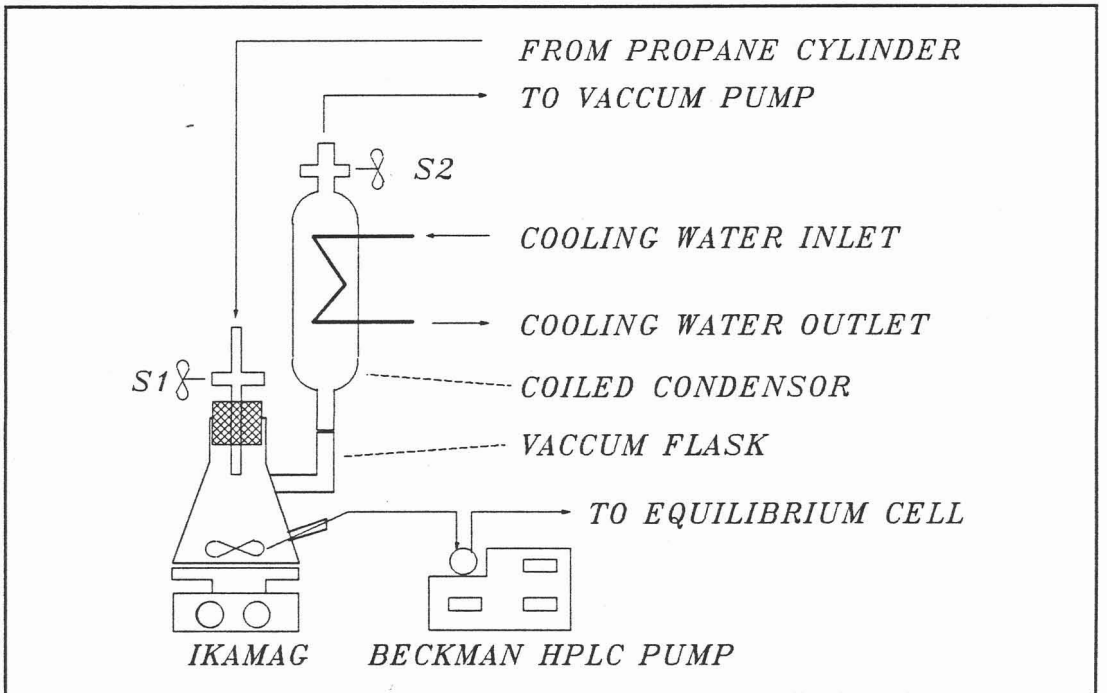

Figure C.5 : Degassing Equipment

C.10 PROPANE COMPRESSION DEVICE

C.10.1 Description Of Propane Compression Device

The construction details of the unit are shown in Figure C.5. The chamber constructed from a stainless steel type 304 billet, received propane from it's cylinder at room temperature and approximately 8 bar. This chamber was heated by three 150 W electric cartridge heaters, positioned longitudinally in the wall of the chamber equi-spaced around the circumference. The heaters were controlled by a RKC controller with a type J thermocouple as its temperature sensing unit. The second chamber, constructed from a 100 mm diameter EN8 Bright (BS 970/SAE AISI 1043) mild steel billet; received air from a compressed air cylinder at approximately 200 bar via a nupro fine metering valve. The two chambers were attached by 12 high tensile, 8 mm mild-steel caphead screws and aligned by a spigot as shown. The pressure created in chamber 2 was transferred to the propane by a double ended stainless steel type 304 piston.

Possible unnoticed contamination of the propane due to an undetected leak across the "O"-ring as could happen in a single piston design was avoided by the use of the double piston.

The pistons were sealed by viton "O" rings in grooves cut to the dimensions for P > 100 bar as recommended by Dowty Seals (1986) for housing assemblies for piston and piston rods (Appendix C.1). The end plates were manufactured to Dowty's recommendations for housing assemblies for axial and triangular sealing applications (Appendix C.1).

C.10.2 Operation Of Propane Compression Device

A schematic diagram of the unit and it's auxilary equipment is shown in Figure C.6.

Chamber 2 was vented to atmosphere by closing V1 and opening V2 and V3. Propane was released into chamber 1 by closing V6 and opening V5 and V6. The propane pressure forced the piston to the end of its travel and filled the chamber. V5 and V4 were closed. The propane was left in chamber 1 for 15 minutes to reach the higher temperature. Valve V2 was closed and V1 opened. The flow rate of air into chamber 1 and hence the rate of movement of the piston, which was graduated, was controlled by the fine metering valve V3. The propane in chamber 1 was compressed and the pressure in the chamber increased. Since the temperature was above the critical temperature the condensation of propane was avoided. When the piston reached the end of its travel V4, V6 and V7 were opened and the propane due to the pressure gradient flowed to the equilibrium cell. V6 and V7 and V1 are shut and V2 and V3 opened. The compressed air now vented from chamber 2. The process was then repeated until the desired equilibrium cell pressure was reached.

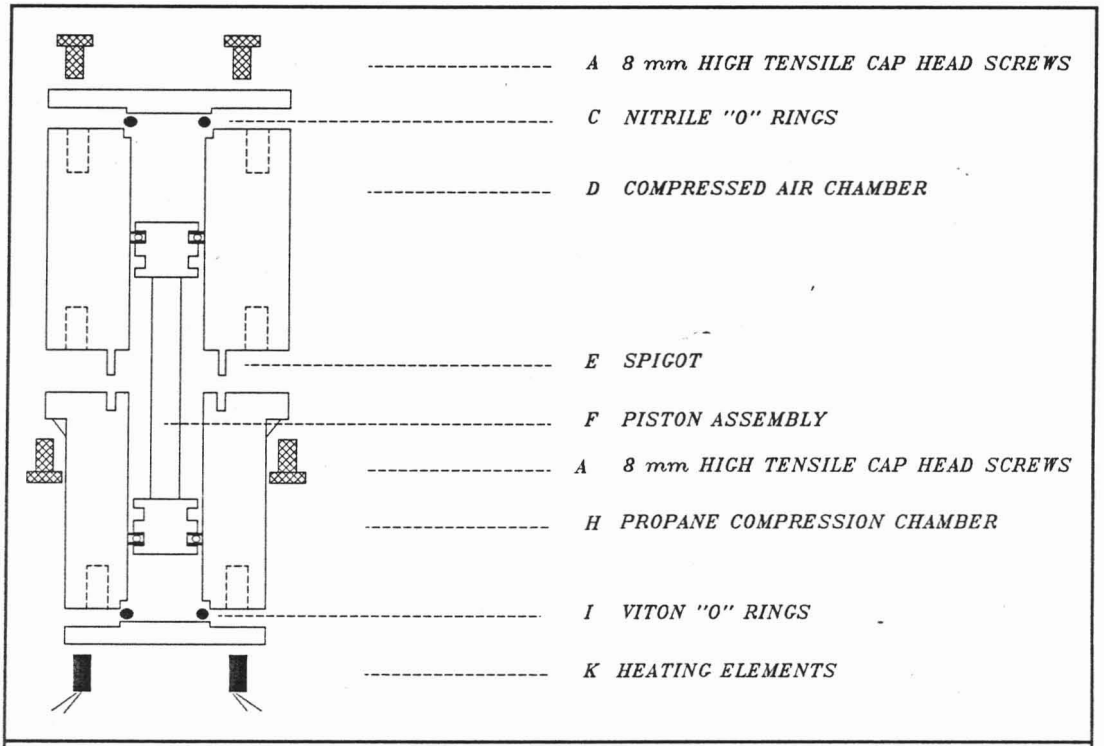

Figure C.6 : Propane Compression Device

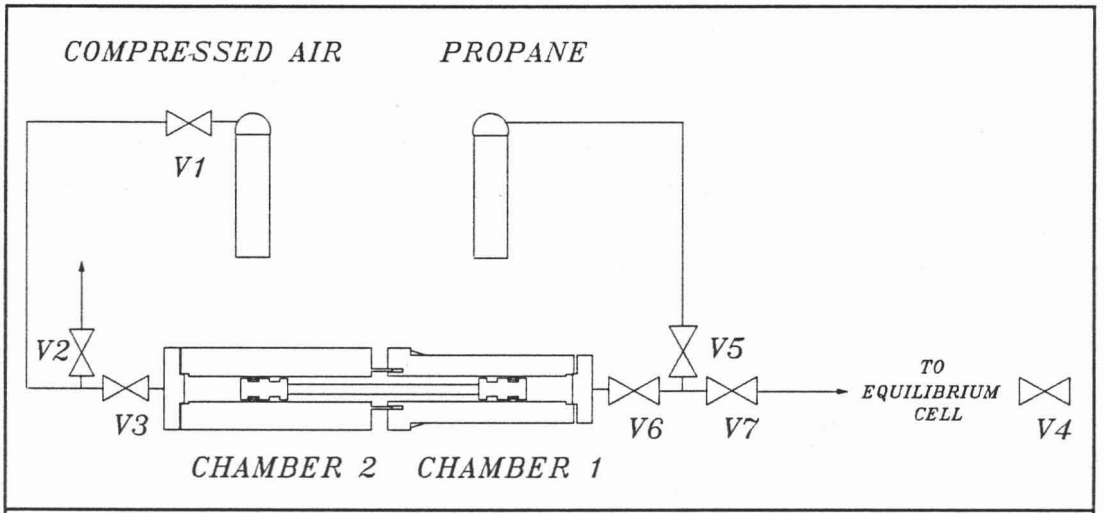

Figure C.7 : Propane Compression Device and Auxilluary Equipment

APPENDIX D

D.1 ASPECTS OF GAS DETECTOR CALIBRATION

The review by Debbrecht (1985) on the qualitative and quantative aspects of gas chromatography was found to be particulary useful.

D.1.1 Qualitative and Quantitative Aspects of Calibration

Qualitative aspects which include the peak shape and the separation of the peaks which are mainly determined by the column and operating conditions chosen. Quantitative aspects include the methods employed to calculate peak areas and calibrate the detectors.

Qualitative Aspects (Peak Separation)

To achieve separate sharp peaks, which allow for most accurate quantitative analysis, experimentation is required to determine the optimum combination of column packing and length) and operating conditions (column carrier gas flow rate and temperature). The column and operating conditions chosen are described in section 4.3.3 (Composition Measurements).

Quantitative Analysis

For both the thermal conductivity and flame ionization detectors used, the detector response at any moment is proportional to the concentration of the component. Thus the area under a peak is representative of the total amount of component present in the sample. To analyse this unknown amount the detector's proportionally or response factor must be found by calibration.

D.1.2 Internal Standardisation Calibration Method

Samples of known concentration, with an internal standard not present in the samples, are injected into the gas chromatograph. The internal standard or reference substance (r) is assigned a value of unity for its response factory (f_r). The response factors of the other component or components are assigned response factors (f_x). The measured peak areas (A_x, A_r) and concentrations (C_x, C_r) may be related to each other knowing that the peak area response of a detector is directly proportional to the concentration :

$$C_x = f_x \; A_x$$

$$C_r = f_r \; A_r$$

The response factors therefore of the components can be calculated from :

$$f_x = \left(\frac{A_r}{A_x}\right)\left(\frac{C_x}{C_r}\right) f_r$$

Before a sample of unknown concentration is analysed, a known amount of standard substance is added directly to the sample. The unknown concentration of a substance is calculated by :

$$C_x(\%) = \left(\frac{A_x}{A_r}\right)(C_s)f_x \times 100$$

D.1.3 Direct Injection Calibration Method

In this method two or more standard solutions of the components of interest are prepared. Given volumes of these are injected into the chromatograph. A calibration curve of peak area versus quantity injected is generated. The calibration curve slope (CSK) can be determined by linear regression if a linear response was observed. The unknown quantity of the component (Q_i) can therefore be calculated from the peak area of the component (A_i) from :

$$Q_i = CSK \times A_i$$

D.2 DIRECT CALIBRATION METHOD AS APPLIED IN THIS PROJECT

D.2.1 Precuations Taken

Gas and liquid syringes

The problem of relying on the reproducibility of injected volumes is partly overcome by using good quality syringes maintained in impeccable working condition. Since volatile/non-volatile binaries were being investigated standard solutions containing a mixture of both components could not be prepared. Separate calibration curves for the gas and liquid components had to be generated.

Two different syringes were used to check that the same injected volumes produced equal peak areas. A inaccurately calibrated syringe was therefore not used for calibration.

The same volume was injected at least 10 times and only the results that correlated to within 1,5 % for the liquid and 1,0 % for the gas injections were used to generate an averaged peak area. All the averaged peak areas when plotted against quantity injected should lie on a straight line. Any spurious points that were discovered during this plotting procedure were repeated.

All syringe needles were regularly checked during calibration for needle blockages due to septa coring. The tightness of piston plunger seal for gas and liquid syringes, and the needle seal for the 1 μl liquid syringe's were regulary checked.

The gas chromatograph septa were replaced after 50 injections during calibration to avoid potential errors due to septum leakages which could be detected by a column head pressure drop.

The gas chromatograph flow-rates of carrier gas, reference, air and hydrogen, were also continuously checked.

Generally only volumes greater than 50 % of the total syringe volume were injected with the gas syringes to negate any errors due to the extra syringe needle volume. Only when absolutely necessary were volumes less than 50 % of the total syringe volume injected.

The regression of the peak area versus volume injected, converted to moles, showed the correlation coefficients of the vapour to be closer to unity than for the liquid, typically 0,9999 versus 0,999.

Sandwich technique for liquid injection

The liquid sample was injected with either a 1 μl or 10 μ *l* liquid syringes manufactured by Dynatech SGE or Hamilton. For the 10 μ *l* syringe the "sandwich" technique was used. A small amount of air was initially drawn into the syringe barrel, usually 2 μ *l*. The desired quantity of liquid was drawn into the syringe barrel followed finally by another layer of air. The liquid was thus contained in a "sandwich" of air and the volume of liquid could be accurately read. This method negated any errors due to the extra liquid volume that would have been contained in the syringe needle had the direct withdrawal and injection method been used.

D.2.2 Gas Component Calibration

The methods used for carbon dioxide and propane calibration are given below. There was essentially little difference between calibration for the vapour phase for the propane/water and propane/1-propanol binaries. Calibration for the liquid phase propane concentrations initially proved problematical. Calibration for the propane/water system required very small quantities of propane. With the avaliability of the Raal detector calibration device (Appendix C.8) the desired propane calibration curves could be obtained.

Calibration for vapour phase mole fractions

Volumes from the gas syringes of sizes 0 to 100 μ *l* and 0 to 1 cm^3 were injected into the gas chromatograph. The volume injected was converted into moles by the truncated two-parameter virial equation of state :

$$n = \frac{V}{\left(\frac{RT}{P} + B\right)} \qquad (D.1)$$

where : V = volume in cm^3

T = temperature in K

P = pressure in kPa

R = universal gas constant 8314

B = second virial coefficient obtained from Dymond and Smith (1980).

The calibration curve of peak area versus moles injected was then plotted.

Calibration for liquid phase mole fractions

The volume of the Raal detector calibration device as a function of piston position was determined. The required amount of propane was displaced into the nitrogen and the mole fraction propane of the mixture calculated. The same calibration calculation (Eq. (D.1)) was used to calculate the calibration for the gas in the liquid phase.

D.2.2.1 Liquid component calibration

The method of water calibration for the vapour phase samples in the propane/water binary required particular attention.

Water calibration

The water had to be diluted in some solvent to generate a calibration curve in the desired peak area range. A major problem with solvents which are mutually soluble with water are that they contain water as an impurity. This water quantity can affect calibration accuracy. The problem is amplified when the sealed solvent bottle is opened. The solvent evaporates and if the climate is particularly humid, water will be absorbed from the environment further increasing the water concentration.

Various techniques were investigated to try to remove the residual traces of water from the solvent. For example a drying agent such as silica gel could be placed in the solvent. Silica gel is however not powerful enough and the more powerful drying agents such as phosphorous pent-oxide tend to chemically attack the solvent. Another option would be to work in an anhydrous environment such as a Dry Box. The setting up of a perfectly functioning Dry Box usually takes 3 to 4 months and none were available in the department.

A method was devised to take into account the impurity of the water in the solvent by calculation. This method is described fully below.

The liquid mixtures, (component of interest + suitable solvent) to achieve the correct concentrations, were made up in 50 m*l* septum vials. The components were added to and the mixture removed from the vial through the septum, to prevent any evaporation of the solvent. The relatively large septum vial volume allowed "large" quantities of solvent and the solute to be used thereby minimizing weighing errors.

Determining water impurities by calculation

Aim : To find water impurity in solvent (X)

X is defined as x g of water (2) / g of solvent (1) i.e. : impurity of solvent

Method :

Add certain quantities of water (m_{21}, m_{22}, m_{23}, ...) to (m_{11}, m_{12}, m_{13}, ...) of solvent where,

m_{2i} is mass water added to solvent.
m_{1i} is mass of solvent + impurity of water.

to get a range of mixtures such that,

mass of water in mixture $= m_{2i} + X\ m_{1i}$
mass of solvent in mixture $= m_{1i} - X\ m_{1i}$

total mass of mixture is therefore m_{total} :

$m_{total} = m_{2i} + m_{1i} + X\ m_{1i} - X\ m_{1i}$

$m_{total} = m_{2i} + m_{1i}$

Mole fraction water (x_2) in mixture, assuming no other major impurity (usually a safe assumption), is therefore :

$$x_2 = \frac{\frac{(m_{2i} + X m_{1i})}{MM_2}}{\frac{(m_{2i} + x m_{1i})}{MM_2} + \frac{(m_{1i} - X m_{1i})}{MM_1}} \qquad (D.2)$$

where MM_1 and MM_2 are the molecular masses of solvent and water respectively.

A certain volume of mixture is injected into the gas chromatograph and peak areas A_1 and A_2 of the solvent water recorded.

Normally a plot of (A_1/A_2) versus (x_1/x_2) should pass through the origin as shown in graph 1 below :

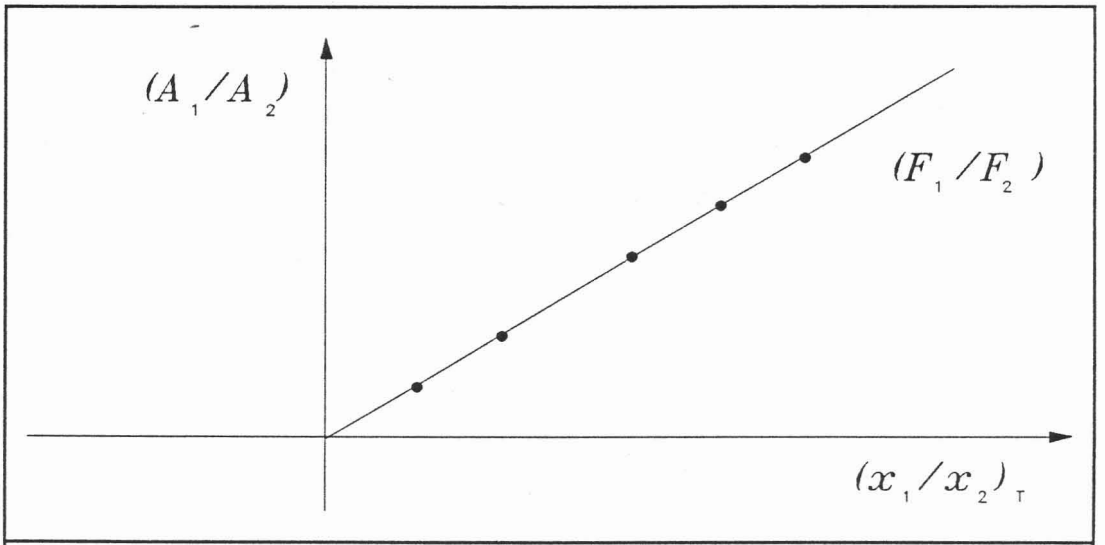

Graph 1 : Peak Area Ratio versus Mole Fraction Ratio

where :

$$\frac{A_1}{A_2} = F\left(\frac{x_1}{x_2}\right) \qquad (D.3)$$

Since mole fraction ratio (x_1/x_2) cannot be calculated as X is unknown the graph of peak area ratio versus the mole fraction ratio X can be represented as shown in graph 2.

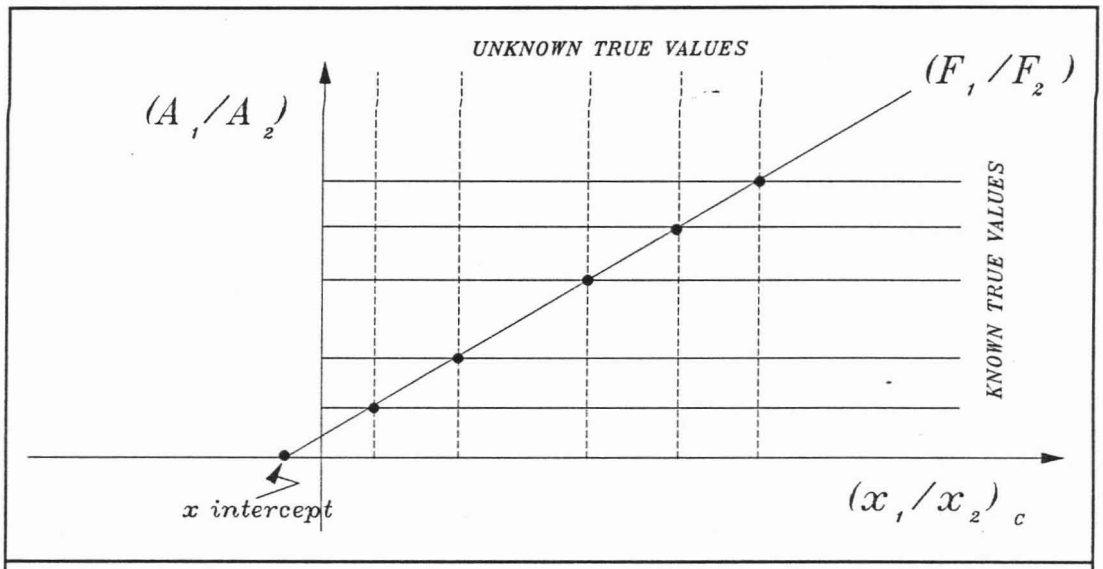

Graph 2 : Peak Area Ratio versus Mole Fraction Ratio

where :

$$\left(\frac{A_2}{A_1}\right) = F\left(\frac{x_2}{x_1}\right)_c + C \qquad (D.4)$$

$$\left(\frac{A_2}{A_1}\right) = F\left(\frac{m_2 - Xm_m}{m_m - Xm_m}\right)\left(\frac{MM_1}{MM_2}\right) + C \qquad (D.5)$$

The A_2/A_1 are known from the various injections. The y intercept is fixed at A_2/A_1 from an injection of pure solvent. This implies that the x intercept would yield the desired X.

The (x_2/x_1) are however not known so a graphical method must be found to solve the X from known values i.e. m_2 and m_m.

Rewriting Eq. (D.5) as :

$$A(m_m - Xm_m) - c(m_m - Xm_m) = F\left(\frac{MM_1}{MM_2}\right)(M_2 + Xm_m) \qquad (D.6)$$

Dividing Eq. (D.6) by m_m

$$A(1 - X) - c(1 - X) = F\left(\frac{MM_1}{MM_2}\right)\left(\frac{m_2}{m_m} + X\right) \qquad (D.7)$$

$$A = F\left(\frac{MM_1}{MM_2}\right)\left(\frac{1}{1-X}\right)\frac{m_2}{m_m} + \frac{\left(XF\left(\frac{MM_1}{MM_2}\right) + C(1+X)\right)}{(1-X)} \qquad (D.8)$$

A plot of A versus m_2/m_m yields the gradient (β) and y intercept (γ) from which X and F can now be solved :

$$\beta = \left(\frac{MM_1}{MM_2}\right)\left(\frac{1}{1-X}\right)F \qquad (D.9)$$

which implies :

$$X = -\left(\frac{1}{\beta}\right)\left(\frac{MM_1}{MM_2}\right)F + 1 \qquad (D.10)$$

and

$$\gamma = \frac{\left(XF\left(\frac{MM_1}{MM_2}\right) + C(1+X)\right)}{(1-X)} \qquad (D.11)$$

Substituting (D.10) into (D.11) yields :

$$\left(\frac{MM_1}{MM_2}\right)^2\left(\frac{1}{\beta}\right)F^2 + \left[\left(\frac{MM_1}{MM_2}\right)\left(\frac{1}{\beta}\right)(C) + \left(\frac{MM_1}{MM_2}\right) + \gamma\left(1 - \left(\frac{MM_1}{MM_2}\right)\frac{1}{\beta}\right)\right]$$

$$F - (C - \gamma) = 0 \qquad (D.12)$$

F^2 can be solved to yield F and hence X is solved from (D.10).

The correct moles of water present can now be plotted against peak area water to generate the calibration curve desired.

1-propanol calibration

Calibration of 1-propanol however did not require such precautions. The 1-propanol was diluted in water which was free of 1-propanol impurities.

D.3 EQUILIBRIUM CELL LIQUID-LEVEL MEASURING DEVICES

Direct measuring methods

(a) **Installation of view window**

This would have required extensive machining and modification of the equilibrium cell and air bath respectively to insert the required view glasses. The present shape and even space limitations in the equilibrium cell are not conducive to the implementation of this solution.

(b) **Fibre optics**

The use of fibre optics to view the cell contents would be a neat solution. The system would be compact and not require the extensive machining of the equilibrium cell required for the window. No modification of the air bath would be required. The optic system would have been difficult to seal and further investigations as to whether they could wihtstand the pressure and temperature specifications of 200 bar and 200 °C would be required. This method and the solid state liquid sensors to be mentioned would require some source of internal light which would be difficult to install

Indirect measuring method

(c) **Measurement of level by Capacitance**

This method has been extensively used in the single vapour and liquid pass experimental method. A limitation of this method is that it is sometimes unresponsive to certain materials as in the case of Lin *et al.* (1985).

A typical capacitance system as described by White and Brown (1942), for example, comprises of a condensor (placed in the equilibrium cell) attached to a high-frequency alternating circuit and balanced against a control condensor in a capacitance bridge. The capacitance of the condensor which depends on the liquid level can be quantified using a cathode ray oscillograph. Wilner (1960) reviews and makes suggestions on the use of Variable Capacitance liquid level sensors for both conductive and non-conductive liquids.

If the condensor can be incorporated as a central draft tube in the equilibrium cell it could be used as an added means of homogenization.

The main problem associated with this method would be the mechanical sealing of the inlet and outlet electric leads and calibrating the capacitor to accurately quantify the liquid level.

Near the critical point problems in the accurate measurement of the liquid level are envisaged as the differences between the physical properties of the phases diminish.

The capacitance measurement is also limited to the time the stirrer is switched of and would not give continuous information as the visual methods would.

(d) **Solid-state liquid level sensors**

Sensors such as those produced by Honeywell can accurately detect liquid levels, have no mechanical parts and are available in miniature sizes. There were however difficulties in the equilibrium cell temperature and pressure specification of 200 °C and 200 bar.

(e) **Float liquid level sensors**

The liquid level interface can be determined by measuring the position of a magnetic float extension. This method is difficult to implemented for the following reasons :

1. It would be difficult to install on the lid of the cell due to space limitations.
2. The stagnant areas that would be created by the float extension are undesirable.
3. The vigourous stirring process and associated vortex formation would in all probability result in mechanical damage to the float and it's extension.

APPENDIX E

TABLE E.1
Impurities Found in Gaseous Materials

Gaseous Material	Maximum Impurity									
	Oxygen ppm	Nitrogen ppm	Water ppm	Carbon monoxide ppm	THC(1) ppm	Sulphur dioxide ppm	Ethane	Propylene	Isobutane	n-butane
Carbon dioxide (2)	10	10	5	1	5	1				
Helium (2)	5	20	2		1					
Nitrogen (2)	5		1				0.007	0.001	0.50	0.05
Propane (Air Products (3)							0.01	0.01	0.35	0.03
Propane (Afrox) (3)(4)										

(1) total hydrocarbon.
(2) impurities by volume.
(3) impurities by weight.
(4) Afrox propane specification was not met.

E.2 PERFORMANCE CHARACTERISTICS OF MILLIPORT MILLI-RO-4 WATER PURIFICATION SYSTEM

TABLE E.2
Millipore Milli-RO-4 Water Specification

Performance Characteristic	Performance
Ion rejection	
Monovalent	90 %
Polyvalent	95 %
Weakly Ionized monovalent	60 %
Particle removal	99 %
Bacterial removal	99 %
Pyrogen reduction	99 %
Organic removal	99 %

APPENDIX F

F.1 CARBON DIOXIDE / TOLUENE DATA

Table F.1

Data Used for the Carbon Dioxide/Toluene Theoretical Analysis

Pressure bar	Mole fraction CO_2 liquid phase x	Mole fraction vapour phase y	Source
Data for CO_2/Toluene System at 38 °C			
3,34	0,030	0,978	Ng & Robinson (1978)
14,89	0,133	0,993	
28,55	0,264	0,997	
40,68	0,406	0,996	
55,78	0,603	0,994	
69,36	0,869	0,992	
73,36	0,931	0,993	
77,43	0,971	0,993	
Data for CO_2/Toluene System at 79 °C			
6,72	0,033	0,887	combined data Kim, *et al* (1986) & Ng & Robinson (1978)
13,33	0,073	0,932	
22,22	0,125	0,958	
28,84	0,166	0,969	
36,28	0,210	0,979	
57,23	0,328	0,981	
83,64	0,491	0,978	
95,57	0,588	0,973	
112,11	0,720	0,961	
116,04	0,749	0,954	
119,22	0,787	0,946	
123,08	0,843	0,931	
8,76	0,0495	0,9300	Present study
17,58	0,1100	0,9675	
31,37	0,1731	0,9775	
54,81	0,3000	0,9820	
55,50	0,3100	0,9820	
86,53	0,5000	0,9820	
103,08	0,6490	0,9725	
105,83	0,6693	0,9720	
109,97	0,7080	0,9650	
3,76	0,021	0,886	Ng & Robinson (1978)
14,00	0,077	0,963	
30,75	0,172	0,978	
57,23	0,328	0,981	
83,64	0,491	0,978	
95,57	0,588	0,973	
112,11	0,720	0,961	
116,04	0,749	0,954	
119,22	0,787	0,946	
123,08	0,843	0,931	

Table F.1 cont.

Data for CO_2/Toluene System at 120 °C			
4,03	0,017	0,0660	Ng & Robinson (1978)
9,89	0,040	0,847	
24,41	0,106	0,926	
52,26	0,231	0,953	
84,26	0,368	0,953	
112,73	0,495	0,943	
138,18	0,621	0,921	
152,93	0,715	0,879	

Table F.2

Data Used for the Propanol/1-Propanol System Theoretical Analysis

Pressure (mm Hg)	Pressure (bar)	Pressure (psi)	Temp (K)	Experimental (x)	Experimental (y)
3397,48	4,52	65,70	354,77	0,0647	0,9212
4897,12	6,52	94,70	354,77	0,0973	0,9438
6133,04	8,17	118,60	354,77	0,1258	0,9530
7869,42	10,52	152,70	354,77	0,1690	0,9665
9602,91	12,80	185,70	354,77	0,2198	0,9665
12085,08	16,11	133,70	354,77	0,2876	0,9701
13688,16	18,25	264,70	354,77	0,3378	0,9736
16118,62	21,49	311,70	354,77	0,4353	0,9778
16790,87	22,38	324,70	354,77	0,4737	0,9831
3438,85	4,58	66,50	378,37	0,0424	0,7189
4581,68	6,10	88,60	378,37	0,0601	0,7924
6345,06	8,45	122,70	378,37	0,0887	0,8489
8103,27	10,18	156,70	378,37	0,1219	0,8800
8284,26	11,04	160,70	378,37	0,1220	0,8825
9602,91	12,80	185,70	378,37	0,1484	0,8985
11671,39	15,56	225,70	378,37	0,1877	0,9129
13119,33	17,49	253,70	378,37	0,2139	0,9165
15187,81	20,24	293,70	378,37	0,2552	0,9190
17308,00	23,07	337,70	378,37	0,3071	0,9245
20410,71	27,21	394,70	378,37	0,3874	0,9294
22608,47	30,14	437,20	378,37	0,4584	0,9300
22737,75	30,31	439,70	378,37	0,4588	0,9300
25840,47	34,45	499,70	378,37	0,5752	0,9300
26616,15	35,48	514,70	378,37	0,5865	0,9300
3397,27	4,52	65,70	393,20	0,0297	0,5826
4793,49	6,39	92,70	393,20	0,0489	0,7364
6913,68	9,21	133,70	393,20	0,0787	0,8200
7538,23	10,04	145,70	393,20	0,0904	0,8445
9964,69	13,28	192,70	393,20	0,1288	0,8690
11878,03	15,83	229,70	393,20	0,1585	0,8765
14980,75	19,97	289,70	393,20	0,2045	0,8900
16842,38	22,45	325,70	393,20	0,2408	0,8999
19893,39	26,52	384,70	393,20	0,2999	0,9080
23409,80	31,21	452,70	393,20	0,3681	0,9160
26228,11	34,96	507,20	393,20	0,4448	0,9265
27526,76	36,72	532,70	393,20	0,4782	0,9270
30235,78	40,31	584,70	393,29	0,5640	0,9335

F.2 CHUEH, *et al* (1965) CONSISTENCY TEST RESULTS

Table F.3						
Comparison of Chueh, *et al* (1965) Consistency Test						
Mole fraction CO_2 liquid phase	Area 1 (1)	Area 2 (2)	Area 3 (3)	LHS	RHS	% Diff
TEMPERATURE 38.11°C						
0,264	1,62	0,08	0,09	1,79	1,52	16,61
0,603	3,57	0,41	0,17	4,14	6,28	-3,13
0,931	4,75	0,97	0,20	5,92	6,10	-3,00
0,985	4,83	1,10	0,21	6,14	6,34	-3,14
TEMPERATURE 79°C						
Ng & Robinson (1978)						
0,172	0,86	0,04	0,10	0,99	1,01	-2,00
0,491	2,33	0,34	0,25	2,92	2,94	-0,69
0,720	3,04	0,76	0,31	4,11	4,17	-1,49
0,787	3,16	0,92	0,32	4,41	4,48	-1,64
0,895	3,26	1,25	0,33	4,3	4,91	-1,62
Kim, *et al* (1986)						
0,166	0,69	0,04	0,08	0,80	0,64	22,50
0,172	0,72	0,04	0,09	0,84	0,44	63,89
0,491	2,19	0,34	0,24	2,77	2,36	15,91
0,720	2,90	0,76	0,30	3,95	3,59	9,74
0,787	3,02	0,93	0,31	4,26	3,90	8,72
0,895	3,12	1,25	0,32	4,68	4,33	7,76
This project						
0,173	0,94	0,04	0,11	1,10	1,17	-6,75
0,310	1,63	0,14	0,19	1,96	1,99	1,27
0,635	2,97	0,58	0,31	3,87	3,73	3,45
0,760	3,32	0,84	0,33	4,50	4,49	0,09
0,840	3,43	1,06	0,34	4,84	4,84	0,10
0,900	3,46	1,25	0,35	5,07	5,07	0,16
TEMPERATURE 120.66°C						
0,106	0,43	0,02	0,07	0,51	0,54	-5,18
0,368	1,51	0,19	0,25	1,95	1,99	-1,69
0,621	2,22	0,56	0,37	3,15	3,25	-3,15
0,790	2,40	0,99	0,41	3,79	3,91	-3,14

F.3 MODELLING OF THE CARBON DIOXIDE/TOLUENE SYSTEM IN THE LITERATURE

Ng and Robinson (1978)

Ng and Robinson (1978) supply temperature independent Peng-Robinson $\delta_{ij} = 0,09$ for the *classical mixing rules* from their experimental data . The δ_{ij} supplied gave the minimum deviation between the experimental bubble point locus and the bubble point locus predicted by the P-R EOS.

Kim, et al (1986)

The experimental data obtained by Kim, *et al* (1986) were used to compare the correlative ability of three different equations.

The direct method was used in conjunction with the original P-R EOS and a modified PACT theory EOS (SPHCT) discussed in Appendix B.6. The combined method was used with UNIFAC for activity coefficients and SPHCT EOS for the fugacity coefficients. The Poynting correction was however neglected.

The SPHCT EOS and P-R EOS interaction parameters were determined by fitting the experimental data onto the respective equations. The SPHCT EOS interaction parameters (k_{ij}) being about 1/5 the magnitude of the P-R EOS δ_{ij}. The SPHCT EOS gave fairly accurate results for both the toluene and carbon dioxide K values even with the neglect of the interaction parameter. The P-R EOS predicted K values for carbon dioxide were however closer to the experimental values than for SPHCT EOS with ($k_{ij} = 0$).

The combined method UNIFAC/SPHCT EOS predicted K toluene values were closer to the experimental values than for the SPHCT EOS with ($k_{ij} = 0,0$).

Mohamed and Holder (1987)

Mohamed and Holder (1987) modelled the experimental data of Ng and Robinson (1978) with their density dependent mixing rules P-R EOS Eq (3.44). Far better agreement in the high pressure region was obtained between the correlational and experimental results using Eq. (3.44) than for the *classical mixing rule* P-R EOS over the temperature range 38 °C to 120 °C.

Fink and Hershey (1990)

Fink and Herskey (1990) used two interaction parameter forms of the P-R and CCOR (Appendix B.5) EOS to model their data as well as the other data in the literature : (Ng and Robinson 1978, Sebastian, *et al* 1980 and Morris and Donohue 1985).

The authors introduced an additional η_{ij} interaction parameter into the P-R EOS in contrast to Mohamed and Holder's (1987) density dependent mixing rule. The interaction parameters of each EOS were obtained by fitting the EOS onto the experimental data. The obtained parameters showed no systematic variation with respect to temperature although the values varied for the different author's data.

The CCOR EOS interaction parameters exhibited more variance with respect to temperature and data source than was observed for the P-R EOS interaction parameters.

The modified two parameter P-R EOS reproduced the experimental data well. The correlated K values of toluene did however show greater deviations from the experimental values than the carbon dioxide K values. The two interaction parameter CCOR EOS however performed poorly. The correlated K values for carbon dioxide were better represented than the K values for toluene which were very poorly represented. The theoretically and computationally more complex CCOR EOS obviously had greater difficulty in conforming to the shape of the coexistence curve than the simpler P-R EOS.

F.4 MODELLING OF PROPANE/ALCOHOL SYSTEM IN THE LITERATURE

Propane/methanol system

The propane/methanol data (Galivel-Solastiouk 1986) at 39,9, 69,9 and 99,9 °C was modelled by the direct method, Schwartzentruber, *et al* (1987). Schwartzentruber, *et al* (1987) used a new empirical three-parameter mixing rule in preference to the Huron-Vidal (1979) mixing rule to describe the alcohol/alkane system. A three parameter mixing rule EOS was necessary to prevent the prediction of non-existant liquid-liquid phase splitting and general lack of flexibility of the *classical mixing rules* that occur with the use of cubic EOS.

The authors achieved satisfactory correlations using the new mixing rules except near the critical point. A systematic deviation in the vapour phase composition was observed for both the new and Huron-Vidal mixing rules. The vapour phase propane composition predictions for the three temperatures lay to the left of the experimental pressure versus propane vapour mole fraction curve.

Propane/ethanol system

The propane/ethanol system was measured and theoretically analysed by Gómez Nieto and Thodos (1978). The direct method in conjunction with the Benedict-Webb-Rubin (BWR) or Soave-Redlich-Kwong (S-R-K) EOS was used to correlate the equilibrium K values.

It would appear that the *classical mixing rules* with interactions parameters derived from the experimental vapour and liquid compositions, were used for the S-R-K EOS. The authors mention that agreement between the correspondingly calculated K and experimental K values was fair for both methods.

No mention was made of any liquid-liquid phase splitting predictions normally associated with the use of the cubic EOS. The authors do mention however that some of the more significant K deviations could be attributed to interactions between propane and ethanol or the lack of adequate mixing rules for polar/non-polar mixtures for the cubic EOS.

Knapp, *et al* (1982) analysed the above data by the BWRS, LKP, S-R-K and P-R EOS by the direct methods. The plot of predicted pressures versus propane mole fraction from the SRK EOS shows the predicted propane liquid phase mole fraction lay to the left of the experimental curve.

Propane/1-propanol system

For the low temperature 19.9 °C and pressure propane/1-propanol data of Nagahama, *et al* (1971) the authors used Barkers method to predict the propane vapour phase mole fractions.